frontiers | Research Topics

Irradiation technologies for vaccine development

Edited by
Viskam Wijewardana, Giovanni Cattoli and Sebastian Ulbert

Published in
Frontiers in Immunology
Frontiers in Veterinary Science

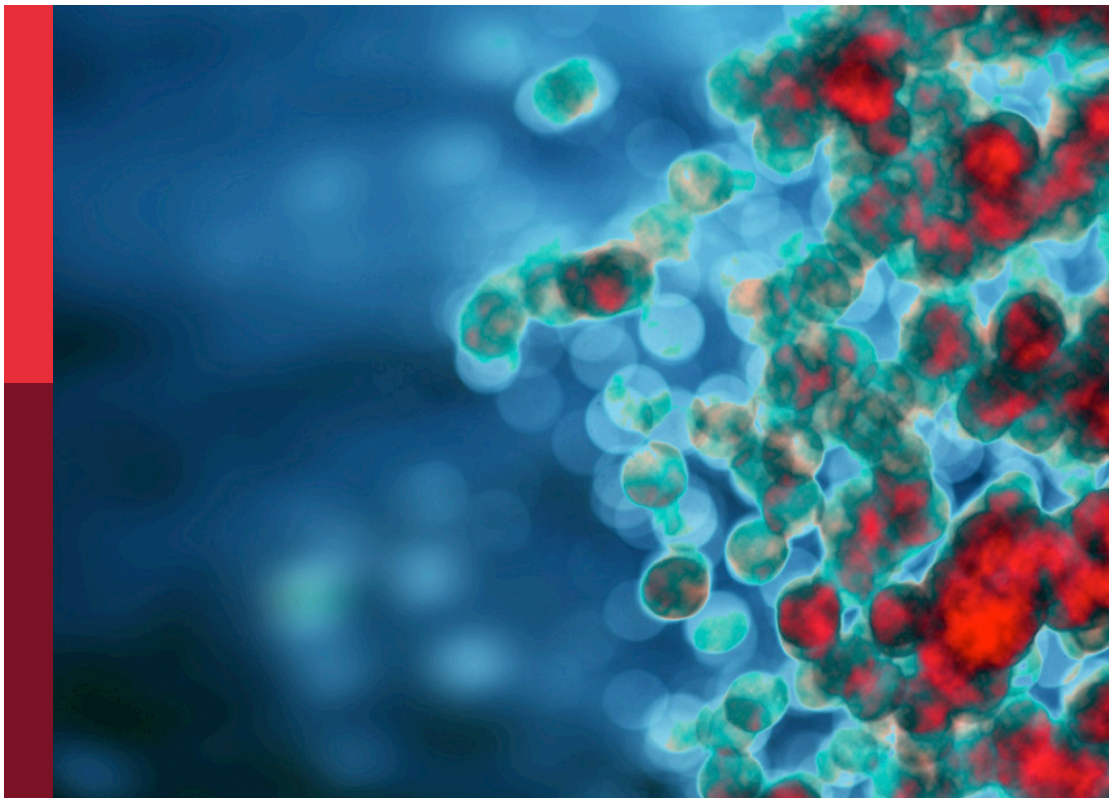

ISSN 1664-8714
ISBN 978-2-83251-547-1
DOI 10.3389/978-2-83251-547-1

About Frontiers

Frontiers is more than just an open access publisher of scholarly articles: it is a pioneering approach to the world of academia, radically improving the way scholarly research is managed. The grand vision of Frontiers is a world where all people have an equal opportunity to seek, share and generate knowledge. Frontiers provides immediate and permanent online open access to all its publications, but this alone is not enough to realize our grand goals.

Frontiers journal series

The Frontiers journal series is a multi-tier and interdisciplinary set of open-access, online journals, promising a paradigm shift from the current review, selection and dissemination processes in academic publishing. All Frontiers journals are driven by researchers for researchers; therefore, they constitute a service to the scholarly community. At the same time, the *Frontiers journal series* operates on a revolutionary invention, the tiered publishing system, initially addressing specific communities of scholars, and gradually climbing up to broader public understanding, thus serving the interests of the lay society, too.

Dedication to quality

Each Frontiers article is a landmark of the highest quality, thanks to genuinely collaborative interactions between authors and review editors, who include some of the world's best academicians. Research must be certified by peers before entering a stream of knowledge that may eventually reach the public - and shape society; therefore, Frontiers only applies the most rigorous and unbiased reviews. Frontiers revolutionizes research publishing by freely delivering the most outstanding research, evaluated with no bias from both the academic and social point of view. By applying the most advanced information technologies, Frontiers is catapulting scholarly publishing into a new generation.

What are Frontiers Research Topics?

Frontiers Research Topics are very popular trademarks of the *Frontiers journals series*: they are collections of at least ten articles, all centered on a particular subject. With their unique mix of varied contributions from Original Research to Review Articles, Frontiers Research Topics unify the most influential researchers, the latest key findings and historical advances in a hot research area.

Find out more on how to host your own Frontiers Research Topic or contribute to one as an author by contacting the Frontiers editorial office: frontiersin.org/about/contact

Irradiation technologies for vaccine development

Topic editors

Viskam Wijewardana — International Atomic Energy Agency, Austria

Giovanni Cattoli — Joint FAO/IAEA Programme of Nuclear Techniques in Food and Agriculture, Austria

Sebastian Ulbert — Fraunhofer Institute for Cell Therapy and Immunology (IZI), Germany

Citation

Wijewardana, V., Cattoli, G., Ulbert, S., eds. (2023). *Irradiation technologies for vaccine development*. Lausanne: Frontiers Media SA.

doi: 10.3389/978-2-83251-547-1

Table of contents

frontiers | Frontiers in Immunology

TYPE Editorial
PUBLISHED 09 January 2023
DOI 10.3389/fimmu.2022.1075335

OPEN ACCESS

EDITED AND REVIEWED BY
Anke Huckriede,
University Medical Center Groningen,
Netherlands

*CORRESPONDENCE
Viskam Wijewardana
V.Wijewardana@iaea.org
Sebastian Ulbert
sebastian.ulbert@izi.fraunhofer.de
Giovanni Cattoli
G.Cattoli@iaea.org

SPECIALTY SECTION
This article was submitted to
Vaccines and Molecular Therapeutics,
a section of the journal
Frontiers in Immunology

RECEIVED 20 October 2022
ACCEPTED 14 December 2022
PUBLISHED 09 January 2023

CITATION
Wijewardana V, Ulbert S and Cattoli G
(2023) Editorial: Irradiation technologies for
vaccine development.
Front. Immunol. 13:1075335.
doi: 10.3389/fimmu.2022.1075335

Editorial: Irradiation technologies for vaccine development

Viskam Wijewardana[1]*, Sebastian Ulbert[2]* and Giovanni Cattoli[1]*

[1]Animal Production and Health Laboratory, Joint Food and Agriculture Organization (FAO)/International Atomic Energy Agency (IAEA) Centre of Nuclear Techniques in Food and Agriculture, International Atomic Energy Agency, Vienna, Austria, [2]Department of Vaccines and Infection Models, Fraunhofer Institute for Cell Therapy and Immunology, Leipzig, Germany

KEYWORDS

gamma irradiation, e-beam irradiation, livestock, vaccine, zoonotic diseases, immune responses

Editorial on the Research Topic
Irradiation technologies for vaccine development

Vaccine development is of high priority in the control of infectious diseases. The impact of vaccination on health is immense; except for the improvement of drinking water quality, no other approach has had such a major effect on mortality reduction and population growth (Rodrigues and Plotkin). However, despite an increase in our knowledge on host-pathogen interactions and the advancement in various cutting-edge technologies in vaccine design, there is still a dearth of effective vaccines against many human and animal diseases. The need to design and generate vaccines in a shorter period against emerging and re-emerging pathogens that are difficult to control by other means is critical for human and animal welfare. The efforts to control current SARS-CoV-2 pandemic is a prime example. Inactivated whole virus vaccines were the first vaccines developed and applied against SARS-CoV-2 and they are still widely used (around 50% of total vaccines delivered), indicating the value of this traditional method of vaccine development (1). At present, chemical inactivation is the most common method to kill pathogens for vaccine preparation. However, in the last decade the use of irradiation (gamma-, X-ray-, electron beam-irradiation) has been considered as a potential, valid alternative for vaccine development. Inactivation by irradiation has some potentially important advantages over chemical inactivation. The compilation of this Research Topic will attract attention to the state-of-the art of irradiation technology in vaccine development.

The two mini reviews that appear in this collection give a comprehensive overview of the technology including historical developments. Despite the fact that irradiation technology is still primarily in the research and development phase, there is an increasing interest in this area as illustrated in the review paper by Bhatia and Pillai that provides a representative list of 24 patents that have been filed for the creation of irradiated vaccines for human and animal bacterial, viral, and protozoan diseases. In the second review paper, Unger et al. discuss the development of irradiated vaccines against livestock diseases with special reference to initiatives from the Animal Production and Health section (APH) of the Joint FAO/IAEA Centre of Nuclear Techniques in Food and Agriculture at the International Atomic Energy Agency. In this paper, information on the dose of irradiation used in various vaccine preparations is also provided. Both these articles show the science behind the ionizing

radiation and its effect on microorganisms. Depending on the dose applied, ionizing radiation can irreparably damage the microbes. Interestingly, the radiation dose can be calibrated in a way that exposed microorganisms are unable to replicate (i.e. to cause infection) but still retain their metabolic activity, resulting in so-called "metabolically active, non-replicating" microorganisms (Hieke and Pillai). The residual functional proteins that yield metabolic activity in these microorganisms induce a broader immune response in the host when vaccinated. This approach was adopted to develop a metabolically active, non-replicating sporozoite vaccine (PfSPZ vaccine) to prevent *Plasmodium falciparum* malaria which is now being tested at phase 2 clinical trials globally (2). While traditionally gamma irradiation was used for the inactivation of pathogens when developing irradiated vaccines, recent technological advances have paved the way for the use of electron (e)-beam or other irradiation techniques in an effort to move away from the use of radioactive material. Moreover, by employing new radio-protectant compounds such as manganese ions (Mn^{2+}) and trehalose, immunogenic epitopes have been better preserved during irradiation inactivation (3).

The antigenic variation of the HA1 domain and its resulting antigenic drift has led to reformulating seasonal influenza vaccines with new strains every year (4). This urge for the development of a universal influenza vaccine that must provide long-lasting cross-protective immunity that can induce both B and T cell responses. In veterinary medicine, the availability of safe and effective avian influenza vaccines suitable for mass applications (e.g. aerosol, drinking water) would facilitate the prevention and control of this disease in poultry. Within this collection there are three articles which aim to investigate if an irradiated influenza vaccine could perform better than chemically inactivated vaccines and/or induce a broader protection. Bortolami et al. investigated the protective efficacy of a H9N2 avian influenza vaccine prototype. In this experiment, birds were vaccinated with an irradiated or a chemical inactivated formulation. The irradiated vaccine group performed as well as the chemical inactivated vaccine group upon challenge when the vaccines were given parenterally. Interestingly, when the vaccine was applied by the mucosal route, the irradiated preparation provided 100% protection at a challenge dose of 3 logs while the chemically inactivated one did not. This indicates the possibility of developing mucosal immunity through irradiated inactivated vaccines which is very difficult to achieve with traditional chemical inactivation. Motamedi Sedeh et al. give further support to this aspect. In their H9N2 avian influenza experiments, both methods of inactivation and routes of administration provided similar levels of protection, but cell-mediated immune responses were more pronounce for the irradiated vaccine formulated with trehalose and given through the mucosal route. In a third article by Singleton et al., the conditions for irradiation were investigated in an H1N1 influenza vaccine experiment. They show not only protection from the vaccine strain but also cross-protection through a gamma irradiated vaccine. Interestingly the induction of higher neutralizing antibodies and more effective cytotoxic T cell responses were correlated with higher temperatures during the irradiation process.

In classical antigen presentation, the exogenous antigen is degraded *via* the endosome pathway and is loaded onto major histocompatibility complex (MHC) class II molecules that presents antigens to CD4 T helper (Th) lymphocytes while inefficient in presenting antigens through MHC class I which is needed to activate CD8 (T cytotoxic) lymphocytes (5). Therefore, traditional inactivated vaccines most often do not yield a pronounced cell-mediated immunity. However, irradiation-inactivated Salmonella gallinarum provided an immune response skewed towards Th1 type (higher IgG2b and IgG3 levels) compared to a formalin inactivated vaccine which led to a protection level similar to a live attenuated vaccine when the challenge was done in chicken (Ji et al.). In another irradiated bacterial vaccine experiment in chicken, Dessalegn et al. showed intranasal or intraocular delivery of gamma irradiated *Pasteurella multocida* provided 100% protection reinforced with higher levels of secretory IgA. Inactivated pathogens are easily cleared by cilia and mucus in the intranasal mucosa unlike live attenuated organisms which can replicate. However, if the structure is maintained along with membrane integrity, this will aid adherence and allow the antigen presenting cells to take up the vaccine antigens. Several groups here investigated the structural integrity following sterilizing irradiation of pathogens when used as vaccine candidates. Electron micrography data showed a high degree of structural integrity when optimum irradiation conditions were used to inactivate Influenza virus (Bortolami et al.) African Swine Fever virus (ASFV) (Pikalo et al.) or *Salmonella gallinarum* (Ji et al.). However, in the case of ASFV, although the irradiated vaccine elicited antibodies when delivered intra-muscularly, there was no protection induced. Since it was shown above that several irradiated vaccines do provide better protection when administered through mucosal rather than parenteral routes, the authors could investigate alternative delivery of the vaccine in future experiments.

One of the bottlenecks which holds back the scaling up and commercial production of irradiated vaccines is the safety and containment requirements for gamma irradiators sourced by radio isotopes. More and more groups are now investigating the use of e-beam or x-ray technologies to produce irradiated vaccines (6). Low-energy electron irradiation (LEEI) which consists of electrons accelerated with up to 500 kilo electron volts (keV) very rapidly delivers high doses necessary for pathogen inactivation, but only requires minimal shielding. Finkensieper et al. showed vaccination with three doses of LEEI inactivated tick-borne encephalitis virus provided complete protection from infection and induced higher antibody titers and avidities as compared to the formalin inactivated virus. E-beam technology can also help in producing biological therapeutics. E-beam irradiated inactivated human rotavirus (HRV) was used as antigen in chickens to produce antibodies against HRV. These egg yolk antibodies and serum derived IgY were effective at neutralizing HRV *in-vitro* (Skrobarczyk et al.). In LEEI processes, determination of the absorbed electron dose is challenging due to the limited, material-dependent penetration depth of the accelerated electrons into the matter. As a solution for this, Schopf et al. proposed the use of bacterial suspensions as biological indicators for electron beam doses.

The use of gamma irradiators has been seen as a hindrance in scaling up of irradiated vaccines against viruses and bacteria, which require relatively high doses. In contrast, eukaryotic cells are several orders of magnitudes more susceptible to ionizing radiation, and consequently a biopharmaceutical production process for attenuation by gamma irradiation has been developed (James et al.) to produce

PfSPZ vaccine against malaria. This process was used for several hundred irradiation events to produce the PfSPZ vaccine candidate in the last 13 years which generated multiple lots released for pre-clinical studies and clinical trials. By studying another unicellular parasite, Kangethe et al. performed experiments to identify genes that are involved in disease establishment by gamma irradiation of *Trypanosoma evansi*. By subjecting parasites to a lower-dose of irradiation than that needed to stop replication, the genes responsible for the repair of the radiation-induced damage and thus potential virulent factors were identified. The authors propose a strategy for a candidate vaccine by deleting some of these virulent genes in the parasite. Radiation-induced mutations were also applied to attenuate the virulence of Salmonella spp. to develop live vaccine strains (Ji et al.). The selected mutant strain (ATOMSal-L6) was almost 10,000 times less virulent than its parent strain. Moreover, attenuation was maintained for over 10 passages. ATOMSal-L6 induced protective immunity upon intramuscular vaccination of mice. Finally, Porfiri et al. explored the immunomodulatory landscape of replication deficient metabolically active Lactobacilli produced through gamma irradiation to be used as novel vaccine adjuvants. There is increasing understanding of the role of vaccine adjuvants and how the formulation of modern vaccines can be better tailored towards the desired clinical benefits. Thus discovery of novel adjuvants that could activate specific immune pathways will aid in the quest for developing vaccines against challenging pathogens (7).

In summary, this Research Topic highlights some of the latest developments, innovations and understanding of the use of irradiation technologies for vaccine development. It also raised scientific and technical questions that need to be answered in future research including the underlying mechanisms involved in the remaining metabolic activity in lethally irradiated microbial cells, generation of better cell mediated immunity compared to chemical inactivation, use of LEEI in bulk vaccine preparations, the best route to deliver irradiated vaccines, discovery of novel radio-protectant compounds to preserve vaccine antigenicity and stabilization of irradiated vaccine formulations. Research and technical innovation are also needed to transfer irradiation technologies for vaccine development from an applied research sector to production and marketing.

Author contributions

All authors listed have made a substantial, direct, and intellectual contribution to the work and approved it for publication.

Acknowledgments

We thank the authors, reviewers and external editors that contributed to this Research Topic. We also thank Dr William Dundon of the International Atomic Energy Agency for editing language of this editorial.

Conflict of interest

The authors declare that the research was conducted in the absence of any commercial or financial relationships that could be construed as a potential conflict of interest.

Publisher's note

References

1. Dolgin E. Omicron thwarts some of the world's most-used COVID vaccines. *Nature* (2022) 601:311. doi: 10.1038/d41586-022-00079

2. Oneko M, Steinhardt LC, Yego R, Wiegand RE, Swanson PA, Kc N, et al. Safety, immunogenicity and efficacy Q13 of PfSPZ vaccine against malaria in infants in western Kenya: a double-blind, randomized, placebo-controlled phase 2 trial. *Nat Med* (2021) 27:1636–45. doi: 10.1038/s41591-021-01470-y

3. Gayen M, Gupta P, Morazzani EM, Gaidamakova EK, Knollmann-Ritschel B, Daly MJ, et al. Deinococcus Mn2+-peptide complex: A novel approach to alphavirus vaccine development. *Vaccine* (2017) 35(29):3672–81. doi: 10.1016/j.vaccine.2017.05.016

4. Petrova VN, Russell CA. The evolution of seasonal influenza viruses. *Nat Rev Microbiol* (2018) 16:47–60. doi: 10.1038/nrmicro.2017.118

5. BlumJS, Wearsch PA, Cresswell P. Pathways of antigen processing. *Annu Rev Q15 Immunol* (2013) 31:443–73. doi: 10.1146/annurev-immunol-032712-095910

6. Fertey J, Bayer L, Grunwald T, Pohl A, Beckmann J, Gotzmann G, et al. Pathogens inactivated by low-energy-electron irradiation maintain antigenic properties and induce protective immune responses. *Viruses* (2016) 8(11). doi: 10.3390/v8110319

7. di Pasquale A, Preiss S, da Silva FT, Garçon N. Vaccine adjuvants: From 1920 to 2015 and beyond. *Vaccines* (2015) 3:320–43. doi: 10.3390/vaccines3020320

frontiers in Immunology

ORIGINAL RESEARCH
published: 16 August 2021
doi: 10.3389/fimmu.2021.717556

Radiation-Inactivated *S. gallinarum* Vaccine Provides a High Protective Immune Response by Activating Both Humoral and Cellular Immunity

Hyun Jung Ji[1,2], Eui-Baek Byun[1], Fengjia Chen[1], Ki Bum Ahn[1], Ho Kyoung Jung[3], Seung Hyun Han[2], Jae Hyang Lim[4,5], Yongkwan Won[3], Ja Young Moon[6], Jin Hur[6] and Ho Seong Seo[1,7]**

[1] Research Division for Radiation Science, Korea Atomic Energy Research Institute, Jeongeup, South Korea, [2] Department of Oral Microbiology and Immunology, and DRI, School of Dentistry, Seoul National University, Seoul, South Korea, [3] Research and Development Center, HONGCHEON CTCVAC Co., Ltd., Hongcheon, South Korea, [4] Department of Microbiology, Ewha Womans University College of Medicine, Seoul, South Korea, [5] Ewha Education & Research Center for Infection, Ewha Womans University Medical Center, Seoul, South Korea, [6] Department of Veterinary Public Health, College of Veterinary Medicine, Jeonbuk National University, Iksan, South Korea, [7] Department of Radiation Science, University of Science and Technology, Daejeon, South Korea

Salmonella enterica subsp. *enterica* serovar Gallinarum (SG) is a common pathogen in chickens, and causes an acute systemic disease that leads to high mortality. The live attenuated vaccine 9R is able to successfully protect chickens older than six weeks by activating a robust cell-mediated immune response, but its safety and efficacy in young chickens remains controversial. An inactivated SG vaccine is being used as an alternative, but because of its low cellular immune response, it cannot be used as a replacement for live attenuated 9R vaccine. In this study, we employed gamma irradiation instead of formalin as an inactivation method to increase the efficacy of the inactivated SG vaccine. Humoral, cellular, and protective immune responses were compared in both mouse and chicken models. The radiation-inactivated SG vaccine (r-SG) induced production of significantly higher levels of IgG2b and IgG3 antibodies than the formalin-inactivated vaccine (f-SG), and provided a homogeneous functional antibody response against group D, but not group B Salmonella. Moreover, we found that r-SG vaccination could provide a higher protective immune response than f-SG by inducing higher Th17 activation. These results indicate that r-SG can provide a protective immune response similar to the live attenuated 9R vaccine by activating a higher humoral immunity and a lower, but still protective, cellular immune response. Therefore, we expect that the radiation inactivation method might substitute for the 9R vaccine with little or no side effects in chickens younger than six weeks.

Keywords: salmonellosis, inactivated vaccine, radiation inactivation, IgG2b, IgG3, CD4+ T cells, fowl typhoid

OPEN ACCESS

Edited by:
Sebastian Ulbert, Fraunhofer Institute for Cell Therapy and Immunology (IZI), Germany

Reviewed by:
Arindam Mitra, Adamas University, India
Asisa Volz, University of Veterinary Medicine Hannover, Germany

***Correspondence:**
Jin Hur
hurjin@jbnu.ac.kr
Ho Seong Seo
hoseongseo@kaeri.re.kr

Specialty section:
This article was submitted to Vaccines and Molecular Therapeutics, a section of the journal Frontiers in Immunology

Received: *31 May 2021*
Accepted: *22 July 2021*
Published: *16 August 2021*

Citation:
Ji HJ, Byun E-B, Chen F, Ahn KB, Jung HK, Han SH, Lim JH, Won Y, Moon JY, Hur J and Seo HS (2021) Radiation-Inactivated S. gallinarum Vaccine Provides a High Protective Immune Response by Activating Both Humoral and Cellular Immunity. Front. Immunol. 12:717556. doi: 10.3389/fimmu.2021.717556

INTRODUCTION

Salmonellosis is a zoonotic disease that can cause gastroenteritis, diarrhea, and systemic typhoid in humans and animals. *Salmonella* species are gram-negative, facultatively flagellated bacteria classified on the basis of 46 lipopolysaccharide (LPS, O) and 114 flagella (H) antigens (1). According to this taxonomy, more than 2,610 serotypes have been identified to date (2). Among them, *Salmonella enterica* subsp. *enterica* serovar Gallinarum (*S.* Gallinarum; SG) is known to cause invasive salmonellosis, or fowl typhoid-like disease, a septic disease that occurs in both acute and chronic forms in chickens, turkeys, and other birds (3). Although SG infection has largely disappeared in the poultry industry in developed countries, it is still widespread in developing countries, causing enormous annual economic losses (4).

Vaccination of chickens has provided promising protection, and there continues to be progress in the development of a safe and efficacious Salmonella vaccine that provides broad cross-protection for enhancing both animal health and food safety (5). The most commonly used vaccine is a commercial live vaccine derived from a stable rough strain of SG 9R that was developed more than 30 years ago (6). Although the protective efficacy of this vaccine has been reported to be extremely high (7), the remaining pathogenicity in this attenuated strain can also lead to severe systemic infections in immunosuppressive groups such as young chicks (8). In addition, the problem of pathogenic reversion due to natural mutation in this strain has also been reported, leading to an increasing demand for additional vaccine development (9). In fact, SG 9R strains from three different Korean animal vaccine companies show different phenotypic characteristics and vaccine efficacy despite having the same original strain (10).

An inactivated vaccine can be considered as a safer alternative to SG 9R. However, several reports have shown that inactivated SG vaccines are not sufficient to provide protection against salmonellosis and less cross-protective against other Salmonella species, such as *Salmonella* Pullorum (SP) or *Salmonella* Enteritidis (SE) because of the low cell-mediated immune response (11, 12). Of the several inactivation methods available for vaccine development, inactivation by irradiation has been reported to enhance the induction of cell-mediated immunity for bacterial and viral vaccines (13, 14). Radiation, such as gamma and X-rays, transfers energy to produce ionization that directly or indirectly damages dsDNA (15). This ionization is completed in picoseconds ($\sim 10^{-12}$ s), so it is thought that it will cause less immunogenic damage that could induce cellular immunity. The major advantages of ionizing radiation in vaccine development, compared to formalin, are the ability to penetrate most biological materials, and the fact that it targets both double- and single-stranded nucleic acids while causing less damage to antigenic surface proteins. Moreover, there is no need to remove any chemical residue after inactivation (16). Gamma-irradiated influenza vaccine was more effective at priming cross-reactive cytotoxic T cells and protected mice against a heterologous influenza virus (17). Irradiated bacterial vaccines, such as against Listeria, Mycobacteria, and Bacillus, which prevent replication but retain their metabolic activity, generate higher cell-mediated immune responses and protect against extracellular and intracellular bacteria (14, 18–20).

In this study, we prepared an SG vaccine using gamma irradiation and analyzed its efficacy by measuring the immune response in mice and chickens. This study demonstrates that gamma irradiation is suitable for developing inactivated vaccines against SG and other infectious diseases.

MATERIALS AND METHODS

Ethics Statement

This study was performed in strict accordance with the recommendations of the Guide for the Care and Use of Laboratory Animals of the National Institutes of Health. All animal experiments were approved by the Committee on the Use and Care of Animals at the Korea Atomic Energy Research Institute (KAERI; approval no. IACUC-2018-007) and performed according to accepted veterinary standards set by the KAERI animal care center. Mice were euthanized by CO_2 inhalation, as specified by the KAERI Institutional Animal Care and Use Committee guidelines.

Bacterial Strains

S. Gallinarum 07Q015 was obtained from the Korea Veterinary Culture Collection (Kimchun, Republic of Korea), and its genome was sequenced using the PacBio RS II platform (Pacific Biosciences, Menlo Park, CA, USA) at Macrogen Co., Ltd. (Seoul, Republic of Korea). The assembled genome of *S.* Gallinarum 07Q015 contained three contigs, one circular genome (4,624,135 bp) and two plasmids (88,418 bp and 56,404 bp). After complete genome assembly, BLAST analysis (v2.7.1) was carried out to identify the species to which each scaffold showed the highest similarity. The best hit was *S. enterica* subsp. *enterica* serovar Gallinarum strain 287/91 (accession number: AM933173.1). The whole genome sequence of *S.* Gallinarum 07Q015 has been deposited at DDBJ/EMBL/GenBank under accession no. CP077760 (Contig 1), CP077761 (Contig 2), CP077762 (Contig 3). In the challenge experiment, we assessed the median lethal dose (LD_{50}) and the optimal challenge dose by monitoring the survival of mice and chicken for two weeks after *S.* Gallinarum 07Q015 inoculation intraperitoneally (i.p.) and orally, respectively. The LD_{50} was calculated using the Reed–Muench method. The optimal challenge doses were at least 10 times higher than LD_{50}, i.e., 5×10^5 CFU for mice and 3×10^7 CFU for chicken.

Preparation of Radiation- or Formalin-Inactivated SG (r-SG or f-SG)

Salmonella was grown in Luria-Bertani (LB; Difco, BD Biosciences, Franklin Lakes, NJ, USA) broth at 37°C and 200 rpm under aerobic conditions. When the bacteria culture reached an optical density (OD_{600}) of 0.8, it was pelleted by centrifugation at 7000 rpm for 20 min at 4°C and resuspended in phosphate-buffered saline (PBS). Harvested SG (10^8–10^9 CFU/mL)

was irradiated using a ^{60}Co-gamma irradiator (point source AECL, IR-79, MDS Nordion International Co., Ottawa, Canada) at the Advanced Radiation Technology Institute of KAERI (Jeongeup, Republic of Korea) with an absorbed dose of 0.5–9 kGy for 1 h at 23°C. f-SG was prepared by incubation with 0.2% formaldehyde solution (JUNSEI; Tokyo, Japan) under mild agitation at 23 - 28°C for 2 h. To confirm inactivation of the prepared vaccines, samples were inoculated in LB broth and cultured for 3 d to assess SG growth.

Quantification of DNA Damage

Genomic DNA was extracted using a G-spin™ Genomic DNA extraction Kit (INTRON Inc., Seoul, Republic of Korea). The genomic DNA concentration was measured using a spectrophotometer (Epoch 2; BioTek, Winooski, VT, USA) and titrated to 100 μg/mL in 10mM Tris-EDTA buffer. To quantify single-strand DNA breaks, a DNA Damage Quantification Kit (Dojindo Laboratories, Kumamoto, Japan) was used according to the manufacturer's instructions. Briefly, genomic DNA (1 μg) was labeled with an aldehyde reactive probe conjugated with biotin, through incubation at 37°C for 1 h. Labeled DNA was immobilized on a 96-well U-bottom microplate (Dojindo) and incubated at 23°C overnight. Bound biotin-conjugated aldehyde reactive probe on immobilized genomic DNA was detected using peroxidase-streptavidin and the OD of the conjugated aldehyde reactive probe was measured at 650 nm after adding 100 μL of 3,3',5,5'-tetramethylbenzidine substrate solution.

Measurement of Protein Carbonylation

SG samples were sonicated using a TECAN sonicator (TECAN; Osaka, Japan) for 1 min on ice. The samples were then centrifuged at 10,000 × g for 15 min at 4°C. Protein concentration and purity were measured using absorbance at 280 nm and 260 nm, respectively. Protein carbonylation was measured using a Protein Carbonyl Colorimetric Assay Kit (Cayman Chemical, Ann Arbor, Michigan, USA) according to the manufacturer's instructions. In brief, 200 μL of the sample was mixed with 800 μL of 2,4-dinitrophenylhydrazine and 800 μL of 2.5 M HCl. After the sample was incubated for 1 h at room temperature, the proteins were precipitated using 20% trichloroacetic acid at 4°C for 5 min. After centrifugation, the pellet was washed with 1 mL of a mixture of ethanol and ethyl acetate (1:1, v/v) and resuspended with protein pellets in 500 μL of guanidine hydrochloride. The OD of the pellet was measured at 360–385 nm.

Scanning Electron Microscope (SEM) Analysis

Live SG, r-SG, and f-SG were fixed with 4% glutaraldehyde overnight at 4°C. After centrifugation (13,000 rpm), the samples were washed three times with PBS and dehydrated through a graded ethanol series (30%, 50%, and 70%) followed by drying the cells. The samples were gold-coated using a gold sputtering unit and then observed using a JEOL JSM-840 scanning microscope (Tokyo, Japan) at the Seoul National University.

Mouse and Chicken Experiments

The animal housing conditions, which were designed for specific pathogen-free animals, and the animal experimental design were approved by the Committee on the Use and Care of Animals at the KAERI and implemented ethically according to the standards accepted by the National Health of Institute. The ventilated housing cage (Orient Bio Inc., Seoul, Republic of Korea) was maintained in an animal biological safety level 2 facility at 22–23°C on a 12 h:12 h light:dark cycle. The cages were covered with high-efficiency particulate air-filtered microisolation lids (Orient Bio Inc.) in a static airflow environment. Bedding (Aspen shavings; Orient Bio Inc.) at an approximate depth of 1.0 cm was changed weekly. Irradiated rodent diet food and sterile water were provided *ad libitum* through a wire cage top. Five-week-old male C57BL/6 mice (weight 19–21 g) were purchased from Orient Bio Inc. Five C57BL/6 mice were randomly assigned to individually ventilated housing cages and immunized i.p. three times at two-week intervals with either PBS, r-SG, or f-SG mixed with the same volume of 2% Alhydrogel® adjuvant (InvivoGen, San Diego, CA, USA). No significant weight loss, mortality, or serious clinical signs were observed after vaccination. Two weeks after the third vaccination, blood was collected to measure SG-specific antibodies, and the spleen was collected to measure SG-specific T cell responses. To examine the protective efficacy of the vaccination, mice were challenged i.p. with *S.* Gallinarum 07Q015 (5×10^5 CFU/mouse) two weeks after the third vaccination. Mouse survival was monitored for 12 d.

Five-week-old female Brown Leghorn chickens (weight 5-6 lb) were purchased from JOIN Inc. (Pyeongtaek, Korea) and placed into chicken isolator (Three-shine Inc.; Daejeong, Korea) containing mesh wire on the floor of the cages. Each cage housed not more than 5 chickens. Chickens were given tap water and commercial chick feed *ad libitum*. Air and light were supplied freely through the hole and windows. All purchased chickens were confirmed to be negative for *Salmonella* infection by confirming with *Salmonella* diagnosis PCR with Primers 3503 (AGC GTA CTG GAA AGG AG) and 5503 (ATA CCG CCA ATA AAG TTC ACA AAG) (21). Chickens adapt to the new environment for one week. All chickens were acclimatized according to the protocols of the Central Animal Research Laboratory at Chunbuk National University (Iksan, Republic of Korea). For vaccination, chickens (n = 10/group) were vaccinated into the breast muscle twice at three-week intervals with r-SG (3×10^8 CFU), f-SG (3×10^8 CFU), or live 9R strain (2×10^7 CFU) of 0.5 mL. Three weeks after the second vaccination, chicken blood was collected 5 mL each from brachial wing vein, and serum was harvested from the supernatant of coagulated blood. All serum were stored at 4°C until performing enzyme-linked immunosorbent assay (ELISA) and opsonophagocytic killing assay (OPKA). For *Salmonella* challenge study, *S.* Gallinarum 07Q015 were inoculated into 10 mL LB and incubated at 37°C with orbital shaking (200 rpm) for 24 h. Subsequently, 0.5 mL of precultures bacteria was transferred into 50 mL LB and incubated with orbital shaking (200 rpm) at 37°C for about 6 h. The challenge inoculum was prepared by diluting *S.* Gallinarum culture in LB to a final viable concentration of 6×10^7

CFU/mL and used immediately for oral infection. The number of *S.* Gallinarum inoculums was determined both before and after challenge. Three weeks after the second vaccination, chickens were orally challenged with 0.5 mL of *S.* Gallinarum 07Q015 (3×10^7 CFU/chicken) as inoculum using a syringe, whereas uninfected chickens were given with the same amount of LB. Chicken survival was monitored daily for 15 d. Any chicken that died or had to be euthanized during the observation period was immediately necropsied and all the remaining chickens at the end of the experiment were euthanized.

Measurement of Lipopolysaccharide (LPS)-Specific Immunoglobulin Levels

Blood samples from mice and chickens were obtained 14 d after the last vaccination. Salmonella antigen lysates were prepared as described previously (22). *Salmonella* Gallinarum (SG), *Salmonella* Typhimurium (ST), *Salmonella* Enteritidis (SE), and *Salmonella* Pullorum (SP) were grown in LB broth and harvested at OD_{600} = 0.8. The pellet was washed with PBS followed by sonication 30 times for 5 s. Samples were centrifuged at 13,000 rpm for 10 min at 4°C, and the supernatants were collected and stored at −70°C. Total protein concentration was measured using the Pierce™ BCA Protein Assay Kit (Thermo Fisher Scientific, Waltham, MA, USA). To examine the levels of SG-specific immunoglobulins (Igs), Salmonella lysate (10 μg/well), group D LPS (1 μg/well; Sigma-Aldrich; St. Louis, MO), and group B LPS (1 μg/well; Sigma-Aldrich) were immobilized on 96-well plates for 16 h at 4°C, followed by blocking with 1% BSA in PBS. After washing three times with PBS containing 0.05% Tween-20 (PBS-T; Sigma-Aldrich), serial two-fold dilutions of mouse or chicken serum (100 μL) were added to each well and incubated at 23°C for 2 h. The plates were washed five times with PBS-T to remove unbound antibodies, and bound antibodies were detected using horseradish peroxidase (HRP)-conjugated anti-mouse Igs (anti-mouse IgM, IgG, IgG1, IgG2a, IgG2b, and IgG3; 1:5000 dilution in PBS-T; Sigma-Aldrich) or HRP-conjugated anti-chicken IgM and IgG (1:5000 dilution in PBS-T; Southern Biotech, Birmingham, AL, USA) for 1 h at room temperature. After washing seven times with PBS-T, 100 μL of 3,3',5,5'-tetramethylbenzidine substrate solution (INTRON) was added, followed by incubation for 5–10 min at 23°C. When the color was sufficiently developed, 50 μL of 2 N H_2SO_4 stop solution (Daejung Chemicals; Siheung, Republic of Korea) was added. The absorbance at 450 nm was measured using an Epoch 2 plate reader (BioTek).

Opsonophagocytic Killing Assay (OPKA)

The functional activity of SG-specific antibodies induced by each vaccine was assessed using OPKA as described previously (23). A 10 μL aliquot of bacteria (100–250 CFU) was incubated with three-fold serially diluted heat-inactivated sera (final 20 μL/well) with OBB (Opsonization buffer B, 1X HBSS buffer containing 0.1% gelatin and 0.5% heat inactivated FBS) at 37°C for 30 min, followed by mixing with 40 μL of differentiated HL60 granulocytic cells (1×10^7 cells; ATCC; Manassas, VA, USA) and 10 μL of 3–4-week-old baby rabbit complement (PelFreeze Biologicals, Rogers, AR, USA). After incubating at 37°C for 45 min, the reaction was stopped by incubating on ice for 20 min. Next, 10 μL of samples were spotted on LB agar plates and the colonies were counted using NIST's Integrated Colony Enumerator software (NICE; Gaithersburg, MD, USA) and opsonic indices (OIs) were analyzed using the Opsonization Index Program ("opsotiter3") kindly provided by Prof. Nahm (University of Alabama at Birmingham).

Splenocyte Analysis by Flow Cytometry

Two weeks after the final immunization, spleens from mice immunized with either the r-SG or f-SG vaccine were isolated and filtered through a cell strainer (70 μm; SPL Life Sciences, Pocheon, Republic of Korea). Red blood cells (RBCs) were lysed with RBC lysis buffer (Sigma-Aldrich) and washed with RPMI-1640 medium containing 10% fetal bovine serum (FBS; Biowest, Nuaillé, France). The cell suspension was seeded into a 48-well plate (2×10^6 cells/well) and stimulated with 10 μg/mL SG lysate, 0.5 μg/mL GolgiStop (BD Bioscience, San Diego, CA, USA), and 0.5 μg/mL GolgiPlug (BD Bioscience) at 37°C for 12 h. The cells were washed with PBS and stained with a Live/Dead Staining Kit (InvivoGen, San Diego, CA, USA), anti-CD8-FITC (BD Bioscience), and anti-CD4-BV421 (BD Biosciences) for 20 min at 23°C to stain T cell surface markers. Cells were fixed and permeabilized using a Cytofix/Cytoperm kit (BD Bioscience) for 20 min at 4°C, and then intracellular cytokines were stained with anti-IFN-γ-PE (BD Biosciences), anti-IL-5-APC (BD Bioscience), and anti-IL-17A-PE-Cy7 (BD Bioscience) for 20 min at 23°C. After staining, the cells were analyzed using a MACS Quant flow cytometer (Miltenyi Biotec, San Diego, CA, USA) and FlowJo software (TreeStar, Ashland, OR, USA).

Cytokine ELISA

Splenocyte culture supernatants prepared as described above were collected, and the levels of IFN-γ, IL-5, IL-17A, TNF-α, IL-10, and TGF-β were measured using an ELISA kit (eBioscience Inc., San Diego, CA, USA).

Adoptive Transfer of $CD4^+$ or $CD8^+$ T Cells

Mouse spleen cell suspensions were prepared by passing spleen specimens through a nylon cell strainer (BD Biosciences), and red blood cells were lysed with FACS Lysing Solution (BD Biosciences). Splenic $CD4^+$ and $CD8^+$ T cells were separated using Miltenyi MACS microbeads conjugated with anti-CD4 and anti-CD8 monoclonal antibodies (Miltenyi Biotec) and a MACS LS column (Miltenyi Biotec). Isolated $CD4^+$ or $CD8^+$ T cells (5×10^5 cells/mouse) were administered i.p. to naïve C57BL/6 mice (n = 7). After 12 h, mice were challenged i.p. with *S.* Gallinarum 07Q015 (5×10^5 CFU/mouse) and mouse survival was monitored for 12 d.

Statistical Analysis

Data are expressed as the mean ± standard deviation (SD). Data in the bar and dot graphs between groups were compared using

an unpaired Student's *t*-test for normal data distribution or the Mann–Whitney non-parametric test for abnormal data distribution using GraphPad Prism (version 7.0; GraphPad Software, Inc., La Jolla, CA, USA). The survival of mice was determined using Kaplan–Meier survival analysis, and the significance of the difference was analyzed using a log-rank test with GraphPad Prism software. $P < 0.05$ was considered statistically significant.

RESULTS

Preparation of an Inactivated *S.* Gallinarum Vaccine

The formalin inactivation method used in this study followed the bacterial vaccine manufacturing protocol of the Korean Animal and Plant Quarantine, in which SG (10^8–10^9 CFU/mL) was treated with 0.2% formaldehyde solution in PBS for 2 h at 37°C. For radiation-inactivated SG vaccines, a value between -10^3 and -10^6 was applied according to the 'Sterility Assurance Level (SAL)' used in the manufacture of sterile viruses (24, 25). To measure the SAL value, harvested SG (10^8–10^9 CFU/mL) in PBS were irradiated with gamma rays at the indicated dose for 1 h, and serially diluted samples were plated onto blood agar plate (BAP) (**Figure 1A**). No bacteria were detected on BAP at 3~4 kGy. SAL values of -10^3 and -10^6 were calculated as assessed by linear regression performed with all viable count data, indicating that SAL values of -10^3 and -10^6 were obtained with doses of 5.442 kGy and 6.879 kGy, respectively. Thus, 6 kGy was chosen as the radiation inactivation dose for SG (**Figure 1B**). After inactivating SG with either formalin or radiation, 1 mL inactivated bacteria was inoculated into 9 mL LB and incubated for 7 d to confirm complete inactivation.

When radiation passes through a cell, it induces an ionization process that produces free radicals *via* the radiolysis of water (26–28), causing DNA damage. To determine whether the radiation inactivation method successfully induced SG DNA damage, Aldehyde Reactive Probe (ARP) was used to examine the DNA single-strand break rate of the SG chromosome (29). As shown in **Figure 1C**, SG DNA damage extensively increased with increased irradiation dose, and approximately (23.252 ± 0.253) sites/100,000 bp damage was detected at 6 kGy. In contrast, only (1.216 ± 0.102) sites/100,000 bp were detected with f-SG, which was comparable to live SG ([0.058 ± 0.001] sites/100,000 bp).

Since formalin- and radiation-induced reactive oxygen species (ROS) can induce protein antigen damage by carbonylation, which can trigger a Th2-biased immune response, the degree of carbonylation was analyzed by a 2,4-dinitrophenylhydrazine (DNPH) immunoassay (30). As shown in **Figure 1D**, r-SG (6 kGy inactivating does) did not show a significant increase in carbonylation ([0.955 ± 0.032] nmol/mL) compared to live SG ([1.602 ± 0.048] nmol/mL). However, 0.2% f-SG exhibited 4.8-fold higher carbonylation ([4.591 ± 0.450] nmol/mL) compared to r-SG (**Figure 1D**). To directly visualize the extracellular structures of live SG, r-SG, and f-SG, scanning electron microscopy (SEM) was performed. As shown in **Figure 1E**, there were no substantial differences in the extracellular structure between the groups.

Vaccination With r-SG Causes a Stronger Humoral Immune Response

Because previous studies indicated that high carbonylation induced by formalin treatment decreased antigen-specific humoral immune responses (31, 32), we compared r-SG with f-SG *in vivo*. Mice (n = 5 per group) were immunized i.p. with either 10^5 or 10^6 CFU of either r-SG or f-SG vaccine three times at two week intervals, then the SG-specific serum antibody titer was measured two weeks after the last immunization (**Figure 2A**). SG-specific IgM and IgG were increased in a dose-dependent manner by immunizing with either r-SG or f-SG. However, the group immunized with 10^6 CFU r-SG showed significant enhancement in SG-specific IgM (4,320 ± 2,170) and IgG (5,760 ± 2,061) compared to the f-SG vaccination group (600 ± 126 for IgM, 800 ± 0 for IgG) (**Figures 2B, C**). To determine whether this SG-specific IgG enhancement by r-SG vaccination was due to a Th1- or Th2-biased IgG response, we analyzed the levels of IgG subclasses. As shown in **Figures 2D, E**, both IgG1 (Th2; 1,020 ± 618) and IgG2a (Th1; 220 ± 78) were modestly increased in the r-SG group, but not significantly when compared to the PBS (188 ± 77 for IgG1, 75 ± 14 for IgG2a) and f-SG (70 ± 12 for IgG1, 50 ± 0 for IgG2a) groups. Surprisingly, T-independent antibodies IgG2b (r-SG: 1,160 ± 682, f-SG: 170 ± 62) and IgG3 (r-SG: 8,990 ± 4,775, f-SG: 70 ± 12) were found to be significantly increased in the r-SG group (**Figures 2F, G**).

To confirm whether the SG-specific immune responses induced by the r-SG vaccine could provide protection against SG, immunized mice (n = 6 per group) were i.p. challenged with 5×10^5 CFU WT SG two weeks after the last immunization. While only 16% of PBS-immunized mice, and 33% of f-SG-immunized mice, survived by 6 d post-injection, 100% of r-SG-immunized mice survived at 12 d post-injection. This suggested that r-SG might induce more potent humoral and protective immune responses than f-SG (**Figure 2H**).

Higher Functional Antibody Responses Induced by r-SG

IgG2b and IgG3 have long been considered the key subclasses produced in response to carbohydrates and other T-independent antigens, such as LPS and pneumococcal polysaccharide. Thus, we next sought to confirm that the higher T-independent humoral immune response observed was due to the immune response to SG serogroup D carbohydrate by measuring homogeneous antibody titers of SG-immunized mouse sera against serogroup D (SE, SP) and serogroup B (ST) strains. Sera isolated from mice immunized with 10^6 CFU of either r-SG or f-SG were used to determine the levels of SE-, SP-, or ST-specific antibody titers by ELISA. As shown in **Figures 3A, B**, serogroup D Salmonella (SE and SP)-specific IgM (r-SG: 425 ± 143, 325 ± 75 f-SG: 80 ± 12, 60 ± 10) and IgG (r-SG: 1,800 ± 503, 325 ± 75 f-SG: 280 ± 48, 60 ± 10) isotype responses increased

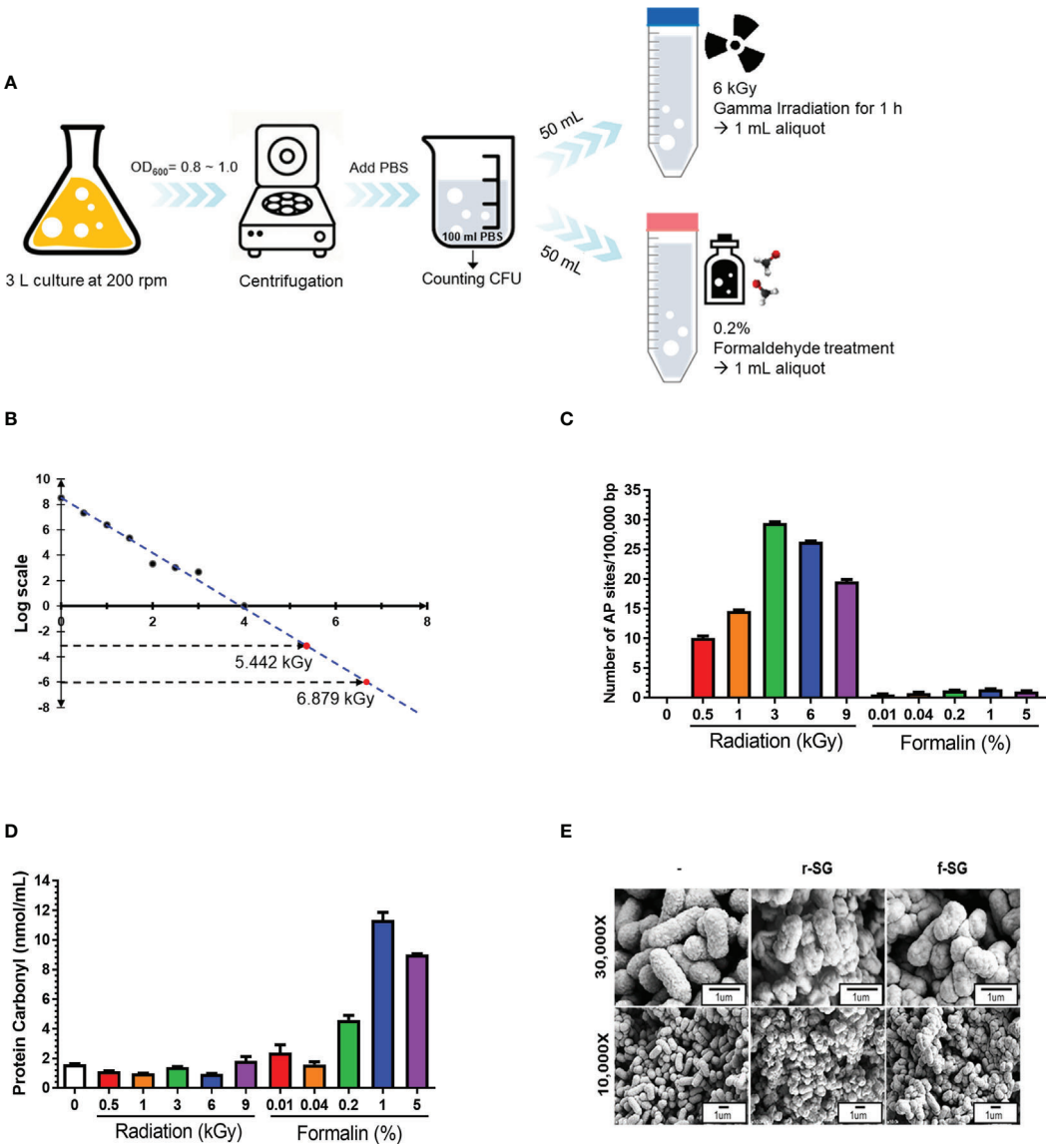

FIGURE 1 | Production and characterization of inactivated SG vaccines. **(A)** Schematic procedure for r-SG and f-SG vaccine production. **(B)** Radiation-inactivated vaccine was produced according to the 'Sterility Assurance Level (SAL).' SG was harvested and re-suspended in PBS and irradiated with the indicated dose of gamma radiation (^{60}Co gamma-ray source) and plated on LB agar to count the number of surviving bacteria. No SG was detected in samples irradiated with doses of gamma radiation >3 kGy. **(C)** Measurement of single strand chromosomal DNA breaks and **(D)** bacterial protein carbonylation after radiation- or formalin-inactivation. **(E)** The surface structure of SG, r-SG, and f-SG visualized by scanning electron microscopy.

significantly in the sera of r-SG-immunized mice. As mentioned above, the major subclasses of IgG were IgG2b and IgG3 against SE and SP. In contrast, no significant levels of IgM (r-SG: 50 ± 0, f-SG: 50 ± 0) and IgG (r-SG: 1,500 ± 619, f-SG: 440 ± 97) were detected in serogroup B Salmonella (ST) (**Figure 3C**). Moreover, we found that these serogroup specific antibodies bound only to serogroup D LPS, not serogroup B LPS (**Supplementary Figure 1**). These data indicate that r-SG-induced IgG2b, and IgG3 antibodies were mostly group D-specific. Furthermore, we found that both r-SG and f-SG boosted high group D LPS-specific IgG and IgM, but not group B LPS-specific antibodies.

To demonstrate that the increase in the homogeneous IgG response was not due to non-specific binding to the immobilized antigen, we measured the functional activity of SG-immunized mouse sera using an OPKA, as described previously (33). Live SG, SE, SP, or ST (100–250 CFU) were incubated for 45 min at 37°C with the pooled SG-immunized sera together with baby rabbit complement and differentiated granulocytes (HL60), and the surviving bacteria were counted on LB agar plates. As shown in **Figure 3D**, the opsonic index (OI; 50% killing serum titer) of PBS-immunized sera (control) was 200, which is the OPKA detection limit in all Salmonella groups. Sera immunized with f-SG showed

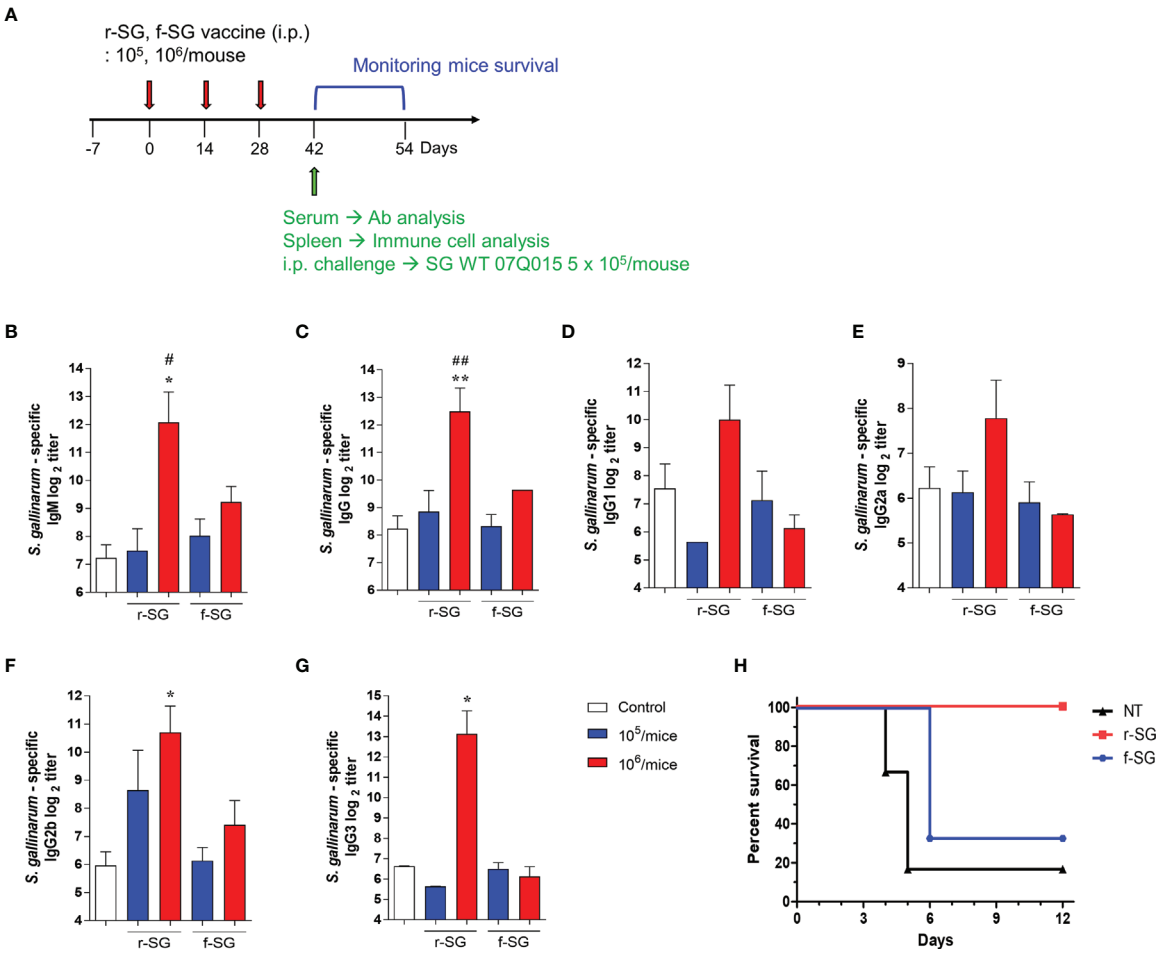

FIGURE 2 | Analysis of humoral immune responses induced by immunization of r-SG or f-SG. Mice (n = 5 per group) were immunized i.p. with either 1 × 10^5 CFU or 1 × 10^6 CFU of r-SG or f-SG three times at two week intervals and sera were collected two weeks after the last vaccination. **(A)** Schematic overview of mice study design. SG-specific **(B)** IgM and **(C)** IgG and IgG subclasses **(D)** IgG1, **(E)** IgG2a, **(F)** IgG2b, and **(G)** IgG3 in sera were measured by ELISA. **(H)** Immunized mice (n = 6 per group) were infected i.p. with 5 × 10^5 CFU SG WT strain and survival was monitored for 12 d. *P < 0.05, **P < 0.01 compared to PBS group. #P < 0.05, ##P < 0.01 compared to f-SG vaccinated group.

OI of 28,970 to SG, but <2,000 for other serogroups. In contrast, sera immunized with r-SG had extremely high OI titers against group D Salmonella: 311,751 (SG), 776,716 (SE), and 1,749,600 (SP); while OI titers to ST were only 200. These results confirmed that the radiation inactivation method induced a higher serotype-specific humoral immune response than the formalin inactivation.

Higher SG-Specific Th17 Cell Immunity Induced by r-SG

To more accurately confirm the immune-induced response to r-SG, we analyzed cell-mediated immune activity in a population of activated $CD4^+$ and $CD8^+$ T cells *in vivo*. Mice (n = 5 per group) were immunized i.p. with PBS, r-SG (10^6 CFU), or f-SG (10^6 CFU) three times at two week intervals, and single cell suspensions of splenocytes were re-stimulated with 10 μg/mL SG lysate followed by analysis of Th1 (IFN-γ-producing $CD4^+$ T cells), Th2 (IL-5-producing $CD4^+$ T cells), Th17 (IL-17A-producing $CD4^+$ T cells), and activated $CD8^+$ T cells (IFN-γ-producing $CD8^+$ T cells) by gating (**Figure 4A**). As shown in **Figure 4B**, any group immunized with either r-SG or f-SG showed no significant difference in IL-5^+CD4^+ cells compared to the PBS group. Only the r-SG-immunized group showed a significant level of IFN-γ^+CD4^+ (r-SG: 7.12 ± 0.56, f-SG: 5.50 ± 0.44; P = 0.005) and IL-$17A^+CD4^+$ cells (r-SG: 1.34 ± 0.19, f-SG: 0.99 ± 0.18; P = 0.03). Both the r-SG and f-SG groups had significant increases in IFN-γ^+CD8^+ cells compared to the PBS group, but no differences were found between the r-SG and f-SG groups.

Next, the levels of cytokines secreted from splenocytes in response to SG lysate stimulation were measured by ELISA (**Figure 4C**). Consistent with the above results, significantly higher levels of IFN-γ and IL-17A were detected in the r-SG group compared to the PBS and f-SG groups, but IL-5 production was not detected in any group. In addition, we

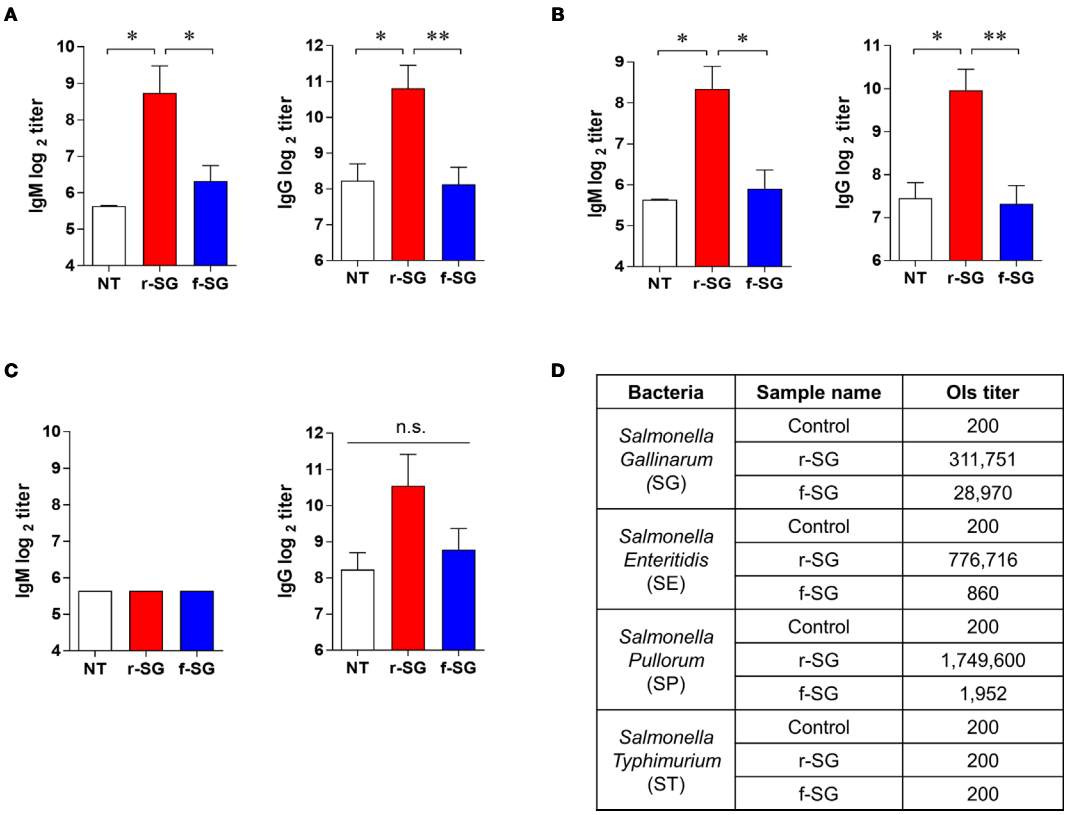

D

Bacteria	Sample name	OIs titer
Salmonella Gallinarum (SG)	Control	200
	r-SG	311,751
	f-SG	28,970
Salmonella Enteritidis (SE)	Control	200
	r-SG	776,716
	f-SG	860
Salmonella Pullorum (SP)	Control	200
	r-SG	1,749,600
	f-SG	1,952
Salmonella Typhimurium (ST)	Control	200
	r-SG	200
	f-SG	200

FIGURE 3 | Homogeneous antibody responses by r-SG against Group D Salmonella. Mice (n = 5 per group) were immunized i.p. with 1 × 10^6 CFU of r-SG or f-SG three times at two week intervals and sera were collected two weeks after the last vaccination. **(A)** SE-specific IgM and IgG, **(B)** SP-specific IgM and IgG, and **(C)** ST-specific IgM and IgG in sera were measured by ELISA. **(D)** Summary of opsonization indices for r-SG and f-SG vaccines against serogroup D (SG, SE, and SP) and serogroup B (ST) Salmonella. *P < 0.05, **P < 0.01, n.s., not significant, compared to unvaccinated mice.

measured the levels of additional cytokines (IL-10 and TNF-α) associated with Salmonella infections (34, 35). TNF-α was significantly increased (r-SG: 359.1 ± 30.53, f-SG: 234.8 ± 12.3; P = 0.0054), but a modest increase of IL-10 was observed in the r-SG group compared to the f-SG group. Although TGF-β is known to be required for class-switching from IgG3 to IgG2b (36), no significant production of TGF-β was detected in either the r-SG or f-SG groups These data confirm that r-SG could induce higher SG-specific immune responses in the direction of Th1 and Th17, and that a higher IgG2b humoral response was not likely to be in the direction of the TGF-β pathway.

To directly examine whether T cells memorized *via* the r-SG or f-SG vaccine could protect against SG infection, either splenic $CD4^+$ or $CD8^+$ T cells were isolated from immunized mice and then transferred to naïve mice *via* the i.p. route. Mice were then challenged with a lethal dose of SG (5 × 10^5 CFU) 16 h after adaptive transfer. As shown in **Figures 4D, E**, the group that received $CD4^+$ T cells from PBS- or f-SG-vaccinated mice died within 5 d after injection, whereas the group that received $CD4^+$ T cells from r-SG-vaccinated mice showed 40% survival during the monitoring period, which was significant compared to the PBS (P < 0.0001) and f-SG (P = 0.003) groups. In contrast, mice that received $CD8^+$ T cells from r-SG- or f-SG-vaccinated donors survived longer than mice in the PBS group, but no significant differences were found between the r-SG and f-SG groups, which correlated with the flow cytometry and ELISA data above. These data suggest that the higher protective immune response induced by the r-SG vaccine could be caused in part by higher activated $CD4^+$ T cells, particularly associated with Th1 and Th17 cells.

Higher Protective Immune Responses by r-SG Vaccination in Chickens

To compare the efficacy of the vaccine between r-SG and f-SG in chickens, five-week-old female Brown Leghorn chickens were immunized with r-SG (3 × 10^8 CFU), f-SG (3 × 10^8 CFU), or commercial 9R live vaccine (2 × 10^7 CFU) twice at three-week intervals (**Figure 5A**). Sera were collected 14 d after the last vaccination, and serogroup D Salmonella (SG, SE, and SP)-specific IgG were measured using ELISA. As shown in **Figure 5B**, all groups immunized with r-SG, f-SG, or 9R showed a significant increase in Group D-specific IgG antibodies (r-SG: 50,220 ± 18,491, f-SG: 57,780 ± 17,779, 9R: 37,260 ± 14,070) compared to the unvaccinated group, but there was no significant difference among the vaccinated

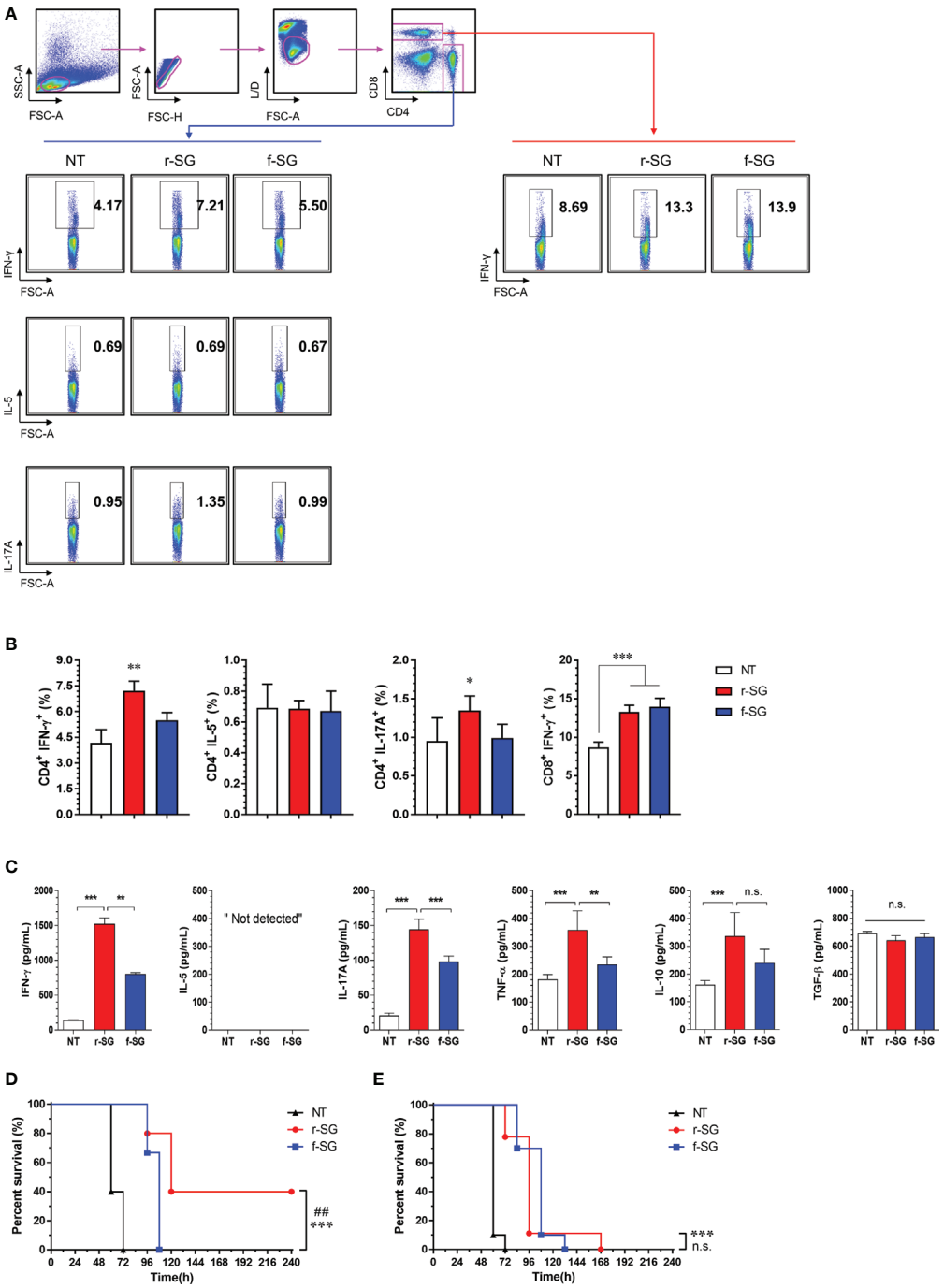

FIGURE 4 | Analysis of SG-specific CD4$^+$ and CD8$^+$ T-cell responses. Mice (n = 5 per group) were immunized i.p. with 1 × 10^6 CFU of r-SG or f-SG three times at two week intervals. Spleen cell suspensions were re-stimulated with 10 μg/mL SG lysate for 12 h and SG-specific Th1 (IFN-γ-expressing CD4$^+$ T cells), Th2 (IL-5-expressing CD4$^+$ T cells), Th17 (IL-17A-expressing CD4$^+$ T cells), and activated CD8$^+$ T cells (IFN-γ-producing CD8$^+$ T cells) were analyzed by intracellular cytokine staining based on the T cell-specific makers (anti-CD4, and anti-CD8). **(A)** Representative plots for Th1, Th2, Th17, and activated CD8$^+$ T cells in spleens from PBS-, r-SG-, and f-SG-vaccinated mice. **(B)** Percentages of Th1, Th2, Th17, and activated CD8$^+$ T cells in spleens of all vaccinated mice. The mean ± SD shown are representative of three independent experiments. **(C)** Single cell suspensions of splenocytes were treated with 10 μg/mL SG lysate for 72 h, and supernatants were collected for determination of SG-specific cytokines (IFN-γ, IL-5, IL-17A, TNF-α, IL-10, and TGF-b) using ELISA. The mean ± SD shown are representative of two independent experiments. *P < 0.05, **P < 0.01, and ***P < 0.001, n.s., not significant, compared with unvaccinated mice **(D)** Splenic CD4$^+$ or **(E)** CD8+ T cells from naïve (n = 7) or r-SG- or f-SG- vaccinated mice were pooled and transferred i.p. to mice. At 12 h after inoculation, mice were challenged i.p. with 5 × 10^5 CFU SG WT strain. Mouse survival was monitored for 10 d. ***P < 0.001, compared with unvaccinated mice. $^{\#\#}$P < 0.01, n.s., not significant, compared with f-SG vaccinated mice.

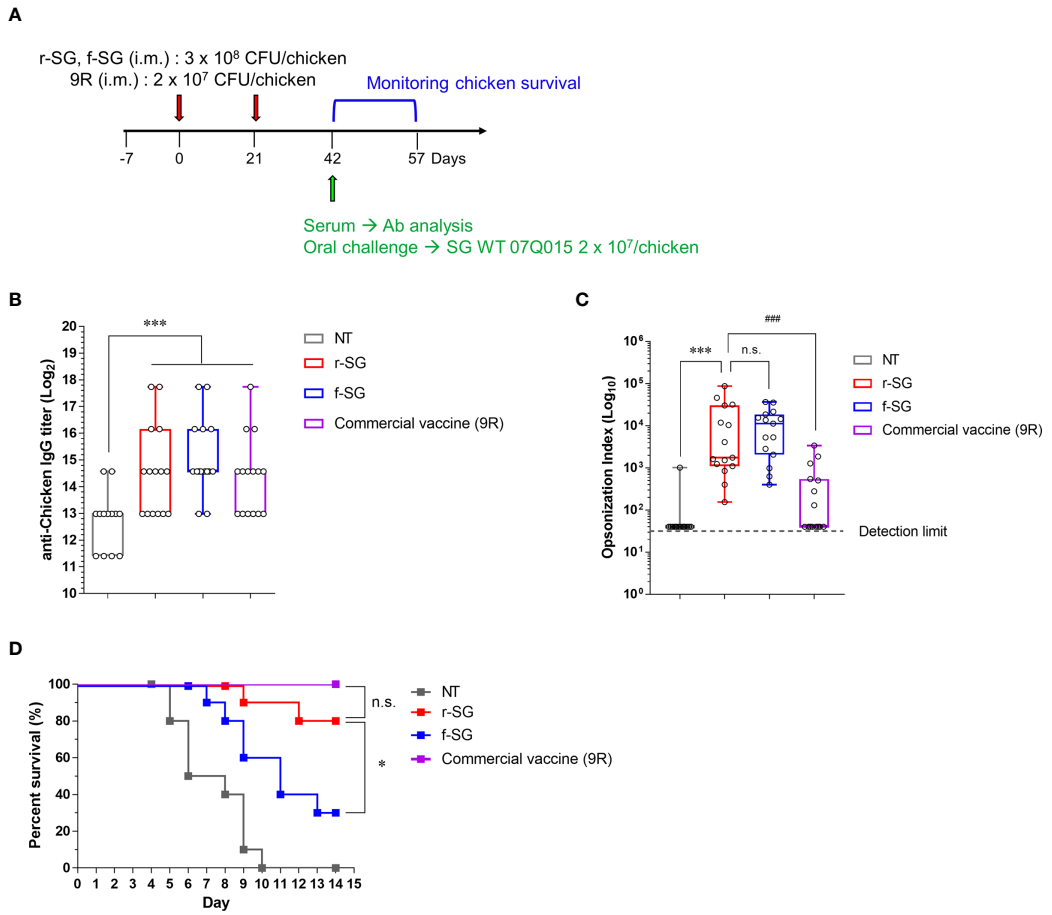

FIGURE 5 | Analysis of humoral immune responses induced by immunization of r-SG or f-SG in chickens. Brown Leghorn chickens (n = 15 per group) were immunized i.m. with the indicated dose of r-SG, f-SG, or live 9R twice at two week intervals. **(A)** Schematic overview of chicken study design. **(B)** A box-and-whisker plot with data points of SG-specific chicken IgG in sera were measured by ELISA and **(C)** Opsonization indices for r-SG, f-SG, and 9R vaccines against *S.* Gallinarum. **(D)** At two weeks after the last vaccination, chickens were orally challenged with 2 x 10^9 CFU SG WT and survival was monitored for 14 d. *P < 0.05, ***P < 0.001, n.s., not significant, compared with unvaccinated chicken. $^{###}$P < 0.001, compared with 9R vaccinated chicken.

groups. Next, we measured the functional activity of SG-immunized chicken sera using OPKA against live SG. As shown in **Figure 5C**, the opsonic index (OI; 50% killing serum titer) was 105 ± 65 (PBS), 15,376 ± 6,332 (r-SG), 12,318 ± 3,069 (f-SG), and 553 ± 245 (9R) indicating that both f-SG and r-SG induced higher functional SG-specific antibodies than the live 9R vaccine (**Figure 5C**).

Two weeks after the last vaccination, the immunized chickens (n = 15) were orally challenged with 3 × 10^7 CFU of *S.* Gallinarum 07Q015 (week 6). All PBS-immunized chickens died within 10 d, but 100% (Live/Dead: 15/15) and 80% (Live/Dead: 12/15) of the 9R- and r-SG-immunized chickens, respectively, were alive for more than 14 d post-challenge (**Figure 5D**). In contrast, only 33% (Live/Dead: 5/15) of the f-SG-immunized chickens survived for 14 d after challenge. Taken together, the data indicated that the higher protective immune response of r-SG vaccination was likely due to both the higher humoral immune response and cellular immune response.

DISCUSSION

Inactivated vaccines have been the most widely used type of vaccine since the 1920s, but due to the recent emergence of new strains and subtypes, it is becoming difficult to sufficiently prevent infectious diseases with inactivated vaccines (37). Instead, live vaccines are being used as alternatives, but their use is extremely limited because of their difficulty in development and high virulence to immunocompromised humans and animals (38). For example, the SG 9R live vaccine against SG has recently been reported as an unpredictable invasive infection (8). Thus, there is an urgent need to develop safe new SG vaccines. In this study, we found that a r-SG vaccine could provide a higher homogeneous protective response against group D Salmonella by activating early humoral responses (IgG2b and IgG3) and Th1/Th17 cell-mediated immunity than f-SG.

Multiple studies have shown that radiation-inactivated vaccines provide better efficacy than conventional vaccines (13).

Furuya et al. reported that influenza vaccines inactivated with gamma radiation significantly enhanced the activity of cytotoxic T cells, which could provide heterosubtypic protection against various influenza subtypes, including the H5N1 avian influenza virus (39). Although ultraviolet radiation was used to inactivate Listeria in a study by Brockstedt et al., they reported that this could induce a potent $CD8^+$ T cell response to increase cellular immunity (40). However, our study found that the r-SG vaccine activates SG-specific Th1/Th17 cells more than cytotoxic T cells, possibly providing high protective immunity. In fact, we recently demonstrated that radiation-inactivated pneumococcal vaccines provide protection *via* Th17-mediated mucosal immune responses (41). Thus, radiation inactivation methods generally provide stronger protective immune responses, but the type of response induced may differ depending on the type of pathogen. As the molecular mechanism underlying the high immune response of radiation-inactivated vaccines is not yet clear, the key determinants leading to the activation of cytotoxic T cells or Th17 cells should also be studied.

Formaldehyde is an electrophilic aldehyde that induces chemical crosslinking of the N-terminal nucleophilic amino group of cysteine, histidine, lysine, tryptophan, and arginine (42). It is well known that the use of formaldehyde, in the form of the aqueous solution formalin, for vaccine production can cause a variety of immunological issues because it can alter the structure of antigenic epitopes (43, 44) and diminish the production of pathogen-specific and functional antibodies. We reported that formalin inactivation could decrease the humoral immune response by impairing the activity of influenza surface antigens hemagglutinin (HA) and neuraminidase (NA) (45). In this study, we also showed that formalin treatment of SG (f-SG) dramatically increased the carbonylation of SG proteins compared to untreated cells or r-SG. Second, formalin is known to increase unpredictable immune responses, such as antibody-dependent enhancement (ADE) (46). For example, a formalin-inactivated respiratory syncytial virus (RSV) vaccine in naïve infants failed to prevent disease, and 80% of vaccine recipients were hospitalized after encountering circulating RSV due to ADE (47). The issue of the SARS-CoV-2 vaccine inducing ADE following structural modifications of the surface S-protein is also a concern (48). Unlike chemical inactivation, radiation inactivation in cells can be caused by direct or indirect action on DNA (49). Radiation can directly cause DNA single-or double-strand breaks (50), while the indirect action causes ionization of water or organic molecules in the cell to produce free radicals which react with DNA bases, leading to DNA damage (51). Thus, the two actions can function together to cause various mutations and break down DNA to quickly inactivate the pathogen. In contrast, cellular damage might be relatively less compared to DNA damage because the physical process of ionizing radiation takes a very short reaction time (about 10^{-15} to 10^{-12} s) (26, 27, 52). Therefore, the high immunological effect of irradiated vaccines may be due to less damage to surface antigens during vaccine manufacturing.

Another surprising finding in our mouse model was that r-SG induced higher titers of SG-specific IgM, IgG2b, and IgG3, and these antibodies are probably anti-group D antigens. IgG2b and IgG3 antibodies are usually considered to be part of the T-independent response and can be induced at a very early stage of infection (53). A previous study showed that LPS stimulation could induce class switching of IgM to IgG3, and LPS induces high levels of IgG2b and low levels of IgA in the presence of TGF-β (54). However, we did not detect the secretion of TGF-β, and there is another, unknown, mechanism for class switching to IgG2b. In addition, both IgG3 and IgG2b are known to have stronger opsonophagocytosis and bactericidal activities than IgG2a and IgG1 (55), therefore the r-SG vaccine may provide early and robust protective humoral immune responses *via* IgG3 and IgG2b. In contrast, we detected a relatively low amount of SG-specific T-dependent antibodies (IgG1, IgG2a) by r-SG vaccination, even with aluminum hydroxide as an adjuvant. Therefore, there is a strong need to investigate the impact of a specific adjuvant combination in increasing the Th1 response.

Although we have not been able to directly analyze the response of cellular immunity after r-SG vaccination in chickens, the increase in protective immunity is likely to be due to an increase in cellular immunity. The role of Th1- and Th17-mediated immune responses has been reported in many infectious diseases, such as those caused by Candida, Salmonella, and Pneumococcus (56–59). Following Salmonella infection, the Th17 response in the $CD4^+$ T cell population shifts to a Th1-biased response, and IL-17A, which is increased by Salmonella infection, stimulates intestinal epithelial cells to enhance the production of antimicrobial proteins and chemokines (60, 61). Thus, the higher protective immune response induced by r-SG might be due to Th17-mediated Th1-biased response. Further analysis of the cellular immune responses should be performed on the spleen of chickens given various doses of r-SG vaccine.

Ionizing radiation primarily damages DNA and consequently, the biological responses depending on the radiation track structure and its energy loss distribution pattern (62). However, because it is difficult to investigate the exact mechanism of ionizing radiation at the atomic level, several modeling and simulation programs, such as Geant4-DNA, have been introduced to predict the effects of cellular oxygenation on the chemical processes involving DNA radicals (63). According to Geant4-DNA simulation, low linear energy transfer radiation can cause 0.04 to 0.010 double-strand breaks/Gy/Mbp, indicating that radiation can penetrate the cell nucleus to induce intracellular oxygenation processes for double-strand breaks in DNA. In contrast, formaldehyde causes external damage to the cell through a diffusion mechanism. Therefore, irradiated microorganisms have the potential to be recognized as living microorganisms in part through the interaction of well-conserved surface antigens with immune cells, which can promote the cell-mediated immune response.

In summary, we are the first to develop a gamma radiation-inactivated vaccine to SG that is safer and more effective than live SG 9R or chemically-inactivated SG vaccines. We found that the r-SG vaccine has the advantage of inducing a higher humoral immune response than the live 9R vaccine and a higher cell-mediated immune response than f-SG. Therefore, the

development of vaccines using gamma irradiation is expected to be applicable to various infectious diseases as an effective vaccine manufacturing method capable of inducing an immune response at an intermediate level between inactive and live vaccines.

DATA AVAILABILITY STATEMENT

The original contributions presented in the study are included in the article/**Supplementary Material**. Further inquiries can be directed to the corresponding authors.

ETHICS STATEMENT

The animal study was reviewed and approved by KAERI-IACUC.

AUTHOR CONTRIBUTIONS

HJJ, JH, SHH, HKJ, and JHL were responsible for conceptualization of the study, HJJ, EBB, FC, KBA, YW, and JYM performed the experiments and analyzed the data. HJJ, SHH, JHL, and HSS wrote the manuscript. HSS supervised the work. HSS, JH, and HKJ were responsible for funding acquisition.

FUNDING

This work was supported in part by National Research Foundation of Korea grants NRF-2017M2A2A6A02020925, NRF-2018K2A206023828, and NRF-2020M2A206023828 to HSS.

SUPPLEMENTARY MATERIAL

The Supplementary Material for this article can be found online at: https://www.frontiersin.org/articles/10.3389/fimmu.2021.717556/full#supplementary-material

Supplementary Figure 1 | Measurement of Serogroup B or D specific LPS antibody responses induced by r-SG. Mice (n = 5 per group) were immunized i.p. with 1 × 10^6 CFU of r-SG or f-SG three times at two week intervals and sera were collected two weeks after the last vaccination. **(A, B)** Serogroup B or D LPS specific antibody levels were measured by ELISA. Serogroup B and D-specific IgM **(A)** and Serogroup B and D-specific IgG **(B)**. *P < 0.05, **P < 0.01, ***P < 0.001, compared to unvaccinated mice or f-SG vaccinated group.

REFERENCES

1. Brenner FW, Willar RG, Angulo FJ, Tauxe R, Swaminathan B. Salmonella nomenclature. *J Clin Microbiol* (2000) 38(7):2465–7. doi: 10.1128/JCM.38.7.2465-2467.2000
2. Dieckmann R, Malorny B. Rapid Screening of Epidemiologically Important Salmonella Enterica subsp. enterica Serovars by Whole-Cell Matrix-Assisted Laser Desorption Ionization-Time of Flight Mass Spectrometry. *Appl Environ Microbiol* (2011) 77(12):4136–46. doi: 10.1128/AEM.02418-10
3. Mdegela RH, Msoffe PL, Waihenya RW, Kasanga JC, Mtambo MM, Minga UM, et al. Comparative Pathogenesis of Experimental Infections With Salmonella gallinarum in Local and Commercial Chickens. *Trop Anim Health Prod* (2002) 34(3):195–204. doi: 10.1023/a:1015226507721
4. Shivaprasad HL. Fowl Typhoid and Pullorum Disease. *Rev Sci Tech* (2000) 19 (2):405–24. doi: 10.20506/rst.19.2.1222
5. Zhang-Barber L, Turner AK, Barrow PA. Vaccination for Control of Salmonella in Poultry. *Vaccine* (1999) 17(20-21):2538–45. doi: 10.1016/s0264-410x(99)00060-2
6. Smith HW. The Use of Live Vaccines in Experimental Salmonella gallinarum Infection in Chickens With Observations on Their Interference Effect. *J Hyg (Lond)* (1956) 54(3):419–32. doi: 10.1017/S0022172400044685
7. Lee YJ, Mo IP, Kang MS. Safety and Efficacy of Salmonella gallinarum 9R Vaccine in Young Laying Chickens. *Avian Pathol* (2005) 34(4):362–6. doi: 10.1080/03079450500180895
8. Silva EN, Snoeyenbos GH, Weinack OM, Smyser CF. Studies on the Use of 9R Strain of Salmonella gallinarum as a Vaccine in Chickens. *Avian Dis* (1981) 25 (1):38–52. doi: 10.2307/1589825
9. Van Immerseel F, Studholme DJ, Eeckhaut V, Heyndrickx M, Dewulf J, Dewaele I, et al. Salmonella gallinarum Field Isolates From Laying Hens Are Related to the Vaccine Strain SG9R. *Vaccine* (2013) 31(43):4940–5. doi: 10.1016/j.vaccine.2013.08.033
10. Hwang JK, Lee YJ. Comparison of the Safety and Immunogenicity of Commercial S. gallinarum 9R Vaccine. *Korean J Vet Res* (2009) 49(2):127–33.
11. Paiva JB, Penha Filho RA, Pereira EA, Lemos MV, Barrow PA, Lovell MA, et al. The Contribution of Genes Required for Anaerobic Respiration to the Virulence of Salmonella Enterica Serovar Gallinarum for Chickens. *Braz J Microbiol* (2009) 40(4):994–1001. doi: 10.1590/S1517-838220090004000035
12. Penha Filho RA, de Paiva JB, Arguello YM, da Silva MD, Gardin Y, Resende F, et al. Efficacy of Several Vaccination Programmes in Commercial Layer and Broiler Breeder Hens Against Experimental Challenge With Salmonella Enterica Serovar Enteritidis. *Avian Pathol* (2009) 38(5):367–75. doi: 10.1080/03079450903183645
13. David SC, Lau J, Singleton EV, Babb R, Davies J, Hirst TR, et al. The Effect of Gamma-Irradiation Conditions on the Immunogenicity of Whole-Inactivated Influenza A Virus Vaccine. *Vaccine* (2017) 35(7):1071–9. doi: 10.1016/j.vaccine.2016.12.044
14. Datta SK, Okamoto S, Hayashi T, Shin SS, Mihajlov I, Fermin A, et al. Vaccination With Irradiated Listeria Induces Protective T Cell Immunity. *Immunity* (2006) 25(1):143–52. doi: 10.1016/j.immuni.2006.05.013
15. Cerutti PA. Effects of Ionizing Radiation on Mammalian Cells. *Naturwissenschaften* (1974) 61(2):51–9. doi: 10.1007/BF00596195
16. Alsharifi M, Mullbacher A. The Gamma-Irradiated Influenza Vaccine and the Prospect of Producing Safe Vaccines in General. *Immunol Cell Biol* (2010) 88 (2):103–4. doi: 10.1038/icb.2009.81
17. Furuya Y, Chan J, Regner M, Lobigs M, Koskinen A, Kok T, et al. Cytotoxic T Cells are the Predominant Players Providing Cross-Protective Immunity Induced by {Gamma}-Irradiated Influenza A Viruses. *J Virol* (2010) 84 (9):4212–21. doi: 10.1128/JVI.02508-09
18. Dubensky TW Jr., Skoble J, Lauer P, Brockstedt DG. Killed But Metabolically Active Vaccines. *Curr Opin Biotechnol* (2012) 23(6):917–23. doi: 10.1016/j.copbio.2012.04.005
19. McFarland HI, Berkson JD, Lee JP, Elkahloun AG, Mason KP, Rosenberg AS. Rescue of CD8+ T Cell Vaccine Memory Following Sublethal Gamma Irradiation. *Vaccine* (2015) 33(32):3865–72. doi: 10.1016/j.vaccine.2015.06.070
20. Yang JD, Mott D, Sutiwisesak R, Lu YJ, Raso F, Stowell B, et al. Mycobacterium Tuberculosis-Specific CD4+ and CD8+ T Cells Differ in Their Capacity to Recognize Infected Macrophages. *PloS Pathog* (2018) 14(5): e1007060. doi: 10.1371/journal.ppat.1007060
21. Kasturi KN, Drgon T. Real-Time PCR Method for Detection of Salmonella spp. In Environmental Samples. *Appl Environ Microbiol* (2017) 83(14): e00644-17. doi: 10.1128/AEM.00644-17
22. Cunningham AF, Gaspal F, Serre K, Mohr E, Henderson IR, Scott-Tucker A, et al. Salmonella Induces a Switched Antibody Response Without Germinal

Centers That Impedes the Extracellular Spread of Infection. *J Immunol* (2007) 178(10):6200–7. doi: 10.4049/jimmunol.178.10.6200
23. Romero-Steiner S, Frasch CE, Carlone G, Fleck RA, Goldblatt D, Nahm MH. Use of Opsonophagocytosis for Serological Evaluation of Pneumococcal Vaccines. *Clin Vaccine Immunol* (2006) 13(2):165–9. doi: 10.1128/CVI.13.2.165-169.2006
24. Furuya Y, Regner M, Lobigs M, Koskinen A, Mullbacher A, Alsharifi M. Effect of Inactivation Method on the Cross-Protective Immunity Induced by Whole 'Killed' Influenza A Viruses and Commercial Vaccine Preparations. *J Gen Virol* (2010) 91(Pt 6):1450–60. doi: 10.1099/vir.0.018168-0
25. Singleton EV, David SC, Davies JB, Hirst TR, Paton JC, Beard MR, et al. Sterility of Gamma-Irradiated Pathogens: A New Mathematical Formula to Calculate Sterilizing Doses. *J Radiat Res* (2020) 61(6):886–94. doi: 10.1093/jrr/rraa076
26. Huttermann J, Lange M, Ohlmann J. Mechanistic Aspects of Radiation-Induced Free Radical Formation in Frozen Aqueous Solutions of DNA Constituents: Consequences for DNA? *Radiat Res* (1992) 131(1):18–23. doi: 10.2307/3578311
27. Wallace SS. Enzymatic Processing of Radiation-Induced Free Radical Damage in DNA. *Radiat Res* (1998) 150(5 Suppl):S60–79. doi: 10.2307/3579809
28. Sevilla MD, Becker D, Kumar A, Adhikary A. Gamma and Ion-Beam Irradiation of DNA: Free Radical Mechanisms, Electron Effects, and Radiation Chemical Track Structure. *Radiat Phys Chem Oxf Engl 1993* (2016) 128:60–74. doi: 10.1016/j.radphyschem.2016.04.022
29. Charret KS, Requena CE, Castillo-Acosta VM, Ruiz-Perez LM, Gonzalez-Pacanowska D, Vidal AE. Trypanosoma Brucei AP Endonuclease 1 Has a Major Role in the Repair of Abasic Sites and Protection Against DNA-Damaging Agents. *DNA Repair (Amst)* (2012) 11(1):53–64. doi: 10.1016/j.dnarep.2011.10.006
30. Krisko A, Radman M. Protein Damage and Death by Radiation in Escherichia coli and Deinococcus radiodurans. *Proc Natl Acad Sci USA* (2010) 107 (32):14373–7. doi: 10.1073/pnas.1009312107
31. Moghaddam A, Olszewska W, Wang B, Tregoning JS, Helson R, Sattentau QJ, et al. A Potential Molecular Mechanism for Hypersensitivity Caused by Formalin-Inactivated Vaccines. *Nat Med* (2006) 12(8):905–7. doi: 10.1038/nm1456
32. Polack FP, Hoffman SJ, Crujeiras G, Griffin DE. A Role for Nonprotective Complement-Fixing Antibodies With Low Avidity for Measles Virus in Atypical Measles. *Nat Med* (2003) 9(9):1209–13. doi: 10.1038/nm918
33. Choi MJ, Noh JY, Cheong HJ, Kim WJ, Lin SM, Zhi Y, et al. Development of a Multiplexed Opsonophagocytic Killing Assay (MOPA) for Group B Streptococcus. *Hum Vaccin Immunother* (2017) 14(1):67–73. doi: 10.1080/21645515.2017.1377379
34. Salazar GA, Penaloza HF, Pardo-Roa C, Schultz BM, Munoz-Durango N, Gomez RS, et al. Interleukin-10 Production by T and B Cells Is a Key Factor to Promote Systemic Salmonella Enterica Serovar Typhimurium Infection in Mice. *Front Immunol* (2017) 8:889. doi: 10.3389/fimmu.2017.00889
35. Tubo NJ, Jenkins MK. CD4+ T Cells: Guardians of the Phagosome. *Clin Microbiol Rev* (2014) 27(2):200–13. doi: 10.1128/CMR.00097-13
36. Collins AM. IgG Subclass Co-Expression Brings Harmony to the Quartet Model of Murine IgG Function. *Immunol Cell Biol* (2016) 94(10):949–54. doi: 10.1038/icb.2016.65
37. Sugaya N, Nerome K, Ishida M, Matsumoto M, Mitamura K, Nirasawa M. Efficacy of Inactivated Vaccine in Preventing Antigenically Drifted Influenza Type A and Well-Matched Type B. *JAMA* (1994) 272(14):1122–6. doi: 10.1001/jama.272.14.1122
38. Rubin LG, Levin MJ, Ljungman P, Davies EG, Avery R, Tomblyn M, et al. 2013 IDSA Clinical Practice Guideline for Vaccination of the Immunocompromised Host. *Clin Infect Dis* (2014) 58(3):309–18. doi: 10.1093/cid/cit816
39. Furuya Y. Return of Inactivated Whole-Virus Vaccine for Superior Efficacy. *Immunol Cell Biol* (2012) 90(6):571–8. doi: 10.1038/icb.2011.70
40. Brockstedt DG, Bahjat KS, Giedlin MA, Liu W, Leong M, Luckett W, et al. Killed But Metabolically Active Microbes: A New Vaccine Paradigm for Eliciting Effector T-Cell Responses and Protective Immunity. *Nat Med* (2005) 11(8):853–60. doi: 10.1038/nm1276
41. Kim HY, Kim SK, Seo HS, Jeong S, Ahn KB, Yun CH, et al. Th17 Activation by Dendritic Cells Stimulated With Gamma-Irradiated Streptococcus Pneumoniae. *Mol Immunol* (2018) 101:344–52. doi: 10.1016/j.molimm.2018.07.023
42. Lu K, Ye W, Zhou L, Collins LB, Chen X, Gold A, et al. Structural Characterization of Formaldehyde-Induced Cross-Links Between Amino Acids and Deoxynucleosides and Their Oligomers. *J Am Chem Soc* (2010) 132(10):3388–99. doi: 10.1021/ja908282f
43. Fan YC, Chiu HC, Chen LK, Chang GJ, Chiou SS. Formalin Inactivation of Japanese Encephalitis Virus Vaccine Alters the Antigenicity and Immunogenicity of a Neutralization Epitope in Envelope Protein Domain III. *PloS Negl Trop Dis* (2015) 9(10):e0004167. doi: 10.1371/journal.pntd.0004167
44. Murphy BR, Walsh EE. Formalin-Inactivated Respiratory Syncytial Virus Vaccine Induces Antibodies to the Fusion Glycoprotein That Are Deficient in Fusion-Inhibiting Activity. *J Clin Microbiol* (1988) 26(8):1595–7. doi: 10.1128/JCM.26.8.1595-1597.1988
45. Chen F, Seong Seo H, Ji HJ, Yang E, Choi JA, Yang JS, et al. Characterization of Humoral and Cellular Immune Features of Gamma-Irradiated Influenza Vaccine. *Hum Vaccin Immunother* (2021) 17(2):485–96. doi: 10.1080/21645515.2020.1780091
46. Ponnuraj EM, Springer J, Hayward AR, Wilson H, Simoes EA. Antibody-Dependent Enhancement, a Possible Mechanism in Augmented Pulmonary Disease of Respiratory Syncytial Virus in the Bonnet Monkey Model. *J Infect Dis* (2003) 187(8):1257–63. doi: 10.1086/374604
47. Kim HW, Canchola JG, Brandt CD, Pyles G, Chanock RM, Jensen K, et al. Respiratory Syncytial Virus Disease in Infants Despite Prior Administration of Antigenic Inactivated Vaccine. *Am J Epidemiol* (1969) 89(4):422–34. doi: 10.1093/oxfordjournals.aje.a120955
48. Nechipurenko YD, Anashkina AA, Matveeva OV. Change of Antigenic Determinants of SARS-CoV-2 Virus S-Protein as a Possible Cause of Antibody-Dependent Enhancement of Virus Infection and Cytokine Storm. *Biophysics (Oxf)* (2020) 65(4):703–9. doi: 10.1134/S0006350920040119
49. Desouky O, Ding N, Zhou G. Targeted and Non-Targeted Effects of Ionizing Radiation. *J Radiat Res Appl Sci* (2015) 8(2):247–54. doi: 10.1016/j.jrras.2015.03.003
50. Olive PL. The Role of DNA Single- and Double-Strand Breaks in Cell Killing by Ionizing Radiation. *Radiat Res* (1998) 150(5 Suppl):S42–51. doi: 10.2307/3579807
51. Dizdaroglu M, Jaruga P. Mechanisms of Free Radical-Induced Damage to DNA. *Free Radic Res* (2012) 46(4):382–419. doi: 10.3109/10715762.2011.653969
52. Zimbrick JD. Radiation Chemistry and the Radiation Research Society: A History From the Beginning. *Radiat Res* (2002) 158(2):127–40. doi: 10.1667/0033-7587(2002)158[0127:RRSRCA]2.0.CO;2
53. Deenick EK, Hasbold J, Hodgkin PD. Switching to IgG3, IgG2b, and IgA Is Division Linked and Independent, Revealing a Stochastic Framework for Describing Differentiation. *J Immunol* (1999) 163(9):4707–14.
54. Deenick EK, Hasbold J, Hodgkin PD. Decision Criteria for Resolving Isotype Switching Conflicts by B Cells. *Eur J Immunol* (2005) 35(10):2949–55. doi: 10.1002/eji.200425719
55. Michaelsen TE, Kolberg J, Aase A, Herstad TK, Hoiby EA. The Four Mouse IgG Isotypes Differ Extensively in Bactericidal and Opsonophagocytic Activity When Reacting With the P1.16 Epitope on the Outer Membrane PorA Protein of Neisseria Meningitidis. *Scand J Immunol* (2004) 59(1):34–9. doi: 10.1111/j.0300-9475.2004.01362.x
56. Lin L, Ibrahim AS, Xu X, Farber JM, Avanesian V, Baquir B, et al. Th1-Th17 Cells Mediate Protective Adaptive Immunity Against Staphylococcus Aureus and Candida Albicans Infection in Mice. *PloS Pathog* (2009) 5(12):e1000703. doi: 10.1371/journal.ppat.1000703
57. Olliver M, Hiew J, Mellroth P, Henriques-Normark B, Bergman P. Human Monocytes Promote Th1 and Th17 Responses to Streptococcus Pneumoniae. *Infect Immun* (2011) 79(10):4210–7. doi: 10.1128/IAI.05286-11
58. Gayet R, Bioley G, Rochereau N, Paul S, Corthesy B. Vaccination Against Salmonella Infection: The Mucosal Way. *Microbiol Mol Biol Rev* (2017) 81(3):e00007-17. doi: 10.1128/MMBR.00007-17
59. Li Y, Wei C, Xu H, Jia J, Wei Z, Guo R, et al. The Immunoregulation of Th17 in Host Against Intracellular Bacterial Infection. *Mediators Inflammation* (2018) 2018:6587296. doi: 10.1155/2018/6587296

60. Clay SL, Bravo-Blas A, Wall DM, MacLeod MKL, Milling SWF. Regulatory T Cells Control the Dynamic and Site-Specific Polarization of Total CD4 T Cells Following Salmonella Infection. *Mucosal Immunol* (2020) 13(6):946–57. doi: 10.1038/s41385-020-0299-1
61. Curtis MM, Way SS. Interleukin-17 in Host Defence Against Bacterial, Mycobacterial and Fungal Pathogens. *Immunology* (2009) 126(2):177–85. doi: 10.1111/j.1365-2567.2008.03017.x
62. Forster JC, Douglass MJJ, Phillips WM, Bezak E. Monte Carlo Simulation of the Oxygen Effect in DNA Damage Induction by Ionizing Radiation. *Radiat Res* (2018) 190(3):248–61. doi: 10.1667/RR15050.1
63. Lampe N, Karamitros M, Breton V, Brown JMC, Sakata D, Sarramia D, et al. Mechanistic DNA Damage Simulations in Geant4-DNA Part 2: Electron and Proton Damage in a Bacterial Cell. *Phys Med* (2018) 48:146–55. doi: 10.1016/j.ejmp.2017.12.008#

Conflict of Interest: Authors HKJ and YW were employed by company HONGCHEON CTCVAC Co., Ltd.

The remaining authors declare that the research was conducted in the absence of any commercial or financial relationships that could be construed as a potential conflict of interest.

Publisher's Note: All claims expressed in this article are solely those of the authors and do not necessarily represent those of their affiliated organizations, or those of the publisher, the editors and the reviewers. Any product that may be evaluated in this article, or claim that may be made by its manufacturer, is not guaranteed or endorsed by the publisher.

frontiers in Immunology

ORIGINAL RESEARCH
published: 24 November 2021
doi: 10.3389/fimmu.2021.761632

Enhanced Immunogenicity of a Whole-Inactivated Influenza A Virus Vaccine Using Optimised Irradiation Conditions

Eve Victoria Singleton[1], *Chloe Jayne Gates*[1], *Shannon Christa David*[1], *Timothy Raymond Hirst*[1,2], *Justin Bryan Davies*[3] *and Mohammed Alsharifi*[1,2*]

[1] Research Centre for Infectious Diseases, Department of Molecular and Biomedical Sciences, University of Adelaide, Adelaide, SA, Australia, [2] Gamma Vaccines Pty Ltd, Yarralumla, ACT, Australia, [3] Irradiations Group, Australian Nuclear Science and Technology Organisation, Lucas Heights, NSW, Australia

OPEN ACCESS

Edited by:
Sebastian Ulbert,
Fraunhofer Institute for Cell Therapy and Immunology (IZI), Germany

Reviewed by:
Paulo J.G. Bettencourt,
Catholic University of Portugal, Portugal
Suresh D. Pillai,
Texas A&M University, United States
Amir Ghaemi,
Pasteur Institute of Iran, Iran

***Correspondence:**
Mohammed Alsharifi
mohammed.alsharifi@adelaide.edu.au

Specialty section:
This article was submitted to Vaccines and Molecular Therapeutics, a section of the journal Frontiers in Immunology

Received: 20 August 2021
Accepted: 08 November 2021
Published: 24 November 2021

Citation:
Singleton EV, Gates CJ, David SC, Hirst TR, Davies JB and Alsharifi M (2021) Enhanced Immunogenicity of a Whole-Inactivated Influenza A Virus Vaccine Using Optimised Irradiation Conditions. Front. Immunol. 12:761632. doi: 10.3389/fimmu.2021.761632

Influenza A virus presents a constant pandemic threat due to the mutagenic nature of the virus and the inadequacy of current vaccines to protect against emerging strains. We have developed a whole-inactivated influenza vaccine using γ-irradiation (γ-Flu) that can protect against both vaccine-included strains as well as emerging pandemic strains. γ-irradiation is a widely used inactivation method and several γ-irradiated vaccines are currently in clinical or pre-clinical testing. To enhance vaccine efficacy, irradiation conditions should be carefully considered, particularly irradiation temperature. Specifically, while more damage to virus structure is expected when using higher irradiation temperatures, reduced radiation doses will be required to achieve sterility. In this study, we compared immunogenicity of γ-Flu irradiated at room temperature, chilled on ice or frozen on dry ice using different doses of γ-irradiation to meet internationally accepted sterility assurance levels. We found that, when irradiating at sterilising doses, the structural integrity and vaccine efficacy were well maintained in all preparations regardless of irradiation temperature. In fact, using a higher temperature and lower radiation dose appeared to induce higher neutralising antibody responses and more effective cytotoxic T cell responses. This outcome is expected to simplify irradiation protocols for manufacturing of highly effective irradiated vaccines.

Keywords: influenza A virus, gamma radiation, vaccine, sterility assurance level (SAL), irradiation conditions, universal influenza A vaccine

INTRODUCTION

Influenza A virus (IAV) is a major health concern and causes significant morbidity and mortality on a global scale. The most at-risk groups for development of serious IAV symptoms or secondary complications are infants, the elderly, the immunocompromised, and pregnant women (1). Vaccination remains the most effective method to combat IAV infection, though current inactivated vaccines have major valency and efficacy limitations. Existing formulations consist of purified IAV surface proteins haemagglutinin (HA) and neuraminidase (NA) of 2 IAV strains and

an additional 1 or 2 influenza B virus strains predicted to circulate in a given year. Whilst effective at protecting against 'vaccine-included' strains, the immune responses induced by current IAV vaccines are antibody-based only and provide minimal protection against strains not included in a given formulation (i.e. non-vaccine strains). In general, current IAV vaccines are ineffective against newly emerging seasonal strains and novel pandemic strains and must also be updated and redistributed every year due to the highly mutagenic nature of IAV surface proteins.

In order to increase vaccine coverage and minimise IAV-related morbidity and economic costs, new cross-protective IAV vaccines must be developed. Our group has previously demonstrated that a gamma (γ)-irradiated whole-inactivated IAV vaccine (γ-Flu) has the ability to induce cross-protective responses against vaccine-included and non-included strains (2). Our previous publications illustrated that mice vaccinated with a single dose of γ-Flu (consisting of a H1N1 strain) were able to survive a lethal dose of a non-vaccine H1N1 strain (drifted), a heterosubtypic H3N2 strain (3), and the highly pathogenic avian H5N1 (4). The ability of γ-Flu to induce cross-protective immunity is specifically due to induction of cytotoxic T-cell responses against conserved internal IAV proteins (5).

In addition to our work on the development of γ-Flu (6, 7), several vaccines using γ-irradiation are currently in clinical trials including vaccines against human immunodeficiency virus (8) and malaria (9, 10). Given these promising results, it is crucial to determine the optimal conditions to ensure both sterility and high immunogenicity of γ-irradiated vaccines. Importantly, all γ-irradiated products intended to come into contact with human tissue must meet the internationally accepted sterility assurance level (SAL) of 10^{-6}, or a one in a million chance that an infectious unit escapes sterilisation (11). In general, while the sterilising dose required to achieve an acceptable Sterility Assurance Leve (DS_{SAL}) is dependent upon starting titre, it is heavily influenced by environmental conditions, particularly irradiation temperature (12). For example, viruses irradiated at lower temperatures (e.g. whilst frozen) are expected to be more resistant to irradiation damage. It is well-established that γ-irradiation causes damage to pathogens *via* two mechanisms, termed the direct and indirect effects. The slower inactivation of frozen materials is due to reduced indirect effects, as the production and movement of damaging free radicals is physically restricted (13, 14). This preserves antigenic epitopes within vaccine preparations (15, 16), but requires increased irradiation doses to achieve sterility. Large-scale irradiation of vaccine materials whilst maintained in a frozen state is likely to pose feasibility issues. Conversely, adopting a higher irradiation temperature (e.g. room temperature) increases viral sensitivity to irradiation damage, resulting in a much lower sterilising doses and faster irradiation time (12). This should increase the practicality of inactivation methods when scaled-up for manufacturing, particularly if vaccine immunogenicity is maintained. However, while faster inactivation at higher temperatures is desirable for most irradiated products (e.g. medical items, foods, etc.), the immunogenicity of vaccines treated in this manner is expected to be reduced due to amplification of indirect effects (17–19). Thus, an appropriate balance between sterilisation requirements and vaccine antigenicity should be assessed. In fact, previous studies did not address vaccine efficacy after irradiating with different doses that achieve the SAL at different irradiation temperatures.

In this study, we calculated the DS_{SAL} for γ-Flu irradiated on dry ice (DI), ice or at room-temperature (RT). We subsequently assessed structural integrity and vaccine efficacy of these three preparations in animal models. Our data show that vaccine efficacy is well maintained when irradiating at higher temperatures using lower doses of sterilising radiation. This could potentially open an avenue to use lower radiation doses to reduce manufacturing time and costs, while suitably maintaining both sterility and vaccine immunogenicity.

MATERIALS AND METHODS

Ethics Statement

This study was conducted in compliance with the *Australian Code of Practice for the Care and Use of Animals for Scientific Purposes* (20). These studies were approved by the University of Adelaide Animal Ethics Committee under ethics approval number S-2018-013.

Virus Stocks

Influenza A/Puerto Rico/8/1934 [H1N1] (A/PR8) and A/California/07/2009 [H1N1] (A/California) were grown in the allantoic cavity of 10-day-old embryonated chicken eggs at 37°C for 48 hours. Eggs were then chilled at 4°C overnight, and infected allantoic fluid was harvested and clarified by centrifugation at 3272 × g for 10 minutes.

Vaccine concentration and purification was performed by haemadsorption as described previously (21). Briefly, infected allantoic fluid was incubated with chicken erythrocytes at 4°C for 1.5 hours to allow virus adsorption to red blood cells (RBCs). Samples were then centrifuged to pellet virus-RBC complexes, and allantoic fluid supernatant was removed. Pellets were resuspended in 0.85% saline and incubated at 37°C for 1.5 hours to allow virus release from RBCs. Samples were then centrifuged to pellet RBCs, and the virus-containing supernatant was collected, aliquoted and stored at -80°C until required. Titres of concentrated IAV stocks were estimated as 3×10^9 $TCID_{50}$/mL and 4×10^7 $TCID_{50}$/mL for A/PR8 and A/California, respectively, by $TCID_{50}$ assay.

Gamma Irradiation of IAV Vaccines

Concentrated IAV stocks of A/PR8 at a $TCID_{50}$ of 3×10^9 $TCID_{50}$/mL were inactivated by γ-irradiation at the following temperature conditions: frozen on dry-ice (DI, approximately -78.5°C), cold on ice water (ice, 4-8°C) or at room temperature (RT, 24-27°C), generating DI-γ-Flu, Ice-γ-Flu, and RT-γ-Flu respectively. Sterilising doses were calculated as described previously to be 35 kGy for DI-γ-Flu and 16 kGy for Ice- and RT-γ-Flu (12).

Irradiation was performed using a cobalt-60 batch-type gamma irradiator at the Australian Nuclear Science and Technology Organisation (ANSTO, NSW). Samples for irradiation were double-contained in cryovials within 10 ml falcon tubes and placed in a 45 litre cooler box, sited in a fixed, reproducible location within the irradiation room. Samples were placed in pre-determined positions in the cooler box at various distances from the radiation source so that multiple doses could be delivered simultaneously. The cooler box was then filled with water (RT), chilled water containing ice blocks, or powdered dry ice for the different temperature conditions. Radiation doses were measured using calibrated Fricke (22) and ceric-cerous dosimeters (23) and dose rates varied from 0.3-1.6 kGy/h.

Temperature was monitored with a calibrated digital temperature probe connected to a data logger (Novus LogBox-AA) for ice and RT samples for the duration of irradiation, and non-irradiated control samples were subject to the same temperature conditions, stored out of the irradiation room. After irradiation, all samples were stored at -80°C until required.

Virus Titrations

IAV was titrated by 50% tissue culture infectious dose ($TCID_{50}$) assay using Madin-Darby canine kidney (MDCK) cells. MDCK cells were maintained in Dulbecco's Modified Eagle's Medium (DMEM) with 10% foetal bovine serum (FBS) and 1% penicillin/streptomycin (P/S). MDCK cells were kept at 37°C with 5% CO_2 and were passaged with trypsin when they reached approximately 90% confluence. For $TCID_{50}$ assay, MDCK cells were seeded in 96-well round-bottomed plates at 5×10^4 cells/well. After 24h incubation, confluent cell monolayers were infected with 10-fold serial dilutions of IAV in DMEM supplemented with 8% trypsin for virus activation. Plates were incubated at 37°C for 3 days, then amplified virus in culture supernatants was detected by the addition of 0.6% packed RBCs based on pellet or mesh formation, with a mesh being considered positive for IAV. 50% infectious doses ($TCID_{50}$/mL) were calculated using the Reed and Muench method (24).

For haemagglutination assays, serial dilutions of IAV were performed in 0.85% saline in a 96-well round-bottomed microtitre plate. 0.6% packed RBCs in 50µL were added to each well and plates were scored for mesh or pellet formation. The reciprocal of the highest virus dilution showing a mesh was used to determine the total haemagglutination units (HAU/mL).

Sterility testing was also performed after γ-irradiation of A/PR8 to ensure that the doses selected were sterile. MDCK cells were plated in 96-well flat-bottomed microtitre plates at 2×10^4 cells/well. γ-Flu was activated with 10µg/mL TPCK-trypsin at 37°C for 30 minutes then diluted 1:10 in DMEM + 1% P/S + 0.5µg/mL TPCK-trypsin. Inoculum was added to MDCK cells at an MOI-equivalent of 600 and cells were then incubated at 37°C for 24 hours to allow virus replication (passage 1). Supernatant was then collected and used to infect fresh MDCK monolayers (passage 2). This was then repeated for passage 3. At the time of collecting supernatant, cells were washed with PBS then fixed and permeabilised with 1:1 acetone:methanol (v/v) at 4°C for 15 minutes. Cells were then stained with polyclonal mouse anti-A/PR8 serum (1:200 dilution in PBS) for 1 hour at 4°C followed by Alexa-fluor® 488 goat anti-mouse IgG secondary antibody (Life Technologies, 1:500 dilution). DAPI was used to stain cell nuclei (1µg/mL in DAPI). Images were taken using the Nikon TiE inverted fluorescence microscope and analysed using NIS elements software (Tokyo, Japan).

Neuraminidase Assay

Two-fold serial dilutions of live and irradiated IAV samples were performed in PBS in triplicate. Samples were then incubated with 0.125mM of 2'-(4-Methylumbelliferyl)-α-D-N-acetylneuraminic acid (4-MUNANA, Sigma M8639) at 37°C for 1 hour, facilitating cleavage of 4-MUNANA by active IAV neuraminidase (NA) into the fluorescent substrate 4-Methylumbelliferyl (4-MU). 4-MU (Sigma M1381) was also included at increasing concentrations to generate standard curves. After 1 hour the assay was stopped with ice-cold 0.5M Na_2CO_3 at pH 10.5 and read using a SpectraMax fluorescent plate reader with an excitation wavelength of 365nm and emission wavelength of 450nm.

Transmission Electron Microscopy

Irradiated IAV at different temperatures was loaded onto 3mm formvar/carbon coated grids (approx. 3 µL/grid) and left to settle for 3 to 5 minutes. Grids were blotted to dry, washed, then stained with 2% uranyl acetate for 3 minutes. Grids were then washed with PBS and blotted to dry prior to visualisation using the FEI Tecnai G2 Spirit TEM (Adelaide Microscopy, University of Adelaide).

Mice

6-8 week old female BALB/c mice were vaccinated intranasally under ketamine anaesthetic (10% ketamine, 1% xylazil in sterile water, inject IP at 10µL/gram of body weight) with 32µL of either PBS (mock-vaccine control) or A/PR8-derived γ-Flu irradiated at different temperatures (9.6×10^7 $TCID_{50}$-equivalent/mouse). Immune serum was collected 20 days post-immunisation by submandibular bleeding. Mice were then challenged intranasally with lethal IAV on day 21 (3 weeks post-immunisation), under ketamine anaesthetic as above. Lethal doses were determined by challenging mice with serially diluted IAV. The lowest virus concentration that gave 100% lethality in mice was selected (data not shown). Challenge doses used were 1.6×10^2 $TCID_{50}$/mouse for A/PR8 and 1.3×10^5 $TCID_{50}$/mouse for the human isolate A/California. A higher dose was required to achieve lethality for A/California. Weight loss was measured daily for a period of 21 days post-challenge, with a 20% loss of starting body weight was used as a humane end point.

Antibody Responses

Enzyme-linked immunosorbent assay (ELISA) was used to measure IgG responses in serum samples from vaccinated and control mice. Plates were coated with A/PR8 in bicarbonate/carbonate coating buffer and incubated overnight at room temperature. Plates were then blocked with 2% skim milk for 2 hours. Serum samples were serially diluted then added to the plate for 2 hours at room temperature. Plates were washed and horseradish peroxidase-conjugated goat anti-mouse IgG

antibody (1:10,000 dilution in blocking buffer, Thermo Scientific) was added to each well. After 2 hours at room temperature, plates were washed, and colour was developed using TMB peroxidase substrate in the dark for 30 minutes then the reaction was stopped with 2M H_2SO_4. Absorbance was measured at 450nm using a Bio-Tek Instruments plate reader. The reciprocal of the highest dilution to give absorbance readings higher than naïve mice + 3 standard deviations was considered the IgG titre.

To measure neutralising antibody responses, a focus-forming inhibition assay was used. Monolayers of MDCK cells were treated with 0.1 MOI of A/PR8 that has been pre-incubated with serial dilutions of immune serum. Virus was allowed 2 hours to adhere to cells then inoculum was removed, and cells were washed with PBS. Fresh media was added, and cells were incubated at 37°C for a further 22 hours. Staining procedure and visualisation were performed as described for sterility testing. For measuring A/California neutralisation, the primary antibody used was polyclonal murine anti-A/California serum (1:200 dilution). Secondary antibody was Alexa-fluor® 488 goat anti-mouse IgG secondary antibody (Life Technologies, 1:500 dilution).

Cytotoxic T Lymphocyte Assay

Cytotoxic T lymphocyte (CTL) assays were performed as described previously (15). Mice were vaccinated intravenously with 3×10^8 $TCID_{50}$-equivalent of γ-Flu. 7 days later, spleens were harvested from naïve donor mice, minced, and pushed through a 70μm filter to generate a single-cell suspension. Cells were then split into equal populations, and one was pulsed with K^d-restricted influenza nucleoprotein (NP) peptide (NPP, sequence: TYQRTRALV) and stained with CFSE (NPP-Pulsed). The second population was stained with cell tracker red (CTR) only (Unpulsed). The cells were mixed at a 1:1 ratio and injected intravenously into vaccinated and non-vaccinated control mice at 10^7 cells/mouse. 24 hours later, all mice were sacrificed, and spleens were harvested and processed into a single-cell suspension prior to fixing using 1% PFA. Labelled pulsed and non-pulsed cells were acquired using the LSRII flow cytometer (BD Biosciences), and data was analysed using FlowJo software (Treestar Incorporated).

Statistical Analysis

Statistical analysis was performed using GraphPad Prism version 8 (GraphPad Software, La Jolla, CA, USA). Quantitative results were expressed as mean ± SEM. One-way ANOVA (with Tukey's multiple comparisons test) was used for comparison of data from 3 or more groups. Survival data were analysed using Fisher's exact test (two-tailed). P-values < 0.05 (95% confidence) were considered statistically significant.

RESULTS

Structural Integrity of γ-Flu

The aim of this study was to compare immunogenicity of vaccines irradiated to the SAL across different temperatures. Sterilising doses required to reduce virus titre to an acceptable SAL of 10^{-6} were calculated as described previously (12). For DI-irradiation, the DS_{SAL} was determined to be 35 kGy (DI-γ-Flu) and for ice- and RT-irradiation the sterilising dose was calculated to be 16 kGy (Ice-γ-Flu, RT-γ-Flu). Sterility testing based on multiple *in vitro* passages was performed to ensure complete inactivation of irradiated materials. Live and irradiated IAV samples were passaged three times in MDCK cells, with supernatants from each treated monolayer (or passage) used to treat the next MDCK monolayer. After 3 passages, monolayers were fixed and stained for IAV infection. No virus infectivity was detected in any of the MDCK monolayers treated with irradiated preparations for all 3 passages, whereas replication of live virus was amplified at each passage (**Figure 1**). The irradiated materials were thus confirmed to be sterile and appropriate for subsequent *in vitro* and *in vivo* experiments.

The structural integrity of the IAV within each vaccine preparation was then assessed by HA and NA functionality assays. While hemagglutination assay show reduced HA activity for all γ-Flu preparations compared to live IAV (**Figure 2A**), no significant difference was detected between the three irradiated samples despite the highly varied temperature conditions used for irradiation. Furthermore, **Figure 2B** demonstrates that the functionality of NA proteins in each γ-Flu preparation was not affected by irradiation, with all three vaccine formulations showing comparable NA enzymatic activity to live IAV. Transmission electron microscopy was then used to examine whole virion structure. Representative images in **Figure 2C** show that virions within all three irradiated preparations were intact and retained spherical IAV structure. This shows that in addition to having minimal impact on surface proteins, exposing IAV to DS_{SAL} at relative temperature conditions does not cause substantial damage to viral envelopes.

Efficacy of γ-Flu in Mice

Given that all three γ-Flu preparations appeared suitably intact in terms of virion structure and protein functionality, we next assessed their efficacy as vaccine candidates in animal models. Initially, mice were vaccinated intranasally with a single dose of each vaccine preparation (DI-γ-Flu, Ice-γ-Flu, or RT-γ-Flu), or with PBS as a mock-vaccine control. 20 days post-immunisation, sera was harvested from all animals and an ELISA was performed to determine IAV-specific IgG titres. As shown in **Figure 3A**, all three γ-Flu preparations induced strong IgG responses above PBS-mock control levels, and no significant difference was detected between IgG titres induced by the three γ-Flu preparations. Interestingly, whilst not significant, there was a trend towards lower IgG responses detected in serum samples from mice vaccinated with DI-γ-Flu.

Following this, a focus-forming inhibition assay was performed to determine the ability of γ-Flu-induced antibodies to inhibit receptor binding and IAV infection. Neutralising antibody responses are crucial for protection against homotypic IAV infection, thus it is important to assess antibody functionality in addition to overall titre. Serum samples from γ-Flu-vaccinated and control mice were used to treat live A/PR8, and virus:serum mixtures were used to infect

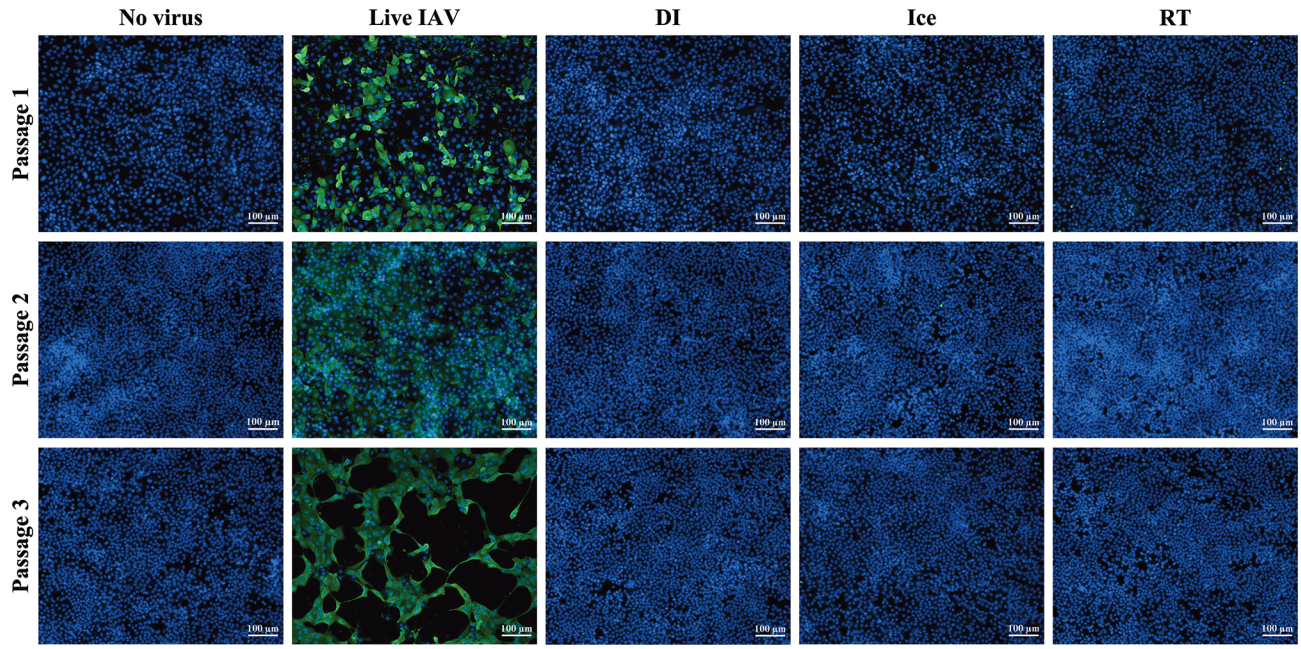

FIGURE 1 | Sterility of γ-irradiated IAV. Sterility of γ-Flu was assessed by multiple passages in MDCK cells. Live A/PR8 or no virus were used as controls. γ-Flu was added to cells at an MOI equivalent of 600. Supernatant from passage 1 was collected 24 hours later and used to infect monolayers of MDCK cells for passage 2, this was then repeated for passage 3. Cell monolayers were stained with DAPI (blue), and IAV-positive cells were visualised with FITC-fluorescence (green). Samples were tested in triplicate and representative images are presented for each group at each passage.

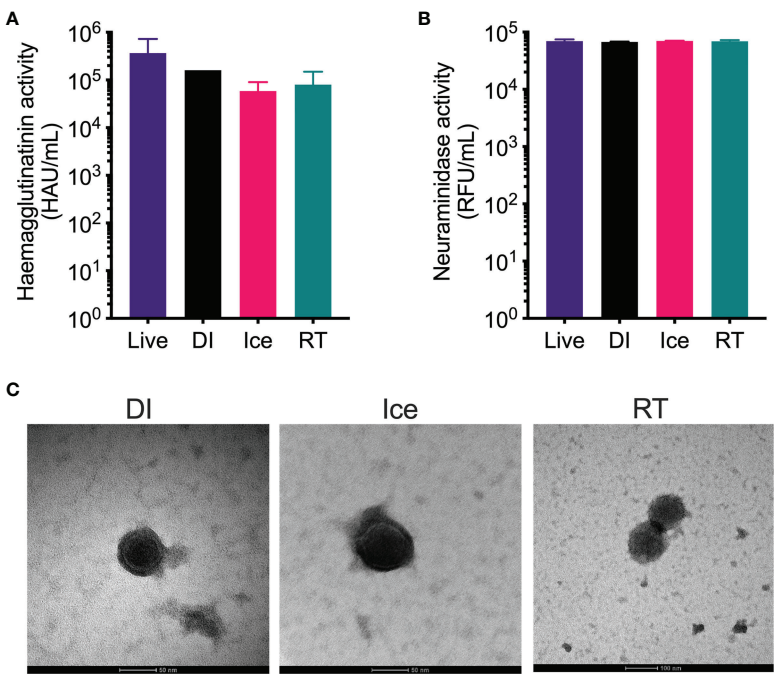

FIGURE 2 | Structural integrity of IAV is maintained after γ-irradiation at different temperatures. γ-Flu preparations were inactivated with either: 16 kGy at RT, 16 kGy on ice, or 35 kGy on DI. Structural integrity of these preparations was then assessed by **(A)** haemagglutination assay, **(B)** neuraminidase assay and **(C)** transmission electron microscopy. Quantitative data is expressed as mean ± SEM (n = 3). Data is analysed by one-way ANOVA and results were not significant.

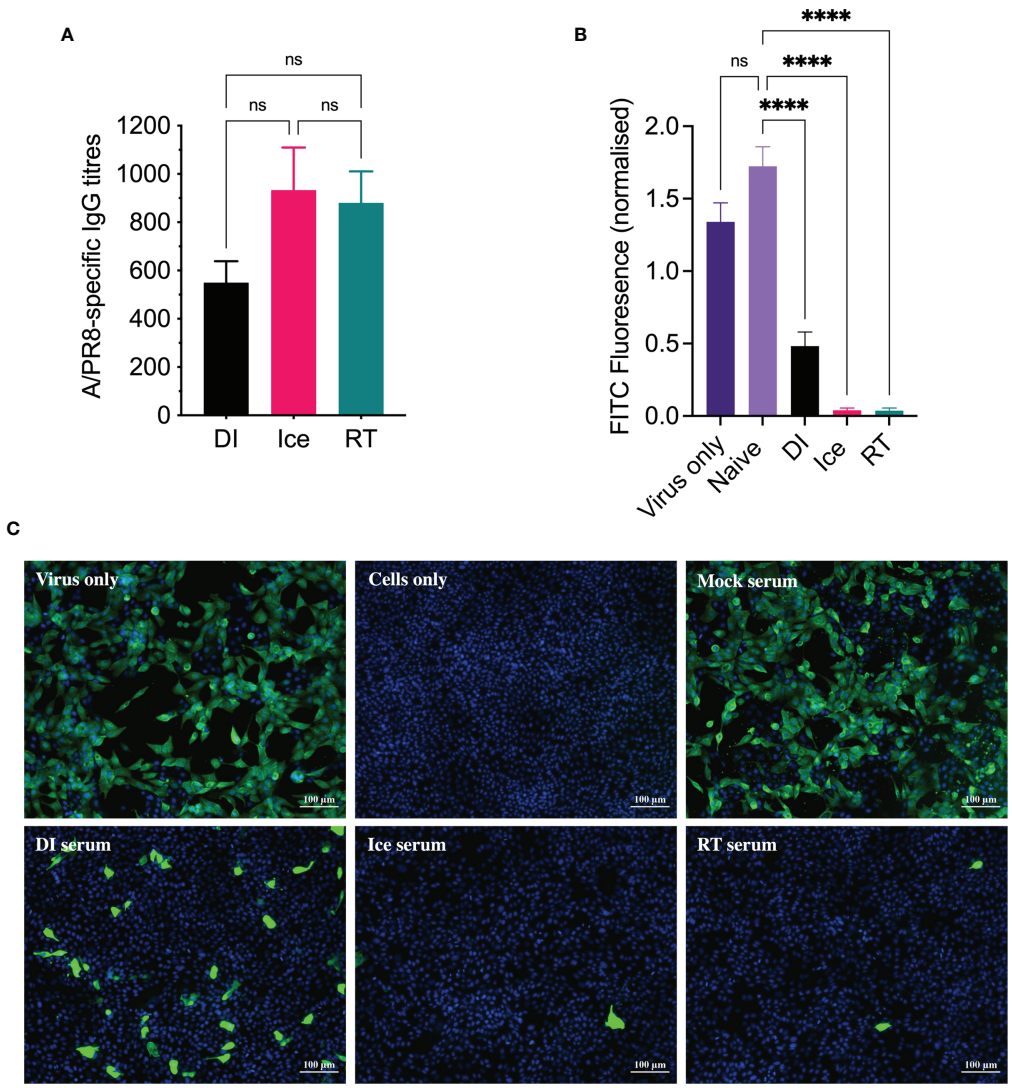

FIGURE 3 | DI-γ-Flu induces reduced neutralising antibody responses when compared to Ice- and RT-γ-Flu. Mice were vaccinated intranasally with DI-γ-Flu, Ice-γ-Flu, RT-γ-Flu or PBS. Serum samples were collected 20 days post-vaccination. **(A)** IgG responses were measured by direct ELISA. Data is collated from two independent experiments (n = 5 mice per repeat) and analysed by One-Way ANOVA (not significant difference). **(B)** Neutralising antibody responses were measured by FFI. Live virus was treated with pooled naïve serum or pooled immune serum from vaccinated mice (n = 10 serum samples pooled within each vaccine group), then virus:serum mixtures were used to infect MDCK cell monolayers at MOI = 0.1. Each virus:serum mixture was tested in triplicate. FITC-fluorescence was quantified as an indicator of IAV infection and was normalised using the corresponding DAPI-fluorescence in each well (indicates the number of cell-nuclei). Data presented as mean FITC fluorescence ± SEM and analysed by one-way ANOVA (****$p < 0.0001$, ns, no significance). **(C)** Representative images from FFI assay showing IAV infectivity levels after treatment with pooled naïve and immune serum at a 1:10 dilution.

monolayers of MDCK cells. After a 22h incubation period, cells were stained with DAPI to visualise cell nuclei, and with murine anti-APR8 and FITC-conjugated anti-murine antibodies to visualise IAV-infected cells. Fluorescence levels of each fluorophore were quantified, and FITC-fluorescence relative to DAPI-fluorescence was calculated to determine the average IAV infectivity per cell. Quantified fluorescence of serum-treated virus samples were then compared to untreated virus only controls. As shown in **Figure 3B**, no reduction in infectivity was detected for virus treated with PBS-mock control sera, indicating that the murine sera from naïve animals had no effect on IAV infectivity. Conversely, infectivity was significantly reduced when A/PR8 was treated with serum from DI-, Ice- and RT-γ-Flu vaccinated mice. Interestingly, immune sera from mice vaccinated with Ice- and RT-γ-Flu was significantly more effective at neutralising A/PR8 when compared to immune sera from mice vaccinated with DI-γ-Flu. Representative images of virus neutralisation were also taken at a 1:10 serum dilution, and similarly demonstrate a clear reduction in foci for all γ-Flu groups, with antibodies induced

by Ice- and RT-γ-Flu vaccination being the most effective (**Figure 3C**). This trend is likely due to the higher titre of total IgG present in immune sera from Ice- and RT-γ-Flu vaccinated animals, compared to those immunised with DI-γ-Flu.

Given the observed differences in functionality of γ-Flu-induced antibodies, we challenged vaccinated animals with live IAV to assess if these variations would translate to detectable differences in protective efficacy. Initially, the ability of DI-, Ice-, and RT-γ-Flu to mediate homotypic protection was investigated. Three weeks post-vaccination, mice were challenged with a lethal dose of homotypic A/PR8. No clinical symptoms were observed and no weight loss was recorded for all vaccinated groups, in contrast to PBS-mock control mice that succumbed to A/PR8 challenge and showed progressive weight loss to reach the humane end point of 20% body weight loss by day 7 post-infection (**Figure 4A**). Importantly, all vaccinated mice, irrespective of vaccine irradiation temperature, show 100% survival based on using 20% bodyweight loss as the humane end point (**Figure 4B**). This indicates that the antibody responses shown in **Figure 3**, though variable, were sufficient to induce robust homotypic protection.

Importantly, a key feature of γ-Flu is its ability to induce cross-protective $CD8^+$ T-cell responses against vaccine and non-vaccine IAV strains. To assess the effect of the differential irradiation temperatures on the induction of $CD8^+$ T-cell responses, an *in vivo* CTL assay was performed. Here, the killing of IAV NPP-pulsed splenocytes (target cells) was assessed in vaccinated and non-vaccinated animals. NP has been identified as a key $CD8^+$ T cell IAV antigen (25). As shown in **Figure 5**, splenocytes from naïve control mice show a 1:1 ratio of pulsed target cells to unpulsed cells, indicating no non-specific killing of targets cells *in vivo*. Conversely, we detected a substantial loss of NPP-pulsed cells relative to unpulsed cells in all three γ-Flu vaccinated groups. This demonstrates the ability of all γ-Flu preparations to induce a robust IAV-specific CTL responses as pulsed target cells were lysed within 24h of injection into immunised animals. Interestingly, animals vaccinated with Ice-γ-Flu and RT-γ-Flu showed significantly more effective CTL responses (97% and 93% killing of IAV-pulsed targets, respectively) compared to animals vaccinated with DI-γ-Flu (73% killing of IAV-pulsed targets).

Enhanced IAV-specific CTL responses should theoretically translate to enhanced cross-protection against newly emerging IAV strains. To assess this, mice were vaccinated intranasally with different γ-Flu preparations (based on A/PR8 [H1N1]), or PBS-mock control. Three weeks later, mice were intranasally challenged with a lethal dose of A/California, the pdmH1N1 strain. As shown in **Figure 6**, all vaccinated and non-vaccinated mice experienced some weight loss following A/California infection, however mice vaccinated with Ice-γ-Flu showed less weight loss and faster recovery than the other vaccine groups. Furthermore, 100% survival was recorded for mice vaccinated with Ice-γ-Flu and RT-γ-Flu, whereas 86% survival occurred in mice vaccinated with DI-γ-Flu (1 out of 7 mice reached the humane end point of 20% weight loss). Overall, while γ-Flu vaccination was associated with significantly less weight loss and faster recovery time in all vaccinated groups, only Ice-γ-Flu and RT-γ-Flu was associated with significantly higher survival rates compared to the unvaccinated group. This outcome is consistent with the enhanced CTL responses (**Figure 5**). To rule out the possibility that the protection demonstrated in **Figure 6** was mediated by neutralising antibody responses, we tested the ability of serum generated by different γ-Flu preparations to neutralise A/California. Live A/California was treated with serial dilutions of serum generated by DI-, Ice- or RT-γ-Flu, or naïve serum as a control. Virus + serum was then added to confluent monolayers of MDCK cells and allowed to adhere for 2 hours before unbound virus was washed away. Cells were incubated for a further 2 hours at 37°C to allow virus growth then cells were fixed and stained with murine anti-A/California serum used as a primary antibody. As expected, we

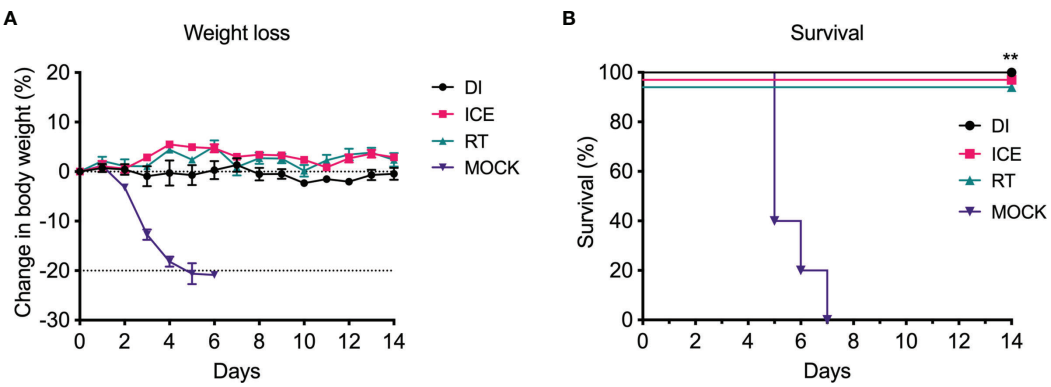

FIGURE 4 | Vaccination with γ-Flu protects against lethal homotypic challenge. Mice were vaccinated intranasally with γ-Flu irradiated at different temperatures (DI, Ice and RT), or PBS-mock control. 21 days later, mice were intranasally challenged with a lethal dose of A/PR8. **(A)** Weight was monitored daily and a 20% loss of starting weight was considered as the humane endpoint (dotted line), at which point mice were euthanised. **(B)** Overall survival was plotted, and a two-tailed Fisher Exact test was used to determine statistical significance compared to the Mock control group (**P < 0.01, n = 5 mice per group).

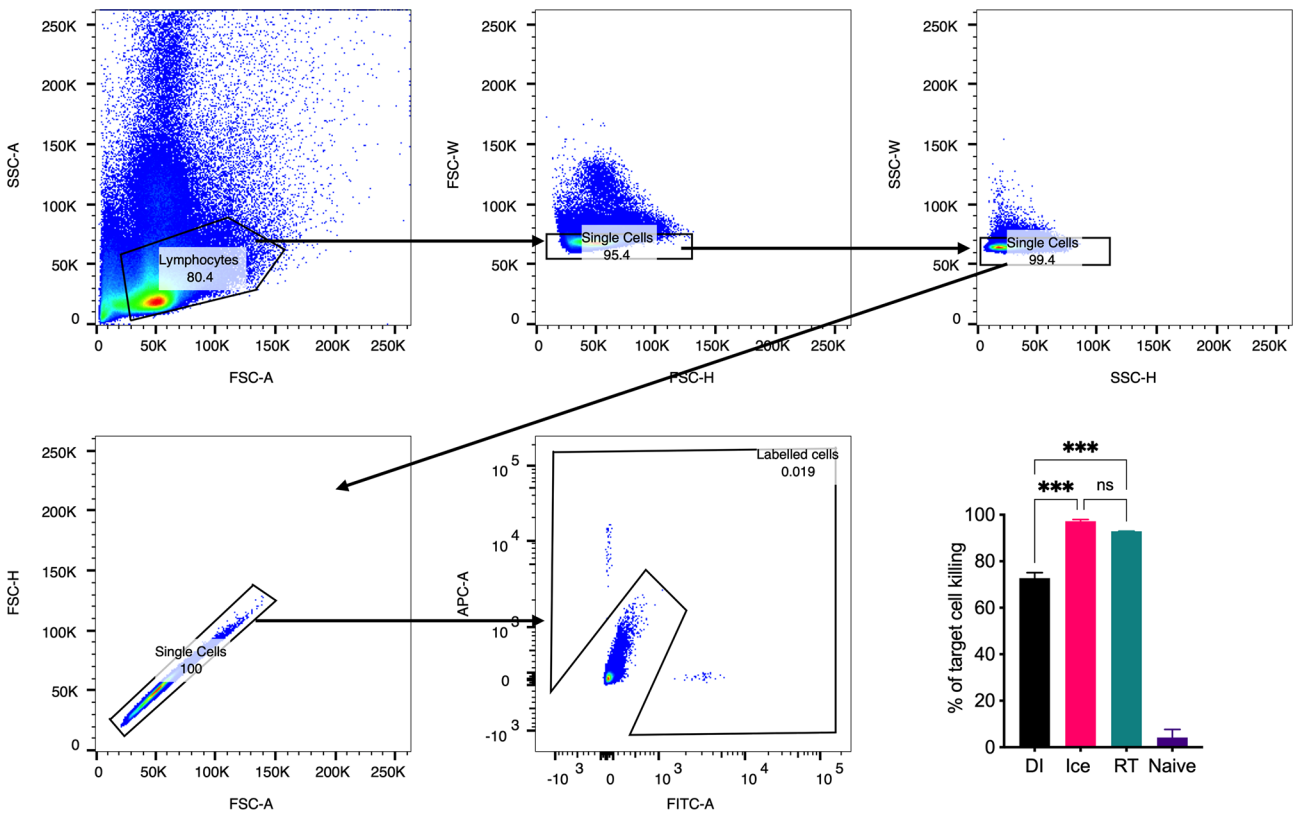

FIGURE 5 | CTL responses are induced by vaccination with γ-Flu. Mice were vaccinated intravenously with γ-Flu preparations (RT-, Ice-, and DI-γ-Flu) or treated with PBS as mock control. 7 days later equal ratios of NPP-pulsed (CFSE labelled) and unpulsed (CTR labelled) splenocytes from naïve donor mice were injected into γ-Flu vaccinated mice or mock-vaccinated controls. 24 hours later splenocytes were harvested, processed and analysed using flow cytometry. Gating strategy is shown. The change in ratio of pulsed to unpulsed splenocytes after injection into vaccinated animals was used to calculate the percentage killing of pulsed cells. Data presented here as mean percentage +/- SEM and analysed using one-way ANOVA (***$p < 0.001$, ns, not significant, n = 3).

observed no cross-neutralisation generated by A/PR8 based γ-Flu preparations against A/California H1N1 (**Figure 7**).

DISCUSSION

IAV remains an important public health concern due to its high mutation rates and potential to cause global pandemics. Current vaccines only offer strain-specific protection due to the reliance on humoral immune responses against highly mutagenic HA and NA surface antigens rather than cross-protective responses against the conserved internal IAV components. We have developed an effective whole-IAV vaccine capable of protecting against multiple IAV strains and subtypes. For this vaccine candidate, IAV is inactivated using γ-irradiation (generating γ-Flu), and the heterosubtypic protection is specifically mediated by induction of cross-reactive cytotoxic T cell responses (5). While previous publications illustrated the underlying mechanisms for the cross-protective immunity, this study aims to improve the immunogenicity of γ-Flu by manipulating irradiation conditions.

Sterilisation of materials for biomedical analysis using γ-radiation is typically performed while the sample is frozen on dry ice to minimise structural damage. For example, serum samples from an Ebolavirus vaccine clinical trial were irradiated frozen at 50 kGy, and antibody binding detected by ELISA was well-maintained after this treatment (26). Bone allografts are also often sterilised whilst frozen, as bones are less brittle when irradiated on dry ice compared to irradiation with the same dose at room temperature (27). Our previous publications describing γ-Flu (2–5, 15, 28), γ-irradiated *Streptococcus pneumoniae* vaccine (γ-PN) (29), and a γ-irradiated rotavirus vaccine (30) all used irradiation on dry ice. Similarly, an experimental Venezuelan Equine Encephalitis Virus vaccine is also γ-irradiated while frozen on dry ice (31). Importantly, we have specifically advocated for DI-irradiation over RT-irradiation when using comparable high irradiation doses, as the use of frozen materials is associated with enhanced structural integrity and immunogenicity (15). However, previous studies did not investigate the immunogenicity of irradiated materials that received different sterilising doses relevant to different irradiation conditions.

It is well established that pathogens are more sensitive to inactivation by γ-irradiation at higher temperatures (17–19), which lowers the total sterilising dose required (12). In fact,

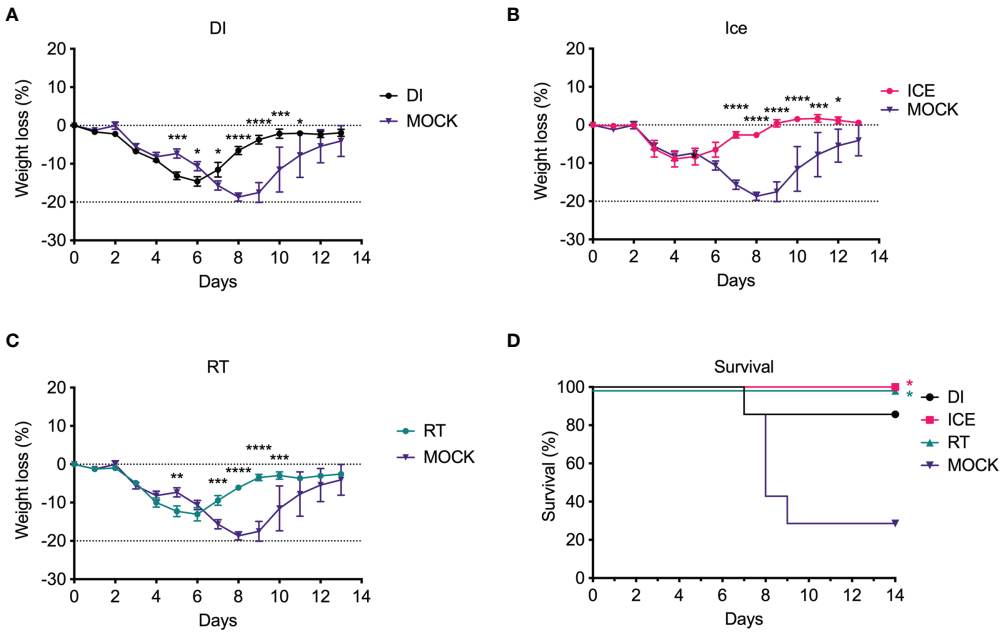

FIGURE 6 | Vaccination with γ-Flu protects against lethal challenge with a drifted IAV strain. Mice were vaccinated intranasally with γ-Flu (γ-A/PR8 H1N1) irradiated at different temperatures, or PBS as mock control. 21 days later mice were challenged intranasally with a lethal dose of A/California H1N1. **(A-C)** Weight loss was measured daily, with a 20% loss of starting weight (dotted line) was considered as the humane end point. Weight loss was analysed by Two-Way ANOVA. **(D)** Survival rates were plotted, and a Two-Tailed Fisher-Exact test was used for analysis by comparing vaccinated groups to the PBS-MOCK vaccinated group (*$p < 0.05$, **$p < 0.01$, ***$p < 0.001$, ****$p < 0.0001$), n = 7 mice/group).

this is the first study to consider the impact of irradiation temperature on the DS_{SAL} and directly compare the immunogenicity of sterile IAV preparations inactivated with different DS_{SAL} doses of γ-rays at different temperatures. Interestingly, our data show improved vaccine immunogenicity when using lower irradiation doses at higher temperatures. While previous studies have shown that more free radicals form and therefore more protein damage would occur when irradiating at higher temperatures (18), the lower dose of radiation required to reach the DS_{SAL} could explain the efficacy of Ice- and RT-γ-Flu. In fact, utilising these conditions would negate the need to keep samples frozen with an added advantage of a faster irradiation process.

To ensure that the heightened efficacy of ice and RT-irradiated samples was not due to residual live virus, sterility was confirmed for each preparation by three passages in MDCK cells. We have previously shown this method of sterility testing to be effective in detecting as little as 2 focus-forming units in a treated sample (30). **Figure 1** clearly shows all three preparations were free from viable virus over multiple passages. Furthermore, we used a very high MOI-equivalent of 600 to demonstrate sterility. Importantly, these data confirm that γ-Flu irradiated at sterilising doses does not have the ability to undergo recombination to produce viable virions.

We subsequently analysed the structural integrity of these sterilised γ-Flu samples by measuring HA and NA function. We found equivalent functionality for all preparations tested (**Figure 2**), which suggests that the γ-Flu preparations would be highly immunogenic due to retained function of key antigens. Furthermore, IFN-I specifically relies on the ability of IAV HA to bind to sialic acid receptors on IFN-I producing cells for virus internalisation (32). In fact, we have previously published the ability of γ-Flu to induce superior IFN-I responses compared to commercial IAV vaccines and demonstrated IFN-1-dependent T cell activation (28).

Of interest, current inactivated IAV vaccines induce antibodies of a narrow breadth, whereas responses to natural IAV infection include a small population of broadly neutralising antibodies against the HA stalk (33), an area that is highly conserved (34). However, antibodies to the HA stalk may still be overcome by mutations (35). We initially tested the effect of irradiation temperature on the ability of γ-Flu to induce neutralising antibody responses and homotypic protection. Interestingly, while all γ-Flu preparations induced strong A/PR8-specific IgG and neutralising responses, Ice-γ-Flu and RT-γ-Flu performed better than DI-γ-Flu (**Figure 3**). Nonetheless, all γ-Flu preparations induced complete protection against homotypic A/PR8 challenge (**Figure 4**).

We found that Ice-γ-Flu and RT-γ-Flu also outperformed DI-γ-Flu for induction of CTL responses (**Figure 5**), and protection against lethal drifted challenge (**Figure 6**). It is well established that live IAV-induces CTL responses that can target the conserved internal NP, matrix and polymerase proteins (36, 37). Our previous work has illustrated that antibodies induced by γ-Flu

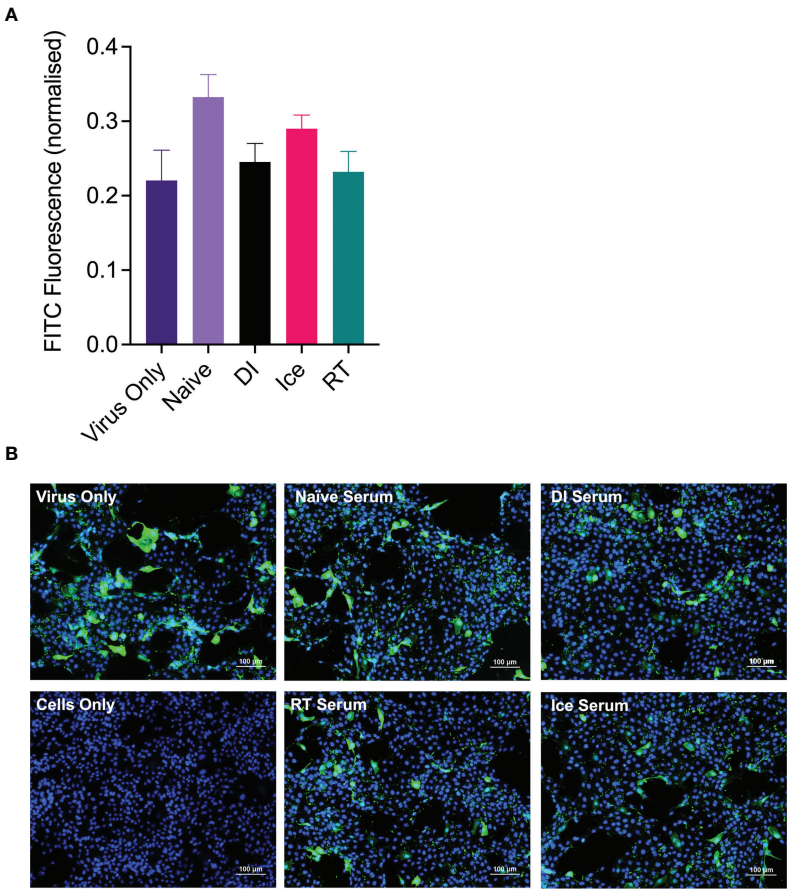

FIGURE 7 | γ-Flu does not induce cross-neutralising antibody responses. Mice were vaccinated intranasally with γ-Flu (γ-A/PR8 H1N1) irradiated at room temperature (RT), on ice water (Ice) or on dry ice (DI). 20 days post-vaccination immune serum was harvested and the ability to neutralise A/California was measured by focus-forming inhibition assay. Live A/California was treated with pooled serum samples from the three vaccine groups or with serum from mock-vaccinated mice. Virus + serum mixtures were used to infect MDCK cell monolayers at MOI of 0.1. **(A)** FITC-fluorescence (green) indicative of A/California replication was measured relative to DAPI-fluorescence (blue), indicative of cell nuclei. **(B)** Representative images of cell monolayers showing A/California infection levels after pre-treatment with a 1:10 dilution of serum samples. Experiments were performed in triplicate and quantitative data was analysed by One-Way ANOVA. Data was not significant.

are strain-specific (3), and that cross-protection arises through cell-mediated responses (5). In the present study we confirm that antibodies generated against all three γ-Flu preparations were unable to neutralise the drifted pdmH1N1 (**Figure 7**), and so protection demonstrated in **Figure 6** is expected to be mediated by the enhanced CTL responses (**Figure 5**).

The reduced efficacy of DI-γ-Flu compared to RT- and ice-irradiated preparations suggest that irradiating frozen materials using high dose may not be the best approach to minimise the damage to viral proteins. Instead, a balanced irradiation process that includes the use of low doses of γ-rays to inactivate unfrozen materials at cold or RT conditions could be utilised to produce highly immunogenic vaccine preparations. Indeed, Cote et al. (38) showed that the irradiation conditions of anthrax spores could be adjusted to meet a SAL of 10^{-6} using room temperature or ice-irradiation while maintaining the biological structure required for biomedical testing. This change in irradiation conditions could overcome biosecurity issues associated with the inadvertent release of live anthrax spores by the US Department of Defense (39). A radiation-attenuated malaria vaccine PfSPZ is reported to receive a low dose of γ-irradiation at RT prior to harvesting the sporozoites from the mosquito (40).

Recently, electron beam (eBeam) irradiation has been employed as an alternative to γ-irradiation. eBeam has several advantages over γ-irradiation including significantly higher dose rates and safety (41). Importantly, our findings demonstrate that liquid samples can be highly immunogenic when irradiating to the DS_{SAL} compared to frozen samples which is expected to simplify manufacturing procedures for irradiated vaccines regardless of the technology used. In fact, these findings may also support the use of eBeam in vaccine development.

In this study, precise calculation of the DS_{SAL} allowed us to prepare highly immunogenic γ-Flu using substantially lower dose of irradiation while maintaining internationally acceptable level of sterility. These data also indicate that ice or RT-irradiation is far less damaging than previously thought if the

concept of the DS_{SAL} is properly applied. These observations offer new and improved insights into the use of γ-irradiation to inactivate viruses for vaccine purposes and they could be utilised to vastly improve the feasibility of scale-up manufacturing.

DATA AVAILABILITY STATEMENT

The original contributions presented in this study are available by request to mohammed.alsharifi@adelaide.edu.au.

ETHICS STATEMENT

The animal study was reviewed and approved by the Animal Ethics Committee, University of Adelaide.

AUTHOR CONTRIBUTIONS

MA and ES conceived and designed the study. ES, CG, SD, and JD performed experiments. ES wrote the manuscript. SD, TH, JD, and MA assisted in experimental design and preparation of the manuscript. MA and JD supervised the study. All authors contributed to the article and approved the submitted version.

FUNDING

This work was supported by the following funding sources, an Australian Institute of Nuclear Science and Engineering (AINSE) Research Award (ALNGRA15517 to MA) and an Australian Government Research Training Program (RTP) Scholarship (to ES).

REFERENCES

1. Mauskopf J, Klesse M, Lee S, Herrera-Taracena G. The Burden of Influenza Complications in Different High-Risk Groups: A Targeted Literature Review. *J Med Economics* (2013) 16:264–77. doi: 10.3111/13696998.2012.752376
2. Furuya Y, Regner M, Lobigs M, Koskinen A, Müllbacher A, Alsharifi M. Effect of Inactivation Method on the Cross-Protective Immunity Induced by Whole 'Killed' Influenza A Viruses and Commercial Vaccine Preparations. *J Gen Virol* (2010) 91:1450. doi: 10.1099/vir.0.018168-0
3. David SC, Norton T, Tyllis T, Wilson JJ, Singleton EV, Laan Z, et al. Direct Interaction of Whole-Inactivated Influenza A and Pneumococcal Vaccines Enhances Influenza-Specific Immunity. *Nat Microbiol* (2019) 4:1316–27. doi: 10.1038/s41564-019-0443-4
4. Alsharifi M, Furuya Y, Bowden TR, Lobigs M, Koskinen A, Regner M, et al. Intranasal Flu Vaccine Protective Against Seasonal and H5N1 Avian Influenza Infections. *PLoS One* (2009) 4:e5336. doi: 10.1371/journal.pone.0005336
5. Furuya Y, Chan J, Regner M, Lobigs M, Koskinen A, Kok T, et al. Cytotoxic T Cells Are the Predominant Players Providing Cross-Protective Immunity Induced by γ-Irradiated Influenza A Viruses. *J Virol* (2010) 84:4212. doi: 10.1128/JVI.02508-09
6. Alsharifi M, Mullbacher A. The Gamma-Irradiated Influenza Vaccine and the Prospect of Producing Safe Vaccines in General. *Immunol Cell Biol* (2010) 88:103–4. doi: 10.1038/icb.2009.81
7. Furuya Y. Return of Inactivated Whole-Virus Vaccine for Superior Efficacy. *Immunol Cell Biol* (2011) 90:571. doi: 10.1038/icb.2011.70
8. Choi E, Michalski CJ, Choo SH, Kim GN, Banasikowska E, Lee S, et al. First Phase I Human Clinical Trial of a Killed Whole-HIV-1 Vaccine: Demonstration of Its Safety and Enhancement of Anti-HIV Antibody Responses. *Retrovirology* (2016) 13:82. doi: 10.1186/s12977-016-0317-2
9. Seder RA, Chang LJ, Enama ME, Zephir KL, Sarwar UN, Gordon IJ, et al. Protection Against Malaria by Intravenous Immunization With a Nonreplicating Sporozoite Vaccine. *Science* (2013) 341:1359–65. doi: 10.1126/science.1241800
10. Ishizuka AS, Lyke KE, DeZure A, Berry AA, Richie TL, Mendoza FH, et al. Protection Against Malaria at 1 Year and Immune Correlates Following PfSPZ Vaccination. *Nat Med* (2016) 22:614–23. doi: 10.1038/nm.4110
11. International Atomic Energy Agency, Sterility assurance level. *Guidelines for Industrial Radiation Sterilisation of Disposable Medical Products (Cobalt-60 Gamma-Irradiation)*, Vienna, Austria: International Atomic Energy Agency. Vol. IAEA-TECDOC-539. (1990). p. 39.
12. Singleton EV, David SC, Davies JB, Hirst TR, Paton JC, Beard MR, et al. Sterility of Gamma-Irradiated Pathogens: A New Mathematical Formula to Calculate Sterilizing Doses. *J Radiat Res* (2020) 61:886–94. doi: 10.1093/jrr/rraa076
13. Ormerod MG. Free-Radical Formation in Irradiated Deoxyribonucleic Acid. *Int J Radiat Biol Relat Stud Phys Chem Med* (1965) 9:291–300. doi: 10.1080/09553006514550341
14. Grieb T, Forng RY, Brown R, Owolabi T, Maddox E, McBain A, et al. Effective Use of Gamma Irradiation for Pathogen Inactivation of Monoclonal Antibody Preparations. *Biologicals* (2002) 30:207–16. doi: 10.1006/biol.2002.0330
15. David SC, Lau J, Singleton EV, Babb R, Davies J, Hirst TR, et al. The Effect of Gamma-Irradiation Conditions on the Immunogenicity of Whole-Inactivated Influenza A Virus Vaccine. *Vaccine* (2017) 35:1071–9. doi: 10.1016/j.vaccine.2016.12.044
16. Kitchen AD, Mann GF, Harrison JF, Zuckerman AJ. Effect of Gamma Irradiation on the Human Immunodeficiency Virus and Human Coagulation Proteins. *Vox sanguinis* (1989) 56:223–9. doi: 10.1111/j.1423-0410.1989.tb02033.x
17. Elliott LH, Mccormick JB, Johnson KM. Inactivation of Lassa, Marburg, and Ebola Viruses by Gamma-Irradiation. *J Clin Microbiol* (1982) 16:704–8. doi: 10.1128/jcm.16.4.704-708.1982
18. Kempner ES, Haigler HT. The Influence of Low Temperature on the Radiation Sensitivity of Enzymes. *J Biol Chem* (1982) 257:13297–9. doi: 10.1016/S0021-9258(18)33445-8
19. Thayer DW, Boyd G. Effect of Irradiation Temperature on Inactivation of Escherichia Coli O157:H7 and *Staphylococcus aureus*. *J Food Prot* (2001) 64:1624–6. doi: 10.4315/0362-028X-64.10.1624
20. H. National and C. Medical Research. *Australian Code of Practice for the Care and Use of Animals for Scientific Purposes*. Canberra: National Health and Medical Research Council (2013).
21. Babb R, Chan J, Khairat JE, Furuya Y, Alsharifi M. Gamma-Irradiated Influenza A Virus Provides Adjuvant Activity to a Co-Administered Poorly Immunogenic SFV Vaccine in Mice. *Front Immunol* (2014) 5:267. doi: 10.3389/fimmu.2014.00267
22. *Practice for Using the Fricke Dosimetry System* Vol. ISO/ASTM 51026. International Organization for Standardization West Conshohocken, PA. (2015).
23. *Practice for Use of Ceric-Cerous Sulfate Dosimetry System* Vol. ISO/ASTM 51205. International Organization for Standardization West Conshohocken, PA. (2017). p. 2017.
24. Reed LJ, Muench H. A Simple Method of Estimating Fifty Per Cent Endpoints. *Am J Epidemiol* (1938) 27:493–7. doi: 10.1093/oxfordjournals.aje.a118408
25. Yewdell JW, Bennink JR, Smith GL, Moss B. Influenza A Virus Nucleoprotein Is a Major Target Antigen for Cross-Reactive Anti-Influenza A Virus Cytotoxic T Lymphocytes. *Proc Natl Acad Sci USA* (1985) 82:1785–9. doi: 10.1073/pnas.82.6.1785
26. Grant-Klein RJ, Antonello J, Nichols R, Dubey S, Simon J. Effect of Gamma Irradiation on the Antibody Response Measured in Human Serum From Subjects Vaccinated With Recombinant Vesicular Stomatitis Virus-Zaire Ebola Virus Envelope Glycoprotein Vaccine. *Am J Trop Med Hyg* (2019) 101:207–13. doi: 10.4269/ajtmh.19-0076

27. Hamer AJ, Stockley I, Elson RA. Changes in Allograft Bone Irradiated at Different Temperatures. *J Bone Joint Surg Br* (1999) 81:342–4. doi: 10.1302/0301-620X.81B2.0810342
28. Furuya Y, Chan J, Wan E-C, Koskinen A, Diener KR, Hayball JD, et al. Gamma-Irradiated Influenza Virus Uniquely Induces IFN-I Mediated Lymphocyte Activation Independent of the TLR7/MyD88 Pathway (Immune Responses to Inactivated Influenza Viruses). *PLoS One* (2011) 6: e25765. doi: 10.1371/journal.pone.0025765
29. David SC, Laan Z, Minhas V, Chen AY, Davies J, Hirst TR, et al. Enhanced Safety and Immunogenicity of a Pneumococcal Surface Antigen A Mutant Whole-Cell Inactivated Pneumococcal Vaccine. *Immunol Cell Biol* (2019) 97:726–39. doi: 10.1111/imcb.12257
30. Shahrudin S, Chen C, David SC, Singleton EV, Davies J, Kirkwood CD, et al. Gamma-Irradiated Rotavirus: A Possible Whole Virus Inactivated Vaccine. *PLoS One* (2018) 13:e0198182. doi: 10.1371/journal.pone.0198182
31. Martin SS, Bakken RR, Lind CM, Garcia P, Jenkins E, Glass PJ, et al. Comparison of the Immunological Responses and Efficacy of Gamma-Irradiated V3526 Vaccine Formulations Against Subcutaneous and Aerosol Challenge With Venezuelan Equine Encephalitis Virus Subtype IAB. *Vaccine* (2010) 28:1031–40. doi: 10.1016/j.vaccine.2009.10.126
32. Miller JL, Anders EM. Virus-Cell Interactions in the Induction of Type 1 Interferon by Influenza Virus in Mouse Spleen Cells. *J Gen Virol* (2003) 84:193–202. doi: 10.1099/vir.0.18590-0
33. Margine I, Hai R, Albrecht RA, Obermoser G, Harrod AC, Banchereau J, et al. H3N2 Influenza Virus Infection Induces Broadly Reactive Hemagglutinin Stalk Antibodies in Humans and Mice. *J Virol* (2013) 87:4728–37. doi: 10.1128/JVI.03509-12
34. Krystal M, Elliott RM, Benz EWJr., Young JF, Palese P. Evolution of Influenza A and B Viruses: Conservation of Structural Features in the Hemagglutinin Genes. *Proc Natl Acad Sci USA* (1982) 79:4800–4. doi: 10.1073/pnas.79.15.4800
35. Wu NC, Thompson AJ, Lee JM, Su W, Arlian BM, Xie J, et al. Different Genetic Barriers for Resistance to HA Stem Antibodies in Influenza H3 and H1 Viruses. *Science* (2020) 368:1335–40. doi: 10.1126/science.aaz5143
36. Gotch F, McMichael A, Smith G, Moss B. Identification of Viral Molecules Recognized by Influenza-Specific Human Cytotoxic T Lymphocytes. *J Exp Med* (1987) 165:408–16. doi: 10.1084/jem.165.2.408
37. Jameson J, Cruz J, Ennis FA. Human Cytotoxic T-Lymphocyte Repertoire to Influenza A Viruses. *J Virol* (1998) 72:8682–9. doi: 10.1128/JVI.72.11.8682-8689.1998
38. Cote CK, Buhr T, Bernhards CB, Bohmke MD, Calm AM, Esteban-Trexler JS, et al. A Standard Method To Inactivate Bacillus Anthracis Spores to Sterility *via* Gamma Irradiation. *Appl Environ Microbiol* (2018) 84:1–19. doi: 10.1128/AEM.00106-18
39. United States Department of Defense (Committee for Comprehensive Review of DoD Laboratory Procedures and Protocols Associated with Inactivating Bacillus Anthracis Spores). *Review Committee Report: Inadvertent Shipment of Live Bacillus Anthracis Spores by DoD, Department of Defense*. Washington DC: US Department of Defense (2015).
40. Epstein JE, Tewari K, Lyke KE, Sim BK, Billingsley PF, Laurens MB, et al. Live Attenuated Malaria Vaccine Designed to Protect Through Hepatic CD8(+) T Cell Immunity. *Science* (2011) 334:475–80. doi: 10.1126/science.1211548
41. Miller RB. Electronic Irradiation of Foods: An Introduction to the Technology. *Springer Sci Business Media* (2006) 43–73.

Conflict of Interest: MA is head of the Vaccine Research Group at the University of Adelaide and the Chief Scientific Officer of Gamma Vaccines Pty Ltd and TH is the Executive Chairman of Gamma Vaccines Pty Ltd. This does not alter adherence to policies on sharing data and materials. Gamma Vaccines Pty Ltd has no role in the study design, data collection and analysis, decision to publish, and preparation of the manuscript.

The remaining authors declare that the research was conducted in the absence of any commercial or financial relationships that could be construed as a potential conflict of interest.

Publisher's Note: All claims expressed in this article are solely those of the authors and do not necessarily represent those of their affiliated organizations, or those of the publisher, the editors and the reviewers. Any product that may be evaluated in this article, or claim that may be made by its manufacturer, is not guaranteed or endorsed by the publisher.

frontiers in Immunology

ORIGINAL RESEARCH
published: 30 November 2021
doi: 10.3389/fimmu.2021.768820

Gamma-Irradiated Fowl Cholera Mucosal Vaccine: Potential Vaccine Candidate for Safe and Effective Immunization of Chicken Against Fowl Cholera

Bereket Dessalegn[1], Molalegne Bitew[2], Destaw Asfaw[1], Esraa Khojaly[3], Saddam Mohammed Ibrahim[1], Takele Abayneh[4], Esayas Gelaye[4], Hermann Unger[5] and Viskam Wijewardana[5]*

[1] College of Veterinary Medicine and Animal Science, University of Gondar, Gondar, Ethiopia, [2] Health Biotechnology Directorate, Ethiopian Biotechnology Institute, Addis Ababa, Ethiopia, [3] MSc Program on Vaccine Production and Quality Control, Pan Africa University for Life and Earth Sciences Institute (PAULESI), University of Ibadan, Ibadan, Nigeria, [4] Vaccine Research and Development Directorate, National Veterinary Institute, Debre Zeit, Ethiopia, [5] Animal Production and Health Section, Joint Food and Agriculture Organization (FAO)/International Atomic Energy Agency (IAEA) Centre of Nuclear Techniques in Food and Agriculture, International Atomic Energy Agency (IAEA), Vienna, Austria

OPEN ACCESS

Edited by:
Sofia A. Casares, Naval Medical Research Center, United States

Reviewed by:
Irina V. Kiseleva, Institute of Experimental Medicine (RAS), Russia
Wayne Robert Thomas, University of Western Australia, Australia

***Correspondence:**
Molalegne Bitew
molalegne23@gmail.com

Specialty section:
This article was submitted to Vaccines and Molecular Therapeutics, a section of the journal Frontiers in Immunology

Received: *01 September 2021*
Accepted: *02 November 2021*
Published: *30 November 2021*

Citation:
Dessalegn B, Bitew M, Asfaw D, Khojaly E, Ibrahim SM, Abayneh T, Gelaye E, Unger H and Wijewardana V (2021) Gamma-Irradiated Fowl Cholera Mucosal Vaccine: Potential Vaccine Candidate for Safe and Effective Immunization of Chicken Against Fowl Cholera. Front. Immunol. 12:768820. doi: 10.3389/fimmu.2021.768820

Fowl cholera (FC) caused by *Pasteurella multocida* is among the serious infectious diseases of poultry. Currently, formalin inactivated FC (FI-FC) vaccine is widely used in Ethiopia. However, reports of the disease complaint remain higher despite the use of the vaccine. The aim of this study was to develop and evaluate gamma-irradiated mucosal FC vaccines that can be used nationally. In a vaccination-challenge experiment, the performance of gamma-irradiated *P. multocida* (at 1 kGy) formulated with Montanide gel/01 PR adjuvant was evaluated at different dose rates (0.5 and 0.3 ml) and routes (intranasal, intraocular, and oral), in comparison with FI-FC vaccine in chicken. Chickens received three doses of the candidate vaccine at 3-week intervals. Sera, and trachea and crop lavage were collected to assess the antibody levels using indirect and sandwich ELISAs, respectively. Challenge exposure was conducted by inoculation at 3.5×10^9 CFU/ml of *P. multocida* biotype A intranasally 2 weeks after the last immunization. Repeated measures ANOVA test and Kaplan Meier curve analysis were used to examine for statistical significance of antibody titers and survival analysis, respectively. Sera IgG and secretory IgA titers were significantly raised after second immunization (p=0.0001). Chicken survival analysis showed that intranasal and intraocular administration of the candidate vaccine at the dose of 0.3 ml resulted in 100% protection as compared to intramuscular injection of FI-FC vaccine, which conferred 85% protection (p=0.002). In conclusion, the results of this study showed that gamma-irradiated FC mucosal vaccine is safe and protective, indicating its potential use for immunization of chicken against FC.

Keywords: chicken, fowl cholera, gamma radiation, mucosal vaccine, *P. multocida*

INTRODUCTION

Poultry production contributes significantly to the livelihoods of farmers and to the national economic system. However, it is hampered by various factors, including poor husbandry practices and poultry diseases (1). Fowl cholera (FC), which is caused by *P. multocida*, is among the serious infectious diseases of poultry. The disease is present globally and endemic to most parts of Ethiopia with significant economic losses associated with reduced production and mortality (2). It is vital and preferable to develop vaccines from locally circulating strains to provide a robust protection (3). Despite the contribution by the locally produced formalin-killed FC vaccine in reducing the disease burden, FC remains to be a big challenge to the poultry sector in the country. This in part can be explained by the fact that the current used formalin-inactivated FC vaccine produced by the National Veterinary Institute (NVI) confers a short duration of protection (4). In addition, owing to its nature of being inactivated parenteral preparation, the vaccine is expected to be a poor inducer of mucosal immunity, which is the desired protective immunity against mucosal pathogens such as avian *Pasteurella* (5).

The route of vaccine administration plays an important and significant role in practical usage. The fact that parenteral vaccines induce little-to-none mucosal immunity makes them poor and ineffective choice to immunize against mucosal pathogens (6). In addition, mucosal vaccines are easy to administer and is preferable in case of vaccination campaigns and in farm settings where there is large number of chickens to be vaccinated (7). In general, parenteral preparations induce short-lived humoral immunity, which necessitates booster doses. However, mucosal vaccines elicit long-lived immunity of both humoral and cellular nature (8). Therefore, there is an urgent need to develop effective and safe mucosal vaccines that confer long duration of protection against mucosal pathogens.

The commonly used chemical inactivation methods has limitations associated with safety (probably correlated with the high endotoxin level) and efficacy due to modification of antigenic components of bacteria, making it less immunogenic and potent. Furthermore, these vaccine antigens are mostly presented through major histocompatibility complex (MHC)-II but not MHC-I pathways by antigen-presenting cells and do not result in an efficient cell-mediated immune response that is crucial against many pathogens. Considering recombinant method of vaccine development against FC might not be a feasible approach for developing countries because they need high technical expertise, high-technical facilities, and resource limitations, as well as the immunity conferred is very limited and narrow (9).

Radiation inactivation of pathogens has potential applications in sterilization and the manufacture of biological reagents and laboratory supplies (10). Exposure to optimum doses of gamma radiation disrupts the genetic material of the pathogens, making the microorganism unable to replicate, so it cannot establish an infection yet leaving some residual metabolic activity. Therefore, the irradiated microorganisms may still find its natural target in the host and could effectively be immunogenic (11). The major advantage of ionizing radiation in vaccine development compared to ultraviolet or chemical agents is its ability to effectively penetrate through most biological materials and specifically target nucleic acids whilst causing less damage to surface antigenic protein, making it preferable to develop safe and simple vaccines (12). Gamma-irradiated vaccines appear to be more effective than formalin-killed vaccines against disease and have the added advantage of a longer storage life than live vaccines (13). Therefore, the present study was aimed to develop an improved gamma-irradiated inactivated vaccine against fowl cholera that stimulates the enhanced mucosal immune response and is easy for application at the rural setting.

MATERIALS AND METHODS

Study Site

The study was conducted at the National Veterinary Institute (NVI), Bishoftu; National Institute for Control and Eradication of Tsetse Fly and Trypanosomosis (NICETT), Addis Ababa; and Ethiopian Biotechnology Institute, Addis Ababa, from November 2020 to June 2021.

Experimental Chicken and Their Management

In this experiment, 250 3-week-old specific antibody negative (SAN) against FC Bovans brown chickens were used. The parent stock was not vaccinated against FC. Chicks used for all the experiments were raised under intensive management system. The animal experiment rooms were cleaned with disinfectants and fumigated with formalin before the introduction of chicks and bedded with disinfected wood shavings. The chickens had access to feed and water *ad libitum* throughout the experiment.

Preparation of Avian *P. multocida* Inoculum: For Preliminary Study, Vaccine Preparation, and the Challenge Study

Working seeds of Avian *P. multocida* biotype A (MK802880, NVI) were used for vaccine preparation. Lyophilized *P. multocida* biotype A was diluted with 2 ml of tryptose soya broth (TSB), homogenized well and then inoculated into sterile tryptose soya agar (TSA) supplemented with 10% horse serum and incubated at 37°C overnight. The identity of this isolate was confirmed by both phenotypic and molecular standard tests. A single colony was transferred to 2 ml tube containing TSB with 10% horse serum and incubated for 7 h at 37°C. Then 0.5 ml of the broth culture was transferred into 30 ml TSB supplemented with 10% horse serum and incubated overnight. The purity of the *P. multocida* type A (PA) inoculum was checked and inoculated into PA production media at the ratio of 7 ml of inoculum, 7 ml of glucose, and 3 ml of serum per 300 ml of *P. multocida* production media, then incubated for 24 h with slow agitation at 80 rpm (14). The culture was harvested at the pH of 5.5 to 6.2, which is known to correspond to the desired titer of 10^9 CFU/ml and above as determined by the plate count method. In addition, avian *P. multocida* strain was used as challenge strains in the test of

the vaccines. Freeze-dried stock was reconstituted with 2 ml tryptose broth (TB), and suspensions were streaked on tryptose soya agar (TSA) plates incubated for 24 h at 37°C. The culture was checked for purity and identity. From the culture on TSA, a typical colony was inoculated to 200 ml TSB and incubated for 7 h at 37°C. These cultures were then adjusted spectrophotometrically at 450 nm (0.475 OD value) and serially diluted in TSB to obtain the desired titer for challenge (3.5×10^9 CFU/ml).

Determination of Appropriate Gamma Radiation Dose for Optimum Inactivation of Avian *P. multocida*

The PA production media containing culture was centrifuged at 4,000×g per minute at 4°C for 20 min after determining the time required to obtain the desired titer (5.6×10^9 CFU/ml). The supernatant was discarded, and the cell pellet was washed twice with PBS and resuspended in PBS with equal volume in falcon tubes and subjected to gamma irradiation with doses ranging from 0.5 to 3 kGy at a dose rate of 1.56 kGy/h using a cobalt 60 irradiation machine (MDS NORDION, Canada) (15, 16).

The falcon tubes containing the culture were placed vertically and securely in the gamma chamber and irradiated for different time periods according to the required doses of gamma rays. The temperature inside the gamma chamber was maintained at 37–40°C. After completion of irradiation, each tube was carefully removed from the gamma chamber and immediately stored at −4°C for further use. Non-irradiated controls underwent the same procedure except irradiation. The facility at the National Institute for Control and Eradication of Tsetse Fly and Trypanosomosis (NICETT) at Addis Ababa was utilized for this purpose. Bactericidal activity of the radiation dose was assessed by subculturing of serial dilution of *P. multocida* cells plated on tryptose soya agar plates to quantify CFU. Various irradiation doses were examined to find the lowest optimum irradiation at the margin of the lethal dose (17).

Safety and Immunogenicity Study of Avian *P. multocida* Irradiated at Different Dose of Gamma Radiation

Avian *P. multocida* preparations irradiated at four consecutive irradiation doses close to complete lethal dose and adjuvanted with 20% of Montanide/01 PR gel adjuvant were evaluated for their immunogenicity and safety. The inoculum preparation of avian *P. multocida* used for challenge was done as indicated in above. Thirty chickens were randomly divided into five groups with six chickens in each group and were intranasally inoculated with 1 ml of candidate mucosal FC vaccine irradiated with 0.9 kGy (group 1), candidate mucosal FC vaccine irradiated with 1 kGy (group 2), candidate mucosal FC vaccine irradiated with 1.1 kGy (group 3), candidate mucosal FC vaccine irradiated with 1.2 kGy (group 4), and control inoculated with PBS (group 5). Following vaccination, chickens were monitored daily for any behavioral changes. Blood samples were collected from the wing vein at days 0, 14, and 21 post-vaccination to determine the antibody titer raised against avian *P. multocida* biotype A (PA) using the indirect ELISA (Product code: PMS-CHICK-5P, IDvet, France). Safety was assessed by monitoring administration site reactions such as pain and swelling, systemic reactions like fever and anorexia, and lesion in the liver and spleen.

Formulation of the Candidate Gamma-Irradiated Mucosal FC Vaccine

The 1 kGy gamma-irradiated avian *Pasteurella multocida* was chosen for the vaccine preparation since it performed best in antibody production using I-ELISA test. The inoculum preparation of avian *P. multocida* was done as mentioned in section 3.2.1. The irradiated culture of avian *P. multocida* (5.6×10^9CFU/ml) was adjuvanted with Montanide/01 PR gel to form the final vaccine preparation. The proportion of Montanide/01 PR gel adjuvant is made to comprise 20% of the antigen preparation as recommended by the adjuvant manufacturer (18). Then, the vaccine was dispensed into vials of 50 ml volume capacity and checked for its purity and sterility by using Gram's stain and culturing on sterility test media such as tryptose agar, tryptose broth, and Sabouraud agar media. Finally, the gamma-irradiated fowl cholera vaccine was found free from any contamination.

Evaluation of the Final Candidate Vaccine

Chickens were allocated into seven groups, G-1 to G-5 based on the dose of candidate mucosal FC vaccine they received and the route of administration. Thirty-six (36) chickens from both G-1 and G-2 received the vaccine intranasally (IN) at a dose of 0.5 and 0.3 ml, respectively. Similarly, 36 chickens from G-3 received the vaccine at a dose of 0.5 ml orally. On the other hand, 20 chickens both from G-4 and G-5 were administered with 0.5 and 0.3 ml of the vaccine intraocularly (IO), respectively. All the chickens (G-1 to G-5) received three doses of the vaccine preparations at 3-week interval. Another two groups of chickens, G-6 (36 chickens) and G-7 (36 chickens), were used as a comparator and placebo control, respectively. Chickens in G-6 were administered three doses of 0.5 ml of the commercial formalin-inactivated FC vaccine (1/20) at 3-week interval intramuscularly. Finally, all chickens from G-7 received PBS (**Figure 1**).

Assessment of the Safety of Mucosal FC Vaccine

Evaluation of the safety of the vaccine was done according to the OIE manual for vaccine safety parameter (3), vaccinated chickens were observed the whole day starting from the time of vaccination up to the end of the experiment on a daily basis, and any deviation from normal health using observation of vital signs was recorded: depression, anorexia, ruffled feather, and any reaction at the site of injection.

Assessment of Serum and Mucosal Antibody Response

Antibody responses, serum IgG, and secretory IgA in chickens were determined by ELISA. Blood samples were collected on days 0, 14,

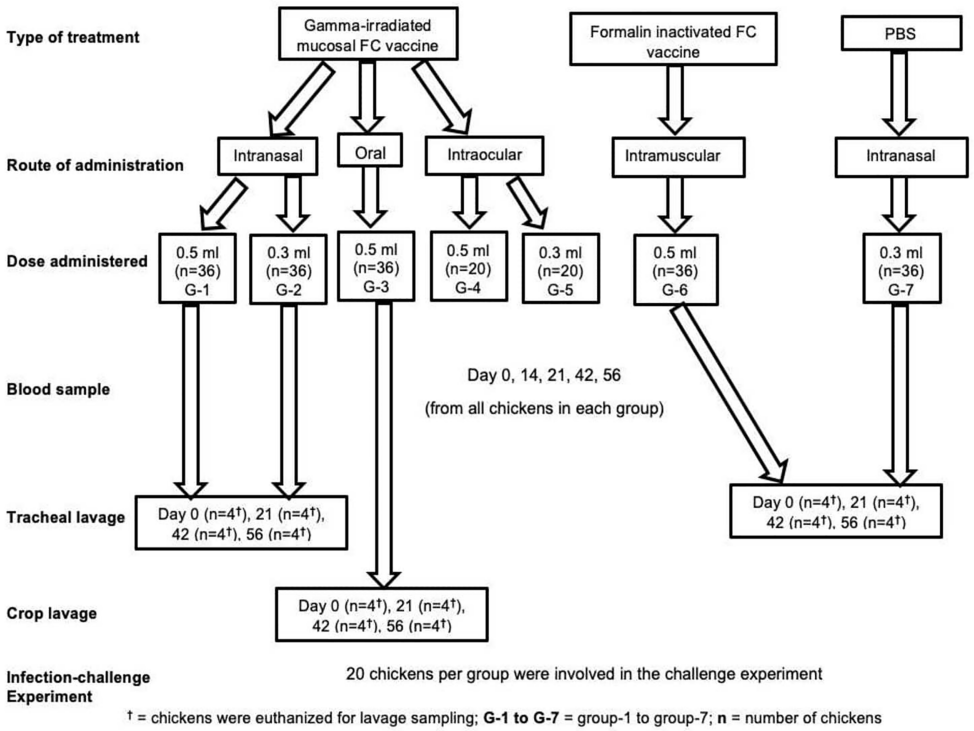

FIGURE 1 | Experimental design groups; treatment, comparator, and control, route of vaccine administration, and number of chickens in each group, number of chickens used in sampling, and number of chickens used in efficacy study.

21, 42, and 56 of the experiments. In addition, four chickens in each group except intraocular route were sampled and euthanized on days 0, 21, 42, and 56 of the experiments, and the tracheal and crop lavage was performed (**Figure 1**). Then, the sera or tracheal and crop lavage solutions were subjected to ELISA procedures. Antibody responses in the chicken sera were determined by measuring of the IgG titers using a commercial indirect ELISA test kit (Product code: PMS-CHICK-5P, IDvet, France). In addition, the secretory IgA was measured using a chicken IgA sandwich ELISA Kit (CAT. No: MBS564152MyBioSource, San Diego, USA). The average antibody titer and the standard error of the mean (SEM) of each group were computed according to the company's recommendation.

Assessment of Efficacy of the Candidate Vaccine

As indicated in **Figure 1**, 20 chickens from all groups were challenged with avian *P. multocida* at a dose of 3.5×10^9 CFU/ml 2 weeks after the final vaccination. Preparation of avian *P. multocida* for challenge study was done as indicated in the above section. The chickens were followed up for clinical signs and mortality for 14 days. Necropsy and bacterial isolation were conducted on dead chickens. The gross lesions were recorded, and lungs, livers, and spleens were collected for bacterial isolation by direct culture using TSA with 10% horse serum followed by identification through morphology, staining, culture, and finally by species-specific PCR.

Data Analysis

GraphPad Prism 9 was used to perform statistical analysis. The antibody titers between the vaccinated groups and the non-vaccinated control group were performed using a repeated measures ANOVA test and Tukey multiple comparisons. The level of significance was recorded at $p<0.05$. The data were presented as individual values for each experimental group. Mean and standard error of means are indicated in lines and error bars. The survival of chickens was compared between different treatment and *in vivo* infection challenge groups using Kaplan-Meier curve analysis.

RESULTS

Effects of Gamma Irradiation on Avian *P. multocida*

Irradiation experiments were conducted to determine the dose required for the inactivation of avian *P. multocida*. An exponential decrease in viability of avian *P. multocida* was observed while increasing the dose of gamma irradiation. After 48 h of culturing, avian *P. multocida* exposed to doses more than or equivalent to 1 kGy of irradiation had fully inhibited replication, and no growth was seen (**Figure 2**). The susceptibility of surface structural proteins to reactive oxygen species (ROS) damage increases when the radiation dose is higher than the level that completely

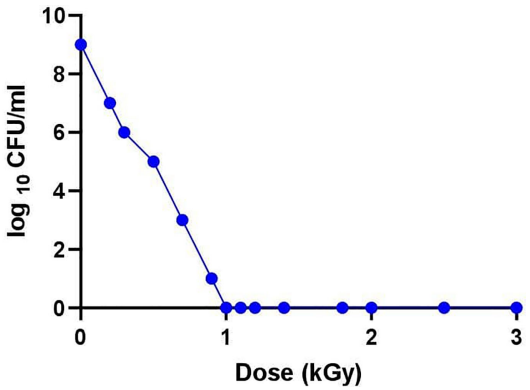

FIGURE 2 | After determination of the desired titer (5.6×109 CFU/ml), the broth culture was centrifuged at 4,000 revolutions per minute at 4°C for 20 min. The supernatant was discarded, and the pellet of cells was washed twice with PBS and resuspended in 5 ml PBS in 15 ml falcon tubes and subjected to gamma irradiation with doses ranging from 0 to 3 kGy at a dose rate of 1.56 kGy/h using a cobalt 60 irradiation machine (MDS NORDION, Canada). Bactericidal activity of the radiation dose was assessed by subcultivation of serial dilution of *P. multocida* cells plated on tryptose soya agar plates to quantify CFU. Various irradiation doses were examined to find the lowest optimum irradiation at the margin of the lethal dose.

abolished avian *P. multocida*. Therefore, the lethal dose (1 kGy) and three doses close to the lethal dose (0.9, 1.1, 1.2 kGy) were used to select immunogenic dose and safety of irradiated avian *P. multocida* in chicken.

Immunogenicity and Safety of Radiation Inactivated Avian *P. multocida* Vaccine Preparations

The safety and immunogenicity of several vaccine preparations made from avian *P. multocida* treated with various doses of gamma radiation adjuvanted with Montanide/01 PR gel (SEPPIC, France) was investigated. Briefly, 30 chickens were assigned into five groups (six chickens per group); four groups were administered 5.6×10^9 CFU/ml of avian *P. multocida* irradiated with 0.9, 1, 1.1, and 1.2 kGy of gamma ray formulated with Montanide/01 PR gel through IN route. Another group of six chickens received PBS and was used as a control. At 14 and 21 days after vaccination, significantly higher levels of PA-specific IgG antibodies were identified in the serum of the four vaccinated groups when compared to the PBS-inoculated control groups (**Figure 3**). In chickens immunized with irradiated avian *P. multocida* at 1 kGy, the average antibody titer was 0.345 ± 0.095 on day 14 and 0.43 ± 0.12 on day 21, while in chickens immunized with 0.9 kGy irradiated was 0.22 ± 0.06 and 0.31 ± 0.11. On the other hand, chickens immunized with 1.1 and 1.2 kGy irradiated avian *P. multocida* produced similar average antibody titer 0.21 ± 0.06 on day 14 and 0.26 ± 0.11 on day 21. When compared to the other vaccinated chickens (different gamma irradiation doses), chickens vaccinated with 1 kGy gamma irradiation candidate vaccine generated significantly higher levels of IgG antibodies in the serum at days 14 and 21 post-vaccination (p=0.0001). Furthermore, chickens vaccinated with 0.9 kGy gamma-irradiated candidate vaccine had higher levels of antibodies as compared to the remaining groups (p=0.04). There was no clinical evidence of sickness or injection site reactions in any of the vaccinated chickens. In all vaccinated groups, no lesion was found in the liver or spleen of chickens. Irradiation at 1 kGy was chosen as optimum irradiation dose based on immunogenicity and safety data.

Evaluation of Serum and Mucosal Antibody Response Against Mucosal FC Vaccine

Determination of serum IgG titers using an indirect ELISA is shown in **Figure 4**. The levels of antibody titers of chickens against FC on day 0 indicated a low cutoff value of 0.2. The levels of chicken serum IgG titers were found to be significantly increased after 2 weeks of the first immunization with the gamma-irradiated or formalin-inactivated vaccine. At the third week, a significant difference was observed among all vaccinated groups, where the average antibody titer of G-2 was 1.13 ± 0.16 compared to 0.97 ± 0.18, 0.59 ± 0.096, 0.61 ± 0.08, 0.77 ± 0.17, and 0.65 ± 0.15 for G-1, G-3, G-4, G-5, and G-6, respectively. After the second vaccination, the titers substantially increased in all chickens and were still significantly higher in the vaccinated chickens of gamma-irradiated mucosal FC vaccine than in the corresponding formalin-inactivated vaccinated group (p=0.037) (**Figure 4**). Furthermore, peak of average antibody titer in G-1, G-2, and G-5 was observed after the second vaccination, which is 1.2 ± 0.18, 1.58 ± 0.29, and 1.26 ± 0.24, respectively. As compared to the other gamma-irradiated FC vaccinated groups, the average antibody titer of group-3 (0.83 ± 0,23) was low and showed significant difference compared to Group-2 (p<0.009). However, there was no significant difference between the mean average antibody titer of groups of chickens vaccinated orally with the irradiated FC vaccine (G-3) and those vaccinated with commercial formalin-inactivated FC vaccine (G-6) throughout the experiment. After the third vaccination dose, the results of mean antibody titer of chickens in all groups were similar with second vaccination dose. On the other hand, the non-immunized group was found to be seronegative to FC, as the average antibody levels throughout the experimental period was lower than the cutoff value. Generally, the results indicated that the gamma-irradiated vaccine formulations are able to induce serum IgG against avian *P. multocida*. With regard to the route of vaccine administration, the average antibody titer levels of group 2 (0.3 ml, intranasal route) generated significantly higher levels of serum IgG throughout the experiment (p=0.001). In addition, group-5 (0.3 ml, intraocular route) produced significantly higher antibody (IgG) titer after booster immunization (p=0.001).

Secretory IgA was also detected in chickens immunized with the candidate gamma-irradiated mucosal fowl cholera vaccine (**Figure 5**). The levels of average IgA titers of chickens against FC on day 0 indicated a low cutoff value of 0.043. At the third week, a significant difference was observed among chickens vaccinated with the gamma-irradiated vaccine intranasally at two dose rates, where the average IgA titer of G-1 and G-2 was 0.32 ± 0.05 and

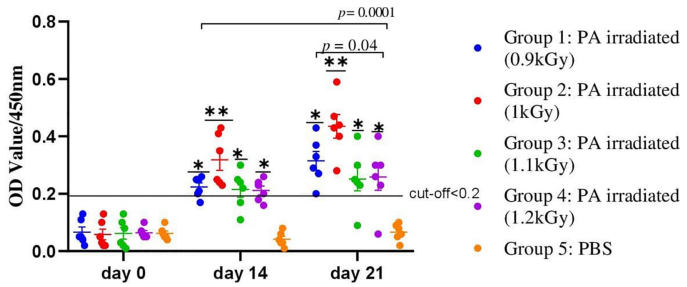

FIGURE 3 | A total of 30 chickens were assigned into five groups, with each group having six chickens. Chickens in groups 1, 2, 3, and 4 received 5.6×10^9 CFU/ml of avian *P. multocida* irradiated with 0.9, 1, 1.1, and 1.2 kGy of gamma rays and adjuvanted with Montanide/01 PR gel, respectively, through IN route. Chickens in group 5 received PBS and were used as a control. Blood samples were taken at days 0, 14, and 21. Serum was analyzed for the presence of IgG. The data were presented as individual values for each experimental group. Mean and standard error of means are indicated in lines and error bars. Asterisk (*) represents the significant differentiation of antibody IgG level compared to the non-vaccinated control group (*$p < 0.05$, **$p < 0.01$).

0.36 ± 0.12 compared to the control group (0.036 ± 0.02). After the second vaccination, the titers substantially increased in all chickens. Comparative evaluation with formalin-inactivated FC vaccine showed that chickens vaccinated with the gamma-irradiated candidate vaccine displayed significantly higher average antibody titer of 1.23 ± 0.06 and 1.46 ± 0.22 in G-1 and G-2, respectively, than the chickens immunized with formalin-inactivated vaccine with 0.46 ± 0.09 mean value. After the third vaccination dose, a significant difference was observed among all vaccinated groups compared to the control group ($p<0.05$). Like that of the serum IgG of chickens, the average IgA titers of the chickens vaccinated with gamma-irradiated FC vaccine orally were low and significantly different compared to the intranasal route ($p=0.026$). In the control groups, no response was observed in antibody titers to avian *P. multocida* throughout the experiment. Generally, significant levels of IgA were detected only in gamma-irradiated mucosal fowl cholera immunized chickens, but not in that of formalin-inactivated fowl cholera immunized chickens ($p=0.034$). These results suggest that gamma-irradiated mucosal fowl cholera vaccine is more potent in enhancing or inducing avian *P. multocida*–specific antibodies on the airway mucosal surface more than formalin-inactivated fowl cholera vaccine.

Evaluation of Protective Efficacy of Mucosal FC Vaccine

A total volume 0.5 ml of bacterial suspension containing 3.5×10^9CFU/ml of avian *P. multocida* biotype A was

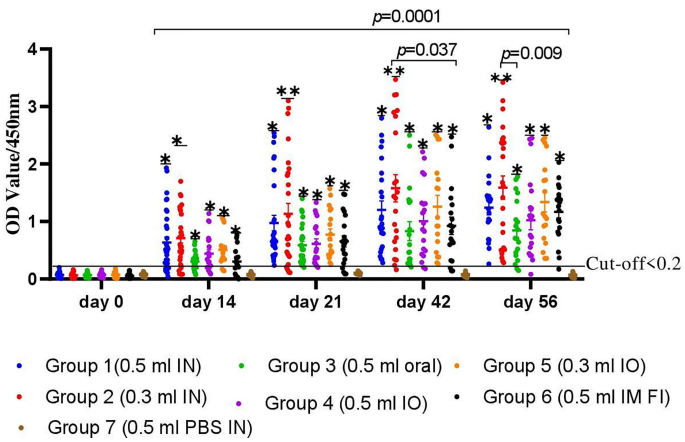

FIGURE 4 | A total of 220 chickens were assigned into seven groups: G-1 to G-5 based on the dose of candidate gamma-irradiated FC vaccine they received and the route of administration. Chickens in both G-1 and G-2 received the vaccine by intranasal route at a dose of 0.5 and 0.3 ml, respectively. Similarly, chickens in G-3 received the vaccine at a dose of 0.5 ml orally. On the other hand, G-4 and G-5 were administered 0.5 and 0.3 ml of the vaccine through the intraocular route (IO), respectively. Another two groups of chickens, G-6 and G-7, received 0.5 ml of the commercial formalin-inactivated FC vaccine intramuscularly and 0.3 ml of PBS intranasally as comparator, respectively. Blood samples were taken at days 0, 14, 21, 42, and 56. Serum was analyzed for the presence of IgG. The data were presented as individual values for each experimental group. Mean and standard error of means are indicated in lines and error bars. Asterisk (*) represents the significant differentiation of antibody IgG level compared to the non-vaccinated control group (*$p < 0.05$, **$p < 0.01$).

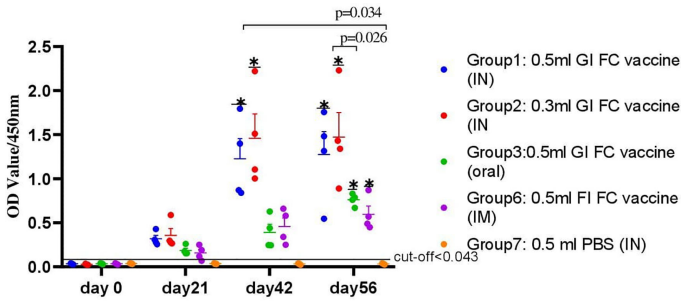

FIGURE 5 | A total of 80 chickens were chosen from all groups. Tracheal (G-1, G-2, G-4, and G-7) and crop lavage (G-3) was taken from four chickens from each group that were euthanized on different period of interval: day 0, 21, 42, and 56 of the experiment; thus, a total of 16 chickens from each group were euthanized for this purpose. Trachea and crop were washed by glycine buffer and analyzed for the presence of IgA. The data were presented as individual values for each experimental group. Mean and standard error of means are indicated in lines and error bars. Asterisk (*) represents the significant differentiation of antibody IgA level compared to the non-vaccinated control group (*p < 0.05).

administered intranasally. Complete protection of the chickens from fowl cholera was conferred by vaccination with the intranasal route of gamma-irradiated fowl cholera vaccine or by intraocular route of gamma-irradiated fowl cholera (0.3 ml/dose) vaccine. The protective efficacy in the chickens immunized with the gamma-irradiated oral vaccine and formalin-inactivated FC vaccine was 85 and 80%, respectively, while in those immunized with the gamma-irradiated intraocular (0.5 ml) vaccine was 90%. According to the log-rank test for equality survival function, vaccinated groups in both vaccine types showed significant difference compared to the control group ($p<0.001$). Furthermore, there was significant difference between the protection conferred by the gamma-irradiated mucosal fowl cholera vaccine and formalin-inactivated FC vaccine ($p<0.001$). In addition, the survival rate of chickens vaccinated with gamma-irradiated FC vaccine intranasally was significantly different compared to chickens vaccinated through the oral route ($p<0.001$).

Based on the curve, there was not any chicken that survived after exposure to the challenge bacterial strain in the control group. The death of chickens started 2 days after challenge, and all of the chickens in this group died within 7 days. In addition, three and four chickens in gamma-irradiated mucosal FC vaccine through oral route and formalin-inactivated immunized groups, respectively, and two chickens in the gamma-irradiated mucosal FC vaccine through intraocular route (0.5 ml/dose) immunized group died within 10 days, respectively (**Figure 6**).

Clinical Signs, Gross Lesions, and Bacterial Isolation

After challenge, no behavioral changes were detected in the groups of chickens immunized with gamma-irradiated mucosal FC vaccine through intranasal and intraocular (0.3 ml/dose) routes. In the control groups, chickens manifested clinical signs at 24 h after the challenge exposure, including depression, anorexia, and severe diarrhea. During the period of 4 days, the severity increased rapidly, resulting in the death of several chickens, and all of the chickens in this group died within 7 days. In addition, seven and eight chickens in the gamma-irradiated mucosal FC vaccine through oral route and formalin-inactivated immunized groups, respectively, and five chickens in the gamma-irradiated mucosal FC vaccine through intraocular route (0.5 ml/dose) immunized group started to display depression and anorexia 5 days after the challenge exposure. Among these chicken, three, four, and two chickens then died within 10 days, respectively.

All of the dead chickens in this investigation had characteristic lesions of fowl cholera, including lung congestion, lung edema, and numerous petechiae in the liver, hemorrhage in the small intestine, splenomegaly, and fibrinopurulent peritonitis, according to necropsy results (**Figure 7**). In addition, the dead chickens were also subjected to isolation and identification of avian *P. multocida*. The findings revealed that avian *P. multocida* was recovered in pure cultures from all of the dead chicken specimens, which was furthermore confirmed by species-specific PCR.

DISCUSSION

Fowl cholera caused by *P. multocida* is a highly contagious disease of poultry presenting as one of the major challenges worldwide. It affects the poultry industry, incurring economic losses due to loss of products (19). The development of vaccine to control FC has proven to be a challenge for years. An effective vaccine must be safe and needs to provide sustained protection with elimination of the challenge infection. Live and formalin-inactivated FC vaccines have been extensively used and succeeded in reducing infection and the prevalence of disease in poultry but have limitations associated with safety and elicit protections of short duration (20). In addition, parenteral vaccines have limited ability of inducing mucosal immunity, which is key in protection against infection or disease by mucosal pathogens. Furthermore, parenterally administered vaccines are stressful to birds and not suitable for mass vaccination, requiring much labor and time. Currently, there is a need for mucosal

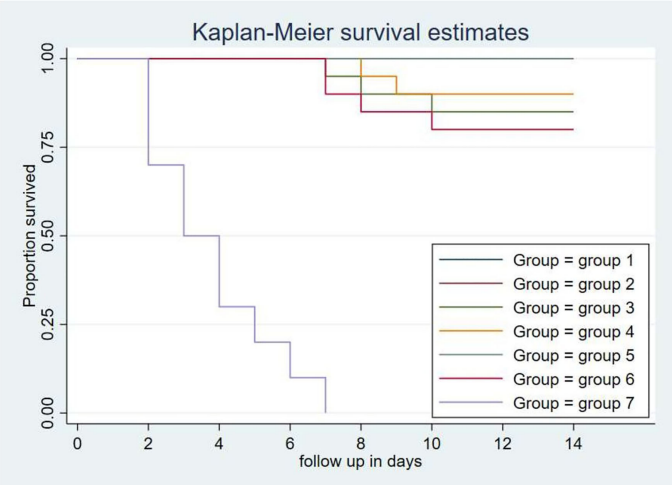

FIGURE 6 | Each group comprises 20 chickens that had been followed for the period of 14 days. The chickens in the treatment and control groups were given 0.5 ml of avian *P. multocida* biotype A. The data were used to determine the Kaplan-Meier estimates (the product limit estimate) of both the control and the treatment groups. The curve takes a step down when the chickens were dead.

vaccines against pathogens that invade *via* the mucosal surfaces. This route of vaccine delivery would also eliminate needle injections (7).

The present study is aimed to develop and evaluate gamma-irradiated mucosal FC vaccine that can be utilized nationally to curb the impact of the disease in Ethiopia as well as in other African countries. In a preliminary study we conducted, fresh cultures of avian *P. multocida* (5.6×10^9 CFU/ml) were irradiated with different doses (0.9, 1, 1.1, and 1.2 kGy) of gamma radiation. Then, the safety and immunogenicity of these preparations [after addition of Montanide gel/01 PR adjuvant (18)] were evaluated in chickens to select the superior radiation dose. Accordingly, irradiation with 1 kGy resulted in safe and immunogenic preparation as evidenced by the higher titer of antibody elicited in chickens and its safety.

Gamma irradiation has been used extensively as an alternative inactivation method of pathogens because of its high penetrability, which allows bacterial inactivation in large

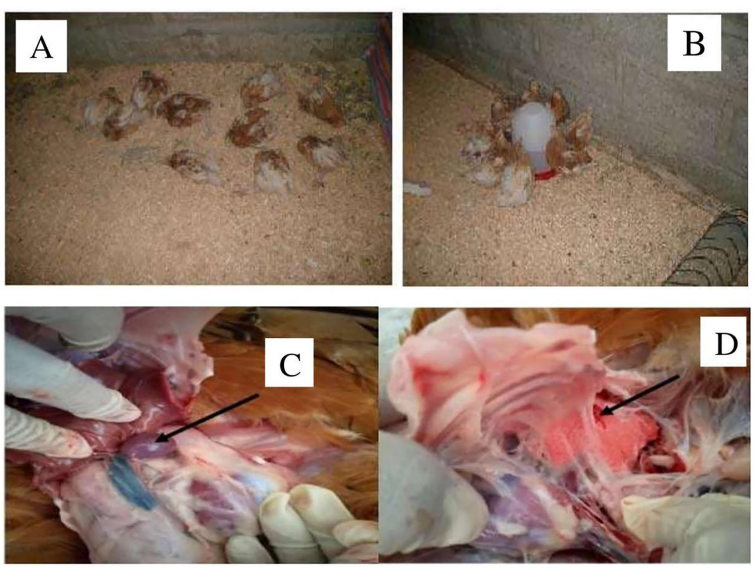

FIGURE 7 | The picture from **(A–D)** indicated the chickens died after challenge with *P. multocida* biotype A at day 56 and the postmortem result. **(A, B)** indicated the dead chickens within 2 weeks. **(C, D)** indicated splenomegaly and petechial and congested lung.

volumes within a short time *via* damage of nucleic acid (11). Several previous reports have suggested that nucleic acids rather than proteins are the primary targets of gamma irradiation to inactivate microorganisms. For example, gamma-irradiated *S. pneumoniae* vaccine produced after inactivation with 10 kGy gamma irradiation elicits strong mucosal and systemic immune responses in mice model, which is indicative of the affectivity of gamma irradiation as a method for the development of a killed whole-cell pneumococcal vaccine (21). Furthermore, sterilization doses for radiation-sensitive organisms could be significantly reduced, which would be expected to reduce damage to epitopes required to develop a protective immune response while maintaining an adequate margin of safety to ensure complete inactivation (22).

In our study, a dose range of 1–3 kGy completely inactivated the avian *P. multocida* as confirmed by the subculturing on TSA and TSB while retaining its immunological properties. There are no available reports on inactivation of avian *P. multocida* using gamma rays. However, *M. haemolytica* was reported to be successfully irradiated using gamma rays of 20 kGy doses, a dose selected to be optimal for vaccine preparation (23). According to our study, radiation with 1 kGy resulted in no avian *P. multocida* cell survival, and the resultant vaccine formulation induced significantly higher antibody response than the formalin-inactivated vaccine. This implies that gamma irradiation efficiently inactivates bacteria with less impact on antigenic structures (determinants), leading to a robust immune response. In contrast, formalin inactivation has been known to induce the formation of methylene bridges between amino groups, resulting in protein cross-linking, affecting antigenicity (24).

One of the key determinants of effectiveness of vaccines is the adjuvant selection. Montanide gel/01 PR is an innovative polymeric adjuvant designed to improve the safety and efficacy of aqueous vaccines. Those adjuvants are based on a dispersion of highly stable gel particles of sodium polyacrylate in water (25). The depot effect with slow release due to polymer adsorption properties improves the recruitment of the innate immune system. It provides a significant enhancement of systemic and mucosal immune responses with a better safety performance than potassium aluminum sulfate (Alum) (26). Based on our finding, it can be speculated that the presence of Montanide gel in our vaccine formulation contributed for its better immunogenicity and efficacy as compared to formalin-inactivated FC vaccine. However, this requires further investigation.

Avian *P. multocida* is known to cause disease in poultry species by infecting or entering through the mucosal surface of the upper respiratory tract. Thus, the first line of defense of the host is invoked against inhaled antigens, making the respiratory route potentially the most effective route for vaccination that is capable of inducing both systemic and mucosal immunity (8). Mucosal vaccines administered through IN route mimics the route of natural infection of mucosal pathogens such as avian *P. multocida*, which in turn would result in protective immune response than injectable preparations (6).

The gamma-irradiated mucosal FC vaccine developed in this study was evaluated for its ability to induce both serum IgG and mucosal IgA in chickens. In chicken sera, IgG is the most common immunoglobulin form, and secretory IgA is produced locally by plasma cells located at mucosal surfaces and plays an important role in mucosal immunity (27). This finding indicated that antibody titers in sera of chickens vaccinated with gamma-irradiated mucosal vaccine were significantly increased after 2 weeks post-vaccination, but significant shooting was recorded at 6 and 8 weeks post-vaccination and is in agreement with (8) and (28), who stated that rOmpH-LTB-based intranasal and irradiated bacterial vaccines generate higher humoral immune responses and protection against extracellular and intracellular bacteria and (29) who registered that vaccines developed by irradiation have been found to be strong inducers for humoral immune responses that make this type of vaccine highly effective.

An interesting finding in our study was the gamma-irradiated mucosal fowl cholera vaccine led to high levels of *P. multocida*–specific serum IgG responses as compared to formalin-inactivated fowl cholera vaccine. This might be due to highly preserved immunogenic properties of protein antigens even after irradiation. However, formalin inactivation can cause crosslinking of several amino acid residues, which leads to a lower immunogenic response (30).

In regard to efficacy, our finding showed that vaccination with intranasal and intraocular (0.3 ml/dose) route of the gamma-irradiated mucosal vaccine resulted in 100% protection against lethal challenge. As compared to the intranasal route, immunization through oral and intraocular route resulted in less efficacy ($p<0.05$) as shown by death of some birds in those groups. This can be due to the local IgA produced in the mucosal airways, which is the natural route and of infection of FC (21).

In this study, the gamma-irradiated fowl cholera vaccine was safe as chickens injected with it were devoid of vaccination side effects and their bodies were maintained normal, and it avoids the drawbacks in vaccinated chickens with chemical inactivated fowl cholera vaccines. We believe that these preliminary findings demonstrate that the gamma-irradiated mucosal fowl cholera vaccine approach is an adaptable vaccine strategy against avian *P. multocida* and that this information will aid in the evaluation of other whole-cell, killed vaccine strategies, as well as identify candidates for recombinant protein vaccine approaches.

In conclusion, the present study showed that gamma-irradiated FC mucosal vaccine is safe and protective, suggesting its potential use for immunization of chicken against FC in chicken. One kGy was identified as a dosage of gamma irradiation that inactivated *P. multocida* replication while retaining immunogenic surface structures. Montanide gel/01 PR showed a significant enhancement of systemic and mucosal immune responses with a safety. In this study, the candidate gamma-irradiated mucosal vaccines induced higher response of both serum IgG and mucosal IgA after three IN doses, the latter (IgA) being highly relevant in the context of protective immunity. In addition to its good immunogenicity,

the candidate vaccine provided protection in challenge experiments. This can be considered a go-on signal to further evaluate the vaccine and approve it for national use.

DATA AVAILABILITY STATEMENT

The original contributions presented in the study are included in the article/supplementary material. Further inquiries can be directed to the corresponding author.

ETHICS STATEMENT

The animal study was reviewed and approved by the animal research ethics committee of the National Veterinary Institute, Ethiopia with the protocol number NVI-AE-008-2020.

AUTHOR CONTRIBUTIONS

BD and EK were involved in the data collection. BD, DA, and SI participated in the study design and in the laboratory analysis, performed data analysis, and drafted the manuscript. MB, EG, TA, VW, and HU assisted in study conception and manuscript revision and also assisted in analysis interpretation and gave inputs in the final manuscript. EG, TA, VW, and HU read and commented on the manuscript and rearranged for publication. All authors contributed to the article and approved the submitted version.

FUNDING

This work was supported by the CRP grant (code D32035) from the International Atomic Energy Agency (IAEA), Vienna, Austria.

ACKNOWLEDGMENTS

The study was supported by a CRP grant from the International Atomic Energy Agency (IAEA). The authors are very grateful for the support provided from Dr Giovanni Cattoli and Dr RichardKangethe of IAEA. Special thanks go to Sebastien Deville of SEPPIC, Air Liquide Healthcare Specialty Ingredients for kindly providing us Montanide/01 PR gel. The authors would like tothank the National Veterinary Institute (NVI) of Ethiopia for availing the laboratory and animal experimentation facilities. The technical support of the staff at the Research and Development directorate of NVI is also highly appreciated. We also thank National Institute for Control and Eradication of Tsetse Fly and Trypanosomosis of Ethiopia for allowing us to use the irradiation facility.

REFERENCES

1. Asfaw YT, Yohannes T, Ameni G, Medhin G, Gumi B, Hagos Y, et al. Poultry Disease Occurrences and Their Impacts in Ethiopia. *Trop Anim Health Production* (2021) 53(1):54. doi: 10.1007/s11250-020-02465-6
2. Molalegne B, Kelay B, Berhe GE, Kyule M. Development and Efficacy Trial of Inactivated Fowl Cholera Vaccine Using Local Isolates of *Pasteurellamultocida*. *Ethiopian Veterinary J* (2009) 13(2):81–98.
3. World organization for animal health. *Manual of Diagnostic Tests and Vaccines for Terrestrial Animals*. Paris, France (2019). Access on: https://www.oie.int/en/produit/manual-of-diagnostic-tests-and-vaccines-for-terrestrial-animals-2019/.
4. Fan YC, Chiu HC, Chen LK, Chang GJ, Chiou SS. Formalin Inactivation of Japanese Encephalitis Virus Vaccine Alters the Antigenicity and Immunogenicity of a Neutralization Epitope in Envelopeproteindomainiii. *PLoSNegl.Trop.Dis.* (2015) 9:10. doi: 10.1371/journal.pntd.0004167
5. Lycke N. Recent Progress in Mucosal Vaccine Development: Potential and Limitations. *Nat Rev Immunol* (2017) 12:592. doi: 10.1038/emm.2014.2
6. Miquel-Clopes A, Bentley EG, Stewart JP, Carding SR. Mucosal Vaccines and Technology. *Clin Exp Immunol* (2019) 196:205–14. doi: 10.1111/cei.13285
7. Thanasarasakulpong A, Poolperm P, Tankaew P, Sawada T, Sthitmatee N. Protectivity Conferred by Immunization With Intranasal Recombinant Outer Membrane Protein H From Pasteurella Multocida Serovar a:1 in Chickens. *J Veterinary Med Sci* (2015) 77(3):321–6. doi: 10.1292/jvms.14-0532
8. Poolperm P, Apinda N, Kataoka Y, Suriyasathaporn W, Tragoolpua K, Sawada T, et al. Protection Against *Pasteurellamultocida* Conferred by an Intranasal Fowl Cholera Vaccine in Khaki Campbell Ducks. *Japanese J Veterinary Res* (2018) 66(4):239–50. doi: 10.14943/jjvr.66.4.239
9. Woodrow KA, Bennett KM, Lo DD. Mucosal Vaccine Design and Delivery. *Annu Rev Biomed.Eng* (2012) 14:17–46. doi: 10.1517/17425247.2013.740008
10. Seo HS. Application of Radiation Technology in Vaccines Development. *Clin Exp Vaccine Res* (2015) 4(2):145. doi: 10.7774/cevr.2015.4.2.145
11. Fertey J, Bayer L, Kahl S, Rukiya M, Burger-Kentischer A, Thoma M, et al. Low-Energy Electron Irradiation Efficiently Inactivates the Gram-Negative Pathogen Rodentibacterpneumotropicus New Method for the Generation of Bacterial Vaccines With Increased Efficacy. *Vaccines* (2020) 8:1–9. doi: 10.3390/vaccines8010113
12. Bayer L, Fertey J, Ulbert S, Grunwald T. Immunization With an Adjuvanted Low-Energy Electron Irradiation Inactivated Respiratory Syncytial Virus Vaccine Shows Immune Protective Activity in Mice. *Vaccine* (2018) 36:1561–9. doi: 10.1016/j.vaccine.2018.02.014
13. Syaifudin M, Tetriana D, Nurhayati S. The Feasibility of Gamma Irradiation for Developingmalariavaccine. *AtomIndonesia* (2011) 37(3):91–101. doi: 10.13170/ajas.4.1.13558
14. National Veterinary institute/SOP. *Fowl Cholera Vaccine Production NVI Standard Operational Procedure*. Debre zeit, Ethiopia (2017) 1–7.
15. Begum RH, Rahman H, Ahmed G. Development and Evaluation of Gamma Irradiated Toxoid Vaccine of *Salmonella Enterica*vartyphimurium. *Veterinary Microbiol* (2011) 153(1–2):191–7. doi: 10.1016/j.vetmic.2011.06.013. Elsevier B.V.
16. Ahmad TA, Rammah SS, Sheweita SA, Haroun M, El-Sayed LH. Development of Immunization Trials Against *Pasteurellamultocida*. *Vaccine* (2014) 32:909–17. doi: 10.1016/j.vaccine.2013.11.068
17. Gaidamakova EK, Elena K, Myles A, McDaniel DP, Fowler CJ, Valdez P, et al. Preserving Immunogenicity of Lethally Irradiated Viral and Bacterial Vaccine Epitopes Using a Radio-Protective Mn2+-Peptide Complex From Deinococcus. *Cell Host Microbe* (2012) 12(1):117–24. doi: 10.1016/j.chom.2012.05.011
18. Seppic. *Technical Bulletin, Montanide TM01 Gel Ready to Use Aqueous Polymeric Adjuvant for Veterinary Vaccines* (2021). Available at: WWW.Seppic.Comhttps://www.seppic.com/sites/seppic/files/2017/02/28/seppic-montanide.pdf.
19. Wubet W, Bitew M, Mamo G, Gelaye E, Tesfaw L, Sori H, et al. Evaluation of Inactivated Vaccine Against Fowl Cholera Developed From Local Isolates of Pasteurellamultocida in Ethiopia. *Afr J Microbiol Res* (2019) 13:500–9. doi: 10.5897/AJMR2019.9096
20. Harper M, Boyce D. The Myriad Properties of *Pasteurellamultocida* Lipopolysaccharide. *Toxin* (2017) 9:254. doi: 10.3390/toxins9080254
21. Jwa MY, Jeong S, Ko EB, Kim R, Seo HS, Yun C, et al. Gamma-Irradiation of Streptococcus Pneumoniae for the Use as an Immunogenic Whole Cell Vaccine. *J Microbiol* (2018) 56(8):579–85. doi: 10.1016/j.micpath.2018.08.015

22. Dollery J, Zurawski V, Gaidamakova E, Matrosova V, Tobin J, Wiggins T, et al. Radiation-Inactivated *Acinetobacterbaumannii*vaccine Candidates. *Vaccines* (2021) 9(2):1–16. doi: 10.3390/vaccines9020096
23. Sahar A, Basem S, Ahmed G, Mahmoud I, Waleed N, Abdel-Rahim EA. Development of Gamma Irradiation Vaccine Against Mannheimiahaemolytica. *Res J Immunol* (2015) 8(1):17–26. doi: 10.3923/rji.2015.17.26
24. Thavarajah R, Mudimbaimannar VK, Elizabeth J, Rao UK, Ranganathan K. Chemical and Physical Basics of Routine Formaldehyde Fixation. *J Oral MaxillofacPathol* (2012) 16:400–5. doi: 10.4103/0973-029X.102496
25. Damiana T, Portuondo D, Loesch M, Batista-Duharte A, CarlosI IZ. A Recombinant Enolase-Montanide TM Petgel a Vaccine Promotes a Protective Th1 Immune Response Against a Highly Virulent *Sporothrixschenckii* by Toluene Exposure. *Pharmaceutics* (2019) 11:144. doi: 10.3390/pharmaceutics11030144
26. Jafari M, Moghaddam M, Taghizadeh M, Masoudi S, Bayat Z. Comparative Assessment of Humoral Immune Responses of Aluminum Hydroxide and Oil-Emulsion Adjuvants in Influenza (H9N2) and Newcastle Inactive Vaccines to Chickens. *Artif Cells Nanomed Biotechnol* (2017) 45:84–9. doi: 10.3109/21691401.2015.1129626
27. Varinrak T, Poolperm P, Sawada T, Sthitmatee N. Cross-Protection Conferred by Immunization With an Romph-Based Intranasal Fowl Cholera Vaccine. *Avian Patho* (2017) 46:515–25. doi: 10.1080/03079457.2017.1321105
28. Tuasikal BJ, Wibawan F, Pasaribu H, Estuningsih S. Bacterial Protein Characterization of *Streptococcus Agalactiae* by SDS-PAGE Method for Subclinical Mastitis Irradiated Vaccine Materials in Dairy Cattle. *Atom Indonesia* (2012) 38:66–70. doi: 10.17146/aij.2012.162
29. Mahmoud HI, Makharita MA, Abbas N. Comparison Between Protective Immunity Induced by Gamma-Irradiated *Brucellaabortus* Field Strain and Commercial *Brucellaabortus* Strain 19 in Mice. *Intl J Microbiol Res* (2016) 7: (3):114–9. doi: 10.5829/idosi.ijmr.2016.114.119
30. Babb R, Chen A, Hirst TR, Kara EE, McColl SR, Ogunniyi AD, et al. Intranasal Vaccination With-Irradiated *Streptococcus Pneumoniae* Whole-Cell Vaccine Provides Serotype-Independent Protection Mediated by B-Cells and Innate IL-17 Responses. *Clin Sci* (2016) 130(9):697–710. doi: 10.1042/CS20150699

Conflict of Interest: The authors declare that the research was conducted in the absence of any commercial or financial relationships that could be construed as a potential conflict of interest.

Publisher's Note: All claims expressed in this article are solely those of the authors and do not necessarily represent those of their affiliated organizations, or those of the publisher, the editors and the reviewers. Any product that may be evaluated in this article, or claim that may be made by its manufacturer, is not guaranteed or endorsed by the publisher.

frontiers in Immunology

MINI REVIEW
published: 11 February 2022
doi: 10.3389/fimmu.2022.845514

Ionizing Radiation Technologies for Vaccine Development - A Mini Review

Sohini S. Bhatia[1] *and Suresh D. Pillai*[1,2*]

[1] National Center for Electron Beam Research, an International Atomic Energy Agency (IAEA) Collaborating Center for Electron Beam Technology, Texas A&M University, College Station, TX, United States, [2] Department of Food Science and Technology, Texas A&M University, College Station, TX, United States

Given the current pandemic the world is struggling with, there is an urgent need to continually improve vaccine technologies. Ionizing radiation technology has a long history in the development of vaccines, dating back to the mid-20th century. Ionizing radiation technology is a highly versatile technology that has a variety of commercial applications around the world. This brief review summarizes the core technology, the overall effects of ionizing radiation on bacterial cells and reviews vaccine development efforts using ionizing technologies, namely gamma radiation, electron beam, and X-rays.

Keywords: ionizing radiation, vaccines, electron beam, gamma irradiation, killed vaccines

OPEN ACCESS

Edited by:
Viskam Wijewardana, International Atomic Energy Agency, Austria

Reviewed by:
Mohammed Alsharifi, University of Adelaide, Australia
Eric James, Sanaria, United States

***Correspondence:**
Suresh D. Pillai
suresh.pillai@ag.tamu.edu

Specialty section:
This article was submitted to Vaccines and Molecular Therapeutics, a section of the journal Frontiers in Immunology

Received: *29 December 2021*
Accepted: *24 January 2022*
Published: *11 February 2022*

Citation:
Bhatia SS and Pillai SD (2022) Ionizing Radiation Technologies for Vaccine Development - A Mini Review. Front. Immunol. 13:845514. doi: 10.3389/fimmu.2022.845514

INTRODUCTION

Vaccination is a cornerstone of public health measures. It promotes human and animal health as well as prevents the spread of communicable diseases in humans and animals. Over one hundred vaccines are currently licensed for human use in the United States (1). Despite this, many infectious diseases, such as Covid-19, HIV, Influenza, Malaria, and Tuberculosis continue to cause severe illness and death globally. In the feed and livestock animal industries, the use of antibiotic growth promoters has been substantially reduced due to fears of multi-drug resistant bacteria, (2–5). However, with the ban of antimicrobial usage, therapeutic usage of antimicrobials increased in Denmark by 33.6% (6) and mortality in weaning pigs increased by 1.5% (2). The resurgence of previously controlled infections and diseases have led to the intensive investigation and commercialization of multiple methods to control and improve animal health, with vaccinations being the most common (3, 7–9).

Current vaccine technologies have their advantages and disadvantages. Live vaccines often elicit strong immune responses, but a balance between attenuation, safety, and protection must be struck. Vaccination with attenuated strains has often been successful, although this option is not suitable for some diseases (10–13). A disadvantage of attenuated vaccines is the fear of regained virulence. Inactivated, or killed vaccines are inactivated using chemicals such as formalin, diethylpyrocarbonate and β-propiolactone. Although there are reduced safety risks associated with chemically inactivated vaccines, they often exhibit reduced immunogenicity due to damaged antigenic epitopes. Toxoids, recombinant vaccines, as well as subunit vaccines are typically considered safe because attenuation is induced by deletions preventing the strain from overgrowing and causing disease (14). The disadvantage of sub-unit vaccines is that only a

singular antigen or at times multiple antigens are presented, generally limiting the cross-protective ability of such vaccines.

Given increased urbanization, climate change and close interaction of animals and humans, there is a continuous need to evaluate vaccine technologies to deal with epidemics, pandemics, and rapidly emerging infectious virus variants. The vaccine technologies should be robust and capable of dealing with multiple pathogens, their possible variants and host species (15). Ionizing radiation technology has benefitted society for over 65 years. Legacy nuclear technologies based on radioactive isotopes such as cobalt-60 and cesium-137 have resulted in significant benefits to human and animal health and agriculture. Besides radioactive isotope based ionizing radiation technology, electron beam (eBeam) and X-ray technologies have grown rapidly in the last decade and are now becoming widely used for a variety of commercial applications. The overall objective of this brief review is to summarize the history and the advances of using ionizing radiation technology for developing vaccines against infectious diseases.

PRINCIPLES OF IONIZING RADIATION

Ionizing radiation is defined as energy capable of removing electrons from atoms and, thereby, causing ionization. The three main ionizing radiation technologies are gamma radiation technology (based on photons), electron beam (eBeam) technology (based on electrons), and X-rays (based on photons) (16). Gamma rays are electromagnetic radiation composed of photons emitted from the nucleus of a radioactive isotope. In most commercial settings, the isotope source is cobalt-60. In some instances, gamma rays are produced from cesium-137 as well. Electron beam (eBeam) technology is based on highly energetic electrons that are produced from regular electricity using industrial equipment called "eBeam accelerators". X-rays are also electromagnetic radiation composed of photons. However, they are generated using energetic electrons from accelerators which are allowed to strike an extremely dense metal such as tantalum or tungsten resulting in the formation of X-ray photons. Cobalt-60 is a radioactive isotope and, therefore, it is of serious security concerns. Also, due to increasing cobalt-60 costs, its stringent safe-guarding requirements, and ultimate disposal needs and costs, this legacy technology is quickly becoming commercially unsustainable. Commercially, gamma radiation technology is being quickly replaced with accelerator-based technologies, namely eBeam and X-ray technologies (16, 17). From a commercial perspective, eBeam technology is an attractive technology because of its relatively overall lower costs and relative ease of adoption. One of the key attractive features of eBeam and X-ray technologies is that they are switch- on/switch-off technologies meaning that they can be switched off when not in use. This is in direct contrast to radioactive isotopes such as cobalt-60 where the emission of gamma ray photons cannot be switched off.

Today, eBeam and X-ray technologies are commercial off the shelf technologies with a diverse array of energy and beam power configurations. In commercial settings, eBeam irradiation is generated using accelerators. In these accelerators, electrons generated from commercial electricity are accelerated to approximately 99.999% of the speed of light resulting in electron energies up to 10 MeV (Mega electron volts) (18). These highly energetic electrons are then focused and pulsed uniformly over a material, solid or liquid (16, 18). When the electrons interact with a molecule leading to its ionization, the ejected electron becomes energized, going on to interact with and ionize an adjacent molecule. This chain reaction continues until the energy has fully dissipated (18). High energy eBeam technology is also currently used in the food and medical device industry for its ability to either pasteurize products or achieve complete sterility. In the food industry, this technology is regularly used for phytosanitary treatment, shelf-life elongation, pathogen inactivation, and occasionally terminal sterilization (16, 17). In the medical device industry, this technology is used to sterilize single-use medical devices and laboratory consumables (19).

EFFECT OF IONIZING RADIATION EXPOSURE ON MICROORGANISMS

Ionizing radiation inactivates microorganisms through direct and indirect methods. Direct damage is caused as a result of interactions between energetic electrons or photons and the molecules within an organism, while indirect damage is caused as a result of interactions with products of water radiolysis (18, 20, 21). When an energized electron from an accelerator (or a gamma photon emitted from a radioactive isotope) interacts with a material, molecules are ionized, ejecting electrons from the outermost valence shells. These ejected electrons in turn cause a cascade of similar ionization events on adjoining atoms until all its energy is fully dissipated. In microorganisms, DNA is the largest molecule, therefore, resulting in it being the primary target of direct ionization events. The ionization of DNA results in the cleavage of the phosphodiester bonds along the DNA backbone. While single-stranded breaks are repairable, extensive double stranded breaks are much harder for an organism to repair and overcome. Due to excessive shearing of the nucleic acid, the microorganism is ultimately inactivated (21). The other major target of ionizing radiation in a microorganism is its cellular water content, leading to the production of radiolytic species. Radiolysis of water generates a diverse array of highly reactive, but short lived free radical species such as hydroxyl radicals, hydrogen peroxide, hydrogen, hydrated electrons, and hydrated protons. The summary equation for water radiolysis is presented below (Equation 1) with the quantity of each product per 100 eV of energy absorbed shown in parenthesis.

$$e^- + H_2O \rightarrow {}^*OH(2.7) + e^-_{aq}(2.7) + {}^*H(0.55) + H_2(0.55) + H_2O_2(0.71) + H_3O^+(2.7) \quad \text{Equation 1}$$

The damage to the cellular components often results indirectly from the interaction of these reactive species as opposed to the direct incident electrons. Hydroxyl radicals (*OH) are extremely short lived. However, during their short time, they can cause significant damage to molecules in their immediate surroundings (22). Superoxide radicals (O_2^{*-}) are also generated by the radiolysis of water, and it is hypothesized that these molecules accumulate within a microbial cell causing severe damage to proteins such as enzymes with exposed iron-sulfur clusters (23, 24). Additionally, methionine and cysteine have been shown to be especially susceptible to ionizing radiation (25). Superoxide radicals also react with endogenous nitric oxide within a cell, forming reactive nitrogen species (RNS) such as a peroxynitrite anion ($ONOO^-$), nitrogen dioxide (NO_2^*), and dinitrogen trioxide (N_2O_3), which cause further damage to the DNA and are the primary agents of damage to proteins within bacterial cells (26). This protein damage can have significant effects on the microorganism's ability to function. Taken together, direct and indirect mechanisms of damage lead to the inactivation of microbial cells due to the high number of single and double strand breaks (21). Assuming a hypothetical genome size of 3.5 million base pairs, a dose of 1 kGy would cause approximately 200 single stranded breaks and 14 double stranded breaks, per copy of a bacteria's genome (18, 27). This extent of DNA damage is irreparable in most microorganisms, resulting in their inactivation due to the inability of the DNA to replicate, thereby, resulting in the microbial population being unable to reproduce. This damage done to microorganisms is extremely rapid. Direct damage due to chemical bonds cleavage is estimated to occur within 10^{-14} – 10^{-12} seconds of exposure. Within one picosecond (10^{-12} s), superoxide and hydrogen peroxide radicals are formed. By about 1 millisecond after exposure, the reactions of most reactive species are hypothesized to be complete (25, 28).

While microbial cells cease to multiply due to damage to their nucleic acids, multiple studies have demonstrated that their cellular membrane remains intact even after exposure to ionizing radiation. It needs to be pointed out the how microbial cells respond to ionizing radiation can be extremely varied depending on the microorganism in question and the ionizing radiation dose applied to the cells. Studies conducted in our laboratory demonstrate that eBeam exposure even at lethal doses does not compromise the bacterial cellular membrane as observed using microscopy (29–33). Similarly, gamma irradiation has also been shown to cause no damage to bacterial cell membranes at lethal doses (34–36). Furthermore, there is now significant evidence that in cells treated with lethal doses of ionizing radiation, there is residual metabolic activity after treatment (33, 35, 37–41). For example, in *Escherichia coli* K-12 metabolic activity of *E. coli* was sustained for up to nine days following treatment, as demonstrated using AlamarBlue™ as well as ATP assays (33). Other studies have demonstrated that gamma radiation also does not significantly hinder cellular functions. Gamma irradiated cells maintained oxidative function and the ability to continue nucleic acid and protein synthesis (35, 38). Furthermore, metabolic activity persists, despite several double stranded breaks of the cell's genome. Researchers hypothesize that there are portions of genomes which are still intact, enough to sustain cellular functions (35, 39, 42). Bacterial cells exposed to eBeam exposure exhibit similar features. Studies examining the metabolomic state of inactivated *E. coli* and *Salmonella* Typhimurium have shown that immediately after treatment, cells are metabolically active with metabolomic fluxes continuing even 24 hours after eBeam treatment (43). Nevertheless, the ability of microbial cells to continue their metabolic activity even after physical damage to their nucleic acids is a scientific conundrum that is worthy of deeper investigation. Taken together, this state in microbial cells where the cells cannot multiply yet remain metabolically active can be termed as a Metabolically Active, yet Non-Culturable (MAyNC) state. In vaccinology, the term that is often used especially with irradiated malarial sporozoites is "Metabolically active, non-replicating". This state has potential broad applications in vaccine development. MAyNC cells are inactivated, but maintain cell membrane integrity, and therefore, function as a killed vaccine. The biological significance of residual metabolic activity on the potency of the vaccine is yet to be completely understood. Because ionizing radiation maintains membrane integrity, MAyNC cells may be specifically well-suited for vaccines against pathogens that require immune recognition of multiple antigenic epitopes. Furthermore, due to the growing availability of eBeam and X-ray technologies which can be installed inline to the manufacturing process, the ability to generate MAyNC cells of varying potency can be extremely valuable for vaccine development.

HISTORY OF VACCINES USING IONIZING RADIATION

The use of ionizing radiation as a method to attenuate or inactive microorganisms for the use as vaccines is not novel, with reports of gamma and x-ray-inactivated vaccine research dating back to the mid-20th century (44–50). The advantage of ionizing-radiation vaccines, or radio-vaccines, is that because they are inactivated, they are able to retain immunogenicity even when stored at non-refrigerated conditions potentially eliminating the need for cold-chain to preserve vaccine potency (31, 51, 52). The ability to store vaccines at ambient or refrigerated storage (as compared to frozen storage) can translate to significantly lower overall costs for vaccine transportation and distribution. The ability to distribute vaccines without the need for cold chain distribution also increases vaccine access in remote areas (53, 54). Importantly, eBeam and X-ray technologies are scalable, with the capability to inactivate large quantities of preparations (55).

Due to the vast commercial capabilities, numerous patents related to "radio-vaccines" have already been filed (**Table 1**). Interest in radio- vaccines has increased significantly recently, with investigations into the creation of vaccines for bacterial, viral, and protozoan diseases (**Table 2**). While many of the researched vaccine candidates are based on gamma-irradiation, there is significantly less research conducted on eBeam or X-ray

TABLE 1 | A selection of patents relating to radio-vaccines.

Patent #	Country	Year	Status[a]	Title
US3657415A	USA	1969	Expired	Canine hookworm vaccines
DE3853854T2	Germany	1988	Expired	Vaccine against group b *Neisseria meningitidis*, gammaglobulin and transfer factor
AU706213B2	Australia	1996	Ceased	Method for obtaining a vaccine with wide protective range against group b *Neisseria meningitidis*, the resulting vaccine, gammaglobulin and transfer factor
AU6320001A	Australia	2001	Published	Gamma irradiation of protein-based pharmaceutical products
KR20030034517A	South Korea	2001	Granted	*Burkholderia gladioli* k4 having antifungal activity, preparation method of its mutant by gamma radiation and the mutant thereof
US20060147460A1	USA	2002	Granted	Anticancer vaccine and diagnostic methods and reagents
KR101173871B1	South Korea	2004	Granted	Modified free-living microbes vaccine compositions and methods of use thereof
US20050175630A1	USA	2004	Abandoned	Immunogenic compositions and methods of use thereof
US8173139B1	USA	2009	Granted	High energy electron beam irradiation for the production of immunomodulators in poultry
CA2733356C	Canada	2009	Granted	Influenza vaccines
US8282942B2	USA	2010	Granted	*Toxoplasma gondii* vaccines and uses thereof
US20130122045A1	USA	2010	Abandoned	Cross-protective influenza vaccine
US20150209424A1	USA	2011	Abandoned	Inactivated varicella zoster virus vaccines, methods of production, and uses thereof
JP2014520117A	Japan	2012	Granted	Vaccine composition comprising inactivated chikungunya virus strain
AU2012211043B2	Australia	2012	Published	Combination vaccines
US10080795B2	USA	2013	Granted	Method for inactivating viruses using electron beams
WO2014155297A2	WIPOb[b]	2014	Published	Systems and methods for viral inactivation of vaccine compositions by treatment with carbohydrates and radiation
WO2014165916A1	WIPO[b]	2014	Published	Methods and compositions for inducing an immune response
DE102015224206B3	Germany	2015	Granted	Irradiation of biological media in transported foil bags
KR20180036987A	South Korea	2016	Published	Vaccine composition
DE102016216573A1	Germany	2016	Published	Inactivation of pathogens in biological media
WO2018167149A1	WIPO[b]	2018	Ceased	Method for irradiating mammalian cells with electron beams and/or x-rays
WO2019191586A2	Canada	2019	Published	Irradiation-inactivated poliovirus, compositions including the same, and methods of preparation
WO2020069942A1	WIPO[b]	2020	Published	Method for inactivating biologically active components in a liquid

[a]*Status as of November, 2020;* [b]*World Intellectual Property Organization.*

inactivated vaccines. This limited amount of information could be attributed to the relatively recent commercial availability of eBeam and X-ray technologies. Among all the research conducted on radio-vaccines, the most progress has been on *Plasmodium* sporozoites attenuated with irradiation to protect against malaria. First examined in 1967 using x-ray irradiation, this idea has evolved considerably over the last 50+ years to its current iteration in phase 2 clinical trials using gamma-attenuated sporozoites (75, 76, 93–97). Studies using gamma-irradiated *Listeria monocytogenes* have demonstrated that unlike other inactivation methods such as heat or formalin, irradiation better maintained antigenic properties and stimulated robust T cell responses (59).

IMMUNE RESPONSES TO RADIO-VACCINES

In multiple studies investigating the immune response to gamma-irradiated *Brucella* spp., investigators found that gamma-irradiated cells were metabolically active and inactivated cells were able to induce a significant cellular immune response and were protective when challenged (34–37, 56, 98). Furthermore, gamma-irradiated cells have even exhibited an ability to act as an adjuvant, increasing the immune response to co-administered antigens (71). A significant amount of research has been conducted on the development of a gamma-inactivated influenza vaccine, demonstrating that this vaccine is effective in eliciting a strong antigen-specific antibody response as well as protecting mice from challenge with heterologous influenza virus (27, 80, 83).

Electron beam (eBeam) technology has been investigated as a method to generate vaccine-like immunomodulators against *Salmonella* Typhimurium using a mice model (31). This concept has been expanded to demonstrating the immunomodulatory and protective effects of eBeam-inactivated *Salmonella* Enteriditis and Typhimurium in chickens and *Rhodococcus equi* in neonatal fouls (29–32, 40, 41, 64, 67). This concept is now been expanded to include the use of low energy eBeam as an inactivation technology for vaccine development with considerable success (73, 77, 82).

ROLE OF ADJUVANTS

For a vaccine formulation to be effective upon challenge, it must be able to induce a prolonged and protective immune response. Live attenuated vaccines that retain their ability to replicate with a host, naturally eliciting a strong CD8+ and CD4+ T cell response, as well as a strong humoral response, while inactivated vaccines often require the assistance of an adjuvant to help the vaccine elicit a stronger immune response in the host. An adjuvant is technically defined as a component that is added to vaccine to enhance an immune response, and typically provides the benefits of increased antibody titers and an increased speed, breadth, and duration of an immune response. Because radio-vaccines are unable to replicate within a host, it has been proposed that their immunogenic potential

TABLE 2 | List of radio-vaccines against bacterial, viral, and protozoan pathogens.

Type of Pathogen	Pathogen	Inactivation Method	Inactivation Dose	Model	Notes	Source
Bacteria	*Brucella abortus*	Gamma	4 kGy	Mice	Irradiated strains induced less of an immune response than live strains	(56)
Bacteria	*Brucella abortus*	Gamma	3 kGy	Mouse	Antigen specific Th1 response	(34)
Bacteria	*Brucella abortus*	Gamma	2.5 kGy	Mice	Stimulated IFN-gamma and Th1 cells	(57)
Bacteria	*Brucella abortus*	Gamma	3.5 kGy	Mice	Protective upon challenge	(58)
Bacteria	*Brucella abortus, B. melitensis, and B. suis*	Gamma	3.5 kGy	Mice	Protective upon challenge	(36)
Bacteria	*Brucella melitensis*	Gamma	3.5 kGy	Mouse	Cytotoxic T cell response and protective against challenge	(35)
Bacteria	*Listeria monocytogenes*	Gamma	6 kGy	Mouse	Induced protective T cell responses	(59)
Bacteria	*Mannheimia haemolytica*	Gamma	2-20 kGy	Rabbit	Protection upon challenge	(60)
Bacteria	*Orientia tsutsugamushi*	Gamma	2 kGy	Mice	Partially protective upon challenge	(61)
Bacteria	*Orientia tsutsugamushi*	Gamma	3 kGy	Mice	Protective upon challenge	(62)
Bacteria	*Pasteurella tularensis*	X-ray	10 kGy	Mice	Partially protective upon challenge	(63)
Bacteria	*Rhodococcus equi*	Electron Beam (High Energy)	4-5 kGy	Horse	Produced cell-mediated and upper respiratory mucosal immune response	(30)
Bacteria	*Rhodococcus equi*	Electron Beam	5 kGy	Horse	Not protective upon challenge	(64)
Bacteria	*Rodentibacter pneumotropicus*	Electron Beam (Low Energy)	20 kGy	Mice	Protective upon challenge and reduced colonization	(65)
Bacteria	*Salmonella* Enteriditis	Electron Beam (High Energy)	2.5 kGy	Chicken	Protective upon challenge and reduced colonization	(66)
Bacteria	*Salmonella* Typhimurium	Electron Beam (High Energy)	2.5 kGy	Chicken	Heterophil-mediated innate immune response	(67)
Bacteria	*Salmonella* Typhimurium	Electron Beam (High Energy)	7 kGy	Mouse	Stimulated innate immune markers and reduced colonization	(31)
Bacteria	*Salmonella* Typhimurium	Gamma	10-80 kGy	Chicken	Protective upon challenge	(68)
Bacteria	*Shigella dysenteriae*	X-ray	Not reported	Rabbits	Bacteria that were treated for a longer time were non-toxic and protective upon challenge	(44)
Bacteria	*Staphylococcus aureus*	Gamma	2.5-2.9 kGy	Mice	Induced specific antibody production, but not protective upon challenge	(69)
Bacteria	*Staphylococcus aureus*	Gamma	25-40 kGy	Mice	Induced B and T cell-dependent protection against challenge	(70)
Bacteria	*Streptococcus pneumoniae*	Gamma	12 kGy	Mice	Protection upon challenge mediated by B-cells and innate IL-17 response	(71)
Bacteria	*Streptococcus pneumoniae*	Electron Beam	25 kGy	Rabbit and Mice	Immunogenic and protective upon challenge	(72)
Protozoa	*Eimeria tenella*	Electron Beam (Low Energy)	0.1-0.5 kGy	Chicken	Partially protective upon challenge	(73)
Protozoa	*Eimeria tenella*	X-ray	0.2 kGy	Chicken	Protective upon challenge	(74)
Protozoa	*Plasmodium berghei*	X-ray	0.02-0.15 kGy	Mouse	Protective upon challenge	(75)
Protozoa	*Plasmodium falciparum*	Gamma	0.12-0.15 kGy	Human	Long-lasting protective immunity	(76)
Protozoa	*Plasmodium gallinaceum*	X-ray	0.005-0.2 kGy	Mosquito	Sporozoites from irradiated oocysts were non-infective	(49)
Virus	Human Respiratory syncytial virus (RSV)	Electron Beam (Low Energy)	20 kGy	Mice	Reduction in viral load upon challenge	(77)
Virus	Influenza A virus	Gamma	12.6 kGy	Mice	Induced cytotoxic T cells and protective upon against challenge	(78)
Virus	Influenza A virus	Gamma	10-40 kGy	Mice	Cross-reactive and cross-protective cytotoxic T cell responses	(79)
Virus	Influenza A virus	Gamma	10 kGy	Mice	Protective upon challenge; freeze-drying did not affect cross-protective immunity	(80)
Virus	Influenza A virus	Gamma	50 kGy	Mice	Intranasal vaccination conferred complete protection	(81)
Virus	Influenza A virus	Electron Beam (Low Energy)	30 kGy	Mouse	Elicited a protective immune response	(82)
Virus	Influenza A virus	Electron Beam	25-40 kGy	Nonhuman primate	Elicited seroconversion	(51)
Virus	Influenza A virus	Gamma	10 kGy	Mice	Protective upon heterotypic challenge	(83)
Virus	Middle Eastern Respiratory Virus (MERS)	Gamma	50 kGy	Mice	Caused lung immunopathology upon challenge	(84)
Virus	Polio Virus	Gamma	45 kGy	Mice	Protective upon challenge	(85)
Virus	Rotavirus	Gamma	50 kGy	Mice	Induced a specific neutralizing-antibody response	(86)
Virus	Severe Acute Respiratory Syndrome coronavirus 2 (SARS-CoV-2)	Gamma	50 kGy	Mice	Adjuvanted vaccine elicited T and B cell responses	(52)
Virus	SARS-CoV-2	Gamma	25 kGy	Mice	Humoral and cellular immune response, induced neutralizing antibodies	(87)
Virus	Vaccinia virus	Gamma	0-15 kGy	Rabbit	Inactivated virus was immunogenic	(48)
Virus	Venezuelan Equine Encephalitis Vaccine	Gamma	80-100 kGy	Guinea Pig	Protective upon challenge	(88)

(Continued)

TABLE 2 | Continued

Type of Pathogen	Pathogen	Inactivation Method	Inactivation Dose	Model	Notes	Source
Virus	Venezuelan Equine Encephalitis Vaccine	Gamma	50 kGy	Mice	Protective against subcutaneous challenge and partially protective against aerosol challenge	(89)
Virus	White Spot Syndrome Virus	Electron Beam	13 kGy	Shrimp	Protective upon challenge	(90)
Virus	Zaire ebola virus	Gamma	100 kGy	Nonhuman primate	Not protective upon challenge	(91)
Virus	Zaire ebola virus	Gamma	60 kGy	Nonhuman primate	Not protective upon challenge	(92)

has to be enhanced by the addition of an adjuvant. There are several reports about coupling radio-vaccines with experimental and commercially available adjuvants. Bayer et al. tested four different adjuvants in combination with Respiratory syncytial virus inactivated with low energy electron beam: Alhydrogel (alum based), MF59 (squalene based), QuilA (saponin based), and Poly IC : LC (synthetic double-stranded RNA based) (77). In their study, strong immune responses and significant reductions in viral loads were detected after immunization and subsequent challenge, although the poly IC : LC adjuvanted vaccine elicited lower titers of neutralizing antibodies than the other adjuvanted vaccines tested (77). Substantial humoral and cellular responses were observed when a gamma-inactivated polio vaccine candidate was combined with an alum adjuvant and when a gamma-irradiated HIN1 vaccine was co-administered with a plasmid encoding mouse interleukin-28B (99, 100). Gamma-inactivated SARS-CoV-2 also benefited from the addition of a GM-CSF adjuvant in order to induce a T cell response (52).

CONCLUSIONS

Though ionizing radiation has been researched as a vaccine technology for nearly a century, only recently have vaccines utilizing ionizing radiation reached commercial development. The general lack of interest in radio-vaccines could be attributed to advances in cloning technologies, mRNA vaccines and gene editing technologies. The recent availability of small footprint, low energy eBeam and X-ray equipment could, however, spur the development of radio-vaccines once again. Commercialization of eBeam and X-ray technologies for the medical device, food, and other industrial applications has led to a decrease in overall technology costs and an increase in technology availability (101). This review highlights the potential of ionizing radiation as a vaccine technology suitable against several pathogens causing diseases in various hosts species. This has been most recently demonstrated in the rapid development of vaccine candidates in response to the COVID-19 pandemic, caused by the virus SARS-CoV-2. Radio-vaccines have even been investigated as a response to previous outbreaks of SARS and MERS, and it was hypothesized that ionizing radiation could be used to rapidly produce a vaccine for SARS-CoV-2 (84, 102–104). Gamma-inactivated SARS-CoV-2 combined with GM-CSF as an adjuvant has demonstrated ability to induce neutralizing antibodies as well as a strong T and B cell response (87, 105).

AUTHOR CONTRIBUTIONS

Major portions of this manuscript have been previously included in a doctoral dissertation by SB (106). SP was involved in writing and editing the manuscript. All authors contributed to the article and approved the submitted version.

FUNDING

This work was supported funds from the USDA-NIFA program administered by Texas A&M AgriLife Research H-87080 as well as funds through contracts from the Pacific Northwest National Laboratories (PNNL).

ACKNOWLEDGMENTS

This work was prepared as part of the activities of the IAEA Collaborating Center for Electron Beam Technology.

REFERENCES

1. FDA. *Vaccines Licensed for Use in the United States* (2021). FDA. Available at: https://www.fda.gov/vaccines-blood-biologics/vaccines/vaccines-licensed-use-united-states (Accessed September 19, 2021).
2. Wierup M. The Swedish Experience of the 1986 Year Ban of Antimicrobial Growth Promoters, With Special Reference to Animal Health, Disease Prevention, Productivity, and Usage of Antimicrobials. *Microb Drug Resist* (2001) 7:183–90. doi: 10.1089/10766290152045066
3. Van Immerseel F, Rood JI, Moore RJ, Titball RW. Rethinking Our Understanding of the Pathogenesis of Necrotic Enteritis in Chickens. *Trends Microbiol* (2009) 17:32–6. doi: 10.1016/j.tim.2008.09.005
4. Maron DF, Smith TJ, Nachman KE. Restrictions on Antimicrobial Use in Food Animal Production: An International Regulatory and Economic Survey. *Global Health* (2013) 9:48. doi: 10.1186/1744-8603-9-48
5. McEwen SA, Angulo FJ, Collignon PJ, Conly J. *Potential Unintended Consequences Associated With Restrictions on Antimicrobial Use in Food-Producing Animals* (2017). World Health Organization. Available at: https://www.ncbi.nlm.nih.gov/books/NBK487949/ (Accessed January 20, 2020).
6. DANMAP. *DANMAP – Use of Antimicrobial Agents and Occurrence of Antimicrobial Resistance in Bacteria From Food Animals, Food and Humans in Denmark* (2010). Available at: http://danmap.org/reports/older.

7. Cheng G, Hao H, Xie S, Wang X, Dai M, Huang L, et al. Antibiotic Alternatives: The Substitution of Antibiotics in Animal Husbandry? *Front Microbiol* (2014) 5:217. doi: 10.3389/fmicb.2014.00217
8. Caly DL, D'Inca R, Auclair E, Drider D. Alternatives to Antibiotics to Prevent Necrotic Enteritis in Broiler Chickens: A Microbiologist's Perspective. *Front Microbiol* (2015) 6:1336. doi: 10.3389/fmicb.2015.01336
9. Marquardt RR, Li S. Antimicrobial Resistance in Livestock: Advances and Alternatives to Antibiotics. *Anim Fron* (2018) 8:30–7. doi: 10.1093/af/vfy001
10. Thompson DR, Parreira VR, Kulkarni RR, Prescott JF. Live Attenuated Vaccine-Based Control of Necrotic Enteritis of Broiler Chickens. *Vet Microbiol* (2006) 113:25–34. doi: 10.1016/j.vetmic.2005.10.015
11. McCullers JA, Dunn JD. Advances in Vaccine Technology And Their Impact on Managed Care. *P T* (2008) 33:35–41.
12. Mishra N, Smyth JA. Oral Vaccination of Broiler Chickens Against Necrotic Enteritis Using a Non-Virulent NetB Positive Strain of Clostridium Perfringens Type A. *Vaccine* (2017) 35:6858–65. doi: 10.1016/j.vaccine.2017.10.030
13. Brisse M, Vrba SM, Kirk N, Liang Y, Ly H. Emerging Concepts and Technologies in Vaccine Development. *Front Immunol* (2020) 11:583077. doi: 10.3389/fimmu.2020.583077
14. Spreng S, Dietrich G, Weidinger G. Rational Design of Salmonella-Based Vaccination Strategies. *Methods* (2006) 38:133–43. doi: 10.1016/j.ymeth.2005.09.012
15. Graham BS, Mascola JR, Fauci AS. Novel Vaccine Technologies: Essential Components of an Adequate Response to Emerging Viral Diseases. *JAMA* (2018) 319:1431–2. doi: 10.1001/jama.2018.0345
16. Pillai SD, Shayanfar S. Electron Beam Technology and Other Irradiation Technology Applications in the Food Industry, in: *Applications of Radiation Chemistry in the Fields of Industry, Biotechnology and Environment Topics in Current Chemistry Collections* (2017). Springer International Publishing (Accessed July 7, 2018).
17. Pillai SD, Bhatia SS. Electron Beam Technology: A Platform for Safe, Fresh, and Chemical-Free Food, in: *Food Safety Magazine* (2018). Available at: https://www.foodsafetymagazine.com/magazine-archive1/aprilmay-2018/electron-beam-technology-a-platform-for-safe-fresh-and-chemical-free-food/ (Accessed January 28, 2019).
18. Miller RB. *Electronic Irradiation of Foods: An Introduction to the Technology*. New York: Springer (2005).
19. IIA and GIPA. *A Comparison of Gamma, E-Beam, X-Ray and Ethylene Oxide Technologies for the Industrial Sterilization of Medical Devices and Healthcare Products* (2017). Available at: http://http://gipalliance.net/wp-content/uploads/2013/01/GIPA-WP-GIPA-iia-Sterilization-Modalities-FINAL-Version-2017-October-308772.pdf (Accessed January 23,2022).
20. Urbain WM. CHAPTER 4 - Biological Effects of Ionizing Radiation. In: WM Urbain, editor. *Food Irradiation*. Academic Press (1986). p. 83–117. doi: 10.1016/B978-0-12-709370-3.50010-5
21. Tahergorabi R, Matak KE, Jaczynski J. Application of Electron Beam to Inactivate Salmonella in Food: Recent Developments. *Food Res Int* (2012) 45:685–94. doi: 10.1016/j.foodres.2011.02.003
22. Mavragani IV, Nikitaki Z, Kalospyros SA, Georgakilas AG. Ionizing Radiation and Complex DNA Damage: From Prediction to Detection Challenges and Biological Significance. *Cancers (Basel)* (2019) 11:1789–818. doi: 10.3390/cancers11111789
23. Keyer K, Imlay JA. Superoxide Accelerates DNA Damage by Elevating Free-Iron Levels. *PNAS* (1996) 93:13635–40. doi: 10.1073/pnas.93.24.13635
24. Popović-Bijelić A, Mojović M, Stamenković S, Jovanović M, Selaković V, Andjus P, et al. Iron-Sulfur Cluster Damage by the Superoxide Radical in Neural Tissues of the SOD1(G93A) ALS Rat Model. *Free Radic Biol Med* (2016) 96:313–22. doi: 10.1016/j.freeradbiomed.2016.04.028
25. Reisz JA, Bansal N, Qian J, Zhao W, Furdui CM. Effects of Ionizing Radiation on Biological Molecules—Mechanisms of Damage and Emerging Methods of Detection. *Antioxid Redox Signal* (2014) 21:260–92. doi: 10.1089/ars.2013.5489
26. Daly MJ. A New Perspective on Radiation Resistance Based on Deinococcus Radiodurans. *Nat Rev Microbiol* (2009) 7:237–45. doi: 10.1038/nrmicro2073
27. Alsharifi M, Müllbacher A. The γ-Irradiated Influenza Vaccine and the Prospect of Producing Safe Vaccines in General. *Immunol Cell Biol* (2010) 88:103–4. doi: 10.1038/icb.2009.81
28. Singh A, Singh H. Time-Scale and Nature of Radiation-Biological Damage: Approaches to Radiation Protection and Post-Irradiation Therapy. *Prog Biophys Mol Biol* (1982) 39:69–107. doi: 10.1016/0079-6107(83)90014-7
29. McReynolds JL, Pillai S, Jesudhasan PRR, Hernandez MLC. High Energy Electron Beam Irradiation for the Production of Immunomodulators in Poultry. (2012) US Patent US8173139B1.
30. Bordin AI, Pillai SD, Brake C, Bagley KB, Bourquin JR, Coleman M, et al. Immunogenicity of an Electron Beam Inactivated Rhodococcus Equi Vaccine in Neonatal Foals. *PloS One* (2014) 9:e105367. doi: 10.1371/journal.pone.0105367
31. Praveen C. Electron Beam as a Next Generation Vaccine Platform: Microbiological and Immunological Characterization of an Electron Beam Based Vaccine Against Salmonella Typhimurium. [Ph.D. Dissertation]. College Station (TX: Texas A&M University (2014).
32. Jesudhasan PR, McReynolds JL, Byrd AJ, He H, Genovese KJ, Droleskey R, et al. Electron-Beam–Inactivated Vaccine Against *Salmonella* Enteritidis Colonization in Molting Hens. *Avian Dis* (2015) 59:165–70. doi: 10.1637/10917-081014-ResNoteR
33. Hieke A-SC, Pillai SD. Escherichia Coli Cells Exposed to Lethal Doses of Electron Beam Irradiation Retain Their Ability to Propagate Bacteriophages and Are Metabolically Active. *Front Microbiol* (2018) 9:2138. doi: 10.3389/fmicb.2018.02138
34. Sanakkayala N, Sokolovska A, Gulani J, HogenEsch H, Sriranganathan N, Boyle SM, et al. Induction of Antigen-Specific Th1-Type Immune Responses by Gamma-Irradiated Recombinant Brucella Abortus RB51. *Clin Diagn Lab Immunol* (2005) 12:1429–36. doi: 10.1128/CDLI.12.12.1429-1436.2005
35. Magnani DM, Harms JS, Durward MA, Splitter GA. Nondividing But Metabolically Active Gamma-Irradiated Brucella Melitensis Is Protective Against Virulent B. Melitensis Challenge in Mice. *Infect Immun* (2009) 77:5181–9. doi: 10.1128/IAI.00231-09
36. Moustafa D, Garg VK, Jain N, Sriranganathan N, Vemulapalli R. Immunization of Mice With Gamma-Irradiated Brucella Neotomae and its Recombinant Strains Induces Protection Against Virulent B. Abortus, B. Melitensis and B. Suis Challenge. *Vaccine* (2011) 29:784–94. doi: 10.1016/j.vaccine.2010.11.018
37. Ahn TH, Nishihara H, Carpenter CM, Taplin GV. Respiration of Gamma Irradiated Brucella Abortus and Mycobacterium Tuberculosis. *Proc Soc Exp Biol Med* (1962) 111:771–3. doi: 10.3181/00379727-111-27917
38. Hiramoto RM, Galisteo AJ, do Nascimento N. And De Andrade, H200 Gy Sterilised Toxoplasma Gondii Tachyzoites Maintain Metabolic Functions and Mammalian Cell Invasion, Eliciting Cellular Immunity and Cytokine Response Similar to Natural Infection in Mice. *F Vaccine* (2002) 20:2072–81. doi: 10.1016/S0264-410X(02)00054-3
39. Secanella-Fandos S, Noguera-Ortega E, Olivares F, Luquin M, Julián E. Killed But Metabolically Active *Mycobacterium Bovis* Bacillus Calmette-Guérin Retains the Antitumor Ability of Live Bacillus Calmette-Guérin. *J Urol* (2014) 191:1422–8. doi: 10.1016/j.juro.2013.12.002
40. Jesudhasan PR, Bhatia SS, Sivakumar KK, Praveen C, Genovese KJ, He HL, et al. Controlling the Colonization of Clostridium Perfringens in Broiler Chickens by an Electron-Beam-Killed Vaccine. *Animals* (2021) 11:671. doi: 10.3390/ani11030671
41. Praveen C, Bhatia SS, Alaniz RC, Droleskey RE, Cohen ND, Jesudhasan PR, et al. Assessment of Microbiological Correlates and Immunostimulatory Potential of Electron Beam Inactivated Metabolically Active Yet Non Culturable (MAyNC) Salmonella Typhimurium. *PloS One* (2021) 16:e0243417. doi: 10.1371/journal.pone.0243417
42. Trampuz A. Effect of Gamma Irradiation on Viability and DNA of Staphylococcus Epidermidis and Escherichia Coli. *J Med Microbiol* (2006) 55:1271–5. doi: 10.1099/jmm.0.46488-0
43. Bhatia SS, Pillai SD. A Comparative Analysis of the Metabolomic Response of Electron Beam Inactivated E. Coli O26:H11 and Salmonella Typhimurium ATCC 13311. *Front Microbiol* (2019) 10:694. doi: 10.3389/fmicb.2019.00694
44. Moore HN, Kersten H. Preliminary Note on the Preparation of Non-Toxic Shiga Dysentery Vaccines by Irradiation With Soft X-Rays. *J Bacteriol* (1936) 31:581–4. doi: 10.1128/jb.31.6.581-584.1936

45. Jordan RT, Kempe LL. Inactivation of Some Animal Viruses With Gamma Radiation From Cobalt-60. *Proc Soc Exp Biol Med* (1956) 91:212–5. doi: 10.3181/00379727-91-22215
46. Tumanyan MA, Duplishcheva AP, Sedova TS. Influence of Massive Doses of $Gamma$-Rays on Immunological Properties of Bacteria of Intestinal Group. *Zhur Mikrobiol Epidemiol i Immunobiol* (1958) 4:3–10.
47. Carpenter CM. Preliminary Report on Vaccines Prepared From Gamma-Irradiated Mycobacterium Tuberculosis and Brucella Suis1, in: *American Review of Tuberculosis and Pulmonary Diseases* (1959). Available at: https://www.atsjournals.org/doi/pdf/10.1164/artpd.1959.79.3.374 (Accessed January 23, 2020).
48. Kaplan C. The Antigenicity of γ-Irradiated Vaccinia Virus. *Epidemiol Infection* (1960) 58:391–8. doi: 10.1017/S0022172400038535
49. Ward RA, Bell LH, Schneider RL. Effects of X-Irradiation on the Development of Malarial Parasites in Mosquitoes. *Exp Parasitol* (1960) 10:324–32. doi: 10.1016/0014-4894(60)90070-9
50. Kalenina EF, Abidov AZ. The Effect of Gamma Rays of Co-60 on Smallpox Vaccine Contaminating Microorganisms(1963). Available at: https://www.osti.gov/biblio/4687625 (Accessed January 23, 2020).
51. Scherließ R, Ajmera A, Dennis M, Carroll MW, Altrichter J, Silman NJ, et al. Induction of Protective Immunity Against H1N1 Influenza A(H1N1)pdm09 With Spray-Dried and Electron-Beam Sterilised Vaccines in Non-Human Primates. *Vaccine* (2014) 32:2231–40. doi: 10.1016/j.vaccine.2014.01.077
52. Sir Karakus G, Tastan C, Kancagi DD, Yurtsever B, Tumentemur G, Demir S, et al. Preliminary Report of Preclinical Efficacy and Safety Analysis of Gamma-Irradiated Inactivated SARS-CoV-2 Vaccine Candidates. (2020). doi: 10.1101/2020.09.04.277426
53. Orr MT, Kramer RM, Barnes LV, Dowling QM, Desbien AL, Beebe EA, et al. Elimination of the Cold-Chain Dependence of a Nanoemulsion Adjuvanted Vaccine Against Tuberculosis by Lyophilization. *J Control Release* (2014) 177:20–6. doi: 10.1016/j.jconrel.2013.12.025
54. Lloyd J, Cheyne J. The Origins of the Vaccine Cold Chain and a Glimpse of the Future. *Vaccine* (2017) 35:2115–20. doi: 10.1016/j.vaccine.2016.11.097
55. Fertey J, Thoma M, Beckmann J, Bayer L, Finkensieper J, Reißhauer S, et al. Automated Application of Low Energy Electron Irradiation Enables Inactivation of Pathogen- and Cell-Containing Liquids in Biomedical Research and Production Facilities. *Sci Rep* (2020) 10:12786. doi: 10.1038/s41598-020-69347-7
56. Surendran N, Hiltbold EM, Heid B, Sriranganathan N, Boyle SM, Zimmerman KL, et al. Heat-Killed and γ-Irradiated Brucella Strain RB51 Stimulates Enhanced Dendritic Cell Activation, But Not Function Compared With the Virulent Smooth Strain 2308. *FEMS Immunol Med Microbiol* (2010) 60:147–55. doi: 10.1111/j.1574-695X.2010.00729.x
57. Oliveira SC, Zhu Y, Splitter GA. Recombinant L7/L12 Ribosomal Protein and Gamma-Irradiated Brucella Abortus Induce a T-Helper 1 Subset Response From Murine CD4+ T Cells. *Immunology* (1994) 83:659–64.
58. Dabral N, Martha-Moreno-Lafont, Sriranganathan N, Vemulapalli R. Oral Immunization of Mice With Gamma-Irradiated Brucella Neotomae Induces Protection Against Intraperitoneal and Intranasal Challenge With Virulent B. Abortus 2308. *PloS One* (2014) 9(9):e107180. doi: 10.1371/journal.pone.0107180
59. Datta SK, Okamoto S, Hayashi T, Shin SS, Mihajlov I, Fermin A, et al. Vaccination With Irradiated Listeria Induces Protective T Cell Immunity. *Immunity* (2006) 25:143–52. doi: 10.1016/j.immuni.2006.05.013
60. Ahmed S, Ahmed BS, Mahmoud GI, Nemr W. And Rahim, E Comparative Study Between Formalin-Killed Vaccine and Developed Gammairradiation Vaccine Against Mannheimia haemolytica in Rabbits. *Turk J Vet Anim Sci* (2016) 40:19–224. doi: 10.3906/vet-1504-34
61. Jerrells TR, Palmer BA, Osterman JV. Gamma-Irradiated Scrub Typhus Immunogens: Development of Cell-Mediated Immunity After Vaccination of Inbred Mice. *Infect Immun* (1983) 39:262–9. doi: 10.1128/iai.39.1.262-269.1983
62. Eisenberg GHG, Osterman JV. Gamma-Irradiated Scrub Typhus Immunogens: Development and Duration of Immunity. *Infect Immun* (1978) 22:80–6. doi: 10.1128/iai.22.1.80-86.1978
63. Gordon M, Donaldson DM, Wright GG. Immunization of Mice With Irradiated Pasteurella Tularensis. *J Infect Dis* (1964) 114:435–40. doi: 10.1093/infdis/114.5.435
64. Rocha JN, Cohen ND, Bordin AI, Brake CN, Giguère S, Coleman MC, et al. Oral Administration of Electron-Beam Inactivated Rhodococcus Equi Failed to Protect Foals Against Intrabronchial Infection With Live, Virulent R. Equi. *PloS One* (2016) 11:1–18. doi: 10.1371/journal.pone.0148111
65. Fertey J, Bayer L, Kähl S, Haji RM, Burger-Kentischer A, Thoma M, et al. Low-Energy Electron Irradiation Efficiently Inactivates the Gram-Negative Pathogen Rodentibacter Pneumotropicus—A New Method for the Generation of Bacterial Vaccines With Increased Efficacy. *Vaccines (Basel)* (2020) 8:113–24. doi: 10.3390/vaccines8010113
66. Jesudhasan PR, McReynolds JL, Byrd AJ, He H, Genovese KJ, Droleskey R, et al. Electron-Beam-Inactivated Vaccine Against Salmonella Enteritidis Colonization in Molting Hens. *Avian Dis* (2015) 59:165–70. doi: 10.1637/10917-081014-ResNoteR
67. Kogut MH, McReynolds JL, He H, Genovese KJ, Jesudhasan PR, Davidson MA, et al. Electron-Beam Irradiation Inactivation of Salmonella: Effects on Innate Immunity and Induction of Protection Against Salmonella Enterica Serovar Typhimurium Challenge of Chickens. *Proc Vaccinology* (2012) 6:47–63. doi: 10.1016/j.provac.2012.04.008
68. Begum RH, Rahman H, Ahmed G. Development and Evaluation of Gamma Irradiated Toxoid Vaccine of Salmonella Enterica Var Typhimurium. *Vet Microbiol* (2011) 153:191–7. doi: 10.1016/j.vetmic.2011.06.013
69. van Diemen PM, Yamaguchi Y, Paterson GK, Rollier CS, Hill AVS, Wyllie DH. Irradiated Wild-Type and Spa Mutant Staphylococcus Aureus Induce Anti- S. Aureus Immune Responses in Mice Which do Not Protect Against Subsequent Intravenous Challenge. *Pathog Dis* (2013) 68:20–6. doi: 10.1111/2049-632X.12042
70. Gaidamakova EK, Myles IA, McDaniel DP, Fowler CJ, Valdez PA, Naik S, et al. Preserving Immunogenicity of Lethally Irradiated Viral and Bacterial Vaccine Epitopes Using a Radio- Protective Mn2+-Peptide Complex From Deinococcus. *Cell Host Microbe* (2012) 12:117–24. doi: 10.1016/j.chom.2012.05.011
71. Babb R, Chen A, Hirst TR, Kara EE, McColl SR, Ogunniyi AD, et al. Intranasal Vaccination With γ-Irradiated Streptococcus Pneumoniae Whole-Cell Vaccine Provides Serotype-Independent Protection Mediated by B-Cells and Innate IL-17 Responses. *Clin Sci* (2016) 130:697–710. doi: 10.1042/CS20150699
72. Pawlowski A, Svenson SB. Electron Beam Fragmentation of Bacterial Polysaccharides as a Method of Producing Oligosaccharides for the Preparation of Conjugate Vaccines. *FEMS Microbiol Lett* (1999) 174:255–63. doi: 10.1111/j.1574-6968.1999.tb13577.x
73. Thabet A, Schmäschke R, Fertey J, Bangoura B, Schönfelder J, Lendner M, et al. Eimeria Tenella Oocysts Attenuated by Low Energy Electron Irradiation (LEEI) Induce Protection Against Challenge Infection in Chickens. *Vet Parasitol* (2019) 266:18–26. doi: 10.1016/j.vetpar.2019.01.001
74. Jenkins MC, Augustine PC, Danforth HD, Barta JR. X-Irradiation of Eimeria Tenella Oocysts Provides Direct Evidence That Sporozoite Invasion and Early Schizont Development Induce a Protective Immune Response(s). *Infect Immun* (1991) 59:4042–8. doi: 10.1128/iai.59.11.4042-4048.1991
75. Nussenzweig RS, Vanderberg J, Most H, Orton C. Protective Immunity Produced by the Injection of X-Irradiated Sporozoites of Plasmodium Berghei. *Nature* (1967) 216:160–2. doi: 10.1038/216160a0
76. Hoffman SL, Goh LML, Luke TC, Schneider I, Le TP, Doolan DL, et al. Protection of Humans Against Malaria by Immunization With Radiation-Attenuated Plasmodium Falciparum Sporozoites. *J Infect Dis* (2002) 185:1155–64. doi: 10.1086/339409
77. Bayer L, Fertey J, Ulbert S, Grunwald T. Immunization With an Adjuvanted Low-Energy Electron Irradiation Inactivated Respiratory Syncytial Virus Vaccine Shows Immunoprotective Activity in Mice. *Vaccine* (2018) 36:1561–9. doi: 10.1016/j.vaccine.2018.02.014
78. Müllbacher A, Ada GL, Hla RT. Gamma-Irradiated Influenza A Virus can Prime for a Cross-Reactive and Cross-Protective Immune Response Against Influenza A Viruses. *Immunol Cell Biol* (1988) 66:153–7. doi: 10.1038/icb.1988.19
79. Furuya Y, Chan J, Wan E-C, Koskinen A, Diener KR, Hayball JD, et al. Gamma-Irradiated Influenza Virus Uniquely Induces IFN-I Mediated Lymphocyte Activation Independent of the TLR7/MyD88 Pathway. *PloS One* (2011) 6:e25765. doi: 10.1371/journal.pone.0025765
80. Furuya Y, Chan J, Regner M, Lobigs M, Koskinen A, Kok T, et al. Cytotoxic T Cells Are the Predominant Players Providing Cross-Protective Immunity Induced by -Irradiated Influenza A Viruses. *J Virol* (2010) 84:4212–21. doi: 10.1128/JVI.02508-09

81. David SC, Lau J, Singleton EV, Babb R, Davies J, Hirst TR, et al. The Effect of Gamma-Irradiation Conditions on the Immunogenicity of Whole-Inactivated Influenza A Virus Vaccine. *Vaccine* (2017) 35:1071–9. doi: 10.1016/j.vaccine.2016.12.044
82. Fertey J, Bayer L, Grunwald T, Pohl A, Beckmann J, Gotzmann G, et al. Pathogens Inactivated by Low-Energy-Electron Irradiation Maintain Antigenic Properties and Induce Protective Immune Responses. *Viruses* (2016) 8:319–33. doi: 10.3390/v8110319
83. Alsharifi M, Furuya Y, Bowden TR, Lobigs M, Koskinen A, Regner M, et al. Intranasal Flu Vaccine Protective Against Seasonal and H5N1 Avian Influenza Infections. *PloS One* (2009) 4:e5336. doi: 10.1371/journal.pone.0005336
84. Agrawal AS, Tao X, Algaissi A, Garron T, Narayanan K, Peng B-H, et al. Immunization With Inactivated Middle East Respiratory Syndrome Coronavirus Vaccine Leads to Lung Immunopathology on Challenge With Live Virus. *Hum Vaccin Immunother* (2016) 12:2351–6. doi: 10.1080/21645515.2016.1177688
85. Tobin GJ, Tobin JK, Gaidamakova EK, Wiggins TJ, Bushnell RV, Lee W-M, et al. A Novel Gamma Radiation-Inactivated Sabin-Based Polio Vaccine. *PloS One* (2020) 15:e0228006. doi: 10.1371/journal.pone.0228006
86. Shahrudin S, Chen C, David SC, Singleton EV, Davies J, Kirkwood CD, et al. Gamma-Irradiated Rotavirus: A Possible Whole Virus Inactivated Vaccine. *PloS One* (2018) 13:e0198182. doi: 10.1371/journal.pone.0198182
87. Turan RD, Tastan C, Kancagi DD, Yurtsever B, Karakus GS, Ozer S, et al. Gamma-Irradiated SARS-CoV-2 Vaccine Candidate, OZG-38.61.3, Confers Protection From SARS-CoV-2 Challenge in Human ACEII-Transgenic Mice. *Sci Rep* (2021) 11, 15799. doi: 10.1038/s41598-021-95086-4
88. Reitman M, Tribble HR, Green L. Gamma-Irradiated Venezuelan Equine Encephalitis Vaccines. *Appl Microbiol* (1970) 19:763–7. doi: 10.1128/am.19.5.763-767.1970
89. Martin SS, Bakken RR, Lind CM, Garcia P, Jenkins E, Glass PJ, et al. Comparison of the Immunological Responses and Efficacy of Gamma Irradiated V3526 Vaccine Formulations Against Subcutaneous and Aerosol Challenge With Venezuelan Equine Encephalitis Virus Subtype IAB. *Vaccine* (2010) 28:1031–40. doi: 10.1016/j.vaccine.2009.10.126
90. Motamedi-Sedeh F, Afsharnasab M, Heidarieh M, Tahami SM. Protection of Litopenaeus Vannamei Against White Spot Syndrome Virus by Electron-Irradiated Inactivated Vaccine and Prebiotic Immunogen. *Radiat Phys Chem* (2017) 130:421–5. doi: 10.1016/j.radphyschem.2016.09.020
91. Marzi A, Halfmann P, Hill-Batorski L, Feldmann F, Shupert WL, Neumann G, et al. An Ebola Whole-Virus Vaccine Is Protective in Nonhuman Primates. *Science* (2015) 348:439–42. doi: 10.1126/science.aaa4919
92. Geisbert TW, Pushko P, Anderson K, Smith J, Davis KJ, Jahrling PB. Evaluation in Nonhuman Primates of Vaccines Against Ebola Virus. *Emerg Infect Dis* (2002) 8:503–7. doi: 10.3201/eid0805.010284
93. Clyde DF. Immunity to Falciparum and Vivax Malaria Induced by Irradiated Sporozoites: A Review of the University of Maryland Studie-75. *Bull World Health Organ* (1990) 68 Suppl:9–12.
94. Rieckmann KH. Human Immunization With Attenuated Sporozoites. *Bull World Health Organ* (1990) 68 Suppl:13–6.
95. Luke TC, Hoffman SL. Rationale and Plans for Developing a Non-Replicating, Metabolically Active, Radiation-Attenuated Plasmodium Falciparum Sporozoite Vaccine. *J Exp Biol* (2003) 206:3803–8. doi: 10.1242/jeb.00644
96. Seder RA, Chang L-J, Enama ME, Zephir KL, Sarwar UN, Gordon IJ, et al. Protection Against Malaria by Intravenous Immunization With a Nonreplicating Sporozoite Vaccine. *Science* (2013) 341:1359–65. doi: 10.1126/science.1241800
97. Arévalo-Herrera M, Vásquez-Jiménez JM, Lopez-Perez M, Vallejo AF, Amado-Garavito AB, Céspedes N, et al. Protective Efficacy of Plasmodium Vivax Radiation-Attenuated Sporozoites in Colombian Volunteers: A Randomized Controlled Trial. *PloS Negl Trop Dis* (2016) 10(10):e0005070. doi: 10.1371/journal.pntd.0005070
98. Vemulapalli R, Cravero S, Calvert CL, Toth TE, Sriranganathan N, Boyle SM, et al. Characterization of Specific Immune Responses of Mice Inoculated With Recombinant Vaccinia Virus Expressing an 18-Kilodalton Outer Membrane Protein of Brucella Abortus. *Clin Diagn Lab Immunol* (2000) 7:114–8. doi: 10.1128/CDLI.7.1.114-118.2000
99. Alamuti MM, Ravanshad M, Motamedi-Sedeh F, Nabizadeh A, Ahmadi E, Hossieni SM. Immune Response of Gamma-Irradiated Inactivated Bivalent Polio Vaccine Prepared Plus Trehalose as a Protein Stabilizer in a Mouse Model. *INT* (2021) 64:140–6. doi: 10.1159/000515392
100. Sabbaghi A, Zargar M, Zolfaghari MR, Motamedi-Sedeh F, Ghaemi A. Protective Cellular and Mucosal Immune Responses Following Nasal Administration of a Whole Gamma-Irradiated Influenza A (Subtype H1N1) Vaccine Adjuvanted With Interleukin-28B in a Mouse Model. *Arch Virol* (2021) 166:545–57. doi: 10.1007/s00705-020-04900-3
101. Pillai SD, Pillai ET. Agriculture: Electron Beam Irradiation Technology Applications in the Food Industry. In: E Greenspan, editor. *Encyclopedia of Nuclear Energy*. Oxford: Elsevier (2021). p. 313–29. doi: 10.1016/B978-0-12-819725-7.00141-0
102. Beniac DR, deVarennes SL, Andonov A, He R, Booth TF. Conformational Reorganization of the SARS Coronavirus Spike Following Receptor Binding: Implications for Membrane Fusion. *PloS One* (2007) 2:e1082. doi: 10.1371/journal.pone.0001082
103. Durante M, Schulze K, Incerti S, Francis Z, Zein S, Guzmán CA. Virus Irradiation and COVID-19 Disease. *Front Phys* (2020) 8:565861. doi: 10.3389/fphy.2020.565861
104. Mullbacher A, Pardo J, Furuya Y. SARS-CoV-2 Vaccines: Inactivation by Gamma Irradiation for T and B Cell Immunity. *Pathogens* (2020) 9:928. doi: 10.3390/pathogens9110928
105. Sir Karakus G, Tastan C, Dilek Kancagi D, Yurtsever B, Tumentemur G, Demir S, et al. Preclinical Efficacy and Safety Analysis of Gamma-Irradiated Inactivated SARS-CoV-2 Vaccine Candidates. *Sci Rep* (2021) 11:5804. doi: 10.1038/s41598-021-83930-6
106. Bhatia SS. *Investigations Into Metabolically Active Yet Non-Culturable (MAyNC) Clostridium Perfringens to Control Necrotic Enteritis in Broiler Chickens* (2021). Available at: https://oaktrust.library.tamu.edu/handle/1969.1/193108 (Accessed November 9, 2021).

Conflict of Interest: The authors declare that the research was conducted in the absence of any commercial or financial relationships that could be constructed as a potential conflict of interest.

frontiers in Immunology

ORIGINAL RESEARCH
published: 15 February 2022
doi: 10.3389/fimmu.2022.851028

A First for Human Vaccinology: GMP Compliant Radiation Attenuation of *Plasmodium falciparum* Sporozoites for Production of a Vaccine Against Malaria

Eric R. James, Steve Matheny, James Overby, B. Kim Lee Sim, Abraham G. Eappen, Tao Li, Ming Lin Li, Thomas L. Richie, Sumana Chakravarty, Anusha Gunasekera, Tooba Murshedkar, Peter F. Billingsley and Stephen L. Hoffman*

Sanaria Inc., Rockville, MD, United States

OPEN ACCESS

Edited by:
Viskam Wijewardana, International Atomic Energy Agency, Austria

Reviewed by:
Takafumi Tsuboi, Ehime University, Japan
Else Bijker, University of Oxford, United Kingdom

***Correspondence:**
Eric R. James
ejames@sanaria.com

Specialty section:
This article was submitted to Vaccines and Molecular Therapeutics, a section of the journal Frontiers in Immunology

Received: *08 January 2022*
Accepted: *25 January 2022*
Published: *15 February 2022*

Citation:
James ER, Matheny S, Overby J, Sim BKL, Eappen AG, Li T, Li ML, Richie TL, Chakravarty S, Gunasekera A, Murshedkar T, Billingsley PF and Hoffman SL (2022) A First for Human Vaccinology: GMP Compliant Radiation Attenuation of Plasmodium falciparum Sporozoites for Production of a Vaccine Against Malaria. Front. Immunol. 13:851028. doi: 10.3389/fimmu.2022.851028

Ionizing radiation (UV, X-ray and ɣ) administered at an appropriate dose to pathogenic organisms can prevent replication while preserving metabolic activity. We have established the GMP process for attenuation by ionizing radiation of the *Plasmodium falciparum* (Pf) sporozoites (SPZ) in Sanaria® PfSPZ Vaccine, a protective vaccine against malaria. Mosquitoes raised and infected aseptically with Pf were transferred into infected mosquito transport containers (IMTC) and ɣ-irradiated using a ^{60}Co source. PfSPZ were then extracted, purified, vialed, and cryopreserved. To establish the appropriate radiation conditions, the irradiation field inside the IMTCs was mapped using radiochromic film and alanine transfer dosimeters. Dosimeters were irradiated for times calculated to provide 120-170 Gy at the minimum dose location inside the IMTC and regression analysis was used to determine the time required to achieve a lower 95% confidence interval for 150 Gy. A formula incorporating the half-life of ^{60}Co was then used to construct tables of irradiation times for each calendar day. From the mapping studies, formulae were derived to estimate the minimum and maximum doses of irradiation received inside the IMTC from a reference dosimeter mounted on the outside wall. For PfSPZ Vaccine manufacture a dose of 150 Gy was targeted for each irradiation event, a dose known to completely attenuate PfSPZ. The reference dosimeters were processed by the National Institute of Standards and Technology. There have been 587 irradiation events to produce PfSPZ Vaccine during 13 years which generated multiple lots released for pre-clinical studies and clinical trials. The estimated doses at the minimum dose location (mean 154.3 ± 1.77 Gy; range 150.0-159.3 Gy), and maximum dose location (mean 166.3 ± 3.65 Gy, range 155.7 to 175.3 Gy), in IMTCs were normally distributed. Overall dose uniformity was 1.078 ± 0.012. There was no siginifcant change in measured dose over 13 years. As of January 2022, 21 clinical trials of PfSPZ Vaccine have been conducted, with 1,740 volunteers aged 5 months to 61 years receiving 5,648 doses of PfSPZ Vaccine totalling >5.3 billion

PfSPZ administered. There have been no breakthrough infections, confirming the consistency and robustness of the radiation attenuation process.

Keywords: radiation, attenuation, malaria, sporozoite, vaccine

INTRODUCTION

Radiation wavelengths shorter than ~124 nm that include far-UV, X-ray and ɣ, induce ionization effects that damage live cells principally through the generation of free radicals and their interaction with proteins, membranes and DNA. The dose of radiation can be selected to render cells or whole organisms metabolically active but incapable of replication. Used on eukaryotic pathogens, irradiation is an ideal method for developing live attenuated vaccines that are immunogenic and for which the ability to cause disease has been abrogated. Ionizing radiation of all three types has been used to attenuate parasitic protozoa and helminths (1–9)[1].

The pioneering studies on attenuation of malaria sporozoites (SPZ) for assessing protective immunity were conducted with X-ray as the irradiation source (10). Subsequent studies used X-rays and ɣ irradiation, sourced either from ^{137}Cs or ^{60}Co (11–14). Sanaria®PfSPZ Vaccine is composed of SPZ, the infective stage of *Plasmodium falciparum* (Pf), that are irradiated in the mosquito using a ^{60}Co source and subsequently extracted from the mosquito salivary glands, purified, formulated with cryoprotectant additives and cryopreserved (15, 16). In clinical trials, PfSPZ Vaccine induces >90% protection against controlled human malaria infection (CHMI) delivered by mosquito bite or by injection (17–19) and significant protection for at least two malaria transmission seasons against natural exposure to malaria in Africa (20). Attenuation by ɣ irradiation was adopted for the manufacture of PfSPZ Vaccine principally due to the ability to deliver a very accurate irradiation dose, shorter irradiation times than X-ray, ease of use, and a history of success in human trials (14) that used PfSPZ administered by the bite of Pf-infected, irradiated mosquitoes for immunizations.

We present here the process for development of a robust and reproducible method for the ɣ-irradiation of PfSPZ-infected mosquitoes delivered by a ^{60}Co source, and the experience of using this method in the manufacture of PfSPZ Vaccine for clinical trials.

MATERIALS AND METHODS

Irradiator

The irradiator, a JL Shepherd model 484-R-2, has three sources, an integral controller incorporating a timer and an air compressor with reservoir. The unit is fabricated principally from cast iron and lead, weighs approximately 6.5 metric tons, and houses the shielded irradiation chamber (**Figure 1**). The unit is calibrated annually by JL Shepherd (San Fernando, CA), and the controller and monitoring systems are calibrated independently every six months.

When installed in 2007, source tunnels 2 (center) and 3 (right) contained cobalt capsules with a total activity of 12,000 Ci. Nine years later, the ^{60}Co had decayed through 1.9 half lives to 3,349 Ci so the ^{60}Co capsule occupying source tunnel 2 was moved into source tunnel 1, and a new capsule with 8,400 Ci activity was added to source tunnel 2 to bring the total activity to 11,749 Ci. Sources are registered with the Nuclear Regulatory Commission and checked annually. In addition to the three source tunnels, the irradiator chamber contains a turntable that rotates at approximately 17 revolutions per minute and can be used at any of five positions at different distances from the irradiation sources. Turntable position 3 is used for IMTC mosquito irradiation (**Figure 1**).

Personnel qualified to operate the irradiator undergo FBI background checks, fingerprinting, and are issued a unique coded card for entry. Other security measures include a second coded door entry, a third door linked to an iris scanner, video surveillance at multiple locations and direct real-time video feed to the County Police Department (CPD) with an on-call Special Weapons and Tactics (SWAT) team.

Residual radiation around the irradiator both at rest and when active is equivalent to background, as indicated by routine dosimetry (processed quarterly) from multiple locations in the irradiator room. However, Sanaria provides operators with personal dosimeters that are maintained by a contract Radiation Safety Officer and processed by Landauer (Beltsville, MD). A survey meter (Technical Associates, Canoga Park, CA) connected to the irradiator controller broadcasts an alarm internally and to the CPD if radiation levels exceed threshold for safety or if the meter is disconnected or disabled. Additional monitoring and alarm systems are integral to the unit.

Infected Mosquito Transport Container (IMTC)

Aseptically-reared PfSPZ-infected *Anopheles stephensi* mosquitoes are transferred to Infected Mosquito Transport Containers (IMTC) for aseptic transport to the irradiator. The IMTC consists of a custom designed outer container (OC) fabricated from polycarbonate and composed of a cylinder with a screw-on base and a screw lid that incorporates a filter (**Figure 2**). The IMTC is assembled with the inner container (IC), a modified 1-pint cardboard cylinder, autoclaved, and mosquitoes are aspirated under aseptic conditions directly into the IC from the adult mosquito containers. Each IMTC is sealed inside a sterility maintenance bag (Steris, Erie, PA) which remains in place during irradiation. IMTCs were fabricated with the base able to fit within the circular wall of the

[1] https://www.vmd.defra.gov.uk/productinformationdatabase/files/QRD_Documents/QRD-Auth_1189554.PDF.

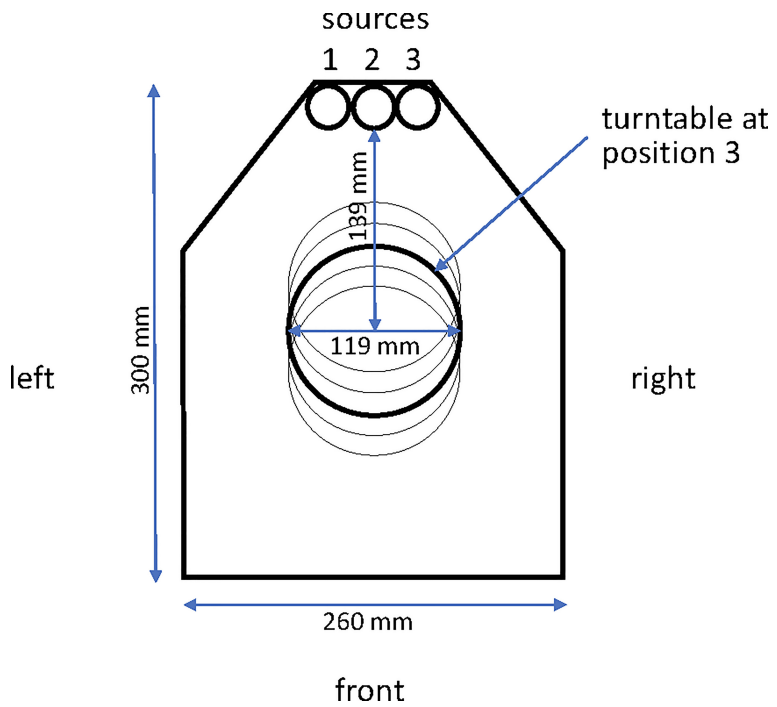

FIGURE 1 | Plan view of the interior of the irradiator chamber. The three source tunnels (left #1, center #2 and right #3) are indicated at the apex of the drawing and the turntable is indicated at position 3 (of 5 potential positions) in the central axis of the chamber.

irradiator chamber turntable and with a base thickness aimed to position the center of the vertical axis of the IC in the center of the irradiation field in the chamber.

Radiochromic Film Mapping of the IMTC

The radiation dose received at any point in the irradiator chamber is inversely proportional to the distance from the sources. Thus the dose delivered inside the IMTC will vary both horizontally and vertically. By mapping the radiation field using radiochromic film, the maximum dose and minimum dose locations inside the IMTC can be identified (21). Two sets of radiochromic film mapping experiments were conducted, the first initially after the irradiator was installed and the second following the irradiator upgrade nine years later.

The first determination of the irradiation field was conducted inside the OC of the IMTC using GAFchromic HD-810 film [International Specialty Products (ISP), Wayne, NJ] rated for a dose range of 10-400 Gy. The film was trimmed to fit vertically into the OC, sandwiched between polystyrene plates and sealed in a black polyethylene pouch. Two different OCs were mapped using an irradiation time (provided by JL Shepherd) to target a dose on that particular day of 150 Gy in the center of the OC when the IMTC was placed on the turntable at position 3. The films were removed from their packaging at the National Institute of Standards and Technology (NIST, Gaithersburg, MD), and scanned into a Pharmacia-LKB 2222 UltroScan XL Laser Densitometer at 633 nm with a spot size of 100 µm. Measurements were made by stepping in both dimensions at a resolution of 0.6 mm. The data output was in arbitrary scanning laser densitometer (SLD) units related to optical absorbance. Average SLD values were determined at the film's center, and the value used to normalize to the whole scan and to express the results in terms of percent increase or decrease relative to the dose at the center.

An additional set of radiochromic film assessments was made following the irradiator upgrade to confirm the distribution of the delivered radiation dose applied to the IC and confirm the minimum and maximum dose locations. Gafchromic Ashland Dose-Map™ film with an upper exposure bound of 50 Gy was sandwiched between Plexiglas sheets and sealed in black polypropylene. This smaller film package was supported inside the IC along the central vertical axis. An alanine transfer dosimeter was also placed on the outside of the OC of the IMTC at location B (**Figure 2**), and the IMTC exposed to a target dose of 50 Gy at the maximum dose location inside the IC.

Alanine Transfer Dosimeter Mapping of the IMTC

To further characterize the distribution of radiation received by the IMTC and to determine the doses received at the minimum and maximum dose locations when targeting a received minimum dose of 150 Gy, the IC of the IMTC was also mapped using alanine transfer dosimeters (22–25). Alanine dosimeters (NIST High Dose Radiation Service, Gaithersburg, MD) were composed of Plexiglas vials each containing four

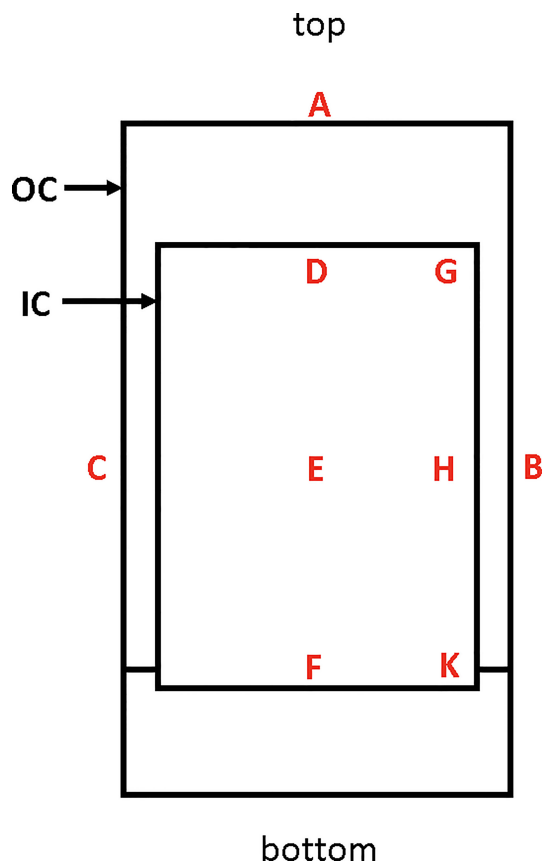

FIGURE 2 | Sagittal sectional schematic diagram of an IMTC. The inner container (IC) is housed inside the outer container (OC), which is a custom machined 1 L polycarbonate container with screw top and screw base. All nine locations used for placement of alanine transfer dosimeters for mapping are indicated. The minimum dose of irradiation was recorded at position F up to the time when a new IC was incorporated when the minimum dose location changed to D. The maximum dose location is position H. The reference dosimeter used in PfSPZ Vaccine manufacturing runs is located at position B. The relationship between the dose received at B to the dose received at D (or previously, F) and between the dose at B and the dose at H are used to generate the formulae for estimating the doses at positions D/F and H during vaccine production.

alanine pellets. The dosimeters were positioned at the locations indicated in **Figure 2**. After irradiation, dosimeters were processed by NIST and the average dose received by the four pellets inside each Plexiglas vial was reported to the nearest whole Gy for that dosimeter.

Dosimetry to Determine the Irradiation Time for the Target Minimum Dose of 150 Gy

Dosimeters located at the minimum dose location were irradiated on a specific date for times calculated to deliver doses ranging from 120 Gy to 170 Gy. Dosimeters were processed as above and the data for irradiation time and dose received by each dosimeter, were used in a regression analysis, including the upper and lower 95% confidence intervals, to determine the time required to deliver 150 Gy of radiation at the minimum dose location on that date. The value was also used to extrapolate back to the reference date when the irradiator was installed. This experiment was repeated after the irradiator source upgrade.

Time Table for Irradiation

Two irradiation time tables were constructed spanning 1) the period from initial installation of the irradiator to the upgrade nine years later, and 2) all dates during the subsequent six years. For both timetables the baseline date was defined as the reference date from which to calculate the times to deliver the target minimum dose on all subsequent days according to the equation:

$$t = x * \left(\frac{1}{0.5^{\left(\frac{y}{T}\right)}} \right) \qquad \text{Equation 1}$$

where:
t = time in minutes for the day of interest,
x = time in minutes at reference date,
y = number of days since reference date, and
T = ½ life of ^{60}Co in days (1925.20 days).

Use of a Reference Dosimeter and Estimation of the Minimum and maximum doses Delivered to Mosquitoes

The minimum and maximum doses of irradiation received by any mosquito inside the IMTC were estimated from the dose received by a dosimeter attached to the outside of the IMTC at location B (reference location) (**Figure 2**). To determine the formulae for estimating the dose received at the minimum dose location (location D or F) and the maximum dose location (location H) inside the IMTC from the dose received at the reference location, dosimeters were mounted on a cardboard scaffold at the three locations in the IC and at the external reference location.

Three sets of data were collected following installation of the irradiator, three more sets were collected when the irradiator was upgraded, and a final three sets were collected when the original IC was replaced by a new IC of slightly different dimensions. This last data set resulted in the minimum dose location changing from location F to location D (**Figure 2**).

In Vitro Assessment of Attenuation

In addition to dosimetry, the 6-day hepatocyte attenuation assay, a biological measure used to confirm attenuation, was performed using irradiated PfSPZ without cryopreservation (26); the result of this assay, along with the dosimetry data, is incorporated into the lot release certificate of analysis for PfSPZ Vaccine.

Irradiation Data From PfSPZ Vaccine Manufacture

A manufacturing campaign for PfSPZ Vaccine consists of multiple sequential irradiation runs, generally up to 16. An alanine dosimeter is included at the reference location on the outside of each IMTC for every irradiation run. The irradiation time for any given date is indicated in the irradiation timetables.

All dosimeters are processed by NIST. The data for the estimated doses delivered to the minimum dose location were calculated for all runs from the doses reported for the reference dosimeter.

RESULTS

Mapping of the Infected Mosquito Transport Container (IMTC) to Determine the Minimum and Maximum Dose Locations

The purpose of these experiments was to determine the relative radiation dose delivered spatially, which is independent of a particular target dose or dose rate. Three pairs of radiochromic film images were recorded for the original study in the OC of the IMTC. After the first pair of images was obtained, the vertical positioning of the OC was adjusted upwards to improve the vertical gradient of received dose. An additional adjustment to the configuration of the IMTC was made after the second pair of images was obtained; results for the third pair are shown in **Figure 3**. Radiation exposure followed a gradient, with the highest dose received at the vertical midpoint on the side wall decreasing to the center of the OC and decreasing further both upwards and downwards along the central vertical axis. The lowest doses were recorded at the top center and bottom center of the OC.

Following upgrading of the irradiator, GAF chromic film was provided cut to fit the inside of the IC. For the three films the mean dose ± SD at the minimum dose location (position F) was 38.8 ± 0.64 Gy, and at the maximum dose location (position H) was 47.1 ± 0.25 Gy (**Figure 4**, **Table 1**). The dose uniformity, the ratio of highest dose to lowest dose, (dose at position H/dose at position F) was 1.216 ± 0.014 for this film using a target dose of 50 Gy.

IMTC (IC) Mapping by Alanine Dosimetry

Experiments were conducted using alanine transfer dosimeters with a dose calculated to deliver 150 Gy to the minimum dose location. The most recent set of these experiments was performed after the changeover to the new IC in the IMTC. These studies used dosimeters placed at the six locations inside the IC (**Figure 2**) to define the minimum and maximum dose locations, and two dosimeters on the exterior of the IMTC at positions A and B (**Figure 2**). In this study, dose uniformity was tighter at 1.09 ± 0.004 (**Table 2**) than seen with GAF chromic film. This alanine dosimeter mapping study also established that the minimum dose was received at location D (154 ± 1.0 Gy) rather than location F (155 ± 1.0 Gy). This change in minimum dose location was a consequence of the changeover to the new IC of the IMTC which was, as indicated above, slightly taller (by 8.7 mm). The position of the base of the IC is fixed, so that the additional height of the IC moved the top of the IC and the minimum dose location higher up the vertical axis of the unit into a lower isodose band. The ratios between the minimum dose and the reference dose (0.834 ± 0.008) and the maximum dose and the reference dose (0.908 ± 0.005) were also established for estimating the minimum and maximum doses delivered during PfSPZ Vaccine production runs. For example, if the dosimeter at the reference location received a dose of 182 Gy, then 151.8 Gy and 165.3 Gy would be received at the minimum and maximum dose locations, respectively, and the dose uniformity (ratio of highest dose to lowest dose), would be 1.089.

Dose Titration

Dosimeters placed at the minimum dose location in the IC of the IMTC were irradiated for different times to deliver doses between 120 and 170 Gy. Regression analysis of irradiation time vs. dose was used to determine the time to deliver a dose of 150 Gy with lower 95% confidence interval (**Figures 5A, B**). This dose was defined as the target minimum dose and the time to deliver this dose extrapolated from the regression analysis as the time on that date to deliver the target dose of irradiation. This time was then extended to the reference date and that value incorporated as the reference time (x in Equation 1) for constructing the calendar of irradiation timetables.

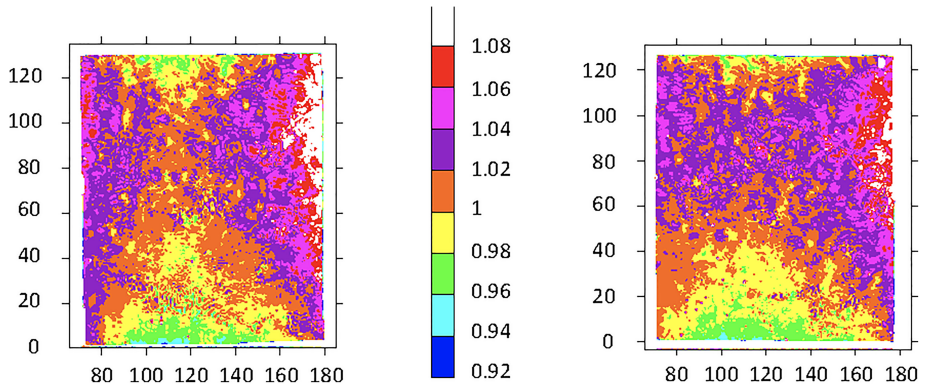

FIGURE 3 | Test film results from two OCs exposed to 150 Gy. The target dose delivered was 150 Gy. The color scale represents proportional arbitrary scanning laser densitometry units normalized to 312 SLD units left, and to 320 SLD units right. The boundary between orange and yellow was assigned a value of 1. Horizontal axis: units in mm relative to the scanner base plate; vertical axis: distance in mm from the bottom of the film/container. See **Figure 2** for the minimum dose locations (position F, bottom center of each film) and maximum dose locations (position H, at the side wall equator of each film).

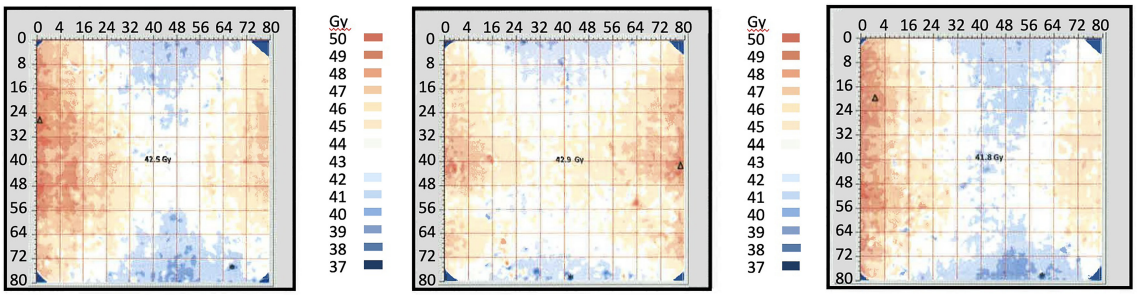

FIGURE 4 | Radiochromic film mapping of the IC of the IMTCs: three runs. The image from run 1 is at left, from run 2 in the center and from run 3 is at right. The dose received at the center of the film (position E) was 42.9 Gy (run 1), 41.8 Gy (run 2) and 42.5 Gy (run 3). See **Table 2** for dose levels recorded for the minimum dose locations (position F, bottom center of each film) and maximum dose locations (position H, at the side wall equator of each film).

Dosimetry for PfSPZ Vaccine Production

The estimated irradiation doses at the minimum dose location (locations F or D) in the IC were calculated using the formulae obtained by dosimetry. Three different sets of conversion factors were used following dosimetry calibration of the irradiator for 1) the period when two sources were active in the irradiator (first 9 years), 2) after the irradiator upgrade when all three sources were active (next 4 years), and 3) after introduction of the new IC (all subsequent times). For all irradiation runs the PfSPZ-infected mosquitoes were irradiated at ambient temperature inside the irradiator chamber which was typically 23°C, a temperature optimum for PfSPZ (26).

For the initial 9-year period the formula for estimating the dose received at location F was x0.8973 and for estimating the maximum dose at location H, the formula used was x0.9471. For the 4 years after the irradiator upgrade the conversion factor used for the dose at location F was x0.845, and for the maximum dose location H, was x0.9141. The current conversion factor used to estimate the minimum dose at location D from the dose received at location B for the period of 2019-present shown in **Table 2** is x0.834, and to convert the dose at location B to the estimated dose at the maximum dose location, location H, the conversion factor is x0.908.

The estimated minimum dose received in each of 587 irradiation events during GMP manufacturing of PfSPZ Vaccine was very consistent (**Figure 6**), ranging from 150.0 Gy to 159.3 Gy, with a mean estimated minimum dose of 154.3 ± 1.77 Gy. The mean estimated maximum dose delivered in all irradiation runs was 166.3 ± 3.65 Gy, (range 155.7 Gy to 175.3 Gy), well below the highest acceptable maximum dose of 190 Gy. The overall dose uniformity was 1.078 ± 0.012.

The viability of PfSPZ in production lots is assessed using a sporozoite membrane integrity assay (SMIA), and is routinely conducted on vaccine bulk product prior to fill-finish. The SMIA results for PfSPZ Vaccine (radiation-attenuated) and PfSPZ Challenge (non-irradiated) have been published previously on several occasions: for example, the viability of PfSPZ after irradiation and prior to cryopreservation was reported as 97% (17) and for non-irradiated PfSPZ prior to cryopreservation the viability has been reported as 98.2% (27).

Clinical Trials of Radiation-Attenuated PfSPZ in PfSPZ Vaccine

In the 21 clinical trials conducted to date using radiation-attenuated PfSPZ, 1,740 volunteers aged 5 months to 61 years have received 5,648 doses of PfSPZ Vaccine, meaning that >5.3 x

TABLE 1 | Radiation doses recorded in the ICs of the IMTCs in the radiochromic film study in **Figure 4**.

Data source	Position in IMTC	Run Number			Mean ± SD
		1	2	3	
		Radiation dose received (Gy)			
Alanine dosimeter	B	49.6	49.7	49.4	49.6 ± 0.15
Radiochromic film	E	42.9	41.8	42.5	42.4 ± 0.56
	F	38.3	38.5	39.5	38.8 ± 0.64
	H	46.9	47.1	47.4	47.1 ± 0.25
		Radiation dose ratio			
Dose uniformity	H/F	1.225	1.223	1.200	1.216 ± 0.014
Adjustment factor, minimum dose	F/B	0.772	0.775	0.800	0.782 ± 0.015
Adjustment factor, maximum dose	H/B	0.946	0.948	0.960	0.951 ± 0.008

The doses received at the center of each film (location E), at the minimum dose location (location F, up to 2019), and the maximum dose location (location H) are shown together with the doses received by the reference alanine dosimeters at location B. Dose uniformity describes the range of dose between the maximum dose location (H) and the minimum dose location (F) expressed as H/F. The adjustment factors for estimating the minimum dose at F and the maximum dose at H from the dose received by the reference dosimeter at B are also included.

TABLE 2 | Mapping of the new ICs.

Data source	Position in IMTC	Run Number			Mean ± SD
		1	2	3	
		Radiation dose received (Gy)			
Alanine dosimeter	B	184.0	184.0	186.0	184.7 ± 1.2
	D	153.0	155.0	154.0	154.0 ± 1.0
	F	154.0	156.0	155.0	155.0 ± 1.0
	H	167.0	168.0	168.0	167.7 ± 0.6
		Radiation dose ratio			
Dose uniformity	H/D	1.0915	1.0839	1.0909	1.0888 ± 0.004
	H/F	1.0844	1.0769	1.0839	1.0817 ± 0.004
Adjustment factor, minimum dose	D/B	0.8315	0.8424	0.8280	0.8340 ± 0.008
	F/B	0.8370	0.8478	0.8333	0.8394 ± 0.008
Adjustment factor, maximum dose	H/B	0.9076	0.9130	0.9032	0.9080 ± 0.005

Irradiation doses received at the two alternative minimum dose locations (positions D and F) and at the maximum dose location (position H) inside the IC of the IMTC, and the dose received at the reference dose location (position B). Also reported are the ratios of the doses received at each location (positions D, F and H) for the three ICs with reference to the doses received at the reference location (B) and the dose uniformity values (H/D and H/F). All runs were performed on 25 July 2019 using an irradiation time of 3.85 minutes to deliver an estimated dose of 150 Gy at position D.

10^9 irradiated PfSPZ have been administered to human subjects. There have been no breakthrough infections. The 100% infectious dose (ID_{100}) for non-irradiated PfSPZ (Sanaria® PfSPZ Challenge (NF54)) administered by direct venous inoculation (DVI) is 3.2 x 10^3 PfSPZ (27), which has been confirmed in 79 of 79 malaria-naive subjects receiving their first CHMI given by injection (28–31). The highest dose of PfSPZ Vaccine administered has been 2.7 x 10^6 PfSPZ, which represents 840x the ID_{100} [(32, 33), Sirima et al, submitted for publication]. Overall, the equivalent of more than 1.6 x 10^6 ID_{100}s have been administered without a breakthrough.

DISCUSSION

We describe here the studies supporting the GMP radiation-attenuation methodology used in the manufacture of PfSPZ Vaccine, a radiation-attenuated, purified and cryopreserved, metabolically-active, non-replicating, whole sporozoite vaccine against malaria which has demonstrated unparalelled efficacy, safety and tolerability. In the 21 clinical trials conducted to date, three trials have shown 100% protection against homologous controlled human malaria infection (CHMI) (17, 19, 20).

Some of the initial concerns considered during development of a radiation-attenuated malaria vaccine were that attenuation by irradiation would be difficult to manage, that the parasites would have the potential to cause infections because of inadequate attenuation, or would cause an inferior and non-protective immune response due to over attenuation. None of these three scenarios has occurred.

Although the precise mechanisms whereby irradiation prevents replication is not understood, it is likely that damage to DNA results in multiple redundant defects providing a high level of assurance that no individual parasite would be capable of replication. Parasite genes that do appear to be downregulated following irradiation include those for DNA repair (34). Thus, with over 5.3 x 10^9 PfSPZ irradiated and subsequently administered to humans, not one has broken through. As the data presented here demonstrate, the manufacturing process for PfSPZ Vaccine maintains a tight control over the attenuation process.

PfSPZ administered directly by the bite of mosquitoes subjected to 150 Gy did not lead to breakthrough infections

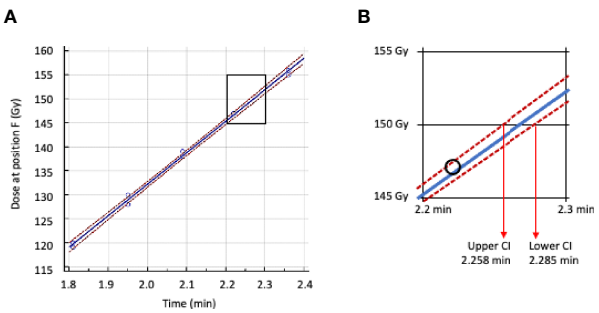

FIGURE 5 | Regression analysis of irradiation time vs dose received at location F (minimum dose location) inside the IMTC. **(A)** Regression line plot in blue, 95% confidence intervals in red. **(B)** Area in A between 145 Gy and 155 Gy enlarged with the lower and upper 95% confidence intervals. The time adopted for calculating the target dose of 150 Gy is 2.285 min.

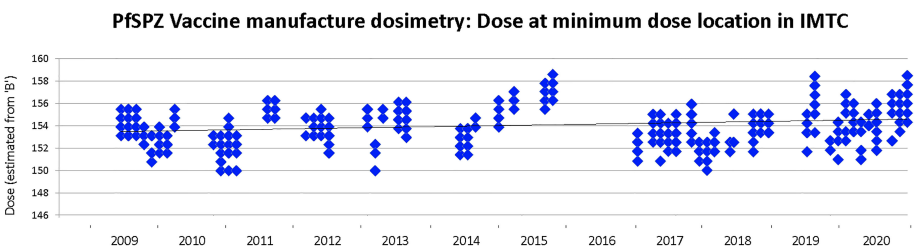

FIGURE 6 | Minimum dose of irradiation received by any mosquito during PfSPZ Vaccine production campaigns between 2009-2020. The target minimum dose is 150 Gy and the minimum acceptable dose is 142.5 Gy. Not all production campaigns were converted into lots released for clinical use, and none of the clinical released lots included PfSPZ irradiated below 150 Gy.

whereas PfSPZ exposed to a dose 120 Gy PfSPZ were not fully attenuated and breakthrough infections occurred (11, 12). In the *in vitro* 6-day hepatocyte attenuation assay, liver stage parasites develop from PfSPZ subjected to 120 Gy, but not after an irradiation dose of 142.5 Gy (data to be published separately). For the rodent malaria parasite, *P. yoelii* (Py), which has a lower tolerance to irradiation than Pf, the minimum predicted dose to achieve full attenuation in mice is 92.4 Gy (35). At a radiation dose of 100 Gy, PySPZ were fully attenuated; injection of $1x10^5$ irradiated PySPZ to each of 41 mice failed to lead to infection, compared to a dose of just 2.78 non-irradiated PySPZ that infected 50% of the mice (33). The minimum attenuating dose for *P. berghei* (Pb) also appears to be 100 Gy (10), although most studies of immunity stimulated by PbSPZ utilize 120-150 Gy (36, 37).

For manufacturing PfSPZ Vaccine, we chose a target minimum dose of 150 Gy with an acceptable minimum dose of 142.5 Gy (5% below the target dose) and a maximum dose of 190 Gy. If over-attenuated, the PfSPZ could potentially lose their ability to stimulate a protective immune response in the liver. For the rodent parasite PySPZ, doubling the attenuating dose (i.e. to 200 Gy) does not lead to a diminution of protection. However, we wanted to provide a tighter range for the PfSPZ so selected, in the absence of any available data, a dose of 190 Gy as the upper threshold for acceptance. In practice, as indicated here, the highest level of irradiation for the PfSPZ has been considerably lower with a range maximum of 175.3 Gy, which is well below the acceptable maximum dose. Overall, the mean estimated minimum dose was 154.3 Gy and the mean estimated maximum dose was 166.3 Gy for vaccine lots.

Irradiation using ^{60}Co is a physical process. When incorporating the defined half life decay of the sources (Equation 1) it should be possible to deliver a precise dose of radiation and for there to be no meaningful variability between runs on the same day or between runs on different days. However, the irradiator has moving parts with some inertia or variability – these include the rotation of the turntable in the irradiator chamber, the position of the reference dosimeter relative to the sources when they are activated during a run, and the speed with which the source rods are elevated by air pressure from the compressor. There are uncertainties in the alanine processing methodology to which NIST assigns a value of ±1.8%. Together some of these factors may account for a portion of the overall ±3.1% (150-159.3 Gy) variability seen between runs (**Figure 6**).

^{60}Co irradiation has proven to be a robust, repeatable and reliable process, but has drawbacks because of attendant security issues which significantly increase the cost, including running personnel background checks, training and certification, and security of controlled access and monitoring. These are fixed costs that would be diluted by scaling up production, however, because of the half life decay, the sources deplete over time and have to be replenished. Our irradiator has undergone one upgrading event at considerable cost. In the future it is likely that ^{60}Co irradiation will be replaced by X-ray irradiation, and Sanaria has begun to explore the process of making this transition.

DATA AVAILABILITY STATEMENT

The original contributions presented in the study are included in the article. Further inquiries can be directed to the corresponding author.

AUTHOR CONTRIBUTIONS

Conceptualization: EJ and SH. Methodology: EJ, SM, JO, BS, AE, TL, ML, PB, TR, SC, AG, and TM. Funding acquisition: EJ and SH. Project administration: EJ and SH. Supervision: EJ and SH. Writing – original draft: EJ. Writing – review & editing: EJ, SH, PB, and TR. All authors contributed to the article and approved the submitted version.

FUNDING

The work was supported by components of several Small Business Research Innovation awards to SH from the National Institute of Allergy and Infectious Disease of NIH, principally 43AI058499 and 44AI058499.

ACKNOWLEDGMENTS

We thank the NIAID/NIH SBIR program for support and Drs Stephen Sletzer, Marc Desrosiers, Lonnie Cumberland and Ileana Pazos of the NIST High Dose Dosimetry Service for providing advice and guidance. We thank Greg Smith ABHP, Sanaria's Radiation Safety Officer, RSO Inc, Laurel, MD, and also Mark A Smith PhD, CHP of Ionaktis LLC, Charlotte, NC, contract Radiation Physicist for data and document reviews.

REFERENCES

1. Jarrett WF, Jennings FW, McIntyre WI, Mulligan W, Urquhart GM. Irradiated Helminth Larvae in Vaccination. *Proc R Soc Med* (1958) 51:743–4. doi: 10.1177/003591575805100912
2. Sharma RL, Bhat TK, Dhar DN. Control of Sheep Lungworm in India. *Parasitol Today* (1988) 4:33–6. doi: 10.1016/0169-4758(88)90061-0
3. Miller TA. Effect of Route of Administration of Vaccine and Challenge on the Immunogenic Efficiency of Double Vaccination With Irradiated *Ancylostoma caninum* Larvae. *J Parasitol* (1965) 51:200–6. doi: 10.2307/3276081
4. Tromba FG. Immunization of Pigs Against Experimental *Ascaris suum* Infection by Feeding Ultraviolet-Attenuated Eggs. *J Parasitol* (1978) 64:651–6. doi: 10.2307/3279954
5. Taylor MG, James ER, Nelson GS, Bickle Q, Dunne DW, Webbe G. Immunisation of Sheep Against *Schistosoma mattheei* Using Either Irradiated Cercariae or Irradiated Schistosomula. *J Helminthol* (1976) 50:1–9. doi: 10.1017/s0022149x00028753
6. Hsü SY, Hsü HF, Burmeister LF. *Schistosoma mansoni*: Vaccination of Mice With Highly X-Irradiated Cercariae. *Exp Parasitol* (1981) 52:91–104. doi: 10.1016/0014-4894(81)90065-5
7. Bushara HO, Hussein MF, Saad AM, Taylor MG, Dargie JD, Marshall TF, et al. Immunization of Calves Against *Schistosoma bovis* Using Irradiated Cercariae or Schistosomula of *S. bovis*. *Parasitol* (1978) 77:303–11. doi: 10.1017/s0031182000050265
8. Ruppel A, Shi YE, Moloney NA. *Schistosoma mansoni* and *S. japonicum*: Comparison of Levels of Ultraviolet Irradiation for Vaccination of Mice With Cercariae. *Parasitol* (1990) 101:23–6. doi: 10.1017/s0031182000079701
9. Sadun EH. Immunization in Schistosomiasis by Previous Exposure to Homologous and Heterologous Cercariae by Inoculation of Preparations From Schistosomes and by Exposure to Irradiated Cercariae. *Ann NY Acad Sci* (1963) 113:418. doi: 10.1111/j.1749-6632.1963.tb40680.x
10. Nussenzweig RS, Vanderberg J, Most H, Orton C. Protective Immunity Produced by the Injection of X-Irradiated Sporozoites of *Plasmodium berghei*. *Nature* (1967) 216:160–2. doi: 10.1038/216160a0
11. Clyde DF, Most H, McCarthy VC, Vanderberg JP. Immunization of Man Against Sporozoite-Induced falciparum Malaria. *Am J Med Sci* (1973) 266:169–77. doi: 10.1097/00000441-197309000-00002
12. Rieckmann KH, Beaudoin RL, Cassells JS, Sell KW. Use of Attenuated Sporozoites in the Immunization of Human Volunteers Against *falciparum* Malaria. *Bull WHO* (1979) 57(Suppl 1):261–5.
13. Edelman R, Hoffman SL, Davis JR, Beier M, Sztein MB, Losonsky G, et al. Long-Term Persistence of Sterile Immunity in a Volunteer Immunized With X-Irradiated *Plasmodium falciparum* Sporozoites. *J Infect Dis* (1993) 168:1066–70. doi: 10.1093/infdis/168.4.1066
14. Hoffman SL, Goh LM, Luke TC, Schneider I, Le TP, Doolan DL, et al. Protection of Humans Against Malaria by Immunization With Radiation-Attenuated *Plasmodium falciparum* Sporozoites. *J Infect Dis* (2002) 185:1155–64. doi: 10.1086/339409
15. Hoffman SL, Billingsley PF, James ER, Richman A, Loyevsky M, Li T, et al. Development of a Metabolically Active, non-Replicating Sporozoite Vaccine to Prevent *Plasmodium falciparum* Malaria. *Hum Vaccin* (2010) 6:97–106. doi: 10.1126/science.1211548
16. Richie TL, Billingsley PF, Sim BKL, James ER, Chakravarty S, Epstein JE, et al. Progress With *Plasmodium falciparum* Sporozoite (PfSPZ)-Based Malaria Vaccines. *Vaccine* (2015) 33:7452–61. doi: 10.1016/j.vaccine.2015.09.096
17. Seder RA, Chang LJ, Enama ME, Zephir KL, Sarwar UN, Gordon IJ, et al. VRC 312 Study Team. Protection Against Malaria by Intravenous Immunization With a Nonreplicating Sporozoite Vaccine. *Science* (2013) 341(6152):1359–65. doi: 10.1126/science.1241800
18. Epstein JE, Paolino KM, Richie TL, Sedegah M, Singer A, Ruben AJ, et al. Protection Against *Plasmodium falciparum* Malaria by PfSPZ Vaccine. *JCI Insight* (2017) 2:e89154. doi: 10.1172/jci.insight.89154
19. Jongo SA, Church LWP, Mtoro AT, Schindler T, Chakravarty S, Ruben AJ, et al. Increase of Dose Associated With Decrease in Protection Against Controlled Human Malaria Infection by PfSPZ Vaccine in Tanzanian Adults. *Clin Infect Dis* (2020) 71:2849–57. doi: 10.1093/cid/ciz1152
20. Sissoko MS, Healy SA, Katile A, Zaidi I, Hu Z, Kamate B, et al. Safety and Efficacy of a Three-Dose Regimen of *Plasmodium falciparum* Sporozoite Vaccine in Adults During an Intense Malaria Transmission Season in Mali: A Randomised, Controlled Phase 1 Trial. *Lancet Infect Dis* (2021) :S1473-3099(21)00332-7. doi: 10.1016/S1473-3099(21)00332-7
21. Devic S. Radiochromic Film Dosimetry: Past, Present, and Future. *Phys Med* (2011) 27:122–34. doi: 10.1016/j.ejmp.2010.10.001
22. McLaughlin WL, Desrosiers MF. Dosimetry Systems for Radiation Processing. *Radiat Phys Chem* (1995) 46:1163–74. doi: 10.1016/0969-806X(95)00349-3
23. Burns DT, Allisy-Roberts PJ, Desrosiers MF, Sharpe PHG, Pimpinella M, Lourenço V, et al. Supplementary Comparison CCRI(I)-S2 of Standards for Absorbed Dose to Water in ^{60}Co γ Radiation at Radiation Processing Dose Levels. *Metrologia* (2011) 48(Tech. Suppl):06009, 1–18.
24. Nagy VYU, Desrosiers MF. A Complex Time Dependence of the EPR Signal of Irradiated L-α -Alanine. *Appl Radiat Isot* (1996) 47:789–93. doi: 10.1016/0969-8043(96)00053-X
25. Humphreys JC, Puhl JM, Seltzer SM, McLaughlin WL, Desrosiers MF, Bensen DL, et al. *Radiation Processing Dosimetry Calibration Services and Measurement Assurance Program*. Gaithersburg, MD: NIST Special Publication (1998) 250–44. doi: 10.6028/NIST.SP.250-44
26. Siu NF, Sedegah M, Hoffman SL. *In Vitro* Survival and Retention of Infectivity of *Plasmodium yoelii* Sporozoites Over Extended Periods of Time. *J Parasitol* (1994) 80(5):826–9. doi: 10.2307/3283266
27. Epstein JE, Tewari K, Lyke KE, Sim BK, Billingsley PF, Laurens MB, et al. Live Attenuated Malaria Vaccine Designed to Protect Through Hepatic CD8$^+$ T Cell Immunity. *Science* (2011) 334(6055):475–80. doi: 10.1126/science.1211548
28. Mordmüller B, Supan C, Sim BKL, Gómez-Pérez GP, Ospina Salazar CL, Held J, et al. Direct Venous Inoculation of *Plasmodium falciparum* Sporozoites for Controlled Human Malaria Infection: A Dose-Finding Trial in Two Centres. *Malar J* (2015) 14:117. doi: 10.1186/s12936-015-0628-0
29. Mordmüller B, Surat G, Lagler H, Chakravarty S, Ishizuka AS, Lalremruata A, et al. Sterile Protection Against Human Malaria by Chemoattenuated PfSPZ Vaccine. *Nature* (2017) 542(7642):445–9. doi: 10.1038/nature21060
30. Gómez-Pérez GP, Legarda A, Muñoz J, Sim BKL, Ballester MR, Dobaño C, et al. Controlled Human Malaria Infection by Intramuscular and Direct Venous Inoculation of Cryopreserved *Plasmodium falciparum* Sporozoites in Malaria-Naive Volunteers: Effect of Injection Volume and Dose on Infectivity Rates. *Malar J* (2015) 14:306. doi: 10.1186/s12936-015-0817-x
31. Murphy SC, Deye GA, Sim BKL, Galbiati S, Kennedy JK, Cohen KW, et al. PfSPZ-CVac Efficacy Against Malaria Increases From 0% to 75% When Administered in the Absence of Erythrocyte Stage Parasitemia: A Randomized, Placebo-Controlled Trial With Controlled Human Malaria Infection. *PloS Pathog* (2021) 17(5):e1009594. doi: 10.1371/journal.ppat.1009594
34. Hoffman BU, Chattopadhyay R. *Plasmodium falciparum*: Effects of Radiation on Levels of Gene Transcripts in Sporozoites. *Exp Prasiitol* (2008) 118(2):247–52. doi: 10.1016/j.exppara.2007.08.014
35. Chattopadhyay R, Conteh S, Li M, James ER, Epstein JE, Hoffman SL. The Effects of Radiation on the Safety and Protective Efficacy of an Attenuated *Plasmodium yoelii* Sporozoite Malaria Vaccine. *Vaccine* (2009) 27(27):3675–80. doi: 10.1016/j.vaccine.2008.11.073
36. Berenzon D, Schwenk RJ, Letellier L, Guebre-Xabier M, Williams J, Krzych U. Protracted Protection to *Plasmodium berghei* Malaria is Linked to Functionally and Phenotypically Heterogeneous Liver Memory CD8+ T Cells. *J Immunol* (2003) 171:2024–34. doi: 10.4049/jimmunol.171.4.2024
37. Parmar R, Patel H, Yadav N, Parikh R, Patel K, Mohankrishnan A, et al. Infectious Sporozoites of *Plasmodium berghei* Effectively Activate Liver CD8 α+ Dendritic Cells. *Front Immunol* (2018) 9:192:192. doi: 10.3389/fimmu.2018.00192
32. Lyke KE, Singer A, Berry AA, Reyes S, Chakravarty S, James ER, et al. Multidose Priming and Delayed Boosting Improve *Plasmodium falciparum* Sporozoite Vaccine Efficacy Against Heterologous *P. falciparum* Controlled Human Malaria Infection. *Clin Infect Dis* (2021) 73(7):e2424–35. doi: 10.1093/cid/ciaa1294
33. Jongo SA, Urbano V, Church LWP, Olotu A, Manock SR, Schindler T, et al. Immunogenicity and Protective Efficacy of Radiation-Attenuated and Chemo-Attenuated PfSPZ Vaccines in Equatoguinean Adults. *Am J Trop Med Hyg* (2021) 104(1):283–93. doi: 10.4269/ajtmh.20-0435

Conflict of Interest: All authors are employed by Sanaria Inc.

Publisher's Note: All claims expressed in this article are solely those of the authors and do not necessarily represent those of their affiliated organizations, or those of the publisher, the editors and the reviewers. Any product that may be evaluated in this article, or claim that may be made by its manufacturer, is not guaranteed or endorsed by the publisher.

frontiers in Immunology

ORIGINAL RESEARCH
published: 07 March 2022
doi: 10.3389/fimmu.2022.825702

Low-Energy Electron Irradiation of Tick-Borne Encephalitis Virus Provides a Protective Inactivated Vaccine

Julia Finkensieper[1†], Leila Issmail[1†], Jasmin Fertey[1], Alexandra Rockstroh[1], Simone Schopf[2], Bastian Standfest[3], Martin Thoma[3], Thomas Grunwald[1] and Sebastian Ulbert[1]*

[1] Department of Vaccines and Infection Models, Fraunhofer Institute for Cell Therapy and Immunology IZI, Leipzig, Germany, [2] Fraunhofer-Institute for Organic Electronics, Electron Beam and Plasma Technology FEP, Dresden, Germany, [3] Department of Laboratory Automation and Biomanufacturing Engineering, Fraunhofer Institute for Manufacturing Engineering and Automation IPA, Stuttgart, Germany

Tick-borne encephalitis virus (TBEV) is a zoonotic flavivirus which is endemic in many European and Asian countries. Humans can get infected with TBEV usually *via* ticks, and possible symptoms of the infection range from fever to severe neurological complications such as encephalitis. Vaccines to protect against TBEV-induced disease are widely used and most of them consist of whole viruses, which are inactivated by formaldehyde. Although this production process is well established, it has several drawbacks, including the usage of hazardous chemicals, the long inactivation times required and the potential modification of antigens by formaldehyde. As an alternative to chemical treatment, low-energy electron irradiation (LEEI) is known to efficiently inactivate pathogens by predominantly damaging nucleic acids. In contrast to other methods of ionizing radiation, LEEI does not require substantial shielding constructions and can be used in standard laboratories. Here, we have analyzed the potential of LEEI to generate a TBEV vaccine and immunized mice with three doses of irradiated or chemically inactivated TBEV. LEEI-inactivated TBEV induced binding antibodies of higher titer compared to the formaldehyde-inactivated virus. This was also observed for the avidity of the antibodies measured after the second dose. After viral challenge, the mice immunized with LEEI- or formaldehyde-inactivated TBEV were completely protected from disease and had no detectable virus in the central nervous system. Taken together, the results indicate that LEEI could be an alternative to chemical inactivation for the production of a TBEV vaccine.

Keywords: vaccine, irradiation, tick-borne encephalitis virus, zoonosis, virus inactivation

OPEN ACCESS

Edited by:
Karl Ljungberg, Eurocine Vaccines AB, Sweden

Reviewed by:
Galina Grigirievna Karganova, Chumakov Institute of Poliomyelitis and Viral Encephalitides (RAS), Russia
Stacey Scroggs, National Institute of Allergy and Infectious Diseases (NIH), United States

****Correspondence:***
Sebastian Ulbert
Sebastian.ulbert@izi.fraunhofer.de

[†]These authors have contributed equally to this work and share first authorship

Specialty section:
This article was submitted to Vaccines and Molecular Therapeutics, a section of the journal Frontiers in Immunology

Received: *30 November 2021*
Accepted: *11 February 2022*
Published: *07 March 2022*

Citation:
Finkensieper J, Issmail L, Fertey J, Rockstroh A, Schopf S, Standfest B, Thoma M, Grunwald T and Ulbert S (2022) Low-Energy Electron Irradiation of Tick-Borne Encephalitis Virus Provides a Protective Inactivated Vaccine. Front. Immunol. 13:825702. doi: 10.3389/fimmu.2022.825702

INTRODUCTION

Tick-borne encephalitis virus (TBEV) belongs to the family *Flaviviridae* of the genus Flavivirus which includes several major human pathogens such as dengue, Japanese encephalitis, Zika, West Nile, or yellow fever viruses (1). These are enveloped, single positive-stranded RNA viruses which are primarily transmitted by arthropod vectors (2). TBEV is transmitted by ticks and is endemic to several European and Asian countries (3). Its natural hosts are small rodents, but also humans can be infected usually *via* tick bites, although they represent dead-end hosts (4). With several thousand clinical cases per year, it is currently the most important tick-borne virus, and disease symptoms range from fever to neurological complications such as meningitis and encephalitis, which in some cases can be fatal (5). Especially older or immunocompromised individuals are at risk of developing severe forms of illness.

Vaccines for the protection from TBEV induced disease are available and widely used in endemic areas (6, 7). They consist of whole viruses, chemically inactivated by formaldehyde (FA), a technology used for decades to generate vaccines against many different pathogens. Other examples include hepatitis A, seasonal influenza, polio, or Japanese encephalitis viruses (8). Although FA-inactivation is relatively simple and well established, the process bears severe disadvantages: the chemical is toxic, which complicates large-scale production processes and generates problems of waste and residual traces in the final product. The usage of only low amounts of FA leads to the need for long inactivation times of several days or weeks (9). In addition, FA acts by crosslinking and modifying structural components like proteins, hence the treatment has been reported to damage antigenic structures impacting antigenicity of vaccines (8, 10, 11). Other chemicals used to inactivate viruses, mostly the alkylating compound β-propiolactone, have less impact on antigenicity but are also highly hazardous (12). Therefore, there is a need for novel inactivation methods as alternatives to chemical treatment.

A technology for the inactivation of pathogens that does not rely on chemical treatment is ionizing radiation, which primarily destroys nucleic acids, but leaves other structural components largely intact (13). It is known that pathogens inactivated by gamma-, high energy electron or X-radiation can induce highly protective immune responses (14–17). However, a major drawback of the existing radiation technologies is the requirement of complex shielding constructions that limit their use to specialized radiation facilities (18). This is due to the high doses necessary to inactivate viruses, which require and/or generate large amounts of radioactivity. As a consequence, ionizing radiation has not been compatible with pharmaceutical production processes, and viral vaccine candidates developed using irradiation remain experimental until today.

We have previously shown that low-energy electron irradiation (LEEI) overcomes these major limitations of other ionizing irradiation technologies. LEEI consists of electrons accelerated with up to 500 kilo electron volts (keV) and very rapidly delivers high doses necessary for pathogen inactivation, but only requires minimal shielding, which enables its use in standard laboratories (19). Different pathogens have been inactivated using LEEI, and the studies showed the potential of the technology to generate efficient vaccines (20–22). In addition, principles for automated processing of LEEI in a biotechnological production setting have been developed (19). Here, we describe the application of LEEI in such an automated process on TBEV and investigate whether LEEI could be an alternative to chemical inactivation in generating a TBEV vaccine.

MATERIALS AND METHODS

Cell and Virus Culture

BHK-21 cells and Vero E6 cells (DSMZ, Braunschweig, Germany) were propagated in Dulbecco's modified Eagle's medium (DMEM, ThermoFisher Scientific, Germany) supplemented with 10% heat inactivated FCS and 1% penicillin/streptomycin (Gibco) at 37°C and 5% CO_2.

TBEV (Hypr 9BMP U39292.1, kindly provided by Uwe Liebert, Institute for Virology, Leipzig University) was cultivated in BHK-21 cells. Cells were infected with a multiplicity of infection of 0.1 TCID50/cell and incubated for 2 days at 37°C and 5% CO_2. The virus was purified from cell culture supernatant by ultracentrifugation (30,000 rpm) on a sucrose cushion (15% (w/v) sucrose in PBS) for 3 h at 4°C.

Titration of TBEV was performed by tissue culture infectious dose 50 (TCID50) assay on BHK-21 cells. In short, for the TCID50 assay 10-fold dilutions of viral stocks were incubated on confluent BHK-21 cell monolayers in a 96-well microwell plate for 4 days. The cells were monitored for cytopathic effects (CPE) and the titer was calculated using the Reed-Muench method (23).

LEEI-Based Inactivation

Virus samples were irradiated as previously described (19). Briefly, irradiation was performed in a custom-built irradiation device situated at the Fraunhofer Institute for Cell Therapy and Immunology (Leipzig, Germany). The device can accommodate different modules that enable an automated LEEI of liquids. A module using disposable bags was used for TBEV irradiation. The bags made of polyethylenterephthalat were filled with 10 ml purified TBEV diluted in PBS containing the stabilizer trehalose at 12% (w/v) and sealed. The filled bags are automatically passed through the irradiation source at a fluid velocity of 50 mm/s. For irradiation the acceleration energy was set to 300 keV and the applied irradiation dose was adjusted by regulating the beam current (in mA). As a control one bag was processed in the module without LEEI (0 kGy). All experiments were performed at 4°C. Afterwards the bags were reopened and the samples were recovered for further experiments.

Chemical Inactivation

Chemical inactivation of TBEV was conducted according to WHO's Good Manufacturing Practice guidelines (24). Briefly, purified TBEV in PBS containing 12% trehalose was mixed with formaldehyde to a final concentration of 0.05% (ThermoFisher Scientific, Germany) and incubated at 22°C for 5 days.

To remove residual formaldehyde the samples were dialyzed against cold PBS for 2 h. Inactivation was verified as described in section *Verification of TBEV Inactivation*.

Verification of TBEV Inactivation

To identify the LEEI-dose necessary for complete inactivation of TBEV, irradiated samples were analyzed on BHK-21 cells seeded in 6-well cell culture plates one day prior to infection. The cells were inoculated with 100 µl of irradiated or active TBEV as a positive control per well (in duplicates). Mock-infected wells served as a negative control. Cells were observed for the appearance of cytopathic effects (CPE) over 3 days. Cell culture supernatants were then passaged onto fresh cells and observed for another 3 days. The sample was regarded as inactivated when no CPE was visible after passage. Samples with visible CPE were titrated in a TCID50 assay to quantify the titer reduction of infectious virus caused by LEEI.

A second experiment was conducted to re-confirm the inactivation of TBEV using 20 kGy. Active TBEV served as a positive control and mock-infected cells as a negative control. BHK-21 cells seeded in 6-well cell culture plates were inoculated with virus samples (in triplicates). After adsorption at 37°C for 1 h, the virus-containing medium was collected, cell monolayers were washed with PBS to completely remove unadsorbed virus and incubated further in fresh cell culture medium for 3 days. Cell culture supernatants were then passaged twice onto fresh cells and incubated for another 3 days per passage. After each passage, 140 µl of cell culture supernatant was used for the extraction of viral RNA using QIAamp viral RNA mini kit following manufacturer's instructions. Isolated RNA was then analyzed using RT-qPCR as described in *Quantification of Viral RNA and Infectious Virus in Organ Homogenates*.

ELISA

The influence of either LEEI-based or formaldehyde inactivation on the antigenicity of TBEV compared to the non-treated controls was tested by an indirect enzyme-linked immunosorbent assay (ELISA). In short, inactivated TBEV samples were coated on a NUNC polysorp 96-microwell plate (ThermoFisher Scientific, Germany) in coating buffer (35 mM Na_2HCO_3 /15 mM Na_2CO_3, pH 9.6), in a total volume of 100 µl per well overnight at 4°C. The plate was washed three times in PBS containing 0.05% (v/v) Tween20 (PBS-T) and wells were blocked with 5% (w/v) skim milk powder in PBS. Sera from two patients tested positive for TBEV by virus neutralization tests (kindly provided by Luisa Barzon, Padova University, Italy, with approval from the local ethical review board) were diluted 1:100 in 100 µl 5% (w/v) skim milk in PBS and added for 2 h at room temperature. After another wash step the plate was incubated with a secondary HRP-conjugated goat anti-human IgG antibody (1:20,000, Dianova, Hamburg, Germany) for 1 h at room temperature. The plate was washed again and TMB-ELISA substrate (Biozol, Eching, Germany) was added for 30 min at room temperature. The reaction was stopped by addition of 1M H_2SO_4. Absorbance was measured at 450 nm and 520 nm reference wave length in a standard ELISA reader (Infinite M200, Tecan, Männedorf, Switzerland).

For the analysis of TBEV-binding antibodies, active TBEV was coated on NUNC PolySorp 96-microwell plates overnight at 4°C. Heat inactivated (56°C for 30 min) sera from the immunized mice were diluted 1:100 in 5% skim milk in PBS, 50 µl were added to each well in duplicates and binding mouse IgG were detected with a HRP-conjugated rabbit anti mouse IgG antibody (1:2000, Dako, Glostrup, Denmark). To test for the avidity of TBEV-binding antibodies in the mouse sera, an additional 3 min washing step using 7 M urea in PBS-T was included after serum incubation. The denaturing urea treatment disrupts weak antibody-antigen complexes and by that dissociates antibodies binding with low affinity. An identical plate without the urea wash served as a reference to calculate the relative avidity with the following formula:

$$relative\ avidity[\%] = \frac{OD_{450/520\ nm} with\ 7M\ urea\ wash}{OD_{450/520\ nm} without\ urea\ wash} \times 100$$

Virus Neutralization Assay

TBEV neutralizing antibodies in mouse sera taken 1 week after the second and third immunization were measured in a focus reduction neutralization test (FRNT). The sera were serially diluted and incubated with 80 focus forming units (FFU) of purified TBEV for 1 h at 37°C. The virus-serum mixture was transferred to Vero E6 cell monolayers in 96-well microwell plates and incubated for another hour. Cells were overlaid with 1% methylcellulose in DMEM with 2% FCS and 1% penicillin/streptomycin and incubated for 2 days. The cells were fixed with 4% formaldehyde in PBS and permeabilized in Perm-Wash buffer (0.1% Saponin and 0.1% BSA in PBS). Immunostaining of TBEV foci was performed using the primary flavivirus antibody 4G2 (Absolute antibody, Oxford, UK) as described previously (25). Neutralizing antibody titer was defined as the reciprocal of the last serum dilution that showed a minimal 50% reduction of TBEV foci compared to sera from sham-immunized mice. Each experiment was performed in duplicates.

TBEV Immunization and Challenge Experiment

All animal experiments were carried out in accordance with the EU Directive 2010/63/EU for animal experiments and were approved by local authorities (No.: TVV 01/20). Female BALB/c mice (8 weeks old) were obtained from Charles River (Germany) and kept in a specific pathogen-free environment in isolated ventilated cages. Groups of eight mice were immunized three times at a two-week interval by intramuscular (i.m.) injection into the hind limbs of 100 µl (2 sites, 50 µl each) of 1:1 mixture of Alhydrogel (aluminum hydroxide gel adjuvant, 10 mg/ml aluminum, InvivoGen, France) with either LEEI- or formalin-inactivated TBEV at a dose of 10^6 TCID50. The immunization schedule with three doses was based on the study by Salat et al. (26), which used the same viral and animal strains. Control mice were sham immunized with vehicle solution (1:1 mixture of Alhydrogel

and PBS + 12% trehalose). Blood was collected from the retrobulbar venous sinus at three time points: one week prior to the first immunization and one week after the second and the third immunization. After collection, blood samples were incubated at room temperature for 30 min and centrifuged at 8000 g for 10 min to obtain serum for analysis of TBEV-binding and neutralizing antibodies. Two weeks after the third immunization, all mice were challenged with 100 µl containing 4.4 x 10^4 TCID50 of purified TBEV *via* intraperitoneal injection. Clinical development of disease was monitored daily for 14 days post-infection and score points were given according to the following criteria: body weight loss (0 points= no weight loss, 5 points= 8-10%, 10 points= 11-19%, 20 points= weight loss ≥20% of initial weight); fur condition (0 points = shiny and clean coat, 2 points = piloerection, 5 points = ruffled fur); eye appearance (0 points= open healthy eyes, 5 points= mildly inflamed, 10 points = highly inflamed and closed); gastrointestinal symptoms due to distention of the intestine (0 points= no symptoms, 5 points= mild, 10 points= moderate abdominal swelling); body posture (0 points= normal posture, 20 points= hunched body posture); activity level and motor function (5 points= slightly reduced activity and reaction, 10 points= coordination disorder and reduced activity, 20 points= apathy and morbidity); neurological symptoms (5 points= mild paralysis of one limb, 10 points= mild paralysis of two limbs, 20 points= complete paralysis of two limbs). Humane endpoints requiring euthanasia were defined as reaching a cumulative score points of 20 for a period of 24 h. Animals acquiring cumulative score points greater than 20 were immediately euthanized.

Quantification of Viral RNA and Infectious Virus in Organ Homogenates

Brains and spinal cords were isolated and homogenized in gentleMACS™ M Tubes (Miltenyi Biotec, Germany) containing 2 ml of ice-cold PBS using gentleMACS Dissociator (Miltenyi Biotec, Germany). Homogenized tissues were cleared of debris by centrifugation at 2000 g and 4°C for 5 min. RNA was isolated from 140 µl of homogenate supernatants using QIAamp-Viral-RNA-Mini Kit (Qiagen, Germany) according to the manufacturer's instructions. 5 µl of isolated RNA was reverse transcribed and analyzed with the QuantiTect probe RT-PCR kit (Qiagen, Germany) using TBEV forward primer (5'-GGGCGGTTCTTGTTCTCC-3'), TBEV reverse primer (5'-ACACATCACCTCCTTGTCAGACT-3') and TBEV probe (5'-TGAGCCACCATCACCCAGACACA-3') labeled with 6-FAM at the 5' end (27). 10-fold dilutions of plasmid DNA containing the TBEV-target sequence were used as standards for the quantification of viral genome copy numbers in mouse samples. The presence of PCR inhibitors in mouse brain and spinal cord homogenates was excluded by performing an RNA isolation from homogenate samples with the addition of an internal RNA extraction control provided in genesig® TBEV advanced kit (Primerdesign™ Ltd, UK). The quantity of added internal RNA control detected by qPCR was within the normal range (Cp values of 28 ± 3) according to the information provided by the manufacturer.

For the detection of infectious virus in brain and spinal cord homogenates, Vero E6 cells were seeded at 2.5 x10^4 cells/well in a 96-well plate in 200 µl of DMEM, 10% FCS, 1% penicillin/streptomycin one day before infection. Next day, the medium was changed to DMEM, 1% penicillin/streptomycin. Serially diluted homogenates were applied in duplicates onto the cells and exchanged for medium after one hour. After two days, TBEV- foci were visualized using immunostaining as described in *Virus Neutralization Assay* section and infectious viral titers were calculated in FFU/ml of homogenate.

Statistical Analysis

Statistical analysis was performed with GraphPad Prism 6.0.7 (GraphPad Software, Inc., La Jolla, CA, USA). Data were checked for normality using the Shapiro-Wilk test. Normally distributed data of the antibody avidity was analyzed using an unpaired t-test. For analyzing not normally distributed antibody data, a Mann-Whitney-U-test was applied. Differences between groups in clinical score and weight loss on each day post-infection and differences in viral loads were analyzed by a Kruskal-Wallis-test followed by a Dunn's *post-hoc* multiple comparison test. Level of significance is indicated with * = $p < 0.05$, ** = $p < 0.01$, *** = $p < 0.001$.

RESULTS

LEEI-Based Inactivation of TBEV

TBEV was purified from cell culture supernatant and treated in liquid solution with different doses of LEEI to determine the dose necessary for complete inactivation of the virus. Irradiation with 10 kGy reduced the amount of TBEV to a titer below the detection limit, but a CPE was still visible after one passage in the inactivation test. A complete viral inactivation resulting in no detectable infectious virus in cell culture after passage was achieved by application of 20 kGy (**Table 1**).

The inactivating dose of 20 kGy was re-confirmed by two rounds of passages of the irradiated material on cells and the measurement of viral RNA every three days. TBEV RNA could be detected in the non-treated sample throughout the experiment. However, in the LEEI treated TBEV, viral RNA was only present in the inoculum, but not after passaging the material (**Figure 1**).

Conservation of Antigenicity Upon Inactivation

The impact of LEEI on antigenic structures of TBEV was analyzed in an ELISA assay. Irradiated TBEV samples were

TABLE 1 | Testing of TBEV inactivation with different doses of LEEI; the detection limit is 100 TCID50/ml.

LEEI dose [kGy]	CPE after 1 passage	Titer of active TBEV [TCID50/ml]
0	+	5 x 10^6
10	+	< 10^2
20	–	< 10^2
30	–	< 10^2

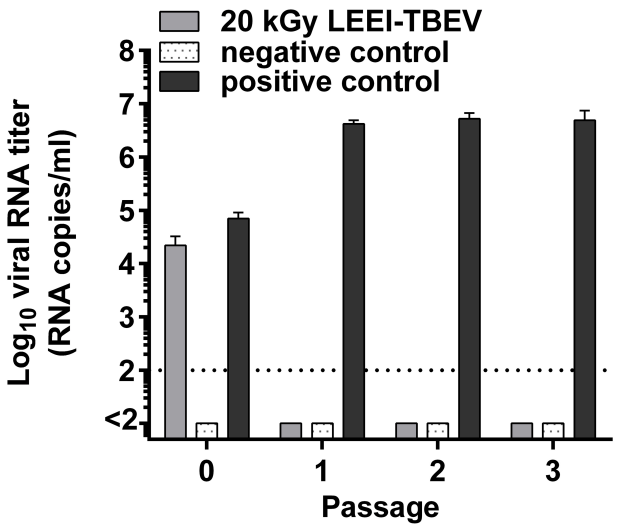

FIGURE 1 | Confirmation of inactivation of LEEI-TBEV samples used for mice immunization. Virus inactivation was performed using a LEEI dose of 20 kGy. Samples were transferred in triplicates to BHK-21 cells and after 3 days the supernatant was passaged onto fresh cells, followed by another passage three days later. Negative control= mock-infected cells; positive control= active TBEV undergoing the LEEI process without irradiation; P0 samples collected at 1 hour post-inoculation; P1= supernatant collected 3 days after inoculation; P2= supernatant collected 3 days after the first passage; P3= supernatant collected 3 days after the second passage. Collected cell culture supernatants were analyzed for TBEV RNA by RT-qPCR. Shown are mean values of triplicates ± standard deviations. The dotted line indicates the limit of detection (100 viral RNA copies).

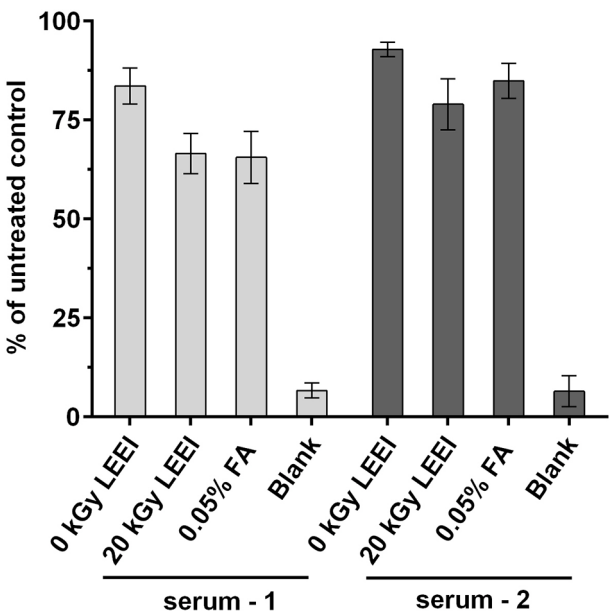

FIGURE 2 | Antigenicity of inactivated TBEV samples. Virus inactivation process was performed either with 20 kGy LEEI or with 0.05% formaldehyde (FA). The ELISA was performed with serum from two TBEV immune individuals. Untreated: virus before inactivation; 0 kGy: virus undergoing the LEEI-process without irradiation; blank: dilution buffer. Shown are mean values of three measurements in duplicates ± standard deviations. Statistical analysis was performed using Kruskal-Wallis test and Dunn's test of multiple comparisons. No statistically significant differences were detected among the groups.

investigated and compared to FA-inactivated TBEV, derived from the same viral stock solution. Untreated TBEV virus stock and the non-irradiated sample passing the process (0 kGy) served as controls. Human sera from two individuals infected with TBEV were added to investigate TBEV antigens (**Figure 2**).

A minor loss in antigenicity was caused by the handling of the virus in the automated LEEI-module, independent from irradiation, as evident from the comparison of untreated (set to 100%) and 0 kGy samples (88.2 ± 5.9%). After application of LEEI, a reduction of signal was detected. Antigen integrity after 20 kGy (72.8 ± 8.5%), which leads to complete inactivation of the virus, was on a similar level as the FA inactivated TBEV (75.2 ± 11.7%).

LEEI and Formaldehyde Inactivated TBEV Elicit Binding and Neutralizing Humoral Immune Responses in Mice

To analyze the potential of LEEI as an alternative inactivation method for providing a safe and immunogenic TBEV vaccine, an immunization study was conducted. TBEV was inactivated either with LEEI or FA and mixed with an aluminium-based adjuvant. Identical titers from the same stock solution were used for both inactivation procedures, in order to ensure that both animal groups received the same amount of inactivated viral particles, equivalent to 10^6 TCID50. BALB/c mice (eight per group) were immunized three times *via* intramuscular injection according to the immunization scheme shown in **Figure 3A**. Mice immunized with buffer and adjuvant only served as sham-immunized controls. TBEV-specific antibodies could be detected in the blood of all immunized mice one week after the second vaccination (**Figure 3**). The value of absorbance corresponds to the amount of TBEV-specific IgG in the sera which bind to antigens on the whole virus. The antibody titers in mice receiving LEEI-inactivated TBEV were significantly higher (unpaired Mann-Whitney U-test; P=0.0006) than those of animals immunized with FA-inactivated TBEV (**Figure 3B**). The third immunization further increased the level of TBEV-binding antibodies in all immunized animals and the difference remained statistically significant (unpaired Mann-Whitney U-test; P=0.028). At any time points no TBEV-specific antibodies could be detected in the control animals.

Additionally, the avidity of the TBEV-binding antibodies was analyzed by measuring the release of TBEV-bound antibodies caused by the treatment with urea as a chaotropic agent in an ELISA assay (**Figure 3C**). The data show a similar pattern compared to the TBEV-binding antibodies. Antibody avidity in the sera of the LEEI-group was significantly higher (unpaired t-test; P=0.0019) after the second immunization than in the group immunized with FA-treated TBEV. The third immunization led to an increase in the antibody-avidity in all mice of both vaccinated groups. The superiority of the antibody-avidity in

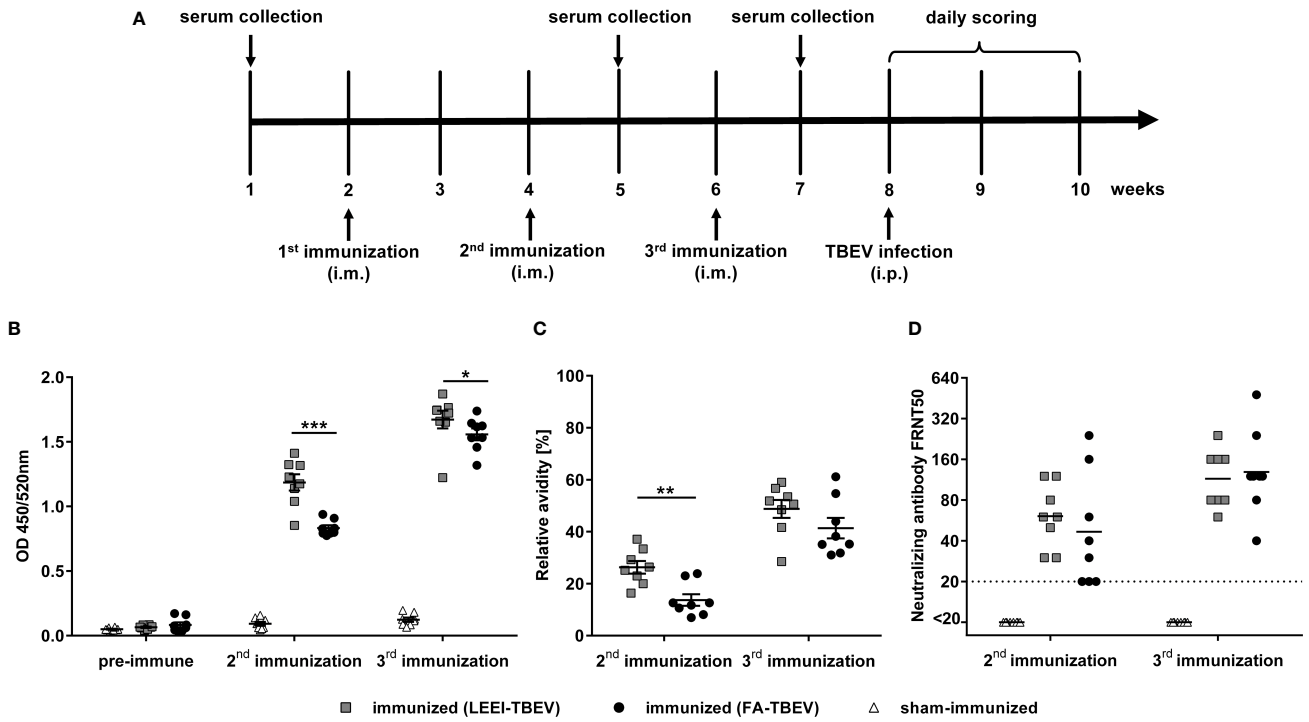

FIGURE 3 | Humoral immune responses after immunization with different inactivated TBEV vaccines. BALB/c mice (n=8) were immunized three times with TBEV inactivated either with 20 kGy LEEI (squares) or 0.05% FA (dots). Sham-immunized mice (triangles) received only buffer and adjuvant. **(A)** scheme of the immunization experiment. **(B, C)** Binding antibodies **(B)** and antibody avidity **(C)** were analyzed in IgG-ELISAs with untreated purified TBEV virions as coating antigen. For avidity measurement, the IgG-ELISA was performed with and without an additional urea wash step after the antibody binding. Both signals were compared in order to calculate the relative antibody avidity. Each data point represents an individual mouse of the same experiment. Data derive from two independent ELISA-assays, each serum sample measured in duplicates per run. Mean values of the groups ± standard error of the mean (SEM) are indicated. **(D)** Neutralizing activities of mouse sera were measured in focus reduction neutralization tests. The dotted line represents the lower detection limit (FRNT50 = 20). Shown are the neutralizing titers of individual mice and the geometric mean of each group. Data derive from two independent FRNT50 assays. All data were tested for normal distribution by a Shapiro-Wilk test. Statistical analysis of normally distributed avidity data was performed by an unpaired t-test. Binding and neutralizing antibodies were analyzed using an unpaired Mann-Whitney U-test (∗p < 0.05; ∗∗p < 0.01; ∗∗∗p < 0.001).

the LEEI- over the FA-group was still visible after the third immunization, however, without statistical significance (unpaired t-test; P=0.178).

Next, induction of neutralizing antibodies after the second and third immunizations was evaluated using a focus-reduction neutralization test (FRNT) (**Figure 3D**). After the second immunization, sera from all LEEI-TBEV immunized mice showed neutralizing activity with an average neutralizing titer of 70, whereas three of the mice immunized with FA-inactivated TBEV had neutralizing titers near the detection limit (FRNT50 = 20). The third immunization increased the neutralizing titers in both immunized groups to a similar level of mean titers of 120. Serum of sham-immunized mice showed no detectable neutralizing activity at both investigated time-points.

LEEI- and Formaldehyde Inactivated TBEV Vaccine Protect Mice Against TBEV Challenge

In order to assess the protective efficacy of the LEEI-inactivated TBEV vaccine, immunized mice were challenged with active TBEV two weeks after the third immunization. Mice were monitored for clinical score and weight loss for 14 days following virus challenge. Starting from 7 days post-infection, sham-vaccinated mice developed first clinical symptoms, like ruffled fur and reduced activity, and began to lose weight. In the following days, the clinical symptoms started to worsen. The symptoms ranged from increased weight loss (up to 11%), abdominal swelling caused by distention of the intestine, ocular inflammation to impaired movement and lethargy, which led to euthanasia of four mice of the control group according to humane endpoints. The remaining four sham-immunized mice all showed symptoms of illness, but were able to survive the infection, which resulted in a 50% (n=4/8) survival rate in the control group. In contrast, none of the mice vaccinated either with LEEI- or FA-inactivated TBEV showed clinical symptoms or weight loss during the entire study duration of 14 days, and all of them survived the infection (**Figures 4A, B**). The differences in cumulative clinical score of both vaccinated groups in comparison to the control vaccinated were statistically significant at day 8, 9 and 10 post-infection (Kruskal-Wallis and

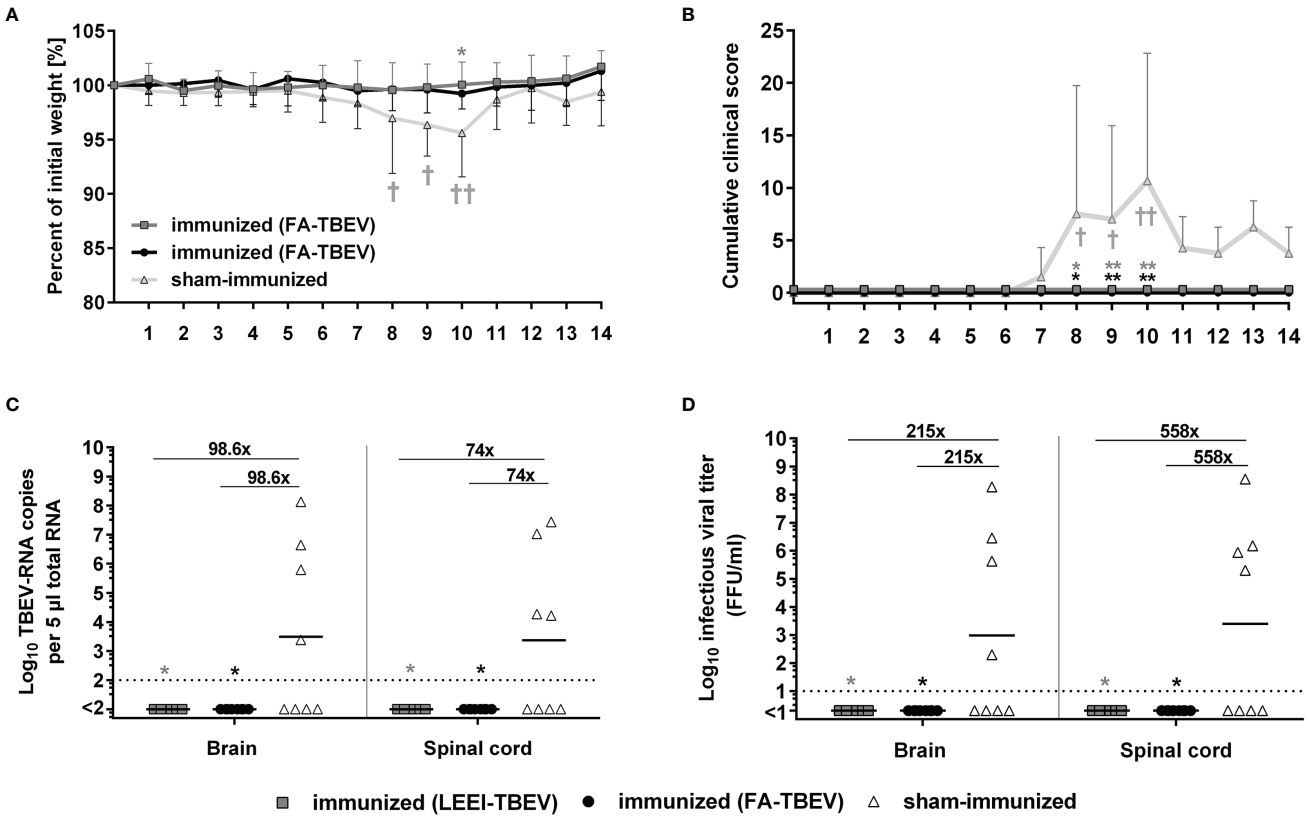

FIGURE 4 | Protective efficacy of inactivated TBEV vaccines against viral-challenge in mice. Immunized mice were infected two weeks after the third immunization with active TBEV. Mice were monitored daily for 14 days post-infection for body weight **(A)**, and clinical score **(B)**. Mice were euthanized upon reaching humane endpoints (marked by a cross) or latest at day 14 post-infection. Body weight and cumulative clinical score are presented as means ± standard errors. After euthanasia, brains and spinal cords were collected and homogenized for viral RNA load analysis using RT-qPCR **(C)** and quantification of infectious virus by a focus-forming assay **(D)**. Shown are viral RNA copy numbers and infectious viral titers of individual mice, geometric means of the groups, and viral reduction compared to the sham-immunized group. Dotted lines indicate limit of detection (= 100 viral genome copies in C and 10 FFU/ml in D). Statistical evaluation of all data was performed using Kruskal-Wallis test and Dunn's pairwise multiple comparison test. The analysis of weight loss and clinical score was performed for each day post-infection and the statistically significant differences are indicated at the corresponding days (∗$p < 0.05$; ∗∗$p < 0.01$).

Dunn's test; P values= 0.0105, 0.0053 and 0.0021, respectively). Upon reaching humane endpoints or the latest on day 14 post-challenge, mice were euthanized, and homogenized brains and spinal cords were used to determine viral load by quantitative RT-PCR and virus growth assays (**Figures 4C, D**). Viral RNA copy numbers remained below the detection limit (100 viral genome copies) in all vaccinated mice, with no differences between both vaccinated groups. In addition, 50% of the sham-immunized control mice that had to be euthanized due to reaching defined humane endpoints showed high viral RNA loads at the time of euthanasia in both brain and spinal cord samples. The surviving mice of the control group had no detectable viral RNA at the end of the experiment. The geometric means of viral RNA load in the brains and spinal cords of all control vaccinated mice were 9.9 x 10^3 and 7.4 x10^3 genome copies in the tested material, respectively. Viral RNA reduction in both vaccinated groups compared to the control vaccinated mice was over 90-fold in the brain samples and 70-fold in the spinal cord samples (Kruskal-Wallis and Dunn's test; P=0.0105). Similar significant reduction (Kruskal-Wallis and Dunn's test; P=0.0105) in infectious viral titers were observed in organ homogenates of vaccinated mice (all below the limit of detection of 10 FFU/ml) in comparison to the control group that showed geometric means of infectious virus of 2.1 x 10^3 and 5.6 x10^3 FFU/ml in brains and spinal cords, respectively.

DISCUSSION

In this study, we analyzed the potential of LEEI as an alternative to chemical treatment for the production of an inactivated TBEV-vaccine. In contrast to other technologies for ionizing radiation, LEEI does not need heavy shielding constructions and therefore has the potential for integration into pharmaceutical production facilities. The major challenge of LEEI is the low penetration depth of the low-energy electrons, which has limited its use so far mainly to the sterilization of surfaces (28). By developing processes to transform liquids into thin films for an

automated application, this problem was solved and LEEI was made applicable for the inactivation of pathogens in solution (19). TBEV was treated with LEEI of different doses, and 20 kGy were found to inactivate the virus completely. This is in line with the related flavivirus Zika virus, for which an LEEI-dose of 20 kGy for a complete inactivation was also established (19). 20 kGy was also reported in a previous publication on gamma-irradiated TBEV (29). However, another study found 50 kGy of gamma-radiation to be required for complete inactivation (30). The discrepancy is likely to be based on different irradiation conditions, such as media or temperature. It has been shown that sensitivity to ionizing radiation increases at higher temperatures (31). Hrusková and this study used samples at room temperature or 4°C, respectively. Feldmann et al., irradiated the virus on dry ice.

When compared to the currently used production process of FA-inactivation, LEEI has important advantages. It does not require any toxic chemicals, and the process is much faster. In the setting presented here, 10 minutes were sufficient to inactivate 10 milliliters of TBEV. Using a recently developed continuous irradiation technology, even multi-liter scale preparations could be inactivated within hours (19). This represents a significant improvement over the 5 days inactivation with FA and would substantially speed up the vaccine production process.

In accordance with previously reported data from other LEEI inactivated pathogens, the antigenicity of TBEV was not substantially changed by the radiation. Consequently, when administered to animals, the LEEI-inactivated virus induced detectable TBEV-binding antibodies. The titers were significantly higher in the mice receiving the LEEI-inactivated TBEV than in the group immunized with FA-inactivated virus. After the second immunization also the avidity of the antibodies, which has been shown to correlate with protection (7, 32), was significantly higher after immunization with LEEI-inactivated TBEV. These observations could be explained by the better preservation of antigens in their natural confirmation during the irradiation-based inactivation process. The impact of FA on the antigenicity of vaccine preparations of several pathogens is known, and also for TBEV it has been demonstrated that treatment with FA leads to the loss of several epitopes within the envelope protein, the most important antigen for flavivirus vaccines (33).

The protective efficacy of the vaccine preparations was analyzed in a viral challenge experiment. When infected with live virus, all animals immunized with LEEI- or FA-inactivated TBEV survived without symptoms, whereas the control mice all developed a clinical score, and 50% of them did not survive. In addition, no viral RNA or infectious virus was found in the brains or the spinal cords of vaccinated animals. Mice immunized with either LEEI- or FA-inactivated TBEV were thus completely protected from virus challenge. On the other hand, it was therefore not possible to detect significant differences in vaccine efficacy between the two inactivation methods. It remains to be determined whether the higher avidity of the antibodies induced by LEEI after two immunizations increases protection over chemically inactivated TBEV. A way to address this further would be the usage of a more stringent challenge and/or less antigen per dose. In addition, an immunization schedule of only two doses could be employed.

Taken together, we show that LEEI efficiently inactivates TBEV while maintaining its antigenic properties. Upon vaccination, LEEI-inactivated TBEV induces antibodies of high avidity and protects animals from symptomatic infection and viral load in the CNS. The results indicate that LEEI is worth being further evaluated as an alternative to chemical inactivation, in order to eventually avoid the usage of hazardous substances for the production of inactivated TBEV vaccines.

DATA AVAILABILITY STATEMENT

The original contributions presented in the study are included in the article/supplementary material. Further inquiries can be directed to the corresponding author.

ETHICS STATEMENT

The animal study was reviewed and approved by Landesdirektion Sachsen, Saxony, Gemany.

AUTHOR CONTRIBUTIONS

SU, TG, LI, and JuF designed the study. JuF and LI performed the virus and animal experiments. SS, JuF, BS, and MT performed irradiation experiments. JuF, LI, TG, JaF, AR, and SU analyzed and interpreted the data. SU, JuF and LI wrote the paper. All authors contributed to the article and approved the submitted version.

ACKNOWLEDGMENTS

We thank Ulrike Ehlert, Anne-Kathrin Donner, Isabell Schulz, Fabian Pappe and Andre Poremba for excellent technical assistance, Dr. Markus Kreuz for statistical evaluation of the data, Prof. Uwe Liebert (Leipzig University) for supplying TBEV, and Prof. Luisa Barzon (Padova University) for supplying serum samples.

REFERENCES

1. Gubler DJ. The Continuing Spread of West Nile Virus in the Western Hemisphere. *Clin Infect Dis an Off Publ Infect Dis Soc Am* (2007) 45 (8):1039–46. doi: 10.1086/521911
2. Heinz FX, Stiasny K. The Molecular Antigenic Structure of the TBEV. In: *Tick-Borne Encephalitis - The Book*. Singapore: Global Health Press Pte. Ltd (2021). doi: 10.33442/26613980_2b-4
3. Mansfield KL, Johnson N, Phipps LP, Stephenson JR, Fooks AR, Solomon T. Tick-Borne Encephalitis Virus - A Review of an Emerging Zoonosis. *J Gen Virol* (2009) 90(Pt 8):1781–94. doi: 10.1099/vir.0.011437-0
4. Dobler G, Gniel D, Petermann R, Pfeffer M. Epidemiology and Distribution of Tick-Borne Encephalitis. *Wiener Med Wochenschr (1946)* (2012) 162(11-12):230–8. doi: 10.1007/s10354-012-0100-5
5. Ruzek D, Avšič Županc T, Borde J, Chrdle A, Ludek E, Karganova G, et al. Tick-Borne Encephalitis in Europe and Russia: Review of Pathogenesis,

Clinical Features, Therapy, and Vaccines. *Antiviral Res* (2019) 164:23–51. doi: 10.1016/j.antiviral.2019.01.014
6. Heinz FX, Stiasny K, Holzmann H, Grgic-Vitek M, Kriz B, Essl A, et al. Vaccination and Tick-Borne Encephalitis, Central Europe. *Emerg Infect Dis* (2013) 19(1):69–76. doi: 10.3201/eid1901.120458
7. Kubinski M, Beicht J, Gerlach T, Volz A, Sutter G, Rimmelzwaan GF. Tick-Borne Encephalitis Virus: A Quest for Better Vaccines Against a Virus on the Rise. *Vaccines* (2020) 8(3). doi: 10.3390/vaccines8030451
8. Sanders B, Koldijk M, Schuitemaker H. Inactivated Viral Vaccines. In: BK Nunnally, VE Turula, RD Sitrin, editors. *Vaccine Analysis: Strategies, Principles, and Control, Bd. 29*. Berlin, Heidelberg: Springer Berlin Heidelberg (2015). p. 45–80.
9. Peetermans J. Production, Quality Control and Characterization of an Inactivated Hepatitis A Vaccine. *Vaccine* (1992) 10 Suppl 1:S99–101. doi: 10.1016/0264-410x(92)90557-z
10. Amanna IJ, Raué H-P, Slifka MK. Development of a New Hydrogen Peroxide–Based Vaccine Platform. *Nat Med* (2012) 18(6):974–9. doi: 10.1038/nm.2763
11. Fan Y-C, Chiu H-C, Chen L-K, Chang G-JJ, Chiou S-S. Formalin Inactivation of Japanese Encephalitis Virus Vaccine Alters the Antigenicity and Immunogenicity of a Neutralization Epitope in Envelope Protein Domain III. *PloS Negl Trop Dis* (2015) 9(10):e0004167. doi: 10.1371/journal.pntd.0004167
12. Uittenbogaard JP, Zomer B, Hoogerhout P, Metz B. Reactions of Beta-Propiolactone With Nucleobase Analogues, Nucleosides, and Peptides: Implications for the Inactivation of Viruses. *J Biol Chem* (2011) 286 (42):36198–214. doi: 10.1074/jbc.M111.279232
13. Alsharifi M, Müllbacher A. The Gamma-Irradiated Influenza Vaccine and the Prospect of Producing Safe Vaccines in General. *Immunol Cell Biol* (2010) 88 (2):103–4. doi: 10.1038/icb.2009.81
14. Furuya Y. Return of Inactivated Whole-Virus Vaccine for Superior Efficacy. *Immunol Cell Biol* (2012) 90(6):571–8. doi: 10.1038/icb.2011.70
15. Jesudhasan PR, McReynolds JL, Byrd AJ, He H, Genovese KJ, Droleskey R, et al. Electron-Beam-Inactivated Vaccine Against Salmonella Enteritidis Colonization in Molting Hens. *Avian Dis* (2015) 59(1):165–70. doi: 10.1637/10917-081014-resnoter
16. Jwa MY, Jeong S, Ko EB, Kim AR, Kim HY, Kim SK, et al. Gamma-Irradiation of Streptococcus Pneumoniae for the Use as an Immunogenic Whole Cell Vaccine. *J Microbiol (Seoul Korea)* (2018) 56(8):579–85. doi: 10.1007/s12275-018-8347-1
17. Seo HOS. Application of Radiation Technology in Vaccines Development. *Clin Exp Vaccine Res* (2015) 4(2):145–58. doi: 10.7774/cevr.2015.4.2.145
18. IAEA. *Radiation Safety of Gamma, Electron and X Ray Irradiation Facilities*. Vienna: INTERNATIONAL ATOMIC ENERGY AGENCY (2010). Available at: https://www.iaea.org/publications/8401/radiation-safety-of-gamma-electron-and-x-ray-irradiation-facilities. Specific Safety Guides.
19. Fertey J, Thoma M, Beckmann J, Bayer L, Finkensieper J, Reißhauer S, et al. Automated Application of Low Energy Electron Irradiation Enables Inactivation of Pathogen- and Cell-Containing Liquids in Biomedical Research and Production Facilities. *Sci Rep* (2020) 10(1):12786. doi: 10.1038/s41598-020-69347-7
20. Bayer L, Fertey J, Ulbert S, Grunwald T. Immunization With an Adjuvanted Low-Energy Electron Irradiation Inactivated Respiratory Syncytial Virus Vaccine Shows Immunoprotective Activity in Mice. *Vaccine* (2018) 36 (12):1561–9. doi: 10.1016/j.vaccine.2018.02.014
21. Fertey J, Bayer L, Grunwald T, Pohl A, Beckmann J, Gotzmann G, et al. Pathogens Inactivated by Low-Energy-Electron Irradiation Maintain Antigenic Properties and Induce Protective Immune Responses. *Viruses* (2016) 8(11). doi: 10.3390/v8110319
22. Fertey J, Bayer L, Kähl S, Haji RM, Burger-Kentischer A, Thoma M, et al. Low-Energy Electron Irradiation Efficiently Inactivates the Gram-Negative Pathogen Rodentibacter Pneumotropicus-A New Method for the Generation of Bacterial Vaccines With Increased Efficacy. *Vaccines* (2020) 8 (1). doi: 10.3390/vaccines8010113
23. Reed LJ, Muench H. A Simple Method of Estimating Fifty Percent Endpoints. *Am J Epidemiol* (1938) 27(3):493–7. doi: 10.1093/oxfordjournals.aje.a118408
24. WHO. *WHO Requirements for Tick-Borne Encephalitis Vaccine (Inactivated)*. WHO (1999). Technical Report Series 889.
25. Berneck BS, Rockstroh A, Fertey J, Grunwald T, Ulbert S. A Recombinant Zika Virus Envelope Protein With Mutations in the Conserved Fusion Loop Leads to Reduced Antibody Cross-Reactivity Upon Vaccination. *Vaccines* (2020) 8 (4). doi: 10.3390/vaccines8040603
26. Salát Jiří, Formanová P, Huňady M, Eyer Luděk, Palus M, Ruzek D. Development and Testing of a New Tick-Borne Encephalitis Virus Vaccine Candidate for Veterinary Use. *Vaccine* (2018) 36(48):7257–61. doi: 10.1016/j.vaccine.2018.10.034
27. Schwaiger M, Cassinotti P. Development of a Quantitative Real-Time RT-PCR Assay With Internal Control for the Laboratory Detection of Tick Borne Encephalitis Virus (TBEV) RNA. *J Clin Virol Off Publ Pan Am Soc Clin Virol* (2003) 27(2):136–45. doi: 10.1016/s1386-6532(02)00168-3
28. Wetzel C, Schönfelder J, Schwarz W, Funk R. Surface Modification of Polyurethane and Silicone for Therapeutic Medical Technics by Means of Electron Beam. *Surface Coatings Technol* (2010) 205:1618–23. doi: 10.1016/j.surfcoat.2010.07.103
29. Hrusková J. Effects of Gamma Radiation on Western Equine Encephalomyelitis and Tick-Borne Encephalitis Viruses. *Acta Virologica* (1969) 13(3):187–92.
30. Feldmann F, Shupert WL, Haddock E, Barri T, Feldmann H. Gamma Irradiation as an Effective Method for Inactivation of Emerging Viral Pathogens. *Am J Trop Med Hygiene* (2019) 100(5):1275–7. doi: 10.4269/ajtmh.18-0937
31. Singleton EV, Gates CJ, David SC, Hirst TR, Davies JB, Alsharifi M. Enhanced Immunogenicity of a Whole-Inactivated Influenza A Virus Vaccine Using Optimised Irradiation Conditions. *Front Immunol* (2021) 12:761632. doi: 10.3389/fimmu.2021.761632
32. Albinsson BO, Vene S, Rombo L, Blomberg J, Lundkvist Åke, Rönnberg B. Distinction Between Serological Responses Following Tick-Borne Encephalitis Virus (TBEV) Infection vs Vaccination, Sweden 2017. *Euro Surveillance Bull Eur sur les maladies transmissibles = Eur Communicable Dis Bull* (2018) 23(3). doi: 10.2807/1560-7917.ES.2018.23.3.17-00838
33. Barrett PN, Schober-Bendixen S, Ehrlich HJ. History of TBE Vaccines. *Vaccine* (2003) 21 Suppl 1:S41–9. doi: 10.1016/s0264-410x(02)00814-9

Conflict of Interest: SU is co-author on the patent WO 2015011265, which describes the inactivation of viruses by low-energy electron irradiation.

The remaining authors declare that the research was conducted in the absence of any commercial or financial relationships that could be construed as a potential conflict of interest.

Publisher's Note: All claims expressed in this article are solely those of the authors and do not necessarily represent those of their affiliated organizations, or those of the publisher, the editors and the reviewers. Any product that may be evaluated in this article, or claim that may be made by its manufacturer, is not guaranteed or endorsed by the publisher.

frontiers in Immunology

ORIGINAL RESEARCH
published: 14 March 2022
doi: 10.3389/fimmu.2022.840077

Electron-Beam Inactivation of Human Rotavirus (HRV) for the Production of Neutralizing Egg Yolk Antibodies

*Jill W. Skrobarczyk[1], Cameron L. Martin[1], Sohini S. Bhatia[1,2], Suresh D. Pillai[2,3] and Luc R. Berghman[1,4]**

[1] Department of Poultry Science, Texas A&M University, College Station, TX, United States, [2] National Center for Electron Beam Research, Texas A&M University, College Station, TX, United States, [3] Department of Food Science and Technology, Texas A&M University, College Station, TX, United States, [4] Department of Veterinary Pathobiology, Texas A&M University, College Station, TX, United States

OPEN ACCESS

Edited by:
Sebastian Ulbert,
Fraunhofer Institute for Cell Therapy and Immunology (IZI), Germany

Reviewed by:
Sankar Renu,
Upkara Inc., United States
Viviana Parreño,
Instituto Nacional de Tecnología Agropecuaria, Argentina

***Correspondence:**
Luc R. Berghman
luc.berghman@ag.tamu.edu

Specialty section:
This article was submitted to Vaccines and Molecular Therapeutics, a section of the journal Frontiers in Immunology

Received: 20 December 2021
Accepted: 21 February 2022
Published: 14 March 2022

Citation:
Skrobarczyk JW, Martin CL, Bhatia SS, Pillai SD and Berghman LR (2022) Electron-Beam Inactivation of Human Rotavirus (HRV) for the Production of Neutralizing Egg Yolk Antibodies. Front. Immunol. 13:840077. doi: 10.3389/fimmu.2022.840077

Electron beam (eBeam) inactivation of pathogens is a commercially proven technology in multiple industries. While commonly used in a variety of decontamination processes, this technology can be considered relatively new to the pharmaceutical industry. Rotavirus is the leading cause of severe gastroenteritis among infants, children, and at-risk adults. Infections are more severe in developing countries where access to health care, clean food, and water is limited. Passive immunization using orally administered egg yolk antibodies (chicken IgY) is proven for prophylaxis and therapy of viral diarrhea, owing to the stability of avian IgY in the harsh gut environment. Since preservation of viral antigenicity is critical for successful antibody production, the aim of this study was to demonstrate the effective use of electron beam irradiation as a method of pathogen inactivation to produce rotavirus-specific neutralizing egg yolk antibodies. White leghorn hens were immunized with the eBeam-inactivated viruses every 2 weeks until serum antibody titers peaked. The relative antigenicity of eBeam-inactivated Wa G1P[8] human rotavirus (HRV) was compared to live virus, thermally, and chemically inactivated virus preparations. Using a sandwich ELISA (with antibodies against recombinant VP8 for capture and detection of HRV), the live virus was as expected, most immunoreactive. The eBeam-inactivated HRV's antigenicity was better preserved when compared to thermally and chemically inactivated viruses. Additionally, both egg yolk antibodies and serum-derived IgY were effective at neutralizing HRV *in vitro*. Electron beam inactivation is a suitable method for the inactivation of HRV and other enteric viruses for use in both passive and active immunization strategies.

Keywords: egg yolk, neutralizing, antibody, rotavirus, electron beam, IgY, chicken

INTRODUCTION

Routine pathogen inactivation methods in the pharmaceutical industry include chemical and thermal treatments. Both are lengthy procedures, and the former requires additional processing to remove chemical residue from the final formulation. Chemical and heat inactivation also pose a greater risk of protein denaturation, thus compromising antigenicity typically defined as the capacity to be recognized by an antigen-specific antibody. Electron beam (eBeam) inactivation of pathogens is a commercially proven method for the inactivation of microorganisms used extensively in the medical device sterilization and food processing industries (1–4). In this technology, highly energetic electrons are accelerated to 99.999% the speed of light, in "accelerators" and guided into a single beam. Microbial inactivation results from both direct damage to the nucleic acids by electrons or indirectly from high reactive radiolytic species produced by the radiolysis of water molecules by the energetic electrons. Both single and double strand breaks can be generated rendering the organism inactive. Studies in our laboratories have shown that bacterial cells when inactivated retain their metabolism for specific periods of time in a state termed, Metabolically Active yet Non-culturable (MAyNC) (4). This technology is used commercially for different applications (2, 3), but its use for pathogen inactivation in pharmaceutical development is relatively new. High energy eBeam (HEEB) equipment are bulky and require large concrete structures and, therefore, often difficult to incorporate into existing production lines. However, major advances in low energy eBeam (LEEB) technology have resulted in equipment that require minimal shielding and with relatively small equipment footprint (3). The availability of LEEB technology now facilitates the adoption of eBeam technology as in-line equipment for the microbial target inactivation in pharmaceutical production (2). Previous studies have compared electron beam irradiation to traditional methods of pathogen inactivation and concluded that eBeam is an effective alternative (2, 3, 5).

Rotavirus is the leading cause of severe gastroenteritis in infants, children, and at-risk adults (6–10). Infection results in severe diarrhea, dehydration, and in some cases, death. With over 111 million cases, 2 million hospitalizations, and 300,000 deaths each year, rotavirus infections are a global issue (11). Vaccination is the primary method of rotaviral diarrhea prevention. RotaTeq™ and Rotarix™ are pentavalent and monovalent, live-attenuated rotavirus commercial vaccines, respectively. They both induce cross-protective antibody responses against multiple virus strains. While these two commercial vaccines are effective in the United States (88% and 90%, respectively), they've had minimal success in developing countries (12). As a result, developing countries have experienced over 80% of all rotavirus-related deaths (11). The poor access to healthcare and costs associated with vaccine storage, transport, and refrigeration make it difficult for these countries to provide adequate protection through vaccination (12, 13). Additional prophylactic strategies should be developed to combat the infection burden in developing countries.

Chickens accumulate antibodies in the egg yolk as a source of maternal immunity for the developing chick (14–16). Egg yolk antibodies (IgY) have a proven record of protecting against viral infections by passive immunity that blocks the adhesion to and invasion of the intestinal mucosa. This is because egg yolk antibodies are more resistant to some of the harsh gut conditions where these infections occur (14, 16). IgY is stable at pH 4-9 and temperatures up to 65°C. Administration as a lyophilized egg yolk powder may further stabilize the antibodies at even lower pH and higher temperatures (17). Additionally, the absence of a hinge region linking the Fab and Fc fragments minimizes cleavage by endogenous proteases (17). Studies have shown that anti-rotavirus egg yolk antibodies are therapeutically effective and significantly reduce the duration of diarrhea in a variety of hosts (16, 18–21). The objective of this study was to explore the utility of eBeam technology for inactivating human rotavirus and generating neutralizing egg yolk antibodies.

MATERIALS AND METHODS

The protocols and approvals by the Texas A&M Institutional Animal Care and Use Committee (IACUC) and the Texas A&M Office of Biosafety served as a guide for all animal and microbiota studies. Animal Use Protocol (AUP) #2018-0127 and Institutional Biosafety Committee (IBC) permit #2019-005 provided support for all animal immunization and rotavirus studies, respectively. Hens were housed at the Texas A&M Poultry Science Research Center and eBeam inactivation was performed at the university's National Center for Electron Beam Research (NCEBR) per biosafety protocols.

Virus and Cells

Tissue culture adapted HRV Wa (G1 P[8]) and fetal monkey kidney derived host cells, MA104, were purchased from ATCC. Cells were maintained in complete Dulbecco's Essential Medium containing 8% Fetal Bovine Serum (Atlanta Biologicals), 1% Glutamax, and 1% antibiotic-antimycotic (10,000 units/mL of penicillin, 10,000 μg/mL of streptomycin, and 25 μg/mL of amphotericin B; Gibco). The virus was activated with trypsin (Gibco) at a concentration of 15μg/ml at 37°C for 1 hour. Next, the activated virus was adsorbed onto monolayers of confluent MA104 cells at 37°C for 90 minutes. The cells were re-fed with serum-free Dulbecco's Modified Essential Medium (Corning) containing 1.5μg/ml trypsin, 1% antibiotic-antimycotic (10,000 units/mL of penicillin, 10,000 μg/mL of streptomycin, and 25 μg/mL of amphotericin B; Gibco), and 25mM HEPES (Gibco), and incubated at 37°C for 7 days or until cytopathic effect (CPE) was observed (22, 23). Virus stocks were titered using a 50% Tissue Culture Infectious Dose (TCID50) assay as described previously (24). The highest dilution of virus that produced CPE in 50% of the infected cells was considered as the endpoint. The titer of the virus was calculated using the Karber method and expressed as $\log_{10}$ TCID50/ml (25).

Electron Beam Inactivation of HRV

The eBeam inactivation was performed at the eBeam facility of NCEBR at Texas A&M University. A 10-MeV, 15-kW linear

accelerator delivered the eBeam dose. An initial dose-response (D-10) study was performed to determine the minimum eBeam dose to achieve a 1-log or 90% reduction in virus titer. Determining the D-10 value is critical when attempting to inactivate large microbial titer preparations. Ensuring that uniform eBeam doses are applied in D-10 studies, three replicates of 5ml of virus were triple-packaged in Whirl-pac bags and sealed for each dose point. An extensive set of preliminary studies was performed to ensure that the bags containing viral cultures could be irradiated effectively with dose-uniformity ratio (DUR) as close to 1.0 as possible. The DUR is the most important criterion in irradiation experiments to ensure dose uniformity within samples. Alanine dosimeters were placed at strategic positions on the sample bags to verify the delivered dose. Dosimetry was performed using validated alanine standards that were traceable to international standards (1, 5). The target doses for virus inactivation in the D-10 study were 0 kGy (non-irradiated control), 2.0 kGy, 5.0 kGy, 10.0 kGy, and 15.0 kGy. The measured doses (as determined by alanine dosimetry standards) were 1.99 kGy, 5.1 kGy, 10.15 kGy, and 15.0 kGy. After irradiation, the virus titers were quantified by TCID50 assay. All treatments were repeated at least 3 times. Based on the D-10 value, the minimum eBeam dose required to achieve complete inactivation in 200 mL of high titer rotavirus preparation for immunization studies was determined. All irradiated virus was subject to titration by TCID50 to confirm complete inactivation.

Chemical and Thermal Inactivation of HRV

Chemical inactivation consisted of incubation of the rotavirus-containing cell culture supernatants at 25°C for 30 minutes with a final concentration of 2% (v/v) formaldehyde followed by 37°C for 30 minutes (26). For thermal inactivation, rotavirus preparations were diluted 1:10 in HBSS prior to incubation at 60°C for 2 hours. After each procedure, the viruses were dialyzed against three changes of PBS for 4 hours at 4°C. The concentrations of both inactivated virus samples were normalized by UV absorbance at 280nm and stored at -80°C.

Production of Chicken Anti-VP8 Antibodies

Five, 18-week -old, single comb, White Leghorn hens housed at the Texas A&M Poultry Science Center, College Station, TX were used to produce HRV viral protein 8 (VP8)-specific antibodies for ELISAs. Immunizations consisted of 50 μg of recombinant VP8 (Bon-Opus) suspended in 0.3 ml PBS, pH 7.4, mixed with Montanide ISA 71 R VG adjuvant (Seppic) in a 3:7 ratio. All immunizations were administered subcutaneously (s.c.) in the wing-web. Birds were boosted every 2 weeks and VP8-specific antibody titers were monitored by ELISA. Once birds were hyperimmunized as determined by indirect ELISA, 5ml of blood was drawn from each bird, pooled and centrifuged (3,000 x g) to collect the serum. The antibodies were precipitated from the pooled serum using 20% (w/v) powdered ammonium sulfate (27). The pellet containing the enriched antibody was dissolved in PBS, pH 7.4 and quantified by absorbance at 280 nm. Half of the antibody was biotinylated using the EZ Link Sulfo-NHS-Biotin kit (ThermoFisher) before storage at -20°C.

Characterization of Chicken Anti-VP8 Antibody

The affinity of the anti-VP8 antibody was determined by indirect ELISA and Western blot. For the ELISA, a flat-bottom ELISA plate (Corning) was coated overnight with 5μg/ml purified HRV VP8. The plate was blocked with 2% BSA in PBS. The anti-VP8 antibody was added to the plate (1:1,000) and incubated for 1 hour at 37°C. After rinsing the plate with PBST, HRP-conjugated goat anti-chicken IgY (1:3,000) was added and incubated for 1 hour at room temperature (Jackson ImmunoResearch). TMB substrate (SeraCare) was used as the enzyme substrate and the plate was read at 450nm. For the Western blot, 5μg of purified recombinant VP8 protein was separated by SDS-PAGE using a 12% Tris-Glycine gel (Invitrogen) and transferred to a PVDF membrane using the TransBlot Turbo Transfer System (BioRad). The membrane was blocked in 2% BSA overnight at 4°C. The purified, biotinylated chicken anti-VP8 antibody served as the primary antibody to confirm immunoreactivity with recombinant VP8 protein. The membrane was incubated with anti-VP8 for 1 hour at room temperature (1:3,000) followed by incubation with streptavidin-conjugated HRP (1:10,000). The membrane was developed with a chemiluminescent substrate solution (Agilent) and imaged on a ChemiDoc (BioRad).

Virus Antigenicity ELISA

The antigenicity of HRV before and after eBeam inactivation was assessed by a sandwich enzyme-linked immunosorbent assay. Briefly, a flat-bottom ELISA plate (Corning) was coated overnight with 5μg/ml purified chicken anti-HRV VP8 as the capture antibody. The use of an antibody raised against one of the outer capsid proteins allowed for the comparison of antibody recognition of an important neutralizing protein. The ability of the purified chicken anti-VP8 antibody to bind to a virus after inactivation indicated that its antigenic integrity was maintained. The plate was blocked with 5% gelatin in PBS. A single batch of four HRV stocks, including live virus, electron beam-inactivated virus, chemically inactivated virus, and thermally inactivated virus, was serially diluted 2-fold starting with a 400μg/ml concentration. The diluted virus preparations were added to the plate and incubated for 1 hour at 37°C. Biotinylated chicken anti-HRV VP8 was added as the detection antibody (1:1,000) and incubated for 1 hour at 37°C. HRP-conjugated neutravidin was added as the enzyme (1:20,000) (ThermoFisher) and TMB substrate (SeraCare) was used to develop the color. Sulfuric acid (50 μl of a 2 M solution) was added to stop the enzymatic reaction and the plate was read at 450nm in a BioTek microplate reader (Synergy H1).

Purification of Virus

The eBeam inactivated HRV was purified by ultracentrifugation using a cesium chloride gradient as described previously (23). After the final spin, the top fraction containing triple-layered virus particles was isolated and dialyzed against sterile PBS, pH

7.4 overnight. The concentration of purified virus particles was normalized by UV absorbance at 280nm and stored at -80°C.

Immunization of Hens and Production of Egg Yolk Antibodies

Five, 18-week-old, single comb, White Leghorn hens housed at the Texas A&M Poultry Science Center, College Station, TX were used to produce HRV-specific antibodies. Immunizations consisted of 50 μg of HRV suspended in 0.3 ml PBS, pH 7.4, mixed with Montanide ISA adjuvant (Seppic) in a 3:7 ratio. All immunizations were administered subcutaneously (s.c.) in the wing-web. Birds were boosted every 2 weeks and blood samples were collected after each boost to quantify HRV-specific antibody levels by ELISA. Four immunizations were administered before the birds were hyperimmunized as determined by indirect ELISA. Eggs were then collected daily for 1 week, and frozen at -20°C until needed. Pre-immune eggs were also collected from each hen before receiving any immunizations.

Purification of IgY From Egg Yolks

Frozen eggs were thawed in room-temperature DI water and yolks were separated from the egg white. To remove the lipids, yolks were pooled and emulsified in DI water before adjusting the pH to 7.0 and freezing again at -20°C. The yolk solution was thawed again the next day and total IgY was precipitated using 20% (w/v) powdered ammonium sulfate (27). The pellet containing highly enriched IgY was dissolved in PBS, pH 7.4, dialyzed against additional PBS, quantified by absorbance at 280 nm and stored at -20°C.

Detection of Anti-HRV Antibodies in Serum and Egg Yolk

The presence of anti-HRV IgY antibodies in serum and egg yolk from hyperimmunized hens was monitored and assayed by a modified indirect ELISA as described previously (28). Briefly, 10 μg/ml of purified HRV was coated on microtiter plates (Corning) overnight and allowed to react with serum and yolk samples diluted 1:1000. In the titration ELISA, the serum and yolk samples were serially diluted three- or five-fold. Antibodies were diluted in PBS, pH 7.4 containing 2% (w/v) BSA. Upon rinsing 3X with 200μl PBST, specifically bound anti-HRV IgY was probed by horseradish peroxidase-conjugated goat anti-chicken IgY (Jackson Immunolabs) at 1:3,000 dilution, followed by detection with Tetramethylbenzidine High Kinetics substrate (BioVision). A positive ELISA value was identified as >2X mean OD450 value of pre-immune IgY (at 1:1,000).

In Vitro Virus Neutralization Assay

The virus neutralization titer of anti-HRV IgY was determined using MA104 cell monolayers by methods described previously (23, 29). The crude serum and egg yolk preparations contained 20 and 5mg/ml of antibody, respectively. The serum and yolk samples were normalized to a concentration of 5mg/ml before diluting 25 microliters of both antibody preparations in 25 microliters of media to create a 2-fold serial dilution for the assay. Two hundred TCID50 units of HRV were incubated with the 2-fold serial dilution of IgY at 37°C for 1 hour. The antibody-virus suspension was layered onto confluent MA104 cell monolayers grown in 96-well microplates (Nunc, USA). After 7 days of incubation at 37°C in a humidified 5% CO_2 atmosphere, the plates were examined for the presence of CPE. The complete absence of CPE was scored as positive for neutralization. Antibody samples were run in triplicate and the reciprocal of the mean highest dilution of IgY was reported as the neutralization titer.

RESULTS

Complete Inactivation of HRV Was Achieved at 15 kGy

The titer of the propagated HRV stock was quantified by TCID50 and reported as 6.5 log TCID50. This titer was maintained for all inactivation and immunization experiments. The propagated virus was purified by ultracentrifugation with a cesium chloride gradient. Purification of HRV yielded two distinct bands in the density gradient corresponding to double and triple layered virus particles. The double and triple layered particles settled at a density of 1.37 g/cm^3 and 1.34 g/cm^3, respectively.

While viruses are more resistant than bacteria to ionizing radiation (because of the smaller genome size), they are, nevertheless, still susceptible to eBeam doses. The dose (± standard error [SE]) required to achieve a 1-log or 90% reduction (D-10 value) in HRV titer was calculated at 2.38 (± 0.017) kGy, while total inactivation of the virus was achieved at 15 kGy (**Figure 1**). The absence of CPE observed after irradiation at 15 kGy indicated no viral replication had occurred and the virus was deemed non-infectious. This eBeam dose was used in all subsequent experiments for complete inactivation of HRV stocks.

Anti-VP8 Chicken Antiserum Detects Recombinant VP8 in ELISA and Immunoblot

The ability of the purified chicken anti-VP8 antibody to bind to recombinant and native VP8 was demonstrated with two assays. The signal of the hyperimmune antiserum was 11 times that of the pre-immune serum indicating that the birds were hyperimmunized and the serum antibodies were specific for the recombinant viral protein (**Figure 2**). In addition, immunoblotting analysis of the recombinant VP8 protein using chicken anti-VP8 produced a single band at the expected apparent molecular weight of 28 kDa (**Figure 3**).

Electron Beam Inactivation Was Effective at Preserving Antigenicity of HRV

A sandwich ELISA using anti-HRV VP8 antibodies was performed to compare the antigenicity of the virus before and after the three different inactivation methods (**Figure 4**). A linear relationship was observed between virus concentration and

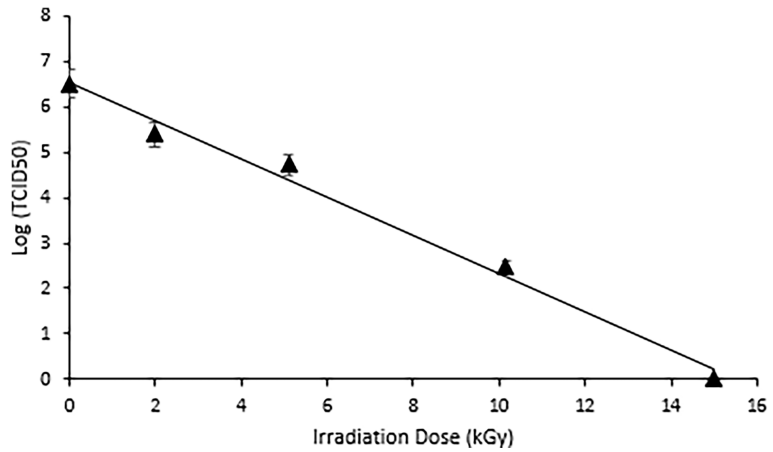

FIGURE 1 | Complete Inactivation of HRV was achieved at 15 kGy. Dose response curve illustrating the effects of electron beam irradiation on HRV stocks. The target doses were set at 0, 2, 5, 10, and 15 kGy and the measured doses were 1.99 kGy, 5.1 kGy, 10.15 kGy, and 15.0 kGy. A TCID50 assay was used to quantify the reduction in viral titer. The D_{10} value, or dose required to achieve a 1-log reduction in viral titer was calculated as 2.38 (± 0.017) kGy. Complete inactivation was achieved at 15kGy.

measured OD450. The live (non-inactivated) control consistently reported the highest OD450 followed by eBeam inactivated, chemically, and thermally inactivated virus preparations. After eBeam inactivation at 15 kGy, the virus was detected at ~75-90% that of non-irradiated live virus control. The chemical and thermal inactivated viruses were detected at ~50-60 and 25-40% that of the live virus, respectively. A signal to noise ratio (SNR) greater than 2 was reported for only the live and eBeam inactivated viruses at 25 μg/ml. When compared to traditional chemical and thermal inactivation methods, eBeam inactivation exhibited improved conservation of antigenicity and chemical and thermal methods of inactivation were more detrimental to the virus' antigenic integrity.

Chickens Reached Maximal Anti-HRV Titers After Three Injections

Following immunization, the hens' HRV specific antibody level was monitored by indirect ELISA. Anti-HRV IgY titers peaked after the third immunization and were maintained thereafter (**Figure 5**). As expected, the response was highly variable between biological replicates. (ELISA S/N values: 4.34, 2.15, 2.55, 3.24, and 1.46). Once the HRV-specific antibody titer

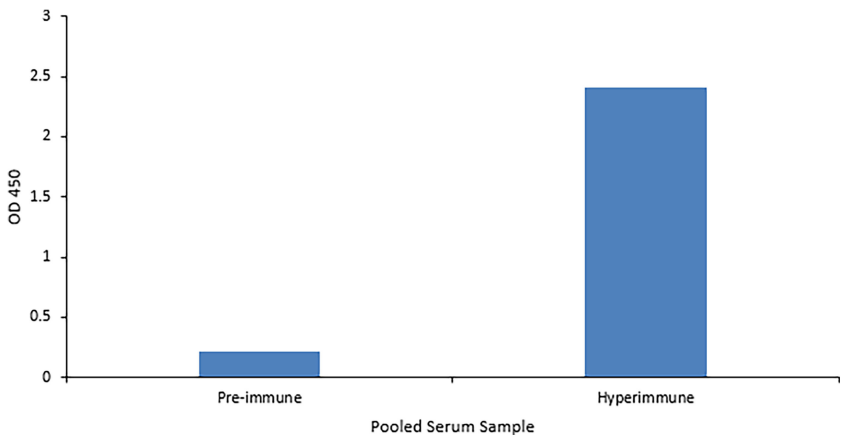

FIGURE 2 | Anti-VP8 chicken antiserum detects recombinant VP8 in an ELISA. Indirect ELISA comparing the affinity of pooled pre- and hyper-immune serum antibodies for the recombinant VP8 antigen. Birds received three immunizations consisting of 50μg purified VP8 with Montanide as an adjuvant. An ELISA plate was coated overnight with 5μg/ml purified HRV VP8 and blocked with 2% BSA in PBS. The pre- and hyper-immune anti-VP8 serum antibodies served as the primary antibody (1:1,000). HRP-conjugated goat anti-chicken IgY was added as the secondary antibody (1:3,000). The hyperimmune serum was specific for the viral protein.

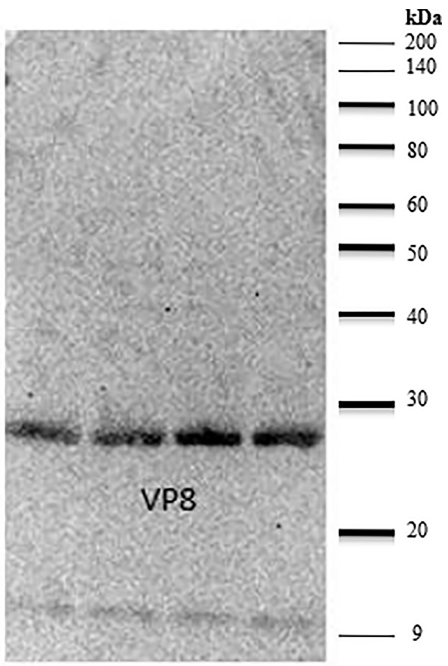

FIGURE 3 | Anti-VP8 chicken antiserum detects recombinant VP8 in a Western blot. Lanes 1-4 were loaded with 5μg of purified recombinant VP8, separated by SDS-PAGE and transferred to a PVDF membrane. The membrane was blocked in 2% BSA. Purified, biotinylated chicken anti-VP8 antibody served as the primary antibody (1:3,000) and streptavidin conjugated HRP was used to detect (1:10,000). Lanes 1-4 were loaded with 5μg of purified recombinant VP8. The purified, biotinylated chicken anti-VP8 antibody recognized the 28 kDa protein at a dilution of 1:3,000.

plateaued, birds were considered hyperimmunized. The maximum titer, defined as the reciprocal of the highest dilution producing a statistically significant indirect ELISA signal was 125,000 (**Figures 6**, **7**).

Serum- and Egg Yolk-Derived IgY Demonstrate *In Vitro* Virus Neutralization Activity

Virus neutralization was defined as the complete absence of CPE. Neutralization titers were reported as the reciprocal of the highest antibody dilution capable of preventing infection or CPE development. Serum neutralization titers were approx. 2-fold higher than corresponding egg yolk titers, ranging from 863-1706 in the serum and 341-768 in the egg yolk (**Table 1**). Pre-immune serum and egg yolk IgY were negative for neutralization.

DISCUSSION

This study outlines the use of eBeam inactivation to produce high-titer neutralizing HRV-specific egg yolk antibodies and analyzes their potential to prevent infection *in vitro*. Hens were immunized with eBeam inactivated HRV particles from the most common human strain, the Wa (G1P[8]) strain. To inactivate the rotavirus, electrons generated from HEEB equipment were utilized to create extensive breaks in the RNA genome. In the D-10 study, the HRV titer decreased as the dose of electron beam radiation increased, demonstrating an inverse but linear relationship. The dose required to inactivate 1-log of virus was reported as 2.38 + (0.017) which was, as expected, significantly higher than the reported D-10 values for bacterial pathogens.

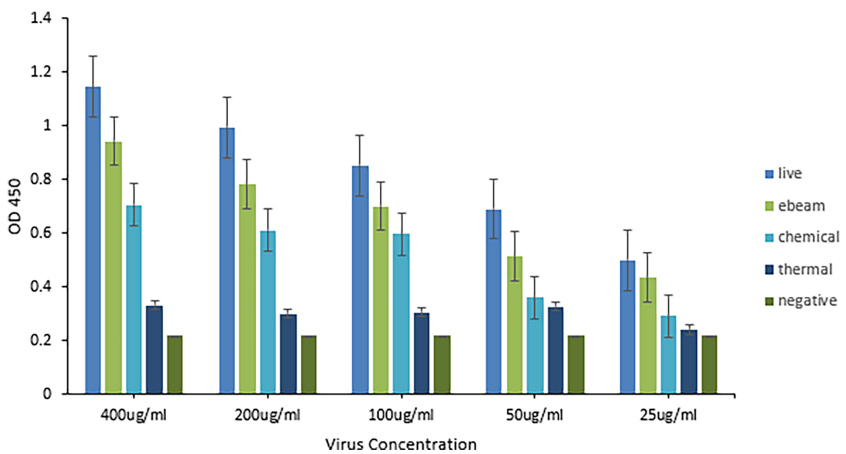

FIGURE 4 | Electron beam inactivation was superior in preserving antigenicity of HRV. Sandwich ELISA titration of inactivated HRV stocks to determine antigenicity. An ELISA plate was coated with purified chicken anti-HRV VP8 as the capture antibody and blocked with 5% gelatin in PBS. Four different HRV stocks including live virus, electron beam-inactivated virus, chemically inactivated virus, and thermally inactivated virus, were serially diluted starting with a 400μg/ml concentration. Biotinylated chicken anti-HRV VP8 served as the detection antibody (1:1,000) and HRP-conjugated neutravidin was used to detect (1:20,000). The eBeam inactivated virus was detected at ~75-90% that of non-irradiated live virus control. The chemical and thermal inactivated viruses were detected at ~50-60 and 25-40% that of the live virus, respectively. Compared to the live virus, antigenicity was best maintained after eBeam inactivation.

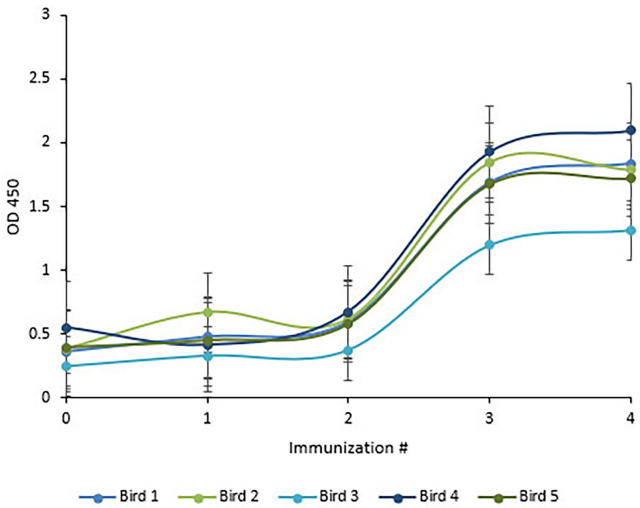

FIGURE 5 | Chickens reached maximal anti-HRV titers after three immunizations. ELISA quantification of chicken anti-HRV specific serum antibody level in response to immunization. An ELISA plate was coated with 10μg/ml of purified HRV and blocked with 2% BSA in PBS. Pre- and hyper-immune serum antibodies served as the primary antibody (1:1000). HRP-conjugated goat anti-chicken IgY served as the secondary antibody (1:3,000). Titers peaked after the third immunization and birds were considered to be hyperimmunized.

This is generally attributed to the smaller viral genome sizes compared to bacteria (2). After exposure to 15 kGy eBeam dose, high titers of HRV exhibited no replication suggesting the efficacy of the technology. Not only was the virus effectively inactivated but it was done so in a fraction of the time that traditional chemical and thermal inactivation methods require. Some chemical processes can take days or even weeks to fully inactivate. Additionally, the viral antigenicity obtained by dose-optimized electron beam inactivation (~80%) markedly exceeded antigenicity after traditional chemical (~60%) and thermal (~40%) treatments. Nucleic acids are the primary target of ionizing radiation based on the larger G-values compared to proteins or lipids (2). The G-value is defined as the amount of radiolytic species produced per 100 eV of absorbed energy. The eBeam-inactivated rotavirus was recognized at levels closest to that of the non-inactivated, live virus control (**Figure 4**) and, when used for antibody generation, produced impressive HRV-specific antibody titers (**Figures 6**, **7**). These data suggest that eBeam inactivation preserves the key epitopes found on the surface of viral proteins and, therefore, retains optimal immunoreactivity (2). The efficacy of eBeam as an inactivation technology for pharmaceutical development observed in this study is in line with previous reports on influenza A, PRRSV, and the gram-negative bacteria *R. pneumotropicus* confirming the notion that eBeam inactivation of pathogens is less damaging (2, 3, 5).

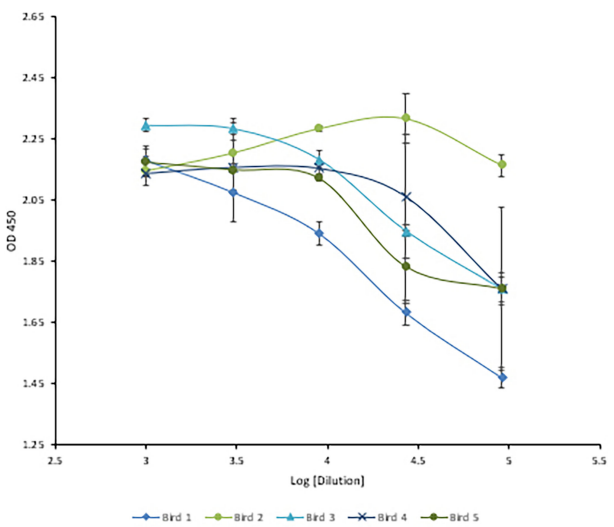

FIGURE 6 | Three-fold serial titration of anti-HRV titers after three immunizations. Titration of hyperimmune anti-HRV serum using a 3-fold serial dilution. An ELISA plate was coated with 10μg/ml of purified HRV and blocked with 2% BSA in PBS. Serum and yolk antibodies were serially diluted three-fold in PBS containing 2% BSA. HRP-conjugated goat anti-chicken IgY served as the secondary antibody (1:3,000). At 1/91,000 [log (4.95)] the signal from bird #2 was still comparable to the undiluted serum.

Not only did the eBeam-inactivated virus maintain antigenicity and generate a high titer of antigen specific antibodies, but these antibodies also demonstrated effective and efficient virus neutralization activity *in vitro*. *In vitro* studies are key to determining drug efficacy in a controlled environment before introduction to a live animal host. These studies allow multiple drugs to be tested at one time and only those that are most effective proceed to *in vivo* studies (30). The serum neutralization titers we observed in this study were approx. 2-fold higher than corresponding egg yolk titers, ranging from 863-1706 in the serum and 341-768 in the egg yolk, which may be

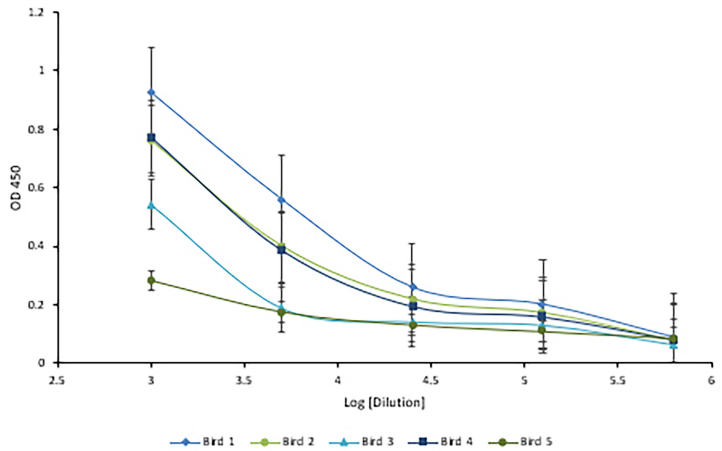

FIGURE 7 | Five-fold serial titration of anti-HRV titers after three immunizations. Titration of hyperimmune anti-HRV serum using a 5-fold serial dilution. An ELISA plate was coated with 10μg/ml of purified HRV and blocked with 2% BSA in PBS. Serum and yolk antibodies were serially diluted five-fold in PBS containing 2% BSA. HRP-conjugated goat anti-chicken IgY served as the secondary antibody (1:3,000). A dilution of 125,000 (log [5.09]) was identified as the detection limit.

TABLE 1 | *In Vitro* Virus Neutralization Titers.

Bird #	Serum	Egg Yolk
1	1706	341
2	1365	512
3	863	424
4	1365	768
5	1024	424

Virus neutralization titers, defined as the reciprocal of the highest antibody dilution capable of preventing in vitro infection or CPE development.

explained by the fact that egg yolk IgY needs to be delipidated, precipitated and dialyzed before it is suitable for addition to eukaryotic cell cultures. Egg yolk IgY is commonly purified by ammonium sulfate precipitation, yielding high levels of antibody at greater than 60-70% purity due to the lack of available affinity purification methods for IgY (27, 31). Although the neutralization titer of the hyperimmune egg yolk antibodies in the present study was lower than that of serum, all neutralization titers were comparable to those reported in the literature (14, 16, 18–21). Egg yolk antibodies represent the most prolific and cost-effective polyclonal antibody platform. Chickens are arguably the most inexpensive animal to house and feed. Depending on the age and breed of chicken and antigen used, up to 80mg of total IgY can be precipitated from one egg. Leghorns can produce over 300 eggs in a year (14, 17, 32). In this study, approximately 60 mg of total IgY was harvested from each egg providing 0.6-6 mg of HRV-specific antibody. It has been reported that 1-10% of egg yolk antibody preparations are antigen specific (16). When combined with eBeam inactivation of viruses, egg yolk antibodies provide a unique tool for passive immunization and an alternative prophylactic strategy to combat rotavirus infections. These data have important implications for the use of electron beam irradiation as an effective method of pathogen inactivation in pharmaceutical development.

DATA AVAILABILITY STATEMENT

The original contributions presented in the study are included in the article/supplementary material. Further inquiries can be directed to the corresponding author.

ETHICS STATEMENT

The animal study was reviewed and approved by Texas A&M Institutional Animal Care and Use Committee (IACUC).

AUTHOR CONTRIBUTIONS

JS performed all experiments, analyzed data, and drafted the manuscript. CM assisted with project design and provided experimental advice. SB provided experimental advice. SP conceived the idea of the study and assisted with project design and data analysis. LB also conceived the idea of the study and assisted with project design, support, data analysis and manuscript writing. All authors read and approved the manuscript.

FUNDING

This study was funded with internal money from both the SP and LB labs.

ACKNOWLEDGMENTS

The electron beam study was performed at the National Center for Electron Beam Research located at Texas A&M University in College Station, TX. The work performed was part of the NCEBR's role as an IAEA Collaborating Center for Electron Beam Technology.

REFERENCES

1. Espinosa AC, Jesudhasan P, Arredondo R, Cepeda M, Mazari-Hiriart M, Mena KD, et al. Quantifying the Reduction in Potential Health Risks by Determining the Sensitivity of Poliovirus Type 1 Chat Strain and Rotavirus SA-11 to Electron Beam Irradiation of Iceberg Lettuce and Spinach. *Appl Environ Microbiol* (2012) 78(4):988–93. doi: 10.1128/AEM.06927-11
2. Fertey J, Bayer L, Grunwald T, Pohl A, Beckmann J, Gotzmann G, et al. Pathogens Inactivated by Low-Energy-Electron Irradiation Maintain Antigenic Properties and Induce Protective Immune Responses. *Viruses* (2016) 8(11):319. doi: 10.3390/v8110319
3. Fertey J, Bayer L, Kähl S, Haji RM, Burger-Kentischer A, Thoma M, et al. Low-Energy Electron Irradiation Efficiently Inactivates the Gram-Negative Pathogen Rodentibacter Pneumotropicus—A New Method for the Generation of Bacterial Vaccines With Increased Efficacy. *Vaccines* (2020) 8 (1):113. doi: 10.3390/vaccines8010113
4. Bhatia SS, Pillai SD. A Comparative Analysis of the Metabolomic Response of Electron Beam Inactivated E. Coli O26:H11 and Salmonella Typhimurium ATCC 13311. *Front Microbiol* (2019) 10:694. doi: 10.3389/fmicb.2019.00694
5. Jesudhasan PR, McReynolds JL, Byrd AJ, He H, Genovese KJ, Droleskey R, et al. Electron-Beam-Inactivated Vaccine Against Salmonella Enteritidis Colonization in Molting Hens. *Avian Dis* (2015) 59(1):165–70. doi: 10.1637/10917-081014-ResNoteR
6. Bines JE, Kirkwood CD. Conquering Rotavirus: From Discovery to Global Vaccine Implementation. *J Paediatr Child Health* (2015) 51:34–9. doi: 10.1111/jpc.12815
7. Estes MK, Cohen J. Rotavirus Gene Structure and Function. *Microbiol Rev* (1989) 53:410–49. doi: 10.1128/mr.53.4.410-449.1989
8. Hammarström L. Passive Immunity Against Rotavirus in Infants. In: *Acta Paediatrica, International Journal of Paediatrics, Supplement*. Oslo, Norway: John Wiley and Sons (1999). 88(430):127–32. doi: 10.1111/j.1651-2227.1999.tb01311.x
9. Hoshino Y, Kapikian AZ. Rotavirus Serotypes: Classification and Importance in Epidemiology, Immunity, and Vaccine Development. *J Health Popul Nutr* (2000) 18(1):5–14.
10. Lieberman JM. Rotavirus and Other Viral Causes of Gastroenteritis. *Pediatr Ann* (1994) 23:529–32. doi: 10.3928/0090-4481-19941001-06
11. Parashar UD, Hummelman EG, Bresee JS, Miller MA, Glass RI. Global Illness and Deaths Caused by Rotavirus Disease in Children. *Emerg Infect Dis* (2003) 9(5):565–72. doi: 10.3201/eid0905.020562
12. Jiang V, Jiang B, Tate J, Parashar UD, Patel MM. Performance of Rotavirus Vaccines in Developed and Developing Countries. *Hum Vaccines* (2010) 6:532–42. doi: 10.4161/hv.6.7.11278
13. Yen C, Tate JE, Hyde TB, Cortese MM, Lopman BA, Jiang B, et al. Rotavirus Vaccines: Current Status and Future Considerations. *Hum Vaccines Immunother* (2014) 10:1436–48. doi: 10.4161/hv.28857
14. Mine Y, Kovacs-Nolan J. Chicken Egg Yolk Antibodies as Therapeutics in Enteric Infectious Disease: A Review. *J Med Food* (2002) 5:159–69. doi: 10.1089/10966200260398198
15. Michael A, Meenatchisundaram S, Parameswari G, Subbraj T, Selvakumaran R, Ramalingam S. Chicken Egg Yolk Antibodies (IgY) as an Alternative to Mammalian Antibodies. *Indian J Sci Technol* (2010) 3(4):468–74. doi: 10.17485/ijst/2010/v3i4.24
16. Pereira EPV, van Tilburg MF, Florean EOPT, Guedes MIF. Egg Yolk Antibodies (IgY)and Their Applications in Human and Veterinary Health: A Review. *Int Immunopharmacol* (2019) 73:293–303. doi: 10.1016/j.intimp.2019.05.015
17. Müller S, Schubert A, Zajac J, Dyck T, Oelkrug C. IgY Antibodies in Human Nutrition for Disease Prevention. *Nutr J* (2015) 14:109. doi: 10.1186/s12937-015-0067-3
18. Sarker SA, Casswall TH, Juneja LR, Hoq E, Hossain I, Fuchs GJ, et al. Randomized, Placebo-Controlled, Clinical Trial of Hyperimmunized Chicken Egg Yolk Immunoglobulin in Children With Rotavirus Diarrhea. *J Pediatr Gastroenterol Nutr* (2001) 32(1):19–25. doi: 10.1097/00005176-200101000-00009
19. Lee SH, Lillehoj HS, Park DW, Jang SI, Morales A, García D, et al. Protective Effect of Hyperimmune Egg Yolk IgY Antibodies Against Eimeria Tenella and Eimeria Maxima Infections. *Vet Parasitol* (2009) 163(1–2):123–6. doi: 10.1016/j.vetpar.2009.04.020
20. Li X, Wang L, Zhen Y, Li S, Xu Y. Chicken Egg Yolk Antibodies (IgY) as Non-Antibiotic Production Enhancers for Use in Swine Production: A Review. *J Anim Sci Biotechnol* (2015) 6:40. doi: 10.1186/s40104-015-0038-8
21. Vega C, Bok M, Saif L, Fernandez F, Parreño V. Egg Yolk IgY Antibodies: A Therapeutic Intervention Against Group A Rotavirus in Calves. *Res Vet Sci* (2015) 103:1–10. doi: 10.1016/j.rvsc.2015.09.005
22. Ward RL, Knowlton DR, Pierce MJ. Efficiency of Human Rotavirus Propagation in Cell Culture. *J Clin Microbiol* (1984) 19(6):748–53. doi: 10.1128/jcm.19.6.748-753.1984
23. Arnold M, Patton JT, McDonald SM. Culturing, Storage, and Quantification of Rotaviruses. *Curr Protoc Microbiol* (2009) 15:15C.3. doi: 10.1002/9780471729259.mc15c03s15
24. Smither SJ, Lear-Rooney C, Biggins J, Pettitt J, Lever MS, Olinger GG. Comparison of the Plaque Assay and 50% Tissue Culture Infectious Dose Assay as Methods for Measuring Filovirus Infectivity. *J Virol Methods* (2013) 193(2):565–71. doi: 10.1016/j.jviromet.2013.05.015
25. Karber G. 50% End Point Calculation. *Archiv Exp Pathol Pharmakol* (1931) 162:480–3. doi: 10.1007/BF01863914
26. Möller L, Schünadel L, Nitsche A, Schwebke I, Hanisch M, Laue M. Evaluation of Virus Inactivation by Formaldehyde to Enhance Biosafety of Diagnostic Electron Microscopy. *Viruses* (2015) 7(2):666–79. doi: 10.3390/v7020666
27. Deignan T, Kelly J, Alwan A, O'Farrelly C. Comparative Analysis of Methods of Purification of Egg Yolk Immunoglobulin. *Food Agric Immunol* (2000) 12 (1):77–85. doi: 10.1080/09540100099643
28. Yolken RH, Leister F, Wee SB, Miskuff R, Vonderfecht S. Antibodies to Rotaviruses in Chickens' Eggs: A Potential Source of Antiviral Immunoglobulins Suitable for Human Consumption. *Pediatrics* (1988) 81 (2):291–5. doi: 10.1542/peds.81.2.291
29. Gauger PC, Vincent AL. Serum Virus Neutralization Assay for Detection and Quantitation of Serum-Neutralizing Antibodies to Influenza a Virus in Swine. *Methods Mol Biol* (2014) 1161:313–24. doi: 10.1007/978-1-4939-0758-8_26
30. Tagle DA. The NIH Microphysiological Systems Program: Developing *In Vitro* Tools for Safety and Efficacy in Drug Development. *Curr Opin Pharmacol* (2019) 48:146–54. doi: 10.1016/j.coph.2019.09.007
31. Ko KY, Ahn DU. Preparation of Immunoglobulin Y From Egg Yolk Using Ammonium Sulfate Precipitation and Ion Exchange Chromatography. *Poult Sci* (2007) 86(2):400–7. doi: 10.1093/ps/86.2.400
32. Pauly D, Dorner M, Zhang X, Hlinak A, Dorner B, Schade R. Monitoring of Laying Capacity, Immunoglobulin Y Concentration, and Antibody Titer Development in Chickens Immunized with Ricin and Botulinum Toxins over a Two-Year Period. *Poult Sci* (2009) 88(2):281–90. doi: 10.3382/ps.2008-00323

Conflict of Interest: The authors declare that the research was conducted in the absence of any commercial or financial relationships that could be construed as a potential conflict of interest.

frontiers in Immunology

MINI REVIEW
published: 28 March 2022
doi: 10.3389/fimmu.2022.853874

Advances in Irradiated Livestock Vaccine Research and Production Addressing the Unmet Needs for Farmers and Veterinary Services in FAO/IAEA Member States

Hermann Unger, Richard T. Kangethe, Fatima Liaqat and Gerrit J. Viljoen*

Animal Production and Health Section, Joint FAO/IAEA Centre of Nuclear Techniques in Food and Agriculture, Department of Nuclear Sciences and Applications, International Atomic Energy Agency (IAEA), Vienna, Austria

The Animal Production and Health section (APH) of the Joint FAO/IAEA Centre of Nuclear Techniques in Food and Agriculture at the International Atomic Energy Agency has over the last 58 years provided technical and scientific support to more than 100 countries through co-ordinated research activities and technical co-operation projects in peaceful uses of nuclear technologies. A key component of this support has been the development of irradiated vaccines targeting diseases that are endemic to participating countries. APH laboratories has over the last decade developed new techniques and has put in place a framework that allows researchers from participating member states to develop relevant vaccines targeting local diseases while using irradiation as a tool for improving livestock resources.

Keywords: irradiated vaccines, FAO/IAEA, coordinated research projects (CRP), member states (MS), livestock

OPEN ACCESS

Edited by:
Maryam Dadar, Razi Vaccine and Serum Research Institute, Iran

Reviewed by:
Nguyen T. K. Vo, Wilfrid Laurier University, Canada
David Dazhia Lazarus, Agricultural Research Council of South Africa, South Africa

****Correspondence:***
Richard T. Kangethe
R.T.Kangethe@iaea.org

Specialty section:
This article was submitted to Vaccines and Molecular Therapeutics, a section of the journal Frontiers in Immunology

Received: *13 January 2022*
Accepted: *07 March 2022*
Published: *28 March 2022*

Citation:
Unger H, Kangethe RT, Liaqat F and Viljoen GJ (2022) Advances in Irradiated Livestock Vaccine Research and Production Addressing the Unmet Needs for Farmers and Veterinary Services in FAO/IAEA Member States. Front. Immunol. 13:853874. doi: 10.3389/fimmu.2022.853874

INTRODUCTION

Vaccines are a mainstay in supporting livestock health both in intensive industrial based animal systems and in the pastoralist livestock industry where they play a crucial role in supporting vulnerable communities. The development of livestock vaccines fits well within the framework of the Sustainable Development Goals specifically SD Goal 2 that aims to end hunger, achieve food security, improve nutrition, and promote sustainable agriculture (1). There are 117 OIE-listed diseases and many of these could be better addressed by a vaccine for control or require an improvement in the current vaccine setup (2, 3). In 2011, FAO declared the eradication of rinderpest globally which was achieved with the use of an attenuated live vaccine, thus emphasizing the importance of livestock vaccines in agriculture (4). The animal health and production laboratory (APHL), a section of the Joint FAO/IAEA center based at Seibersdorf, was involved in sero-monitoring of the Rinderpest vaccination programme and supported the development and validation of diagnostic tests that correlated antibody status with animal or herd level protection (5). This participation led to increasing the activities of the laboratory in different aspects of veterinary vaccine production with the use of irradiation as a tool for researching new vaccine formulations and in serological surveillance for disease eradication programs.

Irradiation has previously been used as a technique to address some of the gaps that exist in developing livestock vaccines but was later abandoned for newer techniques such as recombinant and gene-based vaccines (6). There has only ever been one irradiated livestock vaccine in common use for the cattle lung nematode *Dictyocaulus viviparous* that utilises irradiated L3 stage larvae for vaccination (7–9). Other diseases were not pursued further due to the lack of adequate immunological tools that could assess the effect of using irradiated vaccines. With more recent advances in livestock immunology, there has been a chance to re-examine irradiation for vaccine development with a novel approach targeting replication deficiency while maintaining some metabolic activities and reducing conformational alterations of antigens by employing new radio-protectant compounds such as manganese ions ($Mn2^{+}$) and Trehalose (10, 11). Additional functions for irradiated material have also been explored e.g., as adjuvants (12). A comprehensive summary of the characteristics of irradiated vaccines is found on **Figure 1**.

BACKGROUND ON IRRADIATED VACCINES

Although live attenuated vaccines have been successfully used in preventing diseases, they can trigger side effects in recipients, and in the case of viruses, revert back to infectivity (17, 18). Chemically inactivated and recombinant vaccines are however considered safe but unfortunately are often unable to elicit an effective immune response that is protective in all vaccinated individuals e.g. chemically inactivated vaccines against seasonal flu have an efficacy of only 30- 40% among the elderly (19). Irradiation therefore offers an alternative that can be as effective as live attenuated vaccines yet equally safe as killed or recombinant vaccines (20). The use of irradiation for vaccine development was initiated almost a century ago as an alternative to live attenuated and chemically inactivated *Shigella spp* bacteria (21). In livestock, irradiation experiments using the isotope Cobalt-60 (Co-60) were carried out in the late sixties to study *Trypanosome* spp., the causative agent of Nagana in livestock (22–27). Many of these experiments used higher than necessary irradiation doses to kill their targets rather than rendering them non-infective. Subsequent developments in immunology that described killed but metabolically active bacteria led to the idea that metabolic products produced by living but non-replicating irradiated pathogens made superior antigens compared to those produced by traditional chemical inactivation techniques (17, 18, 28, 29). Irradiation, when compared to chemical methods, is a rapid method of inactivation that requires no post inactivation manipulation and is suitable for industrial production (30). Exposure to radiation randomly causes breaks in single and double stranded nucleic acids that most cellular systems cannot repair, thus eliminating the possibility of reversion back to a virulent state (31). Radiation mediated genetic damage is also comparatively more severe when compared to chemical inactivation (32, 33). The ROS (reactive oxygen species) generated during the inactivation process, whether chemical or irradiation, imparts additional indirect nucleic acid and protein damage (31). Chemical inactivation however, possess the challenge of ineffective membrane penetration by chemical agents and residues in the products that must be eliminated by expensive and time consuming down-stream purification steps (34). The bigger the protein damage during inactivation, the less specific and immunogenic the vaccine becomes due to the loss of conformational epitopes. Epitope damage is more severe for chemically inactivated pathogens when compared to irradiated ones due to radio-protectants employed thus eliciting better responses as has been observed with the Gamma flu vaccine (34, 35). The quality of antigens used for immunization becomes especially important when targeting intracellular parasites where humoral responses have limited efficacy. During *L. monocytogenes* infections, specific neutralizing antibodies fail to clear intracellular infection which is vital to establish infection in the host (36). The recruitment of MHC class I mediated CD8 T cells is necessary for pathogen elimination and can only be induced by vaccines that mimic a natural infection (29). Vaccination with irradiated and killed but metabolically active *Listeria* spp. is able to elicit this crucial response when compared to chemically treated Listeria (17, 37). Using a wider repertoire of conformational epitopes that retain their secondary structures after irradiation becomes even more crucial in diseases where the correlates of immunity are unknown or poorly understood as neutralizing antibodies are not always a marker for protective immunity. The required type of immune response elicited by any radio-vaccine ultimately depends on the pathology pathway in the host vaccinated as it should ultimately strive to mimic the wild-type situation without replication. In the case of bacterial infections, irradiated *Salmonella* elicit T-independent immune protection through both humoral responses (IgG2b, IgG3) and $CD4^{+}$ T-cell mediated responses (Th1, Th17) (38). Numerous other bacterial and parasitic pathogens have been irradiated for vaccine development and are in various stages of vaccine development. These include pathogens such as *E. coli, Brucella, Clostridium, Mycobacterium, Plasmodium, Toxoplasma*, *Ancylostoma*, and *Schistosoma* all observed to be non-dividing but metabolically active after irradiation treatment (16, 39–45). It is clear from these experiments that irradiation generates metabolically active but non-replicative pathogens mainly for bacteria and protozoans, where they resemble a live infective pathogen more closely.

The approach for inactivating viruses using irradiation is however considered different. Viruses, obligate intracellular pathogens, are metabolically dependent on their host for viral replication and reproduction (46). An inactivated virus would essentially be unable to replicate within the host cell even after gaining entry. Gamma inactivated influenza A (γ-flu) can elicit IFN-I dependent partial lymphocyte activation *in vivo* contrary to UV and formalin treated vaccines. This is associated with the synthesis of structural internal viral proteins such as nucleoproteins in the cytosol of antigen presenting cells (47). The IFN-I response elicited by γ-flu can be attributed to the preservation of conformational peptides that are presented *via* MHC class I which trigger a type 1 response that is absent in formulations prepared using formalin or UV. Preparations made with formalin lose peptide moieties that elicit a cell mediated inflammatory response but still maintain

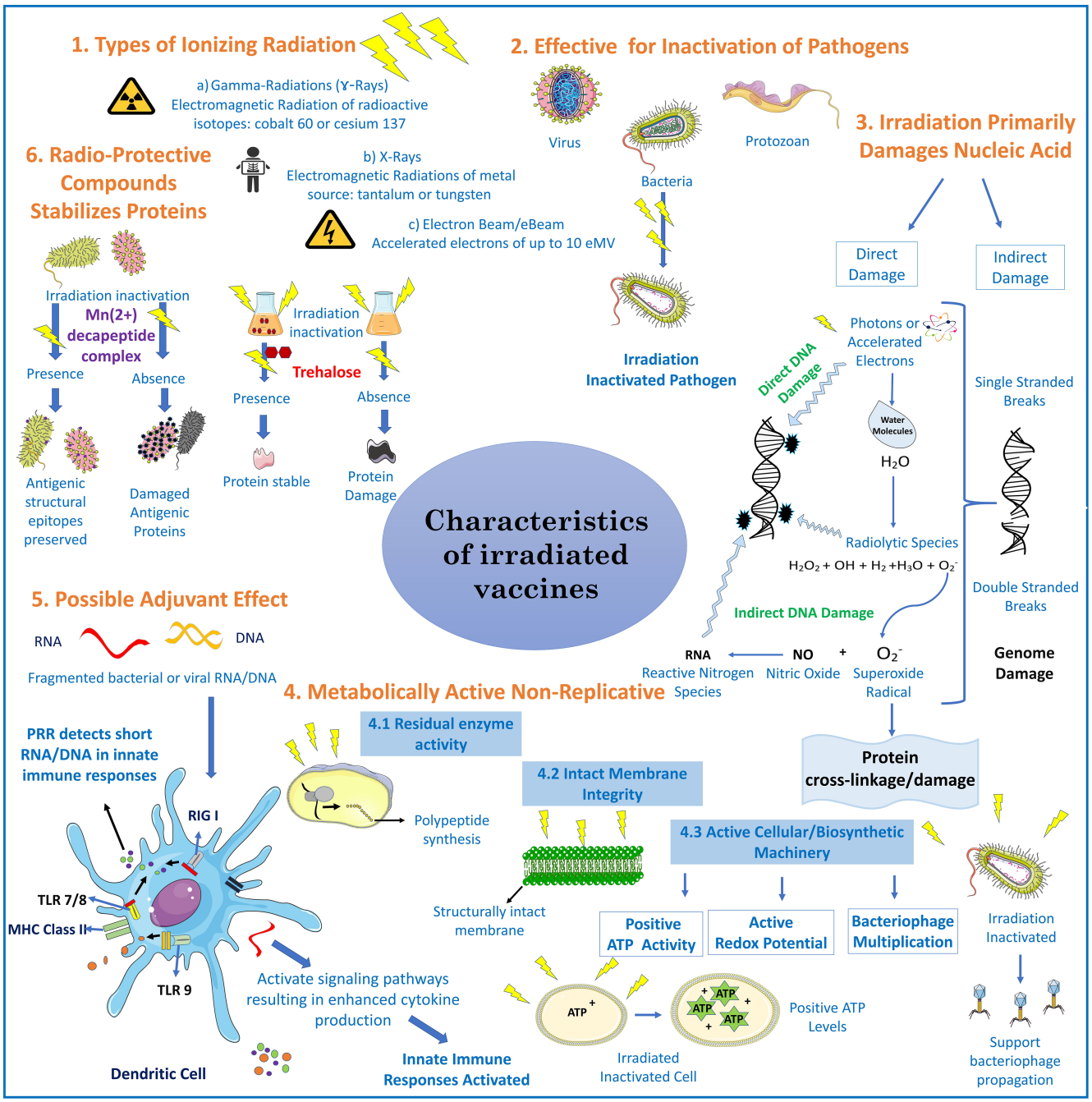

FIGURE 1 | Characteristics of irradiated vaccines: Irradiated vaccines are produced mainly by delivering ionizing radiation through gamma ray, X-ray, or electronic beam (e-Beam) irradiation (13). The mechanism behind inactivation of pathogens is through direct and indirect damage of genetic material (DNA/RNA) and cross linking of proteins. Direct genome damage is by contact of photons (from gamma-rays/X-rays) or accelerated electrons (10eMV mega electron volt) through the breakage of phosphodiester bonds (14). Indirect damage is by highly reactive short lived radiolytic species such as hydrogen peroxide (H_2O_2), hydroxyl radical, hydrogen (H_2) and superoxide radicals (O_2^-), that are the product of endogenous water molecules radiolysis. O_2^- can cause protein cross linkage and upon its reaction with nitric oxide it can generate reactive nitrogen species (RNS) that damages nucleic acids (15). In bacteria and parasites, irradiation stops replication yielding metabolically active organisms that present structural antigens and functional proteins in a vaccine as reported through ATP production, redox potential, or bacteriophage multiplication (16). Irradiation produces short RNA/DNA fragments which activate pathogen pattern recognition receptors (PRR)s, for example retinoic acid-inducible gene I (RIG I) or toll like receptors (TLR's) in the innate immune system thus acting as a vaccine adjuvant (12). Adding radio-protective compounds such Mn2+-decapeptide complex (MDP) derived from *Deinococcus radiodurans* or trehalose preserves immunogenic epitopes (10, 11).

humoral responses which are not effective at preventing disease (19). Given that irradiation leads to major nucleic acid damage when compared to other techniques, the risk of reversion in pathogens with segmented genomes is low. Innocuity testing post irradiation is however required for all formulations before further use to confirm inactivation. In the case of Avian influenza, this is carried out using embryonated chicken eggs which are susceptible to infection and are routinely used for virus isolation during surveillance of the disease (48). Other livestock viruses that have been subjected to irradiation studies with great promise include Bluetongue, Equine encephalitis and rabies amongst others (49–51).

Irradiation has also been used to improve inactivated vaccines from toxin producing pathogens. The best way to currently prevent tetanus is through vaccination using formaldehyde inactivated tetanus toxin (52). In order to overcome the disadvantages of exposing vaccine recipients to long term effects of formaldehyde and associated salts, irradiation was used to inactivate tetanus toxin (53). The toxin was inactivated at 5 kGy but retained immunogenicity at 8 KGy which was the upper limit of irradiation used in the experiment. In addition, pure irradiated toxin retained more than 50% of its enzymatic activity. Future studies will optimize the production process, detoxification and explore its feasibility as an adjuvant (53). Other toxin producing pathogens tested in irradiation studies include *Mycobacterium* spp., Anthrax, Cholera, Coli and paratyphoid B where irradiation does not necessarily inactivate the toxins in contaminated meat (28, 54–56). Irradiation has also been used in the research and production of several snake venom vaccines including African elapid, viperid and Crotalus venoms (57, 58). There are currently no effective treatments or vaccines against prion diseases due to their complex biology (59, 60). Radiation induced protein damage is considered a sterilization method of infectious proteins like prions in aqueous solution and the inactivation of infectious scrapie from transmissible spongiform encephalopathy (33, 61, 62). It was noted that high doses of up to 100 KGy were not enough to completely inactivate prions but instead reduced their quantities by 4 – 5 logs. Diluting the original stock of prion prepared had a stronger effect on reducing the chances of causing disease in mice when compared to irradiation (63). A combination of dilution and irradiation would be considered the best approach to developing antigens for anti-prion vaccines.

TECHNICAL SUPPORT TO MEMBER STATES THROUGH COORDINATED RESEARCH ACTIVITIES

Due to the requirement for basic level research in developing new irradiation vaccine formulations, APHL has initiated several different coordinated research programs (CRP) and technical cooperation projects (TCP) that have run concurrently since 2009 (**Supplementary Table 1**). The initial research project required participating members to establish the basic parameters required to carry out experiments with their chosen diseases. The participants were requested to devise a work plan that included the following points of interest for each disease in the CRP for future experiments.

1. To establish a dose of irradiation for attenuation that is consistent in scale i.e., using KGy as opposed to Krad, due to inconsistencies in groups studying the same pathogen.
2. To determine indicator/s of attenuation of the pathogen to be used for vaccination
3. To describe the representative animals used in vaccine experiments and determine the appropriate sample size.
4. To describe the parameters for vaccination including the amount of pathogen used and number of times and period of duration between inoculations.
5. To describe the parameters for challenge including number of non-irradiated pathogens used, duration of challenge after vaccination and the difference between homologous Vs heterologous.
6. To establish the criteria for protection i.e., full protection or alleviation of pathology associated with the pathogen and parameters to be measured after challenge.
7. To establish a sequence of events starting with safety at dose of irradiation, diagnostic tools available for measuring protection and the performance of the vaccine generated.
8. To identify the immune response important for protection where possible.

As a result of these activities, various basic parameters were established at the end of the first two CRP as shown in **Table 1**. To support participating laboratories further with ongoing activities, APH laboratories also developed tools that could be used in evaluating vaccine efficacy. Quantitative PCR panels that measure innate and adaptive immunity were developed for ruminants, pigs and chicken (70). Quantitative PCR panels are easy to adopt especially where collaborating partners have limited resources to carry out other assays. Similar panels using flow cytometry, ELISA, ELISPOT, Immunofluorescence, microarray and RNAseq technologies are also currently under development. A more complex assay that measures vaccine immunogenicity *in vitro* using bovine monocyte derived dendritic cells was also developed for use as a filter for antigens before proceeding to animal experiments (71). This would be particularly useful in cases where the number of irradiated vaccine candidates was large with limited animal testing facilities.

FUTURE PERSPECTIVES

The future for developing irradiated vaccines in veterinary medicine is bright. Recent advances in delivering ionising radiation using safer methods other than Co-60 have greatly advanced with the development of inactivation techniques like low energy electron beam irradiation that maintains antigenicity for Influenza A (H3N8), Porcine reproductive and respiratory syndrome (PRRSV), Equine herpes (EHV-1), Zika, Respiratory syncytial virus, *Rodentibacter pneumotropicus*, *Bacillus cereus* and *E. coli* (72–74). Irradiated pathogens have also been used

TABLE 1 | Comparison of different irradiation experiments carried out by IAEA and partners.

Species	Strain	Disease	Administered Deactivation dose (KGy)	D10 (KGy)	Post irradiation activity	*In vivo* innoculation/ Challenge	Notes
Brucella abortus	S19	Abortion in pregnant cattle	3.5	NA	alamarBlue®,	$1x10^7$/S2308 strain	Murine Macrophage infection assays
Brucella melitensis	Rev1	Human and bovine disease (zoonotic)	1 - 5	NA	alamarBlue®	NA	cross-species irradiated vaccine?
Theileria annulate	local strain/ Schizont stage vaccine	Theileriosis in ruminants	0.15 - 0.4	NA	NA	NA	To replace schizont stage vaccine, 0.4 KGy used for irradiating blood with 21% parasitaemia (10ml/calf)
Fasciola hepatica	Local strain	Common liver fluke (zoonotic)	3 - 24	NA	NA	NA	(64)
Fasciola gigantica	local strain	Tropical liver disease (zoonotic)	0.030-0.050	NA	NA	metacercaria; 40/ oral dose	
Haemonchus contortus	local strain	Blood feeding nematodes for sheep and goat	0.17 - 170	NA	NA	10.000 larvae	Larvae stage III; 99% protection;
Ichthyophthirius multifiliis	local strain	Protozoan ecto-parasite in fish	1.5	5.2	Lysozyme, alkaline phosphate, protease and Estarases activitiy	100 trophonts/10 fish	(65)
Trypanosoma evansi	RoTat 1.2	Mechanically transmitted blood protozoan parasite	0.2	0.1983	CFSE (replication), Parasite growth	$1x\ 10^4/10^3$ homologous & heterologous Can86K	virulence gene mining
African Swine fever	Estonia 124	African swine fever	30	1.81	NA	$10^{7.25}$HAU/ heterologous Armenia 2008	No protection
Avian Influenza virus	H9N2	Avian influenza	60	5.46	Hemagglutination assay, inoculation in embryonated eggs	128 HAU/10^3,10^4 & 10^6	Protection at lower doses with oral-nasal application
Avian pathogenic Escherichia coli (APEC)	APEC	colibacillosis	1.2	0.89	NA	NA	Ongoing
Lumpy skin disease virus (LSDV)	Various	Lumpy skin disease	30	3.75	NA	NA	Ongoing
Theileria parva	local strain	East Coast fever	0.9	NA	NA	NA	ongoing
Avian Influenza virus	H9N2	LPAI	29.52 (frozen)	3.36	NA	NA	(66)
M. haemolytica	local from pneumonic lungs	Pneumonic mannheimiosis	2-20	NA	NA	$2\times10^{10}/3.6\ x10^{10}$	(67)
Salmonella gallinarum	Field strain	Fowl typhoid	2.4 (RT)	NA	NA	10^8	(68)
White spot syndrome virus	Local	White spot syndrom	15	2.56	NA	NA	(69)
Foot-and-mouth disease virus	Local strain IRN/1/2007	Foot-and-mouth disease	50	4.8	NA	NA	(69)
P. multocida	Local (MK802880, NVI)	Fowl cholera	1	NA	NA	NA	(55)

**NA (Not Available).*

as adjuvants as in the case of gamma irradiated influenza A virus co-administered with Semliki Forest virus where it displayed the potential to enhance immune response against Semliki Forest virus by six-fold in mouse (12). This adjuvant activity is attributed to γ-irradiated influenza A virus which behaves like Poly I:C (synthetic dsRNA) and elicits an interferon type I (IFN-I) humoral response through TLR3 (toll like receptor 3) signaling plus IFN-I mediated lymphocytes activation (12, 75). Irradiated parasite vaccines have also opened new areas of immunological study, as in the case of irradiated *Salmonella gallinarum* protecting mice and chicken from infection and *Haemonchus contortus* where metabolically active irradiated larvae of parasites remain immobilised in the abomasum of vaccinated sheep conferring long term protective response and long term immune stimulation (38, 64). The introduction or generation of unmethylated cytosine–guanine dinucleotide (CpGs) during

irradiation and the application of such vaccines address mucosal immunity and inoculation strategies which are desirable when dealing with intensive farming systems (76). Extensive epitope damage due to high irradiation doses has been mitigated with the development of radio protective compounds such as manganese ions ($Mn2^{+}$) and Trehalose which reduce structural damage of surface epitopes (10, 11).

In summary, recent research over the past 10 years has created a new base for the rational development of irradiated vaccines. New irradiation devices like x-rays or e-beams which do not need special radiation protection and are economically viable can be installed in bio-safety laboratories (73). A broad spectrum of molecular tests replaces traditional cell based immune assays that require expensive equipment and expertise, and the *in vitro* evaluation of immune induction replaces animal experiments where possible (70, 71). This research can effectively be carried out on local diseases in countries that have previously relied on results from advanced laboratories that increasingly cannot prioritise them due to constrains on funding and human resource capacities.

AUTHOR CONTRIBUTIONS

All authors listed have made a substantial, direct, and intellectual contribution to the work, and approved it for publication.

SUPPLEMENTARY MATERIAL

The Supplementary Material for this article can be found online at: https://www.frontiersin.org/articles/10.3389/fimmu.2022.853874/full#supplementary-material

REFERENCES

1. United Nations. Education | Department of Economic and Social Affairs. *Sustain Dev* (2021) 28–9.
2. Meeusen ENT, Walker J, Peters A, Pastoret PP, Jungersen G. Current Status of Veterinary Vaccines. *Clin Microbiol Rev* (2007) 20:489–510. doi: 10.1128/CMR.00005-07
3. Available at: http://www.animalhealthsurveillance.agriculture.gov.ie/oielisteddiseases/ (date accessed 11/01/2022).
4. OIE. *Resolution No. 18: Declaration of Global Eradication of Rinderpest and Implementation of Follow-Up Measures to Maintain World Freedom From Rinderpest*. Paris: 79th Session of the World Assembly of Delegates. (2011).
5. Njeumi F, Taylor W, Diallo A, Miyagishima K, Pastoret PP, Vallat B, et al. The Long Journey: A Brief Review of the Eradication of Rinderpest. *OIE Rev Sci Tech* (2012) 31:729–46. doi: 10.20506/rst.31.3.2157
6. Poulet H, Minke J, Pardo MC, Juillard V, Nordgren B, Audonnet JC. Development and Registration of Recombinant Veterinary Vaccines. The Example of the Canarypox Vector Platform. *Vaccine* (2007) 25:5606–12. doi: 10.1016/j.vaccine.2006.11.066
7. Strube C, Haake C, Sager H, Schorderet Weber S, Kaminsky R, Buschbaum S, et al. Vaccination With Recombinant Paramyosin Against the Bovine Lungworm Dictyocaulus Viviparus Considerably Reduces Worm Burden and Larvae Shedding. *Parasites Vectors* (2015) 8:119. doi: 10.1186/s13071-015-0733-5
8. Jarrett WF, Jennings FW, Mcintyre WI, Mulligan W, Thomas BA, Urquhart GM. Immunological Studies on Dictyocaulus Viviparus Infection: The Immunity Resulting From Experimental Infection. *Immunology* (1959) 2:252–61.
9. McLeonard C, Van Dijk J. Controlling Lungworm Disease (Husk) in Dairy Cattle. *In Pract* (2017) 39:408–19. doi: 10.1136/inp.j4038
10. Gaidamakova EK, Myles IA, McDaniel DP, Fowler CJ, Valdez PA, Naik S, et al. Preserving Immunogenicity of Lethally Irradiated Viral and Bacterial Vaccine Epitopes Using a Radio- Protective Mn2+-Peptide Complex From Deinococcus. *Cell Host Microbe* (2012) 12:117–24. doi: 10.1016/j.chom.2012.05.011
11. Nair CKK, Parida DK, Nomura T. Radioprotectors in Radiotherapy. *J Radiat Res* (2001) 42:21–37. doi: 10.1269/jrr.42.21
12. Babb R, Chan J, Khairat JE, Furuya Y, Alsharifi M. Gamma-Irradiated Influenza a Virus Provides Adjuvant Activity to a Co-Administered Poorly Immunogenic SFV Vaccine in Mice. *Front Immunol* (2014) 5:267. doi: 10.3389/fimmu.2014.00267
13. Pillai SD, Shayanfar S, Venturi M, Pillai s-pillai SD. Electron Beam Technology and Other Irradiation Technology Applications in the Food Industry. *Top Curr Chem* (2016) 375:6. doi: 10.1007/s41061-016-0093-4
14. Miller RB. *Electronic Irradiation of Foods*. Boston, MA: Springer US (2005). doi: 10.1007/0-387-28386-2
15. Tahergorabi R, Matak KE, Jaczynski J. Application of Electron Beam to Inactivate Salmonella in Food: Recent Developments. *Food Res Int* (2012) 45:685–94. doi: 10.1016/j.foodres.2011.02.003
16. Hieke ASC, Pillai SD. Escherichia Coli Cells Exposed to Lethal Doses of Electron Beam Irradiation Retain Their Ability to Propagate Bacteriophages and are Metabolically Active. *Front Microbiol* (2018) 9:2138. doi: 10.3389/fmicb.2018.02138
17. Brockstedt DG, Bahjat KS, Giedlin MA, Liu W, Leong M, Luckett W, et al. Killed But Metabolically Active Microbes: A New Vaccine Paradigm for Eliciting Effector T-Cell Responses and Protective Immunity. *Nat Med* (2005) 11:853–60. doi: 10.1038/nm1276
18. Dubensky TWJr., Skoble J, Lauer P, Brockstedt DG, Dubensky TW, Skoble J, et al. Killed But Metabolically Active Vaccines. *Curr Opin Biotechnol* (2012) 23:917–23. doi: 10.1016/J.COPBIO.2012.04.005
19. Furuya Y. Return of Inactivated Whole-Virus Vaccine for Superior Efficacy. *Immunol Cell Biol* (2012) 90:571–8. doi: 10.1038/icb.2011.70
20. Seo HS. Application of Radiation Technology in Vaccines Development. *Clin Exp Vaccine Res* (2015) 4:145. doi: 10.7774/cevr.2015.4.2.145
21. Moore HN, Kersten H. Preliminary Note on the Preparation of Non-Toxic Shiga Dysentery Vaccines by Irradiation With Soft X-Rays. *J Bacteriol* (1936) 31:581–4. doi: 10.1128/jb.31.6.581-584.1936
22. Duxbury RE, Sadun EH. Resistance Produced in Mice and Rats by Inoculation With Irradiated Trypanosoma Rhodesiense. *J Parasitol* (1969) 55:859–65. doi: 10.2307/3277231
23. Duxbury RE, Anderson JS, Wellde BT, Sadun EH, Muriithi IE. Trypanosoma Congolense: Immunization of Mice, Dogs, and Cattle With Gamma-Irradiated Parasites. *Exp Parasitol* (1972) 32:527–33. doi: 10.1016/0014-4894(72)90071-9
24. Duxbury RE, Sadun EH, Anderson JS. Immunization of Monkeys Against a Recently Isolated Human Strain of Trypanosoma Rhodesiense by Use of Gamma Irradiation. *Trans R Soc Trop Med Hyg* (1973) 67:266–7. doi: 10.1016/0035-9203(73)90172-7
25. Wellde BT, Duxbury RE, Sadun EH, Langbehn HR, Lötzsch R, Deindl G, et al. Experimental Infections With African Trypanosomes: IV. Immunization of Cattle With Gamma-Irradiated Trypanosoma Rhodesiense. *Exp Parasitol* (1973) 34:62–8. doi: 10.1016/0014-4894(73)90063-5
26. Sadun EH, Johnson AJ, Nagle RB, Duxbury RE. Experimental Infections With African Trypanosomes. V. Preliminary Parasitological, Clinical, Hematological, Serological, and Pathological Observations in Rhesus Monkeys Infected With Trypanosoma Rhodesiense. *Am J Trop Med Hyg* (1973) 22:323–30. doi: 10.4269/ajtmh.1973.22.323
27. Duxbury RE, Sadun EH, West JE. Relative Effectiveness of Neutron and Gamma Radiation of Trypanosomes for Immunizing Mice Against African

Trypanosomiasis. *Trans R Soc Trop Med Hyg* (1975) 69:484–5. doi: 10.1016/0035-9203(75)90104-2
28. Skoble J, Beaber JW, Yi G, Lovchik JA, Sower LE, Liu W, et al. Killed But Metabolically Active Bacillus Anthracis Vaccines Induce Broad and Protective Immunity Against Anthrax. *Infect Immun* (2009) 77:1649–63. doi: 10.1128/IAI.00530-08
29. Frankel FR. Vaccine Wakes From the Dead. *Nat Med* (2005) 11:833–4. doi: 10.1038/nm0805-833
30. Singh A, Singh H. Time-Scale and Nature of Radiation-Biological Damage: Approaches to Radiation Protection and Post-Irradiation Therapy. *Prog Biophys Mol Biol* (1982) 39:69–107. doi: 10.1016/0079-6107(83)90014-7
31. Reisz JA, Bansal N, Qian J, Zhao W, Furdui CM. Effects of Ionizing Radiation on Biological Molecules - Mechanisms of Damage and Emerging Methods of Detection. *Antioxidants Redox Signal* (2014) 21:260–92. doi: 10.1089/ars.2013.5489
32. Olive PL. The Role of DNA Single- and Double-Strand Breaks in Cell Killing by Ionizing Radiation. *Radiat Res* (1998) 150:S42–51. doi: 10.2307/3579807
33. Miekka SI, Forng RY, Rohwer RG, MacAuley C, Stafford RE, Flack SL, et al. Inactivation of Viral and Prion Pathogens by γ-Irradiation Under Conditions That Maintain the Integrity of Human Albumin. *Vox Sang* (2003) 84:36–44. doi: 10.1046/j.1423-0410.2003.00256.x
34. Alsharifi M, Müllbacher A. The γ-Irradiated Influenza Vaccine and the Prospect of Producing Safe Vaccines in General. *Immunol Cell Biol* (2010) 88:103–4. doi: 10.1038/icb.2009.81
35. Chen F, Seong Seo H, Ji HJ, Yang E, Choi JA, Yang JS, et al. Characterization of Humoral and Cellular Immune Features of Gamma-Irradiated Influenza Vaccine. *Hum Vaccin Immunother* (2021) 17:485–96. doi: 10.1080/21645515.2020.1780091
36. Jones GS, Bussell KM, Myers-Morales T, Fieldhouse AM, Bou Ghanem EN, D'Orazio SEF. Intracellular Listeria Monocytogenes Comprises a Minimal But Vital Fraction of the Intestinal Burden Following Foodborne Infection. *Infect Immun* (2015) 83:3146–56. doi: 10.1128/IAI.00503-15
37. Datta SK, Okamoto S, Hayashi T, Shin SS, Mihajlov I, Fermin A, et al. Vaccination With Irradiated Listeria Induces Protective T Cell Immunity. *Immunity* (2006) 25:143–52. doi: 10.1016/j.immuni.2006.05.013
38. Ji HJ, Byun E-BB, Chen F, Ahn KB, Jung HK, Han SH, et al. Radiation-Inactivated S. Gallinarum Vaccine Provides a High Protective Immune Response by Activating Both Humoral and Cellular Immunity. *Front Immunol* (2021) 12:717556/BIBTEX. doi: 10.3389/FIMMU.2021.717556/BIBTEX
39. Magnani DM, Harms JS, Durward MA, Splitter GA. Nondividing But Metabolically Active Gamma-Irradiated Brucella Melitensis is Protective Against Virulent B. Melitensis Challenge in Mice. *Infect Immun* (2009) 77:5181–9. doi: 10.1128/IAI.00231-09
40. Bhatia SS. SS. Investigations into Metabolically Active yet Non-Culturable (MAyNC) Clostridium perfringens to Control Necrotic Enteritis in Broiler Chickens. Doctoral dissertation: Texas A&M University (2021). Available at: https://oaktrust.library.tamu.edu/handle/1969.1/193108
41. Yang JD, Mott D, Sutiwisesak R, Lu YJ, Raso F, Stowell B, et al. Mycobacterium Tuberculosis-Specific CD4+and Cd8+T Cells Differ in Their Capacity to Recognize Infected Macrophages. *PloS Pathog* (2018) 14:e1007060. doi: 10.1371/journal.ppat.1007060
42. Luke TC, Hoffman SL. Rationale and Plans for Developing a non-Replicating, Metabolically Active, Radiation-Attenuated Plasmodium Falciparum Sporozoite Vaccine. *J Exp Biol* (2003) 206:3803–8. doi: 10.1242/jeb.00644
43. da Costa A, Zorgi NE, do Nascimento N, Galisteo AJ, de Andrade HF. Gamma Irradiation of Toxoplasma Gondii Protein Extract Improve Immune Response and Protection in Mice Models. *BioMed Pharmacother* (2018) 106:599–604. doi: 10.1016/j.biopha.2018.06.155
44. Fujiwara RT, Loukas A, Mendez S, Williamson AL, Bueno LL, Wang Y, et al. Vaccination With Irradiated Ancylostoma Caninum Third Stage Larvae Induces a Th2 Protective Response in Dogs. *Vaccine* (2006) 24:501–9. doi: 10.1016/j.vaccine.2005.07.091
45. El Ridi R, Tallima H. Why the Radiation-Attenuated Cercarial Immunization Studies Failed to Guide the Road for an Effective Schistosomiasis Vaccine: A Review. *J Adv Res* (2015) 6:255–67. doi: 10.1016/j.jare.2014.10.002
46. Chazal N, Gerlier D. Virus Entry, Assembly, Budding, and Membrane Rafts. *Microbiol Mol Biol Rev* (2003) 67:226–37. doi: 10.1128/mmbr.67.2.226-237.2003
47. Furuya Y, Chan J, Wan EC, Koskinen A, Diener KR, Hayball JD, et al. Gamma-Irradiated Influenza Virus Uniquely Induces IFN-I Mediated Lymphocyte Activation Independent of the TLR7/MyD88 Pathway. *PloS One* (2011) 6:1–12. doi: 10.1371/journal.pone.0025765
48. Woolcock PR, McFarland MD, Lai S, Chin RP. Enhanced Recovery of Avian Influenza Virus Isolates by a Combination of Chicken Embryo Inoculation Methods. *Avian Dis* (2001) 45:1030–5. doi: 10.2307/1592884
49. Campbell CH, Barber TL, Knudsen RC, Swaney LM. Immune Response of Mice and Sheep to Bluetongue Virus Inactivated by Gamma Irradiation. *Prog Clin Biol Res* (1985) 178:639–47.
50. Ceccaldi PE, Marquette C, Weber P, Gourmelon P, Tsiang H. Ionizing Radiation Modulates the Spread of an Apathogenic Rabies Virus in Mouse Brain. *Int J Radiat Biol* (1996) 70:69–75. doi: 10.1080/095530096145346
51. Honnold SP, Bakken RR, Fisher D, Lind CM, Cohen JW, Eccleston LT, et al. Second Generation Inactivated Eastern Equine Encephalitis Virus Vaccine Candidates Protect Mice Against a Lethal Aerosol Challenge. *PloS One* (2014) 9:e104708. doi: 10.1371/journal.pone.0104708
52. Borella-Venturini M, Frasson C, Paluan F, De Nuzzo D, Di Masi G, Giraldo M, et al. Tetanus Vaccination, Antibody Persistence and Decennial Booster: A Serosurvey of University Students and at-Risk Workers. *Epidemiol Infect* (2017) 145:1757–62. doi: 10.1017/S0950268817000516
53. Sartori GP, da Costa A, dos Santos Macarini FL, Mariano DOC, Pimenta DC, Spencer PJ, et al. Characterization and Evaluation of the Enzymatic Activity of Tetanus Toxin Submitted to Cobalt-60 Gamma Radiation. *J Venom Anim Toxins Incl Trop Dis* (2021) 27:1–13. doi: 10.1590/1678-9199-JVATITD-2020-0140
54. Cha SB, Kim WS, Kim JS, Kim H, Kwon KW, Han SJ, et al. Repeated Aerosolized-Boosting With Gamma-Irradiated Mycobacterium Bovis BCG Confers Improved Pulmonary Protection Against the Hypervirulent Mycobacterium Tuberculosis Strain HN878 in Mice. *PloS One* (2015) 10:e0141577. doi: 10.1371/journal.pone.0141577
55. Dessalegn B, Bitew M, Asfaw D, Khojaly E, Ibrahim SM, Abayneh T, et al. Gamma-Irradiated Fowl Cholera Mucosal Vaccine: Potential Vaccine Candidate for Safe and Effective Immunization of Chicken Against Fowl Cholera. *Front Immunol* (2021) 12:768820. doi: 10.3389/fimmu.2021.768820
56. Lawrence EA, Duran-Reynals F. The Effect of Combining Bacterial Toxins and X-Ray Irradiation in the Treatment of a Transplantable Mouse Carcinoma. *Yale J Biol Med* (1941) 14:177–81.
57. de la Rosa G, Olvera F, Cruz E, Paniagua D, Corzo G. Use of Irradiated Elapid and Viperid Venoms for Antivenom Production in Small and Large Animals. *Toxicon* (2018) 155:32–7. doi: 10.1016/j.toxicon.2018.10.001
58. Clissa PB, do Nascimento N, Rogero JR. Toxicity and Immunogenicity of Crotalus Durissus Terrificus Venom Treated With Different Doses of Gamma Rays. *Toxicon* (1999) 37:1131–41. doi: 10.1016/S0041-0101(98)00249-9
59. Mabbott NA. Prospects for Safe and Effective Vaccines Against Prion Diseases. *Expert Rev Vaccines* (2014) 14:1–4. doi: 10.1586/14760584.2015.965691
60. Wisniewski T, Goñi F. Vaccination Strategies. In: *Handbook of Clinical Neurology*. Elsevier. p. 419–30. doi: 10.1016/B978-0-444-63945-5.00023-4
61. Rohwer RG. Scrapie Infectious Agent is Virus-Like in Size and Susceptibility to Inactivation. *Nature* (1984) 308:658–62. doi: 10.1038/308658a0
62. Latarjet R. Inactivation of the Agents of Scrapie, Ceutzfeldt-Jakob Disease, and Kuru by Radiations. In: *Slow Transmissible Diseases of the Nervous System* Amsterdam (1979) 2(60):387–408.
63. Gominet M, Vadrot C, Austruy G, Darbord JC. Inactivation of Prion Infectivity by Ionizing Rays. *Radiat Phys Chem* (2007) 76:1760–2. doi: 10.1016/j.radphyschem.2007.02.099
64. Tadesse A, Eguale T, Ashenafi H, Tilahun G, Ayana D. Enzymatic and Fecundity Evaluation of Fasciola Hepatica Exposed to Different Doses of γ-Irradiation in Ethiopian Sheep. *Ethiop Vet J* (2021) 25:85–114. doi: 10.4314/evj.v25i2.6
65. Heidarieh M, Hedayati Rad M, Mirvaghefi AR, Diallo A, Mousavi S, Sheikhzadeh N, et al. Effect of Gamma Irradiation on Inactivation of Ichthyophthirius Multifiliis Trophonts and its Efficacy on Host Response in Experimentally Immunized Rainbow Trout (Oncorhynchus Mykiss). *Turkish J Vet Anim Sci* (2014) 38:388–93. doi: 10.3906/vet-1312-78
66. Salehi B, Motamedi-Sedeh F, Madadgar O, Khalili I, Langroudi AGC, Unger H, et al. Analysis of Antigen Conservation and Inactivation of Gamma-

Irradiated Avian Influenza Virus Subtype H9N2. *Acta Microbiol Immunol Hung* (2018) 65:163–71. doi: 10.1556/030.65.2018.025
67. Ahmed S, Ahmed B, Mahmoud G, Nemr W, Abdel Rahim E. Comparative Study Between Formalin-Killed Vaccine and Developed Gamma Irradiation Vaccine Against Mannheimia Haemolytica in Rabbits. *Turkish J Vet Anim Sci* (2016) 40:219–24. doi: 10.3906/vet-1504-34
68. Lulie S, Alemayehu H, Nuru A, Abayneh T, Eguale T. Immunogenicity and Protective Efficacy of Irradiated Salmonella Gallinarum Against Homologous Challenge Infection in Bovans Brown Chickens. *Ethiop Vet J* (2020) 24:123–38. doi: 10.4314/evj.v24i2.8
69. Motamedi-Sedeh F, Soleimanjahi H, Jalilian AR, Mahravani H, Shafaee K, Sotoodeh M, et al. Development of Protective Immunity Against Inactivated Iranian Isolate of Foot-and-Mouth Disease Virus Type O/IRN/2007 Using Gamma Ray-Irradiated Vaccine on BALB/c Mice and Guinea Pigs. *Intervirology* (2015) 58:190–6. doi: 10.1159/000433538
70. Sassu EL, Kangethe RT, Settypalli TBK, Chibssa TR, Cattoli G, Wijewardana V. Development and Evaluation of a Real-Time PCR Panel for the Detection of 20 Immune Markers in Cattle and Sheep. *Vet Immunol Immunopathol* (2020) 227:1–10. doi: 10.1016/j.vetimm.2020.110092
71. Kangethe RT, Pichler R, Chuma FNJ, Cattoli G, Wijewardana V. Bovine Monocyte Derived Dendritic Cell Based Assay for Measuring Vaccine Immunogenicity *in Vitro*. *Vet Immunol Immunopathol* (2018) 197:39–48. doi: 10.1016/j.vetimm.2018.01.009
72. Fertey J, Bayer L, Grunwald T, Pohl A, Beckmann J, Gotzmann G, et al. Pathogens Inactivated by Low-Energy-Electron Irradiation Maintain Antigenic Properties and Induce Protective Immune Responses. *Viruses* (2016) 8:319. doi: 10.3390/v8110319
73. Fertey J, Thoma M, Beckmann J, Bayer L, Finkensieper J, Reißhauer S, et al. Automated Application of Low Energy Electron Irradiation Enables Inactivation of Pathogen- and Cell-Containing Liquids in Biomedical Research and Production Facilities. *Sci Rep* (2020) 10:12786. doi: 10.1038/s41598-020-69347-7
74. Fertey J, Bayer L, Kähl S, Haji RM, Burger-Kentischer A, Thoma M, et al. Low-Energy Electron Irradiation Efficiently Inactivates the Gram-Negative Pathogen Rodentibacter Pneumotropicus—A New Method for the Generation of Bacterial Vaccines With Increased Efficacy. *Vaccines* (2020) 8:1–10. doi: 10.3390/vaccines8010113
75. Moresco EMY, LaVine D, Beutler B. Toll-Like Receptors. *Curr Biol* (2011) 21: R488–93. doi: 10.1016/j.cub.2011.05.039
76. Bode C, Zhao G, Steinhagen F, Kinjo T, Klinman DM. CpG DNA as a Vaccine Adjuvant. *Expert Rev Vaccines* (2011) 10:499–511. doi: 10.1586/erv.10.174

Conflict of Interest: The authors declare that the research was conducted in the absence of any commercial or financial relationships that could be construed as a potential conflict of interest.

Publisher's Note: All claims expressed in this article are solely those of the authors and do not necessarily represent those of their affiliated organizations, or those of the publisher, the editors and the reviewers. Any product that may be evaluated in this article, or claim that may be made by its manufacturer, is not guaranteed or endorsed by the publisher.

frontiers | Frontiers in Immunology

ORIGINAL RESEARCH
published: 26 April 2022
doi: 10.3389/fimmu.2022.832264

Vaccination With a Gamma Irradiation-Inactivated African Swine Fever Virus Is Safe But Does Not Protect Against a Challenge

*Jutta Pikalo[1], Luca Porfiri[2], Valerij Akimkin[3], Hanna Roszyk[1], Katrin Pannhorst[4], Richard Thiga Kangethe[2], Viskam Wijewardana[2], Julia Sehl-Ewert[5], Martin Beer[1], Giovanni Cattoli[2] and Sandra Blome[1]**

[1] Institute of Diagnostic Virology, Friedrich-Loeffler-Institut, Greifswald - Insel Riems, Germany, [2] Animal Production and Health Laboratory, Joint FAO/IAEA Centre of Nuclear Techniques in Food and Agriculture, International Atomic Energy Agency (IAEA), IAEA Laboratories, Seibersdorf, Austria, [3] Chemical and Veterinary Investigations, Office Stuttgart, Fellbach, Germany, [4] Institute of Molecular Virology and Cell Biology, Friedrich-Loeffler-Institut, Greifswald - Insel Riems, Germany, [5] Department of Experimental Animal Facilities and Biorisk Management, Friedrich-Loeffler-Institut, Greifswald - Insel Riems, Germany

African swine fever (ASF) is among the most devastating viral diseases of pigs and wild boar worldwide. In recent years, the disease has spread alarmingly. Despite intensive research activities, a commercialized vaccine is still not available, and efficacious live attenuated vaccine candidates raise safety concerns. From a safety perspective, inactivated preparations would be most favourable. However, both historical and more recent trials with chemical inactivation did not show an appreciable protective effect. Under the assumption that the integrity of viral particles could enhance presentation of antigens, we used gamma irradiation for inactivation. To this means, gamma irradiated ASFV "Estonia 2014" was adjuvanted with either Polygen™ or Montanide™ ISA 201 VG, respectively. Subsequently, five weaner pigs per preparation were immunized twice with a three-week interval. Six weeks after the first immunization, all animals were challenged with the highly virulent ASFV strain "Armenia 2008". Although ASFV p72-specific IgG antibodies were detectable in all vaccinated animals prior challenge, no protection could be observed. All animals developed an acute lethal course of ASF and had to be euthanized at a moderate humane endpoint within six days. Indeed, the vaccinated pigs showed even higher clinical scores and a higher inner body temperature than the control group. However, significantly lower viral loads were detectable in spleen and liver of immunized animals at the time point of euthanasia. This phenomenon suggests an immune mediated disease enhancement that needs further investigation.

Keywords: African swine fever virus, gamma irradiation, inactivated vaccine, adjuvant, efficiency, domestic pigs

OPEN ACCESS

Edited by:
Rajko Reljic,
St George's, University of London, United Kingdom

Reviewed by:
Hua-Ji Qiu,
Chinese Academy of Agricultural Sciences, China
Juergen A. Richt,
Kansas State University, United States

***Correspondence:**
Sandra Blome
Sandra.blome@fli.de

Specialty section:
This article was submitted to Vaccines and Molecular Therapeutics, a section of the journal Frontiers in Immunology

Received: *09 December 2021*
Accepted: *25 March 2022*
Published: *26 April 2022*

Citation:
Pikalo J, Porfiri L, Akimkin V, Roszyk H, Pannhorst K, Kangethe RT, Wijewardana V, Sehl-Ewert J, Beer M, Cattoli G and Blome S (2022) Vaccination With a Gamma Irradiation-Inactivated African Swine Fever Virus Is Safe But Does Not Protect Against a Challenge. Front. Immunol. 13:832264. doi: 10.3389/fimmu.2022.832264

INTRODUCTION

The causative agent of African swine fever (ASF) is a large double-stranded DNA virus (1, 2) which belongs to the *Asfivirus* genus of the *Asfarviridae* family. Over the last decade, the disease has become a pandemic threat to domestic and wild pigs. Overall, more than 55 countries on 5 continents are affected (OIE WAHIS, visited online on October 30th 2021) resulting in tremendous socio-economic losses in the pig industry (3). The virus strains involved in this pandemic belong to p72 genotype II and the vast majority shows high virulence, in both domestic pigs and wild boar. However, strains of lower virulence have been reported from Estonia (4, 5), Latvia (6, 7), and more recently from China (8).

The greatest challenge of ASF control is the development of a safe and effective vaccine (9). Until then, strict biosecurity, early detection, and veterinary hygiene are the only tools to prevent and control the disease.

In the past, many traditional approaches to develop a vaccine against ASFV have failed. Up to now, the most promising vaccine candidates are live attenuated (naturally or by deletion) ASFV. These however, have several disadvantages including long-term side effects in some candidates, safety issues related to genetic stability, the requirement for high biocontainment during production, and the lack of suitable cell lines that can be scaled up without leading to changes in the viral genome. The latter remains a key constraint for production (10).

Inactivated vaccines are most interesting from a safety point of view. Unfortunately, they have not yet been shown to be effective (9). Under the assumption that the integrity of viral particles could enhance and facilitate presentation of antigens that are crucial for protection, conservative inactivation protocols have been discussed in the aftermath of different ASF research projects. Among different options of inactivation, gamma irradiation, in combination with a strong adjuvant, was considered a promising approach (11) and thus it was the chosen method for this study. The advantage of inactivation by gamma irradiation is that it damages only the DNA and RNA while preserving both surface antigens and viral structure (12).

Here, we report on a study which was carried out to evaluate the effectiveness of a structure preserving inactivation of ASFV with gamma irradiation and the potential use as a vaccine in combination with two state of the art adjuvants (Polygen™ Adjuvant, MVP Laboratories and Montanide™ ISA 201 VG, SEPPIC).

MATERIAL AND METHODS

Experimental Design

The study included 15 domestic pigs (German Landrace x Large White) of approximately 8-weeks of age, weighing 20-25 kg, and of both sexes, divided in three equally sized groups. All animals were bought from a commercial pig farm and were clinically healthy upon arrival.

All animals were tested negative for ASFV and ASFV specific antibodies prior to enrollment in the study. The animals were kept in the high containment facility of the Friedrich-Loeffler-Institut (FLI), Isle of Riems, Germany. Over the course of the trial, the animals were fed a commercial pig feed with corn and hay-cob supplement and had access to water *ad libitum*. Enrichment material of different matrices was offered over the entire experimental time.

After an acclimatization phase, the domestic pigs were vaccinated intramuscularly with 2 ml of the respective adjuvanted preparation.

Clinical parameters of all animals were assessed daily based on a harmonized scoring system as previously described (13). The sum of the points was recorded as the clinical score (CS) that was also used to define the humane endpoint which was set at 10 clinical score points (moderate humane endpoint).

Blood samples were collected at day (d) 0 prior to vaccination, and at d7, d14, d21, d28, d35, and d42 after the first vaccination. On day 21 after the first vaccination, the pigs received a booster vaccination. On day 42 after the first vaccination/21 days after the second vaccination, the animals were challenged oro-nasally with a highly virulent ASFV genotype II isolate (ASFV "Armenia 08"). After the challenge, blood samples were collected at 4 days post challenge (dpc) and at the day of euthanasia (6 dpc for vaccinated groups and 7 dpc for control group). Animals that reached the humane endpoint or that suffered unacceptably without reaching the endpoint were euthanized through intracardial injection of embutramide (T61, Merck, Darmstadt, Germany) under deep anaesthesia with tiletamine/zolazepam (Zoletil®, Virbac, Carros, France), ketamine (Ketamin 10%, Medistar, Ascheberg, Germany) and xylazine (Xylavet® 20mg/ml, CP-Pharma, Burgdorf, Germany) or ketamine (Ketamin 10%, Medistar, Ascheberg, Germany) and azaperone (Stresnil™ 40mg/ml, Elanco, Bad Homburg, Germany).

Necropsy was performed on all animals to evaluate ASFV induced lesions. Lesions were scored based on the protocol published by Galindo-Cardiel et al. (14) with slight modifications (15). Tissue samples (spleen, kidney, liver, tonsil, bone marrow and lymph nodes) were taken for further analysis and reference material acquisition.

Over the entire study period, all applicable animal welfare regulations, including EU Directive 2010/63/EC and institutional guidelines, were taken into consideration. The animal experiment was approved by the competent authority (Landesamt für Landwirtschaft, Lebensmittelsicherheit und Fischerei (LALLF) Mecklenburg-Vorpommern, Rostock, Germany) under reference number 7221.3-1.1-003/20.

Cells

Blood for the preparation of peripheral blood mononuclear cell (PBMC)-derived macrophages was collected from healthy domestic donor pigs that were kept in the quarantine stable at the FLI. In brief, PBMCs were obtained from EDTA-anticoagulated blood using Pancoll animal density gradient medium (PAN Biotech, Aidenbach, Germany). PBMCs were grown in RPMI-1640 cell culture medium with 4-(2-hydroxyethyl)-1-piperazineethanesulfonic acid (HEPES) and 10% foetal calf serum (FCS) at 37°C in a humidified atmosphere containing 5% CO_2. The medium was supplied

with amphotericin B, streptomycin and penicillin to mitigate bacterial and fungal growth. To facilitate maturation of macrophages, granulocyte macrophage colony-stimulating factor (GM-CSF) (Biomol, Hamburg, Germany) was added to the cell culture medium at a concentration of 2 ng/ml. The cells were used for virus cultivation and hemadsorption test (virus isolation and titration).

Virus Material

The genotype II ASFV isolate "Estonia 2014" (5) was used for gamma irradiation and subsequent vaccination. A virus stock was prepared in PBMCs and the titer was determined by hemadsorption test as previously described (16). The titer amounted to $10^{7.25}$ haemadsorbing units 50% (HAU)/ml. Inactivation of the irradiated virus suspension was verified employing hemadsorption tests.

For challenge infection, a spleen suspension containing genotype II ASFV "Armenia 2008" was used with a final titer of 10^6 HAU per ml. The titer was confirmed by end-point back titration of the inoculum with hemadsorption test.

Gamma Irradiation

The virus stock of ASFV "Estonia 2014" was mixed with 25% of trehalose before irradiation to protect the virus structure during the process. The irradiation was performed with the Model 812 Co-60 irradiator (Foss Therapy Services, Inc., California, USA) in a frozen condition at -80°C where the vials were placed in a Bio bottle with dry ice. For the calculation of the dose and estimation of the time, the GAMMA FOSS Spreadsheet and Dose Tracker software (California, USA), which are connected to the gamma irradiator machine, were used. The software calculates the time of exposure needed based on the emission rate of the Cobalt60 source.

For determination of the inactivation dose, the virus samples were irradiated at 2, 4, 5, 6, 7, 8, 10, 20, 30, 40 and 50 kGy. For the irradiation of the vaccine, a dose of 30 kGy was chosen based on the internationally accepted standard sterility assurance level (SAL) which is 6 times of the D_{10} value. The D_{10} value is the ability of gamma irradiation to reduce an exposed microbial population by 90 per cent (one log10) under standard conditions of time, temperature and dose. The D_{10} value of ASFV "Estonia 2014" vaccine formulation was calculated using the inverse of the slope of the regression lines (-1/slope) of gamma irradiation dose against log virus titer using GraphPad prism 9 (17).

Transmission Electron Microscopy

At 30 kGy irradiated cell culture supernatant containing ASFV supplemented with 25% trehalose was prepared for electron microscopy by negative staining technique as described by Rubbenstroth et al. (18) and analysed in a JEM 1011 transmission electron microscope (JEOL, Freising, Germany) at 80 kv and 200,000-fold magnification.

Adjuvants

Polygen™ (MVP Laboratories, Inc. Omaha, USA) is a low molecular weight copolymer adjuvant that has demonstrated to stimulate significant interferon gamma and interleukin 12 responses when used in a parasite vaccine for cattle (19). Moreover, it has recently been used successfully with an inactivated large DNA virus, i.e. Capripox virus (20).

Montanide™ ISA 201 VG (Seppic, La Garenne-Colombes, France) is a Water-in-Oil-in-Water (W/O/W) formulation, that is a continuous aqueous phase emulsion in which droplets of oil contain a secondary aqueous phase (double emulsion). Due to their structure, they can induce a short and long-term protective immune response. Field trials have shown that such adjuvant can stimulate both humoral and cell mediated immune responses (21).

Preparation of the Vaccine

30 kGy Irradiated ASFV With Polygen™ Adjuvant

For the preparation of the vaccine, the irradiated virus suspension was combined with 20% of Polygen™ adjuvant. For this, the Polygen™ adjuvant was gently mixed for 2 h before the antigen was added to the suspension. During addition of the antigen, the suspension was gently mixed with a magnetic stirrer and stirring was continued for 2 h after complete addition of the antigen. Syringes were filled with 2 ml of the prepared vaccine and stored on ice until further use.

30 kGy Irradiated ASFV With Montanide™ ISA 201 VG

To prepare the vaccine, both phases, the virus suspension and the Montanide™ ISA 201 VG adjuvant, needed to be combined with a 50/50 w/w ratio. The adjuvant was sterilised by 0.2 µm filtration. Both phases were warmed to 32°C. The virus suspension was then slowly added to the adjuvant under magnetic agitation at 32°C. After the addition of the entire volume, the agitation was continued for 5 min at 32°C. After that, the emulsion was cooled down for 1 h to 20°C. Syringes were filled with 2 ml of the prepared vaccine and stored on ice until further use.

Processing of Samples

Serum samples were aliquoted after centrifugation at 2.500 *x g* for 20 min at 20°C and together with aliquoted EDTA samples stored at -80°C until further use.

Tissue samples, which were collected during necropsy, were stored at -80°C. For further processing, tissue samples (a lentil-sized piece) were homogenized in 1 ml phosphate-buffered saline (PBS) with a metal bead using a TissueLyser II (Qiagen®GmbH, Hilden, Germany) at 30 Hz for 3 min before extraction and qPCRs were performed.

Virus Detection

For qPCR, viral nucleic acids were extracted from 100 µl tissue homogenate using the NucleoMag Vet Kit (Machery-Nagel, Düren, Germany) and the KingFisher® extraction platform (Thermo Scientific, Schwerte, Germany) according to the manufacturer's recommendations. qPCRs were performed according to the protocol published by King et al. (22) with slight modifications (addition of a heterologous control DNA). All PCR runs were performed using a C1000™ thermal cycler (BIO-RAD, Hercules, California), with the corresponding

CFX96™ Real-Time System. Results of all qPCR runs were recorded as quantification cycle (cq) values. A cut off >42 was defined for negative results. Using a dilution series of an ASFV DNA standard, genome copy (gc) numbers were estimated.

To verify the integrity of the p72 antigen in the irradiated virus suspension, the Ingezim ® ASFV CROM Ag (Eurofins Technologies Ingenasa) lateral flow assay, which is a double antibody sandwich immunochromatographic assay for the detection of ASFV antigen in blood samples (23) was used. The test procedure was conducted according to the manufacturer's instructions.

Antibody Detection

Sera were tested for the presence of ASFV p72-specific antibodies with the commercially available competitive INGEZIM PPA COMPAC ELISA (Ingenasa, Spain). Additionally, serum samples were tested with an indirect immunoperoxidase test (IIPT) according to standard protocols provided by the European Union Reference Laboratory for ASF (EURL protocol: https://asf-referencelab.info/asf/images/ficherosasf/PROTOCOLOS-EN/2021_UPDATE/SOP-ASF-IPT-1_2021.pdf (accessed on 7 January 2021)) with slight modifications.

Data Analysis

All data were recorded and evaluated using Microsoft Excel 2010 (Microsoft Deutschland GmbH, Munich Germany).

GraphPad Prism 9 (Graphpad Software Inc., San Diego, CA, USA) was used for statistical analysis and graphs. Statistically significant differences were investigated by multiple t-tests with Holm-Sidak's correction for multiple comparisons and with ordinary one-way ANOVA for viral genome detection in blood and organ samples between the groups. Statistical significance was defined as $p < 0.05$ and indicated with an asterisk (*).

RESULTS

Determination of the Inactivation Dose With Irradiation and Integrity of ASFV

In order to determine the exact dose of inactivation, the virus-trehalose suspension was irradiated with different irradiation doses. To quantify the titer reduction and/or to confirm complete inactivation, end-point titrations were performed in quadruplicate (**Figure S1A**) using the hemadsorption test as readout. After an irradiation with 8 kGy, no hemadsorption could be detected. The samples still tested positive by antigen lateral flow device (data not shown) showing an integrity of the p72 antigen.

To account for a substantial safety margin, an irradiation dose of 30 kGy was used in downstream experiments according to the internationally accepted standard sterility assurance level (SAL) which is 6 times of the D_{10} value. The D_{10} was found to be 1.81 kGy (**Figure S1B**).

The structural integrity of the 30 kGy irradiated and inactivated ASFV particles was confirmed with transmission electron microscope as shown in **Figure 1**.

Clinical Findings

Vaccination with irradiated ASFV supplemented with Polygen™ or Montanide™ ISA 201 VG was not associated to adverse reactions except for local erythema between one and two cm in diameter in two out of five animals at the intramuscular injection site after the second vaccination which resolved after three to four days. This lesion was more pronounced in the group that received the vaccine with Montanide™ ISA 201 VG.

To test whether the vaccines were protective, vaccinated pigs and unvaccinated control animals were challenged oro-nasally with 10^6 HAU per ml ASFV strain "Armenia 2008". All animals, whether vaccinated or not, developed severe, unspecific clinical

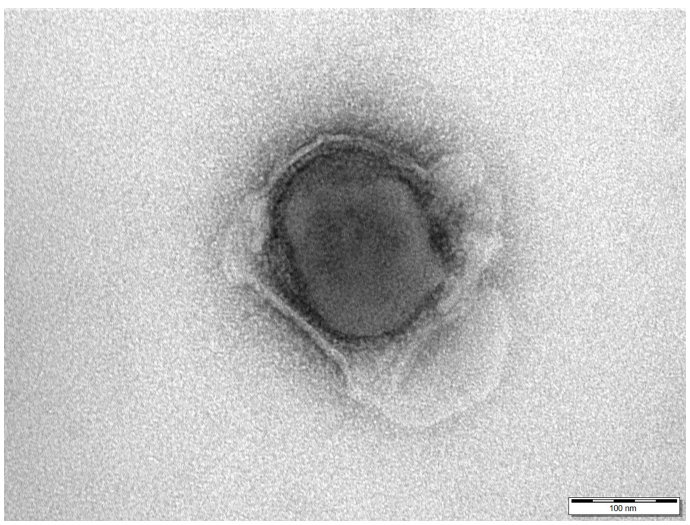

FIGURE 1 | Electron micrograph of a 30 kGy irradiated African swine fever virus shows the integrity of the particle. Negative staining with 1% phosphotungstic acid. Scale bar 100 nm.

signs starting on day 4 post challenge (dpc). Clinical signs included fever, general depression, lack of appetite, curved back, ataxia, increased lying and respiratory distress. Pigs of all groups developed inner body temperatures higher than 40.0°C from day 4 pc (**Figure 2**). Clinical signs worsened more rapidly in the vaccinated animals compared to the control group. The vaccinated groups reached the humane endpoint of 10 score points at 6 dpc while the control group was sacrificed one day later on 7 dpc. The clinical score for each group is shown in **Figure 3**. There was no marked difference between the vaccinated groups and the control group in the final clinical score points at day of euthanasia (humane endpoint).

Virus and Viral Genome Detection

Prior to inoculation, all animals were tested negative for ASFV. After vaccination, no ASFV genome could be detected in blood (data not shown). At 4 dpc, ASFV genome was detectable in blood samples (**Figure 4**) of all groups. In contrast, in one animal (#351) which received Montanide™ ISA 201 VG as adjuvant no viral genome was detectable in blood and only very low genome copies were present in some tissue samples (bone marrow, liver, spleen, lung and Ln. renalis). The vaccinated groups were euthanized on 6 dpc and the control group on 7 dpc. Organ samples obtained from all vaccinated and control animals tested positive in qPCR at day of euthanasia (**Figures 5A–I**). In the vaccinated groups there was significant less genome detectible in the spleen compared to the control group (*** p-Values: < 0.001) at the humane endpoint. The vaccinated group with Montanide™ ISA 201 VG as adjuvant shows significantly less genome copy numbers in the bone marrow compared to the control group (* p-Values: < 0.1) and the vaccinated group which received Polygen™ as adjuvant showed significant less genome copy numbers in the liver compared to the control group (* p-Values: < 0.1). No correlation was found between viremia and clinical score (data not shown).

Pathomorphological Findings

All animals were subjected to full necropsy. Results of macroscopic scoring are shown in **Figure 6**.

Pigs infected with the highly virulent ASFV strain "Armenia 2008" displayed initial ASF lesions (pulmonary edema and enlarged and hemorrhages lymph nodes) typical for a moderate humane endpoint (sum of 10 score points) decision. Incipient hemorrhages and slight to moderate enlargement were continuously observed for the renal and mandibular lymph nodes, and to a lesser extent for the retropharyngeal, tracheobronchial and iliac lymph nodes. Four out of five pigs suffered from mild to severe pulmonary alveolar edema.

Comparable lesions were present in the animal group vaccinated with irradiated ASFV supplemented with Montanide™ ISA 201 VG followed by a challenge infection with ASFV "Armenia 2008". Pulmonary edema, but also pulmonary consolidation of varying severity occurred in all animals, while lymph node lesions were less pronounced when compared to control animals. One pig (#312) developed severe pancreatic necrosis and hemorrhage. Although no viremia was detected in animal #351, pathologic findings did not differ from those of other animals in this group.

Likewise, in the animals that received the vaccine supplemented with Polygen™ and challenged with ASFV strain "Armenia 2008", pathologic changes were indicative for an ASF infection and included mainly mild to severe lymph node hemorrhages, pulmonary edema and consolidation in all affected pigs. No correlation was found between viremia and pathological findings (data not shown).

Antibody Detection

No antibodies were found in the sera prior to inoculation in any of the samples tested *via* ELISA or in the indirect immunoperoxidase test (IIPT). Fourteen days after the first vaccination, antibodies were detected with ELISA in two animals that received the Montanide™ ISA 201 VG adjuvanted vaccine. After the booster vaccination, all animals of this group seroconverted (**Figure 7A**). In the group with Polygen™ as adjuvant the first animals (3/5) with detectible antibodies in the ELISA were found on day 28 post vaccination. On day 46 post vaccination (4 dpc) all animals showed seroconversion (**Figure 7B**). With the IIPT (data not shown),

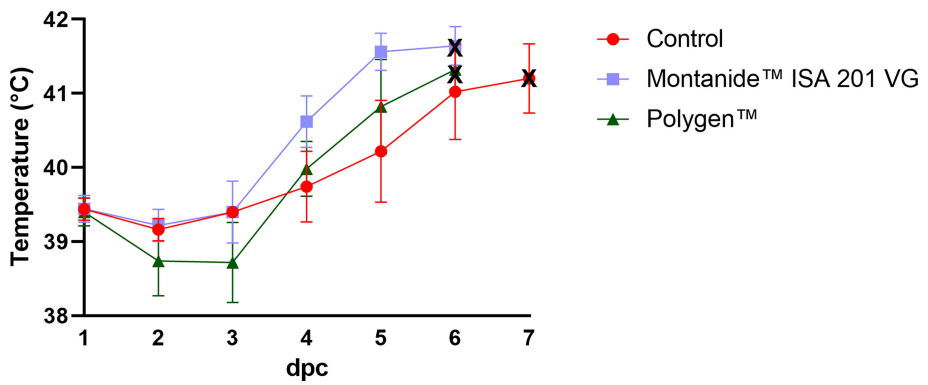

FIGURE 2 | Inner body temperatures depicted as group mean values after challenge (bars indicate standard deviation). Black crosses indicate the day at which the animals reached the moderate humane endpoint. dpc, days post challenge.

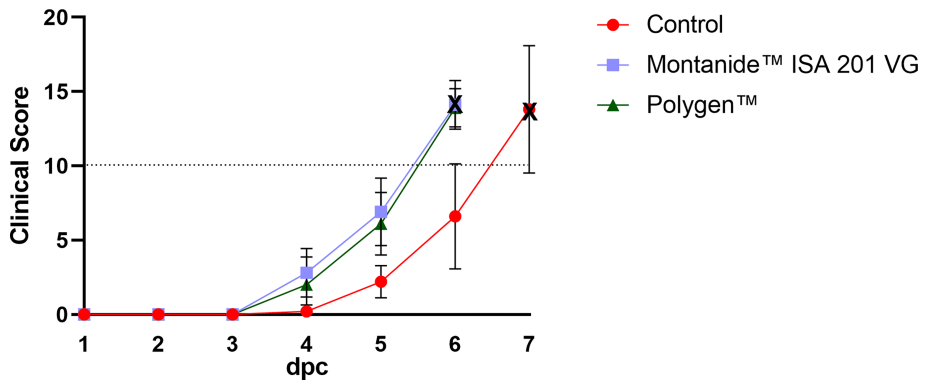

FIGURE 3 | Mean clinical scores (bars indicate standard deviation) of the vaccinated and control groups after challenge. The control group showed a later onset compared to both vaccinated groups. Dotted line indicates the moderate humane endpoint of 10 score points (indicated as dotted horizontal line). The cross marks the day of euthanasia. dpc, days post challenge.

the first antibody positive animals from the Montanide™ ISA 201 VG group could be detected on 7 days post vaccination (dpv) (3/5, 1 questionable). From 14 dpv all animals were positive. In the Polygen™ group only one animal showed a positive immune response on 7 dpv, and on 14 dpv three animals were positive and two questionable. From 21 dpv all animals from the Polygen™ group were antibody positive. No correlation was found between viremia and antibody detection or between clinical score and antibody detection (data not shown).

DISCUSSION

The current ASF pandemic endangers animal health and all branches of global pig industry (24). In the absence of vaccines or treatment options, controlling ASF is proving nearly impossible in many regions of the world (25), and research towards vaccines has been intensified.

For the domestic pig sector, safety is a key requirement and thus, inactivated vaccines, vectored vaccines, and subunit approaches would be favorable. Unfortunately, there has been little success in this direction (3).

In an additional attempt of testing an inactivated vaccine, we explored the use of gamma-irradiation for virus inactivation. After the development of gamma irradiators that can provide precise doses, this technique has been used to develop a variety of proof-of-concept vaccine types. The main advantage of this inactivation technique is its ability to destroy nucleic acids of the pathogen while preserving the proteins and thus the antigenicity. Chemical inactivation which is more frequently used in the current inactivated vaccine production, leads to an increased destruction of pathogen proteins compared to

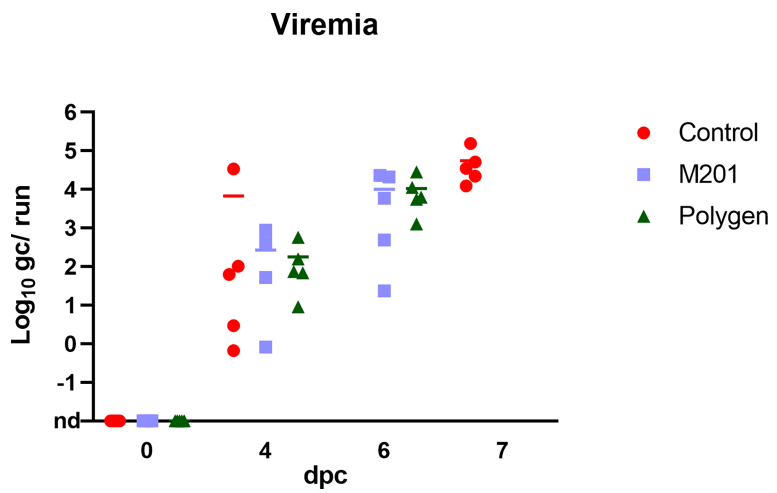

FIGURE 4 | Detection of viral genome in blood samples after challenge infection. Challenge was performed on day 42 after the first vaccination or 21 days after the second vaccination. Blood samples were taken on day 4 pc and at day of euthanasia. Results are expressed as log 10 genome copies (gc)/run. nd, not detected.

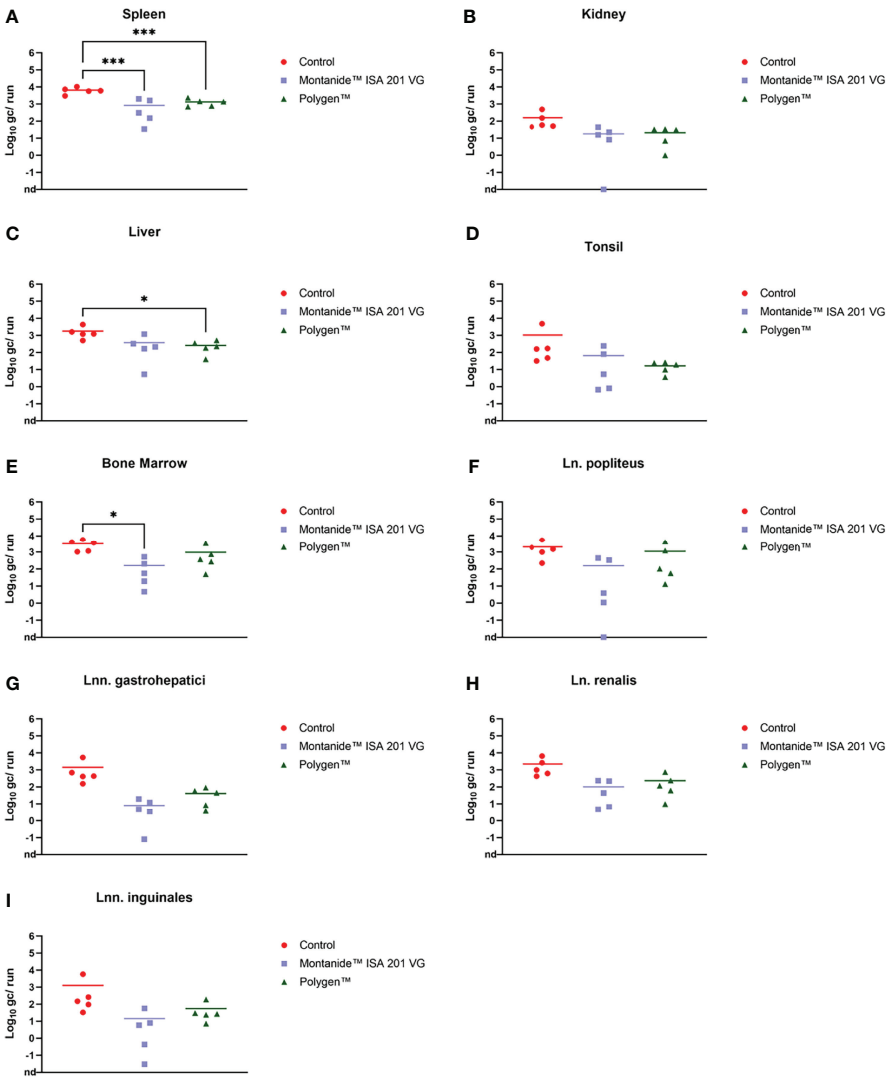

FIGURE 5 | Individual log 10 genome copies (gc)/run obtained by qPCR (King et al., 2003) from spleen **(A)**, kidney **(B)**, liver **(C)**, tonsil **(D)**, bone marrow **(E)**, Ln. popliteus **(F)**, Lnn. gastrohepatici **(G)**, Ln. renalis **(H)** and Lnn. inguinales **(I)** of the vaccinated and control groups. *p-Values: < 0.1; ***p-Values: < 0.001. nd, not detected.

radiation-inactivation. Moreover, following radiation-inactivation, there is no need to remove any chemical residues which increases the safety of the vaccine and makes the whole process simpler and less time-consuming (26). Thus, in this study we aimed at preserving the structure of the virus and the natural presentation of crucial antigens. In addition, we chose two adjuvants with different modes of action, namely "Montanide™ ISA 201" and "Polygen™", that are both known to elicit not only humoral but also cellular responses (20, 21, 27–30). The latter are known to be crucial for protection (31).

In the presented study, inactivation was achieved with doses from 8 kGy onwards with an initial virus titer from $10^{7.25}$ HAU/ml. Given the impact of the disease and biosafety requirements, a considerable safety margin according to the internationally accepted standard SAL was added, and vaccination was carried out with suspensions irradiated with 30 kGy. This dose is still lower than the dose of 50 kGy that was used by McVicar et al. (32) for bulk samples (titers of the selected tissues ranged from $10^{4.6}$ to $10^{7.8}$ HAd_{50}/g). However, McVicar (32) showed that an irradiation dose of 20 kGy was sufficient to inactivate ASFV. The latter is in line with more recent studies by Boudarkov et al. (33), who showed that irradiation doses of 20 kGy and higher completely inactivated ASFV with an initial titer of 10^6 HAd_{50}/cm^3. In the experiment presented here, the infectivity of the irradiated virus was tested by haemadsorption test and complete inactivation was confirmed in the animal trial (no detection of virus in vaccinees). In addition, integrity of the virus particles was confirmed by electron microscopy.

General immunogenicity was shown as all animals developed antibodies against ASFV p72. In detail, the group that received

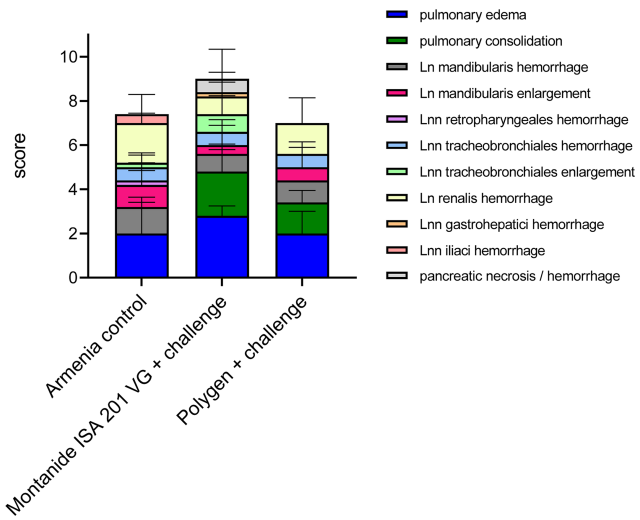

FIGURE 6 | Summary of macroscopic pathological findings in unvaccinated (Armenia control) and vaccinated challenged pigs (Montanide™ ISA 201 VG and Polygen™). The mean values of each individual finding (right legend) from all animals were summarized to form a total score given on the Y-axis.

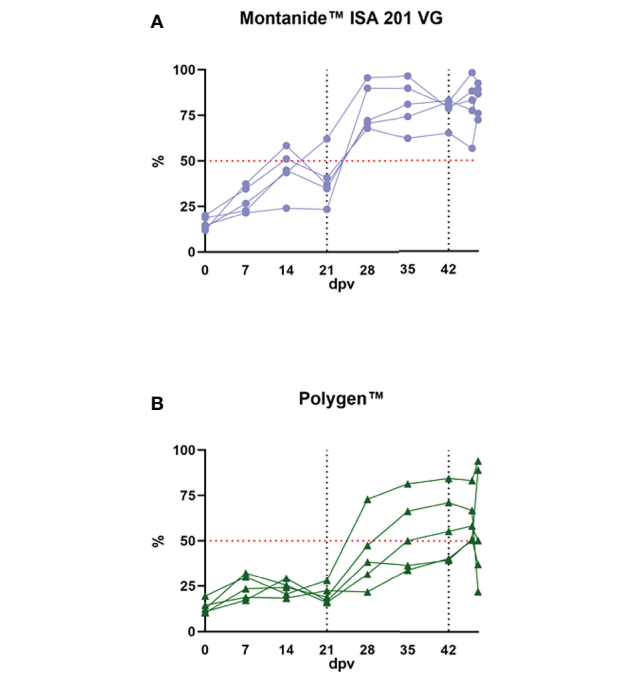

FIGURE 7 | Antibody detection in the vaccinated groups. **(A)** the vaccinated group with Monatide™ ISA 201 VG as adjuvant and **(B)** the vaccinated group with Polygen™ as adjuvant. The ELISA cut off is 50% blocking which is indicated as a red dotted line in both graphs. The first black dotted line indicates the second vaccination and the second dotted line is the time point of the challenge infection.

Montanide™ ISA 201 VG as adjuvant, seroconverted earlier and showed higher ASFV p72 antibody levels when compared to the group that received the vaccine with Polygen™ as adjuvant. Unfortunately, challenge infection showed again that no protective immunity was induced. All vaccinated animals reached the humane endpoint even earlier than the controls and displayed typical ASF lesions. However, lower viral loads were detected in organ samples of the vaccinated animals, especially in spleen, liver and bone marrow. This could be due to a partial protection of antibodies, as the level of antibodies decreased slightly after challenge, indicating consumption. Another explanation could be the fact that the vaccinees had to be euthanized one day earlier than the control group. Jancovich et al. (34), also observed that if animals were vaccinated, decreased levels of ASFV genome in blood and some soft tissues were found after challenge compared to those in control pigs. One pig (# 351) from the Montanide™ ISA 201 VG adjuvanted group showed even no viremia at 4 dpi and very low genome copies in organ samples at the day of euthanasia, although the clinical signs were severe. It cannot be completely ruled out, however, that technical problems during challenge or sampling could have led to the observed difference for this particular pig. These findings of an earlier onset of clinical signs, viremia, and death in vaccinated animals were in line with other studies that showed lacking protective effects in the presence of high antibody levels (9, 35, 36).

The above indicated slightly accelerated clinical course in vaccinated animals in the absence of higher virus replication could indicate an immune-mediated disease enhancement of so far unknown genesis. This phenomenon was also seen in the study with inactivated preparations by Blome et al. (35) and in the study by Lokhandwala et al. (37), which used an Adeno-vectored vaccine. Experiments with DNA vaccines and recombinant proteins have also led to an earlier onset of clinical signs, viremia and death in vaccinated animals after challenge (34, 38, 39). Enhanced susceptibility to certain virus infection due to pre-existing immunity can occur through mechanisms involving antibodies, activated macrophages, CD4+T-cells, and dendritic cells (40, 41). One such mechanism, antibody-dependent enhancement (ADE), is a well-documented phenomenon for viral pathogens such as dengue virus and HIV (42, 43), but also MERS-CoV or SARS-CoV spike S protein (44). For ASFV, the underlying mechanisms remain to be elucidated.

Since this was a proof-of-concept study, groups of animals were restricted for this study in terms of the adjuvants, direct comparison was beyond the scope of our study and we did also not include an adjuvant-only or vaccine-only control. In the end this hampers full evaluation of enhancing effects, but as all animals succumbed, follow-up studies may not be indicated. Taking published studies into account, a detrimental effect of powerful adjuvants cannot be completely excluded.

The route of vaccine administration can also play an important role and is worthy of further research in the context of immunization protocols. For example, it was observed that pigs infected with the naturally tick attenuated genotype I OURT88/3 virus were protected against virulent wild type

OURT88/1 challenge when administered at low to intermediate doses 10^3–10^4 pfu intranasally, but not when administered intramuscularly at the same doses (10). Another route that could be beneficial is the intra-dermal application as antigen-presenting dendritic cells are highly abundant in dermal tissues (45).

Based on the negative results of the use of inactivated vaccines against ASF from previous studies and this one, the use of inactivated vaccines against ASF does not seem to be a viable strategy to date. The lack of neutralizing antibodies plays a major role in the development of an effective inactivated vaccine (9). The insufficiency of inactivated vaccines, along with the lack of efficacy of subunit vaccines, can be explained by the fact that cellular immunity plays a crucial role in protection against ASFV (46, 47). To generate a cellular response, there should be viral replication in the host, which explains effectiveness of live attenuated vaccines (9).

In summary, it can be said that ASF virus inactivated by gamma irradiation cannot be used as a vaccine due to the lack of protection after challenge. The phenomenon of significantly lower viral loads in spleen and liver of immunized animals at the time point of euthanasia, which suggests an immune mediated disease enhancement, needs further investigation.

DATA AVAILABILITY STATEMENT

The raw data that support the findings of this study are available from the corresponding author upon reasonable request.

ETHICS STATEMENT

The animal study was reviewed and approved by Landesamt für Landwirtschaft, Lebensmittelsicherheit und Fischerei (LALLF) Mecklenburg-Vorpommern, Rostock, Germany; reference number 7221.3-1.1-003/20.

AUTHOR CONTRIBUTIONS

Conceptualization, JP, VW, GC, KP, MB, and SB. Methodology, VA, KP, HR, JP, JS-E, LP, and RK. Formal analysis, VA, KP, JP, HR, LP, VW, and SB. Investigation, KP, JP, HR, JS-E, LP, and RK. Resources, VW, GC, MB, and SB. Data curation, VA, KP, JP, HR, LP, and JS-E. Writing—original draft preparation, JP, LP, and SB. Writing—review and editing, GC, SB, and MB. Visualization, JP, HR, LP, and SB. Supervision, VW, GC, SB, and MB. Project administration, JP, VW, MB, and SB. Funding acquisition, GC and SB. All authors have read and agreed to the published version of the manuscript.

ACKNOWLEDGMENTS

The authors would like to thank Sebastien Deville of SEPPIC, Air Liquide Healthcare Specialty Ingredients for providing us Montanide™ ISA 201 VG and all animal caretakers Matthias Jahn, Domenique Lux and Steffen Brenz, and technicians Petra Meyer, Silvia Schuparis, Ulrike Kleinert, Robin Brandt and Christian Loth involved in this study for their excellent work.

SUPPLEMENTARY MATERIAL

The Supplementary Material for this article can be found online at: https://www.frontiersin.org/articles/10.3389/fimmu.2022.832264/full#supplementary-material

Supplementary Figure S1 | (A) Effect of gamma irradiation on the infectivity of ASFV "Estonia 2014". The mean virus titer is calculated in HAU/ml. **(B)** Plot used for calculating the gamma radiation dose required to reduce infectivity of ASFV by 90% (D_{10} value) in kGy.

REFERENCES

1. Alejo A, Matamoros T, Guerra M, Andres G. A Proteomic Atlas of the African Swine Fever Virus Particle. *J Virol* (2018) 92(23):e01293–18. doi: 10.1128/JVI.01293-18
2. Andres G, Charro D, Matamoros T, Dillard RS, Abrescia NGA. The Cryo-EM Structure of African Swine Fever Virus Unravels a Unique Architecture Comprising Two Icosahedral Protein Capsids and Two Lipoprotein Membranes. *J Biol Chem* (2020) 295(1):1–12. doi: 10.1074/jbc.AC119.011196
3. Blome S, Franzke K, Beer M. African Swine Fever - A Review of Current Knowledge. *Virus Res* (2020) 287:198099. doi: 10.1016/j.virusres.2020.198099
4. Nurmoja I, Petrov A, Breidenstein C, Zani L, Forth JH, Beer M, et al. Biological Characterization of African Swine Fever Virus Genotype II Strains From North-Eastern Estonia in European Wild Boar. *Transbound Emerg Dis* (2017) 64(6):2034–41. doi: 10.1111/tbed.12614
5. Zani L, Forth JH, Forth L, Nurmoja I, Leidenberger S, Henke J, et al. Deletion at the 5'-End of Estonian ASFV Strains Associated With an Attenuated Phenotype. *Sci Rep* (2018) 8(1):6510. doi: 10.1038/s41598-018-24740-1
6. Gallardo C, Sanchez EG, Perez-Nunez D, Nogal M, de Leon P, Carrascosa AL, et al. African Swine Fever Virus (ASFV) Protection Mediated by NH/P68 and NH/P68 Recombinant Live-Attenuated Viruses. *Vaccine* (2018) 36(19):2694–704. doi: 10.1016/j.vaccine.2018.03.040
7. Barasona JA, Gallardo C, Cadenas-Fernandez E, Jurado C, Rivera B, Rodriguez-Bertos A, et al. First Oral Vaccination of Eurasian Wild Boar Against African Swine Fever Virus Genotype Ii. *Front Vet Sci* (2019) 6:137. doi: 10.3389/fvets.2019.00137
8. Sun E, Zhang Z, Wang Z, He X, Zhang X, Wang L, et al. Emergence and Prevalence of Naturally Occurring Lower Virulent African Swine Fever Viruses in Domestic Pigs in China in 2020. *Sci China Life Sci* (2021) 64(5):752–65. doi: 10.1007/s11427-021-1904-4
9. Cadenas-Fernández E, Sánchez-Vizcaíno JM, van den Born E, Kosowska A, van Kilsdonk E, Fernández-Pacheco P, et al. High Doses of Inactivated African Swine Fever Virus Are Safe, But Do Not Confer Protection Against a Virulent Challenge. *Vaccines (Basel)* (2021) 9(3):242. doi: 10.3390/vaccines9030242
10. Sang H, Miller G, Lokhandwala S, Sangewar N, Waghela SD, Bishop RP, et al. Progress Toward Development of Effective and Safe African Swine Fever Virus Vaccines. *Front Vet Sci* (2020) 7:84. doi: 10.3389/fvets.2020.00084
11. Salehi B, Motamedi-Sedeh F, Madadgar O, Khalili I, Ghalyan Chi Langroudi A, Unger H, et al. Analysis of Antigen Conservation and Inactivation of Gamma-Irradiated Avian Influenza Virus Subtype H9N2. *Acta Microbiol Immunol Hung* (2018) 65(2):163–71. doi: 10.1556/030.65.2018.025
12. Tobin GJ, Tobin JK, Gaidamakova EK, Wiggins TJ, Bushnell RV, Lee WM, et al. A Novel Gamma Radiation-Inactivated Sabin-Based Polio Vaccine. *PloS One* (2020) 15(1):e0228006. doi: 10.1371/journal.pone.0228006

13. Pietschmann J, Guinat C, Beer M, Pronin V, Tauscher K, Petrov A, et al. Course and Transmission Characteristics of Oral Low-Dose Infection of Domestic Pigs and European Wild Boar With a Caucasian African Swine Fever Virus Isolate. *Arch Virol* (2015) 160(7):1657–67. doi: 10.1007/s00705-015-2430-2
14. Galindo-Cardiel I, Ballester M, Solanes D, Nofrarias M, Lopez-Soria S, Argilaguet JM, et al. Standardization of Pathological Investigations in the Framework of Experimental ASFV Infections. *Virus Res* (2013) 173(1):180–90. doi: 10.1016/j.virusres.2012.12.018
15. Sehl J, Pikalo J, Schäfer A, Franzke K, Pannhorst K, Elnagar A, et al. Comparative Pathology of Domestic Pigs and Wild Boar Infected With the Moderately Virulent African Swine Fever Virus Strain "Estonia 2014". *Pathogens* (2020) 9(8):662. doi: 10.3390/pathogens9080662
16. Fischer M, Mohnke M, Probst C, Pikalo J, Conraths FJ, Beer M, et al. Stability of African Swine Fever Virus on Heat-Treated Field Crops. *Transbound Emerg Dis* (2020) 67(6):2318–23. doi: 10.1111/tbed.13650
17. Jain R, Sarkale P, Mali D, Shete AM, Patil DY, Majumdar T, et al. Inactivation of SARS-CoV-2 by Gamma Irradiation. *Indian J Med Res* (2020) 153:196–8. doi: 10.4103/ijmr.IJMR_2789_20
18. Rubbenstroth D, Peus E, Schramm E, Kottmann D, Bartels H, McCowan C, et al. Identification of a Novel Clade of Group A Rotaviruses in Fatally Diseased Domestic Pigeons in Europe. *Transbound Emerg Dis* (2019) 66 (1):552–61. doi: 10.1111/tbed.13065
19. Andrianarivo AG, Rowe JD, Barr BC, Anderson ML, Packham AE, Sverlow KW, et al. A POLYGEN-Adjuvanted Killed Neospora Caninum Tachyzoite Preparation Failed to Prevent Foetal Infection in Pregnant Cattle Following I.V./I.M. Experimental Tachyzoite Challenge. *Int J Parasitol* (2000) 30(9):985–90. doi: 10.1016/s0020-7519(00)00088-6
20. Wolff J, Moritz T, Schlottau K, Hoffmann D, Beer M, Hoffmann B. Development of a Safe and Highly Efficient Inactivated Vaccine Candidate Against Lumpy Skin Disease Virus. *Vaccines (Basel)* (2020) 9(1):4. doi: 10.3390/vaccines9010004
21. Bouguyon E, Goncalves E, Shevtsov A, Maisonnasse P, Remyga S, Goryushev O, et al. A New Adjuvant Combined With Inactivated Influenza Enhances Specific CD8 T Cell Response in Mice and Decreases Symptoms in Swine Upon Challenge. *Viral Immunol* (2015) 28(9):524–31. doi: 10.1089/vim.2014.0149
22. King DP, Reid SM, Hutchings GH, Grierson SS, Wilkinson PJ, Dixon LK, et al. Development of a TaqMan PCR Assay With Internal Amplification Control for the Detection of African Swine Fever Virus. *J Virol Methods* (2003) 107 (1):53–61. doi: 10.1016/S0166-0934(02)00189-1
23. Sastre P, Gallardo C, Monedero A, Ruiz T, Arias M, Sanz A, et al. Development of a Novel Lateral Flow Assay for Detection of African Swine Fever in Blood. *BMC Vet Res* (2016) 12:206. doi: 10.1186/s12917-016-0831-4
24. Ward MP, Tian K, Nowotny N. African Swine Fever, the Forgotten Pandemic. *Transbound Emerg Dis* (2021) 68(5):2637–9. doi: 10.1111/tbed.14245
25. Turlewicz-Podbielska H, Kuriga A, Niemyjski R, Tarasiuk G, Pomorska-Mól M. African Swine Fever Virus as a Difficult Opponent in the Fight for a Vaccine-Current Data. *Viruses* (2021) 13(7):1212. doi: 10.3390/v13071212
26. Seo HS. Application of Radiation Technology in Vaccines Development. *Clin Exp Vaccine Res* (2015) 4(2):145–58. doi: 10.7774/cevr.2015.4.2.145
27. Andrianarivo AG, Choromanski L, McDonough SP, Packham AE, Conrad PA. Immunogenicity of a Killed Whole Neospora Caninum Tachyzoite Preparation Formulated With Different Adjuvants. *Int J Parasitol* (1999) 29 (10):1613–25. doi: 10.1016/S0020-7519(99)00116-2
28. Jang SI, Lillehoj HS, Lee SH, Lee KW, Park MS, Bauchan GR, et al. Immunoenhancing Effects of Montanide ISA Oil-Based Adjuvants on Recombinant Coccidia Antigen Vaccination Against Eimeria Acervulina Infection. *Vet Parasitol* (2010) 172(3-4):221–8. doi: 10.1016/j.vetpar.2010.04.042
29. Dar P, Kalaivanan R, Sied N, Mamo B, Kishore S, Suryanarayana VV, et al. Montanide ISA™ 201 Adjuvanted FMD Vaccine Induces Improved Immune Responses and Protection in Cattle. *Vaccine* (2013) 31(33):3327–32. doi: 10.1016/j.vaccine.2013.05.078
30. Milian-Suazo F, Gutierrez-Pabello JA, Bojorquez-Narvaez L, Anaya-Escalera AM, Canto-Alarcon GJ, Gonzalez-Enriquez JL, et al. IFN-G Response to Vaccination Against Tuberculosis in Dairy Heifers Under Commercial Settings. *Res Vet Sci* (2011) 90(3):419–24. doi: 10.1016/j.rvsc.2010.07.018
31. Oura CA, Denyer MS, Takamatsu H, Parkhouse RM. *In Vivo* Depletion of CD8+ T Lymphocytes Abrogates Protective Immunity to African Swine Fever Virus. *J Gen Virol* (2005) 86(Pt 9):2445–50. doi: 10.1099/vir.0.81038-0
32. McVicar JW, Mebus CA, Brynjolfsson A, Walker JS. Inactivation of African Swine Fever Virus in Tissues by Gamma Radiation. *Am J Vet Res* (1982) 43 (2):318–9.
33. Boudarkov V, Sereda A, Carpov O, Ponomarev V. Using Gamma Rays to Inactivate African Swine Fever Virus. *Russian Agric Sci* (2016) 42(5):375–7. doi: 10.3103/S1068367416050025
34. Jancovich JK, Chapman D, Hansen DT, Robida MD, Loskutov A, Craciunescu F, et al. Immunization of Pigs by DNA Prime and Recombinant Vaccinia Virus Boost to Identify and Rank African Swine Fever Virus Immunogenic and Protective Proteins. *J Virol* (2018) 92(8):e02219-17. doi: 10.1128/JVI.02219-17
35. Blome S, Gabriel C, Beer M. Modern Adjuvants do Not Enhance the Efficacy of an Inactivated African Swine Fever Virus Vaccine Preparation. *Vaccine* (2014) 32(31):3879–82. doi: 10.1016/j.vaccine.2014.05.051
36. Stone SS, Hess WR. Antibody Response to Inactivated Preparations of African Swine Fever Virus in Pigs. *Am J Vet Res* (1967) 28(123):475–81.
37. Lokhandwala S, Petrovan V, Popescu L, Sangewar N, Elijah C, Stoian A, et al. Adenovirus-Vectored African Swine Fever Virus Antigen Cocktails are Immunogenic But Not Protective Against Intranasal Challenge With Georgia 2007/1 Isolate. *Vet Microbiol* (2019) 235:10–20. doi: 10.1016/j.vetmic.2019.06.006
38. Sunwoo SY, Pérez-Núñez D, Morozov I, Sánchez EG, Gaudreault NN, Trujillo JD, et al. DNA-Protein Vaccination Strategy Does Not Protect From Challenge With African Swine Fever Virus Armenia 2007 Strain. *Vaccines (Basel)* (2019) 28;7(1):12. doi: 10.3390/vaccines7010012
39. Argilaguet JM, Pérez-Martín E, Nofrarías M, Gallardo C, Accensi F, Lacasta A, et al. DNA Vaccination Partially Protects Against African Swine Fever Virus Lethal Challenge in the Absence of Antibodies. *PloS One* (2012) 7(9):e40942. doi: 10.1371/journal.pone.0040942
40. Chapman NM. Prior Immune Exposure can Protect or can Enhance Pathology in the Enteroviruses: What Predicts the Outcome? *Virulence* (2017) 8(6):643–5. doi: 10.1080/21505594.2016.1269048
41. Huisman W, Martina BE, Rimmelzwaan GF, Gruters RA, Osterhaus AD. Vaccine-Induced Enhancement of Viral Infections. *Vaccine* (2009) 27(4):505–12. doi: 10.1016/j.vaccine.2008.10.087
42. Beck Z, Prohászka Z, Füst G. Traitors of the Immune System-Enhancing Antibodies in HIV Infection: Their Possible Implication in HIV Vaccine Development. *Vaccine* (2008) 26(24):3078–85. doi: 10.1016/j.vaccine.2007.12.028
43. Halstead SB. Dengue Antibody-Dependent Enhancement: Knowns and Unknowns. *Microbiol Spectr.* (2014) 2(6):2–6. doi: 10.1128/microbiolspec.AID-0022-2014
44. Ulrich H, Pillat MM, Tárnok A. Dengue Fever, COVID-19 (SARS-CoV-2), and Antibody-Dependent Enhancement (ADE): A Perspective. *Cytomet Part A* (2020) 97(7):662–7. doi: 10.1002/cyto.a.24047
45. Romani N, Flacher V, Tripp CH, Sparber F, Ebner S, Stoitzner P. Targeting Skin Dendritic Cells to Improve Intradermal Vaccination. *Curr Top Microbiol Immunol* (2012) 351:113–38. doi: 10.1007/82_2010_118
46. Argilaguet JM, Pérez-Martín E, Nofrarías M, Gallardo C, Accensi F, Lacasta A, et al. DNA Vaccination Partially Protects Against African Swine Fever Virus Lethal Challenge in the Absence of Antibodies. *PloS One* (2012) 7(9):e40942. doi: 10.1371/journal.pone.0040942
47. Netherton CL, Goatley LC, Reis AL, Portugal R, Nash RH, Morgan SB, et al. Identification and Immunogenicity of African Swine Fever Virus Antigens. *Front Immunol* (2019) 10:1318. doi: 10.3389/fimmu.2019.01318

Conflict of Interest: The authors declare that the research was conducted in the absence of any commercial or financial relationships that could be construed as a potential conflict of interest.

frontiers | Frontiers in Immunology

ORIGINAL RESEARCH
published: 29 April 2022
doi: 10.3389/fimmu.2022.814767

Investigations Into the Suitability of Bacterial Suspensions as Biological Indicators for Low-Energy Electron Irradiation

Simone Schopf, Gaby Gotzmann, Marleen Dietze, Stephanie Gerschke, Lysann Kenner and Ulla König*

Division Medical and Biotechnological Applications, Fraunhofer Institute for Organic Electronics, Electron Beam and Plasma Technology, Dresden, Germany

OPEN ACCESS

Edited by:
Viskam Wijewardana, International Atomic Energy Agency, Austria

Reviewed by:
Suresh D. Pillai, Texas A&M University, United States
Nguyen T. K. Vo, Wilfrid Laurier University, Canada

***Correspondence:**
Simone Schopf
simone.schopf@fep.fraunhofer.de

Specialty section:
This article was submitted to Vaccines and Molecular Therapeutics, a section of the journal Frontiers in Immunology

Received: *14 November 2021*
Accepted: *15 March 2022*
Published: *29 April 2022*

Citation:
Schopf S, Gotzmann G, Dietze M, Gerschke S, Kenner L and König U (2022) Investigations Into the Suitability of Bacterial Suspensions as Biological Indicators for Low-Energy Electron Irradiation. Front. Immunol. 13:814767. doi: 10.3389/fimmu.2022.814767

Low-energy electron irradiation is an emerging alternative technology for attenuated or complete pathogen inactivation with respect to medical, biotechnological, and pharmaceutical applications. Pathogen inactivation by ionizing radiation depends mainly on the absorbed electron dose. In low-energy electron irradiation processes, determination of the absorbed electron dose is challenging due to the limited, material-dependent penetration depth of the accelerated electrons into the matter. In general, there are established dosimetry systems to evaluate the absorbed dose under dry irradiation conditions. However, there is no system for precise dose monitoring of low-energy irradiation processes in liquids or suspensions so far. Therefore, in this study three different bacterial species were investigated as biological dose indicators, especially in the range of low doses (< 6.5 kGy) in aqueous solutions or suspensions. *Escherichia coli*, *Bacillus subtilis*, *and Staphylococcus warneri* were comparatively evaluated for their suitability as biological dose indicators. Thin homogeneous films of the respective bacterial suspensions were irradiated with increasing doses of low-energy accelerated electrons. The average absorbed dose was determined using a colorimetric dosimeter based on a tetrazolium salt solution. The maximum and minimum absorbed doses were measured with a referenced film dosimeter. Subsequently, the inactivation kinetics was determined in terms of inactivation curves and D_{10} values. Thus, the minimum inactivation dose of bacterial growth was assessed for *E. coli* and *S. warneri*. The effect of irradiation with low-energy accelerated electrons on the growth behavior and activity of the bacteria was studied in more detail using impedance spectroscopy. With increasing irradiation doses growth was delayed.

Keywords: bacteria, dosimetry, liquid, inactivation, impedance spectroscopy

INTRODUCTION

The inactivation of microorganisms is a critical step in many aspects of biomedical research, in biotechnological production processes, and in healthcare facilities. Sterilization is a validated process that destroys or eliminates all forms of microbial life, leaving a product free from viable microorganisms. Various physical or chemical processes are used to achieve sterility or to inactivate microorganisms. Amongst physical treatment, ionizing radiation with gamma-rays, X-rays, and high-energy accelerated electrons has been used as technology for pharma applications and to sterilize medical products or pasteurize food (1–4). In recent years, electron beam accelerators have emerged as feasible alternative for industrial processing. Sterilization using accelerated electrons is an accepted technology that meets the requirements of international standards according to (5). For radiation sterilization a minimum dose of 25 kGy is required to achieve sufficient sterilization efficiency. Consequently, microorganisms such as bacteria, viruses, and protozoa can be efficiently inactivated with technologies using accelerated electrons (6–8).

Depending on the kinetic energy of the electrons, electron beam technology can be distinguished either in high-, middle-, or low-energy accelerated electron irradiation (LEEI; ≤ 300 keV) (9). The penetration depth of the electrons is determined by their kinetic energy, by the density, and by the thickness of the treated material. The higher the kinetic energy and the lower the density of the matter, the higher the range of electrons in the material (10). Electrons with high kinetic energy can penetrate products up to several centimeter whereas the penetration depth of low-energy accelerated electrons is limited to a few hundred micrometer (11). Thus, the low penetration depth is a major challenge when using LEEI (12), especially for liquid processing systems. Consequently, the liquid, e.g. a pathogen-containing suspension, has to be processed as a thin film of several microns to ensure homogeneous irradiation through the complete liquid film.

When low-energy accelerated electrons collide with matter their kinetic energy is transferred through physical interactions to excite molecules. This leads to the formation of highly reactive free radicals, such as hydroxyl radicals. These hydroxyl radicals can initiate a cascade of chemical chain reactions leading to the breakdown of structural and functional biomolecules. The most important target for the action of ionizing radiation in the cell is the DNA molecule. The DNA destruction leads to irradiation damage of the cells (13). Furthermore, the inactivation of pathogens can also be attributed to the degradation of nucleic acids, either by direct interaction or indirectly through the radiolysis of water within the cell (4). Hydroxyl radicals are thought to be responsible for 80-90 % of total DNA damage (14).

High-energy electron accelerators generate a large amount of Bremsstrahlung (X-ray radiation). Therefore, these irradiation facilities must be equipped with complex shielding constructions to protect both the personnel and the environment. This makes direct integration of HEEI technologies into pharmaceutical production facilities challenging. In contrast, LEEI technology generates only a low quantity of X-ray radiation, which minimizes undesired side effects and allows for compact radiation protection. In addition, LEEI is a chemical-free, fast process with high overall energy efficiency (11, 15). Previously, LEEI has been shown to be an emerging technology for the development and production of inactivated vaccines (16).

The benefits of LEEI technology are faced with the challenge of determining the absorbed dose in irradiated liquids, especially in the range below 6.5 kGy. In general, there are established dose indicators for measuring the dose under dry irradiation conditions (1, 17). There is a whole range of approved, excellent dosimeters, e.g. the reference standard alanine dosimeter (18), which can be used to calibrate other dosimeters, and the Risø B3 radiochromic film dosimeter for routine dose measurements (19).

However, the radiation-induced response from some routine dosimeters is not stable and changes with time after irradiation (20). Existing film dosimeter systems are susceptible to environmental influences, such as air, humidity, oxygen content in the atmosphere, surrounding temperature, or UV radiation from sun light (21). In addition, the response can vary by up to 30-40 % if the dosimeters have been irradiated under extremely dry or humid conditions, which has a vast impact on the result. For LEEI applications, it is recommended to store and irradiate the film dosimeters under controlled and well-defined conditions (21). A liquid dosimeter currently in use is based on a dye solution that changes its spectral properties after irradiation with low-energy accelerated electrons (8). However, this liquid dosimeter is only reliable for doses above 6.5 kGy. Hence, there is a necessity for a liquid routine dosimeter for low doses of low-energy accelerated electrons.

A biological dose indicator system based on various bacteria (hereafter referred to as bio-dosimeter) could potentially improve the quantification of the dose in liquids after irradiation with low-energy accelerated electrons. The underlying assumption is that bacteria lose their ability to proliferate after being exposed to a certain dose of low-energy accelerated electrons. Consequently, the response of the dosimeter should remain constant and bias due to improper storage of the bio-dosimeter should be avoided.

In this study, three different non-pathogenic bacteria from different taxa and with different physiological characteristics were studied for their suitability as biological dose indicators for LEEI. *Escherichia coli* served as a Gram-negative model organism. *Staphylococcus warneri* and vegetative cells of *Bacillus subtilis* served as Gram-positive representatives. The objective was to characterize the inactivation kinetics of each bacterium and to investigate the impact of LEEI on growth and activity by impedance spectroscopy.

MATERIAL AND METHODS

Strains and Culture Conditions

All bacterial strains used in this study were obtained from the German Collection of Microorganisms and Cell Cultures DSMZ and kept as stock cultures at -20°C. *E. coli* K12 (DSM 498) was cultivated in Standard Nutrient Broth I and vegetative cells of *B. subtilis* (DSM 10) in LB-broth (both Carl Roth GmbH + Co.

KG) at 37°C and 125 rpm shaking. *S. warneri* (DSM 20036) usually appears in conglomerates. To avoid agglomeration of the bacterial cells, CASO-Bouillon (Carl Roth GmbH + Co. KG) was used for cultivation at 37°C and 125 rpm overnight. Prior to each irradiation experiment a fresh overnight culture was grown. To ensure equivalent cell densities, the freshly grown pre-cultures were enumerated with a Neubauer improved counting chamber and diluted to approx. 10^6 bacteria/ml.

A petri dish-based setup was used to irradiate the bacterial suspensions, in which the liquid droplet was covered with a round foil of oriented polypropylene (OPP) to create a thin homogeneous liquid film of 80 µm height (**Figure 1**). Prior to use, the OPP foils were disinfected with 70 % ethanol (v/v) for 15 minutes. 57 µl bacterial suspension was pipetted in three sterile petri dishes in a laminar flow work bench. The fourth petri dish served for routine dosimetry as described below. Briefly, a piece of dosimeter film was fixed in the center of the petri dishes and covered with OPP-foil. The so prepared petri dishes were fixed on one sample holder and covered with high-density polyethylene (HDPE) foil.

The low-energy accelerated electron plant REAMODE ("Reactive Modification with Electrons") with a 200 keV electron beam (KeVac System, Linac Technologies, Orsay, France, 200 kV) was used for irradiation. The conveyor speed was 140 mm/s and the distance of the beam exit window to the specimens was 35 mm. The applied current (0.1-0.85 mA) was used to adjust the intended absorbed dose in a range from 0.1 to 3.5 kGy.

Counting of Viable Cells After Irradiation

30 µl of bacterial suspension was immediately recovered from the petri dish and plated onto respective agar plates to determine the number of colony forming units (CFU). Plates were incubated for 24-48 h at 37°C. To determine the CFU/ml, the mean values of the visible colonies were calculated from three to nine agar plates.

For solely qualitative analysis of bacterial growth after irradiation, 5 ml of sterile nutrition broth was added to the remaining bacterial suspension in the petri dish. The so prepared petri dishes were incubated at the optimum growth temperature for 7 days to monitor the growth of bacteria *via* turbidity.

Routine Measurement of Absorbed Doses and Depth Dose Distribution

The absorbed dose was routinely measured with radiochromic films (**Figure 2A**; Risø B3 dosimeter, Risø High Dose Reference Laboratory, Roskilde, Denmark). The dosimeter films were incubated at 60°C for 8 min after irradiation. The absorbed dose was measured by quantifying the color change at 554 nm using special software with a calibration (RisøScan-System). Irradiation with low-energy accelerated electrons was accompanied by a dose gradient across the thickness of the irradiated dosimeter foil. Therefore, the dose measured with Risø B3 was corrected to Dµ, which corresponds to the absorbed dose in the first micrometer of the absorbing medium (12).

The dose gradient in the irradiated liquid was simulated by a stack of Risø B3 films (depth dose distribution). The total volume of bacterial suspension in the petri dish (57 µl) corresponded to a liquid height of 80 µm. Based on the density of a Risø B3 film (ρ = 1.12 g/cm^3) an equivalent to the density of water was calculated (ρ = 1.0 g/cm^3). Thus, a layer of Risø B3 (18 µm) corresponded to a liquid layer height of 20.1 µm. Consequently, a stack of 5 Risø B3 films was required to simulate a liquid height of 80 µm. Air bubbles between the dosimeter films were avoided.

After irradiation, the maximum irradiation dose was obtained from the response of the dosimeter on the top of the stack. The average dose was calculated from the mean value of 4 dosimeter films. The minimum dose was given as an average of the second last and the bottom dosimeter film. In order to measure the mean irradiation dose of the liquid, a dosimeter based on a solution of 2,3,5-triphenyltetrazolium chloride (TTC; 0.2 % (w/v)) in water was used (**Figure 2B**). The TTC was reduced to red-colored

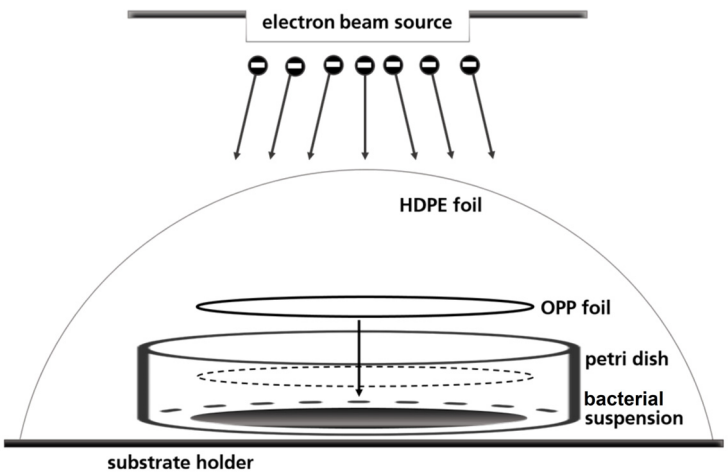

FIGURE 1 | Schematic illustration of the OPP-system used for the irradiation of the bacterial suspensions.

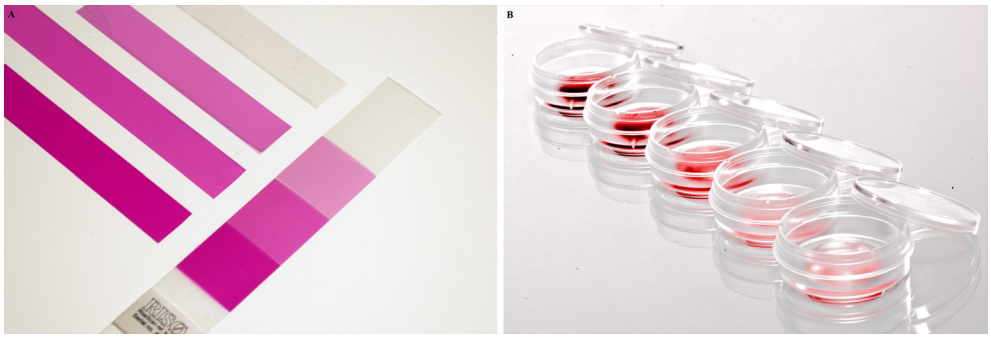

FIGURE 2 | Film and liquid dosimeter. **(A)** Risø B3 film dosimeter. **(B)** TTC-based liquid dosimeter.

formazan upon irradiation. The absorption was measured in transparent 96-well plates at a wavelength of 485 nm (Tecan infinite M200, Tecan Group Ltd.) (8). The TTC was calibrated using the Risø B3 dosimeter. The calibration procedure will be described elsewhere.

Determination of D_{10} Values

The D_{10} value is defined as the dose required to reduce the population by 1 log or decrease it by 90 %. It is calculated from the negative reciprocal of the slope of the regression line that is produced by plotting the number of colony forming units against the absorbed dose. The mean D_{10} value (n = 3) was calculated for each of the three species. From the simulation of the depth dose distribution the maximum and the minimum absorbed doses were measured and calculated. The theoretical inactivation dose was given as the radiation dose that reduced the initial population by 10^6 bacteria/ml or by a 6 log reduction. To calculate the theoretical inactivation dose for each species the D_{10} value was multiplied by 6.

Impedance Spectroscopy

By impedance spectroscopy, the measured change in the electrical conductivity allows the qualitative and quantitative tracing of microorganisms due to the analysis of their microbial activity. Uncharged or weekly charged components of the growth medium are metabolized into smaller charged components by the bacteria, which changes the electrical conductivity of the growth medium and thus the impedance signal. For the measurements carried out in this study, the BacTrac 4100® system (Sy-Lab, Austria) was used with the electrode impedance or E-value (E %). The impedance curve showed the relative change of the E-value as a function of time measured in intervals of 10 minutes.

For *E. coli*, 5970 µl nutrition broth was transferred to an impedance cell. 30 µl of the respective bacterial suspension was added. The suspensions were collected from the petri dish (OPP-system) after irradiation with 0.7, 1.4, 2.1, and 2.8 kGy, respectively. The positive controls (referred to as 0 kGy samples) were not irradiated but handled identically to the irradiated samples. As negative controls sterile growth medium was used.

In an optimized procedure for *S. warneri* and *B. subtilis*, 5700 µl growth medium (CASO bouillon or LB broth) was transferred to an impedance cell. To the (irradiated) bacterial suspension in the petri dish, 513 µl of the respective growth medium was added to the edge of the OPP foil. The petri dish was shaken at 100 rpm for 2 min. 300 µl of the diluted bacterial suspension were rinsed 2-3 times to achieve maximum recovery of bacteria. The collected bacterial suspension was transferred to the impedance cell. All impedance analyses were performed at 37°C.

Statistical Analysis

Data in the figures are given as mean values, and, if indicated, with ± standard deviation (SD). The standard deviation was calculated by the standard error of the arithmetic mean using the MiniTab 20 statistical software. To determine the D_{10} values regression analysis was performed with MiniTab 20 or Excel 2016.

For impedance spectroscopy, all measurements were carried out in triplicates within one series of experiments and additionally at three independent time points (n = 9). Positive controls and negative controls were carried out in triplicates, too.

RESULTS

Dosimetry

Accurate dose measurement was critical for reliable results (**Figure 3**). The intended dose was adjusted by the beam current intensity. The applicable dose range of the Risø B3 film dosimeter is reported to range from 5 to 100 kGy. Since the doses for LEEI inactivation of the used microorganisms are below 5 kGy, which is the Risø B3 lower limit, measuring fluctuations in the dosimeter response can occur. Therefore, dose values from three independent LEEI experiments were plotted against the beam current (**Figure 3A**). There was a linear correlation between beam current and absorbed dose with an R^2 value of 0.989 and a standard deviation of about ± 4 % for the applied doses.

Due to the low penetration depth of the low-energy accelerated electrons, a dose gradient within the bacterial suspension was expected during LEEI. Therefore, experiments were carried out to simulate the depth dose distribution across the liquid using a stack of Risø B3 films as reference dosimeter (**Figure 3B**). The measured and calculated maximum, mean, and minimum dose values are given in **Table 1**. From the maximum

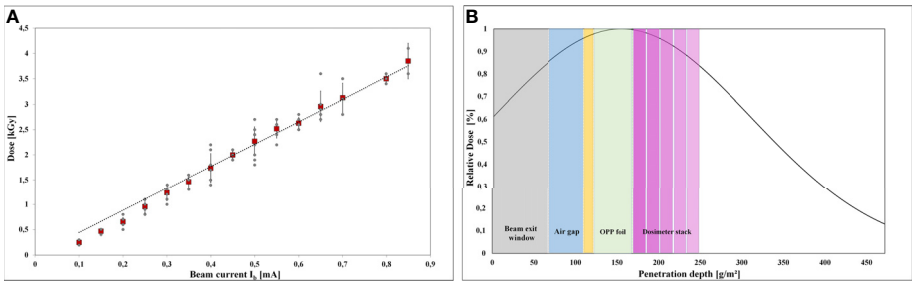

FIGURE 3 | Dose measurements and depth dose distribution: **(A)** Linear correlation between the adjusted beam current and the absorbed dose in the intended dose range from 0 to 3.5 kGy. The red rectangles show the mean values. **(B)** Schematic illustration the depth dose distribution in the OPP-system, simulated by a stack of 5 dosimeter films.

TABLE 1 | Depth dose profile derived from Risø B3 films stacked within the OPP-system.

Nominal dose [kGy]	Absorbed max. dose [kGy]*	Absorbed mean dose [kGy]**	Absorbed min dose [kGy]***	% relative to max. dose	Absorbed mean dose in liquid by TTC [kGy]
20	20.8	20.0	17.9	85.8	20.5
25	24.7	23.4	20.4	82.6	27.1
30	31.5	29.8	26.7	84.8	27.9

**Derived from the uppermost dosimeter film, **the mean value from 4 films, and ***the mean value from the second-last and bottom film. The mean dose determined with the TTC liquid dosimeter is given in the right column.*

absorbed dose (corresponding to 100 %), a relative minimum dose of 84.4 % was derived. This relative percentage value served as calculation basis for the minimum D_{10} value.

As colorimetric dosimeter for liquids, the TTC dye indicator was used. However, with the colorimetric liquid dosimeter, only the average dose related to the total volume of the liquid could be determined. The liquid dosimeter did neither provide information on the dose gradient nor on the maximum and minimum absorbed dose. However, the mean dose values measured with the TTC liquid dosimeter were in good agreement with the mean dose values calculated for the Risø B3 film stack (**Table 1**).

Inactivation Curves and D_{10} Values

LEEI experiments were carried out to determine the dose values required for the inactivation of *E. coli*, *S. warneri*, and *B. subtilis* (**Table 2**). Initially, 10^6 bacteria/ml were irradiated with increasing doses up to 3.5 kGy. Upon irradiation, the bacteria were plated on agar-plates to determine the number of surviving cells. The number of CFU was plotted as a function of the dose to obtain the D_{10} values (**Figure 4**). In all cases, the counts of CFU decreased linearly as the dose increased. The R^2 values from the regression lines were 0.872, 0.903, and 0.871 for *E. coli*, *S. warneri*, and *B. subtilis*, respectively.

Irradiation with low-energy accelerated electrons was associated with dose gradient across the bacterial suspension. Therefore, the maximum and minimum absorbed dose was taken into account.

For *E. coli* (**Figure 4A**) the application of 2.8 kGy reduced the initial cell density of 10^6 cells/ml to 0 CFU. Additionally, no bacterial growth occurred after sterile growth medium was added to the petri dishes for recultivation of potentially surviving or recovering bacteria. Since the media did not become turbid, the presence of multiplying *E. coli* cells was excluded. Thus, 2.8 kGy was experimentally determined as the required dose to inhibit growth. This was in good accordance with the calculated maximum inactivation dose (2.76 kGy), which was derived from the maximum D_{10} value multiplied by 6. The calculated minimum inactivation dose was approximately 2.4 kGy. Furthermore, the maximum and minimum dose to obtain a 1 log reduction for *E. coli* was calculated. The corresponding D_{10} values were 0.46 kGy (derived from the negative reciprocal of the slop from the inactivation line) and 0.39 kGy (84.4 % of the maximum applied dose), respectively.

S. warneri did neither grow on agar-plates nor after adding sterile growth medium to the petri dishes after irradiation with 2.8 kGy. The maximum and minimum inactivation dose was 3.0 kGy and 2.9 kGy, and the corresponding maximum and minimum D_{10} values 0.50 kGy and 0.42 kGy (**Figure 4B**).

Vegetative cells of *B. subtilis* were, according to the calculated doses, supposed to be inhibited in growth in a range from 1.9 kGy to 2.2 kGy, resulting in D_{10} values from 0.31 kGy to 0.37 kGy, respectively (**Figure 4C**). However, the *B. subtilis* inhibition could not clearly be achieved because the turbidimetric test results even at higher doses were not reproducible. The presence of surviving and multiplying *B. subtilis* cells was indicated.

Characterization of Growth *via* Impedance Spectroscopy

Impedance measurement was used to analyze the influence of LEEI on growth and thus metabolic activity of *E. coli*, *S. warneri*, and *B. subtilis* (**Figure 5**). Bacterial suspensions were collected after irradiation with 0.7, 1.4, 2.1, and 2.8 kGy, respectively.

TABLE 2 | D_{10} values and the maximum theoretically and experimentally determined inactivation dose values for *E. coli*, *S. warneri*, and *B. subtilis*.

Bacterium	D-10max [kGy]	D-10min [kGy]	Maximum in activation dose (theoretical) [kGy]	Maximum in activation dose (experimentally) [kGy]
E. coli	0.46	0.39	2.76	2.80
S. warneri	0.50	0.42	2.99	2.80
B. subtilis	0.37	0.31	2.2	n. d.

N. d., not determined.

Samples containing bacterial suspensions, which were handled identically but not irradiated served as controls (0 kGy). As negative control sterile non-inoculated liquid growth medium was used. Those controls did not produce any measurable change in the electrical impedance signal. When bacterial growth occurred, the resulting impedance spectra showed a sigmoidal trend. Positive controls were carried out using a freshly grown pre-culture, which was not handled in the OPP-system. The impedance signals recorded from those controls were similar to the 0 kGy control samples (data not shown). After irradiation of the bacteria with 0.7 kG and 1.4 kGy, growth of *E. coli* and *S. warneri* was measurable in terms of an impedance signal in all samples. Irradiation of *E. coli* and *S. warneri* with 2.1 kGy resulted in a transition state in which two of nine samples were already inactivated, whereas the remaining ones produced an impedance signal (**Figures 5A, B**). After irradiation with 2.8 kGy, basically complete inactivation was achieved, i.e. the impedance signals did not increase.

For *B. subtilis*, impedance analysis revealed a different picture (**Figure 5C**). Complete inactivation could not be reproducibly achieved and growth occurred in some samples even after irradiation with 2.8 kGy was applied.

In general, irradiation with increasing doses from 0.7 to 2.1 kGy resulted in a prolongation of the lag phase. The entry into the exponential phase was delayed, as also summarized in **Table 3**. This finding was very pronounced in *E. coli* and *S. warneri*, whereas it was less evident in *B. subtilis*. However, in all three species studied, the slope of the curve in the exponential growth phase was not significantly affected.

DISCUSSION

It was previously shown that LEEI can successfully be used to inactivate a number of pathogens, such as influenza (H3N8), Equid herpesvirus 1, respiratory syncytial virus (RSV), and bacteria (6, 16, 22). However, up to now, no liquid dosimeter is available for low-energy accelerated electrons and doses below 6.5 kGy. To overcome this issue, the suitability of different bacteria as bio-dosimeter based on their radiation susceptibility was investigated. Therefore, *E. coli*, *S. warneri*, and *B. subtilis* (as vegetative cells) were irradiated with doses < 6.5 kGy to determine the inactivation dose, the D_{10} value, and to investigate the effect of LEEI on the growth behavior in more detail *via* impedance spectroscopy.

Dosimetry

The low penetration depth of LEEI technologies into matter is challenging, when using this technology for biological processes in liquids or suspensions. Therefore, the irradiation process with low-energy accelerated electrons was carried out in a petri dish system using a cover foil of oriented polypropylene (OPP) to achieve a thin homogenous liquid layer (approx. 80 µm) with low dose gradient. The depth dose distribution was determined using the Risø B3 film dosimeter as calibrated reference dosimeter. A transfer of the mean dose measurement data into liquid systems was carried out by using a colorimetric TTC-based liquid dosimeter.

With the implementation of a routine procedure that strictly considers the time of evaluation after irradiation, the TTC-based liquid dosimeter is usable as stable dosimeter for LEEI in a dose range between 6.5 and 40 kGy (8). However, it does not provide optimal results at lower doses. There is an estimated uncertainty range of 11.4 %, especially since the applied the low doses used in this study were outside of the TTC calibration limits.

Inactivation Curves and Minimal Inhibitory Dose

Complete bacterial inactivation, i.e. the inhibition of growth, of defined titers of bacterial cells by lethal electron doses is feasible based on the knowledge of the target organism's D_{10} value (23). Since the applied sources of ionizing radiation and the irradiation conditions differ between studies, a direct comparison is challenging (24). There are several studies dealing with the inactivation of other bacteria by accelerated electrons as source of ionizing radiation, i.e. *Rodentibacter pneumotropicus* (22), *Salmonella enterica* serovar Typhimurium (25), or *Listeria monocytogenes* (26). Using LEEI, a dose of 5 kGy was sufficient to inactivate *E. coli* DH5α from a pre-culture with an OD600 of 3.0 in PBS, reproducibly. Inactivation kinetics (log reduction and D_{10}) were not presented in the previous study using the petri dish system for irradiation (16). In the study shown here, the number of colony forming *E. coli* decreased linearly with increasing doses of low-energy accelerated electrons up to a dose of 2.8 kGy, which was sufficient to inhibit bacterial growth.

In a previously conducted study using high-energy accelerated electrons a dose of 7 kGy was required to prevent a defined titer of *E. coli* K12 from multiplication. It could be shown that the *E. coli* cells stayed metabolically active up to 9 days after irradiation, had intact membranes, and still supported propagation of bacteriophages (27). Another study investigated electron beam technology for food preservation and revealed that a dose of 1.0 kGy reduced the growth of *E coli* in nutrient broth by 3-4 log units (D_{10} = 0.27 kGy). No bacteria were detectable after an irradiation with 2 kGy of high-energy accelerated electrons (10 MeV). However, when grown on meat a dose of 1 kGy caused a reduction of only 2 log units (D_{10} = 0.47 kGy) (28).

The response of the foodborne contaminant *Staphylococcus aureus* towards low-dose gamma-rays as source of ionizing radiation was investigated as a decontamination technology for

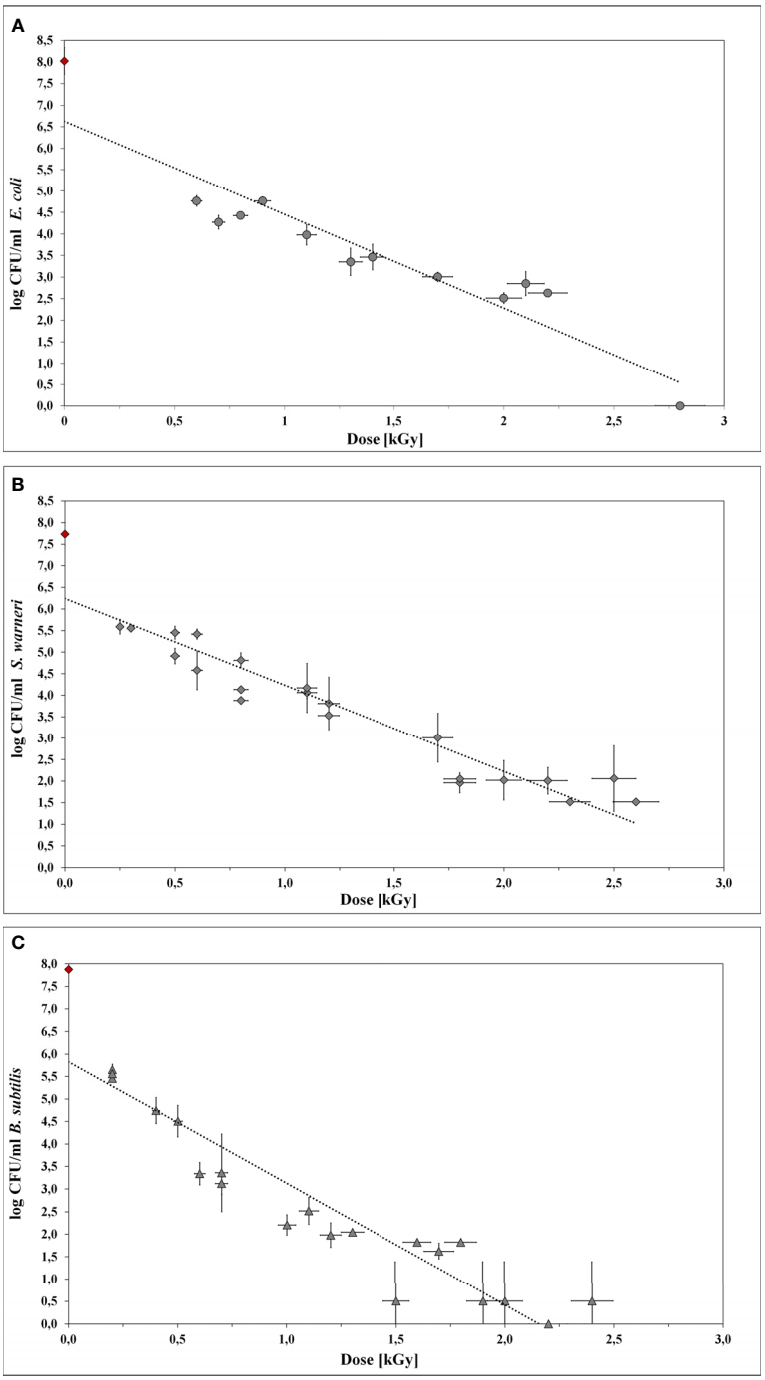

FIGURE 4 | Inactivation curves using LEEI. Each curve represents the mean values of at least three irradiated bacterial suspensions. The initial cell number of the pre-culture (indicated as red rhombus) was approx. 10^8 bacteria/ml. The starting total cell number for the experiments was 10^6 bacteria/ml. **(A)** *E coli.* **(B)** *S. warneri*. **(C)** Vegetative cells of *B. subtilis*.

food preservation (29). Therefore, frozen ham and cheese sandwiches were inoculated with *S. aureus*. Irradiation resulted in an average D_{10} value of 0.625 kGy, indicating that a dose of approximately 3 kGy would result in a 5 log reduction of *S. aureus* in sandwiches.

B subtilis and *B. cereus* spores were reduced to approximately 2 log units when a 10 MeV circular electron accelerator was used with 7.6 kGy (30). The corresponding D_{10} values were in the range of 1 to 4 kGy, which was in good accordance with data from gamma irradiation experiments. It has to be pointed out,

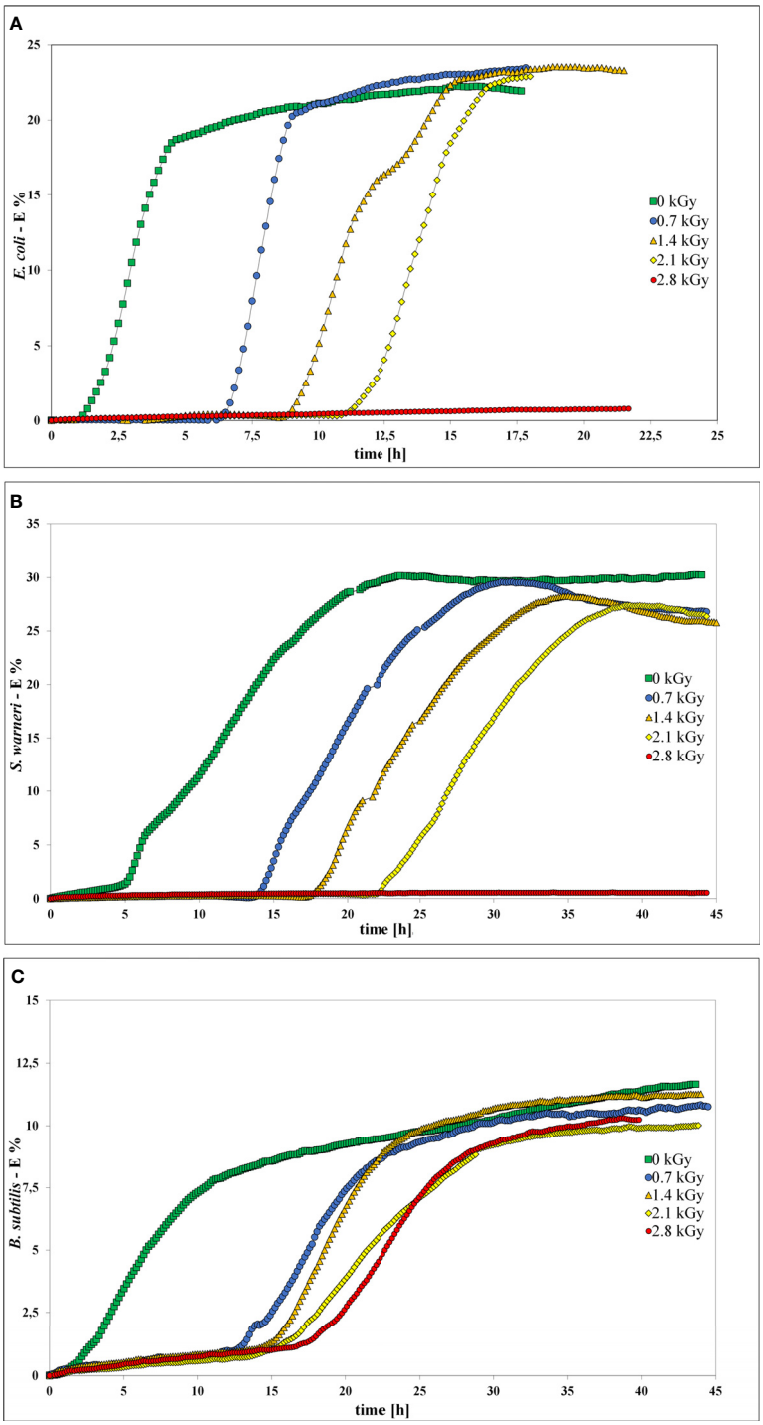

FIGURE 5 | Impedance spectra without (0 kGy, green rectangles) and after irradiation with at 0.7 kGy (blue circles), 1.4 kGy (orange triangles), 2.1 kGy (yellow rhombs), and 2.8 kGy (red rectangles). **(A)** *E. coli*. **(B)** *S. warneri*. **(C)** Vegetative cells of *B. subtilis*.

that in the study of De Lara and coworkers the environmental conditions, like the used type of growth medium, influenced the irradiation efficiency. A previous LEEI study demonstrated, that spore inactivation efficiency was dependent on different external factors, e.g. the sporulation medium used (31). Generally, bacterial spores are more resistant to irradiation than vegetative cells, except for a few very highly radiation-tolerant vegetative bacteria (31). For vegetative *Bacillus* species in

TABLE 3 | Influence of increasing dose values on the start of the exponential phase (start log-phase) given as mean value with the respective standard deviation (SD).

Applied Dose [kGy]	*E. coli*			*S. warneri*			*B. subtilis*		
	Start log-phase [h]	SD	Total IA	Start log-phase [h]	SD	Total IA	Start log-phase [h]	SD	Total IA
0	1.7	± 0.5	0	5.6	± 0.4	0	2.8	± 0.8	0
0.7	6.4	± 0.4	0	14.5	± 0.3	0	12.6	± 3.2	0
1.4	10.6	± 2.5	0	18.5	± 0.6	0	13.9	± 2.1	0
2.1	11.5	± 2.1	2	22.6	± 1.9	2	15.6	± 2.2	1
2.8	14.3	± 3.5	7	23.0	n. d.	8	18	± 5.8	3

The absolute number of complete inactivated bacterial samples is given (total IA). N. d., not determined.

suspension, as used in this LEEI study, there are hardly any data on their radiation sensitivity. 32 summarized some D_{10} values for vegetative *B. cereus* which were in the range of 0.30 to 0.65 kGy in phosphate buffer and 0.575 kGy on nutrition broth. The calculated D_{10} values from the *B. subtilis* used here ranged from 0.31 kGy to 0.37 kGy and the inactivation tests were only partially reproducible. This might indicate the presence of a sporulating sub-population. Similar to the environmental influences, the physiological state of the microorganisms, like their different bacterial growth stages, has a great impact on the subsequent LEEI results. *B. pumilus* spores have been widely used as biological indicator to proof the effect of gamma irradiation sterilization process (31, 33, 34). However, inactivation of *Bacillus* spores suspended in water with high-energy accelerated electrons was shown to be less effective than gamma irradiation (24). Summarizing, this excludes them from practical use as a bio-dosimeter for LEEI processes.

The underlying assumption is that ionizing radiation causes the inactivation of microorganisms by losing their ability to multiply. The mechanisms of radiation sensitivity are not yet completely understood and probably vary between different taxa, species, and even strains. Tolerance mechanisms can include effective DNA repair, compatible solutes, and mechanism to detoxify reactive oxygen species, as well as additional strategies to withstand unpredictable environmental changes (35). Radiation susceptibility of microorganisms is additionally affected by different factors such as medium composition, physiological state of the culture, temperature, gas atmosphere, and pH (32). The data set given in **Figure 4** reveals that growth inhibition by LEEI can reproducibly achieved under defined growth and irradiation conditions at room temperature and in air. However, it also points out a certain response variability of each bacterial species towards ionizing radiation.

Impedance Spectroscopy

Impedance spectroscopy is a rapid and non-invasive method to detect bacterial cells by measuring the change of the electric conductivity. In this study, impedance was used to investigate the response of bacteria to irradiation with low-energy accelerated electrons. *E. coli*, *S. warneri*, and *B. subtilis* showed a delay in growth and the exponential growth phase was entered more slowly with increasing dose. The capability to multiply was affected by an increasing LEEI dose and less surviving (or non-multiplying) bacterial cells remained. This finding was very pronounced in *E. coli* and *S. warneri*, but less evident in *B. subtilis*. Irradiation of *E. coli* and *S. warneri* with 2.8 kGy lead to complete inactivation by inhibition of growth. These results were in good accordance with the inactivation dose experimentally determined by the investigation of the inactivation curves (2.8 kGy). For *B subtilis* growth inhibition was incomplete, which is in accordance with the results from the inactivation kinetics. Although vegetative cells were utilized, a sporulating sub-population may be present, which could explain the inconsistency in determining the inactivation dose.

Impedance spectroscopy has been performed for various applications in microbiology to monitor growth or responses towards environmental changes. To the best of our knowledge, this is the first time that impedance spectroscopy has been successfully used as a method to describe the bacterial response towards irradiation with low-energy accelerated electrons. Whether the irradiated and inactivated bacterial cells have lost their ability to divide, but still show metabolic activity, is yet to be clarified. To investigate the influence of LEEI on the biochemical pathways and gene expression, advanced molecular studies need to be conducted.

CONCLUSION

The aim of the study was to verify the suitability of bacterial suspension as bio-dosimeter for LEEI at a dose below 6.5 kGy. The research results demonstrate that LEEI has the potential to replicable inactivate bacteria at doses below 6.5 kGy. The D_{10} values for *E. coli* and *S. warneri* were determined. However, under the given experimental conditions, vegetative cells of *B. subtilis* were not consistent in their response. Therefore, the applicability as reliable dose indicator is currently still uncertain. A workflow standardization in terms of cultivation and irradiation could overcome these hurdles. The bio-dosimeter could be a promising tool to monitor dynamic LEEI processes within fluids, e.g. LEEI-supported biotechnological processes within a bioreactor.

DATA AVAILABILITY STATEMENT

The original contributions presented in the study are included in the article. Further inquiries can be directed to the corresponding author.

AUTHOR CONTRIBUTIONS

SS, GG, and UK designed the study. MD, SG, and LK performed the experiments. SS, GG, and UK interpreted the data. SS wrote the manuscript. All authors contributed to the article and approved the submitted version.

ACKNOWLEDGMENTS

We thank Sebastian Petzold and Jana Beckmann for their excellent support in laboratory work and Andre´ Poremba for the operation of the Fraunhofer FEP low-energy E-beam facility REAMODE and for excellent technical support on routine dosimetry.

REFERENCES

1. Gotzmann G, Portillo J, Wronski S, Kohl Y, Gorjup E, Schuck H, et al. Low-Energy Electron-Beam Treatment as Alternative for on-Site Sterilization of Highly Functionalized Medical Products – A Feasibility Study. *Radiat Phys Chem* (2018) 150:9–19. doi: 10.1016/j.radphyschem.2018.04.008
2. Hertwig C, Meneses N, Mathys A. Cold Atmospheric Pressure Plasma and Low Energy Electron Beam as Alternative Nonthermal Decontamination Technologies for Dry Food Surfaces: A Review. *Trends Food Sci Technol* (2018) 77:131–42. doi: 10.1016/j.tifs.2018.05.011
3. Pillai SD, Shayanfar S. "Electron Beam Technology and Other Irradiation Technology Applications in the Food Industry". In: M Venturi and M D'Angelantonio, editors. *Applications of Radiation Chemistry in the Fields of Industry, Biotechnology and Environment*. Cham: Springer (2017). doi:: 10.1007/978-3-319-54145-7_9
4. Zhang Y, Huber N, Moeller R, Stülke J, Dubovcova B, Akepsimaidis G, et al. Role of DNA Repair in *Bacillus Subtilis* Spore Resistance to High Energy and Low Energy Electron Beam Treatments. *Food Microbiol* (2020) 87:103353. doi: 10.1016/j.fm.2019.103353
5. Deutsches Institut für Normung/ International Organization for Standardization. (2020). Sterilization of Health Care Products - Radiation - Part 1: Requirements for Development, Validation and Control of a Sterilization Process for Medical Devices (DIN/ISO Standard No. 11137-1:2020-04). Beuth Verlag, Berlin.
6. Bayer L, Fertey J, Ulbert S, Grunwald T. Immunization With an Adjuvanted Low-Energy Electron Irradiation Inactivated Respiratory Syncytial Virus Vaccine Shows Immunoprotective Activity in Mice. *Vaccine* (2018) 36:1561–9. doi: 10.1016/j.vaccine.2018.02.014
7. Thabet A, Schmäschke R, Fertey J, Bangoura B, Schönfelder J, Lendner M, et al. *Eimeria Tenella* Oocysts Attenuated by Low Energy Electron Irradiation (LEEI) Induce Protection Against Challenge Infection in Chickens. *Vet Parasitol* (2019) 266:18–26. doi: 10.1016/j.vetpar.2019.01.001
8. Fertey J, Thoma M, Beckmann J, Bayer L, Finkensieper J, Reißhauer S, et al. Automated Application of Low Energy Electron Irradiation Enables Inactivation of Pathogen- and Cell-Containing Liquids in Biomedical Research and Production Facilities. *Sci Rep* (2020) 10:50. doi: 10.1038/s41598-020-69347-7
9. Tallentire A, Miller A, Helt-Hansen J. A Comparison of the Microbicidal Effectiveness of Gamma Rays and High and Low Energy Electron Radiations. *Radiat Phys Chem* (2010) 79:701–4. doi: 10.1016/j.radphyschem.2010.01.010
10. Urgiles E, Wilcox J, Montes O, Osman S, Venkateswaran K, Cepeda M, et al. Electron Beam Irradiation for Microbial Reduction on Spacecraft Components. *IEEE Aerosp Conf* (2007) 4:1–15. doi: 10.1109/AERO.2007.352739
11. Rögner FH, Wetzel C, Röder O, Gotzmann G. Sterilization of Surgical Instruments Using Mini Electron Accelerators. In: *52nd Annual Technical Conference Proceedings, Society of Vacuum Coaters*. Santa Clara, CA (2009).
12. Helt-Hansen J, Miller A, Sharpe P, Laurell B, Weiss D, Pageau G. Dμ - A New Concept in Industrial Low-Energy Electron Dosimetry. *Radiat Phys Chem* (2010) 79:66–74. doi: 10.1016/j.radphyschem.2009.09.002
13. Riley PA. Free Radicals in Biology: Oxidative Stress and the Effects of Ionizing Radiation. *Int J Radiat Biol* (1994) 65:27–33. doi: 10.1080/09553009414550041
14. Hammad AA. Microbiological Aspects of Radiation Sterilization. In: *Trends in Radiation Sterilization of Health Care Products*, vol. 2008. Vienna: International Atomic Energy Agency (2008).
15. Fan X, Sokorai K, Weidauer A, Gotzmann G, Rögner F-H, Koch E. Comparison of Gamma and Electron Beam Irradiation in Reducing Populations of *E. Coli* Artificially Inoculated on Mung Bean, Clover and Fenugreek Seeds, and Affecting Germination and Growth of Seeds. *Radiat Phys Chem* (2017) 130:306–15. doi: 10.1016/j.radphyschem.2016.09.015
16. Fertey J, Bayer L, Grunwald T, Pohl A, Beckmann J, Gotzmann G, et al. Pathogens Inactivated by Low-Energy-Electron Irradiation Maintain Antigenic Properties and Induce Protective Immune Responses. *Viruses* (2016) 8:319. doi: 10.3390/v8110319
17. Gotzmann G, Beckmann J, Wetzel C, Scholz B, Herrmann U, Neunzehn J. Electron-Beam Modification of DLC Coatings for Biomedical Applications. *Surf Coat Technol* (2017) 311:248–56. doi: 10.1016/j.surfcoat.2016.12.080
18. International Organization for Standardization/ASTM. (2013). Practice for Use of the Alanine-EPR Dosimetry System (ISO Standard No. 51607:2013-06). Geneva, Switzerland.
19. Miller A, Batsberg W, Karman W. A New Radio-Chromic Thin-Film Dosimeter. *Radiat Phys Chem* (1988) 31:491–6. doi: 10.1016/1359-0197(88)90216-0
20. Sharpe P, Miller A. Guidelines for the Calibration of Routine Dosimetry Systems for Use in Radiation Processing. *NPL Rep CIRM* (2009) 29:1–19.
21. Abdel-Fattah AA, Miller A. Temperature, Humidity and Time. Combined Effects on Radiochromic Film Dosimeters. *Radiat Phys Chem* (1996) 47:611–21. doi: 10.1016/0969-806X(95)00037-X
22. Fertey J, Bayer L, Kähl S, Haji RM, Burger-Kentischer A, Thoma M, et al. Low-Energy Electron Irradiation Efficiently Inactivates the Gram-Negative Pathogen *Rodentibacter Pneumotropicus*-A New Method for the Generation of Bacterial Vaccines With Increased Efficacy. *Vaccines* (2020) 8:1-11. doi: 10.3390/vaccines8010113
23. Bhatia SS, Pillai SD. A Comparative Analysis of the Metabolomic Response of Electron Beam Inactivated *E. Coli* O26:H11 and *Salmonella Typhimurium* ATCC 13311. *Front Microbiol* (2019) 10:694. doi: 10.3389/fmicb.2019.00694
24. Pribil W, Gehringer P, Eschweiler H, Cabaj A, Haider T, Sommer R. Assessment of Bacillus Subtilis Spores as a Possible Bioindicator for Evaluation of the Microbicidal Efficacy of Radiation Processing of Water. *Water Environ Res* (2007) 79:720–4. doi: 10.2175/106143007x175889
25. Praveen C, Bhatia SS, Alaniz RC, Droleskey RE, Cohen ND, Jesudhasan PR, et al. Assessment of Microbiological Correlates and Immunostimulatory Potential of Electron Beam Inactivated Metabolically Active Yet Non Culturable (MAyNC) *Salmonella Typhimurium*. *PloS One* (2021) 16: e0243417. doi: 10.1371/journal.pone.0243417
26. Mintier AM, Foley DM. Electron Beam and Gamma Irradiation Effectively Reduce *Listeria Monocytogenes* Populations on Chopped Romaine Lettuce. *J Food Prot* (2006) 69:570–4. doi: 10.4315/0362-028x-69.3.570
27. Hieke A-SC, Pillai SD. *Escherichia Coli* Cells Exposed to Lethal Doses of Electron Beam Irradiation Retain Their Ability to Propagate Bacteriophages and Are Metabolically Active. *Front Microbiol* (2018) 9:2138. doi: 10.3389/fmicb.2018.02138
28. Mayer-Miebach E, Stahl MR, Eschrig U, Deniaud L, Ehlermann DAE, Schuchmann HP. Inactivation of a Non-Pathogenic Strain of *E. Coli* by Ionising Radiation. *Food Control* (2005) 16:701–5. doi: 10.1016/j.foodcont.2004.06.007
29. Lamb JL, Gogley JM, Thompson MJ, Solis DR, Sen S. Effect of Low-Dose Gamma Irradiation on *Staphylococcus Aureus* and Product Packaging in Ready-to-Eat Ham and Cheese Sandwiches. *J Food Prot* (2002) 65:1800–5. doi: 10.4315/0362-028x-65.11.1800
30. De Lara J, Fernandez PS, Periago PM, Palop A. Irradiation of Spores of *Bacillus Cereus* and *Bacillus Subtilis* With Electron Beams. *Innov Food Sci Emerg Technol* (2002) 3:379–84. doi: 10.1016/S1466-8564(02)00053-X
31. Zhang Y, Moeller R, Tran S, Dubovcova B, Akepsimaidis G, Meneses N, et al. *Geobacillus* and *Bacillus* Spore Inactivation by Low Energy Electron Beam Technology: Resistance and Influencing Factors. *Front Microbiol* (2018) 9:2720. doi: 10.3389/fmicb.2018.02720
32. Monk DJ, Beuchat LR, Doyle MP. Irradiation Inactivation of Food-Borne Microorganisms. *J Food Prot* (1994) 58:197–208. doi: 10.4315/0362-028X-58.2.197

33. Prince HN. Stability of *Bacillus Pumilus* Spore Strips Used for Monitoring Radiation Sterilization. *Appl Environ Microbiol* (1976) 31:999–1000. doi: 10.1128/aem.31.6.999-1000.1976
34. Ha TMH, Yong D, Lee EMY, Kumar P, Lee YK, Zhou W. Activation and Inactivation of *Bacillus Pumilus* Spores by Kiloelectron Volt X-Ray Irradiation. *PloS One* (2017) 12(5):e0177571. doi: 10.1371/journal.pone.0177571
35. Koschnitzki D, Moeller R, Leuko S, Przybyla B, Beblo-Vranesevic K, Wirth R, et al. Questioning the Radiation Limits of Life: *Ignicoccus Hospitalis* Between Replication and VBNC. *Arch Microbiol* (2021) 203:1299–308. doi: 10.1007/s00203-020-02125-1

Conflict of Interest: The authors declare that the research was conducted in the absence of any commercial or financial relationships that could be construed as a potential conflict of interest.

Publisher's Note: All claims expressed in this article are solely those of the authors and do not necessarily represent those of their affiliated organizations, or those of the publisher, the editors and the reviewers. Any product that may be evaluated in this article, or claim that may be made by its manufacturer, is not guaranteed or endorsed by the publisher.

frontiers | Frontiers in Immunology

ORIGINAL RESEARCH
published: 13 May 2022
doi: 10.3389/fimmu.2022.852091

Low Dose Gamma Irradiation of *Trypanosoma evansi* Parasites Identifies Molecular Changes That Occur to Repair Radiation Damage and Gene Transcripts That May Be Involved in Establishing Disease in Mice Post-Irradiation

Richard T. Kangethe[1], Eva M. Winger[1], Tirumala Bharani K. Settypalli[1], Sneha Datta[1†], Viskam Wijewardana[1], Charles E. Lamien[1], Hermann Unger[1], Theresa H.T. Coetzer[2], Giovanni Cattoli[1] and Adama Diallo[1,3‡]*

[1] Animal Production and Health Laboratory, FAO/IAEA Agriculture and Biotechnology Laboratory, IAEA Laboratories Seibersdorf, International Atomic Energy Agency (IAEA), Vienna, Austria, [2] Biochemistry, School of Life Sciences, University of KwaZulu-Natal, Pietermaritzburg, South Africa, [3] UMR CIRAD INRA, Animal, Santé, Territoires, Risques et Ecosystèmes (ASTRE), Montpellier, France

The protozoan parasite *Trypanosoma evansi* is responsible for causing surra in a variety of mammalian hosts and is spread by many vectors over a wide geographical area making it an ideal target for irradiation as a tool to study the initial events that occur during infection. Parasites irradiated at the representative doses 100Gy, 140Gy, and 200Gy were used to inoculate BALB/c mice revealing that parasites irradiated at 200Gy were unable to establish disease in all mice. Cytokine analysis of mice inoculated with 200Gy of irradiated parasites showed significantly lower levels of interleukins when compared to mice inoculated with non-irradiated and 100Gy irradiated parasites. Irradiation also differentially affected the abundance of gene transcripts in a dose-dependent trend measured at 6- and 20-hours post-irradiation with 234, 325, and 484 gene transcripts affected 6 hours post-irradiation for 100Gy-, 140Gy- and 200Gy-irradiated parasites, respectively. At 20 hours post-irradiation, 422, 381, and 457 gene transcripts were affected by irradiation at 100Gy, 140Gy, and 200Gy, respectively. A gene ontology (GO) term analysis was carried out for the three representative doses at 6 hours and 20 hours post-irradiation revealing different processes occurring at 20 hours when compared to 6 hours for 100Gy irradiation. The top ten most significant processes had a negative Z score. These processes fall in significance at 140Gy and even further at 200Gy, revealing that they were least likely to occur at 200Gy, and thus may have been responsible for infection in mice by 100Gy and 140Gy irradiated parasites. When looking at 100Gy irradiated parasites 20 hours post-irradiation processes with a positive Z score, we identified genes that were involved in multiple processes and compared their fold change

OPEN ACCESS

Edited by:
Yasuyuki Goto, The University of Tokyo, Japan

Reviewed by:
Ana Paula Cabral Araujo Lima, Federal University of Rio de Janeiro, Brazil
Mariana Waghabi, Instituto Oswaldo Cruz (FIOCRUZ), Brazil

***Correspondence:**
Richard T. Kangethe
R.T.Kangethe@iaea.org

†ORCID:
Sneha Datta
orcid.org/0000-0003-4201-3822

‡Present Address:
Adama Diallo, Laboratoire National d'Elevage et de Recherches Vétérinaires, Institut Sénégalais de Recherches Agricoles (ISRA), Dakar, Senegal

Specialty section:
This article was submitted to Vaccines and Molecular Therapeutics, a section of the journal Frontiers in Immunology

Received: *10 January 2022*
Accepted: *11 April 2022*
Published: *13 May 2022*

Citation:
Kangethe RT, Winger EM, Settypalli TBK, Datta S, Wijewardana V, Lamien CE, Unger H, Coetzer THT, Cattoli G and Diallo A (2022) Low Dose Gamma Irradiation of Trypanosoma evansi Parasites Identifies Molecular Changes That Occur to Repair Radiation Damage and Gene Transcripts That May Be Involved in Establishing Disease in Mice Post-Irradiation. Front. Immunol. 13:852091. doi: 10.3389/fimmu.2022.852091

values at 6 hours and 20 hours. We present these genes as possibly necessary for repair from irradiation damage at 6 hours and suggestive of being involved in the establishment of disease in mice at 20 hours post-irradiation. A potential strategy using this information to develop a whole parasite vaccine is also postulated.

Keywords: *Trypanosoma evansi*, gamma irradiation, TryMS array, vaccine, surra

INTRODUCTION

Trypanosoma evansi, a mechanically transmitted haemoparasitic flagellate from the genus *Trypanosoma*, is geographically the most widely dispersed member of the group and is found in Asia, South America, the Middle East, and Africa, with occasional outbreaks in parts of Europe (1). *T. evansi* has a wide host range and infects many animal species causing Surra in cattle, buffalo, pigs, and donkeys amongst other domesticated animals and is a significant cause of morbidity and mortality in camel populations (1–5). Zoonotic cases have also been reported in humans and are referred to as atypical human trypanosomosis (a-HT) (6). Some a-HT infections were found in individuals that have a fully functional apolipoprotein L1 (ApoL1), the serum lytic factor that prevents African Animal Trypanosomosis (AAT) in humans, suggesting that the parasite is capable of employing other mechanisms that are yet to be elucidated for survival in the human host (7–9). *Trypanosoma evansi* parasites are transmitted by blood sucking flies, which in addition to the tsetse fly, include the horsefly, stable fly, horn fly, and deerfly (*Tabanus* and *Stomoxys* spp.) and by vampire bats in South America (10–12). Infection occurs when an infected fly, a temporary host with parasite contaminated mouthparts, is able to feed on several uninfected mammalian hosts thus quickly establishing disease. The combination of having multiple host animals and a wide range of mechanical vectors has enabled the parasite to spread out of tsetse-infected areas onto four different continents (13, 14).

The symptoms associated with *T. evansi* infections differ depending on the susceptibility of the infected host and include anemia, fever, loss of weight and productivity, as well as abortion (15–17). Like all other extracellular parasites in the genus, *T. evansi* primarily evades mammalian host immunity by switching its variable surface glycoprotein (VSG). At the onset of the infection, initial VSG-induced Th1 responses are followed by T cell exhaustion, altered antigen presentation, defective complement activation and eventually the destruction of the bone marrow, marginal zone, and follicular B cell populations, thus eliminating B cell memory and making the host vulnerable to other secondary diseases (9, 18–21). Vaccinated pigs and water buffalos perform poorly against already vaccinated diseases after acquiring *T. evansi* infections (9, 21). All of these combined factors have hindered the development of potential vaccines against all trypanosome species to date.

There is experimental evidence to show that some animals can undergo self-cure from *T. evansi* infection, an event that is accompanied by qualitative and quantitative changes to their lymphocyte populations (22–24). Studies in buffalo in Indonesia have also shown that in some naturally infected animals, there is a long-term development of immunity that could be enhanced by the use of suitable vaccination methods (25). Approaches to trypanosome vaccine research have included using recombinant subunit targets as antigens. Structural recombinant antigens studied include tubulin, the GPI anchor of VSG, and more recently, an invariant flagellum antigen protein that was successful in mice but with no further developments for affected livestock (26–30). Other promising antigens developed include different Trypanosome proteases as 'anti-disease' targets that alleviate symptoms rather than neutralizing the parasite, but difficulties were encountered in the field due to their complex chemistries (31–36).

Initial studies using irradiation as a tool for developing trypanosome vaccines were made in the early 1970s by destroying the parasite with high irradiation doses of up to 1000Gy (37). Animals inoculated with irradiated parasites developed good humoral immune responses against VSG and were protected against homologous trypanosome challenge but not heterologous variants (37–45). The irradiation doses used were however lethal to the parasite and much higher than those used by current related irradiated parasite vaccines. Previous attempts to develop trypanosome vaccines with irradiation were made using 600Gy, a dose that is four times higher than what had been successful in the development of an irradiated plasmodium vaccine at 150Gy (46). For the non-dividing but metabolically active Schistosoma irradiated vaccine, the effective dose used was between 200- and 500Gy (47). Other studies that measure the effect of using irradiation on the trypanosome spp. have been carried out on *T. cruzi* due to its high tolerance to high doses of irradiation of up to 1500Gy (48–50). Successful developments in malaria have also demonstrated the feasibility of utilizing irradiation as a technique for developing vaccines (46, 51–53). Other potential irradiated parasite vaccines include those for schistosomiasis (47, 54), parasitic bronchitis caused by *dictyocaulus* spp. (55, 56) and Babesia (55, 56).

Following the success of malaria and other parasite irradiated vaccines, we hypothesized that irradiated, metabolically active, but non-replicating parasites could be used as a vaccine. To this end, *T. evansi* was chosen as the representative parasite due to its wide geographical host and vector range with little developmental differences between the vector and mammalian parasite forms. The possibility of restricted strain diversity and the transient nature of infection with *T. evansi* in different transmission vectors, implies that the mechanisms for infection used by the parasite would be universal for all trypanosome spp. Parasites were irradiated at different doses ranging from 100 - 250Gy so that they were temporarily unable to multiply but still

capable of synthesizing many of the proteins that could potentially help the parasite establish disease in mice. Irradiated *T. evansi* parasites were subsequently observed *in vitro* before inoculation and challenge of mice. Doses that produced living and non-infectious parasites were then studied using a whole transcript gene microarray and compared to that of infectious parasites. Data was analyzed to identify genes and processes that are responsible for radiation damage repair and may possibly be involved in enabling the parasites to establish an infection in the mammalian host after recovery.

METHODS

Trypanosome Culture

Bloodstream forms of *T. evansi* RoTat 1.2 wild-type parasites obtained from the Institute of Tropical Medicine, Antwerp, Belgium were isolated in 1982 from a buffalo in Indonesia (ITMAS #020298) . Parasites were cultured in supplemented Iscove's Modified Dulbecco's Medium (IMDM) as previously described (57). Briefly, 1 liter of IMDM containing 3.6 mM $NaHCO_3$ (Thermo Fischer Scientific, Roskilde, Denmark) was supplemented with 1 mM hypoxanthine, 1 mM sodium pyruvate, 0.16 mM thymidine, 0.05 mM bathocuprone sulfate, 1.0 mM L-cysteine and 0.2 mM 2-mercaptoethanol). The pH was adjusted between 7.2 and 7.4 and 10% (v/v) heat inactivated fetal calf serum (Gibco, Paisley, UK) was added before filtration using a 0.2 μm filter. Parasites were seeded at 2 x 10^5 and regularly split at mid logarithmic growth phase. Bloodstream forms of *T. evansi* Can 86K were also obtained from the Institute of Tropical Medicine and were isolated in 1986 from a dog in Brazil (ITMAS #140799B) and used for heterologous challenge studies (58).

Trypanosome Irradiation Parameters

Bloodstream forms of *T. evansi* RoTat 1.2 wild-type parasites (1x10^6 mid log phase) were resuspended in complete IMDM in a 50 mL conical tube filled to the top with no air bubbles and put on ice. Parafilm was used to avoid spillage and contamination. Parasites on ice were then placed in the Gamma irradiator and exposed to the Cobalt 60 source for the calculated length of time it took to deliver the desired dose (Model 812 Co-60 irradiator, Foss Therapy Services, Inc., California, USA). Initial doses ranging from 100Gy to 600Gy were carried out and later on restricted to 100Gy - 250Gy with 20Gy intervals. Irradiated parasites were then pelleted and finally resuspended at 2x10^5 parasites per ml with 1 ml dispensed per well in a 24 well flat-bottomed culture plate and *in vitro* growth was observed. Initial doses of 100Gy, 120Gy, 140Gy, 160Gy, 180Gy, 200Gy, and 250Gy were applied to identify the D10 dose value which is the dose required to reduce parasite load by 90% or 1 log, (59).

Cell Proliferation Assay

Bloodstream forms of *T. evansi* RoTat 1.2 wild-type parasites (1x10^7 mid log phase) were pelleted and re-suspended in 1 mL IMDM containing 5% (v/v) FCS. A volume of 1.1 μL of CFSE stock solution (5 mM 5(6)-Carboxyfluorescein diacetate N-succinimidyl ester; Sigma Aldrich, St. Louis, MO, USA) was mixed with 110 μL of PBS and added to the parasites before gently mixing by inverting the tube. Parasites were incubated with CFSE at 37°C for 5 minutes with gentle mixing 3 to 4 times. The CFSE-labelled parasites were then resuspended in 10 mL IMDM and washed three times with IMDM to remove excess CFSE dye before transfer to a 50 mL conical tube filled to the top with IMDM and used for irradiation at the desired dose on ice. Irradiated CFSE-labelled parasites were then pelleted and finally resuspended at 2x10^5/mL with 1 mL dispensed per well in a 24 well flat-bottomed plate. Cell proliferation was measured using flow cytometry immediately after staining and every 24 hours until the culture was overgrown or had stopped dividing. Flow cytometry data were acquired using the Gallios flow cytometer (Beckman Coulter, USA) and analyzed with Kaluza software (Beckman Coulter, USA). Cell populations were gated by forward and side-light scatter parameters, as shown in **Supplementary Figure 1**.

Mouse Infections

In order to observe what role irradiation plays in *T. evansi* virulence and infection, four groups of 8-week-old BALB/c female mice (8 per irradiation dose) were inoculated twice by intraperitoneal injection using an insulin syringe with 1 ×10^4 *T. evansi* RoTat 1.2 irradiated parasites per mouse resuspended in 50 μl of phosphate buffered saline (PBS). A control group was also infected with 1 × 10^4 *T. evansi* RoTat 1.2 wild type non-irradiated parasites along with a second challenge control group that received 50 μl PBS alone. The two inoculations were carried out at day 0 and day 14. On day 28 post inoculation, surviving mice were challenged with heterologous 1 × 10^3 *T. evansi* Can 86K. A parallel experiment where mice were challenged with homologous 1 × 10^3 *T. evansi* RoTat 1.2 wild type non-irradiated parasites was also performed. Parasitemia was measured on alternative days by bleeding from the tail and the survival and wellbeing of the mice was monitored. Parasite load was estimated in each inoculated mouse using the rapid matching method as previously described (60). Blood samples measured for parasitemia were blinded to the readers. Plasma samples were also collected from the different groups of mice using heparinized capillary tubes over the course of infection and stored at -80°C for further cytokine analysis. Mice were sourced and housed at the University of Veterinary Medicine in Vienna. Infection and care of the infected mice was carried out using protocols approved by the institutional ethics committee of the University of Veterinary Medicine, Vienna, and the national authority according to § 26 of the Austrian Law for Animal Experiments, Tierversuchsgesetz 2012-TVG 2012 under the No. GZ 68.205/0069-WF/II/3b/2014.

Mouse Bio-Plex Cytokine Assay

A custom 10-plex cytokine assay (Bio-Plex: Bio-Rad, Hercules, USA) was used to quantify the plasma levels of 10 cytokines in mouse (Mo) plasma [interferon-gamma (IFN-γ), tumor necrosis factor-alpha (TNF-α), interleukin-1 alpha (IL-1α), IL-1β, IL-4, IL-6, IL-10, IL-12 (p40), IL-12 (p70) and IL-13] as described by

the manufacturer. Briefly, a 1 in 4 dilution of plasma collected from the different groups of mice during inoculation (days 0 to 28) was incubated with beads coupled to monoclonal antibodies specific for each component of the cytokine panel. Samples were washed before adding detection antibodies and developed for reading using the Bio-Plex® 200 suspension array system. Absolute interleukin concentrations were calculated using Bio-Plex Manager™ software and samples were analysed using a one-way ANOVA with Dunn's Multiple Comparison Test in GraphPad Prism 5 for each cytokine. Boxplots were generated using ggplot2 package in R (61).

Trypanosome spp. Whole Transcript Gene Array Design (TrypMS)

A custom *Trypanosome* spp. array that covers the genomes of three trypanosome species, *T. brucei*, *T. evansi* and *T. congolense* was designed by Affymetrix (Santa Clara, California, USA) with input from the authors. Briefly, an expression/tilling array request form for TrypMS (Trypanosoma multi species) was completed describing features desired according to the Affymetrix MyGeneChip™ design guide. The request was sent to the design team along with four Trypanosome genomes (*T. brucei Lister 427, T. brucei TREU 927, T. evansi STIB 805* and *T. congolense IL3000*). All genomes were downloaded from the TriTrypDB datadase (https://tritrypdb.org/tritrypdb/app; accessed on 29.10.2014). A proposal was then prepared by Affymetrix and confirmed. The final array designed contained the fully sequenced *T. brucei* genome as a backbone with selected *T. evansi* and *T. congolense* sequences that do not overlap with the *T. brucei* genome. Approximately 94.9% of *T. evansi* genome is identical to the reference *T. brucei* genome (62). A total of on average 9,300 whole gene transcripts from all three species were targeted with most having 8 to 25 probe pairs per gene. The array was produced using the 16 sample arrays per plate format. Microarray data produced from this experiment is available in the ArrayExpress database (http://www.ebi.ac.uk/arrayexpress) under accession number E-MTAB-11705.

Measurements of RNA Abundance Using the Affymetrix® Whole Transcript Array TrypMS

In order to characterize irradiated parasites, RNA extracted from three or more replicates each at 1, 6, and 20 hours after irradiation at the different indicated doses (0, 100, 140, 200, and 250Gy) was used for hybridisation onto the TrypMS array. RNA extraction was carried out using a RNeasy kit (Qiagen, Hilden, Germany). Extracted RNA was then processed through several amplification cycles, including first-strand cDNA synthesis using a poly dT primer, second-strand cDNA synthesis, *in-vitro* cRNA (copy RNA) synthesis, and final second-cycle single strand cDNA synthesis using GeneChip™ WT PLUS reagent kit by Affymetrix. Single strand cDNA generated was fragmented, labelled, and hybridized to the *Trypanosome* spp. whole transcript array before processing using the Gene Titan® Multi-Channel (MC) instrument from Affymetrix. Intensity CEL files generated after hybridisation and scanning were analysed using Affymetrix® Expression console software and files that passed all quality control parameters were converted into CHIP files that were subsequently interpreted using Affymetrix® Transcriptome Analysis Console (TAC3) Software. Lists of genes were prepared using *T. brucei* annotation with figures on fold change (FC), ANOVA *p-value* and false discovery rate (FDR) adjusted *p-value* assigned to each gene described.

Gene Ontology Analysis

Gene transcript abundance affected by irradiation at different doses after 6 hours and 20 hours were used to query TriTrypDB for gene ontology (GO) enrichment data (63). GO enrichment terms identified were used together with fold changes calculated from the TrypMS array to calculate a Z score using tools from GOplot on R (64). The Z score is a value that indicates whether the GO term associated with a set of genes [biological process (BP)/ molecular function (MF)/cellular components (CC)] is more likely to be decreased or increased and is calculated as $Z = (up - down)/SQRT(Total)$ where *up* and *down* are the number of assigned transcripts up-regulated (logFC > 0) or down- regulated (logFC < 0) in the data set, divided by the square root of the total number of genes associated with the identified GO term. Calculated Z scores versus -log adj *p* values were used to make combined bubble plots (with BP, MF and CC) for 100Gy, 140Gy, and 200Gy at 6 hours and 20 hours post-irradiation. A GO circle plot for the top 10 GO enrichment terms with the most significant *p* values was also plotted for 100Gy at 6 hours and 20 hours. GO chord plots that display the relationship between genes and GO terms was plotted for the ten most significant terms for 100Gy at 20 hours. Gene ontology analysis and visualization was performed using customized python codes and the GO plot manual (http://wencke.github.io/).

Confirmatory Quantitative PCR

Total RNA previously harvested from parasites 1, 6, or 20 hours after irradiation was used to generate copy DNA (cDNA) using random hexamer primers and a Superscript II reverse transcriptase kit (Invitrogen). The synthesized cDNA was used as a template for confirming fold-changes for 17 downregulated and 5 upregulated gene transcripts previously identified using the TrypMS array by relative quantification using TERT as an internal control as previously described (65). The primer sequences used for amplification are listed in **Supplementary Table 1**.

RESULTS

In Vitro and *In Vivo T. evansi* RoTat 1.2 Irradiated Parasite Dynamics

Our initial experiments were carried out to determine the doses at which *T. evansi* parasites survive irradiation but are rendered non-infectious in a mouse infection model. Parasites irradiated at doses above 200Gy did not survive post-irradiation and no cultures were viable after approximately 3 days when irradiated at 250Gy and on average 24 h at 600Gy (**Figure 1**). Less than 10%

TABLE 1 | A comparison of gene transcripts across different doses and time.

Comparison	Down	Up	Total
200Gy (1h vs 6h)	223	261	484
200Gy (1h vs 20h)	179	278	457
100Gy (1h vs 20h)	141	281	422
140Gy (1h vs 20h)	122	259	381
1h vs 20h (all doses)	110	234	344
140Gy (1h vs 6h)	141	184	325
1h vs 6h (all doses)	109	138	247
100Gy (1h vs 6h)	100	134	234
200Gy vs 250Gy	125	71	196
0Gy vs 200Gy	28	134	162
140Gy vs 250Gy	84	57	141
100Gy vs 250Gy	85	46	131
140Gy (6h vs 20h)	3	128	131
0Gy vs140Gy	22	96	118
6h vs 20h	2	114	116
100Gy (6h vs 20h)	4	108	112
200Gy (6h vs 20h)	6	97	103
0Gy vs100Gy	10	85	95
100Gy vs 200Gy	0	47	47
6h (100Gy vs 200Gy)	0	46	46
140Gy vs 200Gy	0	33	33
0Gy vs 250Gy	6	22	28
1h (0 vs 250Gy)	6	22	28
1h (0 vs 200Gy)	8	15	23
20h (100Gy vs 200Gy)	0	18	18
1h (100Gy vs 250Gy)	2	11	13
6h (140Gy vs 200Gy)	0	8	8
1h (140Gy vs 250Gy	1	6	7
1h (0 vs140Gy)	2	4	6
1h (0 vs 100Gy)	2	3	5
1h (100Gy vs 200Gy)	2	2	4
100Gy vs 140Gy	0	4	4
20h (100Gy vs140Gy)	0	3	3
1h (140Gy vs 200Gy)	1	1	2
1h (100Gy vs 140Gy)	1	0	1
20h (140Gy vs 200Gy)	0	1	1
6h (100Gy vs 140Gy)	0	1	1
1h (200Gy vs 250Gy)	0	0	0
Interaction (1h and 6h vs 100Gy and 200Gy)	47	5	52
Interaction (1h and 20h vs 100Gy and 200Gy	22	6	28
Interaction (6h and 20h vs 100Gy and 200Gy)	8	10	18
Interaction (1h and 6h vs 140Gy and 200Gy)	14	1	15
Interaction (1h and 20h vs 100Gy and 140Gy)	7	4	11
Interaction (1h and 6h vs 100Gy and 140Gy)	9	1	10
Interaction (6h and 20h vs 140Gy and 200Gy)	2	4	6
Interaction (6 and 20 vs 100Gy and 140Gy)	2	2	4
Interaction (1 and 20 vs 140Gy and 200Gy)	3	0	3

of parasites (1-2 wells per 24 well plate) irradiated at 200Gy survived 7 days post-irradiation. However, once the parasites survived the week post-irradiation, they were able to divide rapidly and reach log-phase growth rates. Close to a half (43.8%) of the wells plated with parasites irradiated at 140Gy also survived post-treatment. Parasites irradiated at 100Gy all survived treatment and apart from a short period of no division for approximately 48 h, and all wells with parasites, once again, became viable cultures. The D10 dose value for the irradiation of the parasites was calculated as 19.83Gy (**Supplementary Figure 2**). The 100Gy, 140Gy, and 200Gy irradiated parasites were selected for further analysis to represent a deeper range of doses tested (**Supplementary Figure 3**). A CFSE assay that measures replication of cells, confirmed our visual observations by mirroring a similar trend in parasite numbers. Parasites receiving doses above 200Gy were able to divide two to three rounds before death. For the doses at 200Gy and below, the recovery time for irradiated parasites was extended the closer the dose was to 200Gy before the parasites were capable of replication (**Figure 1**).

Irradiated parasites were also used for *in vivo* studies (**Figure 2**). Mice from the group inoculated with parasites irradiated at 100Gy all succumbed to death after developing parasitemia levels similar to the control group that received 0Gy parasites (**Figures 1**, **2A, C**). However, the 100Gy group had a longer prepatent period than the control group, with parasites first appearing on day four rather than day two (**Figure 2A**). The three mice that developed parasitemia in the group inoculated

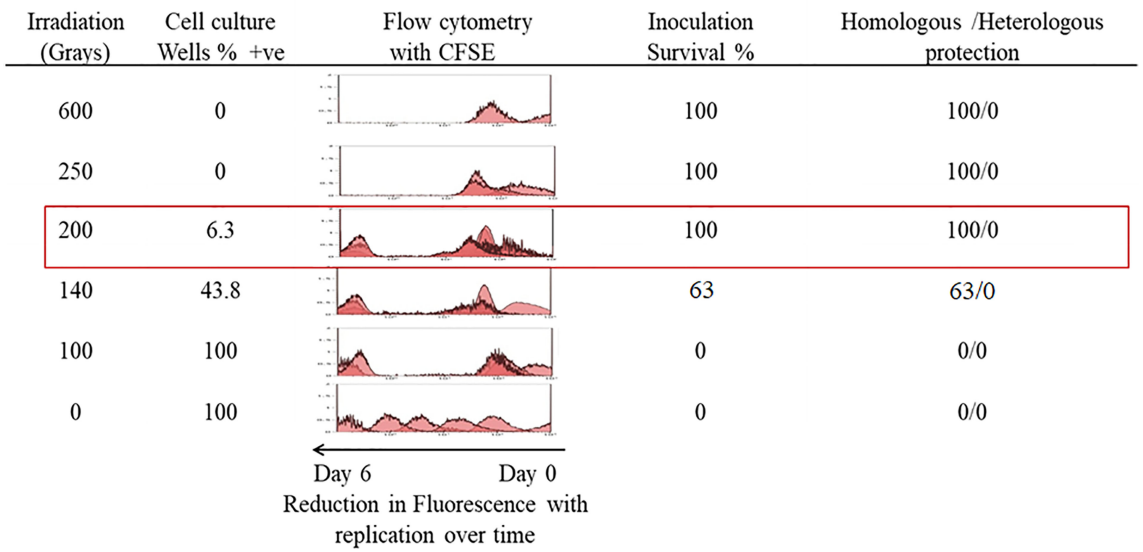

FIGURE 1 | *In-vitro* growth analysis of irradiated parasites. Parasites irradiated at different doses were observed over a 7-day period post-irradiation and 200Gy was identified as the maximum dose applicable. Percentage survival was calculated from the number of wells containing parasites that survived in a 24 well plate. A parallel plate was used to measure replication of parasites labelled with CFSE, which halves in concentration with each doubling of parasites. Eight female BALB/c mice per group were each inoculated with 1 x 10^4 parasites irradiated with doses ranging from 600Gy to 100Gy and a control group received 1 x 10^4 non-irradiated parasites. Surviving mice were further challenged with 1 x 10^3 of either homologous *T. evansi* RoTat 1.2 or heterologous Can 86K strains.

using 140Gy irradiated parasites had an even longer prepatent period with infection first observed after day eight when compared to both 0Gy and 100Gy groups at two and four days, respectively. One of the mice in the 140Gy group showed parasitemia only after the second inoculation and thereafter quickly succumbed to infection (after day 21, **Figure 2A**). All other inoculated mice did not develop any detectable parasitemia even after homologous challenge (results not shown). Heterologous challenge, however, resulted in parasitemia in all groups. The remaining five mice in the 140Gy group developed parasitemia and succumbed much faster than the remaining 200Gy and 250Gy inoculated groups (**Figures 2B, C**). The two groups of mice inoculated with 200Gy and 250Gy irradiated parasites did not show any significant difference compared to the PBS inoculated challenge control group. Plasma samples collected from mice during inoculation revealed that the 200Gy inoculated group displayed statistically significant depressed levels of IFNγ, IL10, IL12b, IL13, IL1b, IL4, when compared to control mice (0Gy, **Figure 3**). The group of mice inoculated using 100Gy irradiated parasites showed similar cytokine levels as the control mice, apart from where levels were significantly higher when compared to groups inoculated with 140Gy and 200Gy irradiated parasites for IL12a and IL6 in the group inoculated with 200Gy irradiated parasites (**Figure 3**).

Gene Transcript Abundance Is Dependent on and Differentially Affected by the Irradiation Dose Applied

Parasites analysed for differential gene transcript abundance after irradiation treatment could only be reliably deciphered after RNA was extracted 6 hours and 20 hours post-irradiation. This was clear after principal components analysis (PCA) of RNA isolated from irradiated parasites processed using TrypMS (**Figure 4A**). All 20 hour and 6 hour delay extracted samples clustered individually and separately from 1 hour delay and non-irradiated 0Gy extracted samples clustered close to each other. Hierarchical clustering of differentially transcribed RNA from 1 hour, 6 hour and 20 hour delay samples separated accordingly as displayed (**Figure 4B**). Samples from the non-irradiated group (0Gy) were used as the baseline for hierarchical clustering.

Further transcriptional analyses of the samples irradiated at 6 hours and 20 hours revealed a higher total number of differential gene transcripts at 20 hours when compared to 6 hours for 100Gy and 140Gy irradiated parasites (**Figure 5A**). For 100Gy irradiated parasites, 134 and 281 gene transcripts were upregulated whereas 100 and 141 were downregulated at 6 hours and 20 hours, respectively. At 140Gy irradiation, 184 and 259 were upregulated and 141 and 122 were downregulated at 6 hours and 20 hours, respectively. Interestingly, 200Gy irradiated parasites showed a reduced number of differential gene transcripts with 261 and 278 upregulated and 223 and 179 downregulated at 6 hours and 20 hours, respectively. In addition, the fold-changes observed at 20 hours were higher in upregulated transcripts when compared to those downregulated for 200Gy irradiated parasites (**Figure 5B**). The calculated individual FDR *p* values also tended to be more significant in the upregulated genes (**Figure 5B**).

When a comparison between 20 hours and 1 hour post-irradiation samples was made, 41.6% of all differential gene transcripts were shared between 100Gy, 140Gy, and 200Gy

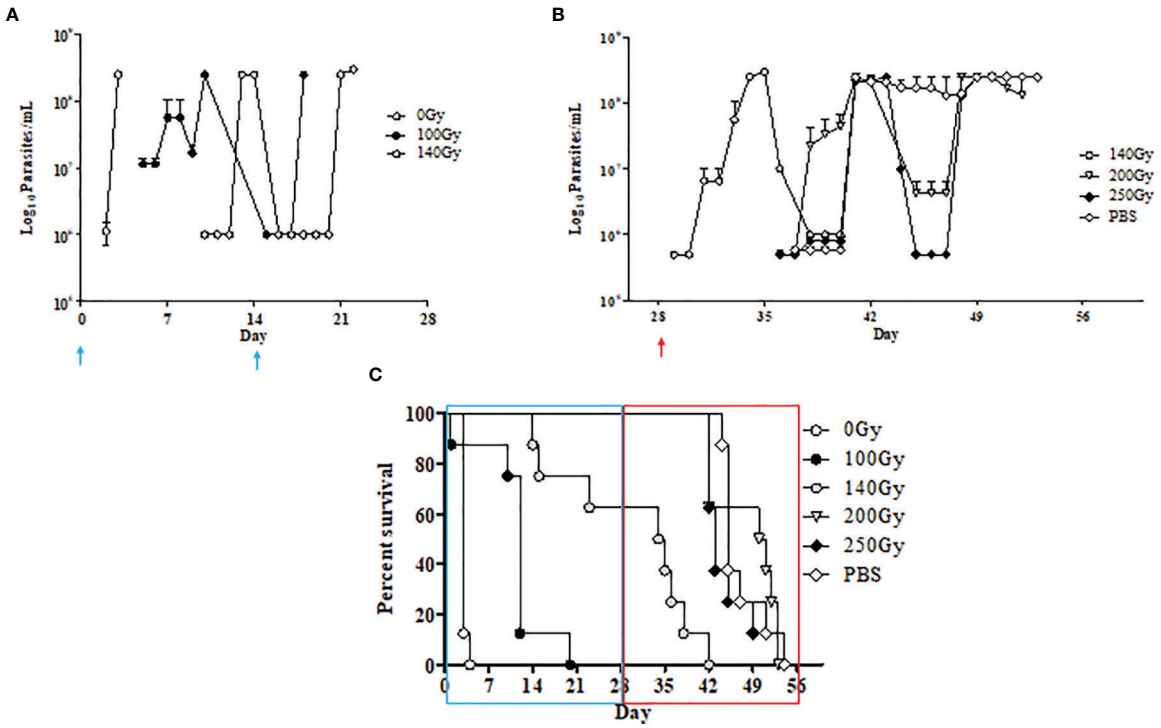

FIGURE 2 | *In-vivo* characteristics of irradiated parasites at different doses. **(A)** Parasite counts in mice that developed an infection after inoculation with *T. evansi* RoTaT1.2 irradiated parasites on days 0 and 14 (↑) are plotted. Mice in groups inoculated with either 0Gy or 100Gy irradiated parasites all developed parasitemia although with a delayed prepatent period at day 4 for mice inoculated with 100Gy irradiated parasites. Only three mice in the group inoculated with 140Gy irradiated parasites were infected with parasites first appearing at day 9. **(B)** Parasite counts in mice that developed an infection after heterologous challenge with *T. evansi* Can 86K on day 28 (↑). **(C)** Kaplan Meier survival analysis shows a 15-day gap between mice inoculated with 0Gy and 100Gy irradiated parasites and the remaining 5 mice in the group inoculated with 140Gy irradiated parasites succumbing faster to heterologous challenge on day 28 compared to the remaining groups.

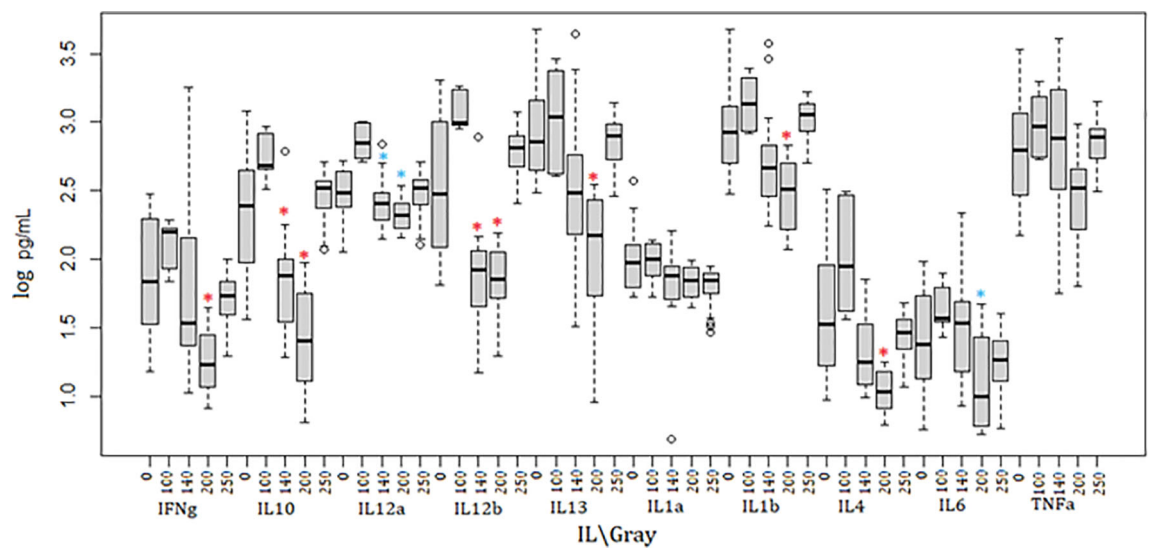

FIGURE 3 | Cytokine dynamics in mice immunized using irradiated parasites. Ten different cytokines were measured through the course of inoculation and challenge. Mice inoculated with 200Gy irradiated parasites had significantly lower levels of IFNγ, IL10, IL12b, IL13, IL1b and IL4 when compared to 0Gy (*). IL12a and IL6 were significantly lower when comparing 200Gy to 100Gy irradiated parasite inoculation (*). Significantly lower IL10, IL12a and IL12b were also observed in mice inoculated with 140Gy irradiated parasites (*). Analyses were calculated using one-way ANOVA for each cytokine, *$p < 0.01$.

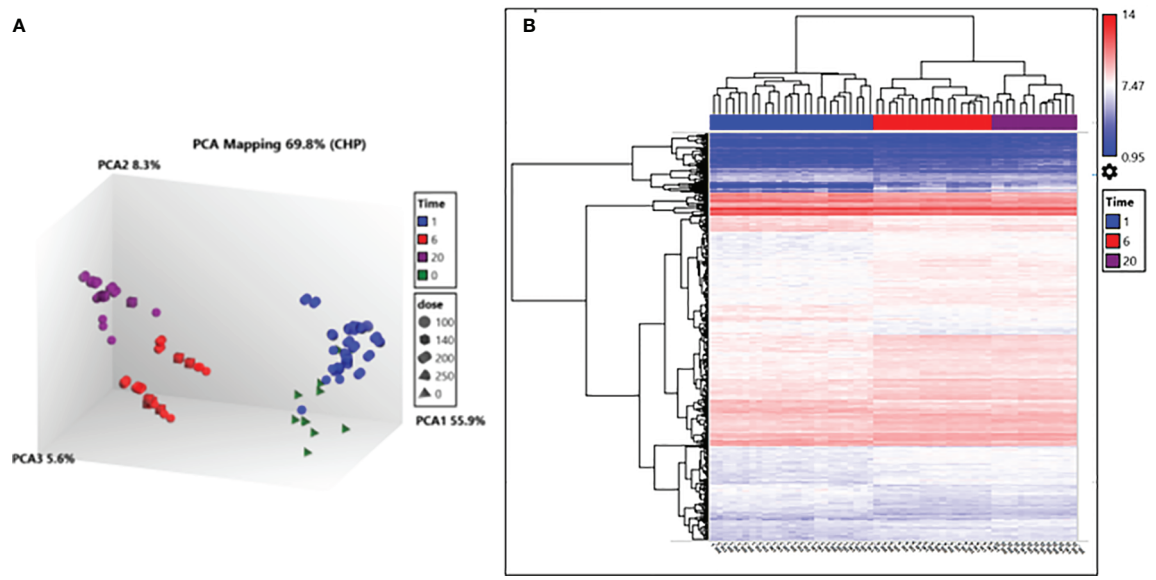

FIGURE 4 | Transcription analysis of irradiated parasites using the TrypMS array. **(A)** PCA mapping separated samples according to time post-irradiation. **(B)** Hierarchical clustering of deferential gene transcripts according to time and further sub clustered using the gene ID. Fold change (FC) cut-off points of > 2 and < 2 were used as the limits for upregulation and downregulation respectively and a gene-level P-value < 0.05.

(ABC; 259 genes on Venn diagram) (**Figure 5C**). Other common differential gene transcripts were observed between 140Gy:100Gy (AB), 200Gy:100Gy (AC), and 200Gy:140Gy (BC) of 25, 36, and 59 respectively. The different doses also had unique differential gene transcripts with 102 for 100Gy, 38 for 140Gy, and 103 for 200Gy irradiation samples. An exhaustive comparison between differential gene transcripts across different doses and times post-irradiation is listed in **Table 1**. All doses showed a higher total difference at 20 hours apart from 200Gy which had its peak of differential expression at 6 hours. Interactions between different doses at different times post-irradiation were highest between 100Gy and 200Gy (**Table 1**). Gene lists for all doses and times post-irradiation with fold changes and FDR *p* values are attached as an excel file in the supplementary section (**Supplementary Table 2**). Further analyses that compared 100Gy- to 200Gy-irradiated parasites' differential gene transcripts between 1 hour and 20 hours is provided in **Supplementary Table 4**. A delta fold change that describes the transcript concentrations of the affected transcripts at ±1.5-fold change was calculated to identify which genes rebound at 20 hours after irradiation between the two representative doses. A total of 75 genes had a + delta difference of 1.5 to 4.32, whereas 157 transcripts had a delta fold change of -1.5 to -3.27. A positive delta fold change designates a higher transcript concentration at 100Gy than 200Gy at 20 hours and inversely for a negative delta fold change (**Supplementary Table 4**).

In order to confirm the integrity of the TrypMS array, a confirmatory qPCR was performed on the same source of RNA used on the array (**Figure 6**). The targets chosen at 100Gy, 140Gy, and 200Gy irradiation had similar profiles with 17 downregulated and 5 upregulated genes in all three irradiation doses. The non-irradiated group (0Gy) was used as the baseline to calculate fold-change (**Figure 6**).

The Effect of Irradiation on Gene Ontology

Although the number of differential gene transcripts at all three doses was similar, ranging from 484 to 234 genes for 200Gy at 6h and 100Gy at 6h, respectively (**Table 1**), the effect on GO term enrichment was dramatically different both in the composition of GO terms affected and the significance in Z score (**Figure 7**). At 6h post-irradiation at 100Gy, GO terms associated with DNA packaging, chromatin assembly, and nucleosome assembly were significantly affected by irradiation. All top ten significant GO terms, except GO:0035328, had a decreasing Z score. A similar pattern was also observed at 140Gy and 200Gy, although with lower significance values at 5 logs and 8 logs less, respectively (**Table 2**). At 20 hours, GO terms associated with translation, ribosome structure, and peptide metabolic process feature prominently with *p* values 10 logs more significant when compared to GO terms affected at 6 hours (**Figure 7**). The GO terms with significantly adjusted *p* values associated with 140Gy at 20 hours are "cell periphery", "plasma membrane", "biological process involved in interaction with host", "biological process involved in interspecies interaction between organisms" and "response to host and response to external biotic stimulus". The GO terms with significant *p* values associated with 200Gy are "cell periphery", "nucleoside diphosphate phosphorylation", "nucleotide phosphorylation", "nucleoside diphosphate metabolic process", "purine nucleotide metabolic process" and "purine nucleoside diphosphate metabolic process". A comprehensive description of all GO terms with associated

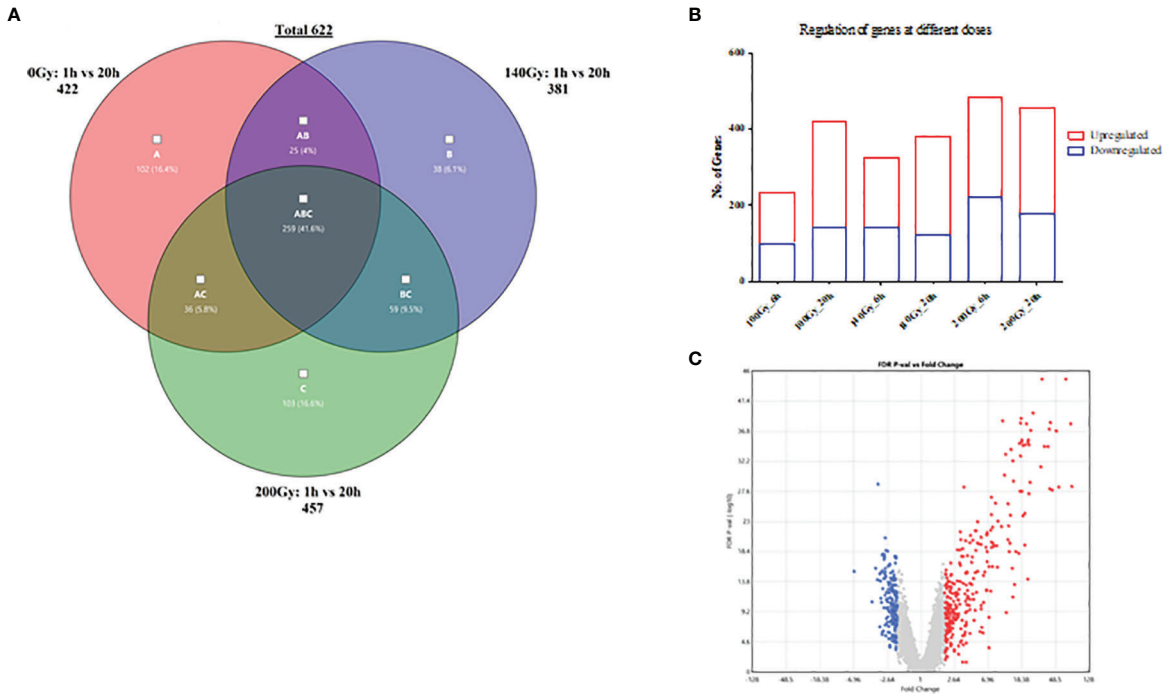

FIGURE 5 | General differences in gene transcript changes according to dose and time post-irradiation. **(A)** Bar graph showing the ratio of gene transcript abundance upregulated to downregulated at different doses at 6 and 20 hours post-irradiation. **(B)** Volcano plot of fold-change (FC) vs false discovery rate (FDR) *p* value for 200Gy irradiated parasites at 20h. **(C)** Venn diagram describing the distribution of 622 differential gene transcripts at 20 hours after irradiation with 259 genes common across all three doses when compared to 1 hour after irradiation, 102, 38 and 103 unique to 100Gy, 140Gy and 200Gy irradiation respectively.

gene IDs, logFC, adjusted *p* values and z scores at different irradiation doses and times post-irradiation (6 hours and 20 hours) is listed in **Supplementary Table 3**.

GO circle plots plotted for the ten most significant enrichment terms for 100Gy at 6 hours shows the associated GO terms mostly have a decreasing Z score apart from G0:0035328; "transcriptionally silent chromatin" (**Figure 8**). However, at 20 hours post-irradiation, some of the most significant GO terms have an increasing Z score, e.g., "cytosolic ribosome" and "cytosolic large ribosomal subunit"; G0:0022626 and G0:0022625, respectively. A deeper look at the GO enrichment terms at 6 hours shows that the processes with the most significantly adjusted *p* values identified and most likely to occur, were all associated with the assembly and packaging of DNA and chromatin (**Table 2**). Similar processes were also found at 140Gy, although not in the top 10 (**Supplementary Table 3**). In addition, there were several logs of lower significance when compared to 100Gy where they featured at the topmost significant GO terms (**Figure 8**). The numbers were even lower when 200Gy was included in the comparison (**Table 2**). At 20 hours, the list of most significant GO processes changes to ribosomal structure, peptide metabolic, and peptide biosynthesis terms (**Table 2**, lower half). The top GO terms for 100Gy at 20 hours are also 10 logs more significant when compared to the top 10 terms at 6 hours at $p < 10^{-20}$ versus $p > 10^{-11}$,respectively. GO terms at 20h for 140Gy and 200Gy averaging with $p > 10^{-5}$ and $p > 10^{-3}$ are more than 20 logs less significant than the same terms at 20 hours post 100Gy irradiation (**Table 2**).

After identifying 100Gy as having a different response profile from the other doses, we identified the genes associated with the positive Z score GO terms (implying upregulation) at 6 hours and 20 hours after irradiation. A chord plot that links GO term to genes involved was constructed to select the most interactive genes and associated processes (**Figure 9**). None of the upregulated processes at 6 hours post 100Gy irradiation was associated with more than one gene, whereas a few genes were involved in multiple processes. For 20 hours, several genes and processes were associated with more than one entity (**Figure 9**). Genes were given a chord plot count ranked according to the fold-change difference between 6 hours and 20 hours (column 6, **Table 3**). Only two genes appeared at both times post-irradiation in the Z score positive GO terms (*Tb927.10.14130* and *Tb927.2.2460*; i and ii respectively in **Table 3**).

DISCUSSION

Previous irradiation studies on trypanosome parasites began in the late 1960s with initial studies targeting *T. b. rhodesiense*, the sub-species responsible for acute trypanosomosis in humans (37). In the *T. b. rhodesiense* study, groups of mice were inoculated with 2 x 10^6 irradiated parasites per animal using

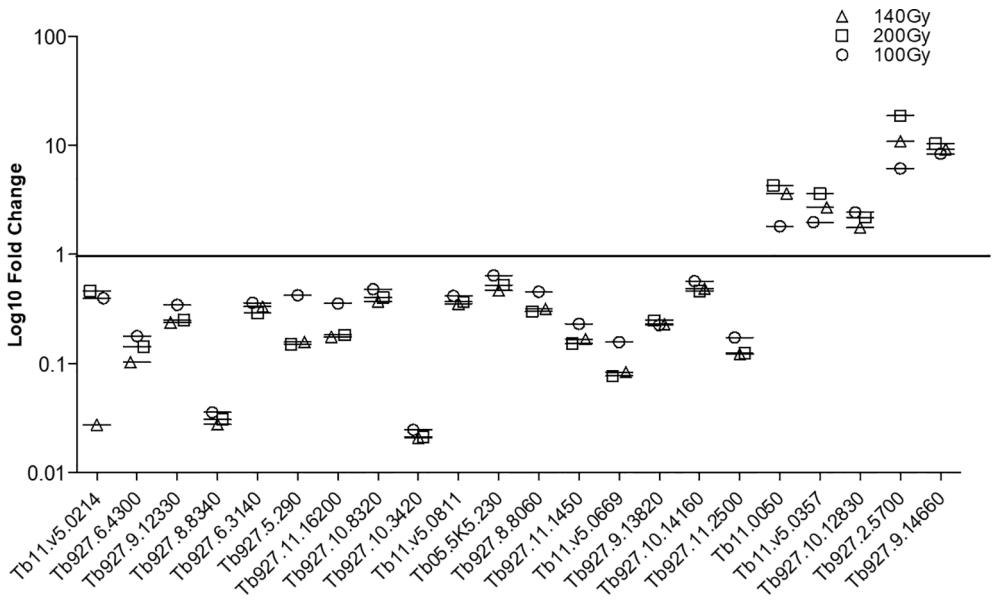

FIGURE 6 | Confirmatory qPCR. Twenty-two genes that were either downregulated (17) or upregulated (5) in all three doses at 20h post-irradiation were amplified using the same RNA samples that had previously been processed using the TrypMS array.

doses ranging from 100Gy to 1000Gy with some groups inoculated up to three times before challenge. After one round of inoculation, only mice inoculated with 100Gy irradiated parasites were infected and this dose was omitted in subsequent experiments. Interestingly, groups of mice inoculated twice with parasites irradiated at 200Gy and 400Gy had a 77% and 90% survival rate with no further mortalities after the third inoculation (37). Subsequent experiments using irradiated *T. b. rhodesiense* in cattle and rhesus monkeys were carried out using 600Gy irradiated parasites (38, 39, 44). In the current study, we used lower numbers of irradiated parasites per mouse and doubled the period between inoculations assuming that subsequent inoculations will not boost any undetectable infections. Similar to the study using *T. b. rhodesiense*, we also measured a dose-dependent delay in the prepatent period as the dose was increased to 200Gy (37). It may be argued that the number of 200Gy irradiated parasites used to inoculate mice was too low with only 6.3% of irradiated parasites surviving post-irradiation but it has previously been shown that as few as 100 - 200 *T. evansi* parasites are more than sufficient to establish an infection in female BALB/c mice (66). In addition, PBS control mice used in the study inoculated with 10^3 parasites rapidly developed parasitemia. We therefore hypothesized that surviving 200Gy irradiated parasites *in vitro* lacked the parasite genes and processes described in 100Gy as necessary for establishing disease *in vivo*. All mice that survived inoculation, survived the subsequent homologous challenge as expected. This could be attributed to an efficient humoral response to the same circulating VSG previously encountered by the mice during inoculation (67).

Using 140Gy as a representative intermediate dose yielded interesting results, with two mice developing parasitemia after one inoculation and a third mouse after the second inoculation. The surviving five mice quickly developed parasitemia when compared to the remaining groups after the heterologous challenge. Previous infection and treatment studies with *T. evansi* that measured host responses after heterologous challenge displayed a prolonged prepatent period and partial protection in rabbits (68, 69). The contradictory results that we observed in mice inoculated with 140Gy irradiated parasites could possibly be explained by the immune- modulating effect of VSG in surviving mice that make them more susceptible to subsequent heterologous challenge (70). In the early stages of infection, carbohydrate moieties associated with soluble VSG released by circulating parasites induce TNF production by activated macrophages leading to trypanosome clearance. Dead parasites expose the VSG lipid moieties which cause overstimulation and subsequent TNF-mediated chronic inflammation in the host (70, 71). We speculate that initial inoculation with 140Gy irradiated parasites behaves similarly to 100Gy irradiated parasites for the three mice that succumbed before challenge, with the remaining five mice efficiently clearing parasites but left with high levels of circulating lipid-associated VSG. The subsequent heterologous challenge of these mice progresses similarly to a chronic infection with the new parasites causing more severe disease in the surviving 140Gy irradiated parasite-infected mice when compared to the PBS control group.

Cytokine profiles across the different irradiated parasite groups were irradiation dose-dependent with 0Gy, 100Gy, and 250Gy consistently producing higher levels of all cytokines apart from IL1a and TNFα when compared to 140Gy and 200Gy. It must be noted that the figures plotted are distributed across different time spans as mice inoculated with 0Gy- and 100Gy

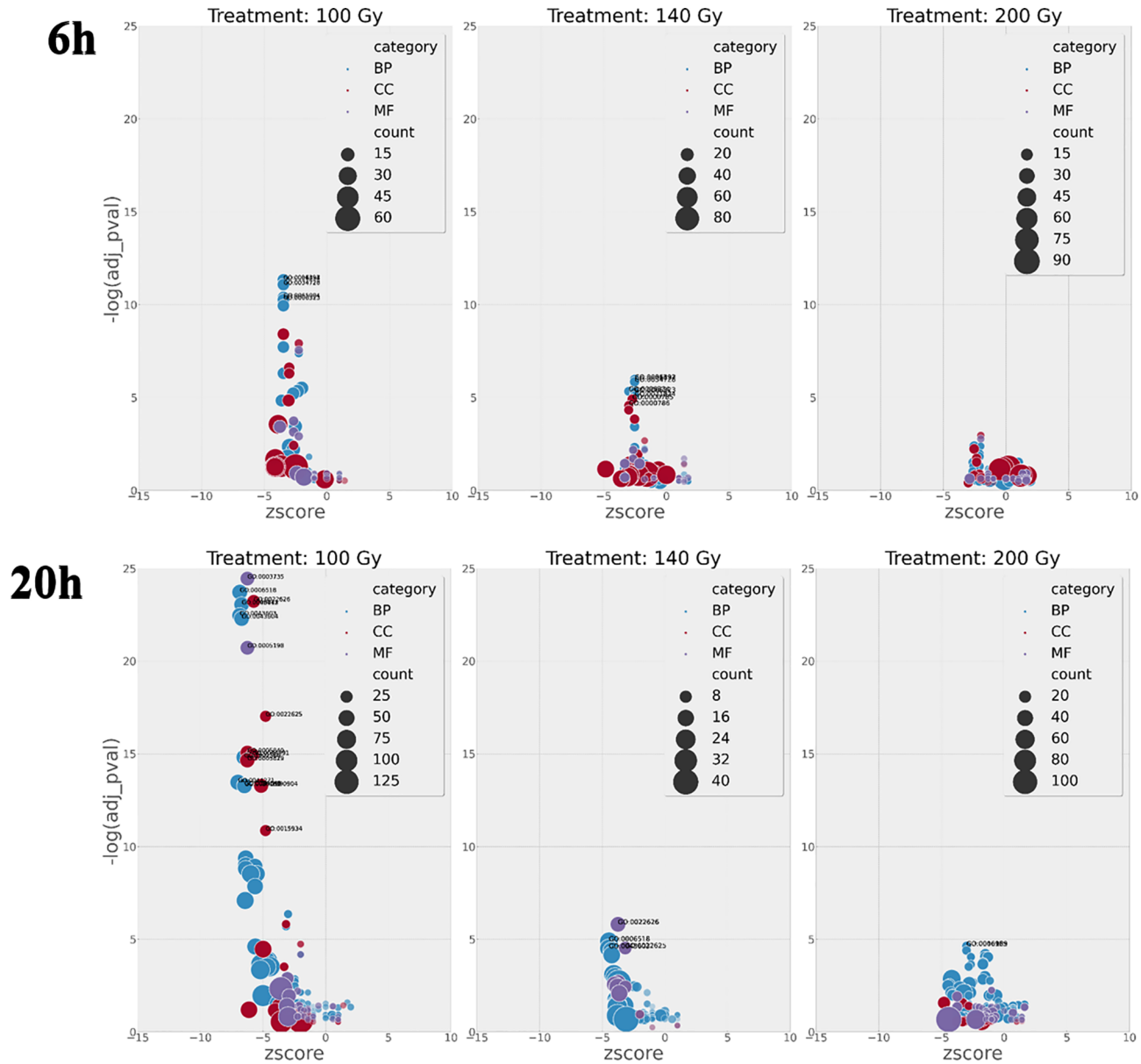

FIGURE 7 | GO enrichment terms with calculated Z scores plotted against FDR *p* value at 6h and 20h hours post-irradiation. The number of terms increases exponentially at 100Gy irradiation after 6h and 20h when compared to 140Gy and 200Gy irradiation with negative log FDR *p* significance values 10 log higher at 100Gy 20h than 100Gy 6h. Adjusted *p* values are important as they designate if a process is more likely to occur.

irradiated parasites survive for a much shorter period than those inoculated with 200Gy- and 250Gy irradiated parasites. Nevertheless, we are still able to estimate the general effect of irradiation. It was noted that mice inoculated with 140Gy irradiated parasites displayed a higher standard deviation when measuring Th1 type responses, mediated by IFNγ and TNFα which are essential when controlling the first peak of infection (72, 73). The deviation is exacerbated by the three mice that succumbed to parasitemia during the first peak and did not have the opportunity for Th2 type responses, mediated by IL10, IL13, IL4, and IL6 to develop. The mice inoculated using 200Gy irradiated parasites showed significantly lower values for the eight cytokines. This is possibly due to the parasites failing to establish disease since the host innate immunity was sufficient to clear the non-virulent parasites used for inoculation, especially in the case of *T. evansi* where type 1 responses are not required to control infection (74, 75). It has been well established in multiple previous studies that the products released by dead and dying Trypanosomes act as immune stimulators in the mammalian host (9, 76, 77). Because we inoculated mice with dead parasites at 250Gy, the products produced by this formulation were able to elicit high cytokine levels. In mice inoculated with 0Gy and

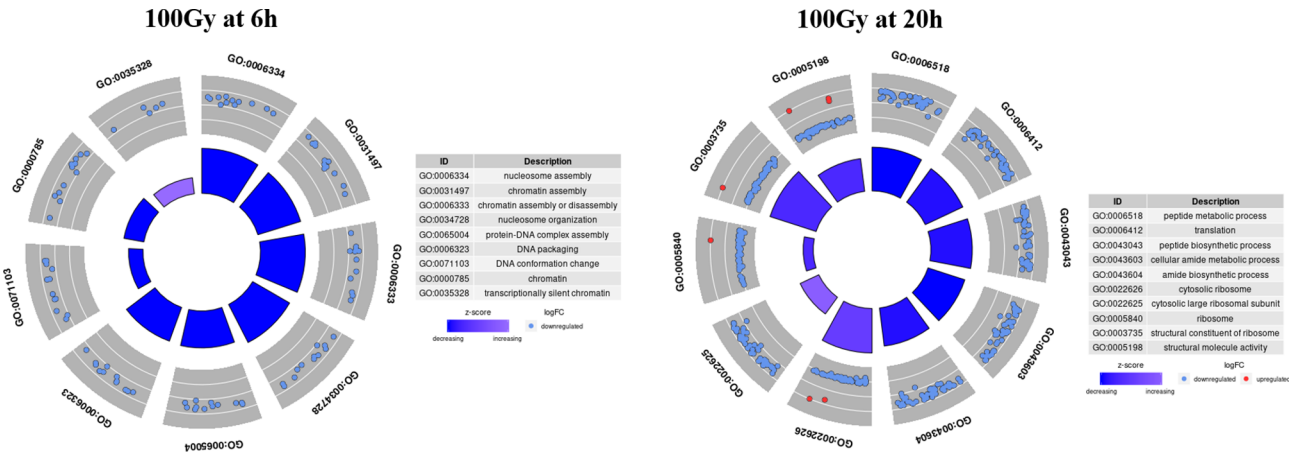

FIGURE 8 | Top 10 most significant GO terms for 100Gy at 6h and 20h post-irradiation. GO circle plots for the top 10 most significant GO enrichment terms with fold-changes of individual genes taken in account and calculated as Z score at 20h post-irradiation. The height of the inner bar chat designates the significance of the GO term plotted. Most processes at both periods post-irradiation were down regulated.

100Gy, mice were also exposed to these products as the initial immune Th1 response in inoculated mice killed off circulating parasites. This trend is however not as clear for 140Gy and 200Gy infected mice where the parasites do not for the most part establish an infection and do not release high amounts of parasite products in the host unlike 0-Gy, 100-Gy, and 250Gy irradiated parasites.

Following the *in vivo* characterization of 100Gy-, 140Gy, and 200Gy- irradiated parasites in mice, we further characterized the effect of irradiation on the parasites by measuring the transcript abundance of different parasite genes using the TrypMS array. We reasoned that since parasites irradiated at 100Gy successfully revived *in vitro* and can infect mice, they were probably able to quickly repair their damaged DNA and proceed to establish disease as critical genes required for both processes were still functional at 6 hours and 20 hours. Furthermore, it was established that these processes were also present in parasites subjected to a dose of 140Gy, albeit at a lower significance value. As the irradiation dose got closer to 200Gy, a much smaller number of parasites could sufficiently repair their DNA. None of the genes necessary to establish disease seemed to sufficiently increase in time to avoid host innate immune responses (21, 78). It could therefore be assumed that any processes with high significance at the 200Gy, 20 hour group are not crucial for establishing disease in mice. In contrast, those at 100Gy, 20 hours are necessary for the parasites after irradiation. Whereas most

TABLE 2 | Comparison of Go Term FDR *p* values across doses at 6h (top half) and 20h (bottom half) post-irradiation.

GO TERM	Description	100Gy Adj *p* value	140 Adj *p* value	200Gy Adj *p* value
GO:0006333	chromatin assembly or disassembly	1.5E-11	2.1E-06	1.6E-02
GO:0006334	nucleosome assembly	1.5E-11	8.4E-06	4.8E-02
GO:0031497	chromatin assembly	1.5E-11	2.1E-06	1.6E-02
GO:0034728	nucleosome organization	2.8E-11	2.8E-06	2.2E-02
GO:0065004	protein-DNA complex assembly	1.4E-10	5.9E-05	1.2E-01
GO:0006323	DNA packaging	1.8E-10	9.8E-06	5.2E-03
GO:0071824	protein-DNA complex subunit organization	3.7E-10	1.6E-05	6.7E-02
GO:0000785	chromatin	1.2E-08	2.5E-05	2.0E-02
GO:0035328	transcriptionally silent chromatin	2.0E-08	2.6E-03	1.4E-03
GO:0031490	chromatin DNA binding	4.7E-08	8.4E-03	2.1E-03
GO:0003735	structural constituent of ribosome	3.5E-25	N/A	1.2E-02
GO:0006518	peptide metabolic process	1.9E-24	1.3E-05	2.8E-03
GO:0022626	cytosolic ribosome	5.9E-24	1.6E-06	2.7E-02
GO:0006412	translation	8.8E-24	4.1E-05	1.0E-02
GO:0043043	peptide biosynthetic process	8.8E-24	4.1E-05	1.0E-02
GO:0043603	cellular amide metabolic process	3.4E-23	3.1E-05	3.2E-03
GO:0043604	amide biosynthetic process	5.0E-23	7.1E-05	7.5E-03
GO:0005198	structural molecule activity	1.9E-21	N/A	4.6E-02
GO:0022625	cytosolic large ribosomal subunit	9.4E-18	3.0E-05	4.0E-02
GO:0005840	ribosome	8.5E-16	2.7E-03	2.7E-01

N/A, Not Available.

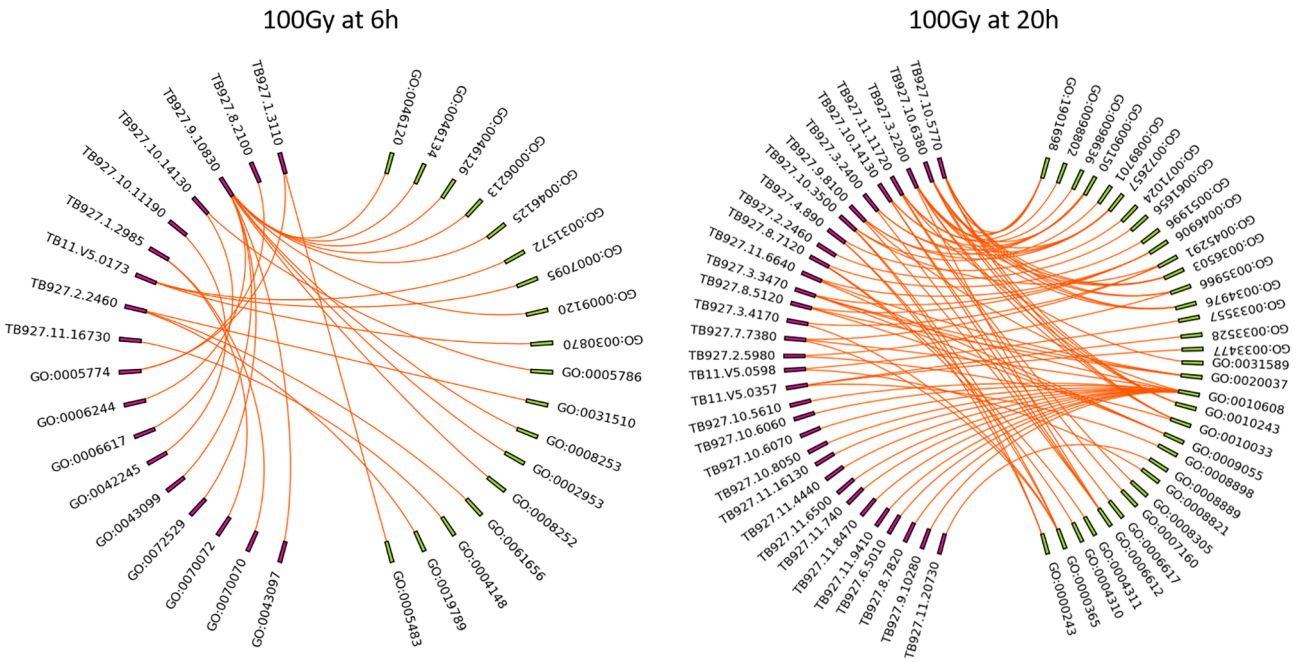

FIGURE 9 | Chord plots for the positive Z score GO enrichment terms and associated genes at 6h and 20h post 100Gy irradiation. All the processes at 6h and 20h post-irradiation were plotted with corresponding genes to identify individual genes involved in multiple processes and given a chord plot count i.e., the higher the count a gene has, the more processes it will be involved with.

eukaryotes control the expression of genes *via* transcription initiation sites at the gene level, kinetoplastid gene expression regulation occurs post-transcriptionally with trypanosome RNA pol II transcribing poly-cistronic RNA transcripts that are processed by trans-splicing and polyadenylation to produce mature mRNA (79, 80). Due to the presence of untranslated RNA intermediates that exist during transcription, we refer to differentially regulated transcripts rather than genes because trypanosome mRNA concentrations do not correlate directly with the concentrations of protein translated (48). In addition, the stability, half-life, degradation, length and copy number of a transcript directly influence on the likelihood of translation (80). We therefore used a GO term approach that used RNA transcript levels to identify the most significant processes enriched at different irradiation doses with a corresponding Z score (64). As expected, the processes involved with DNA binding and chromatin assembly were the most important for 100Gy after 6 hours of irradiation, whereas those involved with ribosome structure and peptide biosynthesis processes at 20 hours. These processes remained significant for 140Gy irradiation at 6 hours and 20 hours but not at 200Gy. When looking at the genes involved in processes with a positive Z score at 6 hours and 20 hours at 100Gy irradiation, most genes identified at 6 hours are for nucleic acid assembly and repair. However, the transcripts identified at 20 hours have more varied functions and include genes such as TPR repeats and Squalene synthase which have been identified as a virulence factor in bacteria and a drug target in *T. cruzi*, respectively (81, 82). Further studies that elucidate the functions of these genes would help develop a genetically manipulated, non-infectious parasite that could potentially be used as a vaccine candidate in the mammalian host as described in **Figure 10**. If successful, an effective vaccine that includes genetically manipulated or irradiated parasites would require quality control measures to ensure safety due to the emergence of resistant parasites.

A comparison of gene transcripts from parasites irradiated at 100Gy and 200Gy at 20 hours with a delta fold change of ±1.5 identified eight genes that have been implicated in a study that described developmental gene regulation events that occur when non-infectious *T. brucei* procyclic insect forms in the tsetse gut and transform first into epimastigotes and subsequently to mammalian infectious metacyclic parasites in a processes known as metacyclogenesis (83). Metacyclogenesis in *T. brucei* can be replicated *in vitro via* the overexpression of RNA-binding protein 6 (RBP6) and has been modified further to skip the intermediate epimastigote stage by overexpressing either RBP6 with a single point mutation (Q109K), or RNA-binding protein 10 (RB10) in procyclic parasites (84–86). Of the eight transcripts identified in this study, one was a positive regulator of metacyclogenesis (Tb927.5.4000; hypothetical protein), and two were negative regulators (Tb927.10.9550 and Tb927.11.1310; hypothetical protein and NADH-cytochrome b5 reductase, putative). The remaining five were considered neutral and not affected by knocking out RBP6 in *T. brucei* procyclics (83). Interestingly, the one positive regulator of metacyclogenesis had a positive delta fold change of 1.67 signifying a higher number of copies in parasites irradiated at 100Gy (**Supplementary Table 4**).

TABLE 3 | Genes found in positive Z score GO terms for 100Gy at 6h and 20h post-irradiation.

Gene ID	Description	Chord plot count	6 vs 1 FC	20 vs 1 FC	6h vs 20h	Time FDR
Tb927.10.14130[i]	SRP19 protein, putative	2	1.69	1.77	0.08	2.07E-16
Tb927.11.16730	Dihydrolipoyl dehydrogenase	1	1.81	1.89	0.08	6.75E-18
Tb927.10.11190	tRNA-splicing ligase RtcB, putative	1	1.89	1.82	-0.07	4.44E-26
Tb11.v5.0173	Hypothetical protein, conserved	3	2.01	1.9	-0.11	1.32E-28
Tb927.1.3110	Soluble N-ethylmaleimide sensitive factor (NSF) attachment protein, putative	2	2.03	1.74	-0.29	2.09E-22
Tb927.9.10830	Metal dependent 5'-nucleotidase	13	2.07	1.75	-0.32	1.21E-29
Tb927.8.2100	Vacuolar ATP synthase 16 kDa proteolipid subunit, putative	1	2.43	2.07	-0.36	6.84E-18
Tb927.2.2460[ii]	Ubiquitin-conjugating enzyme E2, putative	3	2.84	2.38	-0.46	6.58E-18
Tb927.1.2985	ER protein Pkr1, putative	2	1.94	1.47	-0.47	4.87E-24
Tb927.8.7120	Squalene synthase, putative	3	-1.07	1.65	2.72	2.32E-08
Tb927.10.8050	TFIIF-stimulated CTD phosphatase, putative	1	-1.13	1.55	2.68	9.61E-08
Tb927.9.10280	Zinc finger CCCH domain-containing protein 48	1	-1.01	1.56	2.57	1.90E-06
Tb927.11.9410	Hypothetical protein	1	1.6	4.16	2.56	2.36E-17
Tb927.11.4440	Hypothetical protein	1	1.05	2.11	1.06	8.32E-17
Tb927.2.5980	Chaperone protein clpb1, putative	2	2.06	2.76	0.7	1.98E-17
Tb927.8.5120	Cytochrome c	3	-5.3	-4.62	0.68	1.51E-34
Tb11.V5.0357	Homocysteine S-methyltransferase, putative	3	1.09	1.76	0.67	7.40E-18
Tb927.11.8470	Zinc finger protein family member, putative	1	1.29	1.83	0.54	7.51E-05
Tb927.11.20730	Glycerophosphoryl diester phosphodiesterase, putative	1	1.36	1.87	0.51	7.19E-17
Tb11.V5.0598	GIY-YIG catalytic domain containing protein, putative	2	1.7	2.05	0.35	3.33E-26
Tb927.3.4170	CRK9-associated protein	2	1.8	2.13	0.33	4.30E-21
Tb927.11.6640	Cytochrome b5, putative	3	1.24	1.37	0.13	0.0302
Tb927.6.5010	Hypothetical protein, conserved	1	1.95	2.08	0.13	6.64E-28
Tb927.8.7820	'Cold-shock' DNA-binding domain containing protein, putative	1	2.18	2.31	0.13	1.92E-21
Tb927.10.14130[i]	SRP19 protein, putative	4	1.69	1.77	0.08	2.07E-16
Tb927.3.2200	TPR repeat, putative	8	1.58	1.66	0.08	7.27E-20
Tb927.4.890	Small nuclear ribonucleoprotein Sm D3	3	1.72	1.76	0.04	5.33E-15
Tb927.7.7380	U6 snRNA-associated Sm-like protein LSm3	3	1.96	2	0.04	2.51E-24
Tb927.10.5610	40S ribosomal protein S9, putative	1	-2.06	-2.04	0.02	1.84E-15
Tb927.10.3500	Splicing factor u2af 65 kDa subunit	4	2.09	2.1	0.01	7.08E-30
Tb927.11.11720	FG-GAP repeat protein, putative	5	1.87	1.86	-0.01	1.25E-23
Tb927.10.6380	Ring finger containing protein	6	1.83	1.81	-0.02	8.22E-17
Tb927.3.3470	Cytochrome b5, putative	4	1.91	1.84	-0.07	2.61E-19
Tb927.11.6500	40S ribosomal protein S21, putative	1	-1.74	-1.85	-0.11	1.35E-16
Tb927.3.2400	Palmitoyl acyltransferase 10, putative	3	2.34	2.22	-0.12	2.70E-25
Tb927.11.740	Eukaryotic translation initiation factor 5A	1	-1.59	-1.95	-0.36	9.17E-17
Tb927.10.6060	Universal minicircle sequence binding protein 2	1	-1.5	-1.89	-0.39	3.73E-10
Tb927.9.8100	Nascent polypeptide associated complex subunit, putative	4	-1.71	-2.1	-0.39	5.61E-24
Tb927.10.6070	Universal minicircle sequence binding protein 1	1	-2.32	-2.76	-0.44	7.22E-24
Tb927.10.5770	Valosin-containing protein	6	-1.59	-2.05	-0.46	1.34E-16
Tb927.2.2460[ii]	Ubiquitin-conjugating enzyme E2, putative	1	2.84	2.38	-0.46	6.58E-18
Tb927.11.16130	Nucleoside diphosphate kinase	1	-1.26	-2.1	-0.84	1.12E-23

[i] and [ii] found at both 6h and 20h.

Previous studies using irradiated *T. cruzi*, a trypanosome species that is highly resistant to irradiation, compared RNA transcripts to protein differences and found that both analyses complemented rather than confirmed each other (48, 49). A crucial role for the ubiquitin- proteasome system was also described during the repair process initiated after irradiation (87). In this study, ubiquitin-conjugating enzyme E2 is upregulated at both 6 hours and 20 hours post-irradiation at 100Gy. Surprisingly, although upregulated, DNA repair enzymes (RAD-51, BRCA2, MRE2, TOPO IIIα and $RMI_{1/2}$) were not seen to be involved in the initial significant processes after irradiation (88–91). A more precise method of measuring RNA transcripts that are targeted for translation in trypanosome species is ribosome/polysome profiling (92). Ribosome profiling targets the parasite 'translatome' which are ribosome-bound mRNA or polysome when more than one ribosome is bound to the same mRNA moiety (93). The method begins with centrifuging a parasite lysate on a continuous sucrose gradient that separates polysomes from free mRNA ensuring that only ribosome-bound RNA is used for deep sequencing analysis. Fragmented unbound mRNA prepared from the same sample is also sequenced to act as a ribosome footprint library used to orientate sequenced polysomes (93). Although more accurate than total mRNA in terms of what is targeted for expression, it would still be prudent to analyze mRNA transcript levels to identify which target species exist in higher concentrations.

A *T. congolense* RNASeq study that compared parasite gene profiles during development in two distinct tsetse tissues, the cardia and proboscis, showed gene enrichment with GO terms associated with "quorum sensing", "nucleotides", "microtubules", "cell membrane components" and "transport" in parasites colonizing the cardia (94). These terms were deemed essential for long non-dividing procyclic forms that colonize in the gut after a blood feed. Epimastigote and metacyclic forms

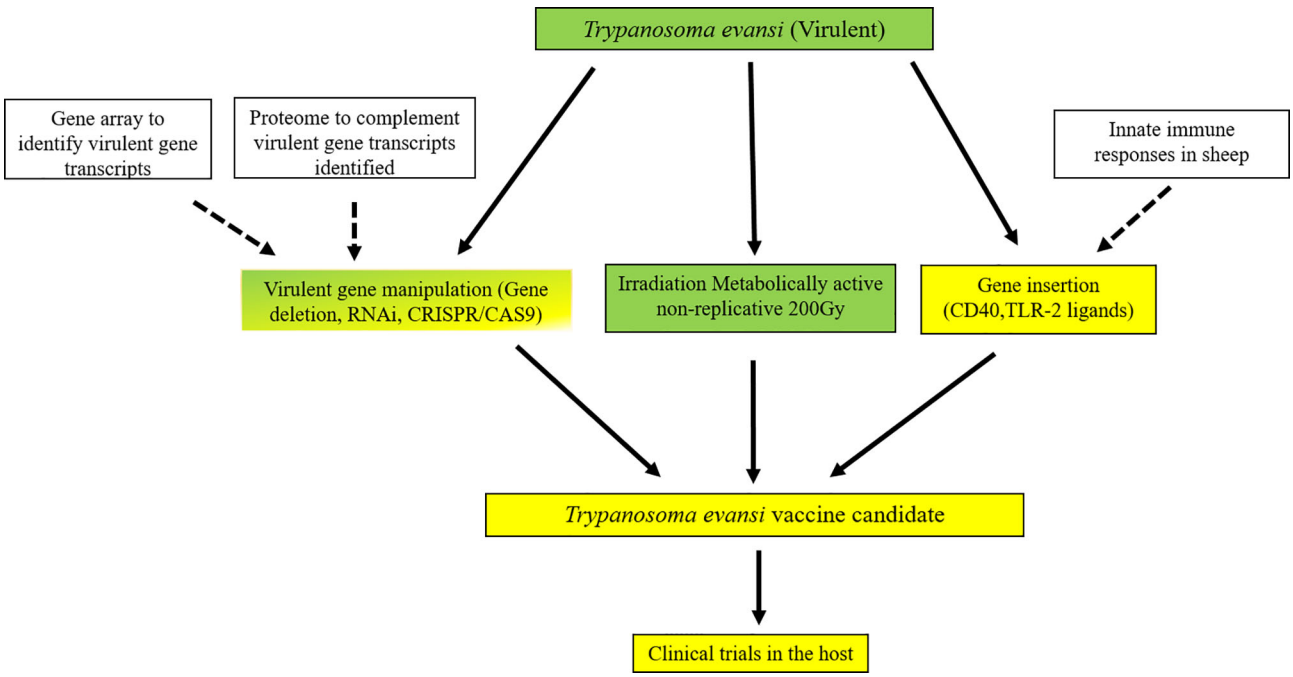

FIGURE 10 | Potential pathway to an effective vaccine for *T. evansi* in livestock. An outline for developing a genetically manipulated and irradiated but metabolically active vaccine against Trypanosomosis in livestock species. Green signifies areas well studied, green/yellow areas are those that have been attempted, yellow are yet to be studied. White boxes are areas that are continuously under study that produce new information for vaccine development. All genes identified across doses were analysed in a matrix that considers the changes in the level of transcription at 100Gy compared to both 140Gy and 200Gy irradiation of *T. evansi* and functional analysis using gene ontology enrichment to identify pathways that are affected by low dose irradiation. Further analysis to look at immune functions of genes identified using gene deletion methods e.g., gene knock-out, RNAi or CRISPR/CAS9. Gene insertion of immune modulation ligands would further enhance immunogenicity of the whole parasite inoculum before testing in the mammalian host.

that are found in the insect mouth parts on the other hand undergo cell division with enrichment terms associated with "nucleosomes", "cytoplasm" and "membrane bound organelles" upregulated in preparation for infection. In addition, many hypothetical cell-surface proteins that have not been functionally characterized were also upregulated (94). When looking at the common terms that were upregulated in both insect parasite forms, "ribosome", "cytosolic ribosomal unit", "structural constituent of ribosome" and "translation" all featured prominently, irrespective of the tissue the parasite was isolated from (94). These terms also feature significantly in the 100Gy irradiated parasites after 20 hours, suggesting that they are important for constitutive processes in all forms of the parasites (**Table 2**). When looking at the most significant processes with a positive Z score, the terms "mRNA trans splicing, *via* spliceosome", "commitment complex", "protein targeting to membrane", and "protein targeting to membrane" feature prominently (**Supplementary Table 2**, circ_100_20 hours), suggesting that these processes are unique to post-irradiation, damage repaired parasites possibly upgrading these processes for establishing disease utilizing specific genes identified and displayed in **Table 3**.

In summary, we irradiated *T. evansi* parasites to identify doses sufficient to produce viable parasites *in vitro* but are defective in causing infection in BALB/c mice. with irradiation doses of 200Gy, 140Gy, and 100Gy producing representative non-infectious, intermediate, and infectious parasites, respectively. Interleukin analyses of inoculated mice revealed that 140- and 200Gy irradiated parasites did not mediate a Th1 response in the host as is expected in regular infection studies. To further characterize the irradiated parasites, we developed a multispecies micro-array, TrypMS, to measure mRNA abundance across the three representative doses at 6 hours and 20 hours post-irradiation. The information gathered from TrypMS was then used to calculate Z scores using a gene ontology approach that measured the enrichment of processes rather than accessing individual genes. Transcript fold changes were also compared between 100- and 200Gy parasites at 20 hours post-irradiation to predict genes that may be involved in establishing an infection after parasite irradiation repair. A list of genes from GO processes upregulated at 20 hours by 100Gy irradiated parasites was also generated for further study and the pathway to a functional irradiated vaccine postulated.

DATA AVAILABILITY STATEMENT

Microarray data produced from this experiment is available in the ArrayExpress database (http://www.ebi.ac.uk/arrayexpress)

under accession number E-MTAB-11705. The TrypMS521152F custom array from Affymetrix has the accession number A-MTAB-695 (95).

ETHICS STATEMENT

The animal study was reviewed and approved by institutional ethics committee of the University of Veterinary Medicine, Vienna, and the national authority according to § 26 of the Austrian Law for Animal Experiments, Tierversuchsgesetz 2012-TVG 2012 under the No. GZ 68.205/0069-WF/II/3b/2014.

AUTHOR CONTRIBUTIONS

RK, EW, and AD conceptualized the work; RK, EW, TS, and HU carried out the experiments; RK, SD, VW, and CL analyzed the data. All authors contributed to the article and approved the submitted version.

SUPPLEMENTARY MATERIAL

The Supplementary Material for this article can be found online at: https://www.frontiersin.org/articles/10.3389/fimmu.2022.852091/full#supplementary-material

Supplementary Figure 1 | Gating strategy for Trypanosome CFSE replication assay.

Supplementary Figure 2 | Calculated D10 for *T. evansi* RoTat 1.2 parasites.

Supplementary Figure 3 | *In vitro* parasite counts post-irradiation. **(A)** Percentage number of wells with viable parasites in a 24 well plate at different doses. **(B)** Log parasite numbers where more than 25% or more of wells in 24 well plates contained motile and viable parasites at different doses.

Supplementary Table 1 | Primer list for 22 genes used to confirm expression.

Supplementary Table 2 | Gene transcripts at different times and doses post-irradiation.

Supplementary Table 3 | Combined GOcirc data.

Supplementary Table 4 | Differential gene transcripts between 1h and 20h for 100Gy- to 200Gy-irradiated parasites.

REFERENCES

1. Aregawi WG, Agga GE, Abdi RD, Büscher P. Systematic Review and Meta-Analysis on the Global Distribution, Host Range, and Prevalence of Trypanosoma Evansi. *Parasit Vectors* (2019) 12:67. doi: 10.1186/s13071-019-3311-4
2. Salah AA, Robertson I, Mohamed A. Estimating the Economic Impact of Trypanosoma Evansi Infection on Production of Camel Herds in Somaliland. *Trop Anim Health Prod* (2015) 47:707–14. doi: 10.1007/s11250-015-0780-0
3. Desquesnes M, Dargantes A, Lai DH, Lun ZR, Holzmuller P, Jittapalapong S. Trypanosoma Evansi and Surra: A Review and Perspectives on Transmission, Epidemiology and Control, Impact, and Zoonotic Aspects. *BioMed Res Int* (2013) 2013:20. doi: 10.1155/2013/321237
4. Dargantes AP, Mercado RT, Dobson RJ, Reid SA. Estimating the Impact of Trypanosoma Evansi Infection (Surra) on Buffalo Population Dynamics in Southern Philippines Using Data From Cross-Sectional Surveys. *Int J Parasitol* (2009) 39:1109–14. doi: 10.1016/j.ijpara.2009.02.012
5. Holland WG, Do TT, Huong NT, Dung NT, Thanh NG, Vercruysse J, et al. The Effect of Trypanosoma Evansi Infection on Pig Performance and Vaccination Against Classical Swine Fever. *Vet Parasitol* (2003) 111(2–3):115–23. doi: 10.1016/S0304-4017(02)00363-1
6. Truc P, Büscher P, Cuny G, Gonzatti MI, Jannin J, Joshi P, et al. Atypical Human Infections by Animal Trypanosomes. *PloS Negl Trop Dis* (2013) 7: e2256. doi: 10.1371/journal.pntd.0002256
7. Van Vinh Chau N, Buu Chau L, Desquesnes M, Herder S, Phu Huong Lan N, Campbell JI, et al. A Clinical and Epidemiological Investigation of the First Reported Human Infection With the Zoonotic Parasite Trypanosoma Evansi in Southeast Asia. *Clin Infect Dis* (2016) 62:1002–8. doi: 10.1093/cid/ciw052
8. Seed JR, Sechelski JB, Ortiz JC, Chapman JF. Relationship Between Human Serum Trypanocidal Activity and Host Resistance to the African Trypanosomes. *J Parasitol* (1993) 79:226–32. doi: 10.2307/3283512
9. Radwanska M, Vereecke N, Deleeuw V, Pinto J, Magez S. Salivarian Trypanosomosis: A Review of Parasites Involved, Their Global Distribution and Their Interaction With the Innate and Adaptive Mammalian Host Immune System. *Front Immunol* (2018) 9:2253. doi: 10.3389/fimmu.2018.02253
10. Hoare CA. Vampire Bats as Vectors and Hosts of Equine and Bovine Trypanosomes. *Acta Trop* (1965) 22:204–16. doi: 10.5169/seals-311269
11. Hoare CA. The Trypanosomes of Mammals: A Zoological Monograph. *Med J Aust* (1973) 1:140–0. doi: 10.5694/j.1326-5377.1973.tb119667.x
12. Sumba AL, Mihok S, Oyieke FA. Mechanical Transmission of Trypanosoma Evansi and T. Congolense by Stomoxys Niger and S. Taeniatus in a Laboratory Mouse Model. *Med Vet Entomol* (1998) 12:417–22. doi: 10.1046/j.1365-2915.1998.00131.x
13. Autyi H, Torr SJ, Michoel T, Jayaraman S, Morrison LJ. Cattle Trypanosomosis: The Diversity of Trypanosomes and Implications for Disease Epidemiology and Control. *OIE Rev Sci Tech* (2015) 34:587–98. doi: 10.20506/rst.34.2.2382
14. Morrison LJ, Vezza L, Rowan T, Hope JC. Animal African Trypanosomiasis: Time to Increase Focus on Clinically Relevant Parasite and Host Species. *Trends Parasitol* (2016) 32:599–607. doi: 10.1016/j.pt.2016.04.012
15. Vickerman K, Myler PJ, Stuart KD. African Trypanosomiasis. In: KS Warren, editor. *Immunology and Molecular Biology of Parasitic Infections*. Cambridge: Blackwell Scientific Publications (1993) 610.
16. Desquesnes M, Holzmuller P, Lai DH, Dargantes A, Lun ZR, Jittaplapong S. Trypanosoma Evansi and Surra: A Review and Perspectives on Origin, History, Distribution, Taxonomy, Morphology, Hosts, and Pathogenic Effects. *BioMed Res Int* (2013) 2013:22. doi: 10.1155/2013/194176
17. FAO. African Animal Trypanosomiasis - PART I. DISEASE AND CHEMOTHERAPY. *Biol World Anim Rev* (1983) 37:1–22.
18. Magez S, Li Z, Nguyen HTT, Torres JEP, Van Wielendaele P, Radwanska M, et al. The History of Anti-Trypanosome Vaccine Development Shows That Highly Immunogenic and Exposed Pathogen-Derived Antigens are Not Necessarily Good Target Candidates: Enolase and Isg75 as Examples. *Pathogens* (2021) 10:1050. doi: 10.3390/pathogens10081050
19. Magez S, Caljon G, Tran T, Stijlemans B, Radwanska M. Current Status of Vaccination Against African Trypanosomiasis. *Parasitology* (2010) 137:2017–27. doi: 10.1017/S0031182010000223
20. Namangala B. How the African Trypanosomes Evade Host Immune Killing. *Parasite Immunol* (2011) 33:430–7. doi: 10.1111/j.1365-3024.2011.01280.x
21. Magez S, Pinto Torres JE, Obishakin E, Radwanska M. Infections With Extracellular Trypanosomes Require Control by Efficient Innate Immune Mechanisms and Can Result in the Destruction of the Mammalian Humoral Immune System. *Front Immunol* (2020) 11:382. doi: 10.3389/fimmu.2020.00382
22. Onah DN, Hopkins J, Luckins AG. Induction of CD4+CD8+ Double Positive T Cells and Increase in CD5+ B Cells in Efferent Lymph in Sheep Infected With Trypanosoma Evansi. *Parasite Immunol* (1998) 20:121–34. doi: 10.1111/j.1365-3024.1998.00125.x

23. Onah DN, Hopkins J, Luckins AG. Changes in Peripheral Blood Lymphocyte Subpopulations and Parasite- Specific Antibody Responses in Trypanosoma Evansi Infection of Sheep. *Parasitol Res* (1999) 85:263–9. doi: 10.1007/s004360050545
24. Onah DN, Hopkins J, Luckins AG. Increase in CD5+ B Cells and Depression of Immune Responses in Sheep Infected With Trypanosoma Evansi. *Vet Immunol Immunopathol* (1998) 63:209–22. doi: 10.1016/S0165-2427(97)00147-5
25. Coen PG, Luckins AG, Davison HC, Woolhouse MEJ. Trypanosoma Evansi in Indonesian Buffaloes: Evaluation of Simple Models of Natural Immunity to Infection. *Epidemiol Infect* (2001) 126:111–8. doi: 10.1017/s0950268801004964
26. Li SQ, Fung MC, Reid SA, Inoue N, Lun ZR. Immunization With Recombinant Beta-Tubulin From Trypanosoma Evansi Induced Protection Against T. Evansi, T. Equiperdum and T. B. Brucei Infection in Mice. *Parasite Immunol* (2007) 29:191–9. doi: 10.1111/j.1365-3024.2006.00933.x
27. Kurup SP, Tewari AK. Induction of Protective Immune Response in Mice by a DNA Vaccine Encoding Trypanosoma Evansi Beta Tubulin Gene. *Vet Parasitol* (2012) 187:9–16. doi: 10.1016/j.vetpar.2012.01.009
28. Lubega GW, Byarugaba DK, Prichard RK. Immunization With a Tubulin-Rich Preparation From Trypanosoma Brucei Confers Broad Protection Against African Trypanosomosis. *Exp Parasitol* (2002) 102:9–22. doi: 10.1016/S0014-4894(02)00140-6
29. Stijlemans B, Baral TN, Guilliams M, Brys L, Korf J, Drennan M, et al. A Glycosylphosphatidylinositol-Based Treatment Alleviates Trypanosomiasis-Associated Immunopathology. *J Immunol* (2007) 179:4003–14. doi: 10.4049/jimmunol.179.6.4003
30. Autheman D, Crosnier C, Clare S, Goulding DA, Brandt C, Harcourt K, et al. An Invariant Trypanosoma Vivax Vaccine Antigen Induces Protective Immunity. *Nature* (2021) 595:96–100. doi: 10.1038/s41586-021-03597-x
31. Authié E, Boulangé A, Muteti D, Lalmanach G, Gauthier F, Musoke AJ. Immunisation of Cattle With Cysteine Proteinases of Trypanosoma Congolense: Targetting the Disease Rather Than the Parasite. *Int J Parasitol* (2001) 31:1429–33. doi: 10.1016/S0020-7519(01)00266-1
32. Kangethe RT, Boulangé AFV, Coustou V, Baltz T, Coetzer THT. Trypanosoma Brucei Brucei Oligopeptidase B Null Mutants Display Increased Prolyl Oligopeptidase-Like Activity. *Mol Biochem Parasitol* (2012) 182:7–16. doi: 10.1016/j.molbiopara.2011.11.007
33. Boulangé AF, Khamadi SA, Pillay D, Coetzer THT, Authié E. Production of Congopain, the Major Cysteine Protease of Trypanosoma (Nannomonas) Congolense, in Pichia Pastoris Reveals Unexpected Dimerisation at Physiological Ph. *Protein Expr Purif* (2011) 75:95–103. doi: 10.1016/j.pep.2010.09.002
34. Coetzer THT, Goldring JPD, Huson LEJ. Oligopeptidase B: A Processing Peptidase Involved in Pathogenesis. *Biochimie* (2008) 90:336–44. doi: 10.1016/j.biochi.2007.10.011
35. Ferreira LG, Andricopulo AD. Targeting Cysteine Proteases in Trypanosomatid Disease Drug Discovery. *Pharmacol Ther* (2017) 180:49–61. doi: 10.1016/j.pharmthera.2017.06.004
36. Moss CX, Brown E, Hamilton A, van der Veken P, Augustyns K, Mottram JC. An Essential Signal Peptide Peptidase Identified in an RNAi Screen of Serine Peptidases of Trypanosoma Brucei. *PloS One* (2015) 10(3):e0123241. doi: 10.1371/journal.pone.0123241
37. Duxbury RE, Sadun EH. Resistance Produced in Mice and Rats by Inoculation With Irradiated Trypanosoma Rhodesiense. *J Parasitol* (1969) 55:859–65. doi: 10.2307/3277231
38. Duxbury RE, Sadun EH, Wellde BT, Anderson JS, Muriithi IE. Immunization of Cattle With X-Irradiated African Trypanosomes. *Trans R Soc Trop Med Hyg* (1972) 66:349–50. doi: 10.1016/0035-9203(72)90237-4
39. Sadun EH, Johnson AJ, Nagle RB, Duxbury RE. Experimental Infections With African Trypanosomes. V. Preliminary Parasitological, Clinical, Hematological, Serological, and Pathological Observations in Rhesus Monkeys Infected With Trypanosoma Rhodesiense. *Am J Trop Med Hyg* (1973) 22:323–30. doi: 10.4269/ajtmh.1973.22.323
40. Duxbury RE, Sadun EH, West JE. Relative Effectiveness of Neutron and Gamma Radiation of Trypanosomes for Immunizing Mice Against African Trypanosomiasis. *Trans R Soc Trop Med Hyg* (1975) 69:484–5. doi: 10.1016/0035-9203(75)90104-2
41. Sadun EH, Anderson JS, Duxbury RE. Experimental Infections With African Trypanosomes. *Am J Trop Med Hyg* (1972) 21:885–8. doi: 10.4269/ajtmh.1972.21.885
42. Wellde BT, Duxbury RE, Sadun EH, Langbehn HR, Lötzsch R, Deindl G, et al. Experimental Infections With African Trypanosomes: IV. Immunization of Cattle With Gamma-Irradiated Trypanosoma Rhodesiense. *Exp Parasitol* (1973) 34:62–8. doi: 10.1016/0014-4894(73)90063-5
43. Duxbury RE, Anderson JS, Wellde BT, Sadun EH, Muriithi IE. Trypanosoma Congolense: Immunization of Mice, Dogs, and Cattle With Gamma-Irradiated Parasites. *Exp Parasitol* (1972) 32:527–33. doi: 10.1016/0014-4894(72)90071-9
44. Duxbury RE, Sadun EH, Anderson JS. Immunization of Monkeys Against a Recently Isolated Human Strain of Trypanosoma Rhodesiense by Use of Gamma Irradiation. *Trans R Soc Trop Med Hyg* (1973) 67:266–7. doi: 10.1016/0035-9203(73)90172-7
45. Morrison WI, Black SJ, Paris J, Hinson CA, Wells PW. Protective Immunity and Specificity of Antibody Responses Elicited in Cattle by Irradiated Trypanosoma Brucei. *Parasite Immunol* (1982) 4:395–407. doi: 10.1111/j.1365-3024.1982.tb00451.x
46. Hoffman SL, Goh LML, Luke TC, Schneider I, Le TP, Doolan DL, et al. Protection of Humans Against Malaria by Immunization With Radiation-Attenuated Plasmodium Falciparum Sporozoites. *J Infect Dis* (2002) 185:1155–64. doi: 10.1086/339409
47. Hewitson JP, Hamblin PA, Mountford AP. Immunity Induced by the Radiation-Attenuated Schistosome Vaccine. *Parasite Immunol* (2005) 27:271–80. doi: 10.1111/j.1365-3024.2005.00764.x
48. Vieira HGS, Grynberg P, Bitar M, Da Fonseca Pires S, Hilário HO, Macedo AM, et al. Proteomic Analysis of Trypanosoma Cruzi Response to Ionizing Radiation Stress. *PloS One* (2014) 9:e97526. doi: 10.1371/journal.pone.0097526
49. Grynberg P, Passos-Silva DG, Mourão M de M, Hirata R, Macedo AM, Machado CR, et al. Trypanosoma Cruzi Gene Expression in Response to Gamma Radiation. *PloS One* (2012) 7:e29596. doi: 10.1371/journal.pone.0029596
50. Regis-da-Silva CG, Freitas JM, Passos-Silva DG, Furtado C, Augusto-Pinto L, Pereira MT, et al. Characterization of the Trypanosoma Cruzi Rad51 Gene and its Role in Recombination Events Associated With the Parasite Resistance to Ionizing Radiation. *Mol Biochem Parasitol* (2006) 149:191–200. doi: 10.1016/j.molbiopara.2006.05.012
51. Luke TC, Hoffman SL. Rationale and Plans for Developing a non-Replicating, Metabolically Active, Radiation-Attenuated Plasmodium Falciparum Sporozoite Vaccine. *J Exp Biol* (2003) 206:3803–8. doi: 10.1242/jeb.00644
52. Plowe CV, Alonso P, Hoffman SL. The Potential Role of Vaccines in the Elimination of Falciparum Malaria and the Eventual Eradication of Malaria. *J Infect Dis* (2009) 200:1646–9. doi: 10.1086/646613
53. Hoffman SL, Billingsley PF, James E, Richman A, Loyevsky M, Li T, et al. Development of a Metabolically Active, non-Replicating Sporozoite Vaccine to Prevent Plasmodium Falciparum Malaria. *Hum Vaccin* (2010) 6:97–106. doi: 10.4161/hv.6.1.10396
54. El Ridi R, Tallima H. Why the Radiation-Attenuated Cercarial Immunization Studies Failed to Guide the Road for an Effective Schistosomiasis Vaccine: A Review. *J Adv Res* (2015) 6:255–67. doi: 10.1016/j.jare.2014.10.002
55. Papatpremsiri A, Junpue P, Loukas A, Brindley PJ, Bethony JM, Sripa B, et al. Immunization and Challenge Shown by Hamsters Infected With Opisthorchis Viverrini Following Exposure to Gamma-Irradiated Metacercariae of This Carcinogenic Liver Fluke. *J Helminthol* (2016) 90:39–47. doi: 10.1017/S0022149X14000741
56. Bain RK. Irradiated Vaccines for Helminth Control in Livestock. *Int J Parasitol* (1999) 29:185–91. doi: 10.1016/S0020-7519(98)00187-8
57. Hirumi H, Hirumi K. Continuous Cultivation of Trypanosoma Brucei Blood Stream Forms in a Medium Containing a Low Concentration of Serum Protein Without Feeder Cell Layers. *J Parasitol* (1989) 75:985–9. doi: 10.2307/3282883
58. Claes F, Agbo EC, Radwanska M, Te Pas MFW, Baltz T, De Waal DT, et al. How Does Trypanosoma Equiperdum Fit Into the Trypanozoon Group? A Cluster Analysis by RAPD and Multiplex-Endonuclease Genotyping Approach. *Parasitology* (2003) 126:425–31. doi: 10.1017/S0031182003002968

59. Singleton EV, David SC, Davies JB, Hirst TR, Paton JC, Beard MR, et al. Sterility of Gamma-Irradiated Pathogens: A New Mathematical Formula to Calculate Sterilizing Doses. *J Radiat Res* (2020) 61:886–94. doi: 10.1093/jrr/rraa076
60. Herbert WJ, Lumsden WHR. Trypanosoma Brucei: A Rapid 'Matching' Method for Estimating the Host's Parasitemia. *Exp Parasitol* (1976) 40:427–31. doi: 10.1016/0014-4894(76)90110-7
61. Vinet L, Zhedanov A. A 'Missing' Family of Classical Orthogonal Polynomials. *J Phys A Math Theor* (2011) 44:85201. doi: 10.1088/1751-8113/44/8/085201
62. Carnes J, Anupama A, Balmer O, Jackson A, Lewis M, Brown R, et al. Genome and Phylogenetic Analyses of Trypanosoma Evansi Reveal Extensive Similarity to T. Brucei and Multiple Independent Origins for Dyskinetoplasty. *PloS Negl Trop Dis* (2015) 9(1):e3404. doi: 10.1371/journal.pntd.0003404
63. Ashburner M, Ball CA, Blake JA, Botstein D, Butler H, Cherry JM, et al. Gene Ontology: Tool for the Unification of Biology. *Nat Genet* (2000) 25:25–9. doi: 10.1038/75556
64. Walter W, Sánchez-Cabo F, Ricote M. GOplot: An R Package for Visually Combining Expression Data With Functional Analysis: Figure 1. *Bioinformatics* (2015) 31:2912–4. doi: 10.1093/bioinformatics/btv300
65. Brenndörfer M, Boshart M. Selection of Reference Genes for mRNA Quantification in Trypanosoma Brucei. *Mol Biochem Parasitol* (2010) 172:52–5. doi: 10.1016/j.molbiopara.2010.03.007
66. De Menezes VT, Oliveira Queiroz A, Gomes MAM, Marques MAP, Jansen AM. Trypanosoma Evansi in Inbred and Swiss-Webster Mice: Distinct Aspects of Pathogenesis. *Parasitol Res* (2004) 94:193–200. doi: 10.1007/s00436-004-1207-4
67. Wellde BT, Schoenbechler MJ, Diggs CL, Langbehn HR, Sadun EH. Trypanosoma Rhodesiense: Variant Specificity of Immunity Induced by Irradiated Parasites. *Exp Parasitol* (1975) 37:125–9. doi: 10.1016/0014-4894(75)90060-0
68. Uche UE, Jones TW. Early Events Following Challenge of Rabbits With Trypanosoma Evansi and T. Evansi Components. *J Comp Pathol* (1993) 109:1–11. doi: 10.1016/S0021-9975(08)80235-6
69. Uche UE, Jones TW. Protection Conferred by Trypanosoma Evansi Infection Against Homologous and Heterologous Trypanosome Challenge in Rabbits. *Vet Parasitol* (1994) 52:21–35. doi: 10.1016/0304-4017(94)90032-9
70. Magez S, Stijlemans B, Baral T, De Baetselier P. VSG-GPI Anchors of African Trypanosomes: Their Role in Macrophage Activation and Induction of Infection-Associated Immunopathology. *Microbes Infect* (2002) 4:999–1006. doi: 10.1016/S1286-4579(02)01617-9
71. Stijlemans B, Caljon G, Van Den Abbeele J, Van Ginderachter JA, Magez S, De Trez C. Immune Evasion Strategies of Trypanosoma Brucei Within the Mammalian Host: Progression to Pathogenicity. *Front Immunol* (2016) 7:233. doi: 10.3389/fimmu.2016.00233
72. Antoine-Moussiaux N, Magez S, Desmecht D. Contributions of Experimental Mouse Models to the Understanding of African Trypanosomiasis. *Trends Parasitol* (2008) 24:411–8. doi: 10.1016/j.pt.2008.05.010
73. Namangala B, Noël W, De Baetselier P, Brys L, Beschin A. Relative Contribution of Interferon-γ and Interleukin-10 to Resistance to Murine African Trypanosomosis. *J Infect Dis* (2001) 183:1794–800. doi: 10.1086/320731
74. Paulnock DM, Freeman BE, Mansfield JM. Modulation of Innate Immunity by African Trypanosomes. *Parasitology* (2010) 137:2051–63. doi: 10.1017/S0031182010001460
75. Baral TN, De Baetselier P, Brombacher F, Magez S. Control of Trypanosoma Evansi Infection Is IgM Mediated and Does Not Require a Type I Inflammatory Response. *J Infect Dis* (2007) 195:1513–20. doi: 10.1086/515577
76. Tizard I, Nielsen KH, Seed JR, Hall JE. Biologically Active Products From African Trypanosomes. *Microbiol Rev* (1978) 42:661–81. doi: 10.1128/mr.42.4.664-681.1978
77. Antoine-Moussiaux N, Biischer P, Desmecht D. Host-Parasite Interactions in Trypanosomiasis: On the Way to an Antidisease Strategy. *Infect Immun* (2009) 77:1276–84. doi: 10.1128/IAI.01185-08
78. Mansfield JM, Paulnock DM. Regulation of Innate and Acquired Immunity in African Trypanosomiasis. *Parasite Immunol* (2005) 27:361–71. doi: 10.1111/j.1365-3024.2005.00791.x
79. Clayton C, Shapira M. Post-Transcriptional Regulation of Gene Expression in Trypanosomes and Leishmanias. *Mol Biochem Parasitol* (2007) 156:93–101. doi: 10.1016/j.molbiopara.2007.07.007
80. Clayton C. Regulation of Gene Expression in Trypanosomatids: Living With Polycistronic Transcription. *Open Biol* (2019) 9:190072. doi: 10.1098/rsob.190072
81. Cerveny L, Straskova A, Dankova V, Hartlova A, Ceckova M, Staud F, et al. Tetratricopeptide Repeat Motifs in the World of Bacterial Pathogens: Role in Virulence Mechanisms. *Infect Immun* (2013) 81:629–35. doi: 10.1128/IAI.01035-12
82. Urbina JA, Concepcion JL, Rangel S, Visbal G, Lira R. Squalene Synthase as a Chemotherapeutic Target in Trypanosoma Cruzi and Leishmania Mexicana. *Mol Biochem Parasitol* (2002) 125:35–45. doi: 10.1016/S0166-6851(02)00206-2
83. Toh JY, Nkouawa A, Sánchez SR, Shi H, Kolev NG, Tschudi C. Identification of Positive and Negative Regulators in the Stepwise Developmental Progression Towards Infectivity in Trypanosoma Brucei. *Sci Rep* (2021) 11:1–14. doi: 10.1038/s41598-021-85225-2
84. Kolev NG, Ramey-Butler K, Cross GAM, Ullu E, Tschudi C. Developmental Progression to Infectivity in Trypanosoma Brucei Triggered by an RNA-Binding Protein. *Science (80-)* (2012) 338:1352–3. doi: 10.1126/science.1229641
85. Shi H, Butler K, Tschudi C, Biochem M, Author P. A Single-Point Mutation in the RNA-Binding Protein 6 Generates Trypanosoma Brucei Metacyclics That are Able to Progress to Bloodstream Forms *In Vitro* Graphical Abstract HHS Public Access Author Manuscript. *Mol Biochem Parasitol* (2018) 224:50–6. doi: 10.1016/j.molbiopara.2018.07.011
86. Mugo E, Clayton C. Expression of the RNA-Binding Protein RBP10 Promotes the Bloodstream-Form Differentiation State in Trypanosoma Brucei. *PloS Pathog* (2017) 13(8):e1006560. doi: 10.1371/journal.ppat.1006560
87. Cerqueira PG, Passos-Silva DG, Vieira-da-Rocha JP, Mendes IC, de Oliveira KA, Oliveira CFB, et al. Effect of Ionizing Radiation Exposure on Trypanosoma Cruzi Ubiquitin-Proteasome System. *Mol Biochem Parasitol* (2017) 212:55–67. doi: 10.1016/j.molbiopara.2017.01.005
88. Davies AA, Masson JY, McIlwraith MJ, Stasiak AZ, Stasiak A, Venkitaraman AR, et al. Role of BRCA2 in Control of the RAD51 Recombination and DNA Repair Protein. *Mol Cell* (2001) 7:273–82. doi: 10.1016/S1097-2765(01)00175-7
89. Powell SN, Willers H, Xia F. BRCA2 Keeps Rad51 in Line: High-Fidelity Homologous Recombination Prevents Breast and Ovarian Cancer? *Mol Cell* (2002) 10:1262–3. doi: 10.1016/S1097-2765(02)00789-X
90. Ohta K, Nicolas A, Furuse M, Nabetani A, Ogawa H, Shibata T. Mutations in the MRE11, RAD50, XRS2, and MRE2 Genes Alter Chromatin Configuration at Meiotic DNA Double-Stranded Break Sites in Premeiotic and Meiotic Cells. *Proc Natl Acad Sci U S A* (1998) 95:646–51. doi: 10.1073/pnas.95.2.646
91. Daley JM, Chiba T, Xue X, Niu H, Sung P. Multifaceted Role of the Topo Iiiα-RMI1-RMI2 Complex and DNA2 in the BLM-Dependent Pathway of DNA Break End Resection. *Nucleic Acids Res* (2014) 42:11083–91. doi: 10.1093/nar/gku803
92. Vasquez J-JJ, Hon C-CC, Vanselow JT, Schlosser A, Siegel TN. Comparative Ribosome Profiling Reveals Extensive Translational Complexity in Different Trypanosoma Brucei Life Cycle Stages. *Nucleic Acids Res* (2014) 42:3623–37. doi: 10.1093/nar/gkt1386
93. Ingolia NT, Ghaemmaghami S, Newman JRSS, Weissman JS. Genome-Wide Analysis *In Vivo* of Translation With Nucleotide Resolution Using Ribosome Profiling. *Science (80-)* (2009) 324:218–23. doi: 10.1126/science.1168978
94. Awuoche EO, Weiss BL, Mireji PO, Vigneron A, Nyambega B, Murilla G, et al. Expression Profiling of Trypanosoma Congolense Genes During Development in the Tsetse Fly Vector Glossina Morsitans Morsitans. *Parasit Vectors* (2018) 11:1–18. doi: 10.1186/s13071-018-2964-8
95. Athar A, Füllgrabe A, George N, Iqbal H, Huerta L, Ali A, et al. ArrayExpress Update - From Bulk to Single-Cell Expression Data. *Nucleic Acids Res* (2019). doi: 10.1093/nar/gky964

Conflict of Interest: The authors declare that the research was conducted in the absence of any commercial or financial relationships that could be construed as a potential conflict of interest.

this article, or claim that may be made by its manufacturer, is not guaranteed or endorsed by the publisher.

frontiers | Frontiers in Veterinary Science

ORIGINAL RESEARCH
published: 18 May 2022
doi: 10.3389/fvets.2022.859124

Irradiated Non-replicative Lactic Acid Bacteria Preserve Metabolic Activity While Exhibiting Diverse Immune Modulation

Luca Porfiri[1†], Johanna Burtscher[2†], Richard T. Kangethe[1], Doris Verhovsek[3], Giovanni Cattoli[1], Konrad J. Domig[2] and Viskam Wijewardana[1]*

[1] Animal Production and Health Section, Joint Food and Agriculture Organization (FAO)/International Atomic Energy Agency (IAEA) Centre of Nuclear Techniques in Food and Agriculture, International Atomic Energy Agency, Vienna, Austria, [2] Department of Food Science and Technology, Institute of Food Science, University of Natural Resources and Life Sciences, Vienna, Austria, [3] VetFarm Medau, University of Veterinary Medicine Vienna, Berndorf, Austria

In the recent years, safety concerns regarding the administration of probiotics led to an increased interest in developing inactivated probiotics, also called "paraprobiotics". Gamma irradiation represents a promising tool that can be used to produce safe paraprobiotics by inhibiting replication while preserving the structure, the metabolic activity, and the immunogenicity of bacteria. In this study, we evaluated the ability of four strains of lactic acid bacteria (LAB: *Lacticaseibacillus casei, Lactobacillus acidophilus, Lactiplantibacillus plantarum,* and *Lacticaseibacillus paracasei*) in preserving the metabolic activity and the immune modulation of swine porcine peripheral blood mononuclear cells, after gamma irradiation or heat inactivation. Our results show that all four strains retained the metabolic activity following gamma irradiation but not after heat inactivation. In terms of immune-modulatory capacity, irradiated *L. acidophilus* and *Lc. paracasei* were able to maintain an overall gene expression pattern similar to their live state, as heat inactivation did with *Lc. casei*. Moreover, we show that the two inactivation methods applied to the same strain can induce an opposed expression of key genes involved in pro-inflammatory response (e.g., IFNα and interleukin-6 for *Lc. casei*), whereas gamma irradiation of *L. acidophilus* and *Lc. paracasei* was able to induce a downregulation of the anti-inflammatory TGFβ. Taken together, our data show that immune modulation can be impacted not only by different inactivation methods but also by the strain of LAB selected. This study highlights that gamma irradiation harbors the potential to produce safe non-replicative metabolically active LAB and identifies immunomodulatory capacities that may be applied as vaccine adjuvants.

Keywords: lactic acid bacteria, gamma irradiation, vaccine adjuvant, immune modulation, metabolic activity

OPEN ACCESS

Edited by:
Anil Kumar Puniya, National Dairy Research Institute (ICAR), India

Reviewed by:
Maryam Dadar, Razi Vaccine and Serum Research Institute, Iran
Alex Galanis, Democritus University of Thrace, Greece
Atte Von Wright, University of Eastern Finland, Finland
Joyce A. Ibana, University of the Philippines Diliman, Philippines

***Correspondence:**
Viskam Wijewardana
v.wijewardana@iaea.org

† These authors have contributed equally to this work

Specialty section:
This article was submitted to Veterinary Infectious Diseases, a section of the journal Frontiers in Veterinary Science

Received: *20 January 2022*
Accepted: *07 April 2022*
Published: *18 May 2022*

Citation:
Porfiri L, Burtscher J, Kangethe RT, Verhovsek D, Cattoli G, Domig KJ and Wijewardana V (2022) Irradiated Non-replicative Lactic Acid Bacteria Preserve Metabolic Activity While Exhibiting Diverse Immune Modulation. Front. Vet. Sci. 9:859124. doi: 10.3389/fvets.2022.859124

INTRODUCTION

Most probiotics belong to the group of gram-positive, non-pathogenic lactic acid bacteria (LAB) (1), which can be found in different niches (e.g., plants, milk, and gastrointestinal tracts) (2) and are able to produce large amounts of lactic acid by fermenting carbohydrates, often linked to health-promoting effects (3). Bifidobacteria and lactobacilli are among the most extensively studied probiotic LAB (4, 5). The generic term "lactobacilli" refers to all genera that were classified as *Lactobacillaceae* until a reclassification and introduction of 25 new genera in 2020 (6). Specifically, some lactobacilli strains, such as the ones evaluated in this study, *Lacticaseibacillus casei, Lactobacillus acidophilus, Lactiplantibacillus plantarum,* and *Lacticaseibacillus paracasei,* have been proven to be particularly capable of stimulating both the intestinal mucosa and the systemic immune response, thus taking the name of "immunobiotics" (7), showing both Th1 and Th2 responses (8–10), which undoubtedly represent remarkable intrinsic adjuvanticity capacities (11, 12). These immunomodulatory effects are exerted through their interaction with different types of immune cells, including lymphocytes, NK cells, and antigen-presenting cells (5, 7). What is intriguing is the capacity of some LAB to induce a balanced pro- and anti-inflammatory action (13). This is achieved by the activation of different pathways leading to a broad and diverse expression of T helper cell subsets, such as Th1, Th2, Th17, and T-regulatory (Treg), inducing the production of different sets of cytokines (14). A broad and diverse immune stimulation is a common characteristic of vaccine adjuvants (15), and some LAB strains have displayed a notable potential for their application in several vaccine formulations (16–18).

Nevertheless, there is an aspect that needs to be considered and evaluated regarding the administration of probiotics, and this regards safety; in fact, although many lactic acid bacteria strains are considered as Generally Recognized as Safe (GRAS), in the recent years, several potential side effects have been documented for some strains, including intestinal probiotic overgrowth, gastrointestinal symptoms (e.g., vomiting, diarrhea, and nausea), bloodstream infection (e.g., bacteremia, sepsis, and peritonitis), excess D-lactate production, dysbiosis, and horizontal gene transfer (19–21). The latter is of particular concern because it can severely contribute to the diffusion of antibiotic resistance, already representing a global threat to human and animal health (22). Considering these factors, current literature review is fostering a debate on whether probiotics need exclusively to be "alive" to induce health benefits to the host organism (23). In fact, more evidence is emerging that also, nonviable probiotic strains are able to provide beneficial effects (24). Since most of the live probiotics ingested are not able to survive the harsh condition of the stomach and intestine, resulting in a severely affected viability of these products (25), most of the health benefits related to probiotics may be attributable to their metabolites and their cell surface components (24), which would therefore be independent from whether they are administered live or inactivated. This noteworthy perspective led to a new interest to explore the application of the so-called paraprobiotics (also called "ghost," or inactivated probiotics) (26), which in addition to being safer (27), which would have advantages in terms of longer shelf life and more favorable storage and transport conditions (24), especially to those areas where strict handling conditions cannot be met (e.g., developing countries) (23).

Among the different methods of inactivation to generate paraprobiotics (26, 28), gamma irradiation technology, which is usually applied to inactivate or sterilize microbes (29), can be used, at optimal doses, to stop the replication of bacteria and parasites while preserving their structure and their metabolic activity (30). This leads to inactivated bacteria which is defined as "metabolically-active non-replicative," potentially preserving all (or most of) the characteristics of the live bacterium while guaranteeing a high level of safety. Evidence showed that gamma irradiation successfully protected surface antigens and cell composition of bacteria compared to other means of inactivation (e.g., heat treatment) (31). Despite the great potential of this technology, few studies in the literature explored the application of gamma irradiation to generate paraprobiotics. Almada et al. (28), for instance, have explored how different strains of lactobacilli (and bifidobacteria) display a different degree of resistance to gamma irradiation, besides investigating several other aspects, such as cultivability, integrity, and physiology. Raz and Rachmilewitz (32) indicated how a mix of paraprobiotics (among which *Lc. casei, Lp. plantarum,* and *L. acidophilus*), obtained by radiation, was more effective in the treatment of colitis in animal models than those inactivated by heat treatment. In contrast, according to Kamiya et al. (33), neither gamma irradiation nor heat inactivation was effective in preserving the inhibitory capacity on visceral pain induced by colorectal distension in rats of *L. reuteri*.

Therefore, in this comparative study, we investigated the ability of four different LAB strains, irradiated with gamma rays, inactivated with heat treatment, and in their live form, to stimulate the immune response of *ex vivo* porcine peripheral blood mononuclear cells (PBMCs), by evaluating the gene expression of 26 immune markers (related to transcription factors, pathogen recognition receptors, innate and adaptive immune response) using quantitative real-time PCR. The application of this panel aims at analyzing the expression of different immune markers involved in different pathways and immunological responses at the same time, providing a broader picture and a more extensive understanding, compared to similar studies, of the immune modulation exerted by this type of lactic acid bacteria.

MATERIALS AND METHODS

Preparation of Bacterial Suspensions

A total of four strains of LAB were used for the experiments in this study: *L. acidophilus* (*L. acidophilus* LMG 9433, type strain), *Lp. plantarum* subsp. *plantarum* (*Lp. plantarum* DSM 20205), *Lc. casei* (*Lc. casei* LMG 6904, type strain), and *Lc. paracasei* subsp. *paracasei* (*Lc. paracasei* LMG 12586). All cultivation steps were performed in Lactobacillus broth acc. to De Man, Rogosa and Sharp (MRS) broth (Merck KGaA, Darmstadt, Germany) under anaerobic conditions using a jar gassing system (gas

mixture containing 80% N_2, 10% CO_2, and 10% H_2; Don Whitley Scientific, West Yorkshire, UK) at 37°C (LMG 9433) or 30°C (DSM 20205, LMG 6904, and LMG 12586). Cell suspensions for inactivation experiments were produced by transferring 800 µl of an overnight culture of each strain into 80 ml of pre-warmed MRS broth followed by an anaerobic incubation for 24 h. MRS broth was removed by centrifugation at 8,000 × *g* for 6 min and by discarding the supernatant. Bacterial biomass was washed by two cycles of resuspension of the biomass in 40 ml of sterile phosphate-buffered saline (PBS, Merck KGaA, Darmstadt, Germany) and subsequent centrifugation as described above. The resulting supernatants were discarded. Subsequently, based on OD measurements at 625 nm, the samples were diluted with PBS to reach the target concentration of 10^8 cfu/ml. The suspension was centrifuged again using the conditions described above, and the resulting biomass without supernatant was resuspended in 75% v/v of the original volume of PBS. The remaining 25% v/v was supplemented with 1 M trehalose, resulting in approximately 80 ml of bacterial suspension containing 10^8 cfu/ml. Aliquots (2.3 ml each) of the final suspension were distributed into 32 cryovials and stored at −80°C until further analysis.

Gamma Irradiation and Heat Inactivation of LAB Strains

Gamma irradiation was performed at International Atomic Energy Agency (IAEA) laboratories in Seibersdorf (Austria) using Cobalt60-source 812 Irradiator from Foss Therapy Services, Inc (34). About eight doses were used to assess the D10 dose: 250, 500, 750, 1,000, 1,500, 2,000, 2,500, and 3,000 Gy. About 50-ml Falcon conical tubes, containing the cryovials, were placed inside a 2.5 l Bio-Bottle (Orange Bio-Bottle; UN Specification Mark: 4GU/Class 6.2) filled with dry ice, to maintain the frozen state, which was eventually inserted into the irradiator. Following irradiation, vials were kept at −80°C until decimal dilutions of all samples. Controls were streaked on MRS agar (Merck KGaA, Darmstadt, Germany) and incubated anaerobically for 72 h to determine viable cell counts in cfu/ml. Next, the survival fraction percentage of each strain of LAB was determined against the different irradiation doses tested to calculate the D10 value.

D10 value is defined as the ability of gamma irradiation to reduce an exposed microbial population by 90%(one $\log_{10}$) under standard conditions of time, temperature, and dose. This value for the different LAB strains was calculated using the inverse of the slope of the regression lines (−1/slope) of gamma irradiation dose against survival fraction (log) (35, 36) using GraphPad Prism version 9.1.2 for (GraphPad Software, San Diego, California USA, www.graphpad.com). Once the D10 value was assessed, the minimum dose needed for the complete inactivation of bacteria was determined by multiplying the D10 value × log concentration of the batch. To have a safety margin and for the easiness of delivering a precise gamma irradiation dose over multiple experiments, we added 1.5 of D10 dose on top of the estimated lethal dose and rounded up to the nearest 500 Gy. These additional irradiation doses provided were herein being termed as "safety inhibitory dose (SID)."

A total of three doses of gamma irradiation were used to assess metabolic activity: a low universal dose to reduce growth (3,000 Gy), a strain-dependent SID, and a high universal dose (10,000 Gy). The procedure described above was then applied to irradiate LAB at these three doses. Additional samples were prepared (and aliquoted) as described above, inactivated *via* heat treatment at 95°C for 10 min, and finally stored at −80°C. Colony counts were done as described above following irradiation at 3,000 Gy, SID, 10,000 Gy, or after heat treatment.

Metabolic Activity and Membrane Integrity

Metabolic activity of live, gamma-irradiated, and heat-inactivated bacteria was determined by measuring redox potential (using the resazurin-based cell-permeable compound Alamar blue) and by adenosine triphosphate (ATP) production. The Alamar blue assay was performed using Alamar blue cell viability reagent (Thermo Fisher: catalog no. DAL1025) according to the manufacturer's protocol. Briefly, frozen LAB samples were thawed and mixed well, and 90 µl bacterial suspension was added to black 96-well assay plates. These plates were incubated at 37°C for 15 min, and then, 10 µl of Alamar blue solution was added and was incubated for another 2 h at 37°C. The metabolic activity was measured as the fluorescence intensity emitted at 590 nm (excitation at 560 nm) using a microplate reader. ATP production was measured with the BacTiter-GloTM Microbial Cell Viability Assay (Promega, Madison, WI, United States) according to the manufacturer's protocol. Briefly, 100 µl of LAB samples was added to opaque-walled 96-well plates and were incubated at 37°C for 15 min. Next, 100 µl of BacTiter-Glo™ Reagent was added, mixed, and then incubated at room temperature for 5 min in a shaker. Following the incubation, the luminescence was measured using a microplate reader. ATP concentrations were calculated from a standard curve.

Membrane integrity was measured using LIVE/DEAD™ BacLight™ Bacterial Viability Kit (Molecular Probes®, Grand Island, NY, United States). This kit contains mixtures of SYTO® 9 green-fluorescent nucleic acid stain and the red-fluorescent nucleic acid stain, propidium iodide. The SYTO 9 stain labels all bacteria in a population while propidium iodide penetrates only bacteria with damaged membranes. The assay was performed according to the manufacturer's protocol with slight modifications. Briefly, 100 µl of 10-fold diluted samples was aliquoted into dark 96-well assay plates, and 1 µl of propidium iodide and SYTO 9 mixture was added and mixed. After 15 min of incubation at 37°C, plates were read at 485/530 (excitation/ emission) and 485/630 (excitation/ emission). The membrane integrity was assessed as fluorescence intensity of SYTO 9/propidium iodide.

Isolation of Swine PBMCs and Their Stimulation

Blood samples were obtained from healthy adult sows, aged between 12 and 48 months, raised in the teaching and research farm of the University of Veterinary Medicine, Vienna, Austria. Whole blood was obtained by puncture of the jugular vein with heparinized Primavette® V Li.-Heparin 10-ml tubes (Kabe Labortechnik GmbH, Germany). Blood collection and animal

handling were performed according to the accepted animal welfare standards (37). None of the animals included in the study showed any signs of clinical disease. The herd is free of Porcine Reproductive and Respiratory Syndrome Virus (PRRSV) and the sows were vaccinated against porcine parvovirus (PPV), porcine circovirus type 2 (PCV-2), and *Erysipelothrix rhusiopathiae*. The blood collection was approved by the University of Veterinary Medicine Vienna's Ethics and Animal Welfare Committee and the Austrian Ministry of Research and Science's Advisory Committee for Animal Experiments (BMBWF-68.205/0192-V3b/2018). Swine PBMCs were isolated and handled as described previously for other species (38). Briefly, fresh blood was first carefully layered over Ficoll-Paque PLUS (Sigma) in a 50-ml Falcon conical tube. Successively, PBMCs were isolated by density gradient centrifugation for 35 min at 800 × *g* at 20°C, allowing the collection at the plasma/Ficoll interface using a Pasteur pipette, and washed three times with PBS to remove the platelets and cell debris. PBMCs were then resuspended in complete medium containing RPMI 1640, 10% fetal bovine serum (FBS), and a solution containing penicillin, streptomycin, and amphotericin B (Antibiotic-Antimycotic, Thermo Fisher Scientific) at a concentration of 10×10^6 cells/ml. Following, cells were incubated at 37°C in an atmosphere of 5% CO_2 for 2 h to remove any contaminating bacteria or molds. Next, antibiotics and antimycotic were removed with two washing cycles using only medium (RPMI 1640), centrifuging at 1,500 rpm at 4°C for 7 min. The resulting cell pellet was resuspended using antibiotic-free medium (RPMI 1640, 10% FBS) at a concentration of 4×10^6 cells/ml, and aliquots of 5 ml per well were distributed in 6-well plates. Next, PBMCs were incubated without (negative control) or with 50 μl of either live, gamma-irradiated, heat-inactivated LAB or various stimulation cocktails as positive controls (concanavalin A or phorbol 12-myristate13-acetate and ionomycin or pokeweed mitogen) at a concentration described previously (38). In each single experiment, PBMCs from one animal were stimulated with all the strains selected (and with various treatments), and the procedure was replicated for each of the five animals. During preliminary experiments, two amounts of LAB stimulation were tested (50 and 250 μl) which showed no difference in immune modulation (data not shown). After 16 h of incubation, PBMCs were harvested and washed with PBS, and resulting cell pellet was resuspended in 700 μl of RLT buffer and stored at −80°C.

Quantitative Expression Analysis by Quantitative Real-Time PCR

RNA extraction of the samples was performed using Direct-Zol RNA Miniprep Plus (ZYMO Research). All steps were performed at room temperature and centrifugation at 10,000 × *g* for 30 s. First, an equal volume (700 μl) of ethanol (95–100%) was added to a sample lysed in RLT buffer and mixed thoroughly. The mixture was transferred into a Zymo-Spin™ IIICG Column2 in a collection tube and centrifuged. The column was transferred into a new collection tube and the flow-through was discarded. For DNase treatment, 400 μl RNA Wash Buffer was added to the column and centrifuged. Then, in an RNase-free tube, 5 μl of DNase I (6 U/μl) and 75 μl DNA digestion buffer were added. After incubation at room temperature (20–30°C) for 15 min, 400 μl of Direct-zol™ RNA PreWash5 was added to the column and centrifuged. About 700 μl of RNA Wash Buffer was then added to the column and centrifuged for 1 min to ensure complete removal of the wash buffer. Eventually, the mix was transferred to the column into an RNase-free tube. Finally, 50 μl of DNase/RNase-Free water was added directly to the column matrix and centrifuged, and the RNA was collected in a 1.5-ml Eppendorf tube. The quantity and purity of RNA were assessed using a NanoDrop ND-1000 Spectrophotometer (Thermo Fisher Scientific, MA, USA). The A260:280 ratio was in a range of 2.0–2.2 for all samples, and RNA was resuspended to a final concentration of 1 μg/μl. Total RNAs from each sample were reverse-transcribed and treated with RNAse using the SuperScriptTM III First-Strand Synthesis System using random hexamer primers (Invitrogen™, Life Technologies™, USA) according to the manufacturer's instruction. Generated complementary DNA (cDNA) was stored at −20°C or used directly for amplification at a working dilution of 1:100 (38).

A panel of 26 immune markers, including 18 cytokines: tumor necrosis factor alpha (TNFα), interferon alpha (IFNα), interferon gamma (IFNγ), interleukin (IL)1α, IL6, IL15, IL17, IL18, IL21, IL1β, IL2, IL23, IL8, IL12β, IL10, IL5, IL13, transforming growth factor beta (TGFβ) related to Th1, Th2, Th17, and T regulatory (Treg) responses; two transcription factor genes: nuclear factor kappa-light-chain-enhancer of activated B cells (NFKb)50, NFKb65; six pathogen-recognition receptors: retinoic acid-inducible gene I (RIG-1), toll-like receptor (TLR)2, TLR3, TLR4, TLR9, cluster of differentiation 163 (CD163), and glyceraldehyde 3-phosphate dehydrogenase (GAPDH) as a housekeeping gene, was generated and used to evaluate gene expression using quantitative real-time PCR (Bio-Rad). Primers were either obtained from previous studies or designed using NCBI-Primer BLAST using targeted swine genes (**Supplementary Table S1**). The primers were validated by melting curve analysis. Quantitative real-time PCR (qPCR) was performed as previously described (38). Briefly, qPCRs were set up for diluted cDNA samples (1:100) in a final volume of 20 μl using iQTM SYBR® Green Supermix (Bio-Rad Laboratories, Hercules, USA) and primers at 1.25 μM concentration. The qPCR was performed in a CFX96TM Real-Time PCR detection system (Bio-Rad) with an initial denaturation step of 3 min at 95°C, followed by 40 cycles of 10 s at 95°C, 20 s at 59°C, and 20 s at 72°C with fluorescence read during extension. The melting curves (Tm) of amplicons were analyzed at 65–95°C with 0.5°C increments for every 5 s. Template controls (NTC) without cDNA template were run in parallel. qPCR for samples and controls ($n = 5$) was run in triplicates. C_q values were noted for further analysis, and the melting temperature (T_m) of each amplicon was verified for specificity. Analysis to determine relative gene expression was done using the comparative C_t (ΔC_t) method, where the expression of each gene was normalized to GAPDH as internal gene, and overall fold change of targeted genes against untreated controls was calculated as $\Delta\Delta C_t$ (39). The choice of GAPDH as the reference gene was made following an efficiency test evaluation of five different housekeeping genes [actin, 18S, GAPDH, cyclophilin, and peptidylprolyl isomerase A (PPIA)] with the web-based tool RefFinder (40) which, by integrating the major available computational programs

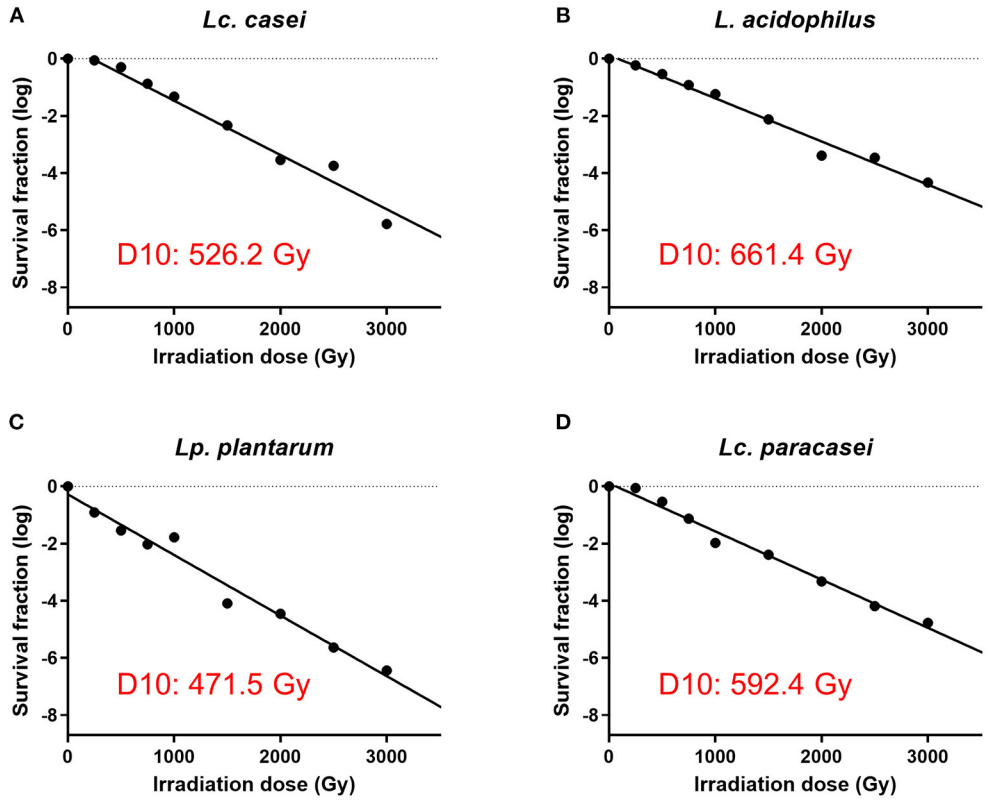

FIGURE 1 | Assessment of surviving fraction at increasing irradiation doses and calculation of the D10 value. The four strains of LAB were irradiated with eight increasing doses of gamma irradiation (250, 500, 750, 1,000, 1,500, 2,000, 2,500, and 3,000 Gy) and the surviving fraction of bacteria was enumerated. D10 value of each strain was calculated using the inverse of the slope of the regression lines (−1/slope) of gamma irradiation dose against survival fraction (log) using GraphPad Prism 9. D10 values are as follows: 526.2 Gy for *Lacticaseibacillus casei* **(A)**, 661.4 Gy for *Lactobacillus acidophilus* **(B)**, 471.5 Gy for *Lactiplantibacillus plantarum* **(C)**, and 592.4 Gy for *Lacticaseibacillus paracasei* **(D)**.

(geNorm, NormFinder, BestKeeper, and the comparative Delta-Ct method), ranked GAPDH as the most stable gene among the ones evaluated (data not shown).

Statistical Analysis

To compare different treatments on PBMCs, one-way ANOVA (Kruskal–Wallis test) followed by Dunn's multiple comparisons test was performed using GraphPad Prism. Statistically significant ($P < 0.05$) gene-expression differences were graphically represented by a separated scatter graph showing individual and mean values. Heat maps showing hierarchical clustering based on one minus Pearson correlation were generated using the software Morpheus (https://software.broadinstitute.org/morpheus).

RESULTS

The Irradiation Dose Needed to Inhibit the Replication Is Strain-Dependent in LAB

In our first experiment, we determined the irradiation dose that is needed to stop the replication of four strains of LAB, namely, *Lc. casei, L. acidophilus, Lc. paracasei, and Lp. plantarum*. This was done by treating LAB with increasing doses of gamma irradiation and enumerating the surviving fraction of bacteria. The D10 values of each strain were calculated, where the D10 value represents the dose of irradiation needed to lower the concentration of an organism by one log. The results showed (**Figure 1** and **Supplementary Figure S1**) that the D10 values assessed were 526.2, 661.4, 592.4, and 471.5 Gy for *Lc. casei, L. acidophilus, Lc. paracasei,* and *Lp. plantarum,* respectively; thus, at concentrations of 10^9 cfu/ml, the minimum dose needed for the complete inhibition of replication was estimated as 4,735.8, 5,952. Gy, 5,331.6, and 4,243.5 Gy, which were then rounded up to 5,500, 7,000, 6,000, and 5,000 Gy, respectively (SID; as explained in the M&M). Colony counts confirmed that there was no growth following treatments at SID, 10,000 Gy, or after heat treatment, whereas at 3,000 Gy, all the strains produced colonies.

Lethal Irradiation Preserves the Membrane Integrity and the Metabolic Activity in LAB

Since few reports (30, 41) have stated the ability of gamma-irradiated replication-incompetent bacteria to maintain residual metabolic activity, an experiment was conducted to assess

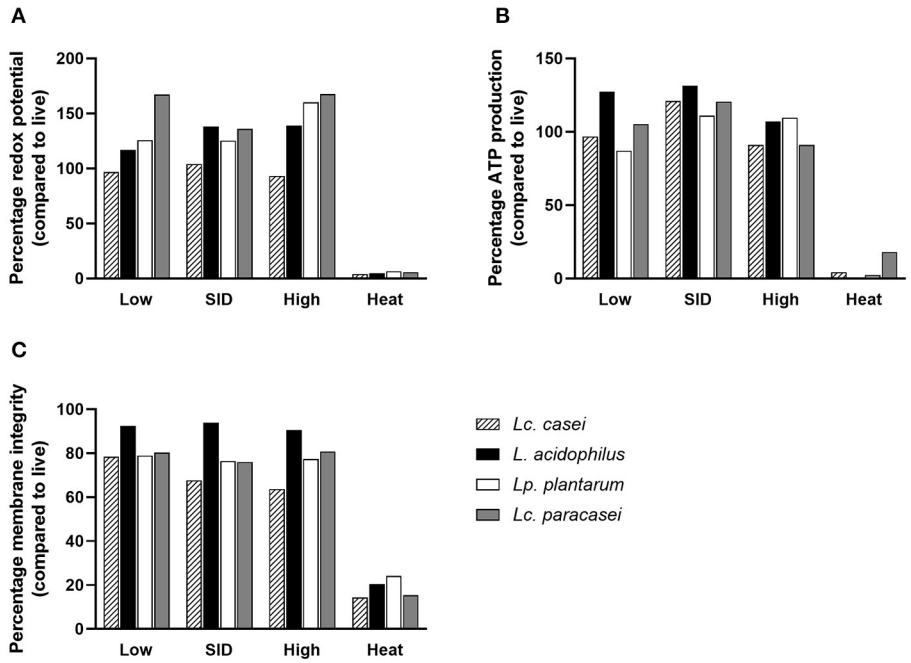

FIGURE 2 | Metabolic activity and membrane integrity. Percentages of redox potential **(A)**, ATP production **(B)**, and membrane integrity **(C)** of irradiated and heat-inactivated *Lacticaseibacillus casei* (pattern-filled), *Lactobacillus acidophilus* (black), *Lactiplantibacillus plantarum* (white), and *Lacticaseibacillus paracasei* (gray) compared to live bacteria are shown. Mean values derived from triplicates are shown in each graph. Irradiation doses: low (3,000 Gy), SID (variable doses according to the strain), high (10,000 Gy); heat treatment: 95°C, 10 min.

whether the LAB strains in our study were able to preserve metabolic activity in comparison with heat-inactivated and live (as a calibrator) lactic acid bacteria. To further characterize the effect of irradiation on the metabolic activity, we irradiated LAB with three levels of gamma irradiation doses: SID (as stated above, variable doses for each strain), or lower (low; 3,000 Gy), or higher (high; 10,000 Gy) irradiation dose. Different doses of gamma rays depend on the exposure time of the sample to the radiation source (^{60}Co). The calculation is based on the *absorbed dose constant,* which is related to the decay energy and time of the radioactive source. For ^{60}Co, it is equal to 0.35 mSv/ (GBq h) at 1 m from the source. This allows the calculation of the equivalent dose, which depends, as described, on distance and activity. Therefore, the three doses were delivered by calculating the exposure time based on the current dose rate (on the day that irradiation was performed) (34). To characterize treated LAB, two parameters were measured: metabolic activity (as redox potential and ATP production) and membrane integrity. Results suggest that metabolic activity of irradiated LAB was preserved at all three doses tested (**Figure 2**), corroborating the findings of other reports. Interestingly, metabolic activity was preserved even at higher doses (10,000 Gy) of irradiation despite delivering a dose nearly that of two times the SID. Surprisingly, we report that the metabolic activity was even higher following irradiation compared to live bacteria in terms of redox potential and ATP production. Conversely, heat inactivation led to less or no metabolic activity post-treatment. In the case of membrane integrity, a parameter that reflects structure preservation, irradiated LAB were able to preserve the membrane integrity although less than the live bacteria (as a percentage), while heat inactivation, as expected, led to a damaged membrane showing minimum membrane integrity.

Immune Modulation of Swine PBMCs by Live and Treated LAB

Immune Modulation by Each Live LAB Has Shared Features but Is Unique to Each Strain

Finally, we investigated whether metabolically active non-replicative LAB could resemble their live counterparts in immunomodulatory function. To this end, the expression of 26 immune markers on porcine PBMCs was measured in an *in vitro* end-point assay. We first aimed to identify the degree of immune-modulation similarity among the four strains of LAB that we investigated in their live form. As shown in **Figure 3A**, according to the hierarchical clustering of immune marker expression heat maps, two disparate similarities were identified. Although being genetically more similar to *Lc. paracasei, Lc. casei* showed similar immune marker expression to *L. acidophilus*, whereas *Lc. paracasei* turned out to be more similar to *Lp. plantarum.*

Preservation of Immune Modulation Following Treatment Is More Common With Gamma Irradiation Compared to Heat Treatment

In a subsequent analysis, we examined how different treatments, such as gamma irradiation or heat inactivation, could alter the ability of each LAB strain in modulating the immune

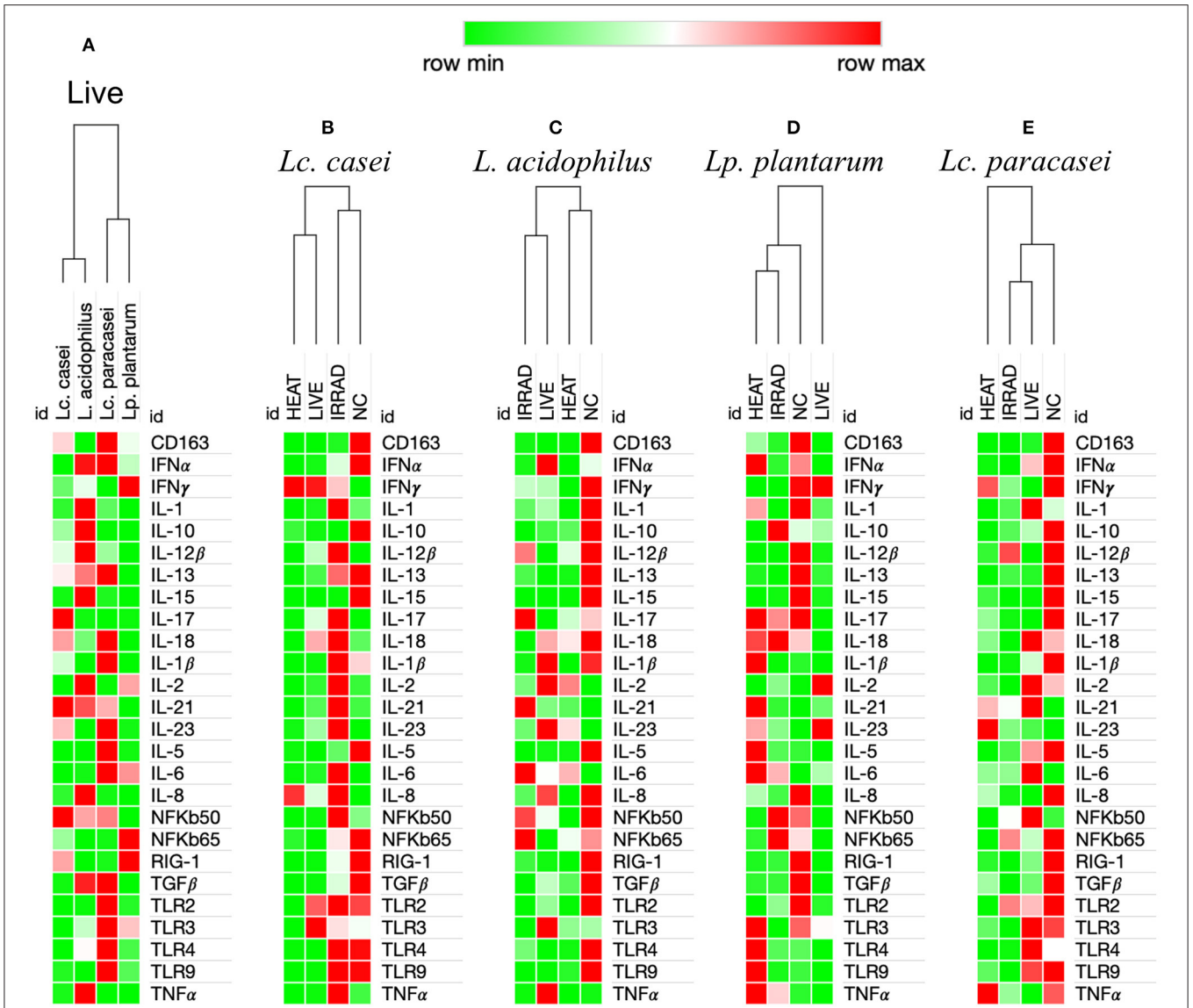

FIGURE 3 | Heat maps analysis of gene expression regulation of 26 immune markers in porcine PBMCs induced by viable and nonviable lactobacilli. Degree of similarity based on one minus Pearson correlation hierarchical clustering in the immune modulation exerted by LAB on the up-(red) or downregulation (green) of 26 immune markers in porcine peripheral blood mononuclear cells. This analysis was performed based upon $\Delta\Delta C_t$ differences among the four live lactobacilli strains **(A)**, and based upon ΔC_t differences among PBMCs unstimulated (NC) and stimulated with live, gamma-irradiated, and heat-treated *Lacticaseibacillus casei* **(B)**, *Lactobacillus acidophilus* **(C)**, *Lactiplantibacillus plantarum* **(D)**, and *Lacticaseibacillus paracasei* **(E)**. Values in the heat map are mapped to colors using the minimum and maximum of each row independently.

system in comparison with their live state. Unstimulated PBMCs were used as the negative control. According to heat map analysis of global expression of the target immune markers, heat-treated and live *Lc. casei* stimulated gene expression in porcine PBMCs similarly; on the contrary, irradiated *Lc. casei* showed less effect in immune modulation, displaying a profile more similar to the negative control (non-stimulated PBMC) as shown in **Figure 3B**. When the expression of each target gene was examined individually (**Figure 4A**), heat-treated *Lc. casei* induced a significant 2.5-fold downregulation of IFNα compared to the negative control, whereas irradiated *Lc. casei* induced a significant 1-fold upregulation of IL-6 compared to the untreated.

Heat maps for *L. acidophilus* (**Figure 3C**) showed that the irradiated strain could preserve similar immune-modulatory characteristics as the live state, whereas heat treatment led to an immune landscape comparable to the untreated, showing less or no effect. In terms of individual gene expression, irradiated *L. acidophilus* was able to induce a significant 1.5-fold upregulation of IL-21 and a significant one-fold downregulation of TGFβ, whereas live *L. acidophilus* induced a significant one-fold downregulation of TLR9 expression (**Figure 4B**).

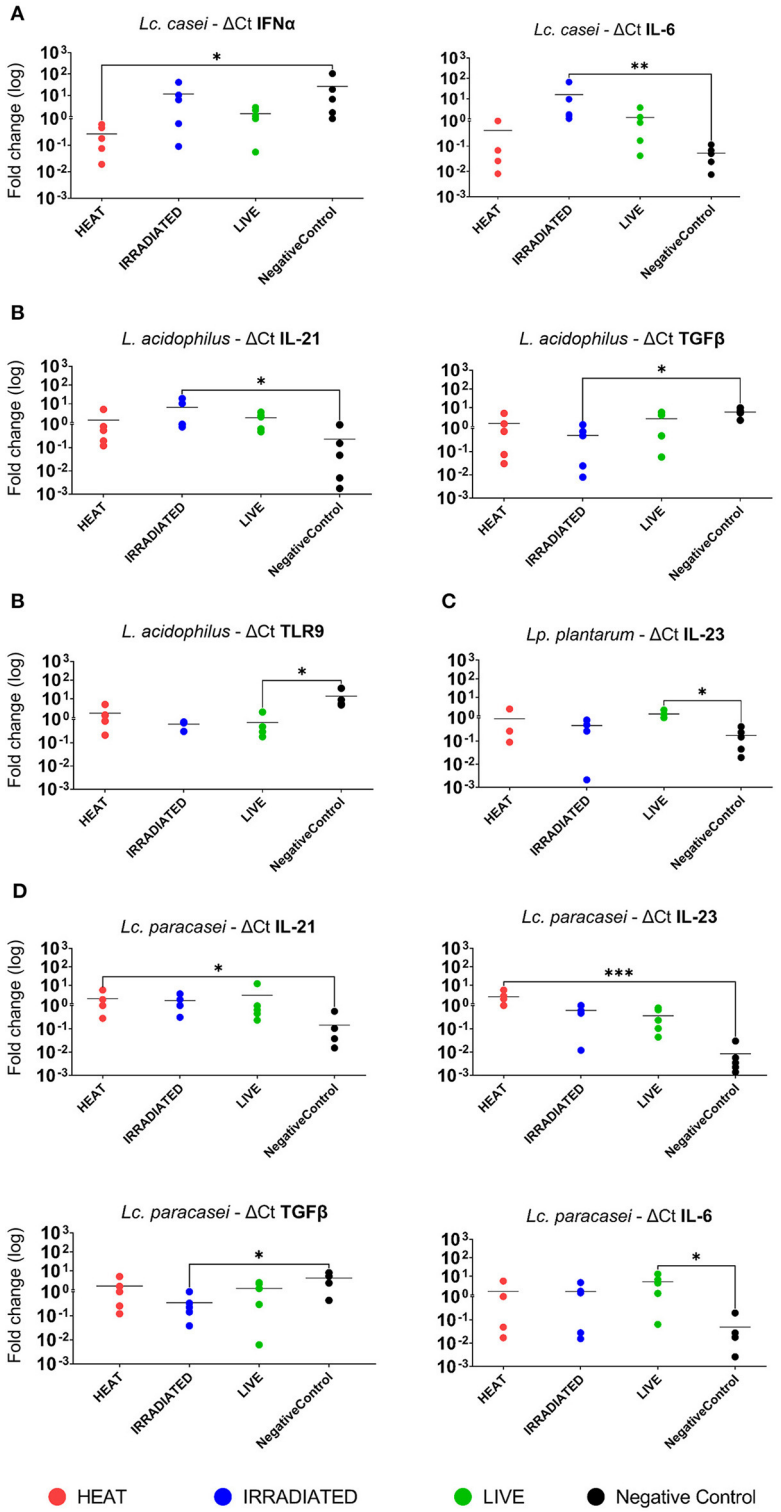

FIGURE 4 | Statistically significant fold change differences in gene expression of immune markers in porcine PBMCs. Logarithmic fold change difference in gene expression comparing individual values (dots) of each animal ($n = 5$) where blood was collected to isolate PBMCs. Here, we report gene expression showing statistical significance highlighted by one-way ANOVA analysis, where * ($P \leq 005$), ** ($P \leq 0.01$), and *** ($P \leq 0.001$) were used to express the degree of significance. Gene expression analysis was performed by comparing unstimulated PBMCs (negative control; black dot) with heat-treated (red dot), gamma-irradiated (blue dot), or live (green dot) *Lacticaseibacillus casei* **(A)**, *Lactobacillus acidophilus* **(B)**, *Lactiplantibacillus plantarum* **(C)**, and *Lacticaseibacillus paracasei* **(D)**.

Gene expression analysis of the different states of *Lp. plantarum* was performed with the same method, showing similarity in terms of overall immune marker expression between the two treatments (irradiation and heat); furthermore, both treated versions of *Lp. plantarum* showed similar overall gene expressions to the untreated cells. Not surprisingly, instead, live *Lp. plantarum* seemed to induce a very different stimulation of gene expression compared to treated strains and to the untreated samples (**Figure 3D**). The only significant difference in gene expression was observed for live *Lp. plantarum,* which was able to induce a 1-fold upregulation of IL-23 compared to untreated PBMCs (**Figure 4C**).

Finally, the same type of analysis was performed for *Lc. paracasei*, showing again that irradiated treatment induced an overall gene expression of the targeted immune markers comparable to the strain's live state. In general, both live and irradiated *Lc. paracasei* were unable to stimulate the whole pool of markers observed for the untreated cells. In contrast, heat-treated *Lc. paracasei* induced a very different stimulation of gene expression compared to the irradiated and live *Lc. paracasei* and compared to the untreated samples (**Figure 3E**). Heat-treated *Lc. paracasei* was able to induce a significant one-fold and a 2.5-fold upregulations of IL-21 and IL-23, respectively, compared to the untreated samples; instead, live *Lc. paracasei* was able to induce a significant two-fold upregulation of IL-6 whereas the irradiated version induced a significant one-fold downregulation of TGFβ (**Figure 4D**).

Taken together these results, as shown in the summary (**Figure 5**), the most affected immune markers by the stimulation of LAB are four pro-inflammatory cytokines (IFNα, IL-6, IL-21, and IL-23), one anti-inflammatory cytokine (TGFβ), and a pathogen recognition receptor (TLR9); two of four LAB strains evaluated in this study were able to maintain an overall gene expression similar to their live state (showed also in **Supplementary Figures S2–S5**) after gamma irradiation; heat treatment and irradiation of *Lc. casei* led to an opposite regulation of key pro-inflammatory cytokines, such as downregulation of IFNα for heat-treated *Lc. casei* and upregulation of IL-6 for irradiated *Lc. casei*; gamma irradiation of *L. acidophilus* and *Lc. paracasei* led to a downregulation of TGFβ.

DISCUSSION

This study aimed at investigating the immune-modulatory effects of gamma irradiated, non-replicative, yet metabolically active LAB. Our study found that irradiated LAB could preserve the immune-modulatory blueprint of their live state more than heat-inactivated bacteria. The end-point gene expression of a broad array of immune markers expressed by porcine PBMCs, evaluated by one minus Pearson correlation hierarchical clustering upon stimulation with irradiated, heat-killed, or live strains of LAB, provides this evidence. However, being metabolically active as their live form does not necessarily implicate similar immune responses when a larger immune landscape is evaluated.

A total of two out of four strains (*L. acidophilus and Lc. paracasei*) were able to induce an overall gene expression similar to that of live LAB following irradiation inactivation. On the other hand, we also observed other outputs, such as a higher degree of similarity between live and heat-killed (*Lc. casei*) LAB, or where both treatments led to a similar change in gene regulation differently from the viable state (*Lp. plantarum*). Similar outputs were also observed in other studies (42, 43), but the type of comparison on immune modulation was either limited to one single strain of LAB, whenever the aim of the study was to compare differences induced by the type of treatment, or to one single type of treatment (heat inactivation) when assessing strain-dependent effects. In addition, key factors, such as selection of LAB strain, dose, duration of the stimulation (incubation), and the number of immune markers evaluated often vary among different studies, influencing the outcome of the research. This heterogeneous landscape in terms of variation contributes to making literature on this topic rather contradictory and confusing. Considering these aspects, we decided to adopt a broad approach, by evaluating four different strains of LAB, with two different methods of inactivation, assessing the metabolic activity and the immune modulation based on the expression of 26 immune markers.

We observed an interesting, varied mosaic of statistically significant differences in the regulation of some of the key genes involved in immune modulation. This variability can be justified by the strain-dependent response to inactivation methods among LAB, as for bacteria in general, documented in previous studies, especially on radiation resistance (28), structure composition (31), immune stimulation (25), and adhesion abilities (23), just to name a few. For example, IFNα, mostly involved in antiviral activity (44), was downregulated by heat-killed *Lc. casei*, whereas IL-6, which is a pivotal pro-inflammatory cytokine responsible for regulating the immune response, playing a key role in stimulating B-cell differentiation (45, 46), was upregulated by live *Lc. paracasei* and gamma-irradiated *Lc. casei*. IL-21, another pro-inflammatory cytokine, which plays a role in Th17 development [whose modulation seems to play an important role in adjuvant development (47)], as well as in the proliferation of T cells and differentiation of B cells into memory cells (48), was found to be upregulated in both gamma-irradiated *L. acidophilus* and in heat-treated *Lc. paracasei*. Live *Lp. plantarum* and heat-treated *Lc. paracasei* were able to upregulate IL-23, which is one of the major effector molecules for Th17 maturation (49). Both gamma-irradiated treated *L. acidophilus* and *Lc. paracasei* induced downregulation of the immunomodulatory TGFβ, which is mainly involved in suppressing T- and B-cell action (50) while activating Treg cell responses (24). Finally, live *L. acidophilus* induced a downregulation of toll-like receptor 9 (TLR9), which has been proven to be essential for probiotics to exert an anti-inflammatory effect (51). The variation in the D10 values and therefore in the dose required to stop the replication depends on the bacterial titer and on the specific strain, as seen in the literature (23, 31). Indeed, the individual animal variation could have masked a better analysis of data in a group of five animals.

Interestingly, we observed that strains, which are more resistant to gamma irradiation and would therefore require a

Strain / Treatment	IFNα	IL-6	IL-21	IL-23	TGFβ	TLR9
***Lc. casei* / Heat**	↓ (*)	-	-	-	-	-
***Lc. casei* / Irradiation**	-	↑ (**)	-	-	-	-
Lc. casei / Live	-	-	-	-	-	-
L. acidophilus / Heat	-	-	-	-	-	-
***L. acidophilus* / Irradiation**	-	-	↑ (*)	-	↓ (*)	-
***L. acidophilus* / Live**	-	-	-	-	-	↓ (*)
Lp. plantarum / Heat	-	-	-	-	-	-
Lp. plantarum / Irradiation	-	-	-	-	-	-
***Lp. plantarum* / Live**	-	-	-	↑ (*)	-	-
***Lc. paracasei* / Heat**	-	-	↑ (*)	↑ (***)	-	-
***Lc. paracasei* / Irradiated**	-	-	-	-	↓ (*)	-
***Lc. paracasei* / Live**	-	↑ (*)	-	-	-	-

FIGURE 5 | Summary of the immune modulation exerted by immunobiotic and paraprobiotic LAB strains. LAB strains and respective treatments are listed in the first column. Strains highlighted in bold were able to induce a statistically significant difference in the up- (↑) or downregulation (↓) of the immune markers listed in the first row. Similarities in overall gene expression modulation, observed in heat maps hierarchical clustering, are indicated by connection lines on the left side of the table. Solid lines show similarity among different states of the same strain whereas the dashed line shows a similarity among live strains of different genera. * $P \leq 0.05$, ** $P \leq 0.01$ and *** $P \leq 0.001$ were used to express the degree of significance.

higher dose to halt replication (as we showed in the D10 values of assessment), are more likely to retain characteristics of the live state. This can be due to the diverse cell surface structure of the different strains, as it is for instance between *L. acidophilus* (coated with S-layer) and *Lp. plantarum* (un-coated) (52). In fact, the presence of S-layer proteins on the bacterial surface has been shown to augment the resistance to gamma irradiation (53), and we hypothesize that representing the outer layer of protection, the S-layer could be able to absorb most of the radiation effects preserving more efficiently the cell wall components responsible of immune modulation.

The major advantage of irradiation is that strains are inactivated by irradiation, are unable to reproduce, and are considered as safe. The inability to replicate impairs the possibility of mutations. For this reason, we decided to add an extra dose of irradiation on top of the minimum inhibitory dose making sure that these bacteria are completely replication-incompetent. For instance, several pathogenic bacteria, such as *Salmonella* or *Staphylococcus aureus,* have been proposed as safer vaccines when irradiated than inactivated with other technologies (54, 55). Ionizing radiation technology, such as gamma or E-beam irradiation, is able to damage the nucleic acid of the organism, by inducing polymerization of the DNA and breaking molecular bonds (56, 57), without affecting cell functions or the main components of the cells (58) which are destroyed in other inactivation methods, such as heat treatment. Irradiated non-replicative lactic acid bacteria share the key features with both live and heat-treated probiotics. On one hand, through this technology, LAB can retain cellular membrane integrity and metabolic activity (in some studies up to 9 days post-irradiation) similar to live strains. In addition, in some studies, cells were even able to maintain oxidative function and protein synthesis. On the other hand, it ensures a high level of safety by making pathogens unable to replicate, as it also occurs when inactivated through conventional practices (i.e., heat treatment, chemical inactivation). The main disadvantage of this technology is surely represented by the safety concern of hosting a radioactive isotope (i.e., cobalt-60) in the facility (55). To ensure radio- and cryo-protection to the cell wall of the LAB used for this study, we added trehalose to our samples prior to irradiation. Our results show that at all three doses of gamma irradiation (low, SID, and high), the metabolic activity was preserved, as it was consistent with other studies (30, 41). Surprisingly, in most of the cases, metabolic activity after irradiation was even higher than the metabolic activity of live bacteria in terms of redox potential and ATP production. Based on the previous studies, where some bacteria have shown the ability to maintain transcription and translation processes for a limited time following gamma irradiation (59), we can hypothesize that the augmented metabolic activity of irradiated LAB can be seen as an effort performed by the cell to counteract the damages caused by ionizing radiation. In fact, according to Acharya et al. (60) and Abomohra et al. (61), the increased metabolic activity indeed reflects a compensatory response in cells damaged by gamma irradiation in an effort to survive. One direct consequence of an upregulated metabolism

is oxidative stress, and irradiation leads to a significant increase in reactive oxygen species/reactive nitrogen species (ROS/RNS) levels. Furthermore, gamma irradiation induces an increased extracellular release of ATP, which stimulates the production of ROS *via* purinergic signaling, leading to the promotion of intracellular antioxidant production, such as pigments and proteins, in response to oxidative stress. We also found that the membrane structural integrity of irradiated LAB is similar to live cells, but different from heat-treated cells. The reason behind, as previously described by other reports (31, 62), is that γ-rays have no impact on membrane lipid profile, nor on peroxidation events, indicating the plausible preservation of the membrane-bound proteins.

A positive correlation between the preservation of metabolic activity after gamma irradiation and immune stimulation capacity was highlighted in some studies, showing better immunogenicity exerted by irradiated compared to heat-inactivated bacteria (41, 63, 64). In addition, studies have demonstrated that compounds of bacterial cells (e.g., teichoic acid, cell wall polysaccharides, and exopolysaccharides) are plausibly the main causative agents for the pro- or anti-inflammatory effects exerted by these microorganisms (21, 26) and that the exposure to high temperatures due to the heat treatment induces denaturation and coagulation of these proteins (58). This does not imply that an immune-modulatory activity of heat-treated strains is not expected. On the contrary, studies have demonstrated that immune modulation can be even more pronounced (25), but that would differ from the viable state.

In this study, we decided to analyze the gene expression of a set of 26 immune markers at a precise time point (16 h after co-incubation), which has been selected also in other studies (65, 66), representing a "snap-shot" of the immune-modulatory action, known to be a dynamic process. This study represents the first screening of the quest for a gamma-irradiated LAB product, which can potentially be incorporated as a vaccine adjuvant or immune therapeutic in the future. The intrinsic immune-modulatory capacity of the LAB combined with the safety conferred by irradiation may generate a product that can be broadly applied to the animal health field, beyond the usage as immune modulators. However, careful strain selection, kinetic gene expression analyses, and additional *in vitro*, *in vivo* as well as protein arrays are encouraged to further evaluate the application of irradiated LAB as vaccine adjuvants or immune-modulatory therapeutics.

DATA AVAILABILITY STATEMENT

The original contributions presented in the study are included in the article/**Supplementary Material**, further inquiries can be directed to the corresponding author.

ETHICS STATEMENT

The animal study was reviewed and approved by University of Veterinary Medicine Vienna's Ethics and Animal Welfare Committee and Austrian Ministry of Research and Science's Advisory Committee for Animal Experiments (BMBWF-68.205/0192-V3b/2018).

AUTHOR CONTRIBUTIONS

VW, KD, LP, and GC: contributed to the conception and design of the study. LP, JB, VW, and RK: performed experiments and analyzed the data. DV: provided veterinary support and provided swine blood. LP and JB: wrote the first draft of the manuscript. All authors contributed to manuscript revision, read, and approved the submitted version.

ACKNOWLEDGMENTS

The authors would like to acknowledge Dr. Hermann Unger (retired from the IAEA) for his kind advice and for obtaining an animal experimental license to collect blood samples and Dr. William Dundon (IAEA) for language editing.

SUPPLEMENTARY MATERIAL

The Supplementary Material for this article can be found online at: https://www.frontiersin.org/articles/10.3389/fvets.2022.859124/full#supplementary-material

REFERENCES

1. Szatraj K, Szczepankowska AK, Chmielewska-Jeznach M. Lactic acid bacteria — promising vaccine vectors: possibilities, limitations, doubts. *J Appl Microbiol.* (2017) 123:325–39. doi: 10.1111/jam.13446
2. Jensen H, Drømtorp SM, Axelsson L, Grimmer S. Immunomodulation of monocytes by probiotic and selected lactic acid bacteria. *Probiotics Antimicrob Proteins.* (2015) 7:14–23. doi: 10.1007/s12602-014-9174-2
3. Huang KY, Yang GL, Jin YB, Liu J, Chen HL, Wang PB, et al. Construction and immunogenicity analysis of *Lactobacillus plantarum* expressing a porcine epidemic diarrhea virus S gene fused to a DC-targeting peptide. *Virus Res.* (2018) 247:84–93. doi: 10.1016/j.virusres.2017.12.011
4. Hill C, Guarner F, Reid G, Gibson GR, Merenstein DJ, Pot B, et al. The International Scientific Association for Probiotics and Prebiotics consensus statement on the scope and appropriate use of the term probiotic. *Nat Rev Gastroenterol Hepatol.* (2014) 11:506–14. doi: 10.1038/nrgastro.2014.66
5. Bermudez-Brito M, Plaza-Díaz J, Muñoz-Quezada S, Gómez-Llorente C, Gil A. Probiotic mechanisms of action. *Ann Nutr Metab.* (2012) 61:160–74. doi: 10.1159/000342079
6. Zheng J, Wittouck S, Salvetti E, Franz CMAP, Harris HMB, Mattarelli P, et al. A taxonomic note on the genus *Lactobacillus*: description of 23 novel genera, emended description of the genus *Lactobacillus* Beijerinck 1901, and union of Lactobacillaceae and Leuconostocaceae. *Int J Syst Evol Microbiol.* (2020) 70:2782–858. doi: 10.1099/ijsem.0.004107
7. Kang HJ, Im SH. Probiotics as an immune modulator. *J Nutr Sci Vitaminol.* (2015) 61(Suppl):S103–5. doi: 10.3177/jnsv.61.S103
8. Gao X, Huang L, Zhu L, Mou C, Hou Q, Yu Q. Inhibition of H9N2 virus invasion into dendritic cells by the S-layer protein from *L. acidophilus* ATCC 4356. *Front Cell Infect Microbiol.* (2016) 6:137. doi: 10.3389/fcimb.2016.00137

9. Tiittanen M, Keto J, Haiko J, Mättö J, Partanen J, Lähteenmäki K. Interaction with intestinal epithelial cells promotes an immunosuppressive phenotype in *Lactobacillus casei*. *PloS ONE*. (2013) 8:e78420. doi: 10.1371/journal.pone.0078420
10. Shida K, Kiyoshima-Shibata J, Nagaoka M, Watanabe K, Nanno M. Induction of interleukin-12 by *Lactobacillus* strains having a rigid cell wall resistant to intracellular digestion. *J Dairy Sci.* (2006) 89:3306–17. doi: 10.3168/jds.S0022-0302(06)72367-0
11. Zhang W, Azevedo MSP, Wen K, Gonzalez A, Saif LJ Li G, Yousef AE, et al. Probiotic *Lactobacillus acidophilus* enhances the immunogenicity of an oral rotavirus vaccine in gnotobiotic pigs. *Vaccine.* (2008) 26:3655–61. doi: 10.1016/j.vaccine.2008.04.070
12. Amdekar S, Dwivedi D, Roy P, Kushwah S, Singh V. Probiotics: multifarious oral vaccine against infectious traumas. *FEMS Immunol Med Microbiol.* (2010) 58:299–306. doi: 10.1111/j.1574-695X.2009.00630.x
13. Lee SI, Kim HS, Koo JM, Kim IH. *Lactobacillus acidophilus* modulates inflammatory activity by regulating the TLR4 and NF-κB expression in porcine peripheral blood mononuclear cells after lipopolysaccharide challenge. *Br J Nutr.* (2016) 115:567–75. doi: 10.1017/S0007114515004857
14. Kaiko GE, Horvat JC, Beagley KW, Hansbro PM. Immunological decision-making: how does the immune system decide to mount a helper T-cell response? *Immunology.* (2008) 123:326–38. doi: 10.1111/j.1365-2567.2007.02719.x
15. Wen K, Li G, Bui T, Liu F, Li Y, Kocher J, et al. High dose and low dose *Lactobacillus acidophilus* exerted differential immune modulating effects on T cell immune responses induced by an oral human rotavirus vaccine in gnotobiotic pigs. *Vaccine.* (2012) 30:1198–207. doi: 10.1016/j.vaccine.2011.11.107
16. Peroni DG, Morelli L. Probiotics as adjuvants in vaccine strategy: is there more room for improvement? *Vaccines*. (2021) 9:811. doi: 10.3390/vaccines9080811
17. Vilander AC, Dean GA. Adjuvant strategies for lactic acid bacterial mucosal vaccines. *Vaccines*. (2019) 7:150. doi: 10.3390/vaccines7040150
18. Davidson LE, Fiorino AM, Snydman DR, Hibberd PL. *Lactobacillus* GG as an immune adjuvant for live-attenuated influenza vaccine in healthy adults: a randomized double-blind placebo-controlled trial. *Eur J Clin Nutr.* (2011) 65:501–7. doi: 10.1038/ejcn.2010.289
19. Pace F, Macchini F, Massimo Castagna V. Safety of probiotics in humans: a dark side revealed? *Dig Liver Dis.* (2020) 52:981–5. doi: 10.1016/j.dld.2020.04.029
20. Besselink MG, van Santvoort HC, Buskens E, Boermeester MA, van Goor H, Timmerman HM, et al. Probiotic prophylaxis in predicted severe acute pancreatitis: a randomised, double-blind, placebo-controlled trial. *Lancet.* (2008) 371:651–9. doi: 10.1016/S0140-6736(08)60207-X
21. Teame T, Wang A, Xie M, Zhang Z, Yang Y, Ding Q, Gao C, Olsen RE, Ran C, Zhou Z. Paraprobiotics and postbiotics of probiotic lactobacilli, their positive effects on the host and action mechanisms: a review. *Front Nutr.* (2020) 7:570344. doi: 10.3389/fnut.2020.570344
22. Imperial ICVJ, Ibana JA. Addressing the antibiotic resistance problem with probiotics: reducing the risk of its double-edged sword effect. *Front Microbiol.* (2016) 7:1983. doi: 10.3389/fmicb.2016.01983
23. Ouwehand AC, Tölkkö S, Kulmala J, Salminen S, Salminen E. Adhesion of inactivated probiotic strains to intestinal mucus. *Lett Appl Microbiol.* (2000) 31:82–6. doi: 10.1046/j.1472-765x.2000.00773.x
24. Taverniti V, Guglielmetti S. The immunomodulatory properties of probiotic microorganisms beyond their viability (ghost probiotics: proposal of paraprobiotic concept). *Genes Nutr.* (2011) 6:261–74. doi: 10.1007/s12263-011-0218-x
25. Adams CA. The probiotic paradox: live and dead cells are biological response modifiers. *Nutr Res Rev.* (2010) 23:37–46. doi: 10.1017/S0954422410000090
26. Vallejo-Cordoba B, Castro-López C, García HS, González-Córdova AF. Hernández-Mendoza A. Postbiotics and paraprobiotics: a review of current evidence and emerging trends. Adv Food Nutr Res. (2020) 94:1–34. doi: 10.1016/bs.afnr.2020.06.001
27. Piqué N, Berlanga M. Miñana-Galbis D. Health benefits of heat-killed (Tyndallized) probiotics: an overview. *Int J Mol Sci.* (2019) 20:2534. doi: 10.3390/ijms20102534
28. Almada CN, Almada-Érix CN, Bonatto MS, Pradella F, dos Santos P, Abud YKD, et al. Obtaining paraprobiotics from *Lactobacilus acidophilus*, *Lacticaseibacillus casei* and Bifidobacterium animalis using six inactivation methods: impacts on the cultivability, integrity, physiology, and morphology. *J Funct Foods.* (2021) 87:104826. doi: 10.1016/j.jff.2021.104826
29. Farkas J. Irradiation for better foods. *Trends Food Sci Technol.* (2006) 17:148–52. doi: 10.1016/j.tifs.2005.12.003
30. Hieke ASC, Pillai SD. *Escherichia coli* cells exposed to lethal doses of electron beam irradiation retain their ability to propagate bacteriophages and are metabolically active. *Front Microbiol.* (2018) 9:2138. doi: 10.3389/fmicb.2018.02138
31. Correa W, Brandenburg J, Behrends J, Heinbockel L, Reiling N, Paulowski L, et al. Inactivation of bacteria by γ-irradiation to investigate the interaction with antimicrobial peptides. *Biophys J.* (2019) 117:1805–19. doi: 10.1016/j.bpj.2019.10.012
32. Raz E, Rachmilewitz D. *Inactivated probiotic bacteria and methods of use thereof* (2005). Available online at: https://patents.google.com/patent/US20050180962A1/en (accessed March 2, 2022).
33. Kamiya T, Wang L, Forsythe P, Goettsche G, Mao Y, Wang Y, et al. Inhibitory effects of *Lactobocillus reuteri* on visceral pain induced by colorectal distension in Sprague-Dawley rats. *Gut.* (2006) 55:191–6. doi: 10.1136/gut.2005.070987
34. Andrew. *Dosimetry for sit: standard operating procedure for Gafchromic^{TM} film dosimetry system for gamma radiation*. Available online at: https://www.iaea.org/ (accessed March 2, 2022).
35. Jain R, Sarkale P, Mali D, Shete A, Patil D, Majumdar T, et al. Inactivation of SARS-CoV-2 by gamma irradiation. *Indian J Med Res.* (2021) 153:196–8. doi: 10.4103/ijmr.IJMR_2789_20
36. Singleton E V, David SC, Davies JB, Hirst TR, Paton JC, Beard MR, et al. Sterility of gamma-irradiated pathogens: a new mathematical formula to calculate sterilizing doses. *J Radiat Res.* (2020) 61:886–94. doi: 10.1093/jrr/rraa076
37. *Animal Welfare Act: The Federal Act on Animal Welfare (Tierschutzgesetz - TSchG), Federal Law Gazette I 2004/118, has been in force since 1 January 2005*. Available online at: https://info.bmlrt.gv.at/en/topics/agriculture/agriculture-in-austria/animal-production-in-austria/animal-welfare-act.html/ (accessed March 14, 2022).
38. Sassu EL, Kangethe RT, Settypalli TBK, Chibssa TR, Cattoli G, Wijewardana V. Development and evaluation of a real-time PCR panel for the detection of 20 immune markers in cattle and sheep. *Vet Immunol Immunopathol.* (2020) 227:110092. doi: 10.1016/j.vetimm.2020.110092
39. Schmittgen TD, Livak KJ. Analyzing real-time PCR data by the comparative CT method. *Nat Protoc.* (2008) 3:1101–8. doi: 10.1038/nprot.2008.73
40. De Spiegelaere W, Dern-Wieloch J, Weigel R, Schumacher V, Schorle H, Nettersheim D, et al. Reference gene validation for RT-qPCR, a note on different available software packages. *PLoS ONE.* (2015) 10:e0122515. doi: 10.1371/journal.pone.0122515
41. Magnani DM, Harms JS, Durward MA, Splitter GA. Nondividing but metabolically active gamma-irradiated *Brucella melitensis* is protective against virulent *B. melitensis* challenge in mice. *Infect Immun.* (2009) 77:5181–9. doi: 10.1128/IAI.00231-09
42. Ma D, Forsythe P, Bienenstock J. Live *Lactobacillus rhamnosus* [corrected] is essential for the inhibitory effect on tumor necrosis factor alpha-induced interleukin-8 expression. *Infect Immun.* (2004) 72:5308–14. doi: 10.1128/IAI.72.9.5308-5314.2004
43. Castro-Herrera VM, Rasmussen C, Wellejus A, Miles EA, Calder PC. *In vitro* effects of live and heat-inactivated *Bifidobacterium animalis* Subsp. *lactis*, BB-12 and *Lactobacillus rhamnosus* GG on Caco-2 cells. *Nutrients*. (2020) 12:1719. doi: 10.3390/nu12061719
44. Zanotti C, Razzuoli E, Crooke H, Soule O, Pezzoni G, Ferraris M, et al. Differential biological activities of swine interferon-α subtypes. *J Interferon Cytokine Res.* (2015) 35:990–1002. doi: 10.1089/jir.2015.0076
45. Shirota K, LeDuy L, Yuan S, Jothy S. Interleukin-6 and its receptor are expressed in human intestinal epithelial cells. *Virchows Arch B Cell Pathol Incl Mol Pathol.* (1990) 58:303–8. doi: 10.1007/BF02890085

46. Wang L, Li X, Wang Y. GSK3β inhibition attenuates LPS-induced IL-6 expression in porcine adipocytes. *Sci Rep.* (2018) 8:15967. doi: 10.1038/s41598-018-34186-0
47. Datta SK, Sabet M, Nguyen KPL, Valdez PA, Gonzalez-Navajas JM, Islam S, et al. Mucosal adjuvant activity of cholera toxin requires Th17 cells and protects against inhalation anthrax. *Proc Natl Acad Sci USA.* (2010) 107:10638–43. doi: 10.1073/pnas.1002348107
48. Liu G, Wang B, Chen Q, Li Y, Li B, Yang N, Yang S, Geng S, Liu G. Interleukin (IL)-21 promotes the differentiation of IgA-producing plasma cells in porcine Peyer's patches *via* the JAK-STAT signaling pathway. *Front Immunol.* (2020) 11:1303. doi: 10.3389/fimmu.2020.01303
49. Xiao Y, Zhang H, Chen J, Chen Y, Li J, Song T, et al. Cloning and expression of the tibetan pig interleukin-23 gene and its promotion of immunity of pigs to PCV2 vaccine. *Vaccines.* (2020) 8:250. doi: 10.3390/vaccines8020250
50. Azevedo MSP, Zhang W, Wen K, Gonzalez AM, Saif LJ, Yousef AE, Yuan L. *Lactobacillus acidophilus* and *Lactobacillus reuteri* modulate cytokine responses in gnotobiotic pigs infected with human rotavirus. *Benef Microbes.* (2012) 3:33–42. doi: 10.3920/BM2011.0041
51. Rachmilewitz D, Katakura K, Karmeli F, Hayashi T, Reinus C, Rudensky B, et al. Toll-like receptor 9 signaling mediates the anti-inflammatory effects of probiotics in murine experimental colitis. *Gastroenterology.* (2004) 126:520–8. doi: 10.1053/j.gastro.2003.11.019
52. Hynönen U, Palva A. Lactobacillus surface layer proteins: structure, function and applications. *Appl Microbiol Biotechnol.* (2013) 97:5225–43. doi: 10.1007/s00253-013-4962-2
53. Kotiranta AK, Ito H, Haapasalo MPP, Lounatmaa K. Radiation sensitivity of *Bacillus cereus* with and without a crystalline surface protein layer. *FEMS Microbiol Lett.* (1999) 179:275–80. doi: 10.1111/j.1574-6968.1999.tb08738.x
54. Ji HJ, Byun EB, Chen F, Ahn KB, Jung HK, Han SH, et al. Radiation-inactivated *S. gallinarum* vaccine provides a high protective immune response by activating both humoral and cellular immunity. *Front Immunol.* (2021) 12:717556. doi: 10.3389/fimmu.2021.717556
55. Bhatia SS, Pillai SD. Ionizing radiation technologies for vaccine development - a mini review. *Front Immunol.* (2022) 13:845514. doi: 10.3389/fimmu.2022.845514
56. Reisz JA, Bansal N, Qian J, Zhao W, Furdui CM. Effects of ionizing radiation on biological molecules–mechanisms of damage and emerging methods of detection. *Antioxid Redox Signal.* (2014) 21:260–92. doi: 10.1089/ars.2013.5489
57. Trampuz A, Piper KE, Steckelberg JM, Patel R. Effect of gamma irradiation on viability and DNA of *Staphylococcus epidermidis* and *Escherichia coli. J Med Microbiol.* (2006) 55:1271–5. doi: 10.1099/jmm.0.46488-0
58. Wong C, Ustunol Z. Mode of inactivation of probiotic bacteria affects interleukin 6 and interleukin 8 production in human intestinal epithelial-like Caco-2 cells. *J Food Prot.* (2006) 69:2285–8. doi: 10.4315/0362-028X-69.9.2285
59. Kato M, Futenma A. Expression of the lacZ gene in *Escherichia coli* irradiated with gamma rays. *J Radiat Res Appl Sci.* (2014) 7:568–71. doi: 10.1016/j.jrras.2014.09.008
60. Acharya MM, Lan ML, Kan VH, Patel NH, Giedzinski E, Tseng BP, et al. Consequences of ionizing radiation-induced damage in human neural stem cells. *Free Radic Biol Med.* (2010) 49:1846–55. doi: 10.1016/j.freeradbiomed.2010.08.021
61. Abomohra AEF, El-Shouny W, Sharaf M, Abo-Eleneen M. Effect of gamma radiation on growth and metabolic activities of *Arthrospira platensis*. *Braz Arch Biol Technol.* (2016) 59:1–11. doi: 10.1590/1678-4324-2016150476
62. Jesudhasan PR, McReynolds JL, Byrd AJ, He H, Genovese KJ, Droleskey R, et al. Electron-beam-inactivated vaccine against salmonella enteritidis colonization in molting hens. *Avian Dis.* (2015) 59:165–70. doi: 10.1637/10917-081014-ResNoteR
63. Sanakkayala N, Sokolovska A, Gulani J, HogenEsch H, Sriranganathan N, Boyle SM, et al. Induction of antigen-specific Th1-type immune responses by gamma-irradiated recombinant *Brucella abortus* RB51. *Clin Diagn Lab Immunol.* (2005) 12:1429–36. doi: 10.1128/CDLI.12.12.1429-1436.2005
64. Secanella-Fandos S, Noguera-Ortega E, Olivares F, Luquin M, Julián E. Killed but metabolically active *Mycobacterium bovis* bacillus Calmette-Guérin retains the antitumor ability of live bacillus Calmette-Guérin. *J Urol.* (2014) 191:1422–8. doi: 10.1016/j.juro.2013.12.002
65. Miettinen M, Matikainen S, Vuopio-Varkila J, Pirhonen J, Varkila K, Kurimoto M, et al. *Lactobacilli* and *Streptococci* induce interleukin-12 (IL-12), IL-18, and gamma interferon production in human peripheral blood mononuclear cells. *Infect Immun.* (1998) 66:6058–62. doi: 10.1128/IAI.66.12.6058-6062.1998
66. Villena J, Suzuki R, Fujie H, Chiba E, Takahashi T, Tomosada Y, et al. Immunobiotic *Lactobacillus jensenii* modulates the Toll-like receptor 4-induced inflammatory response *via* negative regulation in porcine antigen-presenting cells. *Clin Vaccine Immunol.* (2012) 19:1038–53. doi: 10.1128/CVI.00199-12

Conflict of Interest: The authors declare that the research was conducted in the absence of any commercial or financial relationships that could be construed as a potential conflict of interest.

frontiers | Frontiers in Immunology

ORIGINAL RESEARCH
published: 11 July 2022
doi: 10.3389/fimmu.2022.931052

Development of Live Attenuated *Salmonella* Typhimurium Vaccine Strain Using Radiation Mutation Enhancement Technology (R-MET)

Hyun Jung Ji[1,2], *A-Yeung Jang*[3], *Joon Young Song*[3], *Ki Bum Ahn*[1], *Seung Hyun Han*[2], *Seok Jin Bang*[4], *Ho Kyoung Jung*[4], *Jin Hur*[5]* and *Ho Seong Seo*[1,6]*

[1] Research Division for Radiation Science, Korea Atomic Energy Research Institute, Jeongeup, South Korea, [2] Department of Oral Microbiology and Immunology, and Dental Research Institute (DRI), School of Dentistry, Seoul National University, Seoul, South Korea, [3] Department of Internal Medicine, Korea University College of Medicine, Seoul, South Korea, [4] Research and Development Center, HONGCHEON CTCVAC Co., Ltd., Hongcheon, South Korea, [5] Department of Veterinary Public Health, College of Veterinary Medicine, Jeonbuk National University, Iksan, South Korea, [6] Department of Radiation Science, University of Science and Technology, Daejeon, South Korea

OPEN ACCESS

Edited by:
Sebastian Ulbert,
Fraunhofer Institute for Cell Therapy and Immunology (IZI), Germany

Reviewed by:
Palmy Jesudhasan,
United States Department of Agriculture, United States
Rezwanul Wahid,
University of Maryland, United States

***Correspondence:**
Jin Hur
hurjin@jbnu.ac.kr
Ho Seong Seo
hoseongseo@kaeri.re.kr

Specialty section:
This article was submitted to Vaccines and Molecular Therapeutics, a section of the journal Frontiers in Immunology

Received: 28 April 2022
Accepted: 10 June 2022
Published: 11 July 2022

Citation:
Ji HJ, Jang AY, Song JY, Ahn KB, Han SH, Bang SJ, Jung HK, Hur J and Seo HS (2022) Development of Live Attenuated Salmonella Typhimurium Vaccine Strain Using Radiation Mutation Enhancement Technology (R-MET). Front. Immunol. 13:931052. doi: 10.3389/fimmu.2022.931052

Salmonella enterica is a leading cause of food-borne diseases in humans worldwide, resulting in severe morbidity and mortality. They are carried asymptomatically in the intestine or gallbladder of livestock, and are transmitted predominantly from animals to humans *via* the fecal-oral route. Thus, the best preventive strategy is to preemptively prevent transmission to humans by vaccinating livestock. Live attenuated vaccines have been mostly favored because they elicit both cellular and humoral immunity and provide long-term protective immunity. However, developing these vaccines is a laborious and time-consuming process. Therefore, most live attenuated vaccines have been mainly used for phenotypic screening using the auxotrophic replica plate method, and new types of vaccines have not been sufficiently explored. In this study, we used Radiation-Mutation Enhancement Technology (R-MET) to introduce a wide variety of mutations and attenuate the virulence of *Salmonella* spp. to develop live vaccine strains. The *Salmonella* Typhimurium, ST454 strain (ST WT) was irradiated with Cobalt^{60} gamma-irradiator at 1.5 kGy for 1 h to maximize the mutation rate, and attenuated daughter colonies were screened using *in vitro* macrophage replication capacity and *in vivo* mouse infection assays. Among 30 candidates, ATOMSal-L6, with 9,961-fold lower virulence than the parent strain (ST454) in the mouse LD_{50} model, was chosen. This vaccine candidate was mutated at 71 sites, and in particular, lost one bacteriophage. As a vaccine, ATOMSal-L6 induced a *Salmonella*-specific IgG response to provide effective protective immunity upon intramuscular vaccination of mice. Furthermore, when mice and sows were orally immunized with ATOMSal-L6, we found a strong protective immune response, including multifunctional cellular immunity. These results indicate that ATOMSal-L6 is the first live vaccine candidate to be developed using R-MET, to the best of our knowledge. R-MET can be used as a fast and effective live vaccine development technology that can be used to develop vaccine strains against emerging or serotype-shifting pathogens.

Keywords: live vaccine, radiation, R-MET, *Salmonella typhimurium*, mutation- genetics, attenuation

INTRODUCTION

Invasive non-typhoidal *Salmonella* (iNTS) is a leading cause of bacterial bloodstream infections in both humans and animals (1). *Salmonella* infections commonly result in self-limiting diarrheal illness that rarely leads to deaths; however, the case fatality rate increases to 20–25% in infants, elderly, and immunocompromised individuals (2–5). Recent systemic analysis reported that iNTS caused an estimated 535,000 illnesses and 77,500 deaths in 2017 (6), particularly in sub-Saharan Africa, where iNTS is a leading cause of community-onset bloodstream infection (7–9). In that region, iNTS was the second most common invasive bacterial disease, following *Streptococcus pneumoniae* infection (3, 7, 10). Although *Salmonella* can be controlled using antibiotics, an increased prevalence of multidrug-resistant strains has been reported over recent decades (11–13). Vaccines can potentially control the prevalence of *Salmonella* in both humans and animals (14–16). There are two possible vaccination strategies (4); vaccinating high risk groups among humans, such as elderly and/or immunocompromised adults and (5) mass vaccination to poultry and pig to prevent transmission of *Salmonella* to human *via* the consumption of *Salmonella*-contaminated meat.

Approximately 20–36% of *Salmonella* cases in humans were linked to the consumption of eggs, poultry meat, and red meats contaminated with *Salmonella* (17). At present, there is no vaccine that directly targets *S.* Typhimurium in humans, but several types of vaccines have been introduced to pigs and chickens (18–20). Surprisingly, the mass poultry vaccinations carried out in the United Kingdom, which were introduced to combat *Salmonella* infections, has dramatically decreased transmitted illness from 1.6 cases per 1000 persons in 1993 to 0.2 cases per 1,000 persons in 2009 (21). Therefore, vaccinating economically important animals might be the safest and most effective strategy to prevent the spread of *Salmonella* infection in humans.

Primarily, live attenuated vaccines have been favored because they elicit both cellular and humoral immunity, which provide long-term protective immunity (22). To date, several live attenuated vaccines are available worldwide for use in pig and poultry. In Australia, there is only one registered, commercially available live attenuated *S.* Typhimurium vaccine; it was produced by disrupting the *aroA* gene by inserting the Tn10 transposon (23). IDT Biologika licensed Salmovac440 for chickens and Salmoporc for pigs, which are auxotrophic *Salmonella* vaccine strains of both histidine and adenine (24, 25). Recently, whole genome sequencing (WGS) results showed that Salmonvac440 was attenuated by only 6 SNPs, and these mutations dramatically reduced *Salmonella* virulence (26). However, the mutations caused by SNPs easily revert and regain original virulence. To overcome this, a *Salmonella* vaccine strain using LMO (Living Modified Organism) is being developed. CVD1921, which is mutated in both the *guaBA* genes that are involved in the biosynthesis of guanine nucleotides, and the *clpP* gene affecting flagella expression, was shown to be significantly attenuated with decreased shedding, systemic spread, and clinical disease manifestations in the digestive tract of a primate model (rhesus macaque) (27). Nevertheless, LMO vaccines have not been approved for use in the farm in many countries due to environmental contamination risks and transmission of modified genes to environmental microorganisms.

Spontaneous mutations have been extensively used as sources of novel genetic diversity for selecting new, improved organisms (28, 29). However, the appearance of new mutations is a very rare event in bacteria, because the mutation rate of *Escherichia coli* is only 10^{-3} per genome per generation (30). After Hermann Joseph Muller first discovered that exposure to high-energy radiation induces a variety of genetic mutations and can transmit these new mutations to offspring (31, 32), radiation-induced mutation breeding is being widely used to generate genetic variability in various organisms (33). Radiation-induced mutagenesis can be caused by direct or indirect action on the DNA. In the direct action method, the radiation penetrates the cell and hits the DNA causing single-stranded or double-stranded DNA breaks (34). In the indirect action method, the radiation hits the water molecules, the major constituent of the cell, and other organic molecules in the cell, whereby free radicals such as hydroxyl (HO•) and alkoxy (RO•) are produced. Free radicals are characterized by an unpaired electron in the structure, which is highly reactive and reacts with DNA molecules to cause molecular structural damage (35–37). Chemical mutagens and ultraviolet rays have been widely used to accelerate the onset of mutations and develop live attenuated vaccine strains, but SNPs are the major type of mutations and deletions, and insertions are limitedly introduced in the genome (37–39). However, radiation can cause spontaneous DNA mutations including deletions, insertions, and point mutations. In fact, we first introduced radiation mutation enhancement techniques (R-MET) to induce various mutations in cancer targeting *Salmonella* in our previous study (40). However, R-MET has not yet been applied to vaccine development.

In this study, we developed a hyper-attenuated, but immunologically active *Salmonella* vaccine strain ATOMSal-L6 by accelerating mutation using gamma irradiation. ATOMSal-L6 is at least 9,961-fold less virulent than its parent strain, but can enhance both humoral and cellular immune responses, and was found to confer protective immunity in both mice and porcine models. In addition, WGS analysis showed that ATOMSal-L6 introduced many SNPs and deletion/insertion mutations. This newly developed attenuated vaccine strain is a genetically stable vaccine strain that can potentially overcome the shortcomings of existing vaccines and can be easily and quickly developed into bacterial vaccines using radiation.

MATERIALS AND METHODS

Ethics Statement

This study was performed in strict accordance with the recommendations of the Guide for the Care and Use of Laboratory Animals of the National Institutes of Health. All animal experiments were approved by the Committee on the Use and Care of Animals at the Korea Atomic Energy Research Institute (KAERI; approval no. KAERI-IACUC-2020-004,

KAERI-IACUC-2021-003) according to accepted veterinary standards set by the KAERI animal care center. Mice were euthanized by CO_2 inhalation, as specified by the KAERI Institutional Animal Care and Use Committee guidelines.

Bacterial Strains

S. Typhimurium ST454 (ST WT) was obtained from the Korea Veterinary Culture Collection (Kimchun, Republic of Korea), ATOMSal-L6 was derived from ST WT, and gene mutation was induced by gamma-radiation. Their genome was sequenced using the PacBio RS II platform (Pacific Biosciences, Menlo Park, CA, USA) and Illumina Hiseq platform at Macrogen Co., Ltd. (Seoul, Republic of Korea). The assembled genome of ST WT contained two contigs, one circular genome (4,823,318 bp) and one plasmid (109,428 bp). After complete genome assembly, BLAST analysis (v2.7.1) was carried out to identify the species to which each scaffold showed the highest similarity. The best hit was *S. enterica* subsp. *enterica* strain ST1120 (accession number: CP021909.1).

Mutation Rate Analysis

ST WT was grown in Luria-Bertani (LB; Difco, BD Biosciences, Franklin Lakes, NJ, USA) broth at 37°C and 200 rpm under aerobic conditions. The stain attained an optical density (OD_{600}) of 0.5, exposed to 0.5–3.5 kGy for 1 h at room temperature using a ^{60}Co-gamma irradiator (point source AECL, IR-79, MDS Nordion International Co., Ottawa, Canada) at the Advanced Radiation Technology Institute of KAERI (Jeongeup, Republic of Korea). The irradiated samples were concentrated and plated on LB agar plates with 10 μg/mL of kanamycin to select for mutants that acquired kanamycin resistance, as has been described previously (41). The overall mutation rate of the population was calculated using the mean number of mutants.

Macrophage Invasion and Replication Assay

RAW 264.7 cells were purchased from the American Type Culture Collection (ATCC, Manassas, VA, USA), and was grown in high-glucose Dulbecco's modified Eagle's medium (DMEM; Sigma-Aldrich; St. Louis, MO, USA) supplemented with 10% fetal bovine serum (FBS; Biowest, Nuaillé France), and 1% antibiotics (100 U/mL penicillin and 100 μg/mL streptomycin; Gibco; Waltham, MA, USA) at 37°C in the presence of 5% CO_2. RAW 264.7 cell (3×10^4 cells per well) was seeded on 48-well plates (SPL Life Sciences, Pocheon, Republic of Korea) and incubated for 16 h. Attenuated *Salmonella* candidates were cultured in LB at OD_{600} of 1.0 and harvested. The strains were treated to RAW 264.7 cells at multiplicity of infection (MOI) of 10 and incubated for 2 h at 37°CC. The cells were washed with PBS (Welgene, Gyeongsan, Republic of Korea) thrice and transferred to DMEM supplemented with 10% FBS and 100 μg/mL of gentamicin to eliminate extracellular bacteria. After 2 h incubation, the cells were washed three times with PBS and treated with RIPA lysis buffer (Sigma) for invasion assay. For replication assay, the cells were incubated with DMEM supplemented with 10% FBS and 10 μg/mL gentamicin to prevent the leakage of intracellular bacteria. After 16 h incubation, cells were treated with RIPA lysis buffer (Sigma). Subsequently, lysis samples were serially diluted with PBS and spotted on the LB agar plate.

Biochemical Characteristics Analysis

To compare bacterial growth rates with temperature (37°C, 42°C, and 45°C), overnight cultured ST WT and ATOMSal-L6 were re-inoculated into 150 mL LB medium and the bacterial OD_{600} was calculated every 30 min. Overnight cultured ST WT and ATOMSal-L6 were re-inoculated into 20 mL LB medium at OD_{600} of 1.0. Biochemical features of ST454 and ATOMSal-L6 were analyzed using the API ZYM (enzyme activities), API 20NE, and API 50CH (utilization of carbohydrate) kits (bioMerieux, Inc.; Marcy L Etoile, France) according to manufacturer's instructions. In brief, the cultured bacteria were diluted using the provided medium until adequate turbidity was attained. Diluted samples were added into the cupules, and incubated for 48 h at 37°C.

Antimicrobial Susceptibility Test (MIC Test)

The MIC test was measured the antimicrobial susceptibilities of ST WT and ATOMSal-L6 to kanamycin (KAN, 50 mg/mL), tetracycline (TET, 50 mg/mL), erythromycin (ERM, 150 mg/mL), ampicillin (AMP, 100 mg/mL), Cefadroxil (CFR, 1 mg/mL), trimethoprim (TMP, 25 mg/mL), gentamicin (GEN, 0.5 mg/mL), amoxicillin (AMC, 1 mg/mL), amikacin (AMK, 1 mg/mL), streptomycin (STR, 1 mg/mL), spectinomycin (SPT, 1 mg/mL), lincomycin (LIN, 1 mg/mL), clindamycin (CLI, 1 mg/mL), and tobramycin (TOB, 1 mg/mL). Briefly, overnight cultured ST WT and ATOMSal-L6 were re-inoculated into 30 mL LB medium (1:50 dilution), 100 μL of diluted sample was added into round bottom 96 well plate (SPL) with 3-fold diluted antibiotics.

Scanning Electron Microscope Analysis

ST WT and ATOMSal-L6 were fixed with 4% glutaraldehyde solution at 4°C and kept overnight. After centrifuging, the fixed samples were washed thrice with PBS and dehydrated using 30, 50, and 70% ethanol sequentially, following which the samples were dried and coated with gold sputter. The plate was observed using a JEIL JSM-840 Scanning Microscope (Tokyo, Japan) at the Seoul National University.

Motility Assay

Motility medium, which was composed of LB supplemented with 0.4% agar (BD) and 1% triphenyltetrazolium chloride (TTC; Sigma) was poured into the 14 mL round bottom tube (SPL). Overnight cultured ST WT and ATOMSal-L6 were re-inoculated into 3 mL LB medium at an OD_{600} of 1.0. The cultured samples were pierced deeply into the motility medium using the loop (SPL). The tubes were incubated for 3 days at 37°C.

High-Throughput Sequencing and Comparative Genomic Analysis

The location of nucleotide substitutions, deletions, and insertions in the genome of the attenuated strain ATOMSal-L6 was determined using Illumina HiSeq 2000 (150 bp paired-end)

with 825.98–fold coverage. The total length of read bases was 4,088,887,030 bp, which covered 99.98% length of the ST WT strain. The raw reads from the ST WT genome were mapped and aligned to the reference genome sequence using Burrows-Wheeler aligner (BWA-0.7.12) and Picard. Next, the genetic variants were detected using SAMTools (ver. 1.2). All coding variants were identified based on the open reading frames of ST WT. The whole-genome sequences of ST WT (ST454) and ATOMSal-L6 has been deposited in DDBJ/EMBL/GenBank under the accession number CP098438-CP098439. The BioProject accession numbers are PRJNA844490, and PRJNA841760 and the BioSample accession number are SAMN28818465 and SAMN28614156, respectively.

Mouse and Pig Experiments

The animal housing conditions, which were designed for specific pathogen-free animals, and the animal experimental design were approved by the Committee on the Use and Care of Animals at the KAERI and implemented according to the ethical standards accepted by the National Health Institute. The ventilated housing cage (Orient Bio Inc., Seoul, Republic of Korea) was maintained in an animal biological safety level 2 facility at 22–23°C on a 12 h:12 h light:dark cycle. The cages were covered with high-efficiency particulate air-filtered micro-isolation lids (Orient Bio Inc.) in a static airflow environment. Bedding (Beta Chip; Orient Bio Inc.) at an approximate depth of 1.0 cm was changed weekly. Irradiated rodent diet food (5053; Orient Bio Inc.) and sterile water were provided *ad libitum* through a wire cage top. Five-week-old male C57BL/6 or BALB/c mice (weight 19–21 g) were purchased from Orient Bio Inc. Five C57BL/6 mice were randomly assigned to individually ventilated housing cages and immunized i.m. or orally thrice at two-week intervals with either PBS, ATOMSal-L6 (10^5, 10^6, 10^7, 10^8 CFU/mouse) strain vaccine. No significant weight loss, mortality, or serious clinical signs were observed after vaccination. Two weeks after the third vaccination, blood was collected to measure ST-specific antibodies, and the spleen was collected to measure ST-specific T cell responses. To examine the protective efficacy of the vaccination, mice were challenged i.p. with ST WT (5×10^5 CFU/mouse) two weeks after the third vaccination. Mouse survival was monitored for 14 days.

All pigs were acclimatized according to the protocols of the Central Animal Research Laboratory at the Chonbuk National University (Iksan, Republic of Korea). Pregnant sows were divided equally into two groups (n=3). All groups were primed orally during week 8 of pregnancy and boosted orally during week 11 of pregnancy with approximately 2×10^9 CFU of ATOMSal-L6. Blood samples were collected from the pregnant sows in all groups as the same methods mentioned in the previous study (42) at 0 (prior to priming during week 8 of pregnancy), 3 (prior to the booster during week 11 of pregnancy), 5 and 8 (on the day of farrowing) weeks post prime immunization (PPI). Colostrum samples were collected from the sows within 4 h after farrowing. In addition, blood samples were taken from the jugular veins of their suckling piglets 6 days after birth. Three weeks after the second vaccination, the sows and piglets were challenged orally with ST WT (5×10^8 CFU). Survival was monitored for 14 days.

Measurement of *Salmonella*-Specific Immunoglobulin Levels

Blood samples from mice and pigs were obtained 14 days after the last vaccination. *Salmonella* antigen lysates were prepared as was elaborated in previous sections. ST WT was grown in LB broth and harvested at OD_{600} = 0.8. The pellet was washed with PBS followed by sonication 30 times for 5 s. Samples were centrifuged at 13,000 rpm for 10 min at 4°C, and the supernatants were collected and stored at −70°C. Total protein concentration was measured using the Pierce™ BCA Protein Assay Kit (Thermo Fisher Scientific, Waltham, MA, USA). To examine the levels of ST-specific immunoglobulins (Igs), *Salmonella* lysate (10 μg/well) was immobilized on 96-well plates for 16 h at 4°C, followed by blocking with 1% BSA in PBS. After washing thrice with PBS containing 0.05% Tween-20 (PBS-T; Sigma-Aldrich), serial two-fold dilutions of mouse or pig serum (100 μL) were added to each well and incubated at 23°C for 2 h. The plates were washed five times with PBS-T to remove unbound antibodies, and bound antibodies were detected using horseradish peroxidase (HRP)-conjugated anti-mouse Igs (anti-mouse IgM, IgG, IgG1, and IgG2a; 1:5000 dilution in PBS-T; Sigma-Aldrich) or HRP-conjugated anti-pig IgM and IgA (1:5000 dilution in PBS-T; Southern Biotech, Birmingham, AL, USA) for 1 h at room temperature. After washing seven times with PBS-T, 100 μL of 3,3',5,5'-tetramethylbenzidine substrate solution (INTRON Inc., Seoul, Republic of Korea) was added, followed by incubation for 5–10 min at 23°C. When the color was sufficiently developed, 50 μL of 2 N H_2SO_4 stop solution (Daejung Chemicals; Siheung, Republic of Korea) was added. The absorbance at 450 nm was measured using an Epoch 2 plate reader (BioTek).

Splenocytes Analysis by Flow Cytometry

Two weeks after the final immunization, spleens from mice immunized with either the PBS or ATOMSal-L6 vaccine were isolated and filtered through a cell strainer (70 μm; SPL). Red blood cells (RBCs) were lysed with RBC lysis buffer (Sigma-Aldrich) and washed with RPMI-1640 medium containing 10% FBS. The cell suspension was seeded into a 48-well plate (2×10^6 cells/well) and stimulated with 10 μg/mL ST WT lysate, 0.5 μg/mL GolgiStop (BD Bioscience, San Diego, CA, USA), and 0.5 μg/mL GolgiPlug (BD Bioscience) at 37°C for 12 h. To analyse Helper T cells, the cells were washed with PBS and stained with a Live/Dead Staining Kit (L/D; *In vivo*Gen, San Diego, CA, USA), anti-CD8-FITC (BD Bioscience), and anti-CD4-BV421 (BD Biosciences) for 20 min at 23°C to stain T cell surface markers. Cells were fixed and permeabilized using a Cytofix/Cytoperm kit (BD Bioscience) for 20 min at 4°C, and the intracellular cytokines were stained with anti-IFN-γ-PE (BD Biosciences), anti-IL-5-APC (BD Bioscience), and anti-IL-17A-PE-Cy7 (BD Bioscience) for 20 min at 23°C. After staining, the cells were analyzed using a MACS Quant flow cytometer (Miltenyi Biotec, San Diego, CA, USA) and FlowJo software (TreeStar, Ashland, OR, USA). For

further analysis of the multifunctional T cells, the staining was performed in the same method as was described above. Briefly, the T cells surface staining antibodies were used with 7-AAD (7-Amonoactinomysin D; Sigma), anti-CD3e-Alexa Fluro 488 (BD Biosciences), anti-CD4-BV421 (BD Biosciences), and anti-CD8-V500 (BD Biosciences) and intracellular cytokines staining antibodies were stained with anti-IFN-γ-PE (BD Biosciences), anti-TNF-α-APC (BD Bioscience), and anti-IL-2-PE-Cy7 (BD Bioscience).

Adoptive Transfer of Sera, $CD4^+$ or $CD8^+$ T Cells

Individual mouse sera, prepared as described above, were mixed and 100 μL of pooled sera were administrated i.p. to naïve C57BL/6 mice (n = 5). Mouse spleen cells were prepared by passing spleen specimens through a cell strainer (70 μm; SPL), and red blood cells were lysed with RBC lysis buffer (Sigma-Aldrich). Splenic $CD4^+$ and $CD8^+$ T cells were separated using Miltenyi MACS microbeads conjugated with anti-CD4 and anti-CD8 monoclonal antibodies (Miltenyi Biotec) and a MACS LS column (Miltenyi Biotec). Isolated $CD4^+$ or $CD8^+$ T cells (5×10^6 cells or 5×10^5 cells/mouse) were administered i.p. to naïve C57BL/6 mice (n = 5). After 12 h, mice were challenged i.p. with ST WT (5×10^5 CFU/mouse) and mouse survival was monitored for 14 days.

Statistical Analysis

Data are expressed as the mean ± standard deviation (SD). Data in the bar and dot graphs between groups were compared using an unpaired Student's *t*-test for normal data distribution or the Mann–Whitney non-parametric test for abnormal data distribution using GraphPad Prism (version 7.0; GraphPad Software, Inc., La Jolla, CA, USA). The survival of mice was determined using Kaplan–Meier survival analysis, and the significance of the difference was analyzed using a log-rank test with GraphPad Prism software. $P < 0.05$ was considered statistically significant.

RESULTS

Construction of the Attenuated *Salmonella* Strain (ATOMSal-L6) Using R-MET

Radiation mutatin rate was calculated as the rate of generation of antibiotic resistant before and after irradiation (43). To optimize the R-MET condition, ST WT (10^9 - 10^{10} CFU, $A_{600} = 1.0$) was irradiated with the indicated dose of gamma ray and then plated on LB agar with or without kanamycin. As was shown in **Figure 1A**, the number of ST WT on the LB agar plate gradually decreased after irradiation, and no colonies were detected above a radiation dose of 2.5 kGy. In contrast, kanamycin-resistant mutations were not detected before irradiation, but were predominantly present at doses between 0.5–1.5 kGy. We compared the ratio of survived viable and mutated bacteria and selected 1.5 kGy as the optimal radiation dose, because it gave rise to 0.88 ± 0.18 mutants/10^{10} CFU. A schematic procedure for the development of an attenuated *Salmonella* vaccine strain is presented in **Figure 1B**. To construct an attenuated vaccine strain, the ST WT strain was exposed to 1.5 kGy γ-radiation for 1 h followed by plating on LB agar. After incubation for at least 2 days at 28°C, unusual shaped colonies were picked and inoculated into LB broth. This process was repeated 3 or more times to enrich the mutated strains. Finally, 30 colonies were selected as the mutant candidates of ST WT.

The ability of *Salmonella* to invade and replicate in the intracellular vacuoles is crucial for the initial stage of an invasive disease (44). Therefore, we examined the attenuation of mutant candidates by performing cell invasion and replication assays and compared them to the ST WT. RAW264.7 monolayers were infected with each mutant strain (ST WT-IR #) and invasion (2h) and replication (18h) rates were compared to the ST WT strain (**Figure 1C**). Most of the selected mutants showed at least 50% lower levels of invasion and replication capacity than the parent strain (ST WT). We selected five mutants. The mutants #8 and #16 had lower levels of invasiveness (<1%), but higher levels of replication (>25%). Mutants #17 and #18 had high levels of invasiveness (>40%), but low levels of replication (<25%). Mutant #29 was chosen as the control mutant.

To compare virulence, mice (BALB/c; n=5/group) were orally inoculated with the candidates (ST WT-IR #8, #16, #17, #18, #29) and their colonization in cecum and invasion into the spleen and mesenteric lymph node (mLN) were counted 1 day post infection (d.p.i.). Compared to the ST WT, most of the mutants, except #18, had similar levels of colonization in the caecum, spleen, and mLN. Mutant #18 did not show significant change in the level of colonization in the cecum, but showed a significant reduction in organ invasiveness compared to the ST WT (**Figure 1D**). No bacteria were detected in the blood, liver, and lungs (data not shown). Thus, #18 was possibly the most attenuated mutant among the selected candidates. To analyze the lethal dose 50 (LD_{50}), mice (n=3/group) were injected with an increasing dose of #18 or ST WT i.p. LD_{50} was calculated using "Quest Graph LD_{50} calculator", ST WT was 2.71×10^4 CFU/mouse, while #18 was approximately 2.69×10^8 CFU/mouse, making #18 about 9,961 times less virulent than its parent strain (ST WT); therefore, #18 was designated ATOMSal-L6 in this study.

Genetic and Biochemical Characterization of ATOMSal-L6

To confirm the phenotypical stabilization of ATOMSal-L6 strain, it was sequentially cultured 10 times in LB broth and re-examined for virulence. When growth rates were compared with ST WT, ATOMSal-L6 showed a similar growth pattern to ST WT at 37°C and 42°C, but no growth at 45°C (**Figure 2A**). Next, we examined its biochemical characteristics using Analytical Profile Index (API) analysis (**Tables S1–3**). The biochemical profiling of Gram-negative identification (API 20NE) showed no differences; however, esterase (C4) and several carbohydrates utilization profiled (API ZYM, 50CH) were slightly different compared to ST WT. For example,

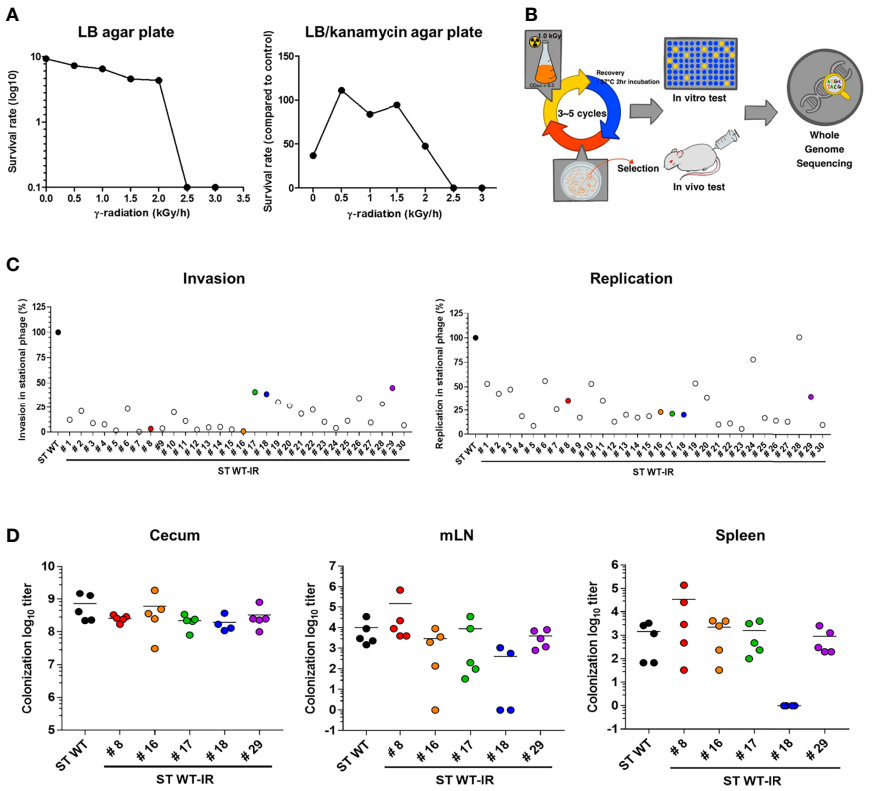

FIGURE 1 | Construction of attenuated *Salmonella* vaccine strain using radiation mutation enhancement techniques (R-MET). **(A)** The radiation dose selection for R-MET. ST WT was irradiated with high-dose ^{60}Co gamma-ray. The ratio of survived/dead bacteria was evaluated by plating on LB plate (left panel) and mutated strains were detected by plating on LB plate with 10 μg kanamycin (right panel). **(B)** Schematic for developing attenuated *Salmonella* vaccine strains. **(C)** *In vitro* virulence test. Macrophages (RAW 264.7 cells) were infected with ST WT or selected candidates (n=30) at a multiplicity of infection of 10 and bacterial viability was evaluated at 2 h (invasion; left panel) or 18 h (replication; right panel). Relative invasion and replication fold of candidates were calculated by comparing with ST WT. Data are representative of three independent experiments and are presented as the mean ± standard deviation. **(D)** *Salmonella* colonization in mice organs. BALB/c mice (n=5) were inoculated orally with 1×10^8 CFU WT and attenuated candidates (8, 16–18, 29). At 72 hpi, the number of bacteria in the cecum (left panel), mLN (middle panel), and spleen (right panel) were counted. Data were presented as the mean ± standard deviation. CFU, colony forming unit; WT, wild type; hpi, hours post-infection; mLN, mesenteric lymph nodes.

ATOMSal-L6 fully utilized esterase and carbon sources (L-arabinose and D-mannose) and showed weak signal at D-ribose, L-rhamnose, and melibiose, but ST WT did not. We tested the antibiotic susceptibility of ST WT and ATOMSal-L6 with MIC (**Table S4**). The MIC of ATOMSal-L6 against KAN, CFR, TMP, and TOB were same with ST WT. The MIC of ATOMSal-L6 against TET, ERM, GEN, AMC, AMK, and STR were 3-fold lower than ST WT. The MIC of ATOMSal-L6 against AMP, SPT, LIN, and CLI were more than 9-fold lower than ST WT. These data indicated that ATOMSal-L6 likely loses its ability to resist antibiotic stress during R-MET process.

To directly visualize the extracellular structure of ATOMSal-L6, Scanning Electron Microscopy (SEM) was performed (**Figure 2B**). Compared with ST WT, ATOMSal-L6 showed no significant difference in size and shape; however, a higher level of flagellin was expressed (**Figure 2B**). To examine whether higher expression of flagellin affected the motility of ATOMSal-L6, we performed swarming assay (Surprisingly, even though ATOMSal-L6 expressed higher flagellin than ST WT, its motility on semi-solid swarming agar media was generally lower than that of ST WT (**Figure 2C**).

The virulence attenuation of ATOMSal-L6 was re-examined *in vitro* and *in vivo*. ATOMSal-L6 or ST WT was added onto RAW 264.7 monolayers at MOIs of approximately 1, 10, or 100 and their invasion and replication abilities were compared as above (**Figure 2D**). As expected, ATOMSal-L6 showed dramatically reduced invasiveness and replication capacity compared to ST WT. When mice (n=5/group) were injected i.p. with ST WT or ATOMSal-L6, all mice infected with ST WT (10^5 CFU/mice) died within 5 days post-infection and only 20% of mice were survived by infecting with extremely high number of ATOMSal-L6 (10^9 CFU/mouse), whereas all mice infected with 1,000-fold higher numbers of ATOMSal-L6 (10^8 CFU/mouse) exhibited 100% survival for more than 14 days (**Figure 2E**).

To analyze the location of mutations in ATOMSal-L6, the complete genome of ATOMSal-L6 was sequenced and compared to ST WT as a reference genome. As shown in **Figure S1A**, we

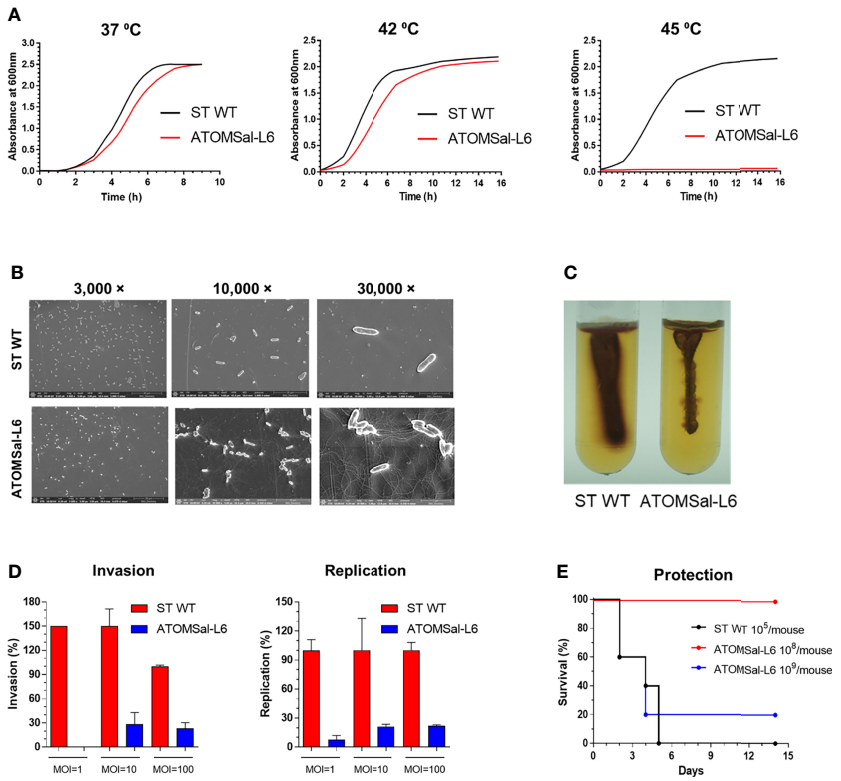

FIGURE 2 | Analysis of biochemical and genetic characteristics of ATOMSal-L6. **(A)** Growth curve of ST WT and ATOMSal-L6 at 37°C, 42°C, and 45°C. **(B)** Morphology analysis of ST WT and ATOMSal-L6 using scanning electron microscopy (SEM; left panel). **(C)** *Salmonella* motility assay for ST WT and ATOMSal-L6 on LB containing 0.4% agar and 1% triphenyltetrazolium chloride at 37°C for 3 days. One *Salmonella* colony on LB agar plate was stabbed once to a depth of ~2 cm in the middle of the motility agar tube (right panel). **(D)** *In vitro* virulence test. Macrophages (RAW 264.7 cells) were infected with ST WT or selected candidates at MOI = 1, 10, 100, and bacterial viability was evaluated at 2 h (invasion; left panel) or 18 h (replication; right panel). Relative invasion and replication fold of candidates were calculated by comparing with ST WT. Data are representative of three independent experiments and are presented as the mean ± standard deviation. **(E)** *In vivo* virulence of ATOMSal-L6. C57BL/6 mice (n=5) were infected i.p. with ST WT (10^5 CFU) or ATOMSal-L6 strain (10^8, 10^9 CFU) and survival was monitored for 14 days.

found 137 mutations in ATOMSal-L6 genome, including 6.56% (n=9) of point mutation (transition and transversion), 90.51% (n=124) of insertion, and 2.92% (n=4) of deletion. Mutation sites were designated to the circular form of ATOMSal-L6 genome (**Figure S1B** and **Table S5**). Surprisingly, only 9 mutations were occurred in A or T nucleotides and the others (n=126) were all mutated in G and T. Of note, we found that ATOMSal-L6 lost one bacteriophage located at 3,440,538 bp - 3,481,579 bp encoded by IS1595 transposase phage genes (gene bank number = CP098438-CP098439). All these data suggested that R-MET introduced many mutations and that these mutations could attenuate its virulence *in vitro* and *in vivo*.

High Immune Response by Immunizing I.M. With ATOMSal-L6 Vaccine in Mice

To determine whether the ATOMSal-L6 could be used as a live attenuated vaccine, the vaccine efficacy of ATOMSal-L6 was examined using a mouse model. Mice (n=5/group) were immunized intramuscularly (i.m.) with 10^5, 10^6, or 10^7 CFU of ATOMSal-L6 and *Salmonella*-specific humoral, cellular, and protective immune response were measured. At 2 weeks after the last immunization, *Salmonella*-specific IgM and IgG were measured with ELISA. As shown in **Figure 3A**, Salmonella-specific IgM was significantly increased in all groups, whereas Salmonella-specific IgG was significantly increased only in the group immunized with 10^7 CFU compared to unvaccinated (NT) group. Furthermore, we found that Th2 response (IgG1) was the dominant immune response over Th1 (IgG2a) in the group immunized with 10^7 CFU (**Figure 3B**).

Next, since both $CD4^+$ and $CD8^+$ T cells are crucial for protection against *Salmonella* infection (45, 46), we evaluated T cell subtypes induced by ATOMSal-L6 vaccination. Mice (n=5/group) were immunized i.m. thrice at 2-week intervals, and single cell splenocytes were re-stimulated with 10 μg of ST WT lysate, followed by analyzing Th1 (IFN-γ-producing $CD4^+$ T cells), Th2 (IL-5-producing $CD4^+$ T cells), Th17 (IL-17A-producing $CD4^+$ T cells), and activated $CD8^+$ T cells (IFN-γ-producing $CD8^+$ T cells) using flow cytometry gating, as shown in **Figure S2**. The population of Th2 and Th17 cells was not changed after immunization (data not shown), but significant

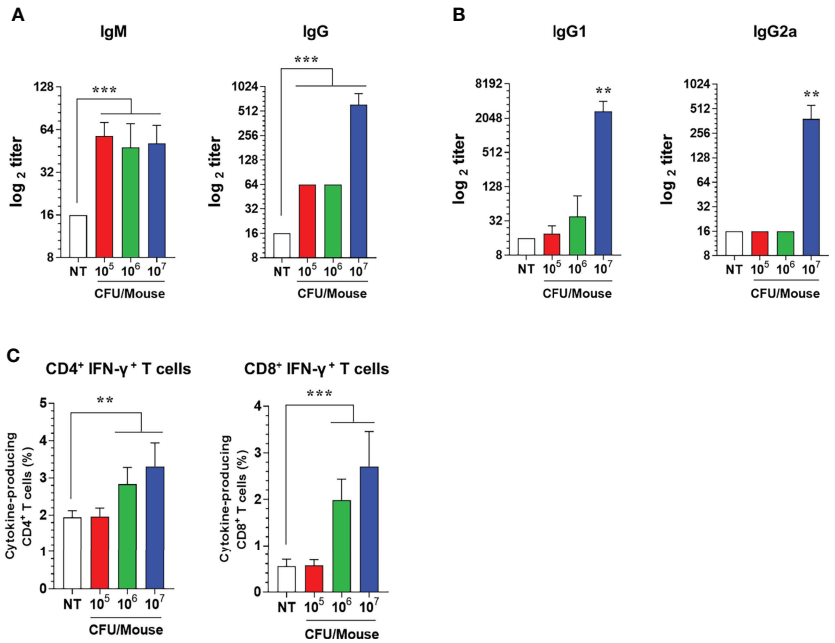

FIGURE 3 | Humoral and cellular immune responses induced by i.m. immunization of ATOMSal-L6. C57BL/6 mice (n = 5 per group) were immunized i.m. with 10^5, 10^6, or 10^7 CFU of ATOMSal-L6 thrice at two-week intervals. **(A, B)** Humoral immune response. Serum levels of *Salmonella*-specific IgG and IgM were analyzed at 7 days following the last immunization **(A)**. Subclass levels of *Salmonella*-specific IgG1 and IgG2a were analyzed at 7 days subsequent to the last immunization **(B)**. Data are representative of three independent experiments and are presented as the mean ± standard deviation. **(C)** Cellular immune response. Single cell suspensions of spleen were re-stimulated with 10 μg/mL ST WT lysate for 12 h and ST-specific $CD4^+$ and $CD8^+$ T cells were analyzed. Percentages of activated $CD4^+$ and $CD8^+$ T cells in spleens of vaccinated mice. Data were presented as mean ± standard deviation. *P < 0.05, **P < 0.01, ***P < 0.001, compared to unvaccinated mice.

enhancement of Th1 (IFN-γ^+ $CD4^+$ T cells) and $CD8^+$ T cells (IFN-γ^+ $CD8^+$ T cells) were detected when immunized with 10^6 or 10^7 CFU ATOMSal-L6 vaccination compared to the NT group (**Figure 3C**).

To investigate whether humoral and cellular immunity induced by ATOMSal-L6 vaccination could provide a protective immune response, ATOMSal-L6 (10^6 CFU) vaccinated mice (n=5/group) were infected i.p. with ST WT (5×10^5 CFU/mouse) and their survival monitored for 14 days. As shown in **Figure 4A**, all unvaccinated mice died at 7 d.p.i, whereas all vaccinated mice survived more than 14 days. In addition, ST WT that invaded the spleen or liver were counted at 1 d.p.i (**Figure 4B**). More than 10^6 CFU/g of invasive bacteria were detected in the spleen and liver from unvaccinated mice, whereas significantly lower number of ST WT were detected in ones from ATOMSal-L6 vaccinated mice.

To test whether the protective immune response was due to humoral or cellular immune responses, sera (100 μL/mouse), $CD4^+$ T cells (5×10^6 cells/mouse), or $CD8^+$ T cells (5×10^5 cells/mouse) were collected from ATOMSal-L6 vaccinated, or unvaccinated mice followed by adopted transfer to naïve mice (n=5/group). After infecting i.p. with ST WT (5×10^5 CFU), all mice transferred with sera or T cells from unvaccinated mice had died at 6–7 d.p.i, whereas all mice transferred with sera from ATOMSal-L6 vaccinated mice survived for more than 14 d.p.i (**Figure 4C**). Although only 40% of the mice that were provided with $CD8^+$ T cells from ATOMSal-L6 vaccinated mice survived, it was not significant, but still marginally higher (p=0.1338) than that of mice transferred with $CD8^+$ T cells from unvaccinated mice (**Figure 4D**). We did not observe a significant difference between $CD4^+$ T cells adopted transferred from different groups (data not shown). All these data suggested that ATOMSal-L6 provided an effective immune response to protect from *Salmonella* infection by activating both humoral and cellular immune responses.

High Immune Response by Immunizing Orally With ATOMSal-L6 Vaccine in Mice

Because oral vaccination of live attenuated *Salmonella* vaccine is recommended for adult pigs and humans (47, 48), we next investigated whether ATOMSal-L6 could be used as an oral vaccine. To examine the virulence of ATOMSal-L6 *via* oral vaccination, mice were immunized orally with ST WT or ATOMSal-L6. No mice died even after oral administration of 10^7 CFU of ST WT or ATOMSal-L6 (data not shown). When intestinal inflammation after ST WT infection, we observed substantial infiltration of immune cells in both the small and large intestine in the ST WT-immunized group (**Figure 5A**). No significant inflammation or damage were observed in the intestinal tissues of ATOMSal-L6 immunized mice, which

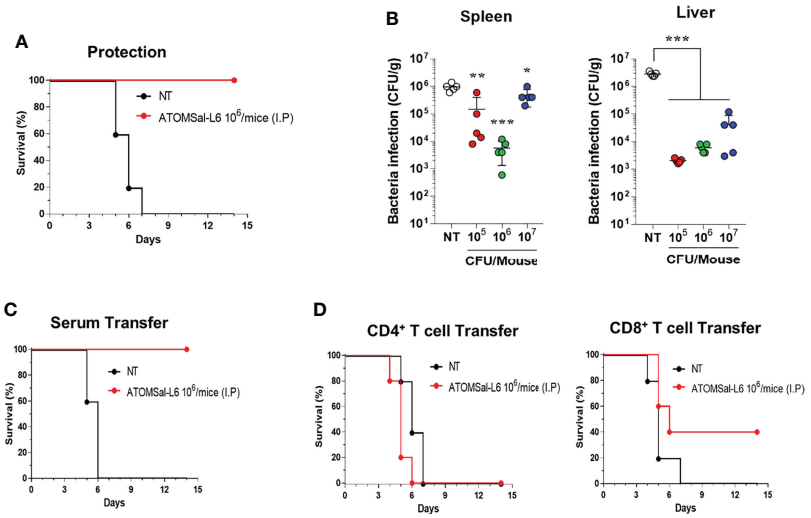

FIGURE 4 | Protective immune responses induced by I.M. immunization of ATOMSal-L6. **(A, B)** Protective immune response. ATOMSal-L6 immunized mice (n=5) were challenged i.p. with 5 × 10^5 CFU ST WT strain and survival was monitored for 14 days **(A)**. Protection of *Salmonella* colonization in mice organs by ATOMSal-L6 vaccination were measured by counting the number of bacteria in the spleen (left panel), and liver (right panel) **(B)**. Data were presented as mean ± standard deviation. *P < 0.05, **P < 0.01, ***P < 0.001, compared to unvaccinated mice. **(C, D)** Protection by the adopted transfer of ATOMSal-L6-vaccinated mice serum **(C)** and $CD4^+$ or $CD8^+$ T cells **(D)** against *Salmonella* infection. Mice were immunized with ATOMSal-L6 thrice at 14-day intervals. Serum (100 µL) or splenic $CD4^+$ (5 × 10^6 cells) or $CD8^+$ T cells (5 × 10^5 cells) from NT or ATOMSal-L6-immunized mice were transferred i.p. into naïve C57BL/6 mice (n=5). At 12 h following inoculation, mice were challenged intraperitoneally with 5 × 10^5 CFU ST WT strain. Mouse survival was monitored for 14 days.

showed similar results to those observed in the NT group (**Figure 5A**). To evaluate whether oral immunization of ATOMSal-L6 elicited *Salmonella*-specific immune response, mice (n=5/group) were immunized orally thrice with 10^6, 10^7, or 10^8 CFU of ATOMSal-L6, and the humoral and cellular immune responses were evaluated. Oral ATOMSal-L6 vaccination resulted in a increase in serum *Salmonella*-specific IgG, and a slight increase in *Salmonella*-specific IgM (**Figure 5B**).

We next analyzed the functional composition of *Salmonella*-specific single- or multi-functional cellular immune responses (49). Mice (n=5/group) were immunized orally thrice at two-weeks interval, following which they were analyzed for *Salmonella*-specific splenic $CD4^+$ T cells and $CD8^+$ T cells using cytometric gating, as shown in **Figure S3**. Only the 10^8 CFU ATOMSal-L6 were found to have significantly increased frequencies of IFN-γ^+CD4^+ (compared to NT group; up to 7.60-fold, p<0.001) and TNF-α^+CD4^+ (compared to NT group; up to 2.05-fold, p=0.005), but no changes were found from IL-2^+CD4^+ T cells. In addition, we found that multifunctional IFN-γ^+ TNF-α^+CD4^+ (compared to NT group; up to 18.15-fold, p=0.007) and IFN-γ^+ IL-2^+CD4^+ (compared to NT group; up to 6.06-fold, p=0.004) were significantly increased upon oral vaccination. Similarly, single- and multi-functional $CD8^+$T cells were significantly increased in the 10^8 CFU ATOMSal-L6 (**Figure 5C**). All these data indicated that oral immunization of live ATOMSal-L6 could induce *Salmonella*-specific humoral and cellular immunities.

To evaluate the protective immunity of ATOMSal-L6 oral vaccination, mice (n=5/group) were immunized orally thrice with ATOMSal-L6 (10^8 CFU) at two-weeks interval, followed by injecting i.p. ST WT (ST454; 5 × 10^5 CFU). As shown in **Figure 5D**, all unvaccinated mice died at 14 d.p.i, but 60% of the vaccinated mice survived for more than 14 d.p.i. To examine whether the protective immune response was due to humoral or cellular immune responses, sera (100 µL/mouse), $CD4^+$ T cells (5 × 10^6 cells/mouse), or $CD8^+$ T cells (5 × 10^5 cells/mouse) were collected from ATOMSal-L6 vaccinated or unvaccinated mice, followed by adopted transfer to naïve mice (n=5/group). After infecting with ST WT (5 × 10^5 CFU), all mice transferred with sera or T cells from unvaccinated mice died at 6 - 7 d.p.i whereas 80%, 40%, and 20% of the mice transferred with sera (**Figure 5E**), $CD4^+$ T cells, and $CD8^+$ T cells (**Figure 5F**), respectively. All these data suggested that oral live ATOMSal-L6 vaccine provided effective immune response to protect from *Salmonella* infection by activating both humoral and cellular immune responses.

High Protective Immune Response by Immunizing I.M. With ATOMSal-L6 Vaccine in Pig

To examine the efficacy of ATOMSal-L6 vaccine (2 × 10^9 CFU/pig) in pig model, pregnant sows were immunized orally with live ATOMSal-L6 twice at three-week intervals. Sera were collected at 3, 6, and 8 weeks, and *Salmonella*-specific IgG antibodies were measured using ELISA. As shown in **Figure 6A**, the vaccinated group showed the increase IgG levels compared to the unvaccinated group. We also collected colostrum on the day of delivery and observed that *Salmonella*-specific IgG and IgA levels were enhanced in the vaccinated group (**Figure 6B**).

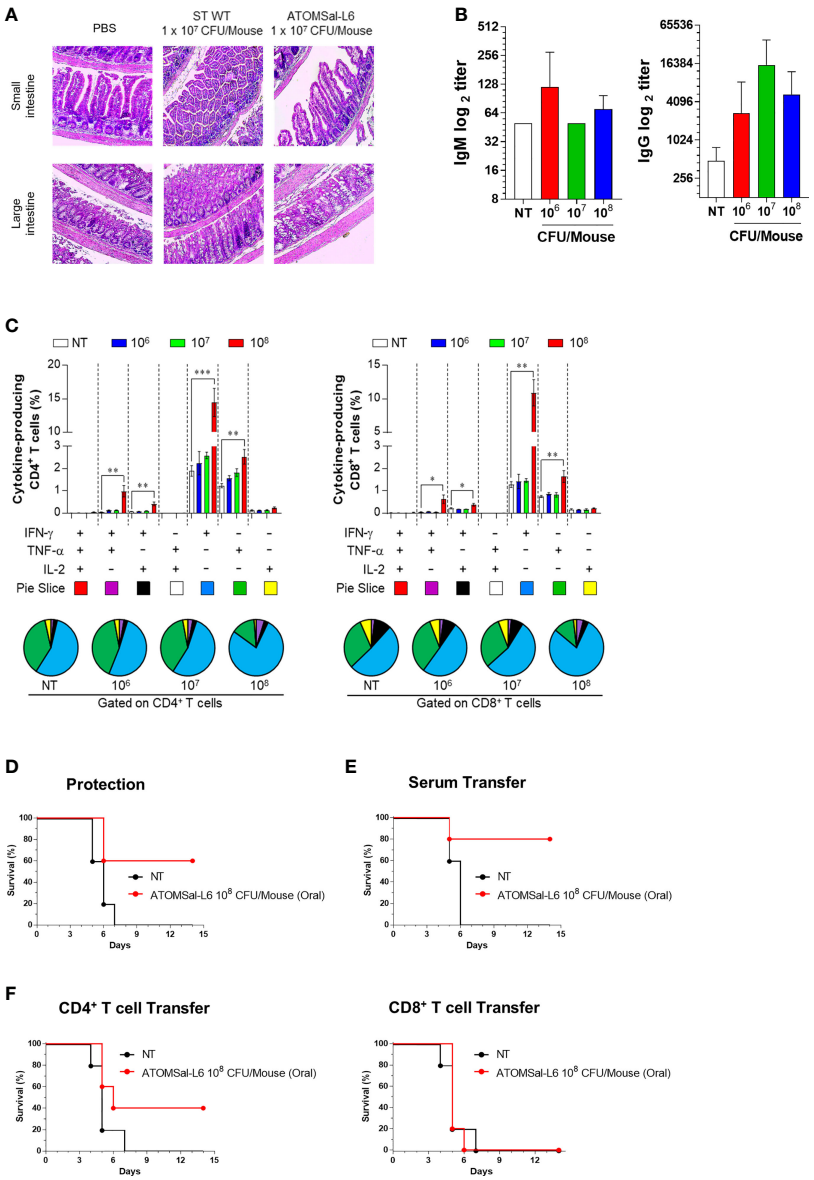

FIGURE 5 | Analysis of humoral and cellular immune responses induced by oral immunization of ATOMSal-L6. **(A)** Safety of ATOMSal-L6 vaccine. Mice were inoculated orally with 10^7 CFU of ST WT or ATOMSal-L6. At 3 d.p.i, mice were sacrificed, and small or large intestinal tissue were stained with H&E. **(B)** Humoral immune response. Mice (n = 5 per group) were orally immunized with 10^6, 10^7, or 10^8 CFU of ATOMSal-L6 thrice at two-week intervals and sera were collected two weeks after the last vaccination. ST-specific IgM (left panel) and IgG (right panel) were measured using ELISA. **(C)** Cellular immune response. Single cell suspensions of spleen were re-stimulated with 10 μg/mL ST WT lysate for 12 h and ST-specific multifunctional $CD4^+$ and $CD8^+$ T cells were analyzed. The percentage of ST-specific total cytokine (IFN-γ, TNF-α, and/or IL-2)-producing cells among splenic $CD4^+CD44^+$ memory T cells (left panel) or $CD8^+CD44^+$ memory T cells (right panel). Pie charts (bottom panel) representing the mean frequencies of cells co-expressing IFN-γ, TNF-α, and/or IL-2. The relative amounts of single-, double-, and triple-functional memory T cells are indicated as pie arcs. Means ± SD (n = 5 mice/group) shown are representative of two independent experiments. *P < 0.05, **P < 0.01, ***P < 0.001, compared to unvaccinated mice. **(D)** Protective immune response. Mice (n=5) were immunized orally with ATOMSal-L6 (1×10^8 CFU) and challenged i.p. with 5×10^5 CFU of ST WT strain and survival was monitored for 14 days. **(E, F)** Protection by the adopted transfer of oral ATOMSal-L6-vaccinated mice serum **(E)** and $CD4^+$ or $CD8^+$ T cells **(F)** against *Salmonella* infection. Mice were immunized orally with ATOMSal-L6 twice at 14-day intervals. Serum (100 μL) or splenic $CD4^+$ (5×10^6 cells) or $CD8^+$ T cells (5×10^5 cells) from NT or ATOMSal-L6-immunized mice were transferred i.p. into naïve C57BL/6 mice (n=5). At 12 h following inoculation, mice were challenged intraperitoneally with 5×10^5 CFU ST WT strain. Mouse survival was monitored for 14 days.

To measure the protective response of ATOMSal-L6 vaccine, vaccinated sows were orally infected with ST WT (5×10^8 CFU/pig) and their diarrheic symptoms were monitored for 14 days. All the vaccinated sows (n=10) were free of diarrheic symptoms, whereas all the unvaccinated sows had severe diarrhea (**Figure 6C**). To determine whether *Salmonella*-specific protective antibodies were delivered from the gilt to the piglet, piglets (n=10) born from vaccinated gilts were infected orally

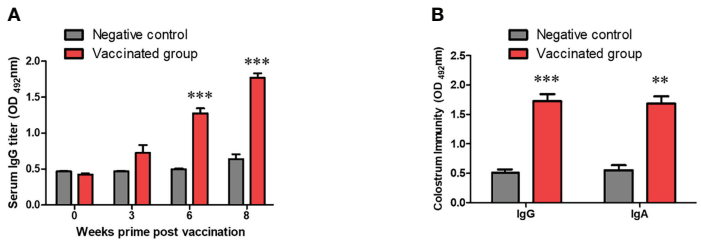

C

	No. of diarrhic sows	Protection (%)
NT	10/10	0 %
ATOMSal-L6	0/10	100%

D

	No. of diarrhic piglets	Protection (%)
NT	10/10	0 %
ATOMSal-L6	3/10	70%

FIGURE 6 | Analysis of humoral immune responses induced by immunization of ATOMSal-L6 in swine. Pregnant sows (n = 3 per group) were immunized orally with 2×10^9 CFU of ATOMSal-L6 twice at three-week intervals. Sera were collected two weeks after the vaccination and colostrum was collected on day of delivery. **(A)** ST-specific serum IgG and **(B)** ST-specific colostrum IgG and IgA were measured using ELISA. **(C)** Sows (n = 10/group; left panel) and **(D)** piglets (n=10/group; right panel) born from vaccinated sows were orally challenged with 5×10^8 CFU of ST WT and monitored for diarrhea symptoms and survival for 14 days. **P < 0.01, ***P < 0.001, compared to unvaccinated group.

with ST WT (5×10^8 CFU/pig) and their survival rates were monitored. As shown in **Figure 6D**, all piglets from the unvaccinated gilts had severe diarrhea and died at 7 d.p.i, but only 30% of piglets born from vaccinated gilts showed lethal and severe diarrhea at 14 d.p.i. We monitored the surviving piglets for more than 21 d.p.i and found no severe diarrheic symptoms. All these data indicated that ATOMSal-L6 could be a safe and effective live attenuated vaccine in pig.

DISCUSSION

The *Salmonella* vaccine program in poultry has been successfully implemented to control the prevalence of human Salmonellosis in the UK (50, 51), and mass vaccine administration to economically important animals is considered the best strategy to prevent transmission of *Salmonella* to animals and humans. However, due to the emergence of new serotypes and multi-drug resistant *Salmonella* worldwide (12, 52–54), more effective and broad-spectrum *Salmonella* vaccines are being developed. Unlike conventional inactivated vaccines, live attenuated vaccines could induce life-long immunity through one or two doses by activating multifunctional cellular immune responses (22, 55, 56). Nevertheless, this type of vaccine has not been widely used against bacteria because it could cause diseases in immunocompromised individuals and the vaccine could potentially re-acquire its pathogenicity by reverting the mutation (57, 58). In addition, rapidly developing the vaccines against newly emerging serotypes or new pathogens has proven difficult. In this study, we introduced a technology to rapidly develop a live attenuated *Salmonella* vaccine, ATOMSal-L6, using R-MET that can be attenuated by accelerating mutation. In addition, because R-MET technology can introduce various forms of mutations (deletion, insertion, SNP), it will be possible to solve the problem of current live vaccines that re-acquired pathogenicity by genetic revertant (40, 59, 60).Due to these mutations, ATOMSal-L6 differed in biochemical properties from its parent strain. For example, it produces more flagellin but less mobility, and cannot be grown at high temperatures (45° C). And it was confirmed that resistance to specific antibiotic resistance was reduced compared to ST WT. The resistance to the aminoglycoside antibiotics did not change significantly, but the resistance to the macrolides antibiotics was reduced more than 3 times compared to the ST WT. This change in antibiotic resistance will be a good standard for separating and analyzing wild-type and vaccine strain in the clinical samples. All these genetic and biochemical changes might have contributed to the attenuation and immunological properties of ATOMSal-L6.

To the best of our knowledge, compared to UV radiation and chemical mutagens, γ-radiation has not been widely used to induce mutations in vaccine industries because it requires a high-dose radiation facility, and all mutations must be detected and selected painstakingly at the phenotypic level. However, in recent years, new and re-emerging infectious diseases have become prevalent. Using R-MET, which can rapidly and effectively develop live vaccines, might be more attractive (40). In addition, recent advances in large-scale genomic analysis techniques have enabled easy analysis of the effects of radiation and the location of mutations in the bacterial genome. In this study, we screened only 30 colonies after irradiation using R-MET and found several attenuated candidates with significantly reduced screening times compared to UV or chemical mutagens. Overall, it took about 4 weeks to develop ATOMSal-L6, as the colony selection process took about 2–3 days and the *in vitro* and *in vivo* virulence examination took about 2–3 weeks. However,

the whole genome sequence with comparative genomics and genetic stabilization tests are time-consuming, often requiring several months to complete. Therefore, a systematic process to speed up these genomic analysis processes must be developed.

Live attenuated Salmonella vaccines must balance attenuation with immunogenicity. In particular, both $CD4^+$ and $CD8^+$ T cells are highly associated with protection against early infection of *Salmonella* (61). $CD4^+$ T cells might play a central role in acquired immunity against *Salmonella* infection and make an additional important contribution to both $CD8^+$ T cell- and B cell-immunities. Therefore, live attenuated *Salmonella* vaccines are preferred over inactivated vaccines that do not have high T-cell immunity. Since ATOMSal-L6 induced protection against ST WT infection by activation of $CD4^+$ and $CD8^+$ T cells in mice, it is a good vaccine candidate with the balance between high immunogenicity to enable cellular and humoral immune response and sufficiently high attenuation of its virulence. Our previous study showed that inactivated *S.* Gallinarum activated moderate $CD4^+$ and $CD8^+$ T cell response, but higher Th17 responses (62). It is known that IL-17, increased by Salmonella infection, stimulates intestinal epithelial cells to enhance the production of antimicrobial proteins and chemokines, thereby inhibiting the early invasion of Salmonella bacteria (63, 64). In contrast, ATOMSal-L6 shows no induction of *Salmonella*-specific Th17 response (data not shown) but does high expression of *Salmonella*-specific $CD4^+$ and $CD8^+$ T cells. We therefore speculate that ATOMSal-L6 may have mutated genes involved in the expression of IL-17-induced antigens during the R-MET process. Therefore, immunization with inactivated *Salmonella* vaccine together or sequentially is another option to increase ATOMSal-L6 efficacy.

ATOMSal-L6 is the first attenuated *Salmonella* vaccine strain developed using R-MET. It is more sensitive to high temperature and showed lower motility compared to its parent strain. In addition, we found 8 SNPs, 3 deletions, 60 insertions, and loss of one bacteriophage upon comparing its genome with its parent strain. Compared to licensed *Salmonella* vaccine strains, its genomic mutations are wide and variable. Although there is no parent strain for comparison with *Salmonella enterica* Serovar Choleraesuis vaccine strain C500 attenuated by chemical mutation, when compared to another WT SC-B67 strain, it was deficient in the *rpoS* gene, a vital transcriptional regulator playing an important role in *Salmonella* infection (65). Salmovac440 developed by IDT Biologika has only 6 SNPs, but lacks the pathogenic plasmid that encodes a number of virulence factors (26, 65, 66). Therefore, the attenuation of Salmovac440 may be due to the amino acid biosynthetic system and other virulence mechanisms involving the lost pathogenic plasmid. In this study, we did not investigate on the degree to which each of these mutations in ATOMSal-L6 affected the virulence attenuation. Thus, to use it as a vaccine strain, accurate biochemical information of ATOMSal-L6 must be acquired, and in particular, additional research on the relationship with the mutation and the virulence must be performed.

In the absence of overt disease, the vaccine strain attenuated in metabolic gene(s) must be metabolically active to reach immune inductive sites and elicit a biologically relevant protective immunity. However, the hyper-attenuation of vaccine strains may result in lower virulence and less effective protective immune responses. Thus, it is necessary to develop a strain that can moderately reduce virulence and induce immunity at a level that does not cause disease. For example, WT05 is the attenuated *S.* Typhimurium vaccine in which the *aroC* gene, involved in aromatic amino acid biosynthesis, and the *ssaV* gene, a component of a Type 3 secretion system (T3SS) apparatus of *Salmonella* pathogenicity island 2 (SPI-2), are deleted. However, this vaccine strain was eliminated through prolonged defecation in healthy volunteers immunized with WT05, thereby failing the phase 1 clinical trial (67, 68). LH1160, a *phoPQ* mutant strain that controls the transcription of multiple genes necessary for intracellular survival, had been tested in phase 1 clinical trials, but an unacceptable fever was reported in two of six volunteers (15, 68, 69). In contrast, CVD1921, which is mutated in the *guaBA* genes that are involved in the biosynthesis of guanine nucleotides and the *clpP* gene affecting flagella expression, was revealed to be notably attenuated with decreased elimination, systemic spread, and clinical disease manifestations in the digestive tract of the non-human primate model (rhesus macaque) used (70, 71). Another advantage of R-MET is that it can be applied to strains that are not sufficiently attenuated to further reduce pathogenicity, allowing it to be used as a vaccine strain. Therefore, further attenuation with R-MET can be attempted in the event of clinically significant safety issues such as those resulting from the use of WT05 and LH1160. In addition, if ATOMSal-L6 has not been sufficiently attenuated, R-MET may be additionally applied. Thus, R-MET will be a very effective and attractive method for live bacterial vaccine development.

DATA AVAILABILITY STATEMENT

The datasets presented in this study can be found in online repositories. The names of the repository/repositories and accession number(s) can be found below: NCBI SRA Biproject accession no for HJL222 (ST WT): PRJNA844490; accession no for ATOMSal-L6: PRJNA841760.

ETHICS STATEMENT

The animal study was reviewed and approved by Korea Atomic Energy Research Institute.

AUTHOR CONTRIBUTIONS

HJJ, AYJ, KBA, SHH, HKJ, JH, and HSS were responsible for conceptualization of the study. HJJ, AYJ, SJB, and JH performed the experiments and analyzed the data. HJJ, KBA, SHH, JYS, and HSS wrote the manuscript. HSS supervised the work. HSS was

responsible for funding acquisition. All authors contributed to the article and approved the submitted version.

FUNDING

This work was supported in part by the Internal R&D program of KAERI (523210) funded by Ministry of Science and ICT (MIST) and the National Research Foundation of Korea grants 2017M2A2A6A02020925, NRF-2018K2A206023828, and NRF-2020M2A206023828 to HS and NRF-2019M2D3A2060217 to KA.

ACKNOWLEDGMENTS

We would like to thank Lina Seo (Kwangju Foreign School, South Korea) for drawing **Figure 1B**.

SUPPLEMENTARY MATERIAL

The Supplementary Material for this article can be found online at: https://www.frontiersin.org/articles/10.3389/fimmu.2022.931052/full#supplementary-material

REFERENCES

1. Albert MJ, Bulach D, Alfouzan W, Izumiya H, Carter G, Alobaid K, et al. Non-Typhoidal Salmonella Blood Stream Infection in Kuwait: Clinical and Microbiological Characteristics. *PloS Negl Trop Dis* (2019) 13(4):e0007293. doi: 10.1371/journal.pntd.0007293
2. Haselbeck AH, Panzner U, Im J, Baker S, Meyer CG, Marks F. Current Perspectives on Invasive Nontyphoidal Salmonella Disease. *Curr Opin Infect Dis* (2017) 30(5):498–503. doi: 10.1097/QCO.0000000000000398
3. Feasey NA, Dougan G, Kingsley RA, Heyderman RS, Gordon MA. Invasive non-Typhoidal Salmonella Disease: An Emerging and Neglected Tropical Disease in Africa. *Lancet* (2012) 379(9835):2489–99. doi: 10.1016/S0140-6736(11)61752-2
4. Wiedemann A, Virlogeux-Payant I, Chausse AM, Schikora A, Velge P. Interactions of Salmonella With Animals and Plants. *Front Microbiol* (2014)5:791. doi: 10.3389/fmicb.2014.00791
5. Majowicz SE, Musto J, Scallan E, Angulo FJ, Kirk M, O'Brien SJ, et al. International Collaboration on Enteric Disease 'Burden of Illness: The Global Burden of Nontyphoidal Salmonella Gastroenteritis. *Clin Infect Dis* (2010) 50(6):882–9. doi: 10.1086/650733
6. Marchello CS, Birkhold M, Crump JAC. C. Vacc-iNTS. Complications and Mortality of non-Typhoidal Salmonella Invasive Disease: A Global Systematic Review and Meta-Analysis. *Lancet Infect Dis* (2022) 22(5):692–705. doi: 10.1016/S1473-3099(21)00615-0
7. Reddy EA, Shaw AV, Crump JA. Community-Acquired Bloodstream Infections in Africa: A Systematic Review and Meta-Analysis. *Lancet Infect Dis* (2010) 10(6):417–32. doi: 10.1016/S1473-3099(10)70072-4
8. Uche IV, MacLennan CA, Saul A. A Systematic Review of the Incidence, Risk Factors and Case Fatality Rates of Invasive Nontyphoidal Salmonella (iNTS) Disease in Africa (1966 to 2014). *PloS Negl Trop Dis* (2017) 11(1):e0005118. doi: 10.1371/journal.pntd.0005118
9. Marchello CS, Dale AP, Pisharody S, Rubach MP, Crump JA. A Systematic Review and Meta-Analysis of the Prevalence of Community-Onset Bloodstream Infections Among Hospitalized Patients in Africa and Asia. *Antimicrob Agents Chemother* (2019) 64(1):e01974-19. doi: 10.1128/AAC.01974-19
10. Ao TT, Feasey NA, Gordon MA, Keddy KH, Angulo FJ, Crump JA. Global Burden of Invasive Nontyphoidal Salmonella Disease, 2010(1). *Emerg Infect Dis* (2015) 21(6):941. doi: 10.3201/eid2106.140999
11. Tack B, Vanaenrode J, Verbakel JY, Toelen J, Jacobs J. Invasive non-Typhoidal Salmonella Infections in Sub-Saharan Africa: A Systematic Review on Antimicrobial Resistance and Treatment. *BMC Med* (2020) 18(1):212. doi: 10.1186/s12916-020-01652-4
12. Crump JA, Sjolund-Karlsson M, Gordon MA, Parry CM. Epidemiology, Clinical Presentation, Laboratory Diagnosis, Antimicrobial Resistance, and Antimicrobial Management of Invasive Salmonella Infections. *Clin Microbiol Rev* (2015) 28(4):901–37. doi: 10.1128/CMR.00002-15
13. Zansky S, Wallace B, Schoonmaker-Bopp D, Smith P, Ramsey F, Painter J, et al. From the Centers for Disease Control and Prevention. Outbreak of Multi-Drug Resistant Salmonella Newport–United States, January-April 2002. *JAMA* (2002) 288(8):951–3. doi: 10.1001/jama.288.8.951-JWR0828-2-1
14. G. B. D. N.-T. S. I. D. Collaborators. The Global Burden of non-Typhoidal Salmonella Invasive Disease: A Systematic Analysis for the Global Burden of Disease Study 2017. *Lancet Infect Dis* (2019) 19(12):1312–24. doi: 10.1016/S1473-3099(19)30418-9
15. Tennant SM, MacLennan CA, Simon R, Martin LB, Khan MI. Nontyphoidal Salmonella Disease: Current Status of Vaccine Research and Development. *Vaccine* (2016) 34(26):2907–10. doi: 10.1016/j.vaccine.2016.03.072
16. Strugnell RA, Scott TA, Wang N, Yang C, Peres N, Bedoui S, et al. Salmonella Vaccines: Lessons From the Mouse Model or Bad Teaching? *Curr Opin Microbiol* (2014) 17:99–105. doi: 10.1016/j.mib.2013.12.004
17. Wessels K, Rip D, Gouws P. Salmonella in Chicken Meat: Consumption, Outbreaks, Characteristics, Current Control Methods and the Potential of Bacteriophage Use. *Foods* (2021) 10(8):1742. doi: 10.3390/foods10081742
18. Baliban SM, Lu YJ, Malley R. Overview of the Nontyphoidal and Paratyphoidal Salmonella Vaccine Pipeline: Current Status and Future Prospects. *Clin Infect Dis* (2020) 71(Suppl 2):S151–4. doi: 10.1093/cid/ciaa514
19. Wales AD, Davies RH. Salmonella Vaccination in Pigs: A Review. *Zoonoses Public Health* (2017) 64(1):1–13. doi: 10.1111/zph.12256
20. Desin TS, Koster W, Potter AA. Salmonella Vaccines in Poultry: Past, Present and Future. *Expert Rev Vaccines* (2013) 12(1):87–96. doi: 10.1586/erv.12.138
21. O'Brien SJ. The "Decline and Fall" of Nontyphoidal Salmonella in the United Kingdom. *Clin Infect Dis* (2013) 56(5):705–10. doi: 10.1093/cid/cis967
22. Tennant SM, Levine MM. Live Attenuated Vaccines for Invasive Salmonella Infections. *Vaccine* (2015) 33 Suppl 3:C36–41. doi: 10.1016/j.vaccine.2015.04.029
23. Alderton MR, Fahey KJ, Coloe PJ. Humoral Responses and Salmonellosis Protection in Chickens Given a Vitamin-Dependent Salmonella Typhimurium Mutant. *Avian Dis* (1991) 35(3):435–42. doi: 10.2307/1591205
24. Springer S, Theuss T, Toth I, Szogyenyi Z. Invasion Inhibition Effects and Immunogenicity After Vaccination of SPF Chicks With a Salmonella Enteritidis Live Vaccine. *Tierarztl Prax Ausg G Grosstiere Nutztiere* (2021) 49(4):249–55. doi: 10.1055/a-1520-1369
25. Schmidt S, Kreutzmann H, Stadler M, Mair KH, Stas MR, Koch M, et al. T-Cell Cytokine Response in Salmonella Typhimurium-Vaccinated Versus Infected Pigs. *Vaccines (Basel)* (2021) 9(8):845. doi: 10.3390/vaccines9080845
26. Tang Y, Davies R, Petrovska L. Identification of Genetic Features for Attenuation of Two Salmonella Enteritidis Vaccine Strains and Differentiation of These From Wildtype Isolates Using Whole Genome Sequencing. *Front Vet Sci* (2019) 6:447. doi: 10.3389/fvets.2019.00447
27. Ault A, Tennant SM, Gorres JP, Eckhaus M, Sandler NG, Roque A, et al. Safety and Tolerability of a Live Oral Salmonella Typhimurium Vaccine Candidate in SIV-Infected Nonhuman Primates. *Vaccine* (2013) 31(49):5879–88. doi: 10.1016/j.vaccine.2013.09.041
28. de Serres FJ, Webber BB. Quantitative and Qualitative Comparisons of Spontaneous and Radiation-Induced Specific-Locus Mutation in the Ad-3 Region of Heterokaryon 12 of Neurospora Crassa. *Mutat Res* (1997) 375(1):37–52. doi: 10.1016/S0027-5107(96)00253-9
29. Sankaranarayanan K. Ionizing Radiation and Genetic Risks IX. Estimates of the Frequencies of Mendelian Diseases and Spontaneous Mutation Rates in Human Populations: A 1998 Perspective. *Mutat Res* (1998) 411(2):129–78. doi: 10.1016/S1383-5742(98)00012-X
30. Foster PL, Lee H, Popodi E, Townes JP, Tang H. Determinants of Spontaneous Mutation in the Bacterium Escherichia Coli as Revealed by Whole-Genome Sequencing. *Proc Natl Acad Sci USA* (2015) 112(44):E5990–9. doi: 10.1073/pnas.1512136112

31. Muller HJ. Artificial Transmutation of the Gene. *Science* (1927) 66(1699):84–7. doi: 10.1126/science.66.1699.84
32. Muller HJ. The Production of Mutations by X-Rays. *Proc Natl Acad Sci USA* (1928) 14(9):714–26. doi: 10.1073/pnas.14.9.714
33. Reed AB. The History of Radiation Use in Medicine. *J Vasc Surg* (2011) 53(1 Suppl):3S–5S. doi: 10.1016/j.jvs.2010.07.024
34. Yokoya A, Shikazono N, Fujii K, Urushibara A, Akamatsu K, Watanabe R. DNA Damage Induced by the Direct Effect of Radiation. *Radiat Phys Chem* (2008) 77(10-12):1280–5. doi: 10.1016/j.radphyschem.2008.05.021
35. Huttermann J, Lange M, Ohlmann J. Mechanistic Aspects of Radiation-Induced Free Radical Formation in Frozen Aqueous Solutions of DNA Constituents: Consequences for DNA? *Radiat Res* (1992) 131(1):18–23. doi: 10.2307/3578311
36. Wallace SS. Enzymatic Processing of Radiation-Induced Free Radical Damage in DNA. *Radiat Res* (1998) 150(5 Suppl):S60–79. doi: 10.2307/3579809
37. Sevilla MD, Becker D, Kumar A, Adhikary A. Gamma and Ion-Beam Irradiation of DNA: Free Radical Mechanisms, Electron Effects, and Radiation Chemical Track Structure. *Radiat Phys Chem Oxf Engl 1993* (2016) 128:60–74. doi: 10.1016/j.radphyschem.2016.04.022
38. Sankaranarayanan K. Ionizing Radiation and Genetic Risks. III. Nature of Spontaneous and Radiation-Induced Mutations in Mammalian *In Vitro* Systems and Mechanisms of Induction of Mutations by Radiation. *Mutat Res* (1991) 258(1):75–97. doi: 10.1016/0165-1110(91)90029-u
39. Li S, Zheng YC, Cui HR, Fu HW, Shu QY, Huang JZ. Frequency and Type of Inheritable Mutations Induced by Gamma Rays in Rice as Revealed by Whole Genome Sequencing. *J Zhejiang Univ Sci B* (2016) 17(12):905–15. doi: 10.1631/jzus.B1600125
40. Gao S, Jung JH, Lin SM, Jang AY, Zhi Y, Bum Ahn K, et al. Development of Oxytolerant Salmonella Typhimurium Using Radiation Mutation Technology (RMT) for Cancer Therapy. *Sci Rep* (2020) 10(1):3764. doi: 10.1038/s41598-020-60396-6
41. Luria SE, Delbruck M. Mutations of Bacteria From Virus Sensitivity to Virus Resistance. *Genetics* (1943) 28(6):491–511. doi: 10.1093/genetics/28.6.491
42. Hur J, Stein BD, Lee JH. A Vaccine Candidate for Post-Weaning Diarrhea in Swine Constructed With a Live Attenuated Salmonella Delivering Escherichia Coli K88ab, K88ac, FedA, and FedF Fimbrial Antigens and its Immune Responses in a Murine Model. *Can J Vet Res* (2012) 76(3):186–94.
43. Pope CF, Gillespie SH, Pratten JR, McHugh TD. Fluoroquinolone-Resistant Mutants of Burkholderia Cepacia. *Antimicrob Agents Chemother* (2008) 52 (3):1201–3. doi: 10.1128/AAC.00799-07
44. Buckner MM, Croxen MA, Arena ET, Finlay BB. A Comprehensive Study of the Contribution of Salmonella Enterica Serovar Typhimurium SPI2 Effectors to Bacterial Colonization, Survival, and Replication in Typhoid Fever, Macrophage, and Epithelial Cell Infection Models. *Virulence* (2011) 2 (3):208–16. doi: 10.4161/viru.2.3.15894
45. Srinivasan A, Foley J, McSorley SJ. Massive Number of Antigen-Specific CD4 T Cells During Vaccination With Live Attenuated Salmonella Causes Interclonal Competition. *J Immunol* (2004) 172(11):6884–93. doi: 10.4049/jimmunol.172.11.6884
46. Labuda JC, Depew CE, Pham OH, Benoun JM, Ramirez NA, McSorley SJ. Unexpected Role of CD8 T Cells in Accelerated Clearance of Salmonella Enterica Serovar Typhimurium From H-2 Congenic Mice. *Infect Immun* (2019) 87(11):e00588-19. doi: 10.1128/IAI.00588-19
47. Schmidt S, Sassu EL, Vatzia E, Pierron A, Lagler J, Mair KH, et al. Vaccination and Infection of Swine With Salmonella Typhimurium Induces a Systemic and Local Multifunctional CD4(+) T-Cell Response. *Front Immunol* (2020) 11:603089. doi: 10.3389/fimmu.2020.603089
48. Kantele A, Pakkanen SH, Siitonen A, Karttunen R, Kantele JM. Live Oral Typhoid Vaccine Salmonella Typhi Ty21a - A Surrogate Vaccine Against non-Typhoid Salmonella? *Vaccine* (2012) 30(50):7238–45. doi: 10.1016/j.vaccine.2012.10.002
49. Horton H, Thomas EP, Stucky JA, Frank I, Moodie Z, Huang Y, et al. Optimization and Validation of an 8-Color Intracellular Cytokine Staining (ICS) Assay to Quantify Antigen-Specific T Cells Induced by Vaccination. *J Immunol Methods* (2007) 323(1):39–54. doi: 10.1016/j.jim.2007.03.002
50. Foley SL, Nayak R, Hanning IB, Johnson TJ, Han J, Ricke SC. Population Dynamics of Salmonella Enterica Serotypes in Commercial Egg and Poultry Production. *Appl Environ Microbiol* (2011) 77(13):4273–9. doi: 10.1128/AEM.00598-11
51. Cogan TA, Humphrey TJ. The Rise and Fall of Salmonella Enteritidis in the UK. *J Appl Microbiol* (2003) 94 Suppl:114S–9S. doi: 10.1046/j.1365-2672.94.s1.13.x
52. Meinen A, Simon S, Banerji S, Szabo I, Malorny B, Borowiak M, et al. Salmonellosis Outbreak With Novel Salmonella Enterica Subspecies Enterica Serotype (11:Z41:E,N,Z15) Attributable to Sesame Products in Five European Countries, 2016 to 2017. *Euro Surveill* (2019) 24(36):1800543. doi: 10.2807/1560-7917.ES.2019.24.36.1800543
53. Miller EA, Elnekave E, Flores-Figueroa C, Johnson A, Kearney A, Munoz-Aguayo J, et al. Emergence of a Novel Salmonella Enterica Serotype Reading Clonal Group Is Linked to Its Expansion in Commercial Turkey Production, Resulting in Unanticipated Human Illness in North America. *mSphere* (2020) 5(2):e00056-20. doi: 10.1128/mSphere.00056-20
54. Carroll LM, Huisman JS, Wiedmann M. Twentieth-Century Emergence of Antimicrobial Resistant Human- and Bovine-Associated Salmonella Enterica Serotype Typhimurium Lineages in New York State. *Sci Rep* (2020) 10 (1):14428. doi: 10.1038/s41598-020-71344-9
55. Clark-Curtiss JE, Curtiss R. 3rd: Salmonella Vaccines: Conduits for Protective Antigens. *J Immunol* (2018) 200(1):39–48. doi: 10.4049/jimmunol.1600608
56. Edrington TS, Arthur TM, Loneragan GH, Genovese KJ, Hanson DL, Anderson RC, et al. Evaluation of Two Commercially-Available Salmonella Vaccines on Salmonella in the Peripheral Lymph Nodes of Experimentally-Infected Cattle. *Ther Adv Vaccines Immunother* (2020) 8:1–7. doi: 10.1177/2515135520957760
57. Detmer A, Glenting J. Live Bacterial Vaccines–a Review and Identification of Potential Hazards. *Microb Cell Fact* (2006) 5:23. doi: 10.1186/1475-2859-5-23
58. Lin IY, Van TT, Smooker PM. Live-Attenuated Bacterial Vectors: Tools for Vaccine and Therapeutic Agent Delivery. *Vaccines (Basel)* (2015) 3(4):940–72. doi: 10.3390/vaccines3040940
59. Yoon WS, Kim S, Seo S, Park Y. Salmonella Typhimurium With Gamma-Radiation Induced H2AX Phosphorylation and Apoptosis in Melanoma. *Biosci Biotechnol Biochem* (2014) 78(6):1082–5. doi: 10.1080/09168451.2014.905173
60. Nuyts S, Van Mellaert L, Barbe S, Lammertyn E, Theys J, Landuyt W, et al. Insertion or Deletion of the Cheo Box Modifies Radiation Inducibility of Clostridium Promoters. *Appl Environ Microbiol* (2001) 67(10):4464–70. doi: 10.1128/AEM.67.10.4464-4470.2001
61. Pham OH, McSorley SJ. Protective Host Immune Responses to Salmonella Infection. *Future Microbiol* (2015) 10(1):101–10. doi: 10.2217/fmb.14.98
62. Ji HJ, Byun EB, Chen F, Ahn KB, Jung HK, Han SH, et al. Radiation-Inactivated S. Gallinarum Vaccine Provides a High Protective Immune Response by Activating Both Humoral and Cellular Immunity. *Front Immunol* (2021) 12:717556. doi: 10.3389/fimmu.2021.717556
63. Clay SL, Bravo-Blas A, Wall DM, MacLeod MKL, Milling SWF. Regulatory T Cells Control the Dynamic and Site-Specific Polarization of Total CD4 T Cells Following Salmonella Infection. *Mucosal Immunol* (2020) 13(6):946–57. doi: 10.1038/s41385-020-0299-1
64. Curtis MM, Way SS. Interleukin-17 in Host Defence Against Bacterial, Mycobacterial and Fungal Pathogens. *Immunology* (2009) 126(2):177–85. doi: 10.1111/j.1365-2567.2008.03017.x
65. Li Q, Hu Y, Xu L, Xie X, Tao M, Jiao X. Complete Genome Sequence of Salmonella Enterica Serovar Choleraesuis Vaccine Strain C500 Attenuated by Chemical Mutation. *Genome Announc* (2014) 2(5):e01022-14. doi: 10.1128/genomeA.01022-14
66. Koerich PKV, Fonseca BB, Balestrin E, Tagliari V, Hoepers PG, Ueira-Vieira C, et al. Salmonella Gallinarum Field Isolates and its Relationship to Vaccine Strain SG9R. *Br Poult Sci* (2018) 59(2):154–9. doi: 10.1080/00071668.2017.1406062
67. Galen JE, Buskirk AD, Tennant SM, Pasetti MF. Live Attenuated Human Salmonella Vaccine Candidates: Tracking the Pathogen in Natural Infection and Stimulation of Host Immunity. *EcoSal Plus* (2016) 7(1):ESP-0010-2016. doi: 10.1128/ecosalplus.ESP-0010-2016
68. Hindle Z, Chatfield SN, Phillimore J, Bentley M, Johnson J, Cosgrove CA, et al. Characterization of Salmonella Enterica Derivatives Harboring Defined aroC and Salmonella Pathogenicity Island 2 Type III Secretion System (Ssav)

Mutations by Immunization of Healthy Volunteers. *Infect Immun* (2002) 70 (7):3457–67. doi: 10.1128/IAI.70.7.3457-3467.2002
69. MacLennan CA, Martin LB, Micoli F. Vaccines Against Invasive Salmonella Disease: Current Status and Future Directions. *Hum Vaccin Immunother* (2014) 10(6):1478–93. doi: 10.4161/hv.29054
70. Sears KT, Galen JE, Tennant SM. Advances in the Development of Salmonella-Based Vaccine Strategies for Protection Against Salmonellosis in Humans. *J Appl Microbiol* (2021) 131(6):2640–58. doi: 10.1111/jam.15055
71. Tennant SM, Schmidlein P, Simon R, Pasetti MF, Galen JE, Levine MM. Refined Live Attenuated Salmonella Enterica Serovar Typhimurium and Enteritidis Vaccines Mediate Homologous and Heterologous Serogroup Protection in Mice. *Infect Immun* (2015) 83(12):4504–12. doi: 10.1128/IAI.00924-15

Conflict of Interest: Authors SJB and HKJ are employed by CTCVAC.

The remaining authors declare that the research was conducted in the absence of any commercial or financial relationships that could be construed as a potential conflict of interest.

Publisher's Note: All claims expressed in this article are solely those of the authors and do not necessarily represent those of their affiliated organizations, or those of the publisher, the editors and the reviewers. Any product that may be evaluated in this article, or claim that may be made by its manufacturer, is not guaranteed or endorsed by the publisher.

frontiers | Frontiers in Veterinary Science

ORIGINAL RESEARCH
published: 11 July 2022
doi: 10.3389/fvets.2022.916108

Protective Efficacy of H9N2 Avian Influenza Vaccines Inactivated by Ionizing Radiation Methods Administered by the Parenteral or Mucosal Routes

Alessio Bortolami[1], Eva Mazzetto[1], Richard Thiga Kangethe[2], Viskam Wijewardana[2], Mario Barbato[2,3], Luca Porfiri[2], Silvia Maniero[1], Elisa Mazzacan[1], Jane Budai[1], Sabrina Marciano[1], Valentina Panzarin[1], Calogero Terregino[1†], Francesco Bonfante[1†] and Giovanni Cattoli[2†]*

[1] Department of Comparative Biomedical Sciences, Istituto Zooprofilattico Sperimentale delle Venezie, Legnaro, Italy, [2] Animal Production and Health Laboratory, Department of Nuclear Sciences and Applications, Joint FAO/IAEA Centre of Nuclear Techniques in Food and Agriculture, International Atomic Energy Agency (IAEA), Vienna, Austria, [3] Department of Animal Science Food and Nutrition–DIANA, Università Cattolica del Sacro Cuore, Piacenza, Italy

OPEN ACCESS

Edited by:
Constantinos S. Kyriakis,
Auburn University, United States

Reviewed by:
Renukaradhya J. Gourapura,
The Ohio State University,
United States
Eric James,
Sanaria, United States

***Correspondence:**
Giovanni Cattoli
G.Cattoli@iaea.org

[†]These authors have contributed equally to this work and share last authorship

Specialty section:
This article was submitted to Veterinary Infectious Diseases, a section of the journal Frontiers in Veterinary Science

Received: 08 April 2022
Accepted: 03 June 2022
Published: 11 July 2022

Citation:
Bortolami A, Mazzetto E, Kangethe RT, Wijewardana V, Barbato M, Porfiri L, Maniero S, Mazzacan E, Budai J, Marciano S, Panzarin V, Terregino C, Bonfante F and Cattoli G (2022) Protective Efficacy of H9N2 Avian Influenza Vaccines Inactivated by Ionizing Radiation Methods Administered by the Parenteral or Mucosal Routes. Front. Vet. Sci. 9:916108. doi: 10.3389/fvets.2022.916108

H9N2 viruses have become, over the last 20 years, one of the most diffused poultry pathogens and have reached a level of endemicity in several countries. Attempts to control the spread and reduce the circulation of H9N2 have relied mainly on vaccination in endemic countries. However, the high level of adaptation to poultry, testified by low minimum infectious doses, replication to high titers, and high transmissibility, has severely hampered the results of vaccination campaigns. Commercially available vaccines have demonstrated high efficacy in protecting against clinical disease, but variable results have also been observed in reducing the level of replication and viral shedding in domestic poultry species. Antigenic drift and increased chances of zoonotic infections are the results of incomplete protection offered by the currently available vaccines, of which the vast majority are based on formalin-inactivated whole virus antigens. In our work, we evaluated experimental vaccines based on an H9N2 virus, inactivated by irradiation treatment, in reducing viral shedding upon different challenge doses and compared their efficacy with formalin-inactivated vaccines. Moreover, we evaluated mucosal delivery of inactivated antigens as an alternative route to subcutaneous and intramuscular vaccination. The results showed complete protection and prevention of replication in subcutaneously vaccinated Specific Pathogen Free White Leghorn chickens at low-to-intermediate challenge doses but a limited reduction of shedding at a high challenge dose. Mucosally vaccinated chickens showed a more variable response to experimental infection at all tested challenge doses and the main effect of vaccination attained the reduction of infected birds in the early phase of infection. Concerning mucosal vaccination, the irradiated vaccine was the only one affording complete protection from

infection at the lowest challenge dose. Vaccine formulations based on H9N2 inactivated by irradiation demonstrated a potential for better performances than vaccines based on the formalin-inactivated antigen in terms of reduction of shedding and prevention of infection.

Keywords: H9N2, vaccines, mucosal, subcutaneous, irradiated, formalin-inactivated

INTRODUCTION

Although wild waterfowl are the natural hosts of avian influenza (AI), H9N2 subtype viruses are relatively uncommon in wild birds (1). In contrast, H9N2 viruses, following their initial spread from South East Asia in the late 1990s, have become globally widespread in poultry over the last two decades, resulting in great economic losses due to their high replicative fitness in Galliformes, associated with severe drops in egg production and moderate mortality, when exacerbated by other pathogens (2, 3). In addition to the severe impact on poultry production, H9N2 viruses have also been implicated in zoonotic transmission to humans, in particular with people in direct contact with live poultry, remarking the importance of vaccination in reducing the circulation of H9N2 viruses, as an indirect measure to prevent zoonotic transmissions and reassortment events between human and AI viruses (4–6). Sustained human-to-human transmission of H9N2 viruses has not been demonstrated, but there is a piece of scientific evidence that only a few molecular changes could be needed to achieve transmissibility by respiratory droplets in humans (7). In addition to the direct involvement in zoonotic infections, H9N2 viruses have also donated the internal gene cassette to other AI viruses responsible for numerous human cases (such as highly pathogenic H5Nx viruses of the Goose/Guangdong/1996-lineage, H7N9 viruses of the Anhui/1/13-lineage, and a zoonotic H10N8 virus), often with fatal outcome (8–10).

There is no widespread consensus on the classification of H9N2 avian viruses; however, epidemiological and phylogenetic analyses of the hemagglutinin (HA) gene of H9N2 influenza viruses revealed that at least two major different lineages can be distinguished, the American and Eurasian lineage. The latter can be further divided into the BJ/94, the Y280/G9, the G1, and possibly a fourth lineage (unrelated to the previous three) found mainly in turkeys reared in Europe (11, 12).

Of the different lineages of H9N2, the G1 lineage, first detected in Hong Kong in 1997 (13) is extremely well adapted to chicken and has rapidly become endemic in poultry species after introduction into parts of Asia, the Middle East, India, Egypt, and Africa (14–17). To control the spread of the disease and to mitigate the severe economic consequences of uncontrolled virus circulation, vaccination has been applied in several endemic countries (17). In regions where these viruses are endemic, such as Asia and the Middle East, genetic and antigenic differences, have been observed within lineages circulating in specific regions (18). The effect of immune selection pressure exerted by vaccination on AI virus evolution has been previously demonstrated for H5N1 and H9N2, showing the rapid emergence of antigenic variants or selection and expansion of a variant that was present at a low prevalence when vaccination was initiated (18, 19). Antigenic drift, in a similar fashion to the antigenic drift observed in H1N1 and H3N2 seasonal human influenza strains, has also been observed in regions where vaccination against H9N2 is common (2).

Vaccines have been used to reduce clinical disease and lower the burden on the poultry industry; however, insufficient attention has been focused on the effect of vaccines on the reduction of viral shedding (2). Highly effective vaccines, able to provide sterilizing immunity, could help in reducing the evolutionary rate and the chances of recombination of H9N2 in endemic countries.

The gamma-irradiation-mediated killing of viruses was explored with little success to develop vaccines since the 1950s. However, a renewed interest in this technology has risen due to: (a) the invention of newer and safer irradiators that can deliver high doses, (b) the introduction of radio-protective compounds that can preserve antigens during irradiation, and (c) a better understanding of the immune system (20). Despite the limitations posed by the need of a radioactive source for the generation of γ-rays, irradiation offers several advantages, mainly related to the better preservation of the antigenic structure of the inactivated pathogen. It has been previously demonstrated that gamma-irradiation-inactivated influenza vaccination in mice resulted in the development of higher antibody titers and a broader spectrum of protection against antigenically different strains compared to a formalin-inactivated influenza vaccine (21–23). However, to the best of our knowledge, detailed efficacy data obtained from challenge studies evaluating irradiated avian influenza vaccines parenterally or mucosally administered to chickens or other avian species are not available in the literature.

In our work, we compared the immunogenicity and the efficacy of H9N2 experimental vaccines based on the antigens inactivated by chemical and irradiation methods, administered by mucosal or intramuscular routes in Specific Pathogen Free (SPF) White Leghorn chickens. The efficacy of the different vaccines and administration routes was measured upon challenge with different doses of an H9N2 isolate belonging to the G1 lineage, aiming to understand if the irradiation technology could improve current vaccination strategies and if the mucosal administration of the inactivated vaccines is able to elicit a protective level of immunity.

MATERIALS AND METHODS

Virus

An AIV H9N2 isolate from the Middle East belonging to the G1 lineage (A/Chicken/Saudi Arabia/3622-31/13) was propagated and titrated in 10-day-old embryonated SPF chicken eggs (Charles Rivers) at 37°C for 72 h. Viral titrations were performed by inoculating 100 μL virus dilutions (10^{-3}-10^{-9}) in 10–11-day-old embryonated chicken eggs in the allantoic fluid. The inoculated eggs were incubated at 37°C and observed every 24 h to detect mortality for 7 days. Allantoic fluids harvested from the eggs were tested by the HA assay to detect viral replication, according to standard procedures (24). Allantoic fluids showing the absence of hemagglutinating activity were considered as negative for virus replication. A 50% egg infectious dose (EID_{50}) was calculated according to the Reed-Muench method (25).

Inactivation of H9N2 by Formalin and Irradiation

Inactivation by irradiation was performed at the International Atomic Energy Agency (IAEA) Laboratories in Seibersdorf, Austria, by following established protocols. The virus stock was mixed with 1M trehalose (trehalose dihydrate; Sigma) 50% V/V, aliquoted into 5 mL volume, and immediately frozen. Frozen samples incubated with dry ice were irradiated using a Model 812 Co-60 irradiator at a dose rate of 66.532 Gy/min (Foss Therapy Services, Inc., California, USA). The irradiator was regularly calibrated using an ionization chamber that also mapped the delivered dose in the location where the samples are irradiated. Initial doses of 5, 10, 15, 20, 25, 30, and 40 kGy were applied to identify the D10 value, the dose required to reduce virus load by 90% or 1 log (26). All samples were labeled with P8100 radiation indicator stickers that progressively change from yellow to purple depending on the dose applied ranging from 3 to 25 kGy (GEX Cooperation, Colorado, USA). The D10 value was used to estimate the inactivation dose. Formalin-inactivated H9N2 was prepared at the Istituto Zooprofilattico Sperimentale delle Venezie (IZSVe) following previously described protocols (27). Briefly, 0.1% V/V formalin in phosphate-buffered saline (PBS) was added to the infectious allantoic fluid and incubated at 37°C for 16 h. To compare vaccine preparations that only differed by the type of inactivation, after formalin treatment, the allantoic fluid was then mixed with 1M trehalose (trehalose dihydrate; Sigma) 50% V/V. Loss of viral infectivity was confirmed by three blind passages of treated viruses in embryonated eggs. The inactivated virus suspensions were stored at −80°C until further use.

Transmission Electron Microscopy (TEM)

Aliquots of untreated, formalin-inactivated, and irradiated viruses were analyzed by negative staining TEM according to standard procedures for viral identification and examination. A formvar/carbon supported copper grid (Electron Microscopy Sciences Formvar/Carbon Copper Grid 200 Mesh) was placed flat on the bottom of the vial and 90 μL of samples were dispensed on the top of the grid. After high-speed centrifugation (28–30 psi or 100,000×*g*) for 15 min (Beckman Air-Driven Ultracentrifuge Airfuge), the grid was placed on a filter paper and stained with 10 μL of 2% phosphotungstic acid (PTA) (pH 7); PTA was left on the grid for a few seconds (8–10 s). The grid was then examined under an EM 208S TEM (Philips) and virus particles were measured using the iTEM software (Olympus SIS).

Animal Experiments

Bird Infectious Dose 50 (BID_{50})

BID_{50} determination was based on the methods described by Swayne and Slemons (28). Birds were challenged with serial dilutions of the selected strains. For each tested dilution, groups of five SPF White Leghorn chickens (*Gallus gallus*) 4–6 weeks old were housed in poultry isolating units (Montair, The Netherlands). All the birds in each group were infected *via* the oronasal route with 100 μL of viral suspension in PBS containing the corresponding EID_{50} dose (one dose per group). Only tracheal swabs (FLmedical, Italy) were collected daily from day 1 to day 5 post-infection (p.i.), as previous experimental results (data not shown) indicated that cloacal shedding was negligible (mean Ct values >30). The samples were then processed for the detection of the M gene by real-time RT-PCR (RRT-PCR) (29). The BID_{50} was defined using the Spearman and Kärber method (30).

Animal Trial 1 (H9N2 Challenge Dose: 10^6 EID_{50}/100 μL)

A total of 40 one-day-old SPF White Leghorn chickens were equally divided into five groups and housed in BSL3 poultry isolators (HM 1900, Montair Andersen BV, Kronenberg, The Netherlands). Two groups were vaccinated oculo-nasally (ON) with either the irradiated-H9N2 (ON-Irr) or the formalin-inactivated H9N2 (ON-For) antigens without adjuvants, respectively. The other two groups were vaccinated subcutaneously (SC) with either irradiated-H9N2 (SC-Irr) or formalin-inactivated H9N2 (SC-For) antigens, respectively, in a water-in-oil (W/O) 7:3 (v/v) emulsion with a commercial adjuvant for poultry (ISA71VG, Seppic). A fifth group served as a negative non-vaccinated control. All groups were vaccinated twice at 14 and 28 days of age and blood samples were taken before each vaccination. The amount of H9N2 antigen given to each bird was standardized to 128 hemagglutinating units (HAU) for each immunization. Two weeks after the second dose (i.e., 42 days of age) blood samples were taken from all the chickens and a homologous challenge was performed by the oronasal route at a dose of 10^6 EID_{50}/100 μL. Tracheal swabs were collected from all the birds on day 2, 4, and 7 p.i. to evaluate viral shedding. Fourteen days p.i. (dpi), a final blood sample was taken from all the birds to evaluate seroconversion.

Animal Trial 2 (H9N2 Challenge Dose: 10^3 and 10^4 EID_{50}/100 μL)

A total of 150 one-day-old SPF White Leghorn chickens were divided into five different experimental groups. The first group was vaccinated ON with irradiated-H9N2 (ON-Irr-Adj) in a 1:1 suspension with the mucosal adjuvant IMS1313 (Seppic, France), the second group received by the ON route a formalin-inactivated H9N2 vaccine in a 1:1 suspension with IMS1313

(ON-For-Adj). The other two groups were vaccinated SC in the same way as in animal trial 1 (SC-Irr, SC-For). The amount of H9N2 antigen given to each bird was standardized to 128 HAU for each immunization. A fifth group served as negative non-vaccinated control. All the vaccinated birds received two doses of the experimental vaccines at 14 and 28 days of age and blood samples were taken before each vaccination. Two weeks after the second dose (i.e., 42 days of age) blood samples were taken, and within each group, birds were equally divided into subgroups of 15 birds each and challenged with either 10^3 or 10^4 EID_{50}/100 μL of the homologous virus. Clinical signs were monitored daily and tracheal swabs for quantification of viral shedding were collected on day 1, 2, 3, 4, 5, 7, and 9 p.i. Fourteen days p.i., a final blood sample was taken from all the birds to evaluate seroconversion.

Assessment of Viral Shedding by Real-Time RT-PCR

RRT-PCR targeting the M-gene was used to determine the BID_{50} and to compare viral shedding in the respiratory tract in each experimental group, in a qualitative and quantitative setup, respectively (29). Swab heads were placed in 500 μL of 1X PBS containing antibiotics and antimycotics (PBS-A) and vortexed for 30 s. Total RNA was purified from 300 μL of sample suspension using the QIAsymphony® DSP Virus/Pathogen Midi Kit on a QIAsymphony® SP instrument (Qiagen). Viral genome amplification was carried out using the QuantiTect Multiplex RT-PCR Kit (Qiagen), 300 nM of each primer, 100 nM of the probe, and 5 μL of template RNA, in a final volume of 25 μL. Each sample was tested in triplicate. Runs were performed on a CFX 96 Deep Well Real-Time PCR System, C1000 Touch (Biorad), under the following cycling conditions: 50°C for 20 min, 95°C for 15 min, followed by 40 cycles at 94°C for 45 s and 60°C for 45 s.

Ten-fold serial dilutions of strain-specific negative-sense *in vitro* transcribed RNA were processed along with each run to develop standard curves and to assess viral shedding. The limit of quantification (LoQ) of the RRT-PCR was preliminarily assessed as being $10^{0.7}$ genome copies.

Viral replication was plotted as the mean viral load ± SD using the Prism 9.1.2 (GraphPad). For graphical and statistical purposes, samples testing negative or with a viral load below the LoQ were given a value of $10^{0.7}$ copies/5 μL of total RNA.

Serological Assays

To detect the humoral immune response of vaccination, hemagglutination inhibition (HI) assays and a commercial ELISA assay targeting the nucleoprotein (NP) of type A influenza viruses were performed on all serum samples collected during animal trials 1 and 2. HI assays were performed according to standard protocol using the homologous vaccine antigen (31). In brief, sera were serially diluted in PBS and mixed with equal volumes (25 μL) of the virus containing 4 HAU, then 25 μL of washed chicken red blood cells were added and incubated for 30 min at room temperature. HI titers were determined as reciprocals of the highest serum dilutions in which inhibition of hemagglutination was observed.

The anti-NP ELISA (ID Screen® Influenza A Nucleoprotein Indirect, IDVet, France) was performed according to the manufacturer's recommendation using positive and negative controls provided with the commercial kit.

Statistical Analyses

The shedding dynamics from 1 to 12 dpi of the control population and those administered with formalin-inactivated and the irradiated vaccines were modeled through General Additive Model (GAM). GAM was performed as implemented in the 'mgcv' R package, which was also used to assess the concurvity and significance of base functions, model selection was performed through the Akaike information criterion (AIC), and the model assumptions were verified through the graphical assessment of the models' residuals using the R package 'gratia' (32–34). A GAM was fitted for each challenge dose (10^3−10^4−10^6) and for each administration route (ON and SC). Shedding observations equal to zero were increased to one (from hereon: Shed01); all observations were then log-transformed. Due to the limits of detection of $10^{0.7}$ copies/5 μL, shedding levels presented a distinct zero-inflation. Consequently, we implemented a two-components mixture GAM where the probability of attaining value 0 (fit0) and the probabilities of the non-0 values (fit1) are modeled separately, and the coefficients from the two models are joined to return a single response model (fit). To compute a different smooth for each unique treatment while allowing for varying intercept, models fit0 and fit1 included the treatment both as a fixed factor and as a factor-smoothing parameter for DPI. The response variable for fit0 was a binary variable describing the presence/absence of measured shedding for each given observation and modeled as logistic regression with a binomial distribution of errors and logit link function. To model fit1, Shed01 was log-transformed and modeled with a Gaussian distribution of errors and log link function. The predicted values from both models were then joined as $\mathbf{fit} = \mathbf{e}^{\log(\mathbf{fit0}) + \log(\mathbf{fit1})}$. Confidence intervals at the 95% confidence level (95% CI) were inferred generating 1,000 bootstrap resampling and applying a bias-corrected CI as implemented in the "coxed" R package (35, 36).

To assess the overall shedding difference significance among treatments for each dose/route combination, general linear mixed models (GLMM) of the log-transformed Shed01 were fitted using treatment as a fixed factor, DPI, and sample ID as random variables as implemented in the "lme4" R package (37). The "emmeans" R package (38) was used to compute the estimated marginal means and the contrast among treatments; the *p*-values associated with the contrast were corrected for multiple comparisons through Honestly Significant Difference (HSD) adjustment.

RESULTS

Inactivation and Preservation of Structural Integrity

The D10 dose was identified as 5.46 kGy (**Supplementary Figure 1**). An inactivation dose of 60 kGy was used for vaccine preparation and was estimated by adding four D10 doses to the minimum inactivation dose estimated at 35.68 kGy to ensure effective sterilization of the virus. The final

dose of 60 kGy, was within the range of the SAL and determined safe for use. Around 12.5 h were taken to deliver this irradiation dose using a gamma irradiator and the sample was kept frozen all the time by refilling dry ice. Indeed, there was a slight difference in each time the inactivation took place as the Co-60 source decayed over time.

Inactivation and safety of formalin-treated and irradiated H9N2 used in the experimental vaccines were confirmed by three blind passages in 10-day-old embryonated eggs. Additionally, no loss in HA titer was observed irrespective of the inactivation method used. Upon Transmission electron microscopy (TEM) examination (**Figure 1**), both formalin and γ-irradiation treatments showed no effect on the integrity of viral particles and normal morphology was preserved. However, after examination of several viral particles, formalin-fixed virions exhibit shorter and less easily detectable projections, representing the immunogenic glycoproteins on their surface than the irradiated viral particles (**Figures 1B,C**, respectively).

BID_{50} of A/Chicken/Saudi Arabia/3622-31/13

To infer the BID_{50} of the challenge virus, we performed multiple infection experiments at different challenge doses (10^{3-6} EID_{50}/100 μL) in poultry isolators units. Following the challenge, tracheal swabs were collected daily and RRT-PCR tests were run to identify infected birds. The results of the challenge are shown in **Table 1** and the BID_{50} was determined as $10^{3.5}$ EID_{50}/100μL.

Vaccination by the Subcutaneous (SC) Route

Formalin-inactivated vaccines represent the most common type of traditional vaccine available for AI. Despite the extensive knowledge of the protection offered by inactivated vaccines when administered SC, control of H9N2 infection is difficult under field conditions and most of the countries in which vaccination is applied are still endemic to H9N2. In our work, we aimed to compare the protective efficacy of formalin-inactivated and irradiation-inactivated H9N2 experimental vaccines against different challenge doses of a homologous virus to the vaccine antigen.

The serological analysis showed that both formulations, when administrated SC, were able to produce high-antibody titers in immunized birds before challenge (i.e., Geometric Mean Titer (GMT) >10 $\log_2$ in all of the immunized groups) according to both HI and NP-ELISA tests. Higher mean HI titers were observed in birds immunized in trial 2 compared to trial 1, possibly due to improved vaccine preparation methods (extended emulsion time, higher shearing speed, and preparation performed on ice), which were adjusted following discussion with the manufacturer. Nonetheless, in SC-For and SC-Irr groups challenged with the same dose, no significant difference was observed in the GMTs.

In animal trial 1, we challenged chickens with a 10^6 EID_{50} dose (i.e., $10^{2.5}$ times greater than the BID_{50}) of the H9N2 isolate. Quantitative RRT-PCR was performed on tracheal swabs collected on days 2, 4, and 7 p.i. showed only partial virological protection in birds, irrespective of the type of inactivation method. However, on day 2 p.i., viral shedding was significantly lower in SC-Irr ($10^{2.38} \pm 10^{2.70}$ copies/5 μL) and SC-For ($10^{3.54} \pm 10^{3.94}$ copies/5 μL) groups than in the control chickens ($10^{4.94} \pm 10^{4.83}$ copies/5 μL), but differences between the two vaccinated groups were not statistically significant. In both vaccinated groups, 75% (6/8) of birds resulted to be positive on day 2 p.i. (**Supplementary Table 1**), as opposed to 100% (8/8) in the control group. In a comparison with the control group, we observed lower mean viral loads for both groups at day 4 p.i. but higher loads at day 7 p.i. (**Figure 2A**). Nonetheless, on day 7 p.i., 3/8 and 1/8 chickens resulted negative in the SC-Irr and SC-For groups, respectively, while in the control groups all birds were found positive. A GLMM statistical approach for the analysis of the viral shedding aggregated data (**Figure 3**) over 12 dpi. was applied to model infection dynamics. The analysis based on the RRT-PCR data showed that the effect of SC vaccination upon challenge with 10^6 EID_{50} mainly affects the initial phases of the infection by reducing the number of infected animals upon challenge for both the vaccines, albeit the effect of vaccination did not reach statistical significance (**Figure 3F**, inset).

We then evaluated the protective efficacy at lower challenge doses (10^3 and 10^4 EID_{50}), below and above the BID_{50}, to better discriminate differences in the ability of these vaccines to prevent an infection. Shedding results showed complete prevention of infection in all challenged birds, resulting in 100% efficacy of both the experimental vaccines in preventing infection (**Figures 2B,C**). Following the challenge, none of the vaccinated birds recorded an increase in the HI titers (**Figures 2D–F**).

Vaccination by the Mucosal (ON) Route

Mucosal vaccination of the upper respiratory tract in poultry is an attractive alternative to SC vaccination due to the potential advantages offered by mass administration and the capacity of mucosal vaccines to elicit mucosal immunity at the site of entry of respiratory viruses. To assess differences in the protective efficacy between irradiated and formalin-inactivated H9N2 antigens administered by the mucosal route, we performed three challenges, including doses of 10^3, 10^4, and 10^6 EID_{50}.

Serological analyses showed variable HI titers before the challenge in all vaccinated birds and no significant differences were observed in terms of HI GMT between formalin inactivated and irradiated vaccinated groups (3.93 $\log_2$ and 4.71 $\log_2$, respectively). Interestingly, NP-ELISA results were clearly distinguishable. The NP-ELISA performed on sera collected before the challenge gave negative results in the irradiated vaccinated groups, while in the formalin inactivated groups few (3/38, 7.9%) chickens seroconverted. After the challenge, the NP-ELISA showed seroconversion in the infected chickens.

As shown in **Figure 4**, at the highest challenge dose 8/8 of the unvaccinated birds infected directly from challenge and high viral titers ($10^{4.94} \pm 10^{4.83}$ copies/5 μL) were detected in tracheal swabs, as early as 2 dpi. In contrast, vaccinated birds showed more heterogeneous shedding titers at the early stages of infection. In particular, a significant reduction in mean viral load was observed in the ON-Irr group compared to controls

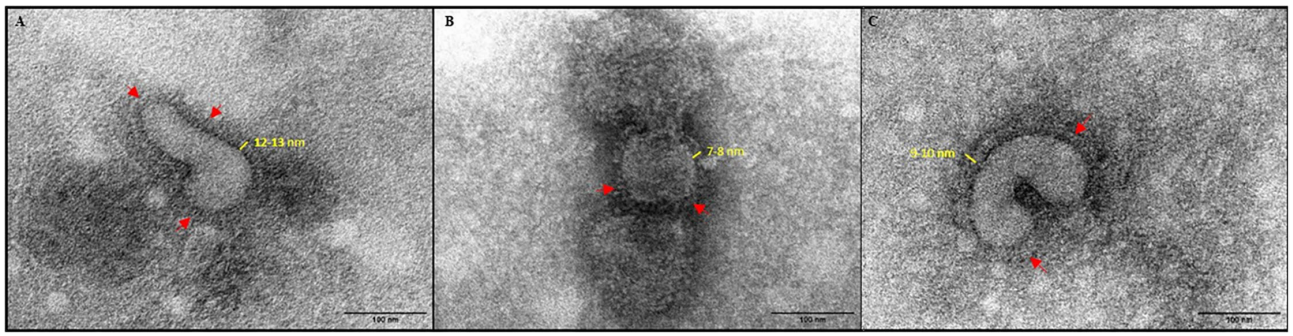

FIGURE 1 | Negative stain TEM images of virus (×180,000). **(A)** Live untreated H9N2. **(B)** formalin-inactivated H9N2; and **(C)** irradiated H9N2. Red arrows indicate viral glycoprotein spikes.

TABLE 1 | BID_{50} determination in 6-weeks-old White Leghorn SPF chickens, each infection experiment was performed by oronasal installation of 100 μL of infectious allantoic fluid diluted in PBS to five ($n = 5$) SPF chickens in different isolator units.

Challenge dose	Positive chickens	Negative chickens	% of infected (Mean Ct of infected chickens at day 1 p.i.)
10^3	2	3	40 (33.2)
10^4	3	2	60 (25.2)
10^5	5	0	100 (21.4)
10^6	5	0	100 (23.1)

The challenge dose is expressed as EID_{50}/100 μL.

on day 2 p.i. (**Figure 4A**). Moreover, in the ON-Irr group, 7/8 challenged birds resulted positive at 2 dpi. However, due to the high transmissibility of the H9N2 virus in chickens, all birds were infected at 4 dpi in all the groups. The GLMM model built on aggregated shedding data shown in **Figure 3C** failed to detect statistically significant differences in terms of overall shedding between groups.

At lower challenge doses, the effect of mucosal vaccination on the prevention of infection was evident, recording fewer positive birds compared to the control group during the first 2 days after the challenge. Upon inoculation with 10^4 EID_{50}, the percentage of positive birds in the ON-Irr-Adj, the ON-For-Adj and the control groups ranged between 23.1% (3/13)−53.8% (7/13), 26.7% (4/15)−46.65 (7/15) and 66.7% (10/15)−86.6% (13/15), respectively (**Supplementary Table 1**). Mean viral loads were significantly higher on day 3 p.i. for the ON-Irr-Adj group, while no statistical difference was recorded for samples at other time points. After day 3, all birds resulted positive at least for two consecutive days (**Supplementary Figure 2**), recording shedding peaks at days 3, 4, and 4 p.i. for ON-Irr-Adj, ON-For-Adj, and controls, respectively.

Upon challenge with 10^3 EID_{50}, the percentage of positive birds in the ON-Irr-Adj, the ON-For-Adj and the control groups ranged between 6.7% (1/15)−0.0% (0/13), 13.3% (2/15)−20.0% (3/15) and 6.7% (1/15)−20.0% (3/15), respectively (**Supplementary Table 1**). In the ON-Irr-Adj group, we observed a transient positivity in one bird at day 1 p.i., while no other animal resulted positive throughout the 12 days. In the ON-For-Adj group the same three infected birds that were positive on day 2 p.i. remained the only animals shedding virus up to day 4 p.i., while on day 5 p.i., five additional subjects resulted positive. In the control group, in addition to the three directly infected birds observed on day 2 p.i. six positive subjects were recorded on day 3 p.i. (**Supplementary Figure 2**). In the ON-For-Adj and the control groups, all birds resulted infected for at least two consecutive days, recording shedding peaks at days 7 and 4 p.i., respectively. HI titers increased after the challenge in all the groups except for the ON-Irr-Adj group challenged with a dose of 10^3 EID_{50}. In this group, the only chicken that transiently shed low viral loads on day 1 p.i. resulted in NP-ELISA positive at 14 dpi.

DISCUSSION

Vaccination to prevent H9N2 AIV infection in poultry has been used extensively since the late 1990s first in China and then in regions that became endemic following the global spread of these poultry-adapted viruses (18, 39, 40). Vaccination programs have relied heavily on traditional vaccines based on oil-emulsified, inactivated whole AIVs (39, 41) to reduce the severe economic consequences of infection. Inactivation of infectious allantoic fluid for the preparation of vaccines destined for the poultry market is usually achieved by formaldehyde treatment (31), which represents an effective well-established method. However, formalin treatment has been demonstrated to affect viral antigenicity by HA polymerization (27) and by reducing the host-immune response to the inoculated antigen. Moreover, formalin, at commercial vaccine concentration levels, has been

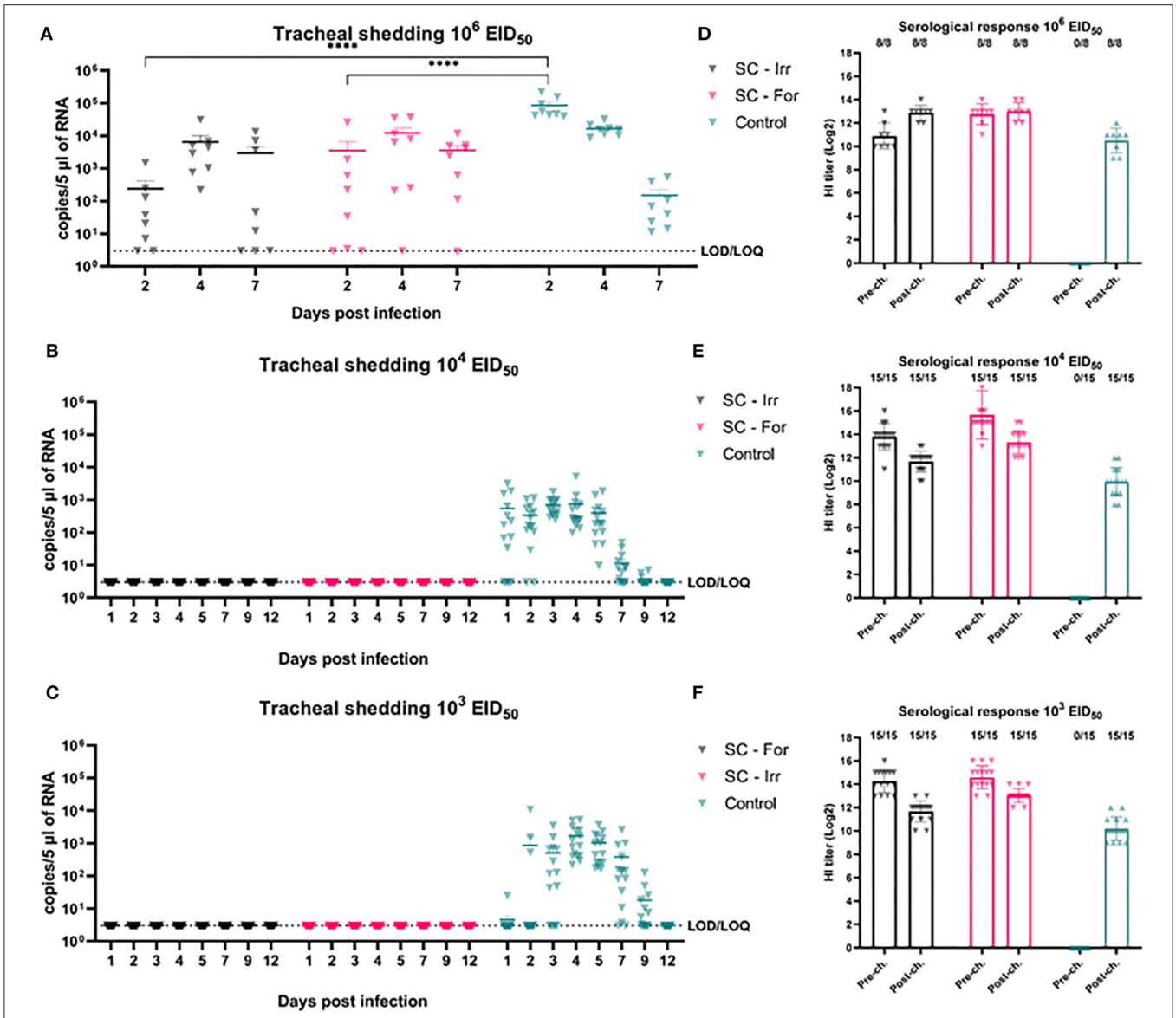

FIGURE 2 | Effects of subcutaneous (SC) vaccination upon infection at different H9N2 challenge doses. **(A–C)** qRRT-PCR results of tracheal swabs collected from all the challenged birds. **(D–F)** Serological test results of blood samplings performed before and after challenge. The numbers above bars indicate a number of NP-ELISA positive birds out of tested birds.

demonstrated to negatively affect production performances in laying hens by causing degeneration in combs, follicles, oviduct, and uterus and lower estradiol levels (42).

In our study, we demonstrated that irradiation is a valid alternative to formalin for the inactivation viruses, as previously demonstrated for other human influenza strains (22) or other pathogenic viruses, such as rotavirus (43), Venezuelan Equine Encephalitis virus (44), and Ebola virus (45). Complete inactivation of an infectious allantoic fluid with a titer of 10^8 EID_{50}, demonstrated by blind passaging in embryonated chicken eggs, was confirmed for irradiation doses higher than 40 kGy. Visualization of inactivated viral particles by TEM imaging suggested that formalin treatment affected more than γ-irradiation of the viral structure by reducing the height of surface immunogenic glycoproteins and by causing a more clustered appearance of H9N2 envelope projections, probably as a result of the cross-linking effect of the formalin treatment (46). The superiority of γ-irradiation to other chemical inactivation methods in the preservation of antigenic structures has been previously demonstrated and is due to the selective damaging effect of irradiation on the RNA genetic material, and the limited impact that irradiation has on proteins if frozen conditions are maintained during the inactivation process (47–49). In our work, to minimize the deleterious effects of γ-irradiation, we also used

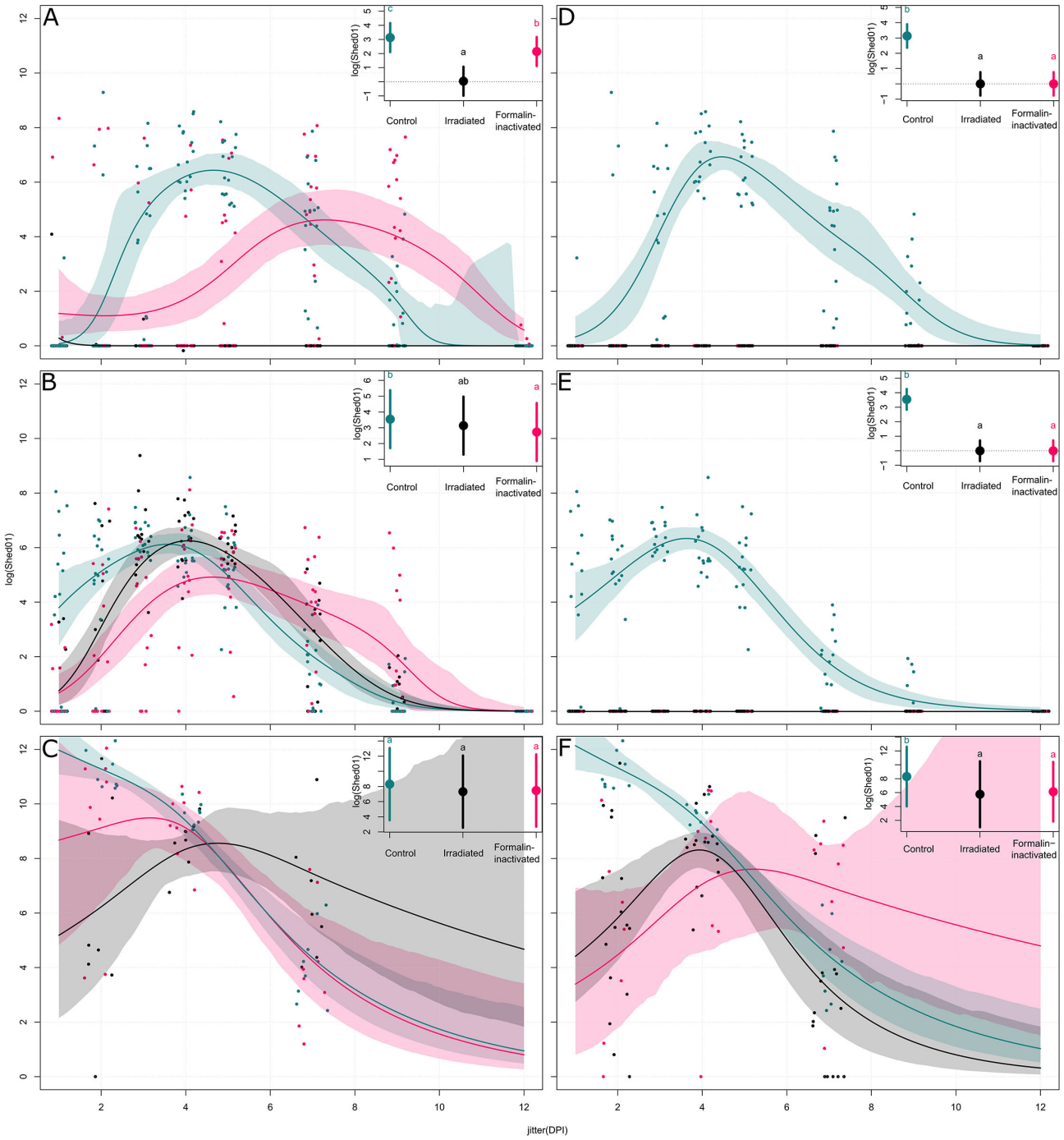

FIGURE 3 | Models of the shedding levels of irradiated and formalin-inactivated vaccines and a non-vaccinated control for 12 days post infection (DPI) for three challenge doses (10^3, 10^4, and 10^6 EID_{50}). For each group, the dots represent the measured observations, the solid line represents the fitted model, and the shaded contour shape represents the 95% confidence intervals of the fitted model. For each plot, the inset compares the overall effect of the group on the shedding, with the solid circle representing the effect value and the vertical bars the 95% confidence interval. Panels **(A–C)** show models of shedding in ON vaccinated birds upon challenge with 10^3, 10^4, and 10^6 EID_{50} of H9N2, respectively; panels **(D–F)** show models of shedding in SC vaccinated birds upon challenge with 10^3, 10^4, and 10^6 EID_{50} of H9N2, respectively.

trehalose as a radio-protectant to preserve the antigenic epitopes during the irradiation process. Trehalose is a well-known cryo-protectant that stabilizes proteins and has been shown to protect DNA during radiation (50). Indeed, trehalose has been used widely in viral vaccine formulations to achieve stabilization of the antigens (51, 52). Moreover, being a sugar it can also aid

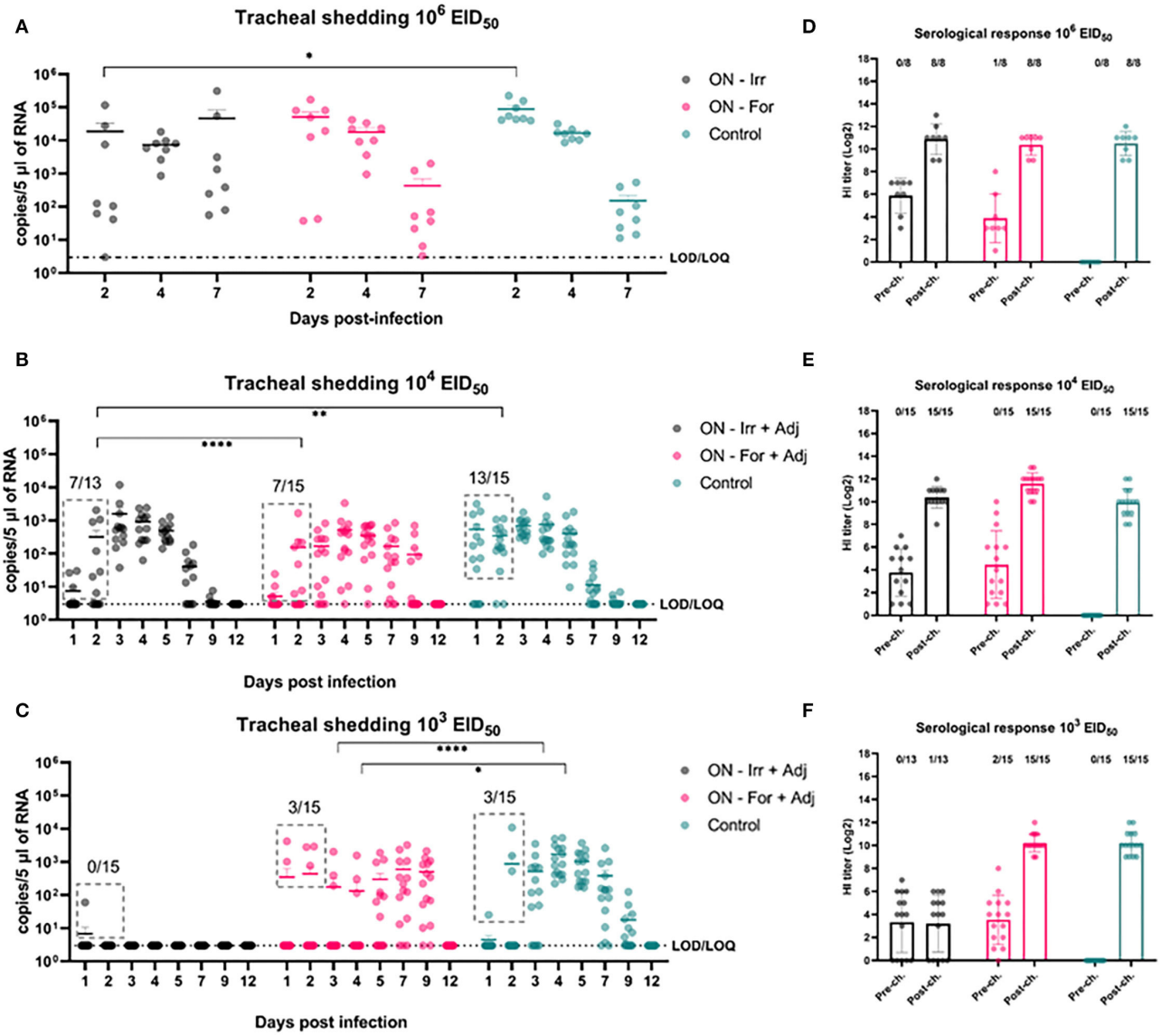

FIGURE 4 | Effects of mucosal (oculo-nasal, ON) vaccination upon infection at different H9N2 challenge doses. **(A–C)** qRRT-PCR results of tracheal swabs collected from all the challenged birds. **(D–F)** Serological test results before and after challenge. The numbers above bars indicates the number of NP-ELISA positive birds out of tested birds.

in increasing the viscosity leading to increased attachment and prolonged presence of vaccine antigens in the mucosae. On the other hand, it should be noted that the addition of trehalose and performing irradiation under frozen conditions could have increased the gamma irradiation dose needed for the inactivation of the virus because of the protective effects exerted both on viral proteins and the viral genome (53). Not surprisingly other groups who used gamma irradiation to inactivate influenza virus at room temperature and without trehalose achieved complete inactivation at 16 KGy (54).

When administered SC, no significant differences were recorded in terms of immunogenicity between the two vaccines. However, HI titers were higher than previously reported for similar antigen concentrations (50, 55), possibly as the result of either optimal vaccine preparation and administration (e.g., type of adjuvant) or due to the presence of trehalose in vaccine batches, whose activity on the modulation of host immunity is well-documented (56). Excellent results of ISA71VG as an adjuvant for AIV vaccine preparation have also been previously demonstrated in a study performed by Lone and colleagues (57) who compared 10 different commercial and experimental adjuvants for use in chickens, identifying ISA71 VG to perform best in terms of clinical protection and reduction of viral shedding in experimentally infected SPF chickens. We believe that the addition of trehalose to mineral oil adjuvants in vaccine formulations

should be further investigated considering its viscosity and adjuvant properties.

When birds were challenged with 10^6 EID_{50}, SC vaccinated groups recorded a significant reduction of shedding ($10^{1.40}$-$10^{2.56}$ fold reduction) in the trachea and a reduced number of positive birds in the early phase of the study, on day 2 p.i. Nonetheless, such reduction did not affect the overall number of birds becoming infected in the vaccinated groups, while it delayed the peak of shedding to day 4 p.i. Interestingly, although mean loads on day 7 p.i. were higher in both vaccinated groups than in the control group, the irradiated and the formalinated vaccines afforded viral clearance in 3/8 and 1/8 animals, respectively, as opposed to the control group in which all birds were still actively shedding the virus. At lower challenges, both vaccines provided sterilizing immunity according to both virological and serological results, achieving a result rarely described in the literature for AI (58). The superior adaptation of H9N2 viruses of the G1 and Y280 lineages to the respiratory epithelia of Galliformes reduces shedding a challenging task for the current inactivated vaccines. In our setting, we proved that even extremely high homologous HI titers could not prevent infection and transmission of infection upon high challenges, reminding us that the traditional approach to AI vaccination *via* IM/SC immunizations with inactivated vaccines might be sufficient to prevent H9N2 infection, only in the presence of moderate loads. High HI titers are known to efficiently curb the commercial impact of H9N2 disease (59, 60), but in our setting proved inefficient in reducing the circulation of a virus characterized by low BID_{50} and high sustained shedding profiles. Altogether, the irradiated antigen performed better than the formalin-inactivated, although differences did not reach statistical significance.

When ON vaccinated groups were challenged with 10^6 EID_{50}, no significant differences were recorded in terms of cumulative shedding in comparison with the control group. However, a significant reduction in shedding was observed in the ON-Irr-adj group at 2 dpi leading to a substantial delay in the shedding dynamic, albeit failing to effectively reduce the circulation of the virus in the flock. This scenario closely replicated what was observed with the SC vaccination. To effectively immunize animals *via* the mucosal route, an inactivated antigen-based vaccine must overcome tissue-specific challenges, in fact, mucosal surfaces display a broad tolerance to antigens and harbor several barriers to the delivery of antigens, such as cilia (mechanical), mucus (chemical), and proteolytic enzymes (biochemical) (61). In an attempt to improve antigen delivery at the level of the mucosa, in the second animal trial, we added to the vaccine formulation IMS1313, an adjuvant with immunostimulatory activity developed for mucosal administration of live vaccines, which showed promising results also with inactivated AIV vaccines (62). When ON immunized chickens were infected with lower doses of H9N2, a stronger reduction in the percentage of positive birds became evident, especially during the first 2 days after the challenge. Both the irradiated and formalinated vaccines dramatically reduced the infection rate against the 10^4 EID_{50} dose. Although overall cumulative shedding did not differ between these two vaccines, the duration was shorter for the ON-Irr-adj group. On the other hand, at the lowest challenge of 10^3 EID_{50}, the irradiated vaccine was the only one affording a complete protection from infection in the entire flock, while the formalinated vaccine did not prevent the infection of 3/15 birds, similarly to what was observed in the control group. Once again, we observed a delayed replication of the virus with high viral loads recorded around 7–9 days from challenge. As we expected that challenges with doses of 10^{3-4} EID_{50} would lead to primary infection in about 40–60% of birds according to BID_{50} for this virus, we assume that the observed higher percentages of RRT-PCR positive birds recorded from 3 dpi in both unvaccinated groups were the result of the secondary spread between primarily infected and primarily non-infected birds.

For this reason, although we could not differentiate primary from secondary infections, we speculate that the number of positive birds identified during the first 2 days after the challenge, might be largely attributable to primarily infected birds. In light of this, the better performance of the irradiated vaccine during the early phases of the lowest challenge with 10^3 EID_{50} suggests the possibility that irradiated antigens administrated *via* the mucosal route might have reduced the primary attack rate more effectively than formalinated ones.

This might depend on the higher avidity/affinity of secretory IgA (S-IgA) mounted against a better preserved antigenic structure inactivated through irradiation (63). A limitation of our study is that we did not assess the IgA levels at the humoral and the mucosal level. Nonetheless, although protection offered by mucosal vaccination cannot be thoroughly measured by the HI assay, lower HI titers in the ON groups correlated with poorer performances when compared to the SC vaccinated animals. The addition of a mucosal adjuvant for live vaccines did not increase mean HI titers, possibly as the result of the lower viscosity of the formulation. Further studies are necessary to test novel mucoadhesive adjuvants (e.g., nanoparticles) and adjuvants targeting receptors of mucosal immune cells that could increase the permanence of inactivated antigens at the mucosal level, and thus increasing interaction with mucosal immune cells and the stimulation of the immune system at a crucial anatomical site for the establishment of infection.

Altogether, our results indicate that vaccination with an antigen inactivated by gamma irradiation achieves excellent results in terms of prevention of infection against low-to-intermediate H9N2 challenges if the vaccine is administrated SC. Moreover, irradiation of the antigen resulted in a shorter duration of shedding when compared to the traditional formalin-inactivated antigen. Additional experimental evidence on the efficacy of irradiated antigens in protecting against H9N2 and other AI subtypes is necessary to confirm our observations and understand whether this method is either comparable or superior to others currently used in vaccine manufacturing. This inactivation method might represent an alternative to the traditional formalin-based approach, especially in light of the recent advancements replacing radioactive material with the safer and cheaper low-energy electron irradiation technology.

Although ON vaccination with an inactivated antigen only partially reduced replication against a high challenge, the performance against a low-to-moderate challenge with a highly infectious strain of H9N2 proved the potential of this innovative delivery route, in particular when the antigen was inactivated by irradiation. Undoubtedly, vaccination by spray or mixing in drinking water can stimulate the mucosae of the upper respiratory and digestive tracts, and is also less expensive and more easily applicable in emergency situations than the SC vaccination and can be designed for periodic boosters. Interestingly, mucosal vaccination with the irradiated H9N2 antigen revealed a complete lack of seroconversion against the structural NP, offering a possible Differentiating Infected from Vaccinated (DIVA) approach that would simply rely on existing commercial anti-NP ELISA assays.

A significant reduction of environmental contamination is one of the secondary goals of vaccination campaigns in endemic countries where human exposure to zoonotic H9N2 viruses is of concern. Noticeable achievements in this sense have been recorded after the deployment of nationwide immunization against H5/H7 HPAI and LPAI viruses in China, with a dramatic drop in the number of H7N9 cases (64, 65). Improving the ability of H9N2 vaccines in reducing shedding, environmental contamination, and increasing the resilience of animals to infection is not only a priority to safeguard poultry production and the access to low-cost proteins in lower-income countries but also a desirable objective from a public health perspective. Mucosal vaccination with either live-vectored vaccines or inactivated antigens might offer the chance to achieve these goals.

DATA AVAILABILITY STATEMENT

The original contributions presented in the study are included in the article/**Supplementary Material**, further inquiries can be directed to the corresponding author/s.

ETHICS STATEMENT

The animal study was reviewed and approved by Istituto Zooprofilattico Sperimentale delle Venezie Ethics Committee and the Italian Ministry of Health.

AUTHOR CONTRIBUTIONS

CT, FB, and GC conceived and designed the study and supervised the study. AB, EM, VW, RK, and FB performed experiments. JB, SMan, EM, LP, and SMar performed laboratory analyses. MB performed statistical analyses of the generated datasets. AB and FB wrote the manuscript. VW, CT, VP, and FB assisted in the experimental design and preparation of the manuscript. All authors contributed to the article and approved the submitted version.

FUNDING

The present work was developed within the framework of the Coordinated Research Project (N° D32033), Irradiation of Transboundary Animal Disease (TAD) Pathogens as Vaccines and Immune Inducers, funded by IAEA.

ACKNOWLEDGMENTS

The authors are grateful to the Sebastien Deville of SEPPIC, the Air Liquide Healthcare Specialty Ingredients for kindly providing us with IMS1313 adjuvant, and to Francesca Ellero for proofreading and language editing of the manuscript.

SUPPLEMENTARY MATERIAL

The Supplementary Material for this article can be found online at: https://www.frontiersin.org/articles/10.3389/fvets.2022.916108/full#supplementary-material

REFERENCES

1. Pusch EA, Suarez DL. The multifaceted zoonotic risk of H9N2 avian influenza. *Vet Sci.* (2018) 5:82. doi: 10.3390/vetsci5040082
2. Sun Y, Pu J, Jiang Z, Guan T, Xia Y, Xu Q, et al. Genotypic evolution and antigenic drift of H9N2 influenza viruses in China from 1994 to 2008. *Vet Microbiol.* (2010) 146:215–25. doi: 10.1016/j.vetmic.2010.05.010
3. Zhao Y, Li S, Zhou Y, Song W, Tang Y, Pang Q, Miao Z. Phylogenetic analysis of hemagglutinin genes of H9N2 Avian influenza viruses isolated from chickens in Shandong, China, between 1998 and 2013. *Biomed Res Int.* (2015) 2015:267520. doi: 10.1155/2015/267520
4. Khan SU, Anderson BD, Heil GL, Liang S, Gray GC. A systematic review and meta-analysis of the seroprevalence of influenza A(H9N2) infection among humans. *J Infect Dis.* (2015) 212:562–9. doi: 10.1093/infdis/jiv109
5. He J, Wu Q, Yu JL, He L, Sun Y, Shi YL, et al. Sporadic occurrence of H9N2 avian influenza infections in human in Anhui province, eastern China: a notable problem. *Microb Pathog.* (2020) 140:103940. doi: 10.1016/j.micpath.2019.103940
6. Song W, Qin K. Human-infecting influenza A (H9N2) virus: A forgotten potential pandemic strain? *Zoonoses Public Health.* (2020) 67:203–12. doi: 10.1111/zph.12685
7. Sorrell EM, Wan H, Araya Y, Song H, Perez DR. Minimal molecular constraints for respiratory droplet transmission of an avian-human H9N2 influenza A virus. *Proc Natl Acad Sci U S A.* (2009) 106:7565–70. doi: 10.1073/pnas.0900877106
8. Guan Y, Shortridge KF, Krauss S, Webster RG. Molecular characterization of H9N2 influenza viruses: were they the donors of the "internal" genes of H5N1 viruses in Hong Kong? *Proc Natl Acad Sci U S A.* (1999) 96:9363–7. doi: 10.1073/pnas.96.16.9363
9. Pu J, Wang S, Yin Y, Zhang G, Carter RA, Wang J, et al. Evolution of the H9N2 influenza genotype that facilitated the genesis of the novel H7N9 virus. *Proc Natl Acad Sci U S A.* (2015) 112:548–53. doi: 10.1073/pnas.1422456112
10. Chen H, Yuan H, Gao R, Zhang J, Wang D, Xiong Y, et al. Clinical and epidemiological characteristics of a fatal case of avian influenza A H10N8 virus infection: a descriptive study. *Lancet.* (2014) 6736:1–8. doi: 10.1016/S0140-6736(14)60111-2
11. Smietanka K, Minta Z, Swietoń E, Olszewska M, Józwiak M, Domańska-Blicharz K, et al. Avian influenza H9N2 subtype in Poland – characterization of the isolates and evidence of concomitant infections. *Avian Pathol.* (2014) 43:427–36. doi: 10.1080/03079457.2014.952221
12. Reid SM, Banks J, Ceeraz V, Seekings A, Howard WA, Puranik A, et al. The detection of a low pathogenicity avian influenza virus subtype H9 infection

in a Turkey breeder flock in the United Kingdom. *Avian Dis.* (2016) 60:126–131. doi: 10.1637/11356-122315-Case.1
13. Fusaro A, Monne I, Salviato A, Valastro V, Schivo A, Amarin NM, et al. Phylogeography and evolutionary history of reassortant H9N2 viruses with potential human health implications. *J Virol.* (2011) 85:8413–21. doi: 10.1128/JVI.00219-11
14. Monne I, Hussein HA, Fusaro A, Valastro V, Hamoud MM, Khalefa RA, et al. H9N2 influenza A virus circulates in H5N1 endemically infected poultry population in Egypt. *Influenza Other Respi Viruses.* (2013) 7:240–3. doi: 10.1111/j.1750-2659.2012.00399.x
15. Davidson I, Fusaro A, Heidari A, Monne I, Cattoli G. Molecular evolution of H9N2 avian influenza viruses in Israel. *Virus Genes.* (2014) 48:457–63. doi: 10.1007/s11262-014-1037-0
16. Gomaa MR, Kandeil A, El-Shesheny R, Shehata MM, McKenzie PP, Webby RJ, et al. Evidence of infection with avian, human, and swine influenza viruses in pigs in Cairo, Egypt. *Arch Virol.* (2018) 163:359–64. doi: 10.1007/s00705-017-3619-3
17. Peacock TP, James J, Sealy JE, Iqbal M, A. global perspective on H9N2 avian influenza virus. *Viruses.* (2019) 11:620. doi: 10.3390/v11070620
18. Lee D. hun, Fusaro A, Song CS, Suarez DL, Swayne DE. Poultry vaccination directed evolution of H9N2 low pathogenicity avian influenza viruses in Korea. *Virology.* (2016) 488:225–31. doi: 10.1016/j.virol.2015.11.023
19. Cattoli G, Fusaro A, Monne I, Coven F, Joannis T, El-Hamid HSA, et al. Evidence for differing evolutionary dynamics of A/H5N1 viruses among countries applying or not applying avian influenza vaccination in poultry. *Vaccine.* (2011) 29:9368–75. doi: 10.1016/j.vaccine.2011.09.127
20. Sims LD, Tripodi A, Swayne DE. Spotlight on avian pathology: can we reduce the pandemic threat of H9N2 avian influenza to human and avian health? *Avian Pathol.* (2020) 49:529–31. doi: 10.1080/03079457.2020.1796139
21. Viljoen GJ, Unger H, Wijewardana V, Naletoski I. Chapter 10: novel developments and next-generation vaccines. In: Metwally S, El Idrissi A, Viljoen G, editors, Veterinary Vaccines: Principles and Applications. Chichester: John Wiley & Sons (2021). p. 119–34.
22. Fertey J, Bayer L, Grunwald T, Pohl A, Beckmann J, Gotzmann G, et al. Pathogens inactivated by low-energy-electron irradiation maintain antigenic properties and induce protective immune responses. *Viruses.* (2016) 8:319. doi: 10.3390/v8110319
23. David SC, Lau J, Singleton E V, Babb R, Davies J, Hirst TR, et al. The effect of gamma-irradiation conditions on the immunogenicity of whole-inactivated Influenza A virus vaccine. *Vaccine.* (2017) 35:1071–9. doi: 10.1016/j.vaccine.2016.12.044
24. Chen F, Seong Seo H, Ji HJ, Yang E, Choi JA, Yang JS, et al. Characterization of humoral and cellular immune features of gamma-irradiated influenza vaccine. *Hum Vaccines Immunother.* (2021) 17.2:485–96. doi: 10.1080/21645515.2020.1780091
25. World Organization for Animal Health [OIE]. *Manual of Diagnostic Tests and Vaccines for Terrestrial Animals*. Paris: OIE (2015).
26. Reed LJ, Muench H, A. simple method of estimating fifty per cent endpoints. *Am J Epidemiol.* (1938) 27:493–7. doi: 10.1093/oxfordjournals.aje.a118408
27. Singleton E V, David SC, Davies JB, Hirst TR, Paton JC, Beard MR, et al. Sterility of gamma-irradiated pathogens: a new mathematical formula to calculate sterilizing doses. *J Radiat Res.* (2020) 61:886–94. doi: 10.1093/jrr/rraa076
28. King DJ. Evaluation of different methods of inactivation of newcastle disease virus and avian influenza virus in egg fluids and serum. *Avian Dis.* (1991) 35:505–14. doi: 10.2307/1591214
29. Swayne DE, Slemons RD. Using mean infectious dose of high- and low-pathogenicity avian influenza viruses originating from wild duck and poultry as one measure of infectivity and adaptation to poultry. *Avian Dis.* (2008) 52:455–60. doi: 10.1637/8229-012508-Reg.1
30. Spackman E, Senne DA, Myers TJ, Bulaga LL, Garber LP, Perdue ML, et al. Development of a real-time reverse transcriptase PCR assay for type A influenza virus and the avian H5 and H7 hemagglutinin subtypes. *J Clin Microbiol.* (2002) 40:3256–60. doi: 10.1128/JCM.40.9.3256-3260.2002
31. Healy MJR, Finney DJ. Statistical method in biological assay. *J R Stat Soc Ser A.* (1979) 142:507–507. doi: 10.2307/2982559
32. World Organization for Animal Health [OIE]. *Manual of Diagnostic Tests and Vaccines for Terrestrial Animal*s. Paris: OIE (2021).
33. Simpson GL. *gratia: Graceful'ggplot'-Based Graphics and Other Functions for GAMs Fitted Using "mgcv." R package version 0.7.3* (2022). Available online at: https://gavinsimpson.github.io/gratia/ (accessed November 29, 2021).
34. Wood SN. Fast stable restricted maximum likelihood and marginal likelihood estimation of semiparametric generalized linear models. *J R Stat Soc Ser B Stat Methodol.* (2011) 73:3–36. doi: 10.1111/j.1467-9868.2010.00749.x
35. Team RDC. *R: A Language and Environment for Statistical Computing*. Vienna: R Foundation for Statistical Computing (2011).
36. DiCiccio TJ, Efron B. Bootstrap confidence intervals. *Stat Sci.* (1996) 11:189–228. doi: 10.1214/ss/1032280214
37. Kropko J, Harden JJ. Beyond the hazard ratio: generating expected durations from the cox proportional hazards model. *Br J Polit Sci.* (2020) 50:303–20. doi: 10.1017/S000712341700045X
38. Bates D, Mächler M, Bolker BM, Walker SC. Fitting linear mixed-effects models using lme4. *J Stat Softw.* (2015) 67:1–48. doi: 10.18637/jss.v067.i01
39. Lenth R, Singmann H, Love J, Buerkner P, Herve M. *Emmeans: Estimated Marginal Means, Aka Least-Squares Means*. R package version 170 (2021). Available online at: https://github.com/rvlenth/emmeans (accessed November 29, 2021).
40. Shen H, Wu B, Li G, Chen F, Luo Q, Chen Y, et al. H9N2 subtype avian influenza viruses in china: current advances and future perspectives. *Br J Virol.* (2014) 1:54–63.
41. Kilany WH, Ali A, Bazid AHI, El-Deeb AH, El-Abideen MAZ, Sayed M. El, El-Kady MF. A dose-response study of inactivated low pathogenic avian influenza H9N2 virus in specific-pathogen-free and commercial broiler chickens. *Avian Dis.* (2016) 60:256–61. doi: 10.1637/11143-050815-Reg
42. Swayne DE, Spackman E, Pantin-Jackwood M. Success factors for avian influenza vaccine use in poultry and potential impact at the wild bird-agricultural interface. *EcoHealth (2014).* (2014) 11:94–108. doi: 10.1007/s10393-013-0861-3
43. Meng D, Hui Z, Yang J, Yuan J, Ling Y, He C. Reduced egg production in hens associated with avian influenza vaccines and formalin levels. *Avian Dis.* (2009) 53:16–20. doi: 10.1637/8343-050208-Reg.1
44. Shahrudin S, Chen C, David SC, Singleton E V, Davies J, Kirkwood CD, et al. Gamma-irradiated rotavirus: a possible whole virus inactivated vaccine. *PLoS ONE.* (2018) 13:e0198182. doi: 10.1371/journal.pone.0198182
45. Martin SS, Bakken RR, Lind CM, Garcia P, Jenkins E, Glass PJ, et al. Comparison of the immunological responses and efficacy of gamma-irradiated V3526 vaccine formulations against subcutaneous and aerosol challenge with Venezuelan equine encephalitis virus subtype IAB. *Vaccine.* (2010) 28:1031–40. doi: 10.1016/j.vaccine.2009.10.126
46. Elliott LH, McCormick JB, Johnson KM. Inactivation of Lassa, Marburg, and Ebola viruses by gamma irradiation. *J Clin Microbiol.* (1982) 16:704–8. doi: 10.1128/jcm.16.4.704-708.1982
47. Pawar SD, Murtadak VB, Kale SD, Shinde P V, Parkhi SS. Evaluation of different inactivation methods for high and low pathogenic avian influenza viruses in egg-fluids for antigen preparation. *J Virol Methods.* (2015) 222:28–33. doi: 10.1016/j.jviromet.2015.05.004
48. Delrue I, Verzele D, Madder A, Nauwynck HJ. Inactivated virus vaccines from chemistry to prophylaxis: merits, risks and challenges. *Expert Rev Vaccines.* (2014) 11:695–719. doi: 10.1586/erv.12.38
49. Abolaban FA, Djouider FM. Gamma irradiation-mediated inactivation of enveloped viruses with conservation of genome integrity: potential application for SARS-CoV-2 inactivated vaccine development. *Open Life Sci.* (2021) 16:558–70. doi: 10.1515/biol-2021-0051
50. Singleton EV, Gates CJ, David SC, Hirst TR, Davies JB, Alsharifi M. Enhanced immunogenicity of a whole-inactivated influenza A virus vaccine using optimised irradiation conditions. *Front Immunol.* (2021) 12:5020. doi: 10.3389/fimmu.2021.761632
51. Yoshinaga K, Yoshioka H, Kurosaki H, Hirasawa M, Uritani M, Hasegawa K. Protection by trehalose of DNA from radiation damage. *Biosci Biotechnol Biochem.* (1997) 61:160–1. doi: 10.1271/bbb.61.160
52. Kim YC, Quan FS, Song JM, Vunnava A, Yoo DG, Park KM, et al. Influenza immunization with trehalose-stabilized virus-like particle vaccine using microneedles. *Procedia Vaccinol.* (2010) 2:15–9. doi: 10.1016/j.provac.2010.03.004
53. Mollaei Alamuti M, Ravanshad M, Motamedi-Sedeh F, Nabizadeh A, Ahmadi E, Hossieni SM. Immune response of gamma-irradiated inactivated bivalent

polio vaccine prepared plus trehalose as a protein stabilizer in a mouse model. *Intervirology*. (2021) 64:140–6. doi: 10.1159/000515392
54. Unger H, Kangethe RT, Liaqat F, Viljoen GJ. Advances in irradiated livestock vaccine research and production addressing the unmet needs for farmers and veterinary services in FAO/IAEA member states. *Front Immunol.* (2022) 13:1310. doi: 10.3389/fimmu.2022.853874
55. Lee DH, Kwon JS, Lee HJ, Lee YN, Hur W, Hong YH, et al. Inactivated H9N2 avian influenza virus vaccine with gel-primed and mineral oil-boosted regimen could produce improved immune response in broiler breeders. *Poult Sci.* (2011) 90:1020–2. doi: 10.3382/ps.2010-01258
56. Sun Y, Pu J, Fan L, Sun H, Wang J, Zhang Y, et al. Evaluation of the protective efficacy of a commercial vaccine against different antigenic groups of H9N2 influenza viruses in chickens. *Vet Microbiol.* (2012) 156:193–9. doi: 10.1016/j.vetmic.2011.10.003
57. Vanaporn M, Titball RW. Trehalose and bacterial virulence. *Virulence.* (2020) 11:1192–202. doi: 10.1080/21505594.2020.1809326
58. Lone NA, Spackman E, Kapczynski D. Immunologic evaluation of 10 different adjuvants for use in vaccines for chickens against highly pathogenic avian influenza virus. *Vaccine.* (2017) 35:3401–8. doi: 10.1016/j.vaccine.2017.05.010
59. Suarez DL. Overview of avian influenza DIVA test strategies. *Biologicals.* (2005) 33:221–6. doi: 10.1016/j.biologicals.2005.08.003
60. Ducatez MF, Becker J, Freudenstein A, Delverdier M, Delpont M, Sutter G, et al. Low pathogenic avian influenza (H9N2) in chicken: Evaluation of an ancestral H9-MVA vaccine. *Vet Microbiol.* (2016) 189:59–67. doi: 10.1016/j.vetmic.2016.04.025
61. Shin JH, Mo JS, Kim JN, Mo IP, Ha B. Do. Assessment of the safety and efficacy of low pathogenic avian influenza (H9N2) virus in inactivated oil emulsion vaccine in laying hens. *J Vet Sci.* (2016) 17:27–34. doi: 10.4142/jvs.2016.17.1.27
62. Wang T, Wei F, Liu J. Emerging role of mucosal vaccine in preventing infection with avian influenza a viruses. *Viruses.* (2020) 12:862. doi: 10.3390/v12080862
63. Ismail NM, El-Deeb AH, Emara MM, Tawfik HI, Wanis NA, Hussein HA, et al. 1313-nanoparticle mucosal vaccine enhances immunity against avian influenza and Newcastle disease viruses. *Int J Poult Sci.* (2018) 17:167–74. doi: 10.3923/ijps.2018.167.174
64. Furuya Y, Regner M, Lobigs M, Koskinen A, Müllbacher A, Alsharifi M. Effect of inactivation method on the cross-protective immunity induced by whole "killed" influenza A viruses and commercial vaccine preparations. *J Gen Virol.* (2010) 91:1450–60. doi: 10.1099/vir.0.018168-0
65. Cheng W, Chong KC, Lau SYF, Wang X, Yu Z, Liu S, et al. Comparison of avian influenza virus contamination in the environment before and after massive poultry H5/H7 vaccination in Zhejiang Province, China. *Open Forum Infect Dis.* (2019) 6:ofz197. doi: 10.1093/ofid/ofz197

Conflict of Interest: The authors declare that the research was conducted in the absence of any commercial or financial relationships that could be construed as a potential conflict of interest.

Publisher's Note: All claims expressed in this article are solely those of the authors and do not necessarily represent those of their affiliated organizations, or those of the publisher, the editors and the reviewers. Any product that may be evaluated in this article, or claim that may be made by its manufacturer, is not guaranteed or endorsed by the publisher.

frontiers | Frontiers in Veterinary Science

ORIGINAL RESEARCH
published: 12 July 2022
doi: 10.3389/fvets.2022.907369

Improved Whole Gamma Irradiated Avian Influenza Subtype H9N2 Virus Vaccine Using Trehalose and Optimization of Vaccination Regime on Broiler Chicken

Farahnaz Motamedi Sedeh[1], Iraj Khalili[2], Viskam Wijewardana[3], Hermann Unger[3], Parvin Shawrang[1], Mehdi Behgar[1], Sayed Morteza Moosavi[1], Arash Arbabi[4] and Sayedeh Maede Hosseini[4]*

[1] Nuclear Agriculture Research School, Nuclear Science and Technology Research Institute (NSTRI), Karaj, Iran, [2] Quality Control Department, Razi Vaccine and Serum Research Institute (RVSRI), Agricultural Research Education and Extension Organization (AREEO), Karaj, Iran, [3] Animal Production and Health Section, Department of Nuclear Sciences and Applications, Joint FAO/IAEA Centre of Nuclear Techniques in Food and Agriculture International Atomic Energy Agency (IAEA), Vienna, Austria, [4] School of Medicine, Tehran University of Medical Science, Tehran, Iran

OPEN ACCESS

Edited by:
Constantinos S. Kyriakis, Auburn University, United States

Reviewed by:
Surya Paudel, City University of Hong Kong, Hong Kong SAR, China
Ahmed Ragab Elbestawy, Damanhour University, Egypt

***Correspondence:**
Farahnaz Motamedi Sedeh
fmotamedi@aeoi.org.ir; farah.motamedi@gmail.com

Specialty section:
This article was submitted to Veterinary Infectious Diseases, a section of the journal Frontiers in Veterinary Science

Received: *29 March 2022*
Accepted: *16 June 2022*
Published: *12 July 2022*

Citation:
Motamedi Sedeh F, Khalili I, Wijewardana V, Unger H, Shawrang P, Behgar M, Moosavi SM, Arbabi A and Hosseini SM (2022) Improved Whole Gamma Irradiated Avian Influenza Subtype H9N2 Virus Vaccine Using Trehalose and Optimization of Vaccination Regime on Broiler Chicken. Front. Vet. Sci. 9:907369. doi: 10.3389/fvets.2022.907369

Gamma (γ)-radiation can target viral genome replication and preserve viral structural proteins compared to formalin inactivation. Thus, a stronger immunity could be induced after the inoculation of the irradiated virus. In this study, γ-irradiated low-pathogenic avian influenza virus-H9N2 (LPAIV-H9N2) was used to immunize the broiler chicken in two formulations, including γ-irradiated LPAIV-H9N2 with 20% Trehalose intranasally (IVT.IN) or γ-irradiated LPAIV-H9N2 plus Montanide oil adjuvant ISA70 subcutaneously (IV+ISA.SC) in comparison with formalin-inactivated LPAIV-H9N2 vaccine intranasally (FV.IN) or formalin-inactivated LPAIV-H9N2 plus ISA70 subcutaneously (FV+ISA.SC). Two vaccination regimes were employed; the first one was primed on day 1 and boosted on day 15 (early regime), and the second one was primed on day 11 and boosted on day 25 (late regime). A challenge test was performed with a live homologous subtype virus. Virus shedding was monitored by quantifying the viral load *via* RT-qPCR on tracheal and cloacal swabs. Hemagglutination inhibition (HI) antibody titration and stimulation index (SI) of the splenic lymphocyte proliferation were measured, respectively, by HI test and Cell Proliferation assay. Cytokine assay was conducted by the RT-qPCR on antigen-stimulated spleen cells. The results of the HI test showed significant increases in antibody titer in all vaccinated groups, but it was more evident in the IVT late vaccination regime, reaching 5.33 $\log_2$. The proliferation of stimulated spleen lymphocytes was upregulated more in the IVT.IN vaccine compared to other vaccines. The mRNA transcription levels of T-helper type 1 cytokines such as interferon-gamma (IFN-γ) and interleukin 2 (IL-2) were upregulated in all vaccinated groups at the late regime. Moreover, IL-6, a pro-inflammatory cytokine was upregulated as well. However, upregulation was more noticeable in the early vaccination than the late vaccination ($p < 0.05$). After the challenge, the monitoring of virus shedding for the H9 gene represented an extremely low viral load. The body weight loss was not significant ($p > 0.05$) among the vaccinated groups.

In addition, the viral load of $<10^{0.5}$ $TCID_{50}$/ml in the vaccinated chicken indicated the protective response for all the vaccines. Accordingly, the IVT vaccine is a good candidate for the immunization of broiler chicken *via* the intranasal route at late regime.

Keywords: avian influenza virus, gamma-radiation, vaccine, immune response, virus shedding

INTRODUCTION

Among the three types of influenza viruses (A, B, and C), only influenza A genus has been isolated from birds and termed as avian influenza virus (LPAIV-H9N2). According to previous studies (1–3), influenza type A viruses are divided into subtypes based on the genetic and antigenic differences in two surface spike proteins, namely, hemagglutinin (HA) and neuraminidase (NA). The subtype LPAIV-H9N2 was initially isolated (1966) from turkeys in the northern state of the United States (4). Then, it was detected in domestic poultry in Europe, Africa, Asia, and the Middle East. Frequent outbreaks have been reported in Asian countries such as Iran, Saudi Arabia, Pakistan, and Iraq (2). After the first reported outbreak (1998), the virus became endemic, which led to a routine vaccination program to control LPAIV-H9N2 (1, 5). H9N2 is commonly co-circulating in poultry with other subtypes of LPAIV-H9N2, including H5 and H7 (6). Live poultry markets are a crucial link in the poultry trade and require close surveillance. H9N2 can be the donor of genes to other AIVs such as H5N1, H5N6, H7N9, and H10N8, which are responsible for high death rates in humans (7). In addition, H9N2 is a low-pathogenic Avian Influenza virus (LPAIV-H9N2) and has a wide host range such as ducks, chickens, pigs, and turkeys (8) with possible transmission from avian to humans (5). It causes considerable economic losses in the poultry industry worldwide (4). H9N2 infection leads to high economic losses in both layers and for breeders due to a drop in egg production. Broilers may also show severe losses during coinfection with other pathogens, especially Infectious Bronchitis Virus (IBV), Newcastle disease virus (NDV), bacteria such as E. coli and Mycoplasma, or even live virus vaccines (9). Therefore, a vaccine yielding a higher level of protection is required to prevent LPAI H9N2 in the poultry industry.

γ-Ray is ionizing radiation emitted from radio isotopes (Cobalt-60 and Cesium-137 isotopes) and high- or low-energy electron beams used for virus inactivation without any changes in viral proteins. The dose of γ-radiation for virus inactivation depends on the radiation temperature, the virus concentration, size of the viral genome, the presence of oxygen, and water content during the irradiation process (10). γ-Rays are at the higher frequency end of the electromagnetic spectrum (the shortest wavelength, but high energy). It is the perfect method for virus inactivation and destroys genetic materials by creating breaks in the genome (breaking ssRNA, dsRNA, or dsDNA).

The potency of γ-radiation has been successfully tested in human clinical trials for radiation-attenuated anti-parasite vaccines against malaria (11). For larger pathogens such as parasites and bacteria, a relatively low dose of γ-irradiation is sufficient for inactivating the organism (e.g., malaria irradiation at 150 Gray, Fasciola irradiation at 30 Gray, and Brucella irradiation at 6 kGy). Conversely, viral pathogens require higher doses, including Rift Valley Fever virus irradiation at 25 kGy (12, 13), LPAIV-H9N2 at 30 kGy (14), foot and mouth disease virus at 45 kGy (15), and poliovirus subtypes 1 and 3 at 35 kGy (16).

The use of these higher doses of irradiation for virus inactivation takes a longer time and results in building up free radicals that could damage the antigenic epitopes of viral proteins, even if that could be lesser extent compared to chemical inactivation (11–15). Although many compounds could be used to rescue this damage which is caused by the free radicals. Trehalose, as a disaccharide, has its own merits as a cryo-protect and a free radical quencher (17–19). Trehalose can stabilize proteins and inhibit protein denaturation by excluding water molecules from the surface of proteins when cells are in a dehydrated condition. The dry state maintains proteins in the folded state by replacing water molecules and forming hydrogen bonds directly with proteins and thus their structure. Trehalose acts as a natural stabilizer of life processes (17–19).

In this research, the LPAIV-H9N2 was irradiated after formulation with Trehalose and employed to immunize the broiler chicken in two formulations and at two vaccination regimes *via* two routes of administration. Virus shedding and immune responses were evaluated for 48 days. The specific objectives of this study are to use Trehalose as a protein stabilizer during LPAIV-H9N2 irradiation, use of irradiated LPAIV-H9N2 plus Trehalose or Montanide ISA70 as an inactivated vaccine, comparison of two vaccination regimes *via* two routes of administration, early and late regimes, vaccine inoculation subcutaneously or intranasal for evaluating immune responses due to irradiated LPAIV-H9N2 vaccine and formalin LPAIV-H9N2 vaccine and comparison of immune responses between irradiated LPAIV-H9N2 vaccine and formalin-inactivated LPAIV-H9N2 vaccine. Furthermore, we can suggest the more protective vaccine, the better route of administration and vaccination regime against LPAIV-H9N2.

MATERIALS AND METHODS

Vaccine Preparation

The isolated LPAIV-H9N2 strain A/chicken/IRN/Ghazvin/2001 was a kind donation from the Razi Vaccine and Serum Research Institute of Iran. The irradiated avian influenza subtype H9N2 vaccine was prepared according to the protocols published by Javan et al. (14) and Salehi et al. (20). Briefly, 3–4 days after the multiplication of the LPAIV-H9N2 on embryonated specific free pathogen (SPF) chicken eggs, the allantoic fluid was collected and tested using a hemagglutination test for HA titration. The infected allantoic fluid was used for virus titration measuring embryo infective dose (EID50) and calculated according to the

formula by Reed and Muench (21). A γ-ray dose of 30 kGy was recommended for the frozen virus suspension (22). Half of the frozen LPAIV-H9N2 stock plus 20% Trehalose (1 M, a disaccharide of glucose and as a protein protectant) and half of the frozen LPAIV-H9N2 stock without Trehalose were irradiated using the gamma irradiator (Nordion Company, Canada, model 220, γ-cell) at a dose rate of 2.07 Gy/s and activity of 8677 Ci for virus inactivation on dry ice. The Laemmli SDS-PAGE system was used to assess the quality of viral proteins in irradiated and non-irradiated viral samples. In this study, the γ-irradiated LPAIV-H9N2 was applied in two formulations. The first one was γ-irradiated LPAIV-H9N2 with 20% disaccharide Trehalose (1 M) as a water suspension (IVT vaccine) and the second one was γ-irradiated LPAIV-H9N2 plus Montanide oil (ISA70) as a water-in-oil (30/70) vaccine (IV+ISA vaccine). A formalin concentration of 0.1% at 25 °C was added to the LPAIV-H9N2 suspension to inactivate the virus for 24 h and employed as the formalin-treated vaccine (FV) according to Razi protocols (20, 22). The FV was used in two formulations. The first one was used as a drop on the nose (FV.IN) by $10^{7.5}$ EID_{50}/100 μl and the second one was an FV plus Montanide oil (ISA70) as a water-in-oil (30/70) vaccine subcutaneously (FV+ISA.SC vaccine). Vaccination was performed in two routes of administration (intranasally and subcutaneously injection on the neck) on broiler chicken. In addition, Montanide ISA 70 was applied as an adjuvant, along with irradiated and formalin vaccines. Injectable vaccine and stable water-in-oil (W/O) emulsions were obtained by mixing Montanide ISA70 and antigenic media (H9N2) under a high shear rate.

Animal Trails

The animal experiments were performed in two steps. The first chicken experiment was conducted on seven chicken groups. A total of forty-two broiler chickens (ROSS 308) were purchased from Alborz hatchery center and allocated into seven groups, each including 6 animals (three chickens were used in each of sampling). The first group was pre-immunization and the second group was the negative control group and was inoculated with sterile PBS intranasally. The third and fourth groups were immunized by irradiated vaccine intranasally or subcutaneously (IV.IN or IV.SC). Moreover, the fifth and sixth groups were vaccinated by irradiated vaccine plus 20% Trehalose intranasally or subcutaneously (IVT.IN or IVT.SC), and the seventh group was inoculated by Trehalose solution (1 M) alone intranasally (T.IN). The amount of each vaccination dose was 100 μl. The sera samples were collected from all chickens 2 weeks after the first and second vaccination for HI antibody titration assay (at days 25 and 38). The splenic lymphocytes of all chicken groups were cultured and stimulated by homologous-inactivated antigens to evaluate the splenic lymphocyte proliferation assay as cellular immunity at days 25 and 38 (three chickens in each group were used for each sampling day).

The second chicken experiment was performed on the other vaccinated bird groups (**Table 1**). A total of 200 and21 broiler chickens (ROSS 308) were purchased and allocated into 17 groups (each including 13 chickens) to evaluate immune responses and virus shedding in the second animal experiment. The first group was pre-immunization, and the second and third groups were inoculated with sterile PBS intranasally or subcutaneously as negative control groups (NC.IN or NC.SC). Further, the fourth to eighth groups were vaccinated with irradiated LPAIV-H9N2 plus Trehalose and the two routes of administration, namely intranasally (IVT.IN) or subcutaneously (IVT.SC), formalin LPAIV-H9N2 intranasally (FV.IN), formalin LPAIV-H9N2 plus ISA70 subcutaneously (FV+ISA.SC), irradiated LPAIV-H9N2 plus ISA70 subcutaneously (IV+ISA.SC), respectively. The vaccination was conducted in two different regimes (**Figure 1**). The first one was primed on day 1 and boosted on day 15 (early regime), and the second one was primed on day 11 and boosted on day 25 (late regime); one hundred and four chickens were used in each regime. The second to eighth groups and the ninth to fifteen groups were vaccinated in the early and late regimens, but the same vaccines. The last two groups (16 and 17 groups) were positive control, without vaccination and challenged with live homologous subtype virus (**Table 1**). The sera samples were collected from all chickens 2 weeks after the second vaccination and before challenge with live virus (at days 30 and 38 for early and late regimes, respectively) for HI antibody titration assay. The splenic lymphocytes of the chicken groups (three chickens in each sampling day, 84 chickens in early and late regimens groups, and 13 chickens in pre-immune group, totally 97 chickens were used for culturing splenic lymphocyte) were cultured and stimulated by homologous-inactivated antigens to measure the splenic lymphocyte proliferation assay as cellular immunity, and cytokines assay at days 30 (before challenge with live virus) and 40 in early regime and at days 38 (before challenge with live virus) and 48 in late regime, respectively.

Challenge of Vaccinated Chicken With the Live Homologous Virus and Virus Shedding

The challenge test with live homologous virus was done in the poultry isolators with Hepa Filter in the biosafety level 2+ laboratory (in Iran Veterinary Organization (IVO), National Diagnosis Center, Reference Laboratories & Applied Studies). All the vaccinated chicken groups in the second animal experiment were challenged with 50 μl live homologous subtype virus ($10^{5.5}$ EID_{50}/ml) through intranasal and ocular routes, except for pre-immunization and negative control groups (1, 2, 3, 9, and 10 groups), including the five early groups on day 30 and the five late groups on day 38 (ten chickens remained in each group for challenge). Furthermore, two positive control groups (each including 13 chickens) were inoculated with 50 μl live homologous subtype virus ($10^{5.5}$ EID_{50}/ ml) *via* intranasal and ocular routes at days 30 and 38 days. Tracheal and cloacal swabs were collected and used for RNA extraction on 2, 4, and 10 days after the challenge from the vaccinated bird groups, negative control and positive control groups to evaluate virus shedding by the RT-qPCR.

Morbidity and body weight loss for all chicken groups were daily monitored for 10 days following the challenge. Similarly, the lung tissue of three chickens in each group was harvested and homogenized 5 days after the challenge, and then the virus titer

TABLE 1 | The second design for the chicken experiment.

No	Vaccine groups	Route- of Adm	Vaccine dose (μl)	Vaccination day	Regime of Vaccination	Challenge-day	Number of chicken	Sampling day for HI antibody titration	Sampling days for SLP assay & cytokine assay / number of chicken	Sampling days after challenge for virus shedding	Sampling days after challenge for virus shedding in lung tissue / Number of chicken
1	Pre-Immune	-	-	-	-	-	13	1	1/13	-	-
2	N.C (PBS)	IN	100	1,15	early	-	13	30	30/3 40/3	2, 4, 10	5/3
3	N.C (PBS)	SC	100	1,15	early	-	13	30	30/3 40/3	2, 4, 10	5/3
4	IVT	IN	100	1, 15	early	30	13	30	30/3 40/3	2, 4, 10	5/3
5	FV	IN	100	1,15	early	30	13	30	30/3 40/3	2, 4, 10	5/3
6	IVT	SC	100	1,15	early	30	13	30	30/3 40/3	2, 4, 10	5/3
7	FV+ISA	SC	100	1,15	early	30	13	30	30/3 40/3	2, 4, 10	5/3
8	IV+ISA	SC	100	1,15	early	30	13	30	30/3 40/3	2, 4, 10	5/3
9	N.C (PBS)	IN	100	11,25	late	-	13	38	38 /3 48/3	2, 4, 10	5/3
10	N.C (PBS)	SC	100	11,25	late	-	13	38	38/3 48/3	2, 4, 10	5/3
11	IVT	IN	100	11, 25	late	38	13	38	38/3 48/3	2, 4, 10	5/3
12	FV	IN	100	11, 25	late	38	13	38	38/3 48/3	2, 4, 10	5/3
13	IVT	SC	100	11, 25	late	38	13	38	38/3 48/3	2, 4, 10	5/3
14	FV+ISA	SC	100	11, 25	late	38	13	38	38/3 48/3	2, 4, 10	5/3
15	IV+ISA	SC	100	11, 25	late	38	13	38	38/3 48/3	2, 4, 10	5/3
16	PC	IN	-	-	-	30	13	-	-	2, 4, 10	5/3
17	PC	IN	-	-	-	38	13	-	-	2, 4, 10	5/3

N.C, negative control; IV, Irradiated Vaccine; IVT, Irradiated Vaccine + Trehalose; IN, Intranasal; SC, Subcutaneous; Adm, Administration; SLP, Splenic Lymphocyte Proliferation Assay; FV, Formalin Vaccine; (FV+ISA), Formalin Vaccine plus Montanide oil ISA70; (IV+ISA), Irradiated Vaccine plus Montanide oil ISA70.

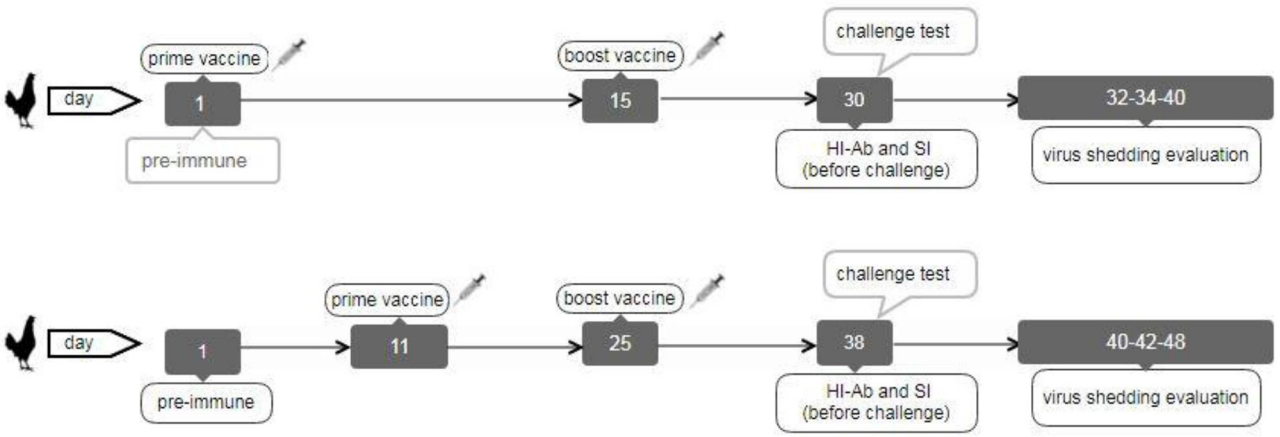

FIGURE 1 | The broiler chicken vaccination diagram in early (top) and late (down) regimes.

was determined using the Madin-Darby canine kidney (MDCK) cells and Hemagglutinin antigen assay (HA assay). To release the virus, the lung tissue homogenates were frozen and thawed three times, and their supernatants, in serial dilution from 10^{-1} to 10^{-7}-fold, were added to triplicate the wells of MDCK cells. After incubation for 1 h, RPMI 1640+ 10% FCS was added to each well and incubated for 48 h at 37 °C in a humidified incubator (New Brunswick, England) containing 5% CO_2. HA was performed on the supernatant of each well by the co-incubation of the culture supernatant with chicken red blood cells. The virus titration in lung tissues was determined by interpolating the dilution endpoint that infected the cells in 50% of the wells and as $\log_{10}$ $TCID_{50}$ (Tissue Culture Infectious Dose 50%).

Evaluation of Immune Responses and Cytokine Assay

The diluted chicken sera (two-fold serially diluted with sterile PBS) were mixed with four hemagglutinin units of virus antigens (the infected allantoic fluids) in 96-well microplates and incubated 30 min at room temperature (23). Chicken red blood cells (0.5%) were added to the mixtures and set for 30 min at room temperature. The reciprocals of the highest serum dilutions showing complete HI were expressed as the HI titration. As explained in **Table 1** for the second chicken experiment, the cellular immunity was measured by the splenic lymphocyte proliferation (SLP) assay at days 30 and 38 for five vaccinated chicken groups and two negative control groups in the early regime, the other five vaccinated chicken groups and two negative control groups in the late regime, respectively (24–26). Briefly, the spleens of the immunized chickens were aseptically removed 2 weeks after the boost immunization (at days 30 and 38), and single splenic lymphocyte suspensions were prepared (25, 26) and incubated in 96-well plates at a density of 2×10^5 cells/well by RPMI 1,640 (Invitrogen, USA) + 10% fetal calf serum (FCS) (ZiSera, Iran) at 37 °C in an incubator with humidified atmosphere containing 5% CO_2. The cells were stimulated by irradiated inactivated homologous LPAIV-H9N2 (3 μl/well) as the specific antigen for the vaccine groups, as well as phytohemagglutinin (5 μg/ml) for the positive control, or without any stimulating antigen in triplicates. Then, 48 h post-stimulation, the supernatant of splenic cells was collected for cell proliferation assay according to the protocol of the cell proliferation MTT kit (Roche, England). The Cell Proliferation MTT Kit is a colorimetric assay for the nonradioactive quantification of cellular proliferation. The tetrazolium salt (MTT) is cleaved to formazan by enzymes of the endoplasmic reticulum. This bio-reduction occurs in viable cells only, and is related to NAD(P)H production through glycolysis. The MTT solution was added (30 μl) per well with a concentration of 5 mg/ml. After 4 h of incubation at 37 °C, 100 μl of dimethyl sulfoxide was added to each well to dissolve formazan crystals. The optical density was measured at 540 nm. Finally, the stimulation index (SI) was calculated for each sample (SI = mean of optical density for stimulated wells/mean of OD unstimulated wells). Additionally, the pellet of splenic cells was collected and suspended in Trizol solution for RNA extraction to assess interleukin 2 (IL-2), IL-6, and interferon-gamma (IFN-γ) production by the real-time polymerase chain reaction (RT-PCR). RNA was extracted by the RNA Mini Kit (Bio&Sell, Germany). The concentration of RNA was measured by the Nanodrop system (Smart, Canada). Then, cDNA was synthesized by the Easy cDNA synthesis kit (Parstous, Iran, Cat A101161). Briefly, the template RNA (1 ng−5 μg), buffer mix-2X (10 μl), enzyme mix (2 μl), and DEPC water (up to 20 μl) were mixed in an RNase- free tube. The above mixture was mixed by the quick vortex, incubated 10 and 60 min at 25 and 47 °C, respectively, stopped the reaction by heating at 85 °C for 5 min, and finally, chilled at 4 °C. According to the manufacturer's protocol, the synthesized cDNA was used for the real-time RT-PCR by IQ SYBR Green Supermix (Bio-Rad, Cat.No.172-5270, United State) at SYBR/FAM channel with a Rotor Gene-Q (Qiagen, German) real-time PCR system. Real-time PCR reactions were set up at 95 °C for 3 min, 40 cycles at 95 °C for 10 s, 59 °C for 20 s, and 72 °C for 20 s. The cycle threshold (Ct) of gene products was

determined and set to the log-linear range of the amplification curve and kept constant. The relative expression of cytokines was calculated as the fold change ($2^{-\Delta\Delta Ct}$) with normalization to the corresponding GAPDH values as the housekeeping gene used in this study (25, 26).

RNA Extraction and CDNA Synthesis

The tracheal and cloacal swabs of vaccinated chicken in the second animal experiment were collected 14 days after the second vaccination and after challenge with live virus in RNX-Plus solution (Sinaclon Iran). The RNA was extracted by the RNA Mini Kit (Bio & Sell, Germany). Briefly, the swab samples were lysed by 400 μl of the lysis solution (in the RNA Mini kit), clarified on Spin Filter E, and centrifuged at 10,000 ×g for two min. The sample was bound on Spin Filter S and washed by the washing solution. Finally, the column was dried, and RNA was eluted in RNase-free water. According to the manufacturer's protocol, the cDNA was synthesized using SCRIPTUM first-strand cDNA synthesis for efficient reverse transcription (Bio & Sell, Germany). The concentration of RNA was measured by the Nanodrop system (Smart, Canada). The specific primer for the HA gene (H9) was used according to Ong et al. (27). Briefly, 50 pg of total RNA, 20 pg of the forward specific primer for the H9 gene (5'-CTACTGTTGGGAGGAAGAGAATGGT-3'), and 20 μl RNase free water were mixed, followed by adding dNTP Mix (5 mM, 1 μl), RT buffer (1X, 4 μl), DTT stock (5 mM, 1 μl), and SCRIPTUM first reverse transcriptase (100 units) and incubating them at 50°C for 30–60 min. The cDNA could now be applied as a template in PCR or stored at −20°C (28). The concentration of cDNA was measured by the Nanodrop system (Smart, Canada).

Conventional RT-PCR and Real-Time Reverse Transcription (RT)-PCR for the H9 Gene

The extracted RNA was reverse transcribed and amplified for conventional RT-PCR using the H9 gene-specific primer pair (F: 5'-CTACTGTTGGGAGGAAGAGAATGGT-3' and R: 5'-TGGGCGTCTTGAATAGGGTAA-3') and AccuPower one-step RT-PCR kit (Bioneer, Daejeon, Korea) (27). Then, the HA gene was deposited with accession number FJ794817, and the PCR products for positive samples were detected as a band with 256 bp in size by agarose gel (1.2%) electrophoresis. The extracted RNA of the LPAIV-H9N2 isolate H9N2/A/chicken/IRN/Ghazvin/2001 (FJ794817) at a viral load of $10^{8.5}$ EID_{50}/ml was used to compare the limit of detection by real-time RT-qPCR and conventional RT-PCR. The conventional RT-PCR and real-time RT-qPCR results for qualification of the H9 gene were compared using the serial dilutions of cDNA (with H9 specific primers), and cDNA concentration was measured by the Nanodrop system (Smart Nano, Canada) (28, 29). Moreover, according to the manufacturer's protocol, the cDNA of all samples for virus gene (H9) quantitation was amplified using QPCR Mix EvaGreen kit (Bio & Sell, Germany). The reaction mixture contained 100 nM of each specific primer pair for the H9 gene, which was used for conventional PCR, and for RT-QPCR we used 5×QPCR mix EvaGreen (4 μl), cDNA as a template (5 μl) and up to 20 μl water (30). The reaction was performed at the initial incubation temperature (94°C) for 3 min, and then 40 three-step cycles (30 s at 94°C for denaturation, 30 s at 58°C for annealing, and 30 s at 72°C for elongation) by the Rotor-Gene Q (QIAGEN) system.

Statistical Analysis

All statistical analyses were conducted by one-way ANOVA and Duncan's multiple range test. The comparisons of means for the antibody titration and SI in the first chicken experiment with sample size: 42 chickens, and the comparisons of means for the antibody titration, SI and cytokines values in the second chicken experiment with sample size: 200 and 21 broiler chickens, were done using SPSS, version 16. All values were expressed as the mean ± standard deviation, and a $p \leq 0.05$ was considered statistically significant.

RESULTS

The virus titer was $10^{8.5}$ EID_{50}/ml, and the HA assay for irradiated and non-irradiated avian influenza A subtype H9N2 virus samples was 10 Log_2, suggesting that irradiation does not lead to a decrease in the HA antigen. The D_{10} value and inactivation dose of γ-radiation were 3.4 and 30 kGy, respectively. The safety test was performed for irradiated LPAIV-H9N2 (at 30 kGy) on SPF eggs by four blind cultures and represented no virus multiplication at 30 kGy (19, 29). Also, the SDS-PAGE electrophoresis showed no change in the viral protein bands (HA and NP proteins) in irradiated and non-irradiated viral samples (**Figure 2**).

The data in the first chicken experiment (**Figure 3**) showed a significant increase in IVT.IN group for HI antibody titration and the proliferation index of stimulated spleen lymphocytes in IVT.IN and IVT.SC groups ($p < 0.05$). The first chicken experiment showed the increasing of the HI antibody titration and stimulation index of stimulated spleen lymphocytes 34 and 15%, in IVT.IN compered to IV.IN vaccine group, respectively.

The data in the second chicken experiment showed a significant increase in HI antibody titration in all vaccinated bird groups relative to the negative control ($p<0.05$), but the most significant increase was observed in the IVT.IN vaccine and the IV+ISA vaccine (SC) groups ($p < 0.05$). The comparison of the antibody titration between two vaccination regimes demonstrated more HI titers in the late-vaccinated groups reaching up to 5.33 log_2 in 2 weeks after the second vaccination. However, these levels were not significantly different in other groups (**Figure 4**).

The proliferation index of stimulated spleen lymphocytes was significantly upregulated in all vaccinated chicken groups in the second chicken experiment ($p < 0.05$). However, the most upregulation was detected in the IVT.IN and the IV+ISA ($p < 0.05$) vaccines in the late vaccinated regime. Based on these data, the cellular immunity induction in the irradiated vaccine groups was more considerable compared to formalin-treated vaccine groups (**Figure 4**). In addition, cytokines mRNA expression was upregulated in all vaccinated groups, and T-helper type 1 (Th1) cytokines such as IFN-γ and IL-2 were expressed more in the late vaccinated chicken regime. In this study, IL-6 was upregulated in

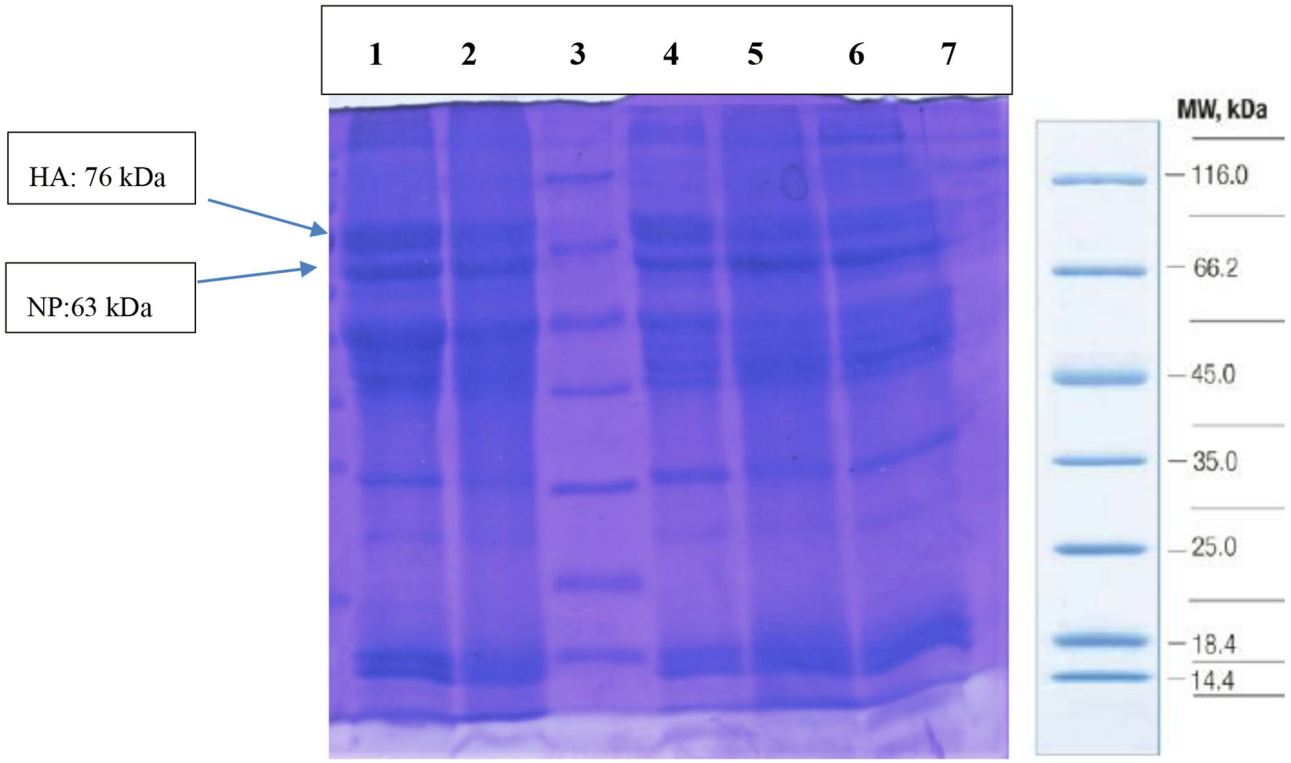

FIGURE 2 | The quality of viral protein by SDS-PAGE in irradiated (Lanes: 4, 5, 6) and non-irradiated (Lanes: 1, 2) LPAIV-H9N2 samples. Lane 3: protein markers (Cat No: SM0431), HA, Hemagglutinin antigen; NP, Nucleoprotein.

all vaccinated chicken groups. However, upregulation was more noticeable in the early vaccination than the late vaccination *($p < 0.05$)* (**Figure 5**). However, IL-6 was down-regulated in all vaccinated chicken groups in early and late regimes before the challenge with the live virus compared to these groups after the challenge.

The Conventional and Real-Time RT-QPCR Results for the H9 Gene

The extracted RNA of the Avian Influenza virus isolate H9N2/A/chicken/IRN/Ghazvin/2001 (FJ794817) at a viral load of 10 $^{8.5}$ EID_{50}/ml was used to compare the limit of detection by real-time RT-qPCR and conventional RT-PCR (28). The conventional RT-PCR and real-time RT-qPCR results for qualification of the H9 gene were compared using the serial dilutions of cDNA (with H9 specific primers), and cDNA concentration was measured by the Nanodrop system (Smart Nano, Canada) and it was from 9,681 −0.05 ng/μl for 10^{0}-10^{-5} dilutions. The detection limit for the H9 gene in the infected allantoic fluid was determined as 1.5 and 127 ng/μl by real-time RT-QPCR (A Ct value of about 27) and conventional RT-PCR (**Figure 6**), respectively.

The monitoring of virus shedding for the H9 gene at 2, 4, and 10 days after the challenge revealed no viral load in the tracheal samples (**Table 2**). The result of cloacal swab samples was the same as that of the tracheal samples. The Ct value for all tracheal and cloacal swab samples in groups 4–8 (early regime) and 11–15 groups (late regime) was more than 27 and negative for virus shedding after challenge. Virus shedding was not observed after challenging the vaccinated chickens with the live virus in tracheal and cloacal swab samples. It indicates that the immunization with irradiated LPAIV-H9N2 and formalin LPAIV-H9N2 can induce a protective response against the live homologous virus.

Viral Load on Lung Tissues and Loss of Body Weight Post-Challenge

The HI antibody titer and SI of splenic lymphocyte proliferation were significantly enhanced in vaccinated chicken groups, especially in the late vaccinated IVT.IN group. To evaluate the clinical protective effect of vaccines, the vaccinated chicken was challenged by the intranasal route on day 14 after the second immunization and monitored for 10 days for body weight loss. According to **Table 3**, the percent of body weight gain in early regime vaccinated groups during 1–30 days was more than 82% and in late regime vaccinated groups during 11–38 days was more than 84%. As expected, all the chickens in positive control groups (without vaccination) showed rapid body weight loss 10 days after the challenge. The percent of body weight gain in the positive control groups was nearly 89% before the challenge (during 1–30 days and 11–38 days), and 10 days after

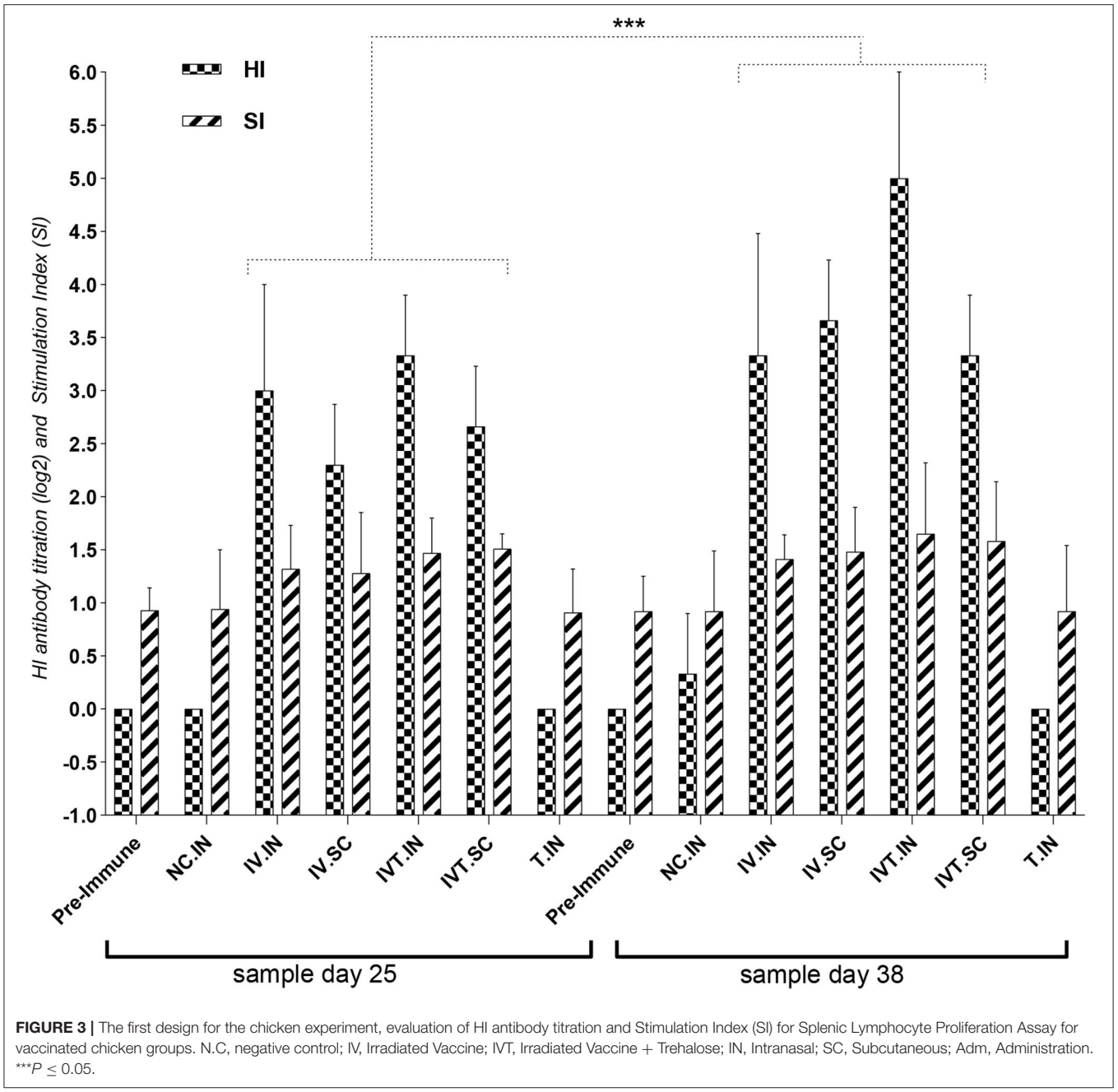

FIGURE 3 | The first design for the chicken experiment, evaluation of HI antibody titration and Stimulation Index (SI) for Splenic Lymphocyte Proliferation Assay for vaccinated chicken groups. N.C, negative control; IV, Irradiated Vaccine; IVT, Irradiated Vaccine + Trehalose; IN, Intranasal; SC, Subcutaneous; Adm, Administration. $^{***}P \leq 0.05$.

the challenge, it decreased to 75%. This data on increasing body weight showed the efficacy of vaccines (**Table 3**). The viral load on lung tissues was assayed 5 days after the challenge. However, body weight loss was not significant among the vaccinated chicken groups *($p>0.05$)*. The viral load in lung tissues was calculated by Reed and Munch's method as $TCID_{50}$/ml. The viral load value in positive control groups was approximately 10^5 $TCID_{50}$/ ml. This value was $<10^{0.5}$ $TCID_{50}$/ ml in the negative control groups (without vaccination and not challenged with live homologous subtype virus) and all vaccinated chicken groups.

DISCUSSION

LPAIV-H9N2 usually causes clinical diseases, including generalized infections, upper respiratory disease, and decreased egg production in the hosts, such as the layer chicken (31–33). In addition, this virus causes specific viral diseases in many bird species. It is also one of the instances of human health risks because it can create disease by contact with infected poultry or meats in humans. Hemagglutinin subtypes H5, H7, and H9 are the most important viruses that may infect humans (33). H9N2 has widely circulated in the poultry population and caused

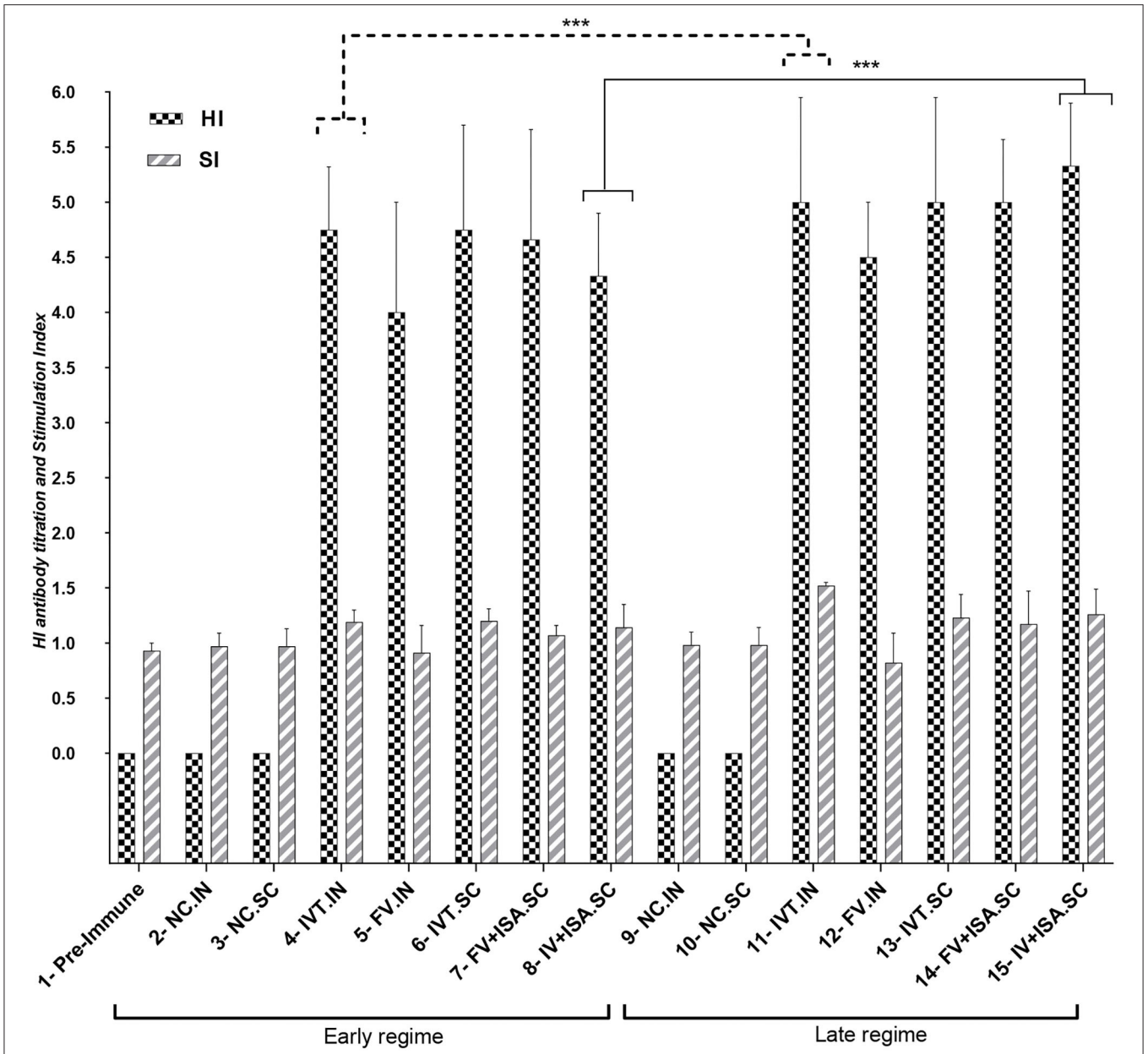

FIGURE 4 | HI antibody titration and Stimulation Index for Splenic Lymphocyte Proliferation Assay for vaccinated chicken groups in the second animal experiment (early regime vaccinated at days 1 and 15, Late regime vaccinated at days 11 and 25), the sampling was done on 30 and 38 days. N.C, negative control; IVT, Irradiated Vaccine + Trehalose; FV, formalin Vaccine; IN, Intranasal; SC, Subcutaneous ($^{**}p \leq 0.05$).

economic losses (34, 35). This virus has low pathogenicity to birds, but it is a severe threat to public health (36). Although prevailing vaccines decrease the disease incidence in birds, they cannot completely prevent the infection and shedding of the LPAIV-H9N2 (14, 37).

H9N2 viruses do not induce viremia in infected poultry (38). They suggested that simultaneous viral and bacterial infections influenced more mortality and egg-laying reduction in the respiratory outbreak. It is necessary to develop safe vaccines to conserve against influenza viruses (38). The vaccination program and biosecurity measures are two important tools for preventing and controlling LPAIV-H9N2s in chickens. An experimental formalin-inactivated oil-emulsion H9N2 LPAIV-H9N2 vaccine was reported by Marandi and Fard (38). The prevention of virus shedding through cloaca was employed as the potency test, revealing that the protective doses of 50% (PD_{50}) of 1, 1/10, and 1/50 of the field dose of the experimental LPAIV-H9N2 vaccine (EAI) were 100, 100, and 96.25%, respectively. The groups receiving <1/50 dose could not prevent virus shedding. Accordingly, the EAI vaccine could even be entirely protective

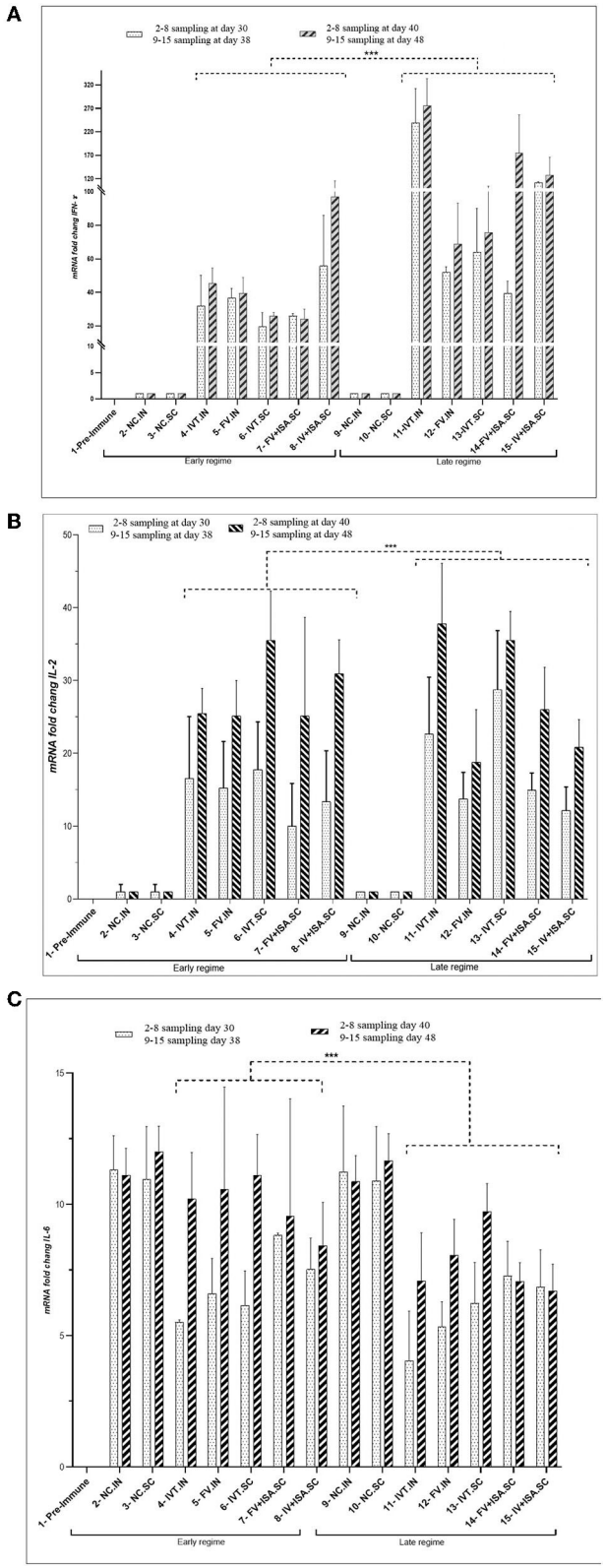

FIGURE 5 | The cytokine assay **(A)** IFN-γ, **(B)** IL-2, and **(C)** IL-6 (cytokines mRNA transcription levels as fold change) in the vaccinated broiler chicken groups in the second animal experiment). Two vaccination regimes were *(Continued)*

FIGURE 5 | performed: the early regime was primed on day 1 and boosted on day 15 (early regime) and sampling was done on 30 and 40 days. The late regime was primed on day 11 and boosted on day 25 (late regime) and sampling was done on 38 and 48 days. N.C, negative control; IVT, Irradiated Vaccine + Trehalose; FV, formalin Vaccine; IN, Intranasal; SC, Subcutaneous ($^{**}p \leq 0.05$).

and efficient in 1/10th dose, leading to a desirable immunity in experimental SPF chickens (39).

Some toxic residues remain in the formalin-inactivated vaccine, and some viruses may escape during chemical inactivation. The typical chemical substances applied for producing inactivated vaccines can cause a reduction in immunogenicity and damage antigenic epitopes (40). γ-Radiation is the perfect method for virus inactivation and the use of ionizing radiation for pathogen inactivation has been developed in the production of effective vaccines (41, 42). γ-Radiation slightly preserves the antigenic construction and can be used in a frozen condition that decreases free radical damage due to water radiolysis (43, 44). Consequently, there are two direct and indirect mechanisms for virus inactivation by γ-irradiation. Direct virus inactivation by γ-irradiation is mainly caused by radiolytic cleavage or cross-linking of genetic materials. The indirect effects of the γ-irradiation stem from the action of free radicals due to the radiolytic cleavage of water. The principal mechanism of virus inactivation by γ-irradiation is damaging viral nucleic acid replication *via* direct and indirect effects (45, 46). One study about LPAIV-H9N2 reported that the virus titer gradually decreased after increasing the dose of γ-radiation (20). The D_{10} value and optimum dose of virus inactivation for LPAIV-H9N2 were calculated by a dose/response curve of 3.36 and 30 kGy, respectively. In addition, the HA antigenicity of γ-irradiated LPAIV-H9N2 subtype H9N2 samples from 0 to 30 kGy represented no change. The safety test for γ-irradiated LPAIV-H9N2 *via* four blind cultures on embryonated eggs showed complete inactivation with γ-ray doses of 30 kGy without any multiplication on the embryonated eggs (20).

Likewise, the γ-irradiation Influenza virus, γ-APC [A/Port Chalmers/1/73(H3N2)], has major immunogenicity, and its protection was 100%, indicating lower weight loss in mice when compared with formalin- or UV-inactivated vaccines (47). Based on their data, γ-ray inactivated virus-induced immunity with high quantitatively and qualitatively to virus preparations inactivated by formalin or UV-irradiation. They further reported that γ-A/PC-vaccinated mice had reduced lung inflammation and viral lung load (47).

This research focused on evaluating both immune responses (humoral and cellular immunity) of the vaccinated broiler chicken in two vaccination regimes (early and late). The HI antibody titration and the proliferation of stimulated spleen lymphocytes had the most upregulation in the IVT and IV+ISA70 vaccine groups at the late vaccination regime 2 weeks after the second vaccination. The first chicken experiment showed the increase of the HI antibody titration and stimulation index of stimulated spleen lymphocytes in IVT.IN compared to

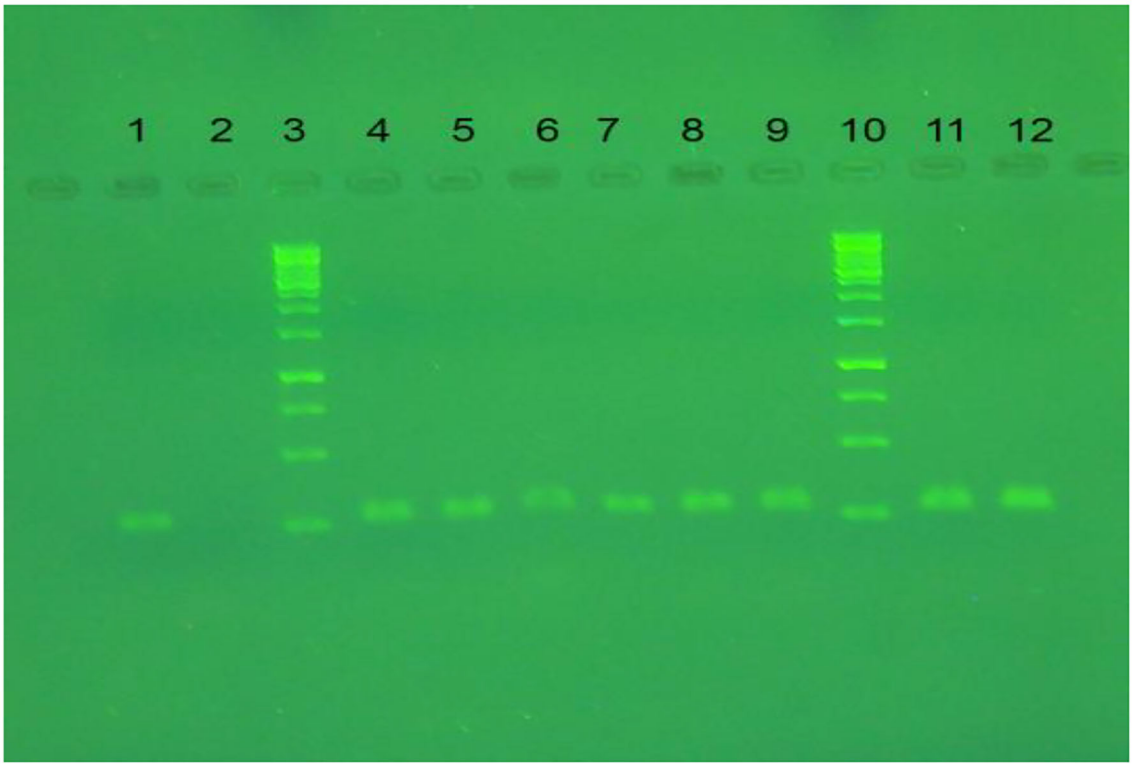

FIGURE 6 | The result of conventional RT-PCR on agarose gel. Lanes 1, 11, and 12 are RT-PCR products of LPAIV-H9N2 *via* specific primer for H9 gene. Lanes 3 and 10 are DNA ladder (SM0313). Lane 2 is a negative control, lanes 4-9 are RT-QPCR products for H9N2 cDNA dilution (10^{-1}-10^{-3}) in duplication.

the IV.IN vaccine group. These findings suggest that the use of γ-rays preferentially targets the viral genome and has little effect on the functional properties of viral proteins and they could indicate characteristics of Trehalose as a protein stabilizer and protein denaturation inhibitor.

Furthermore, the obtained data revealed that cellular immunity induction and cytokine mRNA expression were upregulated more in the irradiated vaccine groups compared to formalin-treated vaccine groups. IL-2 has been studied widely as a vaccine adjuvant and immuno-enhancer because of its role in activating T-cell proliferation (48). Chicken IFN-γ acts as a cytokine with multiple functions and is primarily secreted by T lymphocytes and NK cells. Further, it can modulate macrophage activation in birds, inhibit viral replication, and develop the Th1 response (49). Th1 cytokines such as IFN-γ and IL-2 were expressed more in the vaccinated chicken groups at the late vaccination age. IL-6 is a protein that is produced by various cells. It helps regulate immune responses, making the IL-6 test potentially useful as a marker of immune system activation. Furthermore, IL-6 is mainly made by some T lymphocytes. It causes B lymphocytes to produce more antibodies and causes fever by affecting the areas of the brain that control body temperature. Moreover, this protein is responsible for stimulating acute phase protein synthesis and producing neutrophils in the bone marrow. Moreover, it supports the growth of B cells and is antagonistic to regulatory T cells (50–52). IL-6 is a pleiotropic cytokine acting as a pro-inflammatory cytokine and an anti-inflammatory myokine. In this study, upregulation of IL-6 was more considerable in the early vaccination than in the late regime. Also, IL-6 was down-regulated in all vaccinated chicken groups in early and late regimes before the challenge with the live virus compared to these groups after the challenge. So, it indicates treatment with live LPAIV-H9N2 virus can upregulate IL-6 more than treatment with inactivated LPAIV-H9N2 virus. The lack of virus shedding in the immunized chicken with irradiated LPAIV-H9N2 and formalin-treated LPAIV-H9N2 vaccines after the challenge indicated a protective response against the live homologous virus. In addition, the viral load of $<10^{0.5}$ $TCID_{50}$/ml in the vaccinated chicken confirmed the protective response for all vaccines in this study. Thus, the IVT vaccine can be considered a good candidate for the immunization of broiler chicken *via* the intranasal route at the late regime. The adaptive immune defenses of newly hatched chickens have limited capabilities to control the pathogens (53). Eventually, Bochen reported that the lowest levels of immunity basically occurred from days 6 to 13 in broiler chickens (54). Accordingly, days 11 and 25 can be recommended as the suitable ages of vaccination against LPAIV-H9N2 for inducing the protective response.

One conclusion of this research is that the use of Trehalose as a protein stabilizer during gamma irradiation can prevent viral antigenic damage and is useful for the production of inactivated vaccine with intact immunogenic characteristics. Another conclusion is that two vaccination doses of irradiated

TABLE 2 | The monitoring of virus shedding in vaccinated chickens in the second animal experiment at 2, 4, and 10 days after challenge with homologs subtype virus at tracheal and cloacal swab samples.

No	Vaccine groups	Route- of Adm	Regime of Vaccination	Challenge-day	Sampling days after challenge		
					2	4	10
					Virus shedding CT (log10)		
1	Pre-Immune	-	-	-	-	-	-
2	N.C (PBS)	IN	Early	-	UND	UND	UND
3	N.C (PBS)	SC	Early	-	UND	UND	UND
4	IVT	IN	Early	30	1.543	1.535	1.525
5	FV	IN	Early	30	1.559	1.577	1.485
6	IVT	SC	Early	30	1.532	1.600	1.518
7	FV+ISA	SC	Early	30	1.582	1.549	1.521
8	IV+ISA	SC	Early	30	1.546	1.575	1.527
9	N.C (PBS)	IN	Late	-	UND	UND	UND
10	N.C (PBS)	SC	Late	-	UND	UND	UND
11	IVT	IN	Late	38	1.488	1.487	1.534
12	FV	IN	Late	38	1.492	1.483	1.563
13	IVT	SC	Late	38	1.512	1.554	1.565
14	FV+ISA	SC	Late	38	1.483	1.544	1.549
15	IV+ISA	SC	Late	38	1.512	1.544	1.561
16	PC	IN	-	30	1.308	1.193	UT
17	PC	IN	-	38	1.269	1.209	UT

UND, Undetermined; UT, Un-tested.

TABLE 3 | The % increasing of body weight in early regime vaccinated groups during 1–30 days and in late regime vaccinated groups during 11–38 days.

No	Vaccine groups	Route- of Adm	Regime of Vaccination	Challenge-day	% Increasing of body weight 1–30 and 11–38 days	% Increasing of body weight 1–40 and 11–48 days
1	Pre-Immune	-	-	-	-	-
2	N.C (PBS)	IN	Early	-	89.14	90.14
3	N.C (PBS)	SC	Early	-	88.25	90.33
4	IVT	IN	Early	30	89.52	90.56
5	FV	IN	Early	30	87.26	88.76
6	IVT	SC	Early	30	88.41	89.38
7	FV+ISA	SC	Early	30	82.74	83.33
8	IV+ISA	SC	Early	30	84.55	85.11
9	N.C (PBS)	IN	Late	-	90.52	90.52
10	N.C (PBS)	SC	Late	-	88.75	90.35
11	IVT	IN	Late	38	89.58	91.03
12	FV	IN	Late	38	88.72	89.20
13	IVT	SC	Late	38	89.65	89.65
14	FV+ISA	SC	Late	38	84.20	84.96
15	IV+ISA	SC	Late	38	85.02	86.43
16	PC	IN	-	30	88.94	75.88
17	PC	IN	-	38	88.38	75.14

LPAIV-H9N2 vaccine induce more immune responses than one dose of vaccination. Also, the late vaccination regime induces higher immune responses than the early regime. Finally, we can suggest IVT.IN vaccine in the late regime as the suitable vaccine and comfort to inoculation against IV subtype H9N2.

DATA AVAILABILITY STATEMENT

The datasets presented in this study can be found in online repositories. The names of the repository/repositories and accession number(s) can be found in the article/supplementary material.

ETHICS STATEMENT

The animal study was reviewed and all institutional and national guidelines which were adopted from the horizontal legislation on the protection of animals used for scientific purposes (Directive 2010/63/EU as amended by Regulation (EU) 2019/1010) were approved for implementation Tehran University of Medical Science. Animal trial license number granted by the Tehran University is "IR.TUMS.AEC.1401".

AUTHOR CONTRIBUTIONS

FM, VW, and HU designed the study and helped in interpreting the study results. FM, VW, and SM critically revised the manuscript. IK, AA, and SH carried out the methodology, collected, and analyzed the data. PS and MB have helped in chicken studies and sampling. All authors contributed to the article and approved the submitted version.

FUNDING

This study was supported by the International Atomic Energy Agency (IAEA Coordinated Research Project, CRP No. 22126).

ACKNOWLEDGMENTS

The authors would like to show gratitude to the Department of Nuclear Sciences and Applications, Animal Production and Health Section, International Atomic Energy Agency (IAEA), VIC, Vienna, Austria, for supporting (IAEA Coordinated Research Project, CRP No. 22126).

REFERENCES

1. Rahimirad S, Alizadeh A, Alizadeh E, Hosseini SM. The avian influenza H9N2 at avian-human interface: A possible risk for the future pandemics. *J Res Med Sci*. (2016) 21:51. doi: 10.4103/1735-1995.187253
2. Alexander DJ. An overview of the epidemiology of avian influenza. *Vaccine*. (2007) 25:5637–44. doi: 10.1016/j.vaccine.2006.10.051
3. Szretter KJ, Balish AL, Katz JM. Influenza: propagation, quantification, and storage. *Curr Protoc Microbiol*. (2006) 3:15G.1.1–22. doi: 10.1002/0471729256.mc15g01s3
4. Homme PJ, Easterday BC. Avian Influenza Virus Infections. I. Characteristics of Influenza A-Turkey-Wisconsin-1966 Virus. *Avian Dis*. (1970) 14:66. doi: 10.2307/1588557
5. Alizadeh E, Kheiri M, Bashar R, Tabatabaeian M, Hosseini SM. Avian Influenza (H9N2) among poultry workers in Iran. *Iran J Microbiol*. (2009) 1:3–6.
6. Peacock TP, James J, Sealy JE, Iqbal M. A Global Perspective on H9N2 Avian Influenza. *Virus*. (2019) 11:1–28. doi: 10.3390/v11070620
7. Bi Y, Chen Q, Wang Q, Shi W, Liu D. Genesis evolution and prevalence of h5n6 avian influenza viruses in china genesis, evolution and prevalence of H5N6 Avian Influenza Viruses in China. *Cell Host Microbe*. (2016) 20:1–12. doi: 10.1016/j.chom.2016.10.022
8. Nili H, Asasi K. Avian influenza (H9N2) outbreak in Iran. *Avian Dis*. (2003) 47:828–31. doi: 10.1637/0005-2086-47.s3.828
9. Shaimaa T, Reham R A, Rafa A, Abdel-Daim M M, Elfeil W K. Comparison of the effectiveness of two different vaccination regimes for avian influenza H9N2 in broiler chicken. *Animals (Basel)*. (2020) 10:1875. doi: 10.3390/ani10101875
10. Magnani DM, Harms JS, Durward MA, Splitter GA. Nondividing but metabolically active gamma-irradiated brucella melitensis is protective against virulent B. *melitensis* challenge in mice. *Infect Immun*. (2009) 77:5181–9. doi: 10.1128/IAI.00231-09
11. Hoffman SL, Goh LML, Luke TC, Schneider I, Le TP, Doolan DL, et al. Protection of humans against malaria by immunization with radiation-attenuated Plasmodium falciparum sporozoites. *J Infect Dis*. (2002) 185:1155–64. doi: 10.1086/339409
12. Rojas C, Figueroa JV, Alvarado A, Mejia P, Mosqueda JJ, Falcon A, et al. Bovine babesiosis live vaccine production: Use of gamma irradiation on the substrate. *Ann N Y Acad Sci*. (2006) 1081:405–16. doi: 10.1196/annals.1373.059
13. Dillon GP, Feltwell T, Skelton J, Coulson PS, Wilson RA, Ivens AC. Altered patterns of gene expression underlying the enhanced immunogenicity of radiation-attenuated schistosomes. *PLoS Negl Trop Dis*. (2008) 2:e240. doi: 10.1371/journal.pntd.0000240
14. Javan S, Motamedi-Sedeh F, Dezfulian M. Reduction of viral load of avian influenza A virus (H9N2) on SPF eggs and cell line by gamma irradiation. *Bulg J Vet Med*. (2021) 24:144–51. doi: 10.15547/bjvm.2019-0094
15. Motamedi-Sedeh F, Soleimanjahi H, Jalilian AR, Mahravani H, Shafaee K, Sotoodeh M, et al. Development of Protective Immunity against Inactivated Iranian Isolate of Foot-and-Mouth Disease Virus Type O/IRN/2007 Using Gamma Ray-Irradiated Vaccine on BALB/c Mice and Guinea Pigs. *Intervirology*. (2015) 58:190–6. doi: 10.1159/000433538
16. Mollaei Alamuti M, Ravanshad M, Motamedi-Sedeh F, Nabizadeh A, Ahmadi E, Hossieni SM. Immune response of gamma-irradiated inactivated bivalent polio vaccine prepared plus trehalose as a protein stabilizer in a mouse model. *Intervirology*. (2021) 64:140–6. doi: 10.1159/000515392
17. Martinon D, Borges VF, Gomez AC, Shimada K. Potential fast COVID-19 containment with trehalose. *Front Immunol*. (2020) 11:1623. doi: 10.3389/fimmu.2020.01623
18. Richards AB, Krakowka S, Dexter LB, Schmid H, Wolterbeek APM, Waalkens-Berendsen DH, et al. Trehalose: a review of properties, history of use and human tolerance, and results of multiple safety studies. *Food Chem Toxicol*. (2002) 40:871–98. doi: 10.1016/S0278-6915(02)00011-X
19. Lee HJ, Yoon YS, Lee SJ. Mechanism of neuroprotection by trehalose: controversy surrounding autophagy induction. *Cell Death Dis*. (2018) 9:1–12. doi: 10.1038/s41419-018-0749-9
20. Salehi B, Motamedi-Sedeh F, Madadgar O, Khalili I, Ghalyan Chi Langroudi A, Unger H, et al. Analysis of antigen conservation and inactivation of gamma-irradiated avian influenza virus subtype H9N2. *Acta Microbiol Immunol Hung*. (2018) 65:163–71. doi: 10.1556/030.65.2018.025
21. Reed LJ, Muench H. A simple method of estimating fifty per cent endpoints. *Am J Epidemiol*. (1938) 27:493–7. doi: 10.1093/oxfordjournals.aje.a118408

22. Raie Jadidi B, Erfan-Niya H, Ameghi A. Optimizing the process of inactivating influenza virus subtype H9N2 by formalin in the production of killed avian influenza vaccine. *Arch Razi Inst.* (2017) 72:43–9.
23. Statement E. EFSA Panel on Animal Health and Welfare (AHAW); EFSA Panel on Animal Health and Welfare (AHAW). *EFSA J*. (2015) 13.
24. Health [OIE] World Organisation for Animal. Avian influenza (infection with avian influenza viruses). Man diagnostic tests vaccines. *Terr Anim.* (2015).
25. Motobu M, El-Abasy M, Na KJ, Hirota Y. Detection of Mitogen-Induced Lymphocyte Proliferation by Bromodeoxyuridine(BrdU)incorporation in the Chicken. *J Vet Med Sci.* (2002) 64:377–9. doi: 10.1292/jvms.64.377
26. Sandbulte MR, Roth JA. Methods for analysis of cell-mediated immunity in domestic animal species. *J Am Vet Med Assoc.* (2004) 225:522–30. doi: 10.2460/javma.2004.225.522
27. Ong WT, Omar AR, Ideris A, Hassan SS. Development of a multiplex real-time PCR assay using SYBR Green 1 chemistry for simultaneous detection and subtyping of H9N2 influenza virus type A. *J Virol Methods.* (2007) 144:57–64. doi: 10.1016/j.jviromet.2007.03.019
28. Mosleh N, Dadras H, Mohammadi A. Molecular quantitation of H9N2 avian influenza virus in various organs of broiler chickens using TaqMan real time PCR. *J Mol Genet Med.* (2009) 03:152–7. doi: 10.4172/1747-0862.1000027
29. Ward CL, Dempsey MH, Ring CJA, Kempson RE, Zhang L, Gor D, et al. Design and performance testing of quantitative real time PCR assays for influenza A and B viral load measurement. *J Clin Virol.* (2004) 29:179–88. doi: 10.1016/S1386-6532(03)00122-7
30. Ben Shabat M, Meir R, Haddas R, Lapin E, Shkoda I, Raibstein I, et al. Development of a real-time TaqMan RT-PCR assay for the detection of H9N2 avian influenza viruses. *J Virol Methods.* (2010) 168:72–7. doi: 10.1016/j.jviromet.2010.04.019
31. Motamedi Sedeh F, Shadi J, Dezfoolian M, Wijewardana V. Evaluation of Immune Responses and Histopathological Effects against Gamma Irradiated Avian Influenza (Sub type H9N2) Vaccine on Broiler. *Brazil Archiv Biolo Technol*. (2020) 63:1–9. doi: 10.1590/1678-4324-2020200094
32. Fouchier RAM, Rimmelzwaan GF, Kuiken T, Osterhaus ADME. Newer respiratory virus infections: human metapneumovirus, avian influenza virus, and human coronaviruses. *Curr Opin Infect Dis.* (2005) 18:141–6. doi: 10.1097/01.qco.0000160903.56566.84
33. Qiang L. Dong-ying L, Zhan-qiu Y. Characteristics of human infection with avian influenza viruses and development of new antiviral agents. *Acta Pharmacolo Sinica.* (2013) 34:1257–69. doi: 10.1038/aps.2013.121
34. Yoon SW, Webby RJ, Webster RG. Evolution and ecology of influenza a viruses. *Curr Top Microbiol Immunol.* (2014) 385:359–75. doi: 10.1007/82_2014_396
35. Xu KM, Smith GJD, Bahl J, Duan L, Tai H, Vijaykrishna D, et al. The genesis and evolution of H9N2 influenza viruses in poultry from southern China, 2000 to 2005. *J Virol.* (2007) 81:10389–401. doi: 10.1128/JVI.00979-07
36. Munir M, Zohari S, Abbas M, Shabbir M Z, Nauman Zahid M, Latif M S, et al. Isolation and characterization of low pathogenic H9N2 avian influenza A virus from a healthy flock and its comparison to other H9N2 isolates. *Indian J Virol.* (2013) 24:342–8. doi: 10.1007/s13337-013-0144-1
37. Monne I, Ormelli S, Salviato A, Battisti C De, Bettini F, Salomoni A, et al. Cattoli G. Development and validation of a one-step real-time PCR assay for simultaneous detection of subtype H5, H7, and H9 Avian Influenza Viruses. *J Clin Microbiol*. (2008) 46:1769–73. doi: 10.1128/JCM.02204-07
38. Marandi MV, Fard MHB. Isolation of H9N2 subtype of avian influenza viruses during an outbreak in chickens in Iran. *Iran Biomed J.* (2002) 6:13–7.
39. Moghaddam Pour M, Momayez R, Akhavizadegan MA. The efficacy of inactivated oil-emulsion H9N2 avian influenza vaccine. *Iran J Vet Res.* (2006) 7:85–8.
40. Sohini S. Bhatia1 and Suresh D. Pillai. Ionizing Radiation Technologies for Vaccine Development -A Mini Review. *Front Immunol*. (2022) 13:1–9, doi: 10.3389/fimmu.2022.845514
41. Ohshima H, Iida Y, Matsuda A, Kuwabara M. Damage induced by hydroxyl radicals generated in the hydration layer of γ-irradiated frozen aqueous solution of DNA. *J Radiat Res.* (1996) 37:199–207. doi: 10.1269/jrr.37.199
42. Dorey S, Gaston F, Dupuy N, Barbaroux M, Marque RA, Dorey S, et al. Reconciliation of pH, conductivity, total organic carbon with carboxylic acids detected by ion chromatography in solution after contact with multilayer films after γ -irradiation To cite this version : HAL Id : hal-01764846. *Eur J Pharm Sci*. (2018) 117:216–26. doi: 10.1016/j.ejps.2018.02.023
43. Alsharifi M, Müllbacher A. The γ-irradiated influenza vaccine and the prospect of producing safe vaccines in general. *Immunol Cell Biol.* (2010) 88:103–4. doi: 10.1038/icb.2009.81
44. Lomax ME, Folkes LK, Neill PO. Biological consequences of radiation-induced DNA damage : relevance to radiotherapy statement of search strategies used and sources of information why radiation damage is more effective than endogenous damage at killing cells ionising radiation-induced do. *Clin Oncol.* (2013) 25:578–85. doi: 10.1016/j.clon.2013.06.007
45. Hume AJ, Ames J, Rennick LJ, Duprex WP, Marzi A, Tonkiss J, et al. Inactivation of RNA viruses by gamma irradiation: a study on mitigating factors. *Viruses.* (2016) 8:204. doi: 10.3390/v8070204
46. Summers WC, Szybalski W. Gamma-irradiation of deoxyribonucleic acid in dilute solutions: II. Molecular mechanisms responsible for inactivation of phage, its transfecting DNA, and of bacterial transforming activity. *J Mol Biol.* (1967) 26:227–35. doi: 10.1016/0022-2836(67)90293-8
47. Furuya Y, Regner M, Lobigs M, Koskinen A, Müllbacher A, Alsharifi M. Effect of inactivation method on the cross-protective immunity induced by whole "killed" influenza A viruses and commercial vaccine preparations. *J Gen Virol.* (2010) 91:1450–60. doi: 10.1099/vir.0.018168-0
48. Hilton LS, Bean AGD, Kimpton WG, Lowenthal JW. Interleukin-2 directly induces activation and proliferation of chicken T cells in vivo. *J Interf cytokine Res*. (2002) 22:755–63. doi: 10.1089/107999002320271341
49. Cardenas-Garcia S, Dunwoody RP, Marcano V, Diel DG, Williams RJ, Gogal Jr RM, et al. Effects of chicken interferon gamma on Newcastle disease virus vaccine immunogenicity. *PLoS ONE.* (2016) 11:e0159153. doi: 10.1371/journal.pone.0159153
50. Schneider K, Klaas R, Kaspers B, Staeheli P. Chicken interleukin-6: cDNA structure and biological properties. *Eur J Biochem.* (2001) 268:4200–6. doi: 10.1046/j.1432-1327.2001.02334.x
51. Fernando FS, Okino CH, Silva KR, Fernandes CC, Gonçalves M, Montassier MFS, et al. Increased expression of interleukin-6 related to nephritis in chickens challenged with an avian infectious bronchitis virus variant. *Pesqui Veterinária Bras.* (2015) 35:216–22. doi: 10.1590/S0100-736X2015000300002
52. Nishimichi N, Kawashima T, Hojyo S, Horiuchi H, Furusawa S, Matsuda H. Characterization and expression analysis of a chicken interleukin-6 receptor alpha. *Dev Comp Immunol.* (2006) 30:419–29. doi: 10.1016/j.dci.2005.05.007
53. Alkie TN, Yitbarek A, Hodgins DC, Kulkarni RR, Taha-Abdelaziz K, Sharif S. Development of innate immunity in chicken embryos and newly hatched chicks: a disease control perspective. *Avian Pathol.* (2019) 48:288–310. doi: 10.1080/03079457.2019.1607966
54. Song B, Tang D, Yan S, Fan H, Li G, Shahid MS, et al. Effects of age on immune function in broiler chickens. *J Anim Sci Biotechnol.* (2021) 12:1–12. doi: 10.1186/s40104-021-00559-1

Conflict of Interest: The authors declare that the research was conducted in the absence of any commercial or financial relationships that could be construed as a potential conflict of interest.

Frontiers in Immunology

Explores novel approaches and diagnoses to treat immune disorders.

The official journal of the International Union of Immunological Societies (IUIS) and the most cited in its field, leading the way for research across basic, translational and clinical immunology.

Discover the latest Research Topics

See more →

Frontiers

Avenue du Tribunal-Fédéral 34
1005 Lausanne, Switzerland
frontiersin.org

Contact us

+41 (0)21 510 17 00
frontiersin.org/about/contact